

Umpolung Amide Synthesis Mechanistic Studies, Development of a
New *N*-Aryl Amide Synthesis, and α -Oxy- and α -Thio-nitroalkanes in
the BAM-Catalyzed aza-Henry Reaction

By

Michael Crocker

Dissertation

Submitted to the Faculty of the
Graduate school of Vanderbilt University
in partial fulfillment of the requirements
for the degree of
DOCTOR OF PHILOSOPHY

in

Chemistry

March 31st, 2021

Nashville, Tennessee

Approved:

Jeffrey N. Johnston

Steven D. Townsend

Craig W. Lindsley

Ned A. Porter

Acknowledgments

I will be forever grateful to all those who I was lucky enough to receive guidance and support from both leading up to and during my graduate education. Graduate school is an incredibly formative and challenging experience and so much of what I learned and accomplished would have been inaccessible without the relationships I made along the way.

The wealth of expertise and experience of the professors I have interacted with in combination with their willingness to teach and help has been invaluable. Specifically, Prof. Jeffrey Johnston's dedication to the fundamentals of organic chemistry both in class and as a research advisor is unrivaled. As a researcher, I will never forget Dr. Johnston's lessons to never give up and leave no stone unturned. I have learned so much about chemistry as well as what type of scientist I am and strive to be, and for that I cannot thank him enough.

I also want to thank the other members of my committee who each brought unique and valuable perspectives to my graduate career. Prof. Steven Townsend was an incredible teacher, exciting personality, and all-around supportive person. Prof. Craig Lindsley brought a down to earth mindset with excellent suggestions and broad awareness of the field. Prof. Ned Porter contributed an exquisite mechanistic knowledge as well as a friendly and helpful attitude.

My committee were not the only people at Vanderbilt who were vital to my academic and personal growth. Profs. Alissa Hare, Nathan Schley, and Brian Bachmann all taught me so much while always being encouraging and receptive to questions. Prof. Nathan Schley also very generously helped me with crystal structures on several occasions; his instruments and skill led to valuable advancements in my work. Dr. Donald Stec's work to keep the NMR facilities running

smoothly and, just as importantly, his ability and willingness to help with advanced techniques was impressive and serves as a foundation for the whole department.

The importance of my fellow lab members also cannot be understated. I consider myself lucky to have worked alongside every single member I overlapped with past and present from our most experienced postdocs to our greenest undergraduates. Dr. Jade Bing and Dr. Matt Knowe each served as true mentors and great friends for me. Jade was supportive both in and out of the lab and would never hesitate to go above and beyond expectations to address any question or problem I brought up to her. Matt always had a level head, good advice, and truly cared about his peers. I'm also grateful to him for bringing the occasional excitement in the form of a soccer game or rocket launch viewing into the lab. Although my time alongside him was shorter, Dr. Ken Schwieter was my first guide in the lab, and I could not be the researcher I am today without him. Dr. Thomas Struble, Dr. Suzanne Batiste and Sangjun Park are great people and labmates as well. Karan Goyal also deserves a lot of thanks for his contributions to the lab as well as extraordinarily positive and lively character he put into everything he did. I'll never see SpongeBob again without thinking of Karan's antics.

The postdocs I got to spend the most time with were Dr. Kazuyuki Tokumaru, Dr. Mahesh Vishe, Dr. Kalisankar Bera, and Dr. Rashanique Quarels. Each brought a different skillset and personality without which the lab would not have felt the same. Kazu's work overlapped with some of mine, and he was always so knowledgeable when I came to him with questions. I also remember and praise Kazu's generosity every time I take a melting point.

Just as losing (as coworkers) each of the former lab members mentioned above was difficult, a hard part about reaching this point is leaving current group members. Jenna Payne was

always a friend and sounding-board, and I frequently enjoyed dinner or brunch with her and Dom. Abby Smith was always kind, efficient, and a lot of fun to work through problems with on our white boards (not to mention a dream-team subgroup partner). Jade Izaguirre was up for any challenge and an animated desk buddy and conversationalist. I'm glad the group star wars figures have such an enthusiastic home.

I've never known someone more persevering than Ron Benning. He was a great benchmate and friend and always kept my spirits up. Ron and Jade Bing also knew how to throw a party. Another superlative: Jade Williams is the most excited and passionate chemist I've ever met. It was always so refreshing to have an engaged, positive discussion about any development or topic with her. While my time spent alongside Zihang Deng, Madelaine Thorpe, and David Almond was far too short we were still able to have good times together. Zihang is a great chemist (and I'm not just saying that because a reaction he developed was key to one of my syntheses) and a fun friend. I really enjoyed the occasions we got to hang out around a fire and talk about everything from Chinese history to Mr. Mistoffelees.

My friends Amy Zheng and Matt Miletich were a great part of living in Nashville and will always be some of my best friends. I want to thank them for always stopping by on their walks to say "hi", and being all-around good people always interested in talking about whatever was going on in my life. That's not even to mention how generous they have been to regularly invite me over for wonderful home-cooked meals.

There were many people involved with my pre-graduate education who instilled in me my love of the field and scientific foundation. In high school, Mary Lohr and Jana Layne first got me interested in science. I studied at the Gatton Academy which was full of amazing people who

created a culture of learning and support. Derick Strode and Tim Gott were just a couple of the people making that opportunity possible. At the university level, Dr. Jeremy Maddox, Dr. Lester Pesterfield, Dr. Ru-Jong Jeng, Dr. Chad Snyder, and Dr. Mark Meier were but some of the mentors who taught me the basics of scientific research and chemistry.

Most of all, I want to thank my family. Graduate school is so taxing physically, mentally, socially, and emotionally. It offers incredible opportunity to learn and progress, but it requires a great deal of sacrifice from the researcher and those close to them. I'm so thankful that those closest to me were willing to support me in every way they could through the process. My fiancé Krysta Waldrop was going through a parallel experience in a different program, but always had time for me. She encouraged me to never lose hope and was an example of strength throughout. Having my best friend to come home to and have dinner or watch TV with was an inexhaustible source of happiness even in the darkest of times. I'm grateful that we were able to earn our degrees together, and I'm not sure I could have done it without her support.

My parents as well were unwavering pillars as I pursued my degree. Even as a child they encouraged me to study what interested me and worked hard to make sure I had opportunities to do so. Their faith in me has been such a source of strength and confidence. They were always understanding of the pressures I faced and, at the same time, always prioritized spending time together. They never hesitated to bear any burden they could for me and frequently traveled to Nashville even just for short visits. They afforded me a lifestyle of more comfort than a typical graduate stipend allows for, and my mom, a former English teacher, always offered to proofread my documents. My brother Clay recently finished a Ph.D. program and consequently always had

great advice. More importantly though, he was a source of fun and relaxation for me as we frequently played video games together and talked about our similar interests.

Lastly, none of this work would have been possible without the financial support of the National Science Foundation, National Institutes of Health, Vanderbilt University, Vanderbilt Institute of Chemical Biology, and Warren Foundation.

Table of Contents

	Page
Acknowledgments.....	ii
Table of Contents.....	vii
List of Figures.....	xiv
List of Tables.....	xxvi
List of Schemes.....	xxvii
Chapter	
Chapter 1. Development of Enantioselective BAM-Catalyzed aza-Henry Reactions.....	1
1.1 Introduction.....	1
1.1.1 Aza-Henry Reaction.....	1
1.1.2 Bis-Amidine Catalysis in Aza-Henry Reactions.....	5
1.1.3 α -Sulfanyl, α -Alkoxy, and Sulfonyl Nitroalkanes.....	7
1.2 α -Oxy- and α -Thio Nitroalkane Addition to <i>N</i> -Boc Aryl Aldimines.....	11
1.2.1 Aza-Henry Reactions with α -Sulfanyl, α -Alkoxy, and Sulfonyl Nitroalkanes.....	16
1.3 Conclusions.....	22
Chapter 2. Mechanistic Investigation of Umpolung Amide Synthesis; Evidence for the Halo-Amino-NitroAlkane (HANA) Tetrahedral Intermediate.....	25
2.1 Introduction.....	25
2.1.1 Amide Bond Formation.....	25
2.1.2 Umpolung Amide Synthesis.....	32
2.2 Mechanism Investigations Using α -Sulfanyl, α -Alkoxy, and Sulfonyl Nitroalkanes.....	40
2.2.1 UmAS Reactions with α -Sulfanyl, α -Alkoxy, and Sulfonyl Nitroalkanes.....	40
2.2.2 Study of the Epimerization of an Active Ester in Traditional Amide Synthesis.....	42

2.3 Mechanism Investigations by HaloAminoNitroAlkane (HANA) Preparation	44
2.3.1 HANA Synthesis.....	48
2.3.2 HANA Competency for Amide Formation.....	54
2.3.3 Coproduct Analysis.....	55
2.3.4 ¹⁸ O Labeling Experiments.....	57
2.3.5 Probing the Nature of Nitro-Nitrite Isomerization.....	60
2.3.6 Kinetics Experiments	65
2.3.7 Theoretical-Computational Analysis	69
2.3.8 Application of Fluoro Nitroalkanes to Study Diverted UmAS.....	76
2.3.9 Conclusions.....	78
Chapter 3. New Applications for HANAs	80
3.1 Introduction	80
3.2 Expansion of Umpolung Heterocycle Access	81
3.2.1 Umpolung Heterocycle Access.....	81
3.2.2 Investigation of an Unexpected Product from Standard UmAS Applied to an <i>N</i> -Methyl α -Amino Ester.....	87
3.2.3 Attempted Umpolung Synthesis of Indazoles and Triazoles from Diazonium Salts...	90
3.2.4 Attempted Umpolung Synthesis of Thiadiazoles and Thiazoles	94
3.2.5 Conclusions.....	97
3.3 Umpolung Synthesis of <i>N</i> -Aryl Amides	99
3.3.1 <i>N</i> -Aryl Amides.....	99
3.3.2 Reaction Discovery	102
3.3.3 Reaction Optimization	113
3.3.4 Mechanistic Insights	123

3.3.5 Reaction Scope and Application	134
3.3.6 Conclusions.....	147
References.....	149
Appendix A: Experimental	164
General Procedure for Aza-Henry Reactions.....	165
<i>tert</i> -Butyl ((1 <i>R</i>)-2-(benzyloxy)-1-(4-chlorophenyl)-2-nitroethyl)carbamate (19).....	165
<i>tert</i> -Butyl (1-(4-chlorophenyl)-2-nitro-2-(phenylthio)ethyl)carbamate (22).....	166
<i>tert</i> -Butyl ((1 <i>R</i>)-1-(4-chlorophenyl)-2-nitro-2-(phenylsulfonyl)ethyl)carbamate (23).....	167
General Procedure for Aza-Henry Reactions to Prepare Racemic Standards	168
Competition Reaction Between α -OBn and α -SPh Nitromethane.....	169
Competition Reaction Between α -OBn Nitromethane and Nitrobutane	169
Example α -Nitrosulfone Reduction Leading to Oxime (E)-2-phenyl-1-(phenylsulfonyl)ethan-1-one (S1).....	169
Ozonolysis of 23 for ee Determination	170
Desulfonylation of 23 for ee Determination	171
S-Phenyl (<i>R</i>)-2-((<i>tert</i> -butoxycarbonyl)amino)-2-(4-chlorophenyl)ethanethioate (69).....	171
Conventional Amide Synthesis from Thioester	173
General Procedure for UmAS Reactions	173
Use of Fluoronitroalkane in UmAS	173
General Procedure for Halogen Screening in the Tetrahedral Intermediate (TI') Synthesis ..	174
1-Chloro-4-(chloro(nitro)methyl)benzene (77c).....	174
Chloro Nitroalkane in the Tetrahedral Intermediate (TI') Synthesis.....	175
Bromo Nitroalkane in the Tetrahedral Intermediate (TI') Synthesis.....	176
Evaluation of Imide Stability	176

General Procedure for Tetrahedral Intermediate Conversion	176
Diethyl 1-(4-chlorobenzoyl)hydrazine-1,2-dicarboxylate (79a).....	177
Diethyl 1-benzoylhydrazine-1,2-dicarboxylate (79b).....	177
Diethyl 1-(4-fluorobenzoyl)hydrazine-1,2-dicarboxylate (79c).	178
Diethyl 1-(4-(trifluoromethyl)benzoyl)hydrazine-1,2-dicarboxylate (79d).....	179
Diethyl 1-(4-nitrobenzoyl)hydrazine-1,2-dicarboxylate (79e).	179
Conversion of (-)-85e.....	180
TI' Conversion in the Presence of TEMPO.....	180
Chemically Induced Dynamic Nuclear Polarization (CIDNP) Experiment.....	181
Cyclopropane Radical Probe Experiments.....	181
(<i>trans</i> -2-(Nitromethyl)cyclopropyl)benzene (S2).....	181
(<i>trans</i> -2-((<i>R</i>)-Fluoro(nitro)methyl)cyclopropyl)benzene (103).....	182
Diethyl 1-(<i>trans</i> -2-phenylcyclopropane-1-carbonyl)hydrazine-1,2-dicarboxylate (104)...	183
(<i>cis</i> -2-(Nitromethyl)cyclopropyl)benzene (S3).	183
(<i>cis</i> -2-(Fluoro(nitro)methyl)cyclopropyl)benzene (105).	184
Diethyl 1-(<i>cis</i> -2-phenylcyclopropane-1-carbonyl)hydrazine-1,2-dicarboxylate (106).	185
(((<i>cis</i> -2-(Fluoro(nitro)methyl)cyclopropyl)methoxy)methyl)benzene (107).....	186
Diethyl 1-(<i>cis</i> -2-((Benzyloxy)methyl)cyclopropane-1-carbonyl)hydrazine-1,2-dicarboxylate (108).....	187
General procedure for Tetrahedral Intermediate Synthesis.....	187
Diethyl 1-((4-chlorophenyl)fluoro(nitro)methyl)hydrazine-1,2-dicarboxylate (85a).....	188
Diethyl 1-(fluoro(nitro)(phenyl)methyl)hydrazine-1,2-dicarboxylate (85b).....	188
Diethyl 1-(fluoro(4-fluorophenyl)(nitro)methyl)hydrazine-1,2-dicarboxylate (85c).	189

Diethyl 1-(fluoro(nitro)(4-(trifluoromethyl)phenyl)methyl)hydrazine-1,2-dicarboxylate (85d).....	190
Diethyl 1-(fluoro(nitro)(4-nitrophenyl)methyl)hydrazine-1,2-dicarboxylate (85e).	190
(-)-Diethyl 1-(fluoro(nitro)(4-nitrophenyl)methyl)hydrazine-1,2-dicarboxylate ((-)-85e). 191	
Diisopropyl 1-((4-chlorophenyl)fluoro(nitro)methyl)hydrazine-1,2-dicarboxylate (88). ..	191
Control Reaction with Diacyl Hydrazine	192
Control Reaction with Diacyl Hydrazine and Oxidant	192
General Procedure for Preparation of Tetrahedral Intermediate Synthesis Byproducts	193
Diethyl 1-(4-chlorobenzoyl)hydrazine-1,2-dicarboxylate (93).	193
Diethyl 1,2-bis(4-chlorobenzoyl)hydrazine-1,2-dicarboxylate (94).....	194
Diethyl 1-(4-chlorobenzoyl)-2-nitrosohydrazine-1,2-dicarboxylate (95a).	194
Diethyl 1-benzoyl-2-nitrosohydrazine-1,2-dicarboxylate (95b).	195
Diethyl 1-(4-chlorobenzoyl)hydrazine-1,2-dicarboxylate (96).	196
Diethyl 1-(4-chlorobenzoyl)hydrazine-1,2-dicarboxylate (97).	196
Conversion of 95a in the Presence of $^{18}\text{OH}_2$	197
Ethyl (Z)-2-(fluoro(4-nitrophenyl)methylene)hydrazine-1-carboxylate (120).....	197
Tetrahedral Intermediate NMR Conversion Experiments	200
Conversion of 85a in Wet Oxygenated Solvent.....	200
Conversion of 85a in Dry Oxygenated Solvent	200
Conversion of 85a in Dry Degassed Solvent	201
Conversion of 85a in Degassed Solvent	202
Conversion of 85b in Degassed Solvent	203
General Procedure for 85c Conversion Comparison Experiments: Sample Preparation ...	205
Conversion of 85c in Dry Degassed Solvent	205

Conversion of 85c in Degassed Solvent	206
Conversion of 85c in Dry Oxygenated Solvent	207
Conversion of 85d in Degassed Solvent	208
Conversion of 85e in Degassed Solvent	209
(2 <i>S</i>)-1-Fluoro-2-(methoxymethoxy)-1-nitroheptane (S4).....	210
(2 <i>S</i>)-1-Chloro-2-(methoxymethoxy)-1-nitroheptane (S5).	211
Isopropyl (<i>S</i>)-2-((2-(methoxymethoxy)heptanoyl)imino)propanoate <i>N</i> -oxide (138).	212
Procedure for HCl/NaNO ₂ Diazotization.....	212
General Procedure for HNO ₃ /KNO ₂ Diazotization.....	213
1-((4-Chlorophenyl)(nitro)methylene)-2-phenylhydrazine (S6).	214
1-(3-Methoxyphenyl)-2-(1-nitroethylidene)hydrazine (151).....	214
CTAN Deprotection of S6.....	215
(<i>E</i>)-1-(4-Fluorophenyl)-3-tosyltriaz-1-ene (171).....	216
(<i>S</i>)-2-(4-([1,1'-Biphenyl]-2-yl)-1 <i>H</i> -1,2,3-triazol-1-yl)-1,1-diphenylpropan-1-ol (183).	216
(<i>S</i>)- <i>N</i> -(2-(4-([1,1'-Biphenyl]-2-yl)-1 <i>H</i> -1,2,3-triazol-1-yl)-1,1-diphenylpropyl)benzamide (187).....	217
(<i>S</i>)-4-([1,1'-Biphenyl]-2-yl)-1-(1-benzamido-1,1-diphenylpropan-2-yl)-3-phenethyl-1 <i>H</i> - 1,2,3-triazol-3-ium bromide (179).	218
<i>N</i> ,2-bis(4-Chlorophenyl)- <i>N</i> -hydroxyacetamide (196).	219
General Procedure for <i>N</i> -Aryl Hydroxylamine Synthesis	220
General Procedure for Umpolung <i>N</i> -Aryl Amide Synthesis.....	221
X-ray of Single Crystal of 88	247
X-ray of Single Crystal of 120	253
Computational Methods	257

Single Point Energies, Enthalpy, and Entropy Data	258
Cartesian Coordinates	260
Additional Structural Data	314
Hydrolysis of F-N=O	322
Appendix B: Spectral Data and HPLC Traces.....	327

List of Figures

Figure	Page
1. Biologically active natural products and small molecules synthesized using the aza-Henry reaction	3
2. Some important BAM catalysts	6
3. Biologically active compounds with β -amino ethers or thioethers.....	12
4. Significant structures in the Johnston and Hayashi mechanistic proposals for UmAS	16
5. Structures of several representative amide coupling reagents	26
6. Possible structures for the electrophilic amine	35
7. Hayashi <i>N</i> -haloamine complex bond lengths	37
8. Rate of epimerization of 69 in dilute ethanol solution at rt	43
9. Structure of PTAD	51
10. X-Ray crystal structure of <i>rac</i> -88 (TI') establishing C-NO ₂ (nitro) regiochemistry rather than C-ONO (nitrite ester)	52
11. Examination of a series of nitroalkanes by X-ray structural analysis: correlation of C-N bond length with sum of angles at tetrahedral carbon	54
12. Minor co-products formed from the reaction of 32a with DEAD	55
13. Hammett plot generated from observing HANA consumption during the thermal conversion of 85a-e to their corresponding amide products plotted against A) σ^+ and B) σ substituent constants.....	67
14. Energy profiles corresponding to 1,2-migration and heterolytic C-F bond cleavage. Calculated relative free energies at 298 K (kcal mol ⁻¹) include single-point energy corrections at the IEFPCM(DMSO)/B3LYP/6-311++G(2d,2p)//IEFPCM(DMSO)/B3LYP/6-31G(d) level. The inlet scheme depicts homolytic C-N bond cleavage and associated bond-dissociation energy ΔH (kcal mol ⁻¹).....	71

15. Energy profile corresponding to stepwise nitro to nitrite isomerization pathway leading to amide from formation of nitrite ester (black line) or water capture (red line). Calculated relative free energies at 298 K (kcal mol ⁻¹) include single-point energy corrections at the IEFPCM(DMSO)/uB3LYP/6-311++G(2d,2p)//IEFPCM(DMSO)/uB3LYP/6-31G(d) level	72
16. Transition states associated with Figure 15	73
17. Example thiazole-containing antibiotic (thiocillin I)	83
18. Nitron product initially assigned as oxazole	88
19. Examples of α -stereocenter containing <i>N</i> -aryl amides of pharmaceutical relevance – difficult couplings	99
20. Examples of α -stereocenter containing <i>N</i> -aryl amides of pharmaceutical relevance	100
21. Energy profiles corresponding to 1,2-migration and heterolytic C-F bond cleavage. Calculated relative free energies at 298 K (kcal mol ⁻¹) include single-point energy corrections at the IEFPCM(DMSO)/uM06-2X/6-311++G(2d,2p)//IEFPCM(DMSO)/uB3LYP/6-31G(d) level. The inlet scheme depicts homolytic C-N bond cleavage and associated bond dissociation energy (ΔH in kcal mol ⁻¹).	316
22. Energy profile corresponding to stepwise nitro to nitrite isomerization pathway leading to amide from formation of nitrite ester (black line) or water capture (red line). Calculated relative free energies at 298 K (kcal mol ⁻¹) include single-point energy corrections at the IEFPCM(DMSO)/uM06-2X/6-311++G(2d,2p)//IEFPCM(DMSO)/uB3LYP/6-31G(d) level. .	317
23. Energy profiles corresponding to 1,2-migration and heterolytic C-F bond cleavage. Calculated relative free energies at 298 K (kcal mol ⁻¹) include single-point energy corrections at the IEFPCM(DMSO)/uPBEPBE/6-311++G(2d,2p)//IEFPCM(DMSO)/uB3LYP/6-31G(d) level. The inlet scheme depicts homolytic C-N bond cleavage and associated bond dissociation energy (ΔH in kcal mol ⁻¹).	318
24. Energy profile corresponding to stepwise nitro to nitrite isomerization pathway leading to amide from formation of nitrite ester (black line) or water capture (red line). Calculated relative free energies at 298 K (kcal mol ⁻¹) include single-point energy corrections at the IEFPCM(DMSO)/uPBEPBE/6-311++G(2d,2p)//IEFPCM(DMSO)/uB3LYP/6-31G(d) level..	319

25. Energy profiles corresponding to 1,2-migration and heterolytic C-F bond cleavage. Calculated relative free energies at 298 K (kcal mol ⁻¹) include single-point energy corrections at the IEFPCM(DMSO)/uMPW1PW91/6-311++G(2d,2p)//IEFPCM(DMSO)/uB3LYP/6-31G(d) level. The inset scheme depicts homolytic C-N bond cleavage and associated bond dissociation energy (ΔH in kcal mol ⁻¹).	320
26. Energy profile corresponding to stepwise nitro to nitrite isomerization pathway leading to amide from formation of nitrite ester (black line) or water capture (red line). Calculated relative free energies at 298 K (kcal mol ⁻¹) include single-point energy corrections at the IEFPCM(DMSO)/uMPW1PW91/6-311++G(2d,2p)//IEFPCM(DMSO)/uB3LYP/6-31G(d) level.	321
27. Energy profile corresponding to hydrolysis of F-N=O. Calculated relative free energies at 298 K (kcal mol ⁻¹) include single-point energy corrections at the IEFPCM(DMSO)/uB3LYP/6-311++G(2d,2p)//IEFPCM(DMSO)/uB3LYP/6-31G(d) level.	323
28. Energy profile corresponding to hydrolysis of F-N=O. Calculated relative free energies at 298 K (kcal mol ⁻¹) include single-point energy corrections at the IEFPCM(DMSO)/uM06-2X/6-311++G(2d,2p)//IEFPCM(DMSO)/uB3LYP/6-31G(d) level.	324
29. Energy profile corresponding to hydrolysis of F-N=O. Calculated relative free energies at 298 K (kcal mol ⁻¹) include single-point energy corrections at the IEFPCM(DMSO)/uPBEPBE/6-311++G(2d,2p)//IEFPCM(DMSO)/uB3LYP/6-31G(d) level.	325
30. Energy profile corresponding to hydrolysis of F-N=O. Calculated relative free energies at 298 K (kcal mol ⁻¹) include single-point energy corrections at the IEFPCM(DMSO)/uMPW1PW91/6-311++G(2d,2p)//IEFPCM(DMSO)/uB3LYP/6-31G(d) level.	326
31. ¹ H NMR (400 MHz, CDCl ₃) of 19	328
32. ¹³ C NMR (100 MHz, CDCl ₃) of 19	329
33. ¹ H NMR (400 MHz, CDCl ₃) of 22	330
34. ¹³ C NMR (100 MHz, CDCl ₃) of 22	331

35. ^1H NMR (400 MHz, CDCl_3) of 23	332
36. ^{13}C NMR (100 MHz, CDCl_3) of 23	333
37. ^1H NMR (400 MHz, CDCl_3) of 69	334
38. ^{13}C NMR (100 MHz, CDCl_3) of 69	335
39. ^1H NMR (400 MHz, CDCl_3) of 77c	336
40. ^{13}C NMR (100 MHz, CDCl_3) of 77c	337
41. ^1H NMR (600 MHz, CDCl_3) of 79a	338
42. ^{13}C NMR (150 MHz, CDCl_3) of 79a	339
43. ^1H NMR (600 MHz, CDCl_3) of 79b	340
44. ^{13}C NMR (150 MHz, CDCl_3) of 79b	341
45. ^1H NMR (400 MHz, CDCl_3) of 79c	342
46. ^{13}C NMR (100 MHz, CDCl_3) of 79c	343
47. ^{19}F NMR (376 MHz, CDCl_3) of 79c	344
48. ^1H NMR (400 MHz, CDCl_3) of 79d	345
49. ^{13}C NMR (100 MHz, CDCl_3) of 79d	346
50. ^{19}F NMR (376 MHz, CDCl_3) of 79d	347
51. ^1H NMR (600 MHz, CDCl_3) of 79e	348
52. ^{13}C NMR (150 MHz, CDCl_3) of 79e	349
53. ^1H NMR (400 MHz, DMSO-d_6) of 85a	350
54. ^{13}C NMR (100 MHz, DMSO-d_6) of 85a	351
55. ^{19}F NMR (376 MHz, CDCl_3) of 85a	352
56. ^1H NMR (600 MHz, CDCl_3) of 85b	353
57. ^{13}C NMR (150 MHz, CDCl_3) of 85b	354
58. ^{19}F NMR (376 MHz, CDCl_3) of 85b	355

59. ^1H NMR (600 MHz, CDCl_3) of 85c	356
60. ^{13}C NMR (150 MHz, CDCl_3) of 85c	357
61. ^{19}F NMR (376 MHz, CDCl_3) of 85c	358
62. ^1H NMR (400 MHz, DMSO-d_6) of 85d	359
63. ^{13}C NMR (100 MHz, DMSO-d_6) of 85d	360
64. ^{19}F NMR (376 MHz, CDCl_3) of 85d	361
65. ^1H NMR (600 MHz, CDCl_3) of 85e	362
66. ^{13}C NMR (150 MHz, CDCl_3) of 85e	363
67. ^{19}F NMR (376 MHz, CDCl_3) of 85e	364
68. ^1H NMR (600 MHz, CDCl_3) of 88	365
69. ^{13}C NMR (150 MHz, CDCl_3) of 88	366
70. ^{19}F NMR (376 MHz, CDCl_3) of 88	367
71. ^1H NMR (600 MHz, CDCl_3) of 93	368
72. ^{13}C NMR (150 MHz, CDCl_3) of 93	369
73. ^{19}F NMR (376 MHz, CDCl_3) of 93	370
74. ^1H NMR (600 MHz, CDCl_3) of 94	371
75. ^{13}C NMR (150 MHz, CDCl_3) of 94	372
76. ^1H NMR (600 MHz, CDCl_3) of 95a	373
77. ^{13}C NMR (150 MHz, CDCl_3) of 95a	374
78. ^1H NMR (600 MHz, CDCl_3) of 95b	375
79. ^{13}C NMR (150 MHz, CDCl_3) of 95b	376
80. ^1H NMR (400 MHz, CDCl_3) of 96	377
81. ^{13}C NMR (150 MHz, CDCl_3) of 96	378
82. ^1H NMR (600 MHz, CDCl_3) of 97	379

83. ^{13}C NMR (150 MHz, CDCl_3) of 97	380
84. ^1H NMR (400 MHz, CDCl_3) of 103	381
85. ^{13}C NMR (100 MHz, CDCl_3) of 103	382
86. ^{19}F NMR (376 MHz, CDCl_3) of 103	383
87. ^1H NMR (400 MHz, CDCl_3) of 104	384
88. ^{13}C NMR (150 MHz, CDCl_3) of 104	385
89. ^1H NMR (400 MHz, CDCl_3) of 105	386
90. ^{13}C NMR (100 MHz, CDCl_3) of 105	387
91. ^{19}F NMR (376 MHz, CDCl_3) of 105	388
92. ^1H NMR (400 MHz, CDCl_3) of 106	389
93. ^{13}C NMR (100 MHz, CDCl_3) of 106	390
94. ^1H NMR (600 MHz, CDCl_3) of 107	391
95. ^{13}C NMR (150 MHz, CDCl_3) of 107	392
96. ^{19}F NMR (376 MHz, CDCl_3) of 107	393
97. ^1H NMR (400 MHz, toluene- d_8) of 108	394
98. ^{13}C NMR (150 MHz, toluene- d_8) of 108	395
99. ^1H NMR (600 MHz, CDCl_3) of 120	396
100. ^{13}C NMR (150 MHz, CDCl_3) of 120	397
101. ^{19}F NMR (376 MHz, CDCl_3) of 120	398
102. ^1H NMR (600 MHz, CDCl_3) of 121	399
103. ^{13}C NMR (150 MHz, CDCl_3) of 121	400
104. ^1H NMR (600 MHz, CDCl_3) of 138	401
105. ^{13}C NMR (150 MHz, CDCl_3) of 138	402
106. ^1H NMR (400 MHz, CDCl_3) of 151	403

107.	^{13}C NMR (100 MHz, CDCl_3) of 151	404
108.	^1H NMR (400 MHz, CDCl_3) of 171	405
109.	^{13}C NMR (100 MHz, CDCl_3) of 171	406
110.	^{19}F NMR (376 MHz, CDCl_3) of 171	407
111.	^1H NMR (600 MHz, CDCl_3) of 179	408
112.	^{13}C NMR (150 MHz, CDCl_3) of 179	409
113.	^1H NMR (400 MHz, CDCl_3) of 183	410
114.	^{13}C NMR (100 MHz, CDCl_3) of 183	411
115.	^1H NMR (400 MHz, CDCl_3) of 187	412
116.	^{13}C NMR (100 MHz, CDCl_3) of 187	413
117.	^1H NMR (400 MHz, $\text{DMSO}-d_6$) of 196	414
118.	^{13}C NMR (100 MHz, $\text{DMSO}-d_6$) of 196	415 ¹⁰⁹ .
119.	^1H NMR (400 MHz, acetone- d_6) of 215	416
120.	^{13}C NMR (100 MHz, acetone- d_6) of 215	417
121.	^1H NMR (400 MHz, $\text{DMSO}-d_6$) of 216	418
122.	^{13}C NMR (100 MHz, $\text{DMSO}-d_6$) of 216	419
123.	^1H NMR (400 MHz, CDCl_3) of 220	420
124.	^{13}C NMR (100 MHz, CDCl_3) of 220	421
125.	^{19}F NMR (376 MHz, CDCl_3) of 220	422
126.	^1H NMR (400 MHz, CDCl_3) of 222	423
127.	^{13}C NMR (100 MHz, CDCl_3) of 222	424
128.	^{19}F NMR (376 MHz, CDCl_3) of 222	425
129.	^1H NMR (400 MHz, CDCl_3) of 223	426
130.	^{13}C NMR (100 MHz, CDCl_3) of 223	427

131. ¹⁹ F NMR (376 MHz, CDCl ₃) of 223	428
132. ¹ H NMR (400 MHz, DMSO- <i>d</i> ₆) of 230	429
133. ¹³ C NMR (100 MHz, DMSO- <i>d</i> ₆) of 230	430
134. ¹ H NMR (400 MHz, DMSO- <i>d</i> ₆) of 232	431
135. ¹³ C NMR (100 MHz, DMSO- <i>d</i> ₆) of 232	432
136. ¹ H NMR (400 MHz, DMSO- <i>d</i> ₆) of 233	433
137. ¹³ C NMR (100 MHz, DMSO- <i>d</i> ₆) of 233	434
138. ¹ H NMR (400 MHz, DMSO- <i>d</i> ₆) of 234	435
139. ¹³ C NMR (100 MHz, DMSO- <i>d</i> ₆) of 234	436
140. ¹ H NMR (400 MHz, DMSO- <i>d</i> ₆) of 237	437
141. ¹³ C NMR (100 MHz, DMSO- <i>d</i> ₆) of 237	438
142. ¹ H NMR (600 MHz, DMSO- <i>d</i> ₆) of 238	439
143. ¹³ C NMR (150 MHz, DMSO- <i>d</i> ₆) of 238	440
144. ¹ H NMR (400 MHz, DMSO- <i>d</i> ₆) of 239	441
145. ¹³ C NMR (100 MHz, DMSO- <i>d</i> ₆) of 239	442
146. ¹ H NMR (400 MHz, DMSO- <i>d</i> ₆) of 24	443
147. ¹³ C NMR (100 MHz, DMSO- <i>d</i> ₆) of 24	444
148. ¹⁹ F NMR (376 MHz, DMSO- <i>d</i> ₆) of 240	445
149. ¹ H NMR (400 MHz, DMSO- <i>d</i> ₆) of 241	446
150. ¹³ C NMR (100 MHz, DMSO- <i>d</i> ₆) of 241	447
151. ¹ H NMR (400 MHz, DMSO- <i>d</i> ₆) of 24	448
152. ¹³ C NMR (100 MHz, DMSO- <i>d</i> ₆) of 24	449
153. ¹ H NMR (400 MHz, DMSO- <i>d</i> ₆) of 244	450
154. ¹³ C NMR (100 MHz, DMSO- <i>d</i> ₆) of 24	451

155. ¹ H NMR (400 MHz, DMSO- <i>d</i> ₆) of 245	452
156. ¹³ C NMR (100 MHz, DMSO- <i>d</i> ₆) of 245	453
157. ¹ H NMR (600 MHz, DMSO- <i>d</i> ₆) of 24	454
158. ¹³ C NMR (150 MHz, DMSO- <i>d</i> ₆) of 24	455
159. ¹⁹ F NMR (376 MHz, DMSO- <i>d</i> ₆) of 246	456
160. ¹ H NMR (400 MHz, DMSO- <i>d</i> ₆) of 247	457
161. ¹³ C NMR (100 MHz, DMSO- <i>d</i> ₆) of 247	458
162. ¹ H NMR (600 MHz, CDCl ₃) of 249	459
163. ¹³ C NMR (150 MHz, CDCl ₃) of 249	460
164. ¹⁹ F NMR (376 MHz, CDCl ₃) of 249	461
165. ¹ H NMR (400 MHz, CDCl ₃) of 25	462
166. ¹³ C NMR (100 MHz, CDCl ₃) of 25	463
167. ¹ H NMR (600 MHz, CDCl ₃) of 253	464
168. ¹³ C NMR (150 MHz, CDCl ₃) of 253	465
169. ¹ H NMR (400 MHz, CDCl ₃) of 254	466
170. ¹³ C NMR (100 MHz, CDCl ₃) of 254	467
171. ¹ H NMR (400 MHz, CDCl ₃) of 25	468
172. ¹³ C NMR (100 MHz, CDCl ₃) of 25	469
173. ¹ H NMR (600 MHz, CDCl ₃) of 260	470
174. ¹³ C NMR (150 MHz, CDCl ₃) of 260	471
175. ¹⁹ F NMR (376 MHz, CDCl ₃) of 260	472
176. ¹ H NMR (600 MHz, CDCl ₃) of 261	473
177. ¹³ C NMR (150 MHz, CDCl ₃) of 261	474
178. ¹ H NMR (600 MHz, CDCl ₃) of 263	475

179.	^{13}C NMR (150 MHz, CDCl_3) of 263a	476
180.	^1H NMR (400 MHz, CDCl_3) of 27	477
181.	^{13}C NMR (100 MHz, CDCl_3) of 27	478
182.	^{19}F NMR (376 MHz, CDCl_3) of 271	479
183.	^1H NMR (400 MHz, CDCl_3) of 27	480
184.	^{13}C NMR (100 MHz, CDCl_3) of 27	481
185.	^1H NMR (400 MHz, CDCl_3) of 27	482
186.	^{13}C NMR (100 MHz, CDCl_3) of 27	483
187.	^1H NMR (400 MHz, CDCl_3) of 27	484
188.	^{13}C NMR (100 MHz, CDCl_3) of 27	485
189.	^1H NMR (400 MHz, CDCl_3) of 28	486
190.	^{13}C NMR (100 MHz, CDCl_3) of 28	487
191.	^1H NMR (400 MHz, CDCl_3) of 28	488
192.	^{13}C NMR (100 MHz, CDCl_3) of 28	489
193.	^1H NMR (600 MHz, CDCl_3) of 29	490
194.	^{13}C NMR (150 MHz, CDCl_3) of 29	491
195.	^1H NMR (600 MHz, CDCl_3) of 29	492
196.	^{13}C NMR (150 MHz, CDCl_3) of 29	493
197.	^1H NMR (600 MHz, CDCl_3) of 29	494
198.	^{13}C NMR (150 MHz, CDCl_3) of 29	495
199.	^1H NMR (400 MHz, CDCl_3) of S1	496
200.	^{13}C NMR (100 MHz, CDCl_3) of S1	497
201.	^1H NMR (400 MHz, CDCl_3) of S2	498
202.	^{13}C NMR (100 MHz, CDCl_3) of S2	499

203. ^1H NMR (400 MHz, CDCl_3) of S3	500
204. ^{13}C NMR (100 MHz, CDCl_3) of S3	501
205. ^1H NMR (400 MHz, CDCl_3) of S4	502
206. ^{13}C NMR (100 MHz, CDCl_3) of S4	503
207. ^{19}F NMR (376 MHz, CDCl_3) of S4	504
208. ^1H NMR (400 MHz, CDCl_3) of S5	505
209. ^{13}C NMR (100 MHz, CDCl_3) of S5	506
210. ^1H NMR (600 MHz, CDCl_3) of S6	507
211. ^{13}C NMR (150 MHz, CDCl_3) of S6	508
212. ^1H NMR (600 MHz, $\text{DMSO-}d_6$) of S7	509
213. ^{13}C NMR (150 MHz, $\text{DMSO-}d_6$) of S7	510
214. ^1H NMR (400 MHz, $\text{DMSO-}d_6$) of Conversion of 85a in degassed solvent; t = 0, 15, 60, 180, 240 minutes (bottom to top).....	511
215. ^1H NMR (400 MHz, $\text{DMSO-}d_6$) of Conversion of 85b in degassed solvent; t = 0, 15, 60, 120 minutes (bottom to top).....	512
216. ^1H NMR (400 MHz, $\text{DMSO-}d_6$) of Conversion of 85c in dry degassed solvent; t = 0, 15, 60, 150 minutes (bottom to top).....	513
217. ^1H NMR (400 MHz, $\text{DMSO-}d_6$) of Conversion of 85c in degassed solvent; t = 0, 15, 60, 150 minutes (bottom to top).....	514
218. ^1H NMR (400 MHz, $\text{DMSO-}d_6$) of Conversion of 85c in dry oxygenated solvent; t = 0, 15, 60, 150 minutes (bottom to top).....	515
219. ^1H NMR (400 MHz, $\text{DMSO-}d_6$) of Conversion of 85d in degassed solvent; t = 0, 90, 360, 950 minutes (bottom to top).....	516
220. ^1H NMR (400 MHz, $\text{DMSO-}d_6$) of Conversion of 85e in degassed solvent; t = 0, 90, 270, 520, 2240 minutes (bottom to top).....	517

221. Selective ^1H NMR NOE on a mixture of 272 and 291 (600 MHz, CDCl_3) irradiating minor (purple, <i>Z</i> , 3% enhancement) and major (green, <i>E</i> , 3% enhancement) isomers with isolated minor (red, <i>Z</i>) and major (blue, <i>E</i>) for reference	518
222. HPLC traces of 19 (racemic top; enantioenriched bottom)	519
223. HPLC traces of 22 (racemic top; enantioenriched bottom)	520
224. HPLC traces of 24 (racemic top; enantioenriched bottom)	521
225. HPLC traces of 25 (racemic top; enantioenriched bottom)	522
226. HPLC traces of 69 (racemic top; enantioenriched bottom)	523
227. HPLC traces of 260 (racemic top; enantioenriched bottom)	524
228. HPLC traces of 261 (racemic top; enantioenriched bottom)	525
229. HPLC traces of 263a (racemic top; enantioenriched bottom)	526
230. HPLC traces of 282 (racemic top; enantioenriched bottom)	527
231. HPLC traces of 85e (racemic top; t=0 min bottom)	528
232. HPLC traces of 85e continued (t=20 top; t=140 min bottom)	529
233. HPLC traces of 85e continued (t=1400 min)	530

List of Tables

Table	Page
1. Bond dissociation energies of relevant carbon-heteroatom bonds	14
2. Yields of UmAS with various α -halo nitroalkanes	15
3. Benzyloxy nitromethane aza-Henry results	17
4. pKa values for some substituted nitroalkanes in DMSO	18
5. Thiophenyl nitromethane aza-Henry results	20
6. Phenylsulfonyl nitromethane aza-Henry results	21
7. Catalyzed reaction of α -halo nitroalkanes with an azodicarboxylate electrophile (DEAD) ^a ...	48
8. A survey of conditions targeting α -NO ₂ hydrazones	91
9. Early optimization of the hydroxylamine <i>N</i> -aryl amide synthesis.....	118
10. Final optimization of the hydroxylamine <i>N</i> -aryl amide synthesis	121
11. Reaction scope of umpolung <i>N</i> -aryl amide synthesis	136
12. Single point energies, enthalpies and entropies for structures	258
13. Single point energies for structures. Geometry optimizations and frequency calculations were performed at the uB3LYP/6-31G(d) level of theory. Single point energies were calculated at the uB3LYP/6-311++G(2d,2p), uM06-2X/6-311++G(2d,2p), uPBEPBE/6-311++G(2d,2p) and uMPW1PW91/6-311++G(2d,2p) level of theory. Solvent effects were evaluated with the integral equation formalism polarizable continuum model (IEFPCM).	314
14. Single point energies for the structures associated with the hydrolysis of F–N=O. Geometry optimizations and frequency calculations were performed at the uB3LYP/6-31G(d) level of theory. Single point energies were calculated at the uB3LYP/6-311++G(2d,2p), uM06-2X/6-311++G(2d,2p), uPBEPBE/6-311++G(2d,2p) and uMPW1PW91/6-311++G(2d,2p) level of theory. Solvent effects were evaluated with the integral equation formalism polarizable continuum model (IEFPCM).	322

List of Schemes

Scheme	Page
1. Selected examples of aza-Henry reactions	2
2. Early work on enantioselective aza-Henry reactions	4
3. Nef-type ozonolysis of nitronates	8
4. Examples of nitronate ozonolysis in synthesis	8
5. Palladium catalyzed nitrosulfone additions	9
6. Reported desulfonylations of α -nitrosulfones	10
7. Possible transformations and applications of novel nitroalkanes	13
8. Competition reactions between benzyloxy nitromethane, nitrobutane, and thiophenyl nitromethane	19
9. Ozonolysis of 23 for ee determination	21
10. Thiophenyl nitromethane in the bisamidine catalyzed aza-Henry reaction	23
11. Benzyloxy nitromethane in the bisamidine catalyzed aza-Henry reaction	24
12. Epimerization of active esters with α - <i>N</i> -acyl groups	28
13. Enantioselective routes to non-natural amino acids	29
14. A survey of amide forming reactions	31
15. Illustration of UmAS's unique reversal of polarity	33
16. Proposed UmAS mechanism	33
17. Mechanistic insight from diverted UmAS reaction	35
18. Proposed oxidative amidation mechanism	38
19. Johnston UmAS and Hayashi oxidative amidation reaction conditions	39

20. Results from UmAS reactions with unexplored α -substituted nitroalkanes	40
21. Limited mechanistic pathways resulting from α -SR/OR/SO ₂ R substituents.....	41
22. Traditional amide synthesis with epimerizable active ester	42
23. Attempted synthesis of UmAS tetrahedral intermediate analogue	45
24. Discovery of oxadiazole formation in bromo nitroalkane addition to DEAD.....	45
25. Electrophilic behavior of DEAD	46
26. Consideration of nitrogen electronics on intermediate stability	48
27. Reactions of α -fluoro nitroalkane with amine and azodicarboxylate	49
28. Control reactions validating umpolung behavior of C-N bond formation.....	50
29. Mechanistic hypotheses for observed co-products	57
30. ¹⁸ O-Labeling experiments.....	58
31. Additional ¹⁸ O-Labeling experiments.....	59
32. The nitro-nitrite isomerization and possible pathways contributing to partial ¹⁸ O-label loss	61
33 Investigation of possible reversible conversion of 32e, illustrated by the potential intermediacy of carbon radical 49.....	62
34. Cyclopropane substrates used to probe radical intermediacy.....	64
35. Cyclopropane substrate used previously in UmAS	65
36. Representative pathways that were explored using computational methods.....	74
37. The nitro-nitrite isomerization and possible pathways contributing to partial ¹⁸ O-label loss	76
38. Unified hypothesis for HANA collapse pathways and factors determining outcome	78
39. General scheme for diverted UmAS alongside proposed expansions	81
40. Thiazole access from conventional methods and umpolung methods.....	84
41. Azo to hydrazine rearrangement.....	85
42. Suspected oxazole formation in UmAS.....	87

43. Possible mechanism leading to nitron product.....	89
44. Conditions applied to hydrazone cyclization.....	93
45. Thiadiazole synthesis using diverted UmAS conditions	95
46. Attempted diverted UmAS synthesis of thiazoles	97
47. UmAS conditions unsuccessfully applied to aryl amines.....	103
48. UmAS conditions applied to aryl amines with Se activation	105
49. Exploration of Fe catalyzed amination using hydroxylamine	106
50. Hypothesis and results of attempted nitronate addition into internal azide nitrogen.....	107
51. Zincate amination via nitroarene partial reduction and its proposed adaptation to nitroalkanes	109
52. Other nitrogen electrophiles tried in <i>N</i> -aryl amide synthesis.....	111
53. <i>In situ</i> hydrazide activation.....	112
54. Ooi amination of enolates and its application to amide formation	113
55. NMR studies of trichloroacetimidate formation.....	113
56. Ending sequence for the synthesis of Ooi's triazolium catalyst	116
57. Experiments probing the umpolung nature of this amination.....	123
58. Experiments probing various nitrogen sources in the amidation.....	124
59. Additional justification for α -fluoro nitron assignment	125
60. Crossover experiment demonstrating aryl group origin in amide product	126
61. Partial mechanistic hypothesis.....	127
62. Azoxy formation from hydroxylamine and nitroso compounds.....	127
63. UmAS analogy mechanism for α -fluoro nitron to amide conversion.....	128
64. ^{18}O labeling experiments.....	130
65. New route to ^{18}O labeled hydroxylamine	131

66. Possible mechanisms for α -F nitron collapse.....	132
67. ^{18}O -labeling in preformed nitron collapse.....	132
68. Detailed mechanistic hypothesis.....	133
69. A comparison of conventional amide synthesis to UmAS for regiospecific <i>N</i> -aryl amide formation.....	137
70. Epimerization studies.....	137
71. Aryl glycine product epimerization	138
72. Retrosynthetic analysis of published routes to non-racemic Eli Lilly glucokinase inhibitors	141
73. Retrosynthetic analysis for 263a.....	142
74. The synthesis of an Eli Lilly glucokinase activator	143
75. Attempted early-stage alternatives.....	144
76. Stereochemical outcome in List nitroalkene reduction as it relates to alkene geometry	144
77. Established organocatalytic enantioselective nitroalkene reduction.....	145
78. <i>Z</i> -Nitroalkene reduction using catalyst 281	145
79. Other analogues in the Eli Lilly glucokinase activator series.....	147

Chapter 1. Development of Enantioselective BAM-Catalyzed aza-Henry Reactions

1.1 Introduction

1.1.1 Aza-Henry Reaction

The formation of carbon-carbon bonds is central to the construction of complex small molecules from simple starting materials. It is of particular value when the new carbon framework is decorated with functionality conducive to further manipulation or which is present in the final product such as groups with carbon-nitrogen sigma bonds. It is for this reason that the aza-Henry (or nitro-Mannich) reaction is of significant value to the scientific community. The reaction has been known since the late 1800's and was initially shown to have utility in the synthesis of some non-aromatic heterocycles (Scheme 1, eq 1), nitroalkenes (Scheme 1, eq 2), and nitroalkanes (Scheme 1, eq 3) among other synthetically applicable motifs.^{1,2,3,4,5,6,7,8}

¹ Noble, A.; Anderson, J. C. *Chem. Rev.* **2013**, *113*, 2887.

² Henry, L. *Bull. Cl. Sci., Acad. R. Belg.* **1896**, *32*, 33.

³ Hurd, C. D.; Strong, J. S. *J. Am. Chem. Soc.* **1950**, *72*, 4813.

⁴ Blomquist, A. T.; Shelley, T. H. *J. Am. Chem. Soc.* **1948**, *70*, 147.

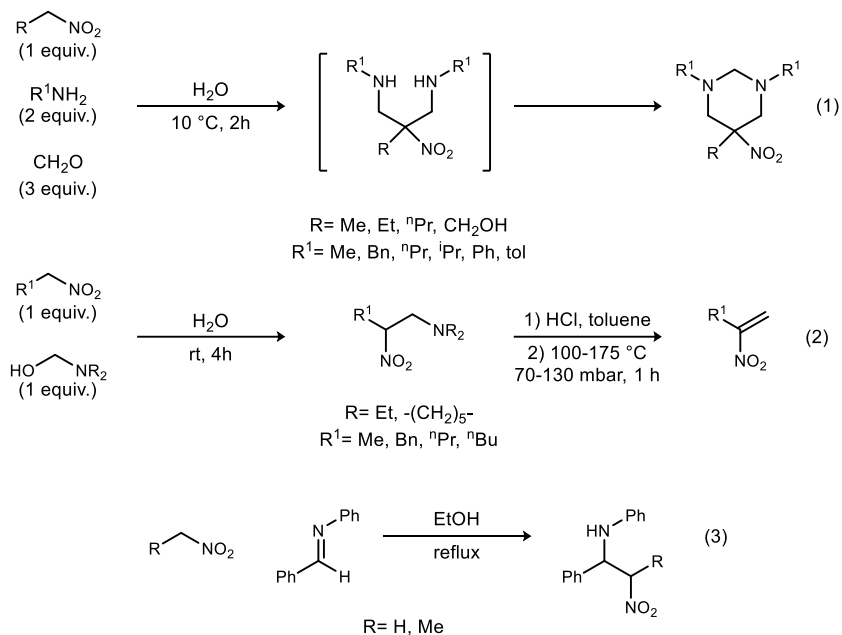
⁵ Senkus, M. *J. Am. Chem. Soc.* **1946**, *68*, 1611.

⁶ Kobayashi, S.; Ishitani, H. *Chem. Rev.* **1999**, *99*, 1069.

⁷ Adams, H.; Anderson, J. C.; Peace, S.; Pennell, A. M. *J. Org. Chem.* **1998**, *63*, 9932.

⁸ Faisca Phillips, A. M.; Guedes da Silva, M. F. C.; Pombeiro, A. J. *Front. Chem.* **2020**, *8*, 30.

Scheme 1. Selected examples of aza-Henry reactions

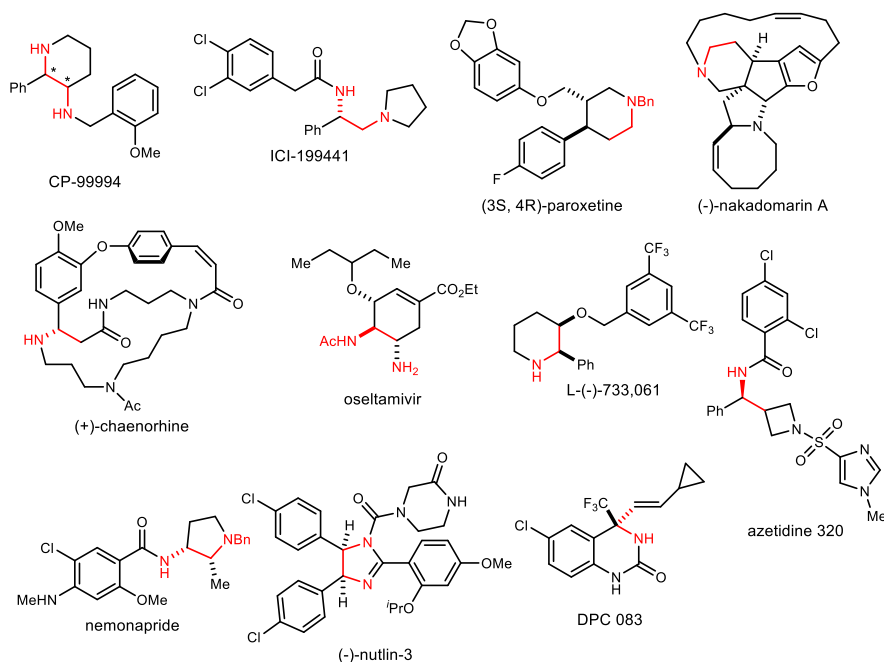


These early transformations demonstrated some of the power of this reaction, but advances were reported infrequently and the field did not receive much attention until diastereoselective examples were discovered in the late 1990's. Work by the Anderson group demonstrating the first diastereoselective aza-Henry on acyclic substrates seems to have stimulated the field to expand rapidly to include many variants of this important reaction.^{1,7} One valuable transformation demonstrated in Anderson's work was the conversion of β -nitroamines resulting from the aza-Henry to bis-amines through the reduction of the nitro group with SmI_2 , but one can envision the intermediacy of β -nitroamines towards a number of significant groups including amines⁹ and α -

⁹ Shen, B.; Johnston, J. N. *Org. Lett.* **2008**, *10*, 4397.

amino carbonyls.^{10,11} The ability to set two stereocenters while creating a carbon-carbon bond has led to a number of syntheses taking advantage of the versatile aza-Henry products. The products of several of those schemes are shown below (Figure 1).^{1,9,12,13,14,15,16,17,18,19,20,21,22}

Figure 1. Biologically active natural products and small molecules synthesized using the aza-Henry reaction



¹⁰ Noland, W. E. *Chem. Rev.* **1955**, *55*, 137.

¹¹ Lucet, D.; Le Gall, T.; Mioskowski, C. *Angew. Chem. Int. Ed.* **1998**, *37*, 2580.

¹² Tsuritani, N.; Yamada, K.-i.; Yoshikawa, N.; Shibasaki, M. *Chem. Lett.* **2002**, *31*, 276.

¹³ Xu, X.; Furukawa, T.; Okino, T.; Miyabe, H.; Takemoto, Y. *Chem. Eur. J.* **2006**, *12*, 466.

¹⁴ Hynes, P. S.; Stuppel, P. A.; Dixon, D. J. *Org. Lett.* **2008**, *10*, 1389.

¹⁵ Jakubec, P.; Cockfield, D. M.; Dixon, D. J. *J. Am. Chem. Soc.* **2009**, *131*, 16632.

¹⁶ Weng, J.; Li, Y.-B.; Wang, R.-B.; Li, F.-Q.; Liu, C.; Chan, A. S. C.; Lu, G. *J. Org. Chem.* **2010**, *75*, 3125.

¹⁷ Kumaraswamy, G.; Pitchaiah, A. *Tetrahedron* **2011**, *67*, 2536.

¹⁸ Davis, T. A.; Danneman, M. W.; Johnston, J. N. *Chem. Commun.* **2012**, *48*, 5578.

¹⁹ Handa, S.; Gnanadesikan, V.; Matsunaga, S.; Shibasaki, M. *J. Am. Chem. Soc.* **2010**, *132*, 4925.

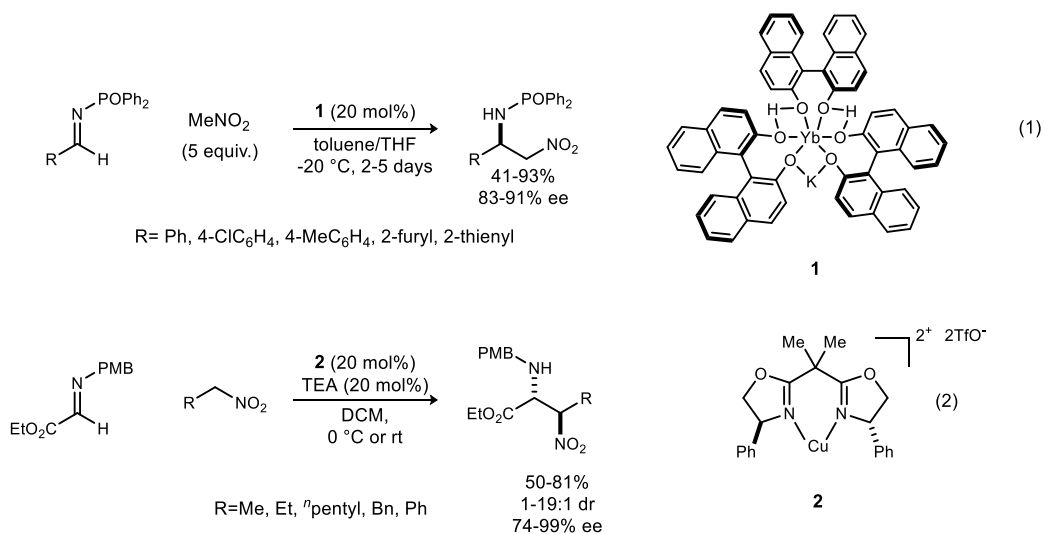
²⁰ Davis, T. A.; Johnston, J. N. *Chem. Sci.* **2011**, *2*, 1076.

²¹ Xie, H.; Zhang, Y.; Zhang, S.; Chen, X.; Wang, W. *Angew. Chem. Int. Ed.* **2011**, *50*, 11773.

²² Lindsley, C.; Hallett, D.; Wolkenberg, S. Azetidine Glycine Transporter Inhibitors. WO2005110983, November 25, 2005.

The first enantioselective aza-Henry reactions came shortly after initial diastereoselective examples. In 1999, Shibasaki and coworkers demonstrated that a $\text{Yb}^{\text{III}}/\text{K}^{\text{I}}$ catalyst with binaphthol ligands, **1**, was able to provide several β -nitro *N*-phosphinoyl-benzyl amines in good to excellent yields with good enantioselectivity (Scheme 2, eq 1).²³ Another significant early enantioselective aza-Henry was reported by the Jørgenson group which showed the conversion of α -iminoesters to β -nitroamines with the use of a Cu(II)-Ph-BOX catalyst, **2**, and catalytic amine base (Scheme 2, eq 2).²⁴

Scheme 2. Early work on enantioselective aza-Henry reactions



²³ Yamada, K.-i.; Harwood, S. J.; Gröger, H.; Shibasaki, M. *Angew. Chem. Int. Ed.* **1999**, *38*, 3504.

²⁴ Nishiwaki, N.; Rahbek Knudsen, K.; Gothelf, K. V.; Jørgensen, K. A. *Angew. Chem. Int. Ed.* **2001**, *40*, 2992.

Takemoto's group was among the first to successfully apply an organocatalyst to an enantioselective aza-Henry. They demonstrated that a thiourea catalyst could give moderate enantioselectivity in the reaction of *N*-phosphinoyl-aryl imines with simple nitroalkanes.²⁵ In similar work, Jacobson introduced the use of *N*-Boc imines which quickly became the preferred functional group in much of the further exploration of the organocatalyzed aza-Henry.²⁶ Fairly extensive work has been done on urea-based catalysts, and one other notable organocatalytic approach is the phase transfer conditions utilizing a cinchona-derived catalyst introduced by both Palomo and Ricci.^{27,28}

1.1.2 Bis-Amidine Catalysis in Aza-Henry Reactions

Simultaneously to the disclosure of Takemoto's initial thiourea catalysis, a new class of catalysts was introduced; the chiral proton catalysts. The bis-amidine (BAM) structure of these catalysts is proposed to hold an otherwise solvent-coordinated Brønsted acid in a chiral environment.²⁹ The initial report of enantioselective aza-Henry reactions was promising but required the solvent to be the nitroalkane, was quite slow, and gave only moderate yields. Two major improvements have made BAM catalysis a highly effective route to enantioenriched β -nitroamines. First, it was discovered that switching from the original HQuin-BAM scaffold to the more basic H,⁴PyrrolidineQuin-Bam (PBAM) (Figure 2) resulted in a much more reactive catalyst

²⁵ Okino, T.; Nakamura, S.; Furukawa, T.; Takemoto, Y. *Org. Lett.* **2004**, *6*, 625.

²⁶ Yoon, T. P.; Jacobsen, E. N. *Angew. Chem. Int. Ed.* **2005**, *44*, 466.

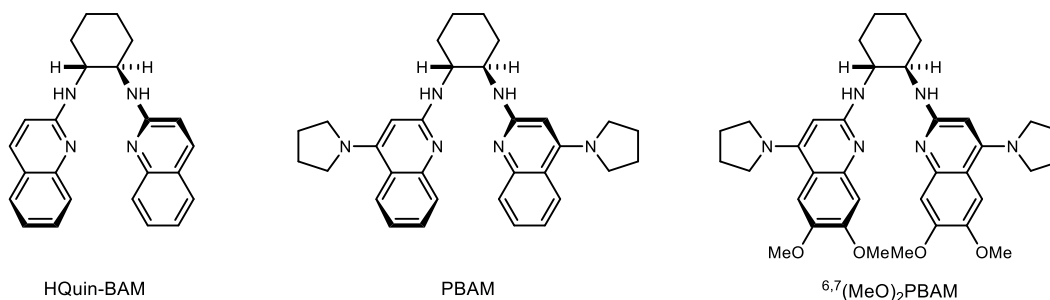
²⁷ Palomo, C.; Oiarbide, M.; Laso, A.; López, R. *J. Am. Chem. Soc.* **2005**, *127*, 17622.

²⁸ Fini, F.; Sgarzani, V.; Pettersen, D.; Herrera, R. P.; Bernardi, L.; Ricci, A. *Angew. Chem. Int. Ed.* **2005**, *44*, 7975.

²⁹ Nugent, B. M.; Yoder, R. A.; Johnston, J. N. *J. Am. Chem. Soc.* **2004**, *126*, 3418.

that produced higher yields and dr's while allowing for a reduction of nitroalkane equivalents to only 1.5.³⁰ Further modification of the catalyst to ^{6,7}(MeO)₂PBAM (Figure 2) expanded the scope of the chemistry to include aryl nitroalkanes.²⁰

Figure 2. Some important BAM catalysts



The power of BAM catalyzed aza-Henry reactions with ^{6,7}(MeO)₂PBAM was demonstrated through the construction of the *cis*-stilbene motif in (–)-Nutlin-3 (Figure 1). The easily modified and optimized structure of the catalyst class has proven useful for the synthesis of Azetidine 320^{18,22,31} (Figure 1) and expansion of the chemistry to nitroalkanes bearing heteroatom substituents α to the nitro group.³²

Both α -nitroesters and α -nitrophosphonates have been successfully incorporated into the scope of nitroalkanes applicable to BAM catalysis. Secondary nitroesters could be converted to the corresponding *anti*- α,β -diamino acids with an asymmetric, anthracene-containing BAM catalyst and subsequent treatment with NaBH₄ and CoCl₂.³³ Tertiary nitroesters underwent

³⁰ Davis, T. A.; Wilt, J. C.; Johnston, J. N. *J. Am. Chem. Soc.* **2010**, *132*, 2880.

³¹ Senter, T. J.; O'Reilly, M. C.; Chong, K. M.; Sulikowski, G. A.; Lindsley, C. W. *Tetrahedron Lett.* **2015**, *56*, 1276.

³² Shen, B.; Makley, D. M.; Johnston, J. N. *Nature.* **2010**, *465*, 1027.

³³ Singh, A.; Yoder, R. A.; Shen, B.; Johnston, J. N. *J. Am. Chem. Soc.* **2007**, *129*, 3466.

analogous transformations with only the addition of a methoxy group at the 4-position of the quinoline of the catalyst for increased basicity.³⁴ α -Nitrophosphonates, in contrast, could be reacted with *N*-Boc aryl aldimines using just the HQuin-BAM scaffold to give good yield, dr, and ee.³⁵ The value of adding a di-functionalized carbon into an imine in a stereoselective fashion has been highlighted by the synthesis of (+)-chaenorhine (Figure 1).⁹ The route involved the addition of a secondary α -nitroester to an *N*-Boc aryl aldimine followed by denitration to give the β -aminoester as a useful intermediate towards the final natural product.

Given recent interest in umpolung amide synthesis (UmAS) (discussed in Chapter 2), another valuable product class produced by BAM catalyzed aza-Henry reactions is the α -bromo nitroalkane. The synthesis of one such compound in the seminal work on UmAS from an *N*-Boc aryl aldimine using the same catalyst that was used in the secondary α -nitroester additions, gave good yield with excellent ee.³²

1.1.3 α -Sulfanyl, α -Alkoxy, and Sulfonyl Nitroalkanes

Surprisingly little work has been done with nitro compounds bearing sulfanyl, sulfonyl, or alkoxy substituents at the α -position. Possibly the most established chemistry involving nitro compounds with these α -substituents is the use of substituted nitro alkenes (bearing no stereocenters β to the nitro group) as Michael acceptors.^{36,37} Several possible manipulations of

³⁴ Singh, A.; Johnston, J. N. *J. Am. Chem. Soc.* **2008**, *130*, 5866.

³⁵ Wilt, J. C.; Pink, M.; Johnston, J. N. *Chem. Commun.* **2008**, *0*, 4177.

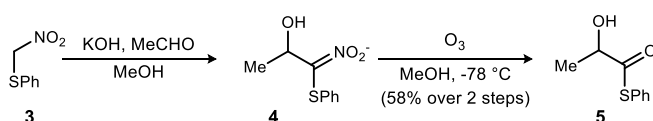
³⁶ Banks, B. J.; Barrett, A. G. M.; Russell, M. A. *J. Chem. Soc., Chem. Commun.* **1984**, 670.

³⁷ Barrett, A. G. M.; Cheng, M. C.; Spilling, C. D.; Taylor, S. J. *J. Org. Chem.* **1989**, *54*, 992.

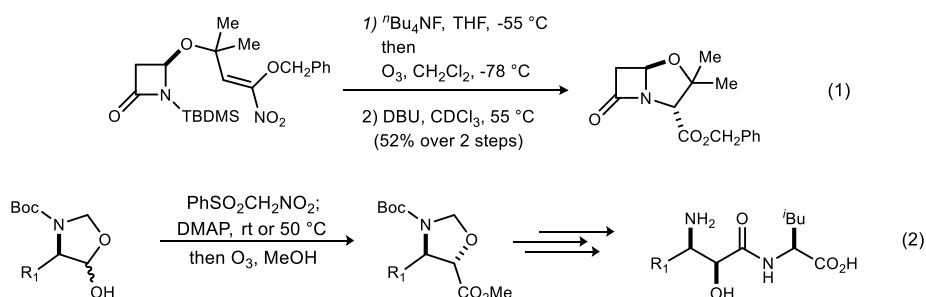
these motifs suggest that, in conjunction with enantioselective aza-Henry reactions, they could be useful and desirable intermediates in future organic syntheses.

One of the more common derivatizations of nitroalkanes with any of these substituents is the Nef-type ozonolysis of the nitronate of the nitromethyl group, **4**, to a carbonyl, **5**. The acidic proton in these compounds makes this a relatively simple process. The procedure (Scheme 3), which was initially developed on an α -sulfanyl nitroalkane, has been applied in the synthesis of an

Scheme 3. Nef-type ozonolysis of nitronates



Scheme 4. Examples of nitronate ozonolysis in synthesis



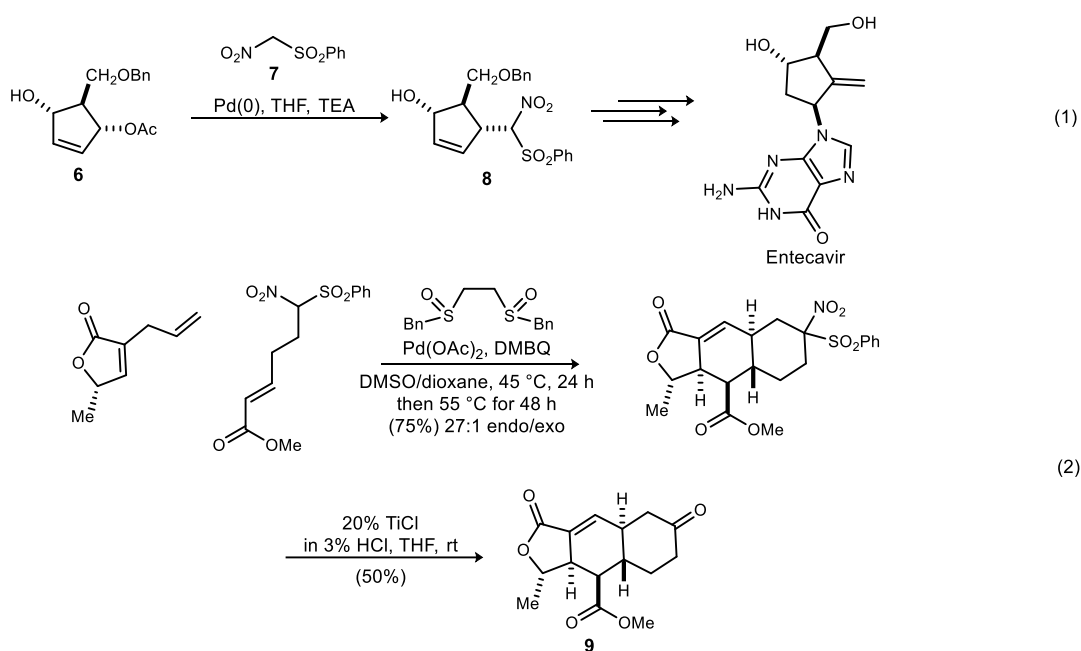
oxapenam core relevant to β -lactam antibiotics (Scheme 4, eq 1) as well as the anticancer and antibacterial agent, bestatin, and some of its analogues (Scheme 4, eq 2).^{36,37,38}

Furthermore, both secondary and tertiary α -nitro sulfones are valuable nucleophiles in palladium-aided carbon-carbon bond forming reactions. This type of reaction allows for one

³⁸ Seo, Y.; Kim, H.; Chae, D. W.; Kim, Y. G. *Tetrahedron: Asymmetry* **2014**, *25*, 625.

carbon of the newly formed bond to be at the ketone oxidation state with substituents with distinct reactivity. Synthetically applicable examples include the Tsuji-Trost reaction between nitromethyl sulfone **7** and cyclopentene derivative **6** used in a route to the antiviral Entecavir (Scheme 5, eq 1).³⁹ Also, the construction of the tricyclic core **9** common to several members of the galbulimima class of alkaloids with a tandem C-H activation/Diels-Alder cycloaddition (Scheme 5, eq 2) has been reported.⁴⁰

Scheme 5. Palladium catalyzed nitrosulfone additions



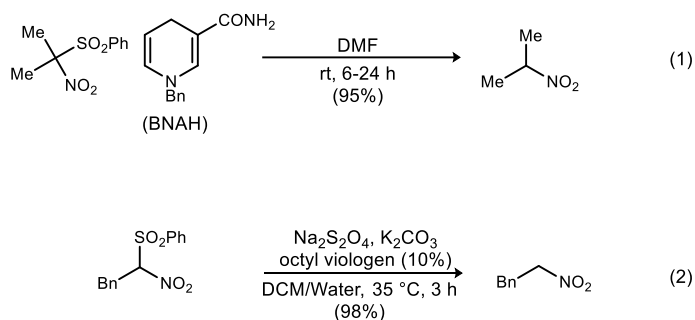
Finally, several procedures for the selective desulfonation of α -nitro sulfones exist. Using the single electron transfer agent *N*-benzyl-1,4-dihyronicotinamid (BNAH) Ono was able to show

³⁹ Process for Preparing the Antiviral Agent [1s-(1alpha, 3 Alpha, 4 Beta)]-2-Amino-1,9-Dihydro-9-[4-Hydroxy-3-(hydroxymethyl)-2-Methylenecyclo. WO2004052310 (A2), June 24, 2004.

⁴⁰ Howell, J. M.; Liu, W.; Young, A. J.; White, M. C. *J. Am. Chem. Soc.* **2014**, *136*, 5750.

desulfonylation of a limited scope of α -nitrosulfones (Scheme 6, eq 1).⁴¹ Also using a single electron transfer reagent, Park disclosed the utility of viologens in the desulfonylation of α -nitrosulfones (Scheme 6, eq 2).⁴² While mechanistic evidence is not overwhelming, the Choi group suggests that the first step in the reduction involves the transfer of an electron to the nitro group followed by loss of sulfonate anion to generate a carbon radical. The carbon-hydrogen bond is then formed by another one-electron reduction and protonation. It would be expected that the Ono conditions follow a similar mechanism. The ability of the reductant in those conditions (BNAH) to reduce the carbon-nitrogen bond of nitro groups activated by a cyano, an ester, or a ketone group suggests both that the initial one-electron reduction requires an electron withdrawing group α to the nitro group and the selectivity is related to leaving group ability.⁴³

Scheme 6. Reported desulfonylations of α -nitrosulfones



⁴¹ Ono, N.; Tamura, R.; Tanikaga, R.; Kaji, A. *J. Chem. Soc., Chem. Commun.* **1981**, 0, 71.

⁴² Park, K. K.; Lee, C. W.; Choi, S. Y. *J. Chem. Soc., Perkin Trans. 1* **1992**, 601.

⁴³ Ono, N.; Kaji, A. *Synthesis* **1986**, 1986, 693.

1.2 α -Oxy- and α -Thio Nitroalkane Addition to *N*-Boc Aryl Aldimines

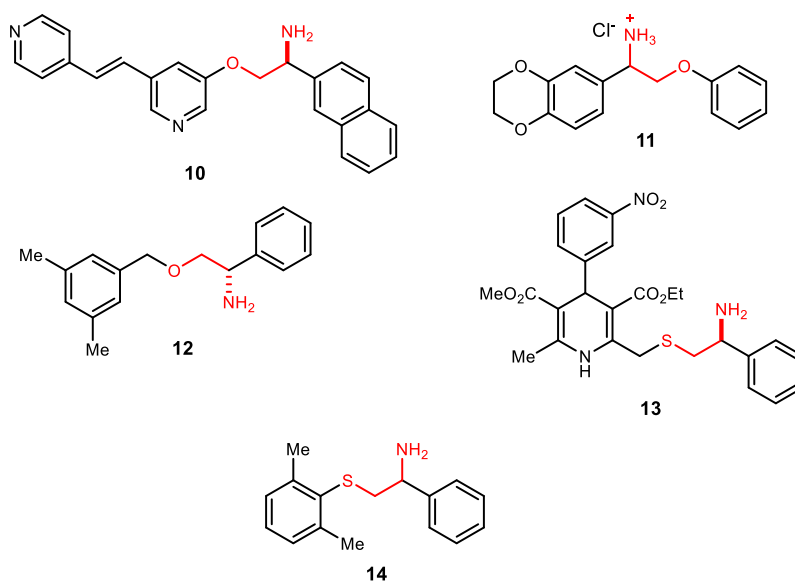
Given the intrinsic value to organic synthesis in creating a C-C bond in an enantioselective fashion with nitrogen substituents in differing oxidation states on each carbon (amine vs. nitro), the intense recent interest in enantioselective aza-Henry reactions is well-deserved. Many synthetic routes take advantage of this reaction, and several demonstrate the utility of bringing in functional groups through their incorporation at the α -position of the nitroalkane. This observation highlights the benefits of developing highly enantioselective aza-Henry reactions between imines and nitroalkanes with α -substituents unexplored in this chemistry. The work already done in this group suggests that using BAM catalysis and *N*-Boc imines could be a very effective route to enantioenriched β -amino nitroalkanes with new synthetic handles at the α -position.

It has been one main goal of this work to perform BAM catalysis with alkoxy, sulfanyl, and sulfonyl nitroalkanes in a geminal relationship with the nitro group. The products of such reactions would be amenable to a number of interesting transformations. α -Amino esters and thioesters would be acquired through the direct ozonolysis of the nitronate of the aza-Henry products (Scheme 7, eq 1-2). Apart from synthesis, such a compound could be used to gauge the susceptibility to epimerization of active esters relatable to the Hayashi-Lear (H-L) mechanistic proposal for UmAS (see chapter 2).⁴⁴ Another desirable motif that could be derived from the products of aza-Henry reactions proposed herein through denitration is the β -amino ether or thioether (Scheme 7, eq 3). A number of compounds explored as potential small-molecule

⁴⁴ Li, J.; Lear, M. J.; Kwon, E.; Hayashi, Y. *Chem. Eur. J.* **2016**, 22, 5538.

therapeutics have aryl amines β to ethers or thioethers. Figure 3 shows the structures of a PKB/Akt1 inhibitor (**10**), a potassium channel blocker (**11**), an NK₁ receptor antagonist (**12**), an analogue of the commercially available calcium channel antagonists Nifedipine and Nitrendipine (**13**), and an analogue of the commercially available Class IB anti-arrhythmia drug Mexiletine (**14**).^{45,46,47,48,49}

Figure 3. Biologically active compounds with β -amino ethers or thioethers



⁴⁵ Dong, X.; Zhou, X.; Jing, H.; Chen, J.; Liu, T.; Yang, B.; He, Q.; Hu, Y. *Eur. J. Med. Chem.* **2011**, *46*, 5949.

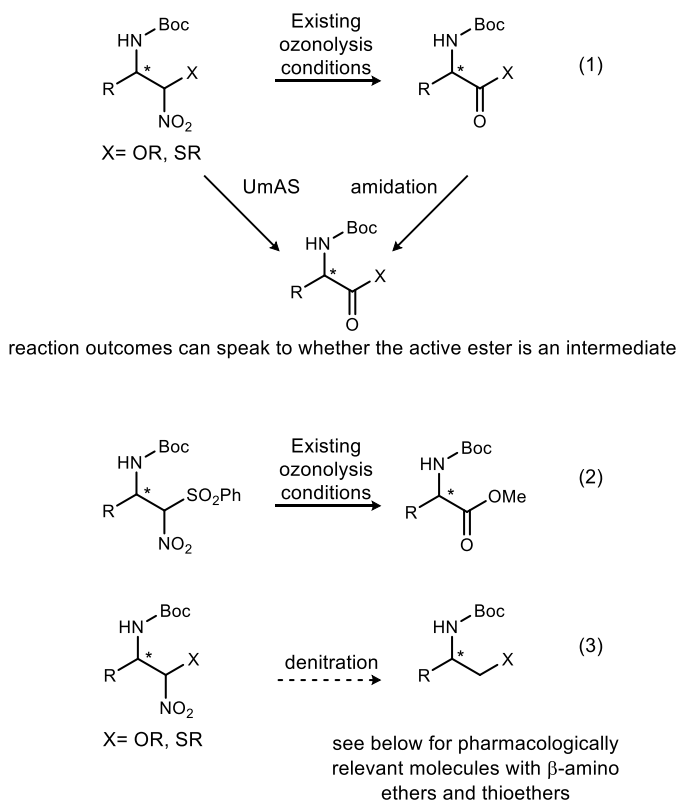
⁴⁶ Liu, H.; Gao, Z.-B.; Yao, Z.; Zheng, S.; Li, Y.; Zhu, W.; Tan, X.; Luo, X.; Shen, J.; Chen, K.; Hu, G.-Y.; Jiang, H. *J. Med. Chem.* **2007**, *50*, 83.

⁴⁷ Owens, A. P.; Williams, B. J.; Harrison, T.; Swain, C. J.; Baker, R.; Sadowski, S.; Cascieri, M. A. *Bioorg. Med. Chem. Lett.* **1995**, *5*, 2761.

⁴⁸ Galletti, F.; Zheng, W.; Gopalakrishnan, M.; Rutledge, A.; Triggle, D. J. *Eur. J. Pharmacol.* **1991**, *195*, 125.

⁴⁹ Carrieri, A.; Muraglia, M.; Corbo, F.; Pacifico, C. *Eur. J. Med. Chem.* **2009**, *44*, 1477.

Scheme 7. Possible transformations and applications of novel nitroalkanes



Lastly, as already discussed (Section 1.1.3), α -nitro sulfones have proven to be useful nucleophiles for palladium catalyzed carbon-carbon bond formation. The ability to arrive at nitrosulfones with adjacent enantioenriched, nitrogen-substituted chiral centers could be a useful way to bring that motif into a more complex molecule. The nitrosulfone functionality could then be transformed either through the Lewis acid conditions in Scheme 5, eq 9 or sulfone reduction followed by hydrodenitration.

In addition to the transformations in Scheme 7, the development of this chemistry was largely motivated by the interest in the group for further probing the mechanism and reactivity of UmAS. As can be seen from Table 1, the bond dissociation energies of carbon bonded to benzyloxy and thiophenyl groups would lead one to suspect the possibility that they would be viable substitutions for the halogen in UmAS.^{50,51} There is precedence in the group for using non-bromine substitutions α to the nitro group in UmAS in an attempt to find a balance between reactivity and stability of the intermediates. This prior work suggests substituents with bond dissociation energies similar to chlorine or bromine could behave optimally in UmAS (Table 2).⁵² This work seeks to use these substituents to allow for the same or similar chemistry to take place but with sufficiently perturbed reactivity such that intermediates or mechanistically telling products could be obtained.

Table 1. Bond dissociation energies of relevant carbon-heteroatom bonds

Entry	Bond	Bond dissociation energy ΔH_{298}^\ddagger (kcal/mol)
1	H ₃ C-I	56
2	H ₃ C-Br	70
3	H ₃ C-Cl	84
4	H ₃ C-F	108
5	H ₃ C-OBn	67
6	H ₃ C-SPh	68

One rationale for this proposed substitution is the fact that the absence of an exchangeable halogen on the nitroalkane entering the reaction excludes the potential for homo-

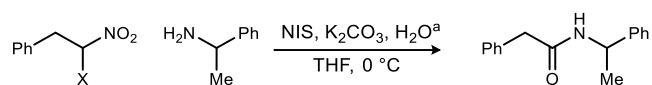
⁵⁰ Benson, S. W. *J. Chem. Educ.* **1965**, *42*, 502.

⁵¹ Dean, J. A. *Lange's handbook of chemistry*; McGraw-Hill, 1992.

⁵² Shen, B. PhD. Dissertation, Vanderbilt University, 2010

disubstituted nitroalkane (Table 2, **16**) formation en route to amide bond formation. It was found in prior work⁵³ that these intermediates, while competent precursors to amide, lie off-pathway. The overall rate is thereby slowed through nitronate sequestration. Notably, the role of these intermediates was misunderstood in the Hayashi-Lear hypothesis which assigns them a central role.⁴⁴ In this context, a successful amide bond forming reaction using these substrates would be evidence for the mechanism proposed by the Johnston group.³² Additionally, the direct

Table 2. Yields of UmAS with various α -halo nitroalkanes



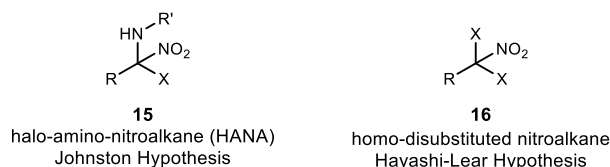
entry	X	Yield (%)
1	F	48 ^b
2	Cl	74
3	Br	75
4	I	51

^aNIS (1 equiv.), K₂CO₃ (2 equiv.), amine (1.2 equiv.), H₂O (5 equiv.), and nitroalkane (1 equiv, 0.2 M in THF) were stirred until complete conversion of the nitroalkane. ^bReaction conducted at room temperature.

observation of a stabilized tetrahedral intermediate was an appealing possibility. The existence of a halo-amino-nitroalkane tetrahedral intermediate (Figure 4, **15**) is a key part of the Johnston hypothesis as it firmly establishes a reactivity umpolung thereby differentiating it from the Hayashi-Lear hypothesis.

⁵³ Schwieter, K. E.; Shen, B.; Shackleford, J. P.; Leighty, M. W.; Johnston, J. N. *Org. Lett.* **2014**, *16*, 4714.

Figure 4. Significant structures in the Johnston and Hayashi mechanistic proposals for UmAS

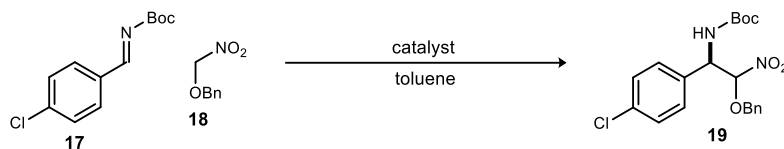


1.2.1 Aza-Henry Reactions with α -Sulfanyl, α -Alkoxy, and Sulfonyl Nitroalkanes

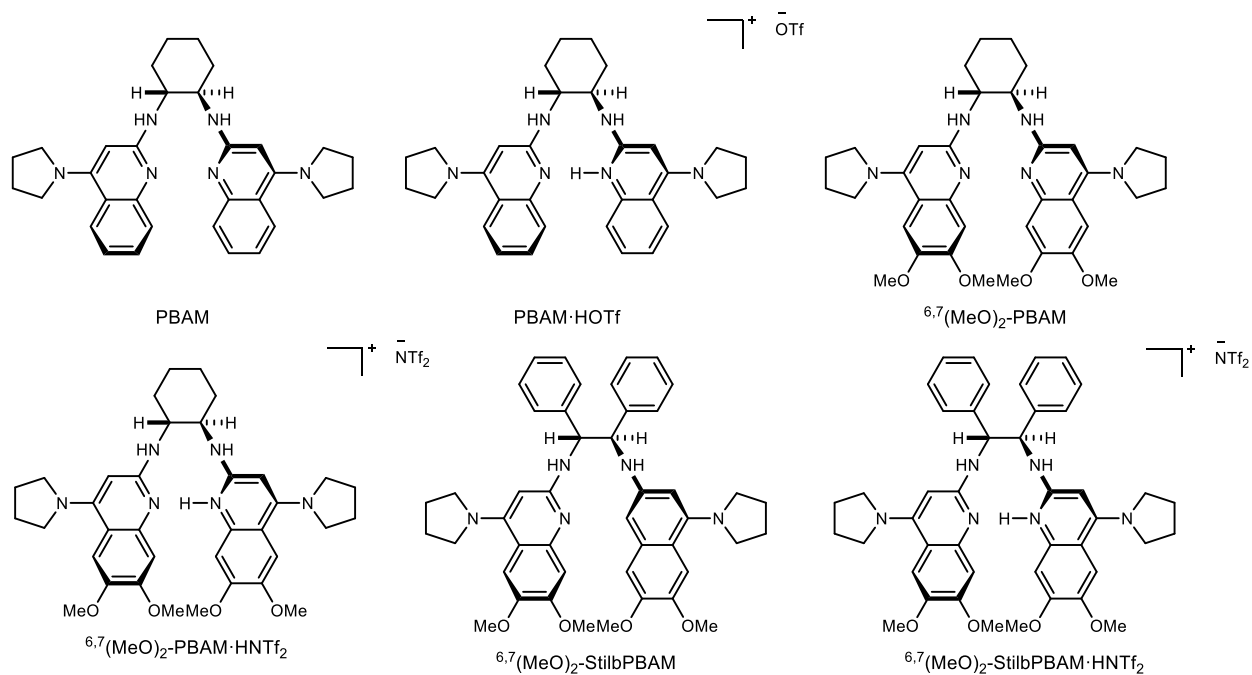
All of the substrates attempted to this point with BAM catalyzed aza-Henry reactions ultimately gave moderate to good yields of the desired α -substituted- β -amino-nitroalkanes with fair to excellent enantioselectivity. For these reactions, *N*-Boc aryl aldimines were used based on the general observation from previous work in BAM catalysis, as well as other enantioselective aza-Henry reactions, that this is a protecting group conducive to high enantioselectivity. Additionally, the simple and epimerization-free deprotection conditions of this group (HCl/dioxane) make it very suitable for potential applications of the products. Phenylsulfonyl nitromethane, benzyloxy nitromethane, and thiophenyl nitromethane were selected as substrates for aza-Henry investigations due to these compounds being known in the literature while still satisfying the bond dissociation energy criteria discussed earlier (Table 1). As will be expanded upon below, the benzyloxy substituent led to a high diastereomeric ratio under some conditions, while the thiophenyl analogue did not and the dr could not be determined for the products of several aza-Henry reactions between phenylsulfonyl nitromethane and *N*-Boc aryl aldimines.

In the case of reactions between benzyloxy nitromethane (Table 3, **18**) and the *N*-Boc aryl aldimine bearing a 4-chlorophenyl substituent (Table 3, **17**), relatively low yields of **19** were obtained even after very extended reaction times at -20 °C for both PBAM and the 1:1 triflic acid

Table 3. Benzyloxy nitromethane aza-Henry results



entry	Catalyst	Temperature (°C)	Time (h)	Yield (isolated)	ee major/minor	dr
1	PBAM	-20	140	56	58/59	2.3:1
2	PBAM·HOTf	-20	140	52	98/86	9:1
3	^{6,7} (MeO) ₂ -PBAM	-20	90	61	68/57	4.1:1
4	^{6,7} (MeO) ₂ -PBAM·HNTf ₂	20	24	69	94/93	7.7:1
5	^{6,7} (MeO) ₂ -StilbPBAM	-20	45	59	24/24	5.5:1
6	^{6,7} (MeO) ₂ -StilbPBAM·HNTf ₂	-20	46	58	61:44	20:1



salt of PBAM (Table 3, entries 1-2). An analysis of the pK_a's of substituted nitroalkanes (Table

4) implies that benzyloxy nitromethane should be marginally less reactive than nitroethane.^{54,55} With that in mind, the catalyst was switched to ^{6,7}(MeO)₂-PBAM and its triflimide salt. The switch was justified by the results obtained in early BAM catalysis studies that showed moving to a more basic catalyst allowed for shorter reaction times, higher yields, and smaller excess of nitroalkane in the reaction between *N*-Boc aryl aldimines and nitroalkanes with no heteroatom substituents.^{29,30}

Table 4. pKa values for some substituted nitroalkanes in DMSO



entry	R	pKa
1	Me	16.7
2	OBn	17.1
3	SPh	12.0
4	SO ₂ Ph	7.2
5	Br	12.5

With the more basic catalysts (Table 3, entries 3-4), improved yields up to 69% were observed with lower reaction times. Good enantiomeric excess (93%) and fair dr (~8:1) were observed even at 20 °C with the triflimide salt. In the case of both the original (Table 3, entries 1-2) and more basic catalysts (Table 3, entries 3-4), the acid salt versions (Table 3, entries 2 and 4) of the catalyst gave much better ee than the free base versions (Table 3, entries 1 and 3). Also explored was a similar series of BAM catalysts with a stilbene rather than cyclohexane backbone.

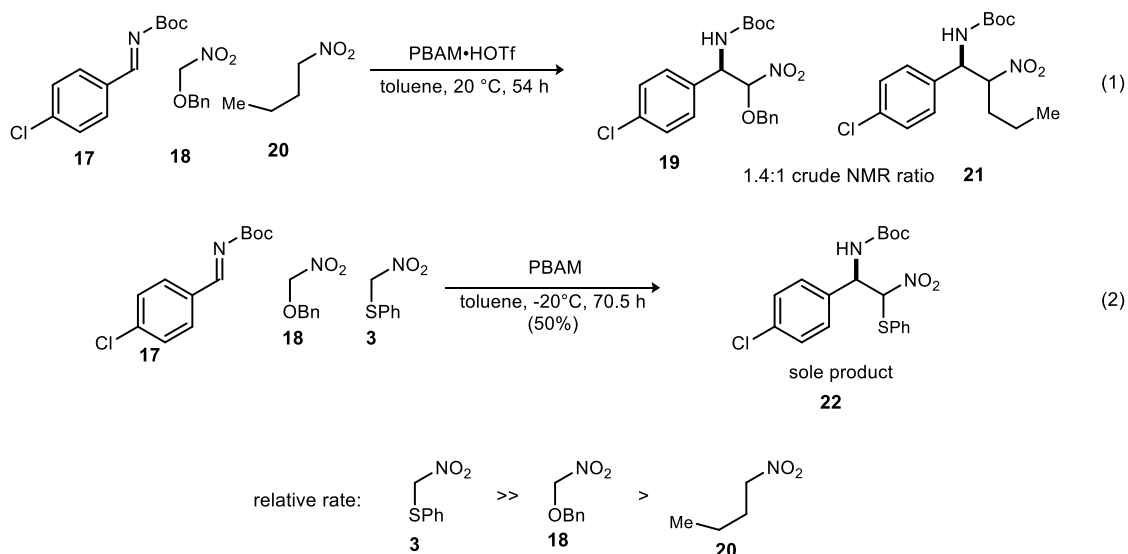
⁵⁴ Bordwell, F. G.; Bartmess, J. E. *J. Org. Chem.* **1978**, *43*, 3101.

⁵⁵ Bordwell, F. G.; Satish, A. V. *J. Am. Chem. Soc.* **1994**, *116*, 8885.

Despite observing a higher dr in the product (up to 20:1) when using the stilbene backbone, yields were slightly decrease to ~60% and ee's were much lower at up to 61% (Table 3, entries 5 and 6).

In order to have a more quantified understanding of the relative reactivities of α -substituted nitroalkanes, competition experiments were performed between benzyloxy nitromethane (**18**), nitrobutane (**20**), and thiophenyl nitromethane (**3**) (Scheme 8). As anticipated, the simple nitroalkane (**3**) had similar reactivity to benzyloxy nitromethane (**18**) in this reaction (Scheme 8, eq 1). Also of interest was the finding that the thiophenyl nitromethane adduct **22** was the sole product in the competition experiment between **3** and benzyloxy nitromethane (**18**). This result highlights the significance of pK_a for the prediction of reactivity of nitroalkanes and shows that the rate of the aza-Henry with thiophenyl nitromethane (**3**) is much greater than that with benzyloxy nitromethane (**18**) which is in turn greater than nitro butane (**20**) (Scheme 8).

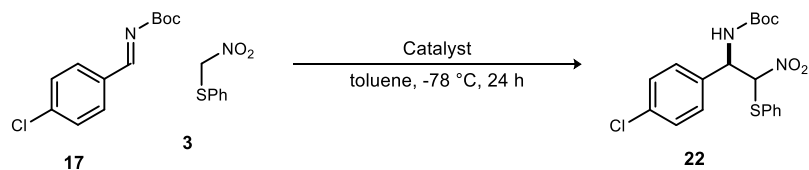
Scheme 8. Competition reactions between benzyloxy nitromethane, nitrobutane, and thiophenyl nitromethane



The reaction of thiophenyl nitromethane (**3**) with the same imine as reported above (**17**) does, as would be expected, lead to much faster conversion of starting material than reactions with

benzyloxy nitromethane. These reactions were completed at -78 °C in less than 24 hours with only PBAM and its triflic acid salt. Notable distinctions between this set of experiments (Table 5) and those using the less reactive benzyloxy nitromethane are the lower dr and subtle, yet reversed, impact of the presence of catalyst-bound acid on ee. The dr for all entries of Table 5 are about 2:1 or less which is in contrast to the dr's of 2-9:1 in Table 3. One theory for this difference is the higher hydrogen bond accepting ability of oxygen compared to that of sulfur. If a hydrogen bond is forming at the substituent on the nitronate carbon, then that could help dictate its orientation as it approaches the imine. The weak influence of using the protonated catalyst implies that the enantioselectivity in this case (Table 5) is not dependent on two-point contact between one of the substrates and the corresponding amidine. Similarly, unpromising trends to those observed in analogous reactions with benzyloxy nitromethane (Table 3, entries 5-6) were also observed when applying the stilbene backbone catalysts to this substrate combination (Table 5, entries 3-4).

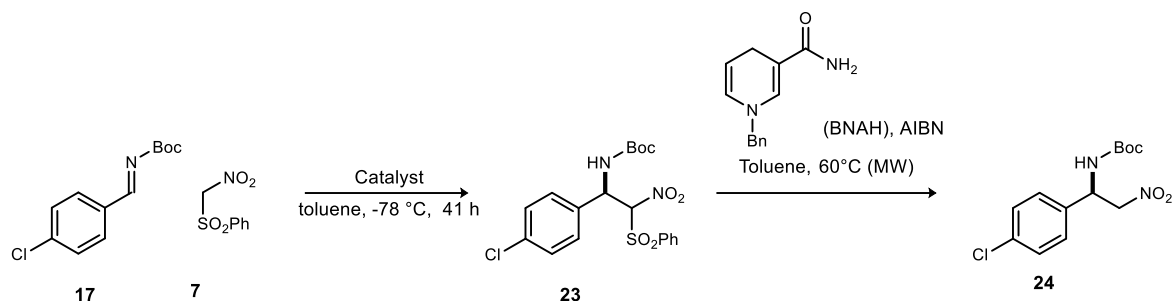
Table 5. Thiophenyl nitromethane aza-Henry results



entry	Catalyst	Yield (isolated)	ee major/minor	dr
1	PBAM	72	95/95	1.7:1
2	PBAM·HOTf	85	93/91	1.4:1
3 ^a	StilbPBAM	67	3/2	1:1
4 ^b	StilbPBAM·HNTf ₂	63	42/49	2.4:1

^a48 h reaction time; ^b70 h reaction time

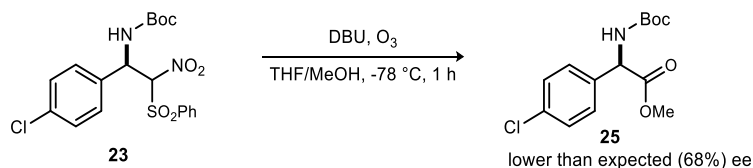
Unexpectedly, when moving to the even more acidic phenylsulfonyl nitromethane (**7**), yield dropped and longer reaction times were required for complete conversion (Table 6). Unfortunately, the β -amino nitro sulfone (**23**) proved to be unsuitable for chiral-HPLC analysis.

Table 6. Phenylsulfonyl nitromethane aza-Henry results

entry	Catalyst	Yield (isolated)	ee (24) ^a	dr (23)
1	PBAM	46	78	1.2:1
2	PBAM·HOTf	63	60	1.2:1

^aSee text for discussion of enantiomeric excess determination

Additionally, analogues of **17** with *meta*-cyano, methoxy, nitro, and methyl substituents on the phenyl ring instead of *para*-chloro failed to completely resolve by chiral-HPLC, so a transformation was required in order to analyze ee for the material. Several reductions failed to give amine products. Those attempted on **15** or an analogue were zinc dust with ammonium chloride,⁵⁶ zinc dust with HCl,⁵⁷ SnCl₂,⁵⁸ CoCl₂/NaBH₄,⁵⁹ and Pd/C with H₂. Several of these conditions gave conversion to an oxime, but only in very low yield and these were not pursued.

Scheme 9. Ozonolysis of **23** for ee determination

⁵⁶ Yang, D.; Fan, M.; Zhu, H.; Guo, Y.; Guo, J. *Synthesis* **2013**, 45, 1325.

⁵⁷ Bera, K.; Namboothiri, I. N. N. *J. Org. Chem.* **2015**, 80, 1402.

⁵⁸ Xu, M.-L.; Huang, W. *Synth. Commun.* **2014**, 44, 3435.

⁵⁹ Uraguchi, D.; Kinoshita, N.; Nakashima, D.; Ooi, T. *Chem. Sci.* **2012**, 3, 3161.

Also attempted were the ozonolysis/esterification conditions used by Kim and coworkers in their synthesis of bestatin analogues.⁶⁰ This method gave the desired methyl ester which allowed for ee determination, but the surprisingly low ee implied that the active ester formed as an intermediate was epimerizing under the basic conditions (Scheme 9). Since later derivations gave material with higher ee, that assumption seems likely. While the desulfonylation method in Table 6 eq 1 was successful, the viologen-mediated desulfonylation conditions shown in Scheme 6, eq 2 showed no reaction on this substrate.

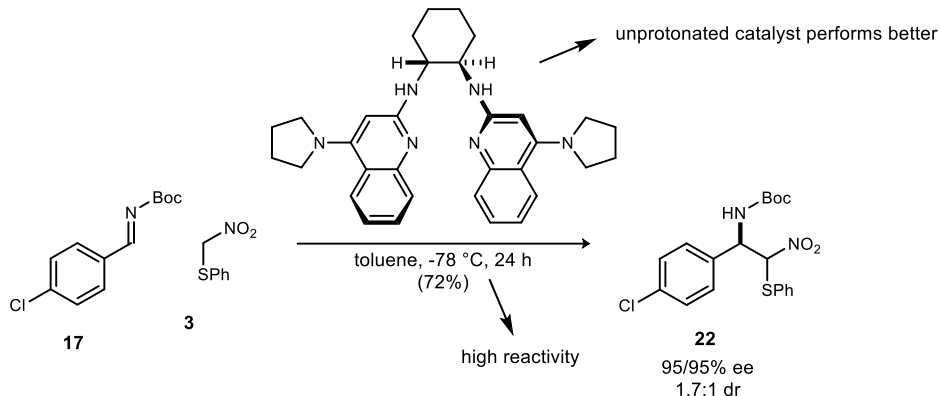
1.3 Conclusions

Several nitroalkanes with underexplored α -heteroatom substitution have been prepared and tested in the aza-Henry reaction. The highly-acidic thiophenyl nitromethane was very reactive, giving high ee and yield in only one day even at $-78\text{ }^{\circ}\text{C}$ when catalyzed by BAM catalysts (Scheme 10). Notably, unprotonated BAM ligands gave the best results for this substrate. This is in-line with previous observations of BAM catalyzed aza-Henry reactions where sufficiently acidic nitroalkanes can serve as the proton source for the Brønsted-basic catalyst.⁶¹

⁶⁰ Seo, Y.; Lee, S.; Kim, Y. G. *Applied Chemistry for Engineering* **2015**, 26, 111.

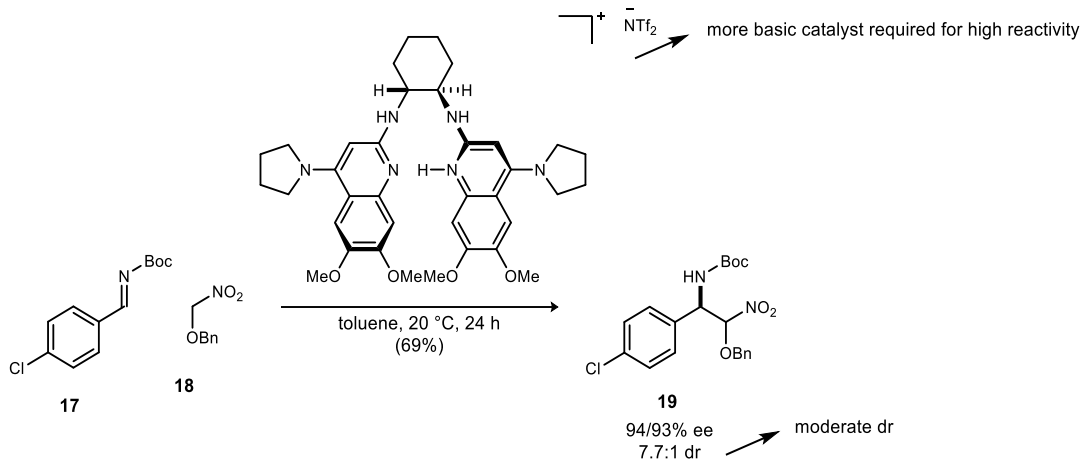
⁶¹ Lim, V. T.; Tsukanov, S. V.; Stephens, A. B.; Johnston, J. N. *Org. Synth.* **2016**, 93, 88.

Scheme 10. Thiophenyl nitromethane in the bisamidine catalyzed aza-Henry reaction



Benzyloxy nitromethane was significantly less reactive in aza-Henry reactions than thiophenyl nitromethane. This relative rate can be seen in competition reactions (Scheme 8), and manifests itself by requiring higher temperatures and more-basic BAM catalysts for the reaction to be complete in a similar timeframe (Scheme 11). The difference in reactivity can be easily explained on the basis of pKa's. Thiophenyl nitromethane is significantly more acidic than benzyloxy nitromethane (~5 pKa units) and can be deprotonated by the catalyst much more easily. The yield and ee for this substrate were very comparable to those obtained with thiophenyl nitromethane, being moderate and high respectively, but the dr was a notable difference. Moderate dr's were observed in the aza-Henry reaction between imine **7** and benzyloxy nitromethane using several conditions (Table 3). The exact origin of this effect is unknown but we speculate that the increased hydrogen bond accepting capacity of ethers compared to thioethers allows the catalyst to control the nucleophile orientation in addition to the consistently-controlled facial selectivity.

Scheme 11. Benzyloxy nitromethane in the bisamidine catalyzed aza-Henry reaction



Finally, phenylsulfonyl nitromethane was somewhat of an exception to the established trends. Despite a highly acidic (~ 5 pKa units more so than thiophenyl nitromethane) α -proton, the reactivity of this substrate was lower than that of thiophenyl nitromethane. Two explanations seem reasonable to explain this departure from the acidity/reactivity correlation. It is possible that the electronics of this substrate are so far on one side of the spectrum that acidity no longer contributes to the rate-limiting step of the reaction. Instead, the lowered nucleophilicity of the nitronate resulting from the stabilizing effect of the sulfone could be serving to decrease reactivity. This hypothesis would not, however, explain the only moderate ee's observed in Table 6. Alternatively, a sterics argument can be made to explain the lowered reactivity and ee. The sulfone substituent is by-far the largest of those studied in this work. Its size could be interfering with catalyst binding leading to the loss in ee and reactivity that is observed experimentally.

Overall, benzyloxy nitromethane and thiophenyl nitromethane perform well in aza-Henry reactions catalyzed by standard BAM catalysts. These reactions give access to β -oxy/thio amines with excellent stereocontrol at the amine carbon. In the case of benzyloxy nitromethane, moderate dr could also be obtained. Factors impacting reaction outcome were determined and are consistent

with previous observations of BAM catalyzed reactions. Derivatizations of the products, particularly nitronate ozonolysis, are promising in the context of providing a tangible point of comparison between umpolung and traditional amide synthesis. These tool compounds will be vital for determining the mechanism of UmAS in the following chapter.

Chapter 2. Mechanistic Investigation of Umpolung Amide Synthesis; Evidence for the Halo-Amino-NitroAlkane (HANA) Tetrahedral Intermediate⁶²

2.1 Introduction

2.1.1 Amide Bond Formation

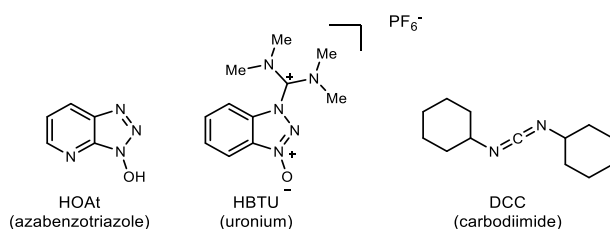
The amide is a particularly ubiquitous functional group in chemistry. Given the group's presence in a great number of secondary metabolites and many pharmacologically relevant molecules, amide synthesis remains of great importance and, indeed, is a thoroughly developed field. Their significance is exemplified by the fact that 10 of the top 10 and 134 of the top 200 pharmaceutical products by retail sales in 2016 (as compiled by the Njardarson group)⁶³ contain this functional group. By far the most widely-used (in nature and the lab) route to the construction

⁶² Section 2.3 of this chapter is adapted from “Direct Observation and Analysis of the Halo-Amino-Nitro Alkane Functional Group” published in *Chem.* and has been reproduced with the permission of the publisher and my co-authors Hayden Foy, Kazuyuki Tokumaru, Travis Dudding, Maren Pink, and Jeffrey Johnston: Crocker, M. S.; Foy, H.; Tokumaru, K.; Dudding, T.; Pink, M.; Johnston, J. N. *Chem* **2019**, 5, 1248.

⁶³ McGrath, N. A.; Brichacek, M.; Njardarson, J. T. *J. Chem. Educ.* **2010**, 87, 1348.

of amides is through nucleophilic acyl substitution with an amine and an active ester. This approach is synergistic with the existence of countless enantiopure amino acids. However, it is not without drawbacks. Some effort typically must be committed to optimizing the reaction, and acceptable reactivity often requires hazardous coupling reagents such as azabenzotriazoles, uronium containing reagents, or carbodiimides (Figure 5).⁶⁴ Uronium coupling agents have been specifically identified recently as a liability for process development applications.⁶⁵

Figure 5. Structures of several representative amide coupling reagents



Coupling reagents in general are a mainstay in amide coupling, and there has been significant development in the area spanning more than a century.⁶⁶ Many classes of reagents experience regular use in peptide synthesis, but none satisfactorily provides good reactivity while avoiding epimerization and not adding safety or operational difficulties. Among the most used reagents are acyl-chloride generating reagents (such as SOCl₂) which generate HCl, anhydride producing reagents (such as pivaloyl chloride) which can lead to regioselectivity issues associated with mixed anhydrides, carbodiimides (such as DCC) which are sensitizers, and benzotriazoles

⁶⁴ Dunetz, J. R.; Magano, J.; Weisenburger, G. A. *Org. Process Res. Dev.* **2016**, *20*, 140.

⁶⁵ Zhao, W.; Guizzetti, S.; Schwindeman, J. A.; Daniels, D. S. B.; Douglas, J. J.; Petit, S.; Knight, J. *Org. Process Res. Dev.* **2020**, *24*, 115.

⁶⁶ Fischer, E.; Otto, E. *Ber. Deutsch. Chem. Ges* **1903**, *36*, 2106.

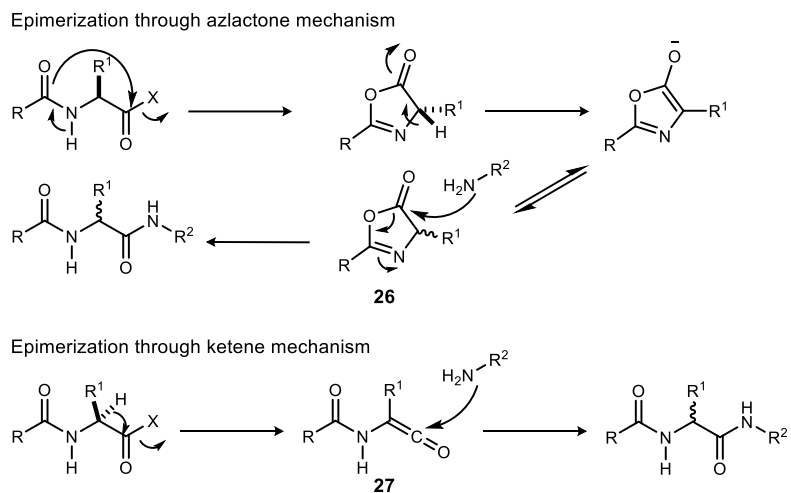
(such as HOBt) which tend to be explosive and/or expensive.⁶⁴ In addition to the hazards associated with coupling reagents, they are often high molecular mass additives used in stoichiometric or super-stoichiometric amounts: a shortcoming that has been cited by the ACS GCI Pharmaceutical Roundtable as a key research area.⁶⁷

Even with coupling reagents and conditions designed to minimize epimerization, the active ester intermediates involved in condensative amide synthesis can lose stereopurity at the carbon α to the carbonyl. This complication arises from the basic conditions common to amide synthesis, combined with the acidification of α protons when a carboxylic acid is activated for nucleophilic acyl substitution. The epimerization of active esters with the common α -*N*-acyl motif can be explained mechanistically by the intermediacy of an azlactone (**26**) or a ketene (**27**) species (Scheme 12).⁶⁸ Loss of enantio or diastereopurity is especially important in the context of medicinally relevant compounds where there is a high demand for stereochemically-pure compounds.

⁶⁷ Constable, D. J.; Dunn, P. J.; Hayler, J. D.; Humphrey, G. R.; Leazer Jr, J. L.; Linderman, R. J.; Lorenz, K.; Manley, J.; Pearlman, B. A.; Wells, A. *Green Chem.* **2007**, *9*, 411.

⁶⁸ Goodman, M.; McGahren, W. J. *J. Am. Chem. Soc.* **1966**, *88*, 3887.

Scheme 12. Epimerization of active esters with α -N-acyl groups



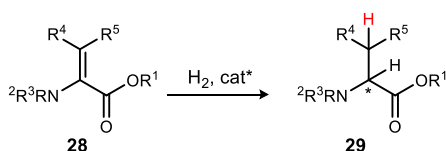
With the growing interest in non-natural amino acids for protein engineering and bioactive small molecules has come an increased need to be able to form the requisite α -amino amides using enantioselective catalysis. There are now many effective routes to these unnatural amino acid building blocks in enantioenriched form. Despite this development, however, unnatural amino amides still generate synthetic challenges, especially aryl glycinamide precursors.⁶⁹

⁶⁹ Schwieter, K. E.; Johnston, J. N. *J. Am. Chem. Soc.* **2016**, *138*, 14160.

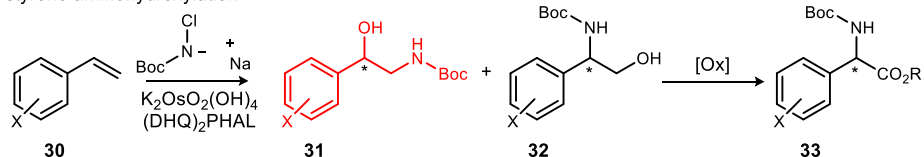
Reduction of the corresponding dehydroamino amide (**28**) has been a workhorse for this purpose; however, this method excludes aryl or tertiary substituents at the stereogenic center in **29**.⁷⁰ Scheme 13 shows the general transformations for this and the following established α -amino acid/ester forming reactions. The weaknesses of each approach are colored red. Aminohydroxylation of styrenes (**30**) is an established route to quickly access aryl glycine derivatives (**33**), but poor regioselectivity (**31-32**) is a major drawback when observed, and it is

Scheme 13. Enantioselective routes to non-natural amino acids

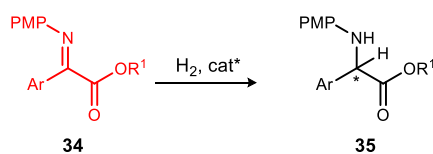
enamine reduction



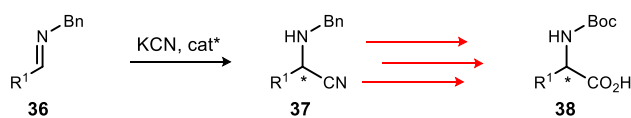
styrene aminohydroxylation



imine reduction



Strecker synthesis



⁷⁰ Najera, C.; Sansano, J. M. *Chem. Rev.* **2007**, *107*, 4584.

not compatible with *N*-Fmoc protection.⁷¹ Reduction of α -keto ester derived imines (**34**) provides a good alternative with low catalyst loading and no issues with regiocontrol, but the starting material is less readily available.⁷² The Strecker synthesis has been found to be amenable to catalytic asymmetric variants to produce α -amino acids (**38**) when thiourea catalysts are used, but typically involves multiple steps (hydrolysis, protection/deprotection, and amide coupling) to generate α -amino amides.⁷³ Two final transition-metal catalyzed routes that will be mentioned here are the N-H insertion of α -diazo esters into carbamates and the aryl boronic acid addition into α -aldimino esters.^{74,75} Significantly, all of these routes produce α -amino acids or esters and still rely on traditional condensative amide synthesis when making α -amino amides or coupling to peptide chains.

⁷¹ Reddy, K. L.; Sharpless, K. B. *J. Am. Chem. Soc.* **1998**, *120*, 1207.

⁷² Shang, G.; Yang, Q.; Zhang, X. *Angew. Chem. Int. Ed.* **2006**, *45*, 6360.

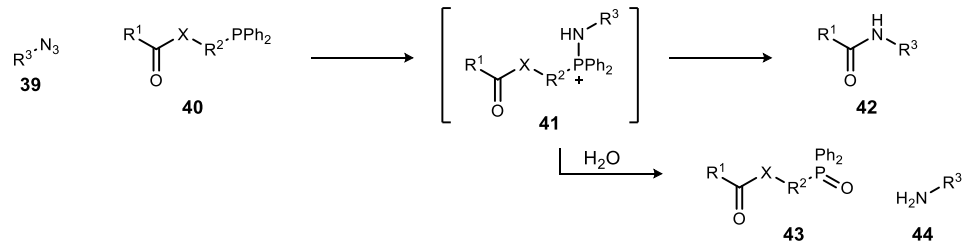
⁷³ Zuend, S. J.; Coughlin, M. P.; Lalonde, M. P.; Jacobsen, E. N. *Nature* **2009**, *461*, 968.

⁷⁴ Beenen, M. A.; Weix, D. J.; Ellman, J. A. *J. Am. Chem. Soc.* **2006**, *128*, 6304.

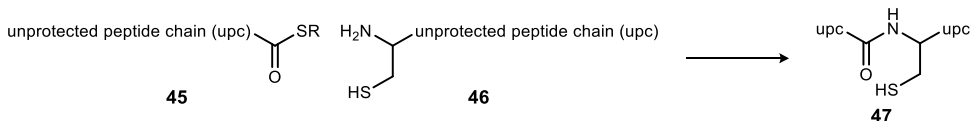
⁷⁵ Lee, E. C.; Fu, G. C. *J. Am. Chem. Soc.* **2007**, *129*, 12066.

Scheme 14. A survey of amide forming reactions

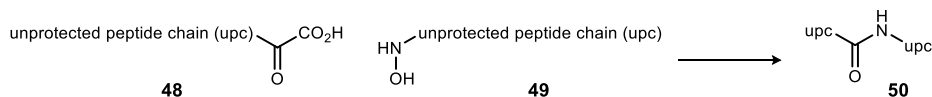
traceless Staudinger ligation



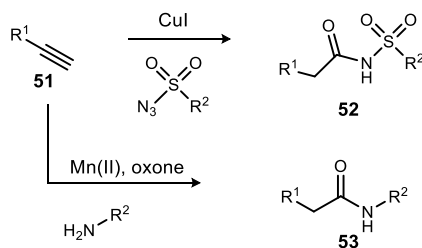
native chemical ligation



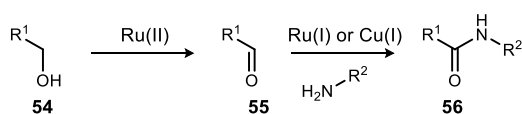
from α -ketoacids



from alkynes



from aldehydes/alcohols



As discussed, amide bond synthesis is a highly researched field, so various creative reactions and procedures distinct from but related to “traditional” condensative methods have been advanced to accomplish that goal. Several examples (discussed below) can be seen in Scheme 14. The Staudinger ligation is one such reaction but suffers from the possibility of competitive

hydrolysis of the aza-ylides (**41**) and the use of engineered substrates (**40**).⁷⁶ Similarly, a unique, selective ligation, native chemical ligation, has been significant in the field of chemical biology, but is useful only for coupling peptides with *N*-terminal cysteines (**46**).⁷⁷ Amides may also be synthesized from α -ketoacids (**48**) via decarboxylative ligation,⁷⁸ terminal alkynes (**51**) through azide coupling or oxidative amination,^{79,80} or aldehydes/alcohols (**54-55**) using other oxidative aminations,^{81,82} but all of these reactions require transition metal catalysts and are not without other hurdles and issues. The variety these methods bring to amide bond formation is valuable, however it is clear that new methods, particularly any which allow for retention of enantiopurity in otherwise epimerization-prone couplings, would be of great use.

2.1.2 Umpolung Amide Synthesis

Due to large interest in developing new routes to amide bond formation, particularly for the formation of peptide bonds, the Johnston group developed umpolung amide synthesis.³² Not only does this reaction allow for the amides to be formed from feedstock distinct from the traditional routes involving nucleophilic acyl substitution, but also it is proposed to proceed through a fundamentally different mechanistic paradigm (Scheme 15). As will be expanded upon in the mechanistic discussion, this reaction incorporates conditions leading to an electrophilic nitrogen that is attacked by the nucleophilic nitronate (the carbon of which is ultimately the

⁷⁶ Saxon, E.; Armstrong, J. I.; Bertozzi, C. R. *Org. Lett.* **2000**, *2*, 2141.

⁷⁷ Dawson, P. E.; Muir, T. W.; Clark-Lewis, I.; Kent, S. B. *Science* **1994**, *266*, 776.

⁷⁸ Bode Jeffrey, W.; Fox Ryan, M.; Baucom Kyle, D. *Angew. Chem. Int. Ed.* **2006**, *45*, 1248.

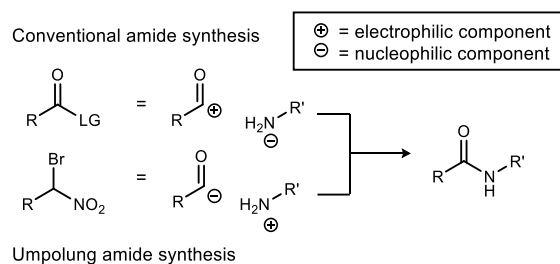
⁷⁹ Cho, S. H.; Yoo, E. J.; Bae, I.; Chang, S. *J. Am. Chem. Soc.* **2005**, *127*, 16046.

⁸⁰ Chan, W.-K.; Ho, C.-M.; Wong, M.-K.; Che, C.-M. *J. Am. Chem. Soc.* **2006**, *128*, 14796.

⁸¹ Yoo, W.-J.; Li, C.-J. *J. Am. Chem. Soc.* **2006**, *128*, 13064.

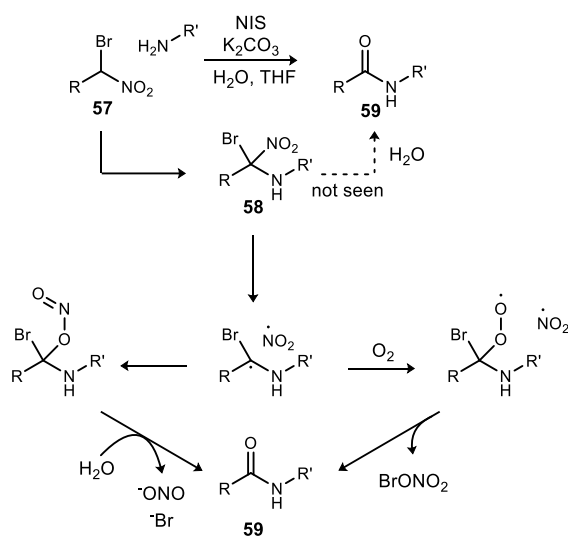
⁸² Gunanathan, C.; Ben-David, Y.; Milstein, D. *Science* **2007**, *317*, 790.

Scheme 15. Illustration of UmAS's unique reversal of polarity



carbonyl carbon of the final amide). Furthermore, when coupled with existing chemistry (aza-Henry reactions,^{83,84} Henry reactions,⁸⁵ Michael additions,⁸⁶ hydride reductions⁸⁷), cheap starting materials can be converted into enantioenriched building blocks for complex amides.

Scheme 16. Proposed UmAS mechanism



⁸³ Schwieter, K. E.; Johnston, J. N. *ACS Catalysis* **2015**, *5*, 6559.

⁸⁴ Schwieter, K. E.; Johnston, J. N. *Chem. Sci.* **2015**, *6*, 2590.

⁸⁵ Leighty, M. W.; Shen, B.; Johnston, J. N. *J. Am. Chem. Soc.* **2012**, *134*, 15233.

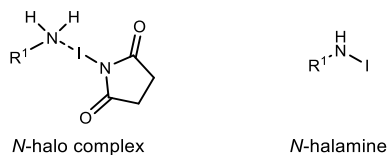
⁸⁶ Vishe, M.; Johnston, J. N. *Chem. Sci.* **2019**, *10*, 1138.

⁸⁷ Martin, N. J. A.; Ozores, L.; List, B. *J. Am. Chem. Soc.* **2007**, *129*, 8976.

The mechanism proposed for UmAS (Scheme 16) notably excludes an active ester intermediate, which can provide epimerization pathways for stereocenters at the α carbon of the eventual amide.⁸⁸ Additionally, sufficiently weak base is required such that epimerization through deprotonation at the amide product chiral center is typically not of concern. The mechanistic hypothesis laid out by a series of studies involves the formation of an *N*-halamine or *N*-halo complex (Figure 6) upon reaction of an amine with an electrophilic halogen source (NIS for example) followed by attack on the halamine by the nitronate of the bromo-nitroalkane **57**. The resulting tetrahedral intermediate (**58**) can then collapse via an anaerobic or aerobic pathway to form the amide (**59**). Oxygen labeling studies confirm that the source of the amide oxygen can be either from molecular oxygen or the nitro group, but not water, which is present in the reaction conditions.⁸⁸ As an additional advantage to this chemistry, it was noted that the aerobic collapse of the tetrahedral intermediate generates an electrophilic halogen, and consequently, conditions were developed for the reaction to use sub-stoichiometric quantities of NIS.⁵³

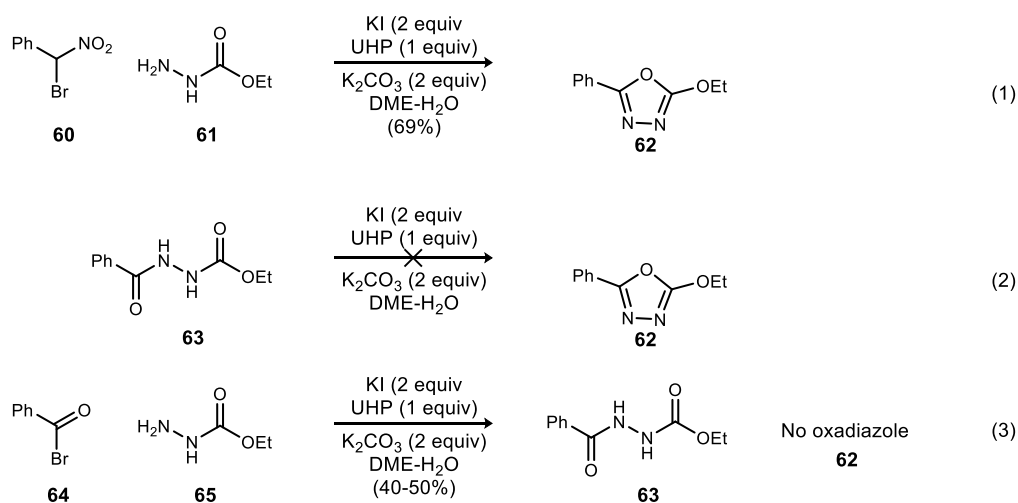
⁸⁸ Shackleford, J. P.; Shen, B.; Johnston, J. N. *Proc. Natl. Acad. Sci. U. S. A.* **2012**, *109*, 44.

Figure 6. Possible structures for the electrophilic amine



Other evidence for the mechanism in Scheme 16 lies in the fact that no active ester was observed when the reagent mixture in the absence of amine is monitored, and addition of amine after bromo-nitroalkane is consumed is not viable towards amide. Also, the reagent mixture is not viable towards ester formation with benzyl alcohol in the place of amine.³² A final piece of

Scheme 17. Mechanistic insight from diverted UmAS reaction



evidence from the group that supports the original mechanistic hypothesis excluding an active ester is the work by Tokumaru and Johnston showing that the reaction of a hydrazide (**61**), halonium generated *in situ* from an oxidant and iodide, and a bromonitroalkane (**60**) generates an oxadiazole (**62**) (Scheme 17, eq 1) while neither a diacyl hydrazine (**63**) or an active ester (**64**) and hydrazide

(65) under similar conditions do (Scheme 17, eq 2-3).⁸⁹ Taken together, this evidence suggests that there is some intermediate formed in Scheme 17, eq 1 prior to conversion to the diacyl hydrazine expected from UmAS (63) which can be intercepted intramolecularly to generate an oxadiazole. The early-stage C-N bond formation intrinsic in that assertion is extremely difficult to rationalize without assuming an electrophilic nitrogen is being attacked by a nucleophilic carbon (umpolung behavior)⁹⁰ which is a central claim in the UmAS mechanistic proposal.

While the reactivity seen in UmAS is largely unprecedented, some literature analogy can be made to individual mechanistic steps. The nucleophilic behavior of nitronates requires no justification, but some comment should be made in relation to the behavior of the *N*-halo complex. The original disclosure of UmAS discusses an *N*-haloamine or an *N*-haloamine succinimide complex as the likely source of electrophilic nitrogen in the reaction and presents some evidence for such a species existing in the reaction conditions.³² The Hayashi group has since provided experimental support for the existence of an *N*-haloamine succinimide complex present in UmAS in that allyl amine and NIS form a crystalline complex with the bond lengths shown in Figure 7.⁹¹ The halogen being more closely held by succinimide in this case is also in line with the recent halonium affinity scale advanced by Borhan and coworkers, but it should be noted that the crystal structure is not necessarily representative of what is occurring in solution.⁹² For reference, the

⁸⁹ Tokumaru, K.; Johnston, J. N. *Chem. Sci.* **2017**, *8*, 3187.

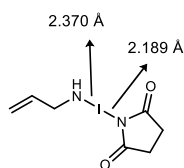
⁹⁰ Seebach, D. *Angew. Chem. Int. Ed.* **1979**, *18*, 239.

⁹¹ Li, J.; Lear, M. J.; Kawamoto, Y.; Umemiya, S.; Wong, A. R.; Kwon, E.; Sato, I.; Hayashi, Y. *Angew. Chem. Int. Ed.* **2015**, *54*, 12986.

⁹² Ashtekar, K. D.; Marzijarani, N. S.; Jaganathan, A.; Holmes, D.; Jackson, J. E.; Borhan, B. *J. Am. Chem. Soc.* **2014**, *136*, 13355.

energy change as described by the Borhan model when Cl^+ attaches to succinimide anion is 290.1 kcal/mol while the corresponding figure for Cl^+ and allyl amine is 152.8 kcal/mol. While the best known *N*-halo amines behave as electrophilic sources of halogen (NIS for example), there are certainly many cases in which they function as sources of electrophilic nitrogen.^{93,94,95} Hayashi and coworkers also demonstrate that the *N*-iodo complex in Figure 7 can serve as a source of electrophilic iodine by reacting with the potassium nitronate of an iodo nitroalkane to generate a di-iodo nitroalkane, but there is no evidence to suggest species of that type are viable towards amine rather than non-productive resting state sources of iodonium used to regenerate an electrophilic amine.⁹¹ Whatever its exact nature, the complex present in UmAS conditions would be expected to be an ambident electrophile where nucleophilic attack could result in halogenation or amination.

Figure 7. Hayashi *N*-haloamine complex bond lengths

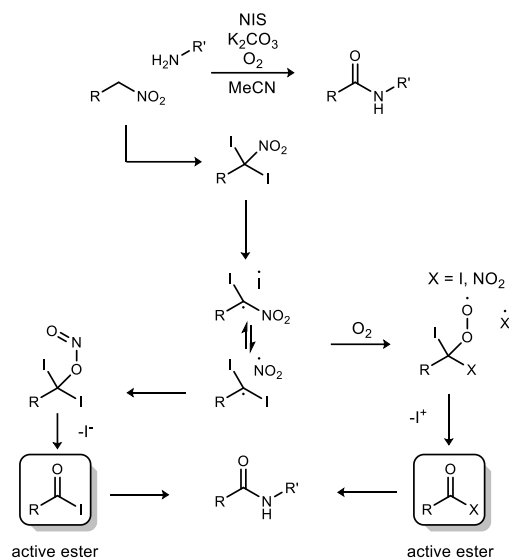


⁹³ Erdik, E. *Tetrahedron* **2004**, *60*, 8747.

⁹⁴ Kovacic, P.; Lowery, M. K.; Field, K. W. *Chem. Rev.* **1970**, *70*, 639.

⁹⁵ He, C.; Chen, C.; Cheng, J.; Liu, C.; Liu, W.; Li, Q.; Lei, A. *Angew. Chem. Int. Ed.* **2008**, *47*, 6414.

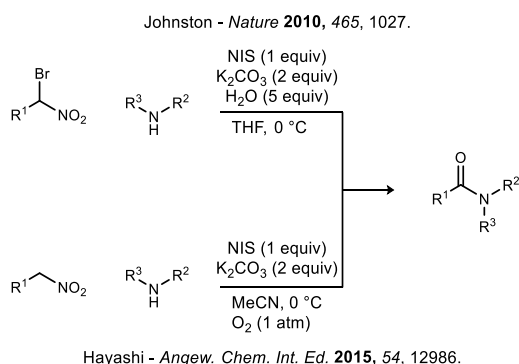
Scheme 18. Proposed oxidative amidation mechanism



Recently, Hayashi published work on an oxidative amidation of nitroalkanes which was proposed to go through a non-umpolung pathway involving the intermediacy of an active ester (Scheme 18).⁹¹ Because of the extremely similar reaction conditions of this work to the work establishing UmAS, it was apparent to both groups involved that there were, in all likelihood, now two contradicting mechanistic proposals for the same reaction. The conditions of the two reactions can be directly compared in Scheme 19 and only differ in solvent, intentional incorporation of O₂, and *in situ* halogenation of the nitroalkane. Indeed, a paper the next year by the Hayashi group reported a mechanistic study directly applying data and observations obtained by each group to both proposals.⁴⁴ It was established that the existing oxygen labeling studies represented no direct contradictions to either mechanism and additional observations were made that supported both mechanisms (such as a radical clock experiment indicating the existence of a carbinyl radical at the expected carbon and evidence for a nitro-nitrite isomerization). It should be noted that Tokumaru et. al. has convincingly ruled out active esters in an oxadiazole forming reaction with

highly analogous conditions to UmAS (Scheme 17).⁸⁹ Also, it was shown that the potassium nitronate of an α -iodonitroalkane could produce a di-iodonitroalkane when treated with a complex of an amine and NIS. Again, this finding provides no rationale for assuming such a di-halo intermediate is en route to amide formation rather than an off-pathway intermediate in equilibrium with other, directly productive intermediates. In fact, unpublished work by Dr. Ken Schwieter has suggested that the di-halo compounds are not intermediates along the direct path to amide. This work shows a higher yield of amide is observed when mono-bromo nitroalkanes are subjected to UmAS conditions compared to when dibromo nitroalkanes are subjected to the same conditions. If monobromo nitroalkanes were converted to dibromo nitroalkanes along the path to amides, one would expect the opposite trend to be observed.

Scheme 19. Johnston UmAS and Hayashi oxidative amidation reaction conditions



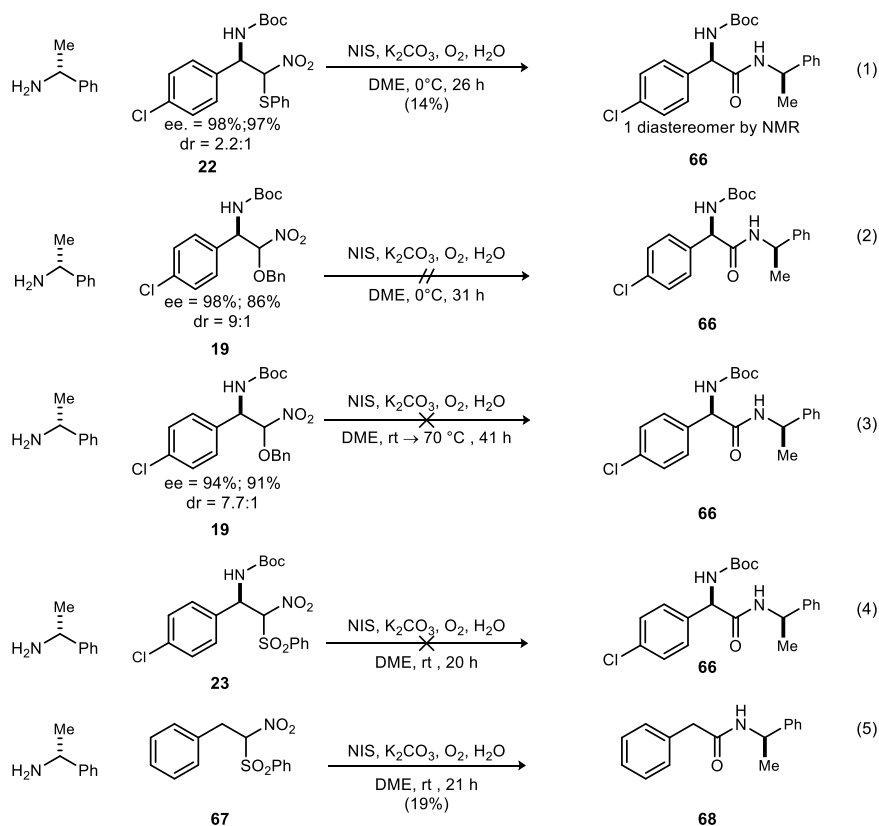
Clearly there is suggestive evidence for each mechanism, however direct evidence of either the active ester in the Hayashi-Lear mechanism or the tetrahedral intermediate in the UmAS mechanism has been completely elusive. Since the existence of each of those intermediates is paramount to the claims about underlying reactivity, any evidence suggesting which one is indeed present or viable in amide production would have pivotal mechanistic implications.

2.2 Mechanism Investigations Using α -Sulfanyl, α -Alkoxy, and Sulfonyl Nitroalkanes

2.2.1 UmAS Reactions with α -Sulfanyl, α -Alkoxy, and Sulfonyl Nitroalkanes

As discussed in Section 1.2, a major motivation for the work described above on aza-Henry reactions with various α -substituents was the window that the products of such reactions open for

Scheme 20. Results from UmAS reactions with unexplored α -substituted nitroalkanes

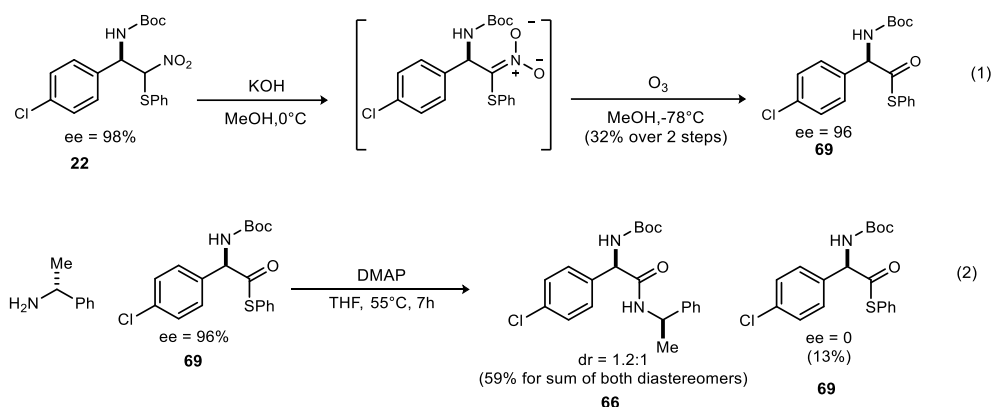


mechanistic investigation of a seemingly unrelated reaction (UmAS). The first potential avenue to that end we probed was the observation of a stabilized intermediate in the reaction or telling byproducts. While the bond dissociation energy of the C-S/C-O bond replacing the C-X bond in

2.2.2 Study of the Epimerization of an Active Ester in Traditional Amide Synthesis

With **22** available in high ee, it was apparent that a series of experiments could be designed as a somewhat direct comparison between UmAS and traditional amide synthesis. Compound **22** nor the bromo-nitroalkane analogue showed any sign of epimerization under UmAS conditions, and a single diastereomer of the α -methyl-benzylamine-derived amide **66** was obtained. Through the ozonolysis of **22**, an active ester precursor to **66** could be obtained (Scheme 22, **69**). Based on the rationale in Scheme 21, **69** must be the active ester operative if the Hayashi mechanistic hypothesis (Scheme 18) is accurate.

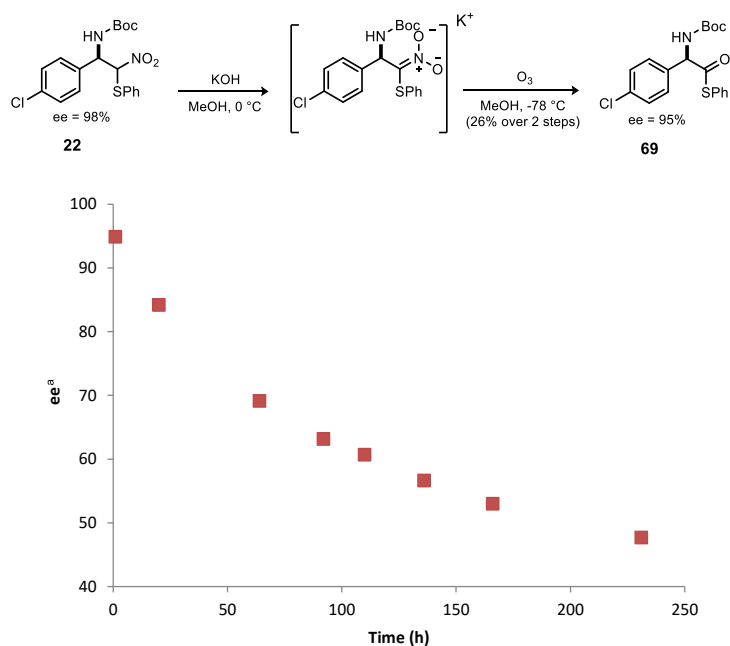
Scheme 22. Traditional amide synthesis with epimerizable active ester



The active ester can then be subjected to traditional amide synthesis and observations made about the enantiopurity and diastereopurity of the product (**66**) and recovered starting material (**69**). It was found that the starting material had been totally racemized while the dr of the amide was nearly one to one. This is a reminder of a limitation of active ester-based amide synthesis and is evidence against the Hayashi-Lear proposal for UmAS. One can imagine that **69** would be the operative active ester formed if applying the Hayashi-Lear mechanism to the **22**→**66** transformation. Due to the results in Scheme 22, it is then reasonable to suspect that, if going

through intermediate **69** and then engaging in traditional amide synthesis, some degradation of enantiopurity would occur giving a lowered dr in the product **66**. Since using UmAS conditions leads to **66** as a single diastereomer, it seems likely the operative mechanism does not involve **69**. Furthermore, if one is considering a mechanism that would involve active ester **69** (such as the Hayashi-Lear proposal) then they would note that reactivity under UmAS conditions was high, giving complete conversion at 0 °C in < 26 h, while traditional amide synthesis required elevated temperature to convert at all. Experiments probing the stability of **69** did also show that it epimerizes upon sitting (Figure 8) with a $t_{1/2}$ of 203 h.

Figure 8. Rate of epimerization of **69** in dilute ethanol solution at rt



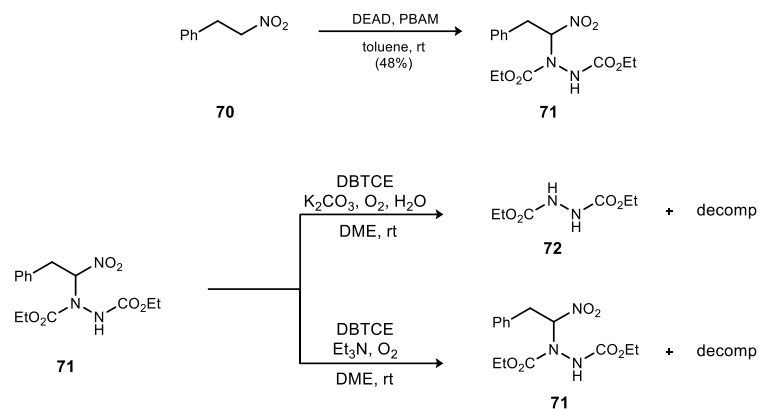
^a ee of a purified sample dissolved in MeOH (1mg/mL) at 20 °C was monitored using Chiralpak IA, 5% IPA/hexanes, 1.0 mL/min

2.3 Mechanism Investigations by HaloAminoNitroAlkane (HANA) Preparation

The pursuit of direct evidence (spectroscopic) for the UmAS tetrahedral intermediate has long been a goal of the Johnston program. The assumed short lifetime and instability of this species is thought to be the reason that this goal has gone unrealized. Dr. Ken Schwieter and Jessica Shackleford have attempted a synthesis of a stand-in for the desired functionalized carbon center by adding in the nitronate of a nitroalkane to electrophilic sources of nitrogen such as DEAD. One such successful reaction of this type led to an α -amino nitroalkane (**71**), but subsequent bromination attempts were all unsuccessful (Scheme 23).

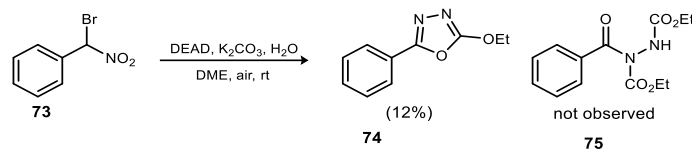
Also relevant to the synthesis of the UmAS tetrahedral intermediate is the work done by Dr. Kazuyuki Tokumaru which showed that an oxadiazole could be formed from the addition of a bromo nitroalkane into DEAD (Scheme 24). Since the formation of this oxadiazole is proposed to involve the desired tetrahedral intermediate, this result is a promising finding. Together these experiments suggest that azodicarboxylates are compatible electrophiles for nitronate nucleophiles.

Scheme 23. Attempted synthesis of UmAS tetrahedral intermediate analogue



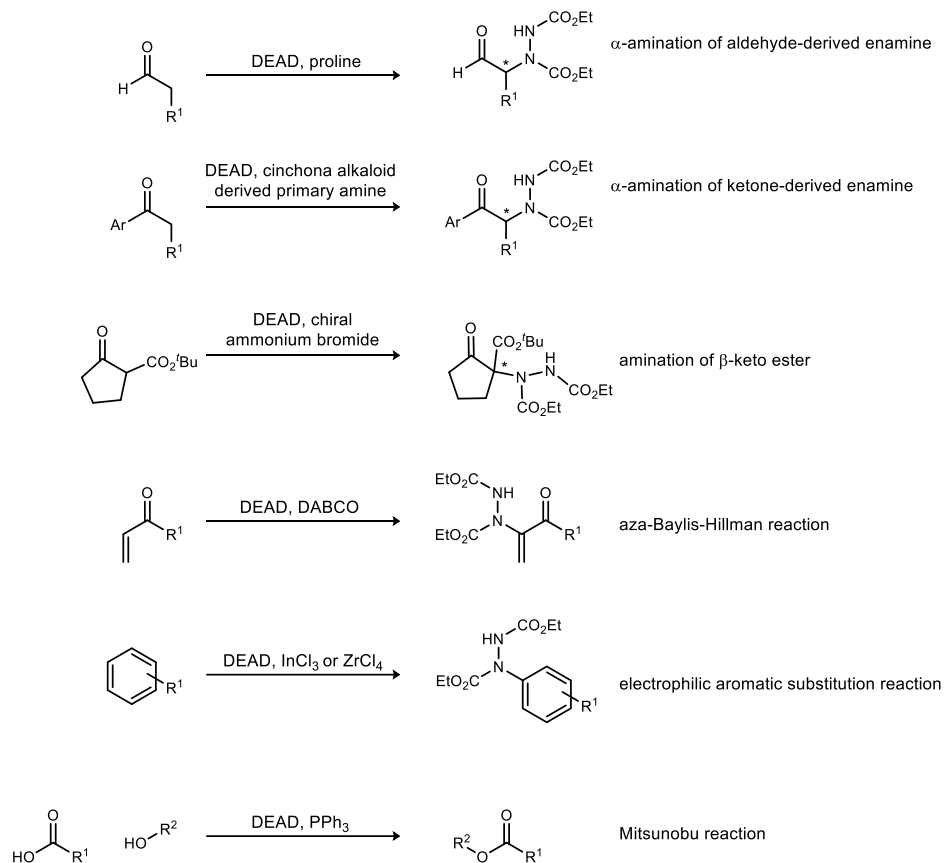
It is possible that the higher bond dissociation energy of fluorine-carbon bonds leads to the lower reactivity of fluoro nitroalkanes in UmAS (Table 1, Table 2). With that effect in mind, it was noted that an appealing option for further attempts to observe a stabilized intermediate would

Scheme 24. Discovery of oxadiazole formation in bromo nitroalkane addition to DEAD



be the addition of a fluoro nitroalkane to an electrophilic source of nitrogen. It was not without notice that fluorine also provides a useful analytical advantage when compared to other halogens (^{19}F NMR).

Scheme 25. Electrophilic behavior of DEAD



DEAD was chosen as the electrophile for a number of reasons. First, it shows promise in terms of reactivity when considering reactions in Scheme 23 and Scheme 24. Second, a departure from the standard *N*-halamine system was needed because fluoro nitroalkanes have already been applied to UmAS conditions with no observation of intermediates. Third, this electrophile is established as a simple and well-behaved *N*-electrophile.⁹⁶ Examples (Scheme 25) of azodicarboxylates serving as *N*-electrophiles include α -aminations of aldehyde and ketone derived

⁹⁶ Stoner, E. J.; Hart, A. C. *Encyclopedia of Reagents for Organic Synthesis* **2001**.

enamines,^{97,98} amination of β -keto esters,⁹⁹ aza-Baylis-Hillman reactions,¹⁰⁰ electrophilic aromatic substitution reactions,^{101,102} and Mitsunobu reactions.¹⁰³ Unlike conditions with amine and *N*-halamine ambident electrophile all in equilibrium, any products or intermediates observed with an azodicarboxylate can be confidently assumed to have come from an electrophilic source of nitrogen.

Finally, the electron withdrawing groups on the nitrogens of DEAD were expected to help in the stabilization of the HANA. The first step in collapse of the key intermediate is C-NO₂ bond homolysis (Scheme 16), and this step is rationalized on the basis of the captodative effect (Scheme 26, eq 1).¹⁰⁴ It follows that removing the stabilizing effect that an electron withdrawing halogen and an electron donating amine have when α to a carbon-centered radical (**76**) could increase the energetic barrier to collapse of the species of interest. A less available nitrogen lone pair should accomplish this goal. Additionally, if there is an elimination step occurring in the pathway from HANA to amide, another incentive for reducing electron density on nitrogen would be apparent (Scheme 26, eq 2).

⁹⁷ Bøgevig, A. J. *Angew. Chem. Int. Ed* **2002**, *41*, 1790.

⁹⁸ Liu, T.-Y.; Cui, H.-L.; Zhang, Y.; Jiang, K.; Du, W.; He, Z.-Q.; Chen, Y.-C. *Org. Lett.* **2007**, *9*, 3671.

⁹⁹ Lan, Q.; Wang, X.; He, R.; Ding, C.; Maruoka, K. *Tetrahedron Lett.* **2009**, *50*, 3280.

¹⁰⁰ Kamimura, A.; Gunjigake, Y.; Mitsudera, H.; Yokoyama, S. *Tetrahedron Lett.* **1998**, *39*, 7323.

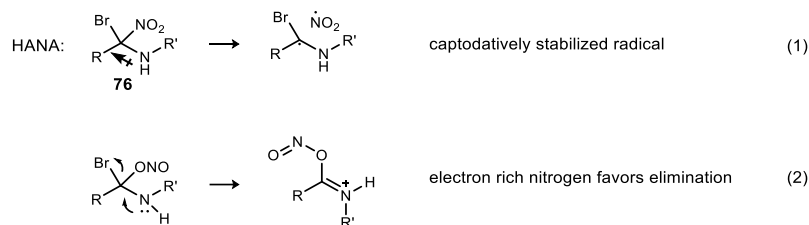
¹⁰¹ Yadav, J.; Reddy, B. S.; Kumar, G. M.; Madan, C. *Synlett* **2001**, *2001*, 1781.

¹⁰² Bombek, S.; Požgan, F.; Kočevár, M.; Polanc, S. *J. Org. Chem.* **2004**, *69*, 2224.

¹⁰³ Mitsunobu, O.; Yamada, M. *Bull. Chem. Soc. Jpn.* **1967**, *40*, 2380.

¹⁰⁴ Viehe, H. G.; Janousek, Z.; Merenyi, R.; Stella, L. *Acc. Chem. Res.* **1985**, *18*, 148.

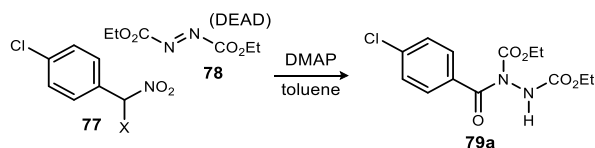
Scheme 26. Consideration of nitrogen electronics on intermediate stability



2.3.1 HANA Synthesis

To test the theory that halogen-carbon bond strength may be a significant contributor to reaction outcome, nitroalkanes with α -iodo, bromo, chloro, and fluoro substituents were reacted with DEAD in the presence of substoichiometric amounts of base (Table 7). An α -iodo substituted nitroalkane (Table 7, entry 1) proved highly reactive, but produced only complex mixtures with no evidence for imide (amide) formation. The typical α -bromo nitroalkane donor, however, provided encouraging evidence for the formation of the imide in the crude reaction mixture (Table 7, entry 2). The amount formed was considerably higher when using the α -chloro nitroalkane, but still rather low at 20% yield (Table 7, entry 3). The imide, isolated in the reaction described by entry 3, most notably had a ^{13}C peak corresponding to the amide carbonyl at 170.2 ppm and a pair

Table 7. Catalyzed reaction of α -halo nitroalkanes with an azodicarboxylate electrophile (DEAD)^a



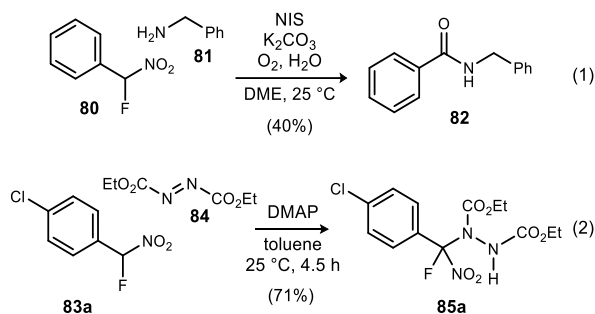
entry	X		yield (%)
1	I	a	-
2	Br	b	trace
3	Cl	c	20 ^b

^aGeneral procedure: DEAD (1.1 equiv.), DMAP (0.22 equiv.), and nitroalkane (1 equiv, 0.1 M in toluene) were stirred for 1 h (**77a**), 25 h (**77b**) or 17 h (**77c** in CH_3CN). ^bIsolated yield.

of N-H peaks by $^1\text{H-NMR}$ arising from the amide conformations. These tell-tale N-H peaks were the clearest indication that imide was formed in Table 7 entry 2, particularly when $\text{DMSO-}d_6$ was used as the NMR solvent. None of these reactions gave evidence for a metastable intermediate, but an encouraging trend was emerging.

The fluoro nitroalkane was first established as a competent substrate in standard UmAS conditions (Scheme 27, eq 1) before its application to this system. Examination of α -fluoro nitroalkane additions with diethyl azodicarboxylate was also made at room temperature, but in contrast to UmAS, water was not included due to its nonessential role in converting nitroalkane to amide.⁵³ A new material was isolated and assigned as the addition product (Scheme 27, eq 2). $^{19}\text{F-}$

Scheme 27. Reactions of α -fluoro nitroalkane with amine and azodicarboxylate

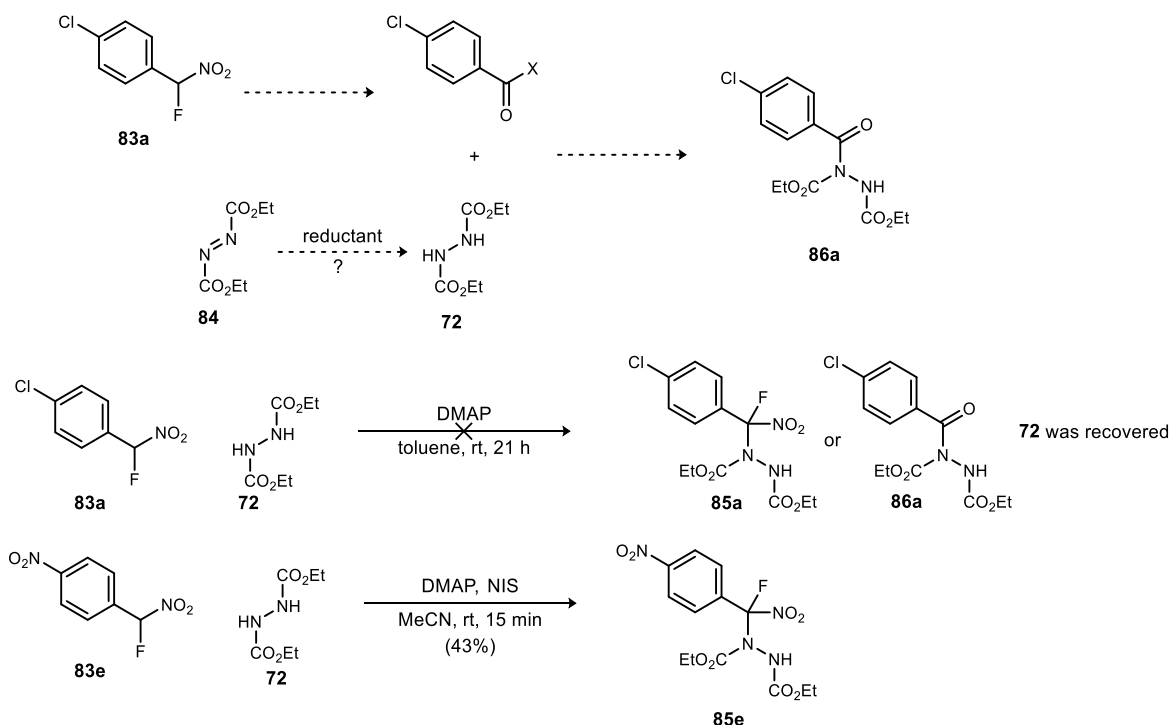


NMR of this product exhibited a resonance at -103.1 ppm, while a quaternary carbon (d, $^1J_{\text{CF}} = 265$ Hz) at 119.4 ppm by $^{13}\text{C-NMR}$ was also consistent with **85a**. The NMR data was not without ambiguity, owing to significant broadening, and in some cases doubling, of peaks. The complexity observed in the NMR is in line with literature precedence for hindered hydrazine derivatives and

has been attributed to a combination of hindered carbamate C-N bond rotation and hindered N-N bond rotation.^{105,106}

Despite our belief that this reaction excluded any source of nucleophilic nitrogen, we sought further evidence that the C-N bond formation is umpolung in nature. We explored the possibility that reduction of DEAD *in situ* would produce a nucleophilic diacyl hydrazine (Scheme 28, **72**). The necessity for electrophilic nitrogen was thus validated by the observation that **72** in place of DEAD produces no conversion to **85** or **86**. Significantly, using diacyl hydrazine plus an

Scheme 28. Control reactions validating umpolung behavior of C-N bond formation



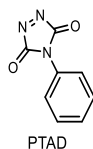
¹⁰⁵ Anderson, J.; Lehn, J. *Tetrahedron* **1968**, *24*, 123.

¹⁰⁶ Anderson, J.; Lehn, J. *Tetrahedron* **1968**, *24*, 137.

exogenous oxidant (NIS) did lead to significant production of the adduct product **85**. This presumably occurs through oxidation of the diacyl hydrazine to DEAD.

In the course of establishing the standard method for TI' synthesis, other bases such as potassium carbonate were found to be competent but lead to reaction mixtures in which the desired product was less abundant. Other fluoro nitroalkanes (including those with alkyl rather than aryl substituents) were also tested, and, while evidence for HANA formation was obtained, the intermediates produced from these reagents were even less stable than **85**, so they were not pursued. **83a** also failed to generate any identifiable adduct products when reacted with the related electrophile 4-phenyl-1,2,4-triazole-3,5-dione (PTAD, Figure 9).

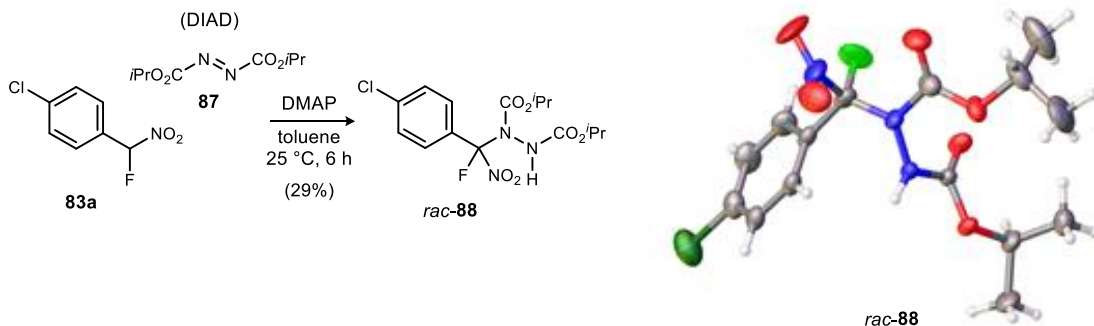
Figure 9. Structure of PTAD



Although the spectroscopic data was consistent with addition product **85a**, it did not differentiate the nitro and nitrite ester regioisomers. On the basis of literature precedence

documenting nitro-nitrite isomerizations,^{107,108,109,110,111,112,113,114,115,116,117,118} we proposed both

Figure 10 X-Ray crystal structure of *rac-88* (TI') establishing C-NO₂ (nitro) regiochemistry rather than C-ONO (nitrite ester)



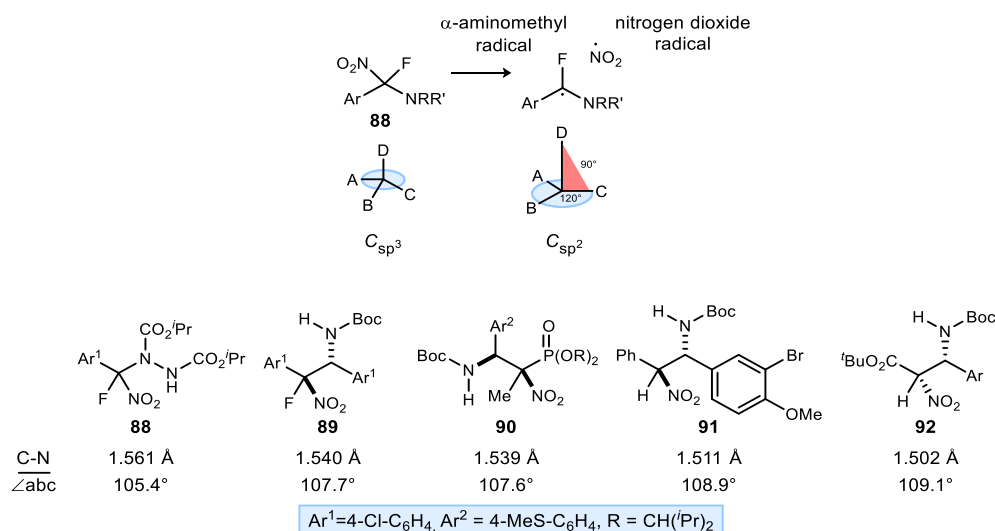
along the pathway to amide.⁸⁸ Adduct **85a** did not yield to crystallization attempts, but the analogous addition product using DIAD (**87**) produced a material with nearly identical characteristics, one that could be crystallized from diethyl ether/heptane. X-Ray diffraction of the DIAD adduct (**88**) confirmed the identity of this product as TI' (Figure 10). Two chemically identical, but crystallographically distinct, molecules were observed (one shown in Figure 10, with bond lengths and angles provided later as averages).

-
- ¹⁰⁷ Amin, M. R.; Dekker, L.; Hibbert, D. B.; Ridd, J. H.; Sandall, J. P. B. *J. Chem. Soc., Chem. Commun.* **1986**, 658.
¹⁰⁸ Baum, K.; Archibald, T. G.; Tzeng, D.; Gilardi, R.; Flippen-Anderson, J. L.; George, C. *J. Org. Chem.* **1991**, *56*, 537.
¹⁰⁹ Hartshorn, M.; Robinson, W.; Wright, G.; Cheng, L. *Aust. J. Chem.* **1989**, *42*, 1569.
¹¹⁰ Hochstein, W.; Schöllkopf, U. *Ann.* **1978**, *1978*, 1823.
¹¹¹ Khrapkovskii, G.; Nikolaeva, E.; Chachkov, D.; Shamov, A. *Russ. J. Gen. Chem.* **2004**, *74*, 908.
¹¹² Nguyen, M. T.; Le, H. T.; Hajgato, B.; Veszpremi, T.; Lin, M. *J. Phys. Chem. A* **2003**, *107*, 4286.
¹¹³ Nguyen, N. V.; Baum, K. *Tetrahedron Lett.* **1992**, *33*, 2949.
¹¹⁴ Saito, I. **1975**.
¹¹⁵ Saxon, R. P.; Yoshimine, M. *Can. J. Chem.* **1992**, *70*, 572.
¹¹⁶ Soto, J.; Arenas, J. F.; Otero, J. C.; Pelaez, D. *J. Phys. Chem. A* **2006**, *110*, 8221.
¹¹⁷ Yim, W.-L.; Liu, Z.-f. *J. Am. Chem. Soc.* **2001**, *123*, 2243.
¹¹⁸ Zhang, C.; Wang, Q. *Macromol. Rapid Commun.* **2011**, *32*, 1180.

The formation of this intermediate from a substrate recognized as an electrophilic nitrogen supports the hypothesis that an electrophilic nitrogen species reacts similarly with nitronate in UmAS when using conditions favorable for halamine formation.⁹⁴ The preparation of **88** from nitronate and DIAD, and its characterization by X-ray diffraction, provides a tangible point of study within this context. There is some structural evidence that **88** is disposed toward nitro-nitrite isomerization when considering bond angles and lengths located at the tetrahedral carbon. As weakening of the C-NO₂ bond occurs, one would expect to see its length increase and the three associated bond angles to approach 90° as the attached carbon approaches sp² hybridization. Figure 11 illustrates this effect by diagram, charting the C-NO₂ bond lengths alongside the mean of the three X-C-NO₂ bond angles (a-c) for nitroalkanes **88-92**.^{9,35,85,119} Although the magnitude of the bond length and angle change is relatively small, the trend is clear and consistent along this series. The increasing bond lengths and decreasing bond angles in the direction of **92**→**88** correspond to increasingly electron withdrawing substituents and, presumably, an increasingly weak C-NO₂ bond.

¹¹⁹ Davis, T. *Org. Lett.* **2010**, *12*, 5744.

Figure 11. Examination of a series of nitroalkanes by X-ray structural analysis: correlation of C-N bond length with sum of angles at tetrahedral carbon



2.3.2 HANA Competency for Amide Formation

Preparation and structural confirmation of a tetrahedral intermediate (TI') provided an opportunity to use it as an analogy to TI. TI' exhibited the key features attributed to an UmAS-productive TI: nitro, amine, and halogen at a single carbon. A key difference is the nitrogen substituent: an alkyl for TI vs. an acyl/nitrogen for TI'. The use of fluorine in exchange for bromine may have strengthened the carbon-halogen bond, but its relevance to UmAS was validated by its behavior under typical conditions (Scheme 27, eq 1). Focus therefore shifted to the reactivity of this compound and its competency as a precursor to imide **86**. It was first noted that imide **86a** was observed in low yield (10%) alongside **85a** under the conditions in Scheme 27, however much higher yields of **86a** were realized when heat was applied. Imide **86a** was obtained in as high as 54% yield when isolated **85a** was heated in a J-Young tube with DMSO-*d*₆.

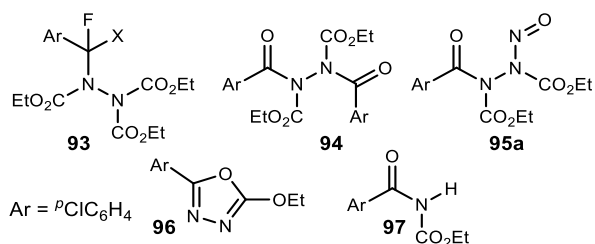
Control reactions with imide **86a** show that it is stable under the reaction conditions which further indicates **85a** is an intermediate towards **86a**. Comparison experiments were performed

first with **85a**, but ultimately in a more rigorous manner with **85c** in order to facilitate ^{19}F -NMR monitoring. In these experiments $\text{DMSO-}d_6$ from an ampule was used to prepare samples within a glovebox, and the solutions were degassed before heating and NMR observation. Through parallel experiments with the intentional incorporation of an oxygen atmosphere or water, it was observed that O_2 had little impact on the appearance of the crude reaction mixture, but water led to fewer co-products alongside conversion to amide.

2.3.3 Coproduct Analysis

The reaction of **85a** with DEAD was chosen for careful inspection to identify co-products whose formation might provide mechanistic insight. Figure 12 lists those compounds isolated from the addition of **85a** into DEAD (**93-97**). These were identified over the course of numerous reactions focused on the factors affecting production of **85a**, so relative yields from a single reaction are not available, but certainly $<10\%$ in general, with some as low as 1%. Hydrazines with additional acylation (**93** and **94**) indicate the possibility of acyl transfer between either DEAD or the major product (**85a**) and TI'. Imide **93** is another TI', and although it was not rigorously established as the nitro-regioisomer, its spectroscopic characteristics are quite similar to **85** for which X-ray structure determination was used to establish the nitro isomer (Figure 10). Nitroso **95a** was identified tentatively by analogy to imide **86a**, as it exhibited similar spectroscopic characteristics, but lacked ^1H NMR or IR evidence for an N-H bond; HRMS indicated the mass of

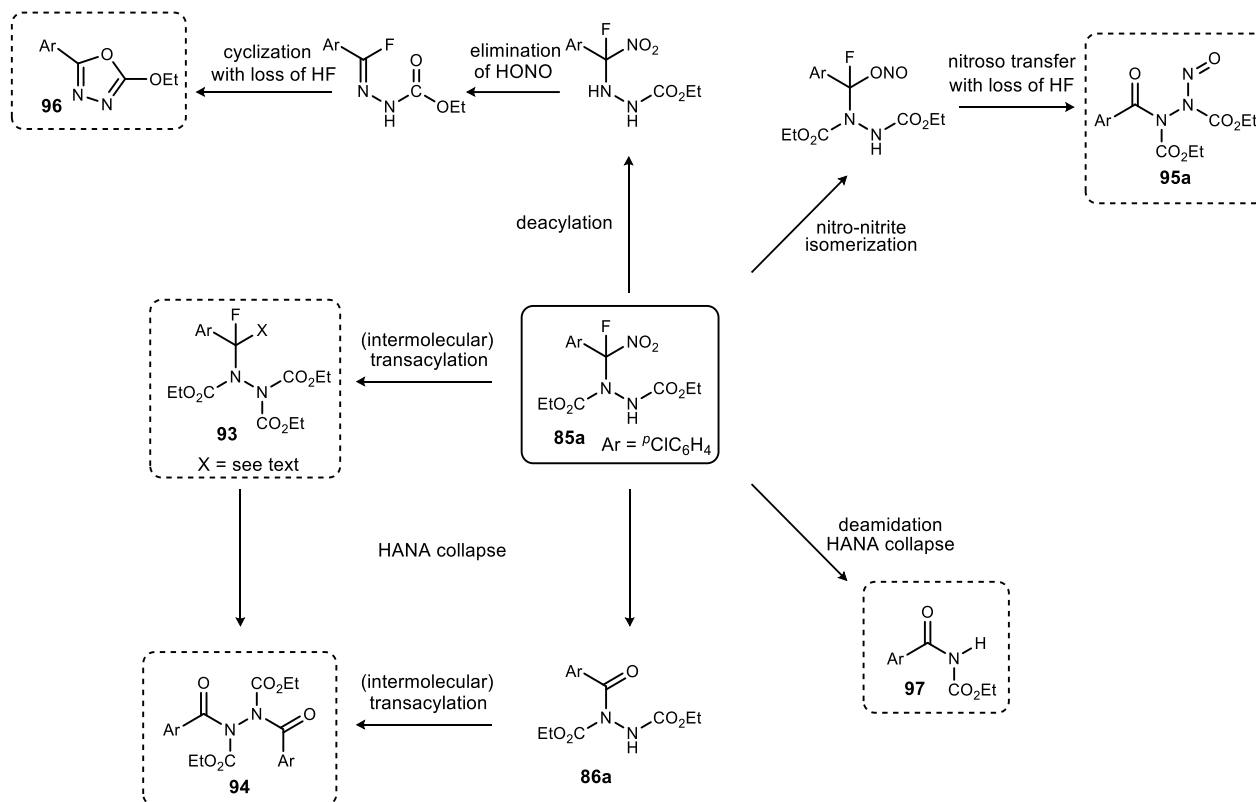
Figure 12. Minor co-products formed from the reaction of **32a** with DEAD



amide **32a** with the expected H to NO substitution. The ultimate assignment also benefits from the preparation of nitroso **95a** from amide **86a** using nitrosonium tetrafluoroborate. Its formation is highly suggestive that a nitrite ester is indeed formed as an intermediate, consistent with the nitro-nitrite isomerization mechanistic hypothesis that was itself based on isotopic labeling experiments.⁸⁸ The pathway to **95a** would involve nitrosyl transfer from the nitrite ester to carbamate nitrogen. Its conversion to **86a** during storage or heating was noted; the use of water in a typical UmAS protocol would likely promote the conversion of nitrosyl **95a** to product. Oxadiazole **96** was identified as well, consistent with our recent descriptions of diverted UmAS.^{89,120} Its formation here suggests a mechanistic intersection between UmAS and diverted UmAS as the overlapping monikers foreshadowed. Quite unusual, however, was the isolation of imide **97**, as it results from cleavage of the N-N bond. Formation of **97** might indicate nitrene formation at some point in the reaction, but insofar as it is the only N-N cleavage product observed, and in low yield, its significance should not be overstated. A mechanistic hypothesis for the formation of **93-97** can be seen in Scheme 29.

¹²⁰ Tokumaru, K.; Bera, K.; Johnston, J. N. *Synthesis* **2017**, *49*, 4670.

Scheme 29. Mechanistic hypotheses for observed co-products

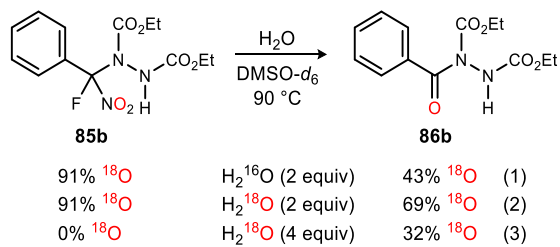


2.3.4 ^{18}O Labeling Experiments

Past mechanistic studies of UmAS used ^{18}O -labeled substrates and reagents to uncover the source of the amide oxygen.⁸⁸ Labeled **85b** (91% ^{18}O in the nitro group arising from an 82:18:0 ratio of di:mono:unlabeled molecules) was subjected to conditions typical of the above reactions, leading to the corresponding amide with 43% ^{18}O -incorporation. High resolution mass spectrometry confirmed its incorporation as depicted in Scheme 30. This indicates that nearly half of the amide oxygen originates from the nitro group under the conditions outlined here. As with our earlier studies of UmAS by ^{18}O -labeling, at least one additional oxygen source competes. The lack of apparent effect by molecular oxygen led us to investigate the possibility that water-oxygen

is involved, despite its lack of involvement in early UmAS mechanistic studies.⁸⁸ Repeating the

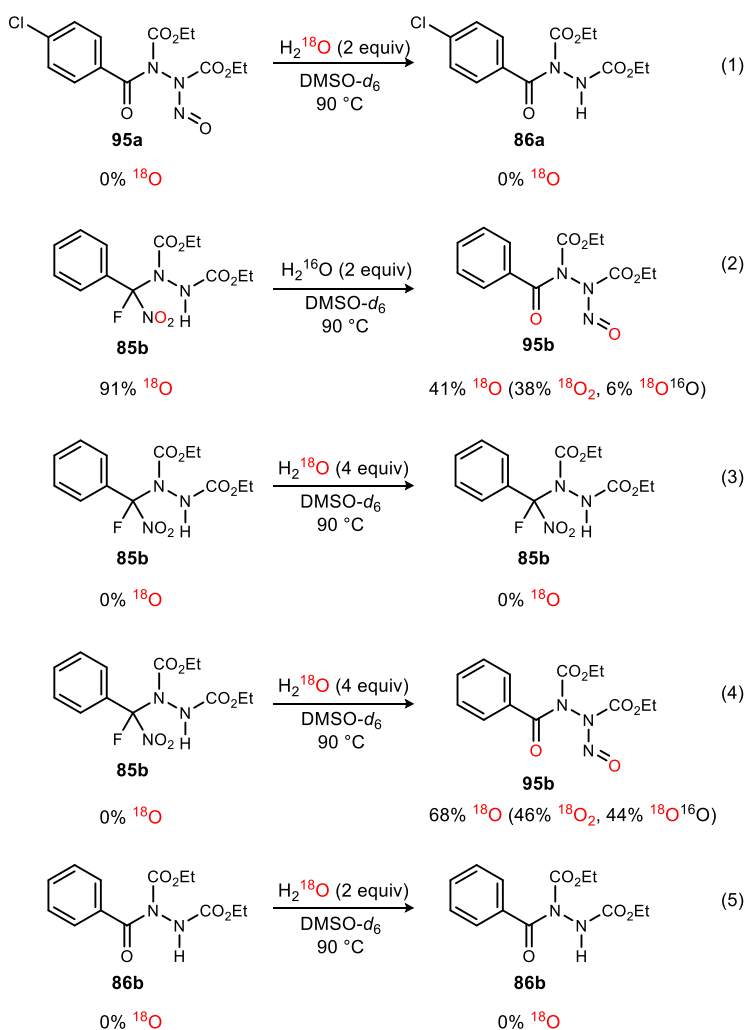
Scheme 30. ¹⁸O-Labeling experiments



labeled **85b** decomposition with H₂¹⁸O led to amide with 69% ¹⁸O-incorporation, highlighting the likely effect of nitrogen group on the fate of each type of HANA. The increase from 43% to 69% is significant and indicates the involvement of water in conservation of the label, either by slowing the introduction of an ¹⁶O source, or supplying an alternative ¹⁸O source to a key intermediate. The lack of complete retention of labeling may be attributed to unlabeled water present in the system or competing minor pathways to amide.

Additional ^{18}O labeling experiments were used to acquire greater detail regarding the oxygen sources in the reaction. Isolated *N*-nitroso species **95a** could be converted to imide **86a** by heating in wet DMSO, and no labeling in **86a** was observed when the water source was highly ^{18}O enriched (Scheme 31, eq 1). This finding suggests that **95a** lies past some irreversible oxygen-source-determining mechanistic step. Interestingly, when the *N*-NO compound **95b** was isolated

Scheme 31. Additional ^{18}O -Labeling experiments



from Scheme 31, eq 2 it also showed signs that water is serving as an oxygen source. **95b** was 41% labeled arising from a distribution of molecules that was 38% doubly labeled and 6% mono

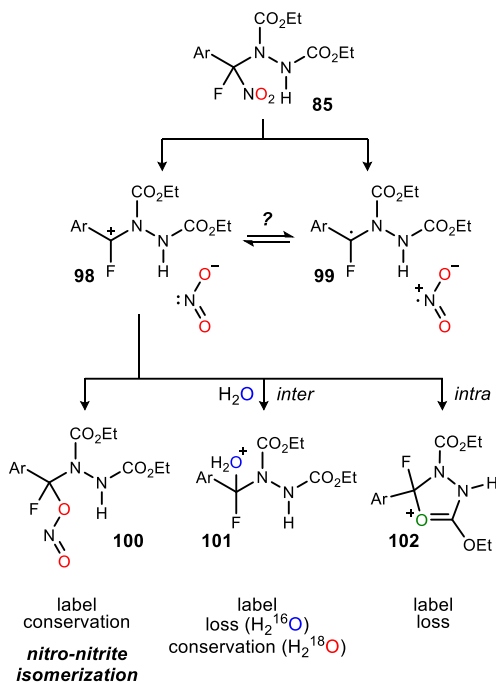
labeled. This finding suggests that the nitro nitrite isomerization itself provides an opportunity for oxygen exchange between water and the NO_2^- or HNO_2 that is generated. Notably, the recovered starting material from Scheme 31, eq 3 (**85b**) had no enrichment of ^{18}O and the *N*-nitroso **95b** had 68% ^{18}O incorporation arising from a distribution of molecules that was 46% doubly labeled and 44% mono labeled (Scheme 31, eq 4). It was also validated that the heavy isotope of oxygen was introduced at some point between **85** and **86** by subjecting isolated, unlabeled product (**86b**) to the reaction conditions in the presence of H_2^{18}O (Scheme 31, eq 5). This experiment confirmed that no oxygen exchange between water and the product was occurring. The exact nature of the oxygen incorporation into **95b** is unclear, but it is apparent that water and the nitro group of **85** are both significant contributors to labeling outcome in both **95** and **86**.

2.3.5 Probing the Nature of Nitro-Nitrite Isomerization

At this point in the study all indications were consistent with nitronate reaction with an electrophilic nitrogen followed by conversion of the tetrahedral intermediate nitro to nitrite. The homolytic nature of the nitro-nitrite isomerization rests on literature precedent and the observation that oxygen can serve as the source for amide oxygen in UmAS.⁸⁸ Both radical and carbenium ion formation, however, are reasonable in this system. Unlike the labeling outcomes in amide formation,⁸⁸ the findings in Scheme 30 involving imide formation determined that H_2^{18}O can contribute to amide oxygen. The nitrogen in these hydrazine intermediates is electronically and sterically different than that in a typical UmAS.

Possible intermediates and pathways to rationalize the differences are outlined in Scheme 32. The question whether nitro-nitrite isomerization is heterolytic (giving **98**) or homolytic (giving **99**) aside, *N*-acyl iminium **98** can form directly or indirectly. Recombination to form nitrite accounts for the majority of label retention in Scheme 30. Evidence for nitrite ester intermediacy (**100**) is further supported by the observation of efficient conversion of **85b** to the corresponding *N*-nitroso species (**95b**) (70% NMR yield) when the reaction is performed in dry toluene-*d*₈. That labeled water increases conservation of label is explained by reaction of the *N*-acyl iminium with water intermolecularly (**98**→**101**). We speculate that the remaining label loss could be due to intramolecular cyclization of the distal carbamate oxygen (**98**→**102**), and then adventitious water

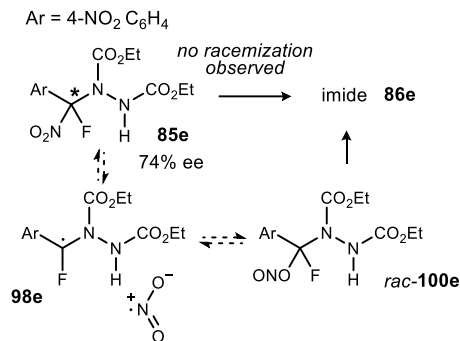
Scheme 32. The nitro-nitrite isomerization and possible pathways contributing to partial ¹⁸O-label loss



or workup eventually provides the imide product. Unfortunately, we were unable to prepare a labeled azodicarboxylate that might firmly support the involvement of **102** but note its similarity

to the concept of diverted UmAS. Regardless of any uncertainty, the iminium-like behavior of the

Scheme 33 Investigation of possible reversible conversion of **32e**, illustrated by the potential intermediacy of carbon radical **49**



amide's precursor is observed here for the first time.

Additional evidence for reversible TI' conversion, and possible evidence for C-NO₂ homolytic cleavage was sought via an epimerization study of **85e** at partial conversion to **86e** inspired by the work of Cheng.¹⁰⁹ In the epimerization study, bis(amidinium) catalysis²⁹ was found to be effective at providing enantioenriched **85e** (Scheme 33). As determined by chiral HPLC at partial conversion, there was no loss of enantioenrichment (% ee) through the course of the reaction. This indicates that consumption of the intermediate is faster than any rate of **85e** reformation, anticipated to occur through the possible formation of radical **98e** (or carbenium ion equivalent). A short-lived radical that leads irreversibly to the nitrite, or a solvent cage effect that provides a high degree of retention of stereochemistry in the forward and backward transformations, cannot be entirely excluded. The cage effect resulting in retention of stereochemistry in reactions of ion and radical pairs is well established (e.g. Stevens and

Meisenheimer rearrangements among others), but complete retention would be unprecedented.^{121,122,123,124,125,126}

To fully rule out the intermediacy of a radical species, a number of established radical probing techniques were applied and all gave negative results. For starters, the conversion of **85a** to **86a** was not significantly perturbed by the inclusion of TEMPO in the reaction mixture. Additionally, a chemically induced dynamic nuclear polarization effect¹²⁷ was not observed here when **85a** was heated in DMSO within a temperature-controlled NMR probe. Finally, only the stereo-conserved products were obtained when several cyclopropane containing fluoro nitroalkanes were reacted with DEAD (Scheme 34). Interestingly, these substrates were quite unreactive using standard conditions employed for HANA preparation, but bis(amidine) catalysts could carry out the additions (though be it in lower yields). In these cases, evidence for the HANAs could be observed in crude reaction mixtures, but they proved to be unstable and were never isolated. This is unsurprising considering how much more electron donating an alkyl substituent is compared to an aryl one. Even electron-rich aryl substituents were sufficiently destabilizing that HANAs could not be isolated.

¹²¹ Franck, J.; Rabinowitsch, E. *Transactions of the Faraday Society* **1934**, *30*, 120.

¹²² Greene, F. D.; Berwick, M. A.; Stowell, J. C. *J. Am. Chem. Soc.* **1970**, *92*, 867.

¹²³ Engstrom, J. P.; Greene, F. D. *J. Org. Chem.* **1972**, *37*, 968.

¹²⁴ Lorand, J. P.; Grant, R. W.; Samuel, P. A.; O'Connell, S. E. M.; Zaro, J.; Pilotte, J.; Wallace, R. W. *J. Org. Chem.* **1973**, *38*, 1813.

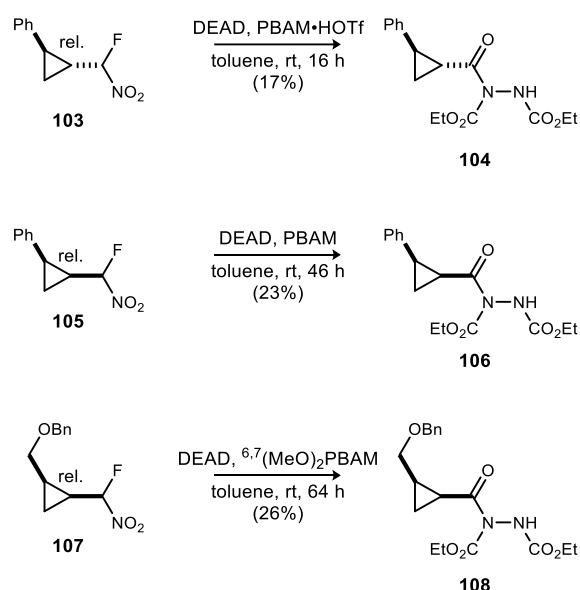
¹²⁵ Zhang, Y.; Reynolds, N. T.; Manju, K.; Rovis, T. *J. Am. Chem. Soc.* **2002**, *124*, 9720.

¹²⁶ Sweeney, J. B. *Chem. Soc. Rev.* **2009**, *38*, 1027.

¹²⁷ Ward, H. R. *Acc. Chem. Res.* **1972**, *5*, 18.

The *trans* cyclopropane **103** was chosen for initial study due to ease of preparation, but no sign of the *cis* cyclopropane product **104** was observed. Of course the *cis* product would be the thermodynamically less favorable product, so we considered whether the low yield would preclude any chance to observe the epimerized product despite the intermediacy of a radical. The analogous reaction was run using **105** to address this concern. In this series as well, no erosion to cyclopropane stereopurity was observed in the transformation from fluoro nitroalkane to imide **106**. Using both stereoisomers also provided authentic standards that increased our confidence that

Scheme 34. Cyclopropane substrates used to probe radical intermediacy

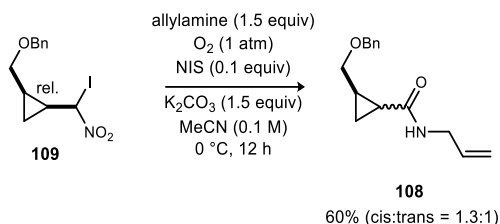


no epimerization occurred during either reaction.

The phenyl substituent on the cyclopropanes **103** and **105** was chosen out of convenience but also because the stability of a benzyl radical resulting from ring opening would be expected to increase the odds of finding evidence for a radical if one was operative in the mechanism. It is true though that radicals have a preference to generate radicals of opposing polarity, especially in

radical polymerizations.^{128,129} To account for the possibility that forming the electrophilic benzylic radical was disfavored due to the electrophilic nature of the proposed α -fluoro, α -carbamate radical, we sought the electronically differentiated radical probe **107**. This compound is also identical (except for the halogen) to one used previously to investigate UmAS which did show

Scheme 35. Cyclopropane substrate used previously in UmAS



epimerization (Scheme 35, **109**).⁴⁴ Its validated applicability to a similar system makes it the best possible candidate for observing evidence for a radical intermediate. The results of reacting **107** with DEAD, however, show no sign of radical formation in that only the *cis* product **108** was observed. These experiments as well as others above referenced convinced us to consider that the mechanism of this HANA collapse is perturbed from that of the standard UmAS case.

2.3.6 Kinetics Experiments

Due to ¹⁸O labeling indications of iminium-like behavior and the lack of evidence to support a radical or reversible nitro-nitrite isomerization, we next sought kinetics data to get more information on the steps leading from **85** to imide. Conversion of **85a** (TI') to amide **86a** was monitored by ¹H NMR to develop a kinetic analysis. Plotting ln(concentration) vs. time gave a

¹²⁸ Alfrey Jr, T.; Price, C. C. *Journal of Polymer Science* **1947**, 2, 101.

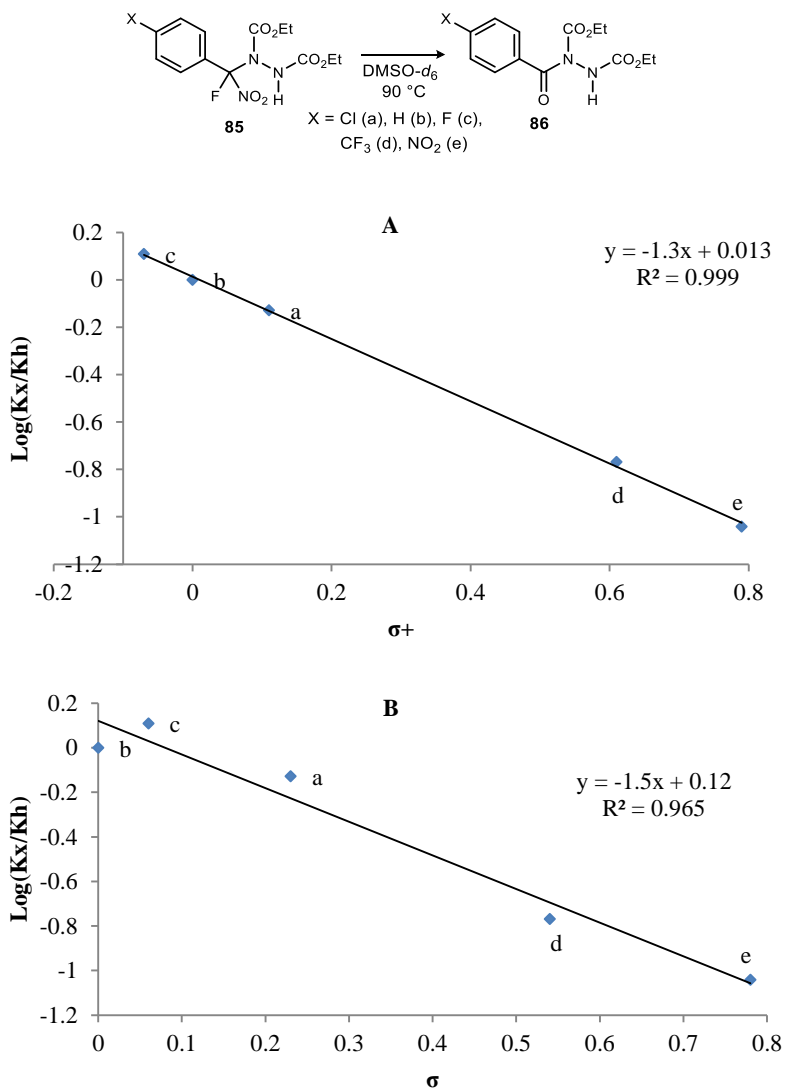
¹²⁹ De Vleeschouwer, F.; Van Speybroeck, V.; Waroquier, M.; Geerlings, P.; De Proft, F. *Org. Lett.* **2007**, 9, 2721.

linear trendline consistent with a rate-limiting step that is first order. Additionally, the slope of the fitted line provided $k(\mathbf{85a}) = 0.013 \text{ min}^{-1}$. Preparation of the electron-deficient **85e** and measurement of its rate of conversion provided $k(\mathbf{85e}) = 0.0016 \text{ min}^{-1}$, clearly establishing rate deceleration by an electron-withdrawing substituent. The synthesis of **85e** was unique from the synthesis of all the other TI's in this series as it had to be run in MeCN rather than toluene. This did take some optimization to determine, and the observation of a small amount of precipitate immediately upon addition of the base was the feature that, once noticed, led to the solution. It is suspected that nitronate solubility for this fluoro nitroalkane is prohibitively low. This lesson proved important in several unrelated instances involving α -aromatic substituted halo nitroalkanes.

Attempts to acquire kinetic data for the tetrahedral intermediate bearing an electron-donating *para*-methoxy group were unsuccessful due to the difficulties in isolating this more reactive species. Several other analogues were successfully prepared and analyzed, leading to a Hammett plot with a ρ constant of -1.3 (Figure 13 top). The linear fit using the standard substituent constants was very good ($R^2 = 0.965$, Figure 13 bottom), but application of the σ^+ constants gave significant improvement and an exceptional fit ($R^2 = 0.999$).¹³⁰

¹³⁰ Hansch, C.; Leo, A.; Taft, R. *Chem. Rev.* **1991**, *91*, 165.

The negative slope of the Hammett plot is consistent with an *N*-acyl iminium ion (and, to
Figure 13. Hammett plot generated from observing HANA consumption during the thermal conversion of **85a-e** to their
 corresponding amide products plotted against A) σ^+ and B) σ substituent constants



a lesser extent, radical) intermediates. Moreover, the improvement in fit when switching to the σ^+ constants (designed for systems with transition states having positive charge character able to engage in resonance stabilization with ring substituents) is highly suggestive of a benzylic cation forming in the rate-limiting step of the reaction. For context, the solvolysis of

phenyldimethylcarbinyl chlorides (the reaction from which σ^+ is derived) has a ρ of -4.62 (90% aq acetone) which is more pronounced than the effect seen here but of consistent sign.¹³¹

Qualitative analysis of the effect of the electronics of the R group on stability, and the magnitude of the slope demonstrates that the effect is significant. Notably, the linear fit in the Hammett plot is very good and the slope is not near zero, indicating a linear effect from substituents. Reactions involving radical transition states are typically not well correlated by the application of simple Hammett substituent constants and significant effort has been placed on separating out and accounting for resonant radical stabilization.^{128, 132, 133, 134, 135, 136, 137, 138, 139, 140, 141, 142, 143, 144} This typically culminates in a two-parameter Hammett analysis. The fact that no such analysis was necessary to produce a good linear fit in this system suggests that no radical character is involved in the transition state of the rate limiting step (the homolytic loss of NO₂ is not involved in evolution to amide). It should be pointed out, however, that certain radical reactions, especially those involving generation of a benzylic radical through the action of an electrophilic radical, are dominated by polar effects and correlated

¹³¹ Okamoto, Y.; Brown, H. C. *J. Org. Chem.* **1957**, *22*, 485.

¹³² Adam, W.; Harrer, H. M.; Kita, F.; Korth, H.-G.; Nau, W. M. *J. Org. Chem.* **1997**, *62*, 1419.

¹³³ Creary, X. *Acc. Chem. Res.* **2006**, *39*, 761.

¹³⁴ Ađirbas, H.; Jackson, R. A. *Journal of the Chemical Society, Perkin Transactions 2* **1983**, 739.

¹³⁵ Tvaroška, I.; Bleha, T. In *Adv. Carbohydr. Chem. Biochem.*; Elsevier: 1989; Vol. 47, p 45.

¹³⁶ Dust, J. M.; Arnold, D. R. *J. Am. Chem. Soc.* **1983**, *105*, 1221.

¹³⁷ Fisher, T.; Meierhoefer, A. *J. Org. Chem.* **1978**, *43*, 224.

¹³⁸ Ito, R.; Migita, T.; Morikawa, N.; Simamura, O. *Tetrahedron* **1965**, *21*, 955.

¹³⁹ Jiang, X.; Ji, G. *J. Org. Chem.* **1992**, *57*, 6051.

¹⁴⁰ Leigh, W. J.; Arnold, D. R.; Humphreys, R. W.; Wong, P. C. *Can. J. Chem.* **1980**, *58*, 2537.

¹⁴¹ Sakurai, H.; Hayashi, S.-i.; Hosomi, A. *Bull. Chem. Soc. Jpn.* **1971**, *44*, 1945.

¹⁴² Spivack, K. J.; Walker, J. V.; Sanford, M. J.; Rupert, B. R.; Ehle, A. R.; Tocyloski, J. M.; Jahn, A. N.; Shaak, L. M.; Obianyo, O.; Usher, K. M. *J. Org. Chem.* **2017**, *82*, 1301.

¹⁴³ Streitwieser, A.; Perrin, C. *J. Am. Chem. Soc.* **1964**, *86*, 4938.

¹⁴⁴ Yamamoto, T. *Bull. Chem. Soc. Jpn.* **1967**, *40*, 642.

well by traditional Hammett approaches.^{145,146,147} Consequently, it cannot be concluded that this kinetics data is entirely inconsistent with a homolytic pathway.

2.3.7 Theoretical-Computational Analysis¹⁴⁸

We called on computational tools to provide quantitative insight into the mechanism of the collapse of **85** to **86** along pathways consistent with the experiment outcomes outlined above. Calculations were performed at the IEFPCM(DMSO)/B3LYP/6-311++G(2d,2p)//IEFPCM(DMSO)/B3LYP/6-31G(d) level using **110** (methyl ester) as the modeled substrate by analogy to **85b** (ethyl ester). Our rationale for using B3LYP is based on its well-validated use for organic systems and robust nature for simulating many important molecular and reaction properties, e.g., bond energies, geometries, and barrier heights. For comparison, several other functionals were used to validate the trends reported herein using B3LYP. With the outcome of ¹⁸O-labeling experiments at the forefront, C–N or C–F cleavage and C–O bond formations were envisioned through four principal pathways: 1) concerted nitro to nitrite isomerization via 1,2-migration (Figure 14, Pathway 1), 2) heterolytic cleavage of the C–F bond (Figure 14, Pathway 2), 3) homolytic C–NO₂ bond cleavage affording radical species (Figure 14, Pathway 3) and 4) stepwise nitro to nitrite isomerization of the nitro group, possibly interrupted by addition of water

¹⁴⁵ Jaffé, H. H. *Chem. Rev.* **1953**, *53*, 191.

¹⁴⁶ Wells, P. R. *Chem. Rev.* **1963**, *63*, 171.

¹⁴⁷ Muizebelt, W. J.; Nivard, R. J. F. *Journal of the Chemical Society B: Physical Organic* **1968**, 913.

¹⁴⁸ Please note that the computational work in this section was performed by Hayden Foy and Travis Dudding (Department of Chemistry, Brock University, St. Catharines, ON, Canada). Overseeing project goals and directions and interpreting results within the context of this mechanistic study was performed jointly at Brock and Vanderbilt.

(Figure 15, Pathway 4). A simplified graphical representation of those pathways can be seen in Scheme 36.

Concerted nitro to nitrite isomerization was investigated due to the observation that such a process would rectify the evidence for a nitrite ester with the failure to acquire direct radical evidence, and because it is a major pathway discussed in theoretical assessments of the decomposition of nitro compounds.^{112,115,116,117,149,150} We were most interested in an evaluation of the homolytic mechanism's energy landscape, as this rationalizes the ¹⁸O-labeling observations in our original study (amide oxygen origination from nitro and O₂, but not H₂O) and has substantial theoretical and experimental precedence.^{107,109,110,112,113,115,116,117,149,150,151} We were open, however, to the possible differences introduced here, based largely on the involvement of H₂O in the studies described above (Scheme 30). The last pathway, stepwise nitro to nitrite isomerization, involving heterolytic nitrite ionization was considered as it is a hybrid pathway that could introduce ¹⁶O from water starting with labeled nitro TI'.

¹⁴⁹ Nikolaeva, E.; Shamov, A.; Khrapkovskii, G. *Russ. J. Gen. Chem.* **2014**, *84*, 2076.

¹⁵⁰ Zhang, C.; Wang, X.; Zhou, M. *J. Comput. Chem.* **2011**, *32*, 1760.

¹⁵¹ Dieter, R. K. *Tetrahedron* **1999**, *55*, 4177.

Figure 14. Energy profiles corresponding to 1,2-migration and heterolytic C-F bond cleavage. Calculated relative free energies at 298 K (kcal mol⁻¹) include single-point energy corrections at the IEFPCM(DMSO)/B3LYP/6-311++G(2d,2p)//IEFPCM(DMSO)/B3LYP/6-31G(d) level. The inset scheme depicts homolytic C-N bond cleavage and associated bond-dissociation energy ΔH (kcal mol⁻¹)

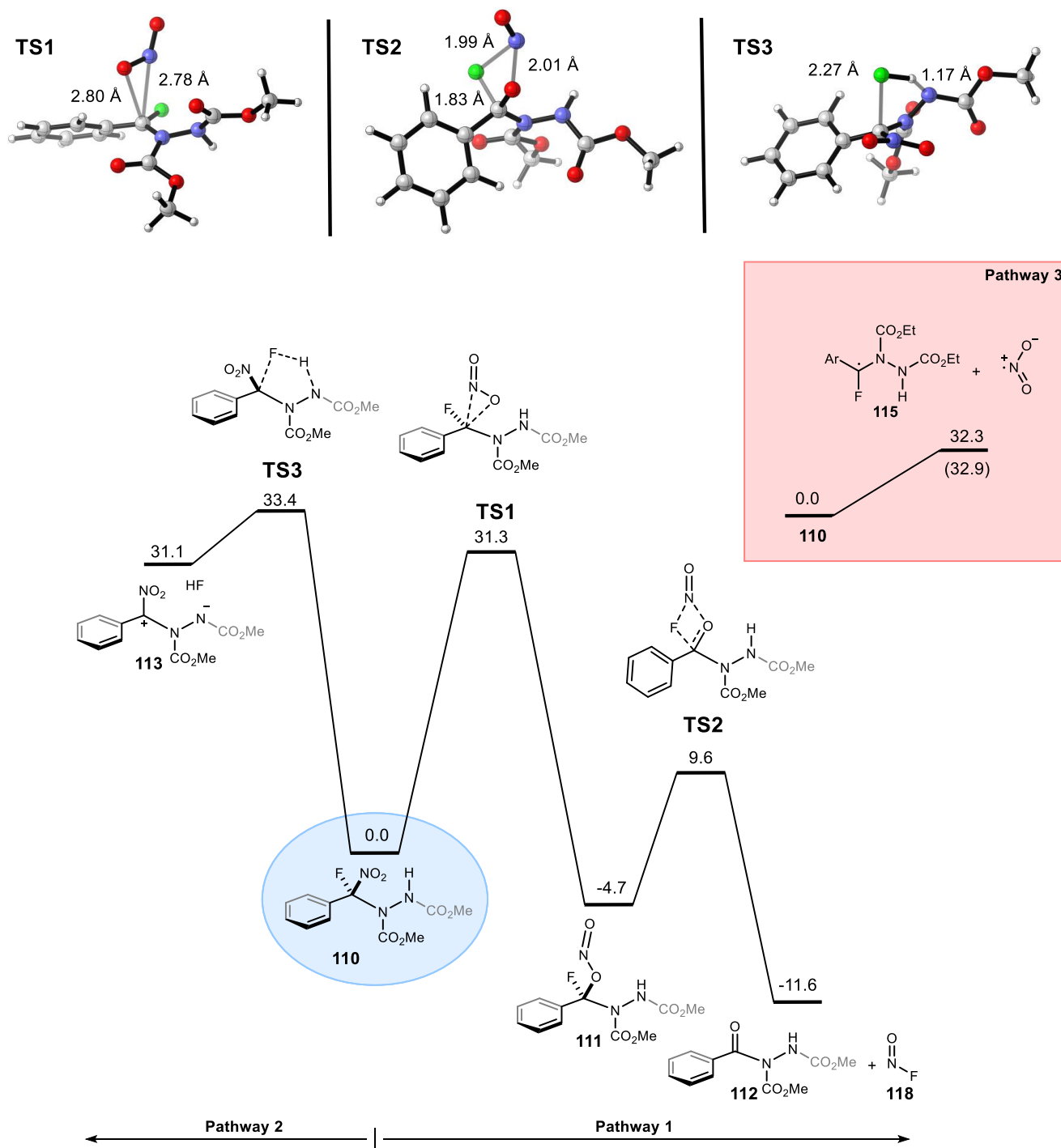
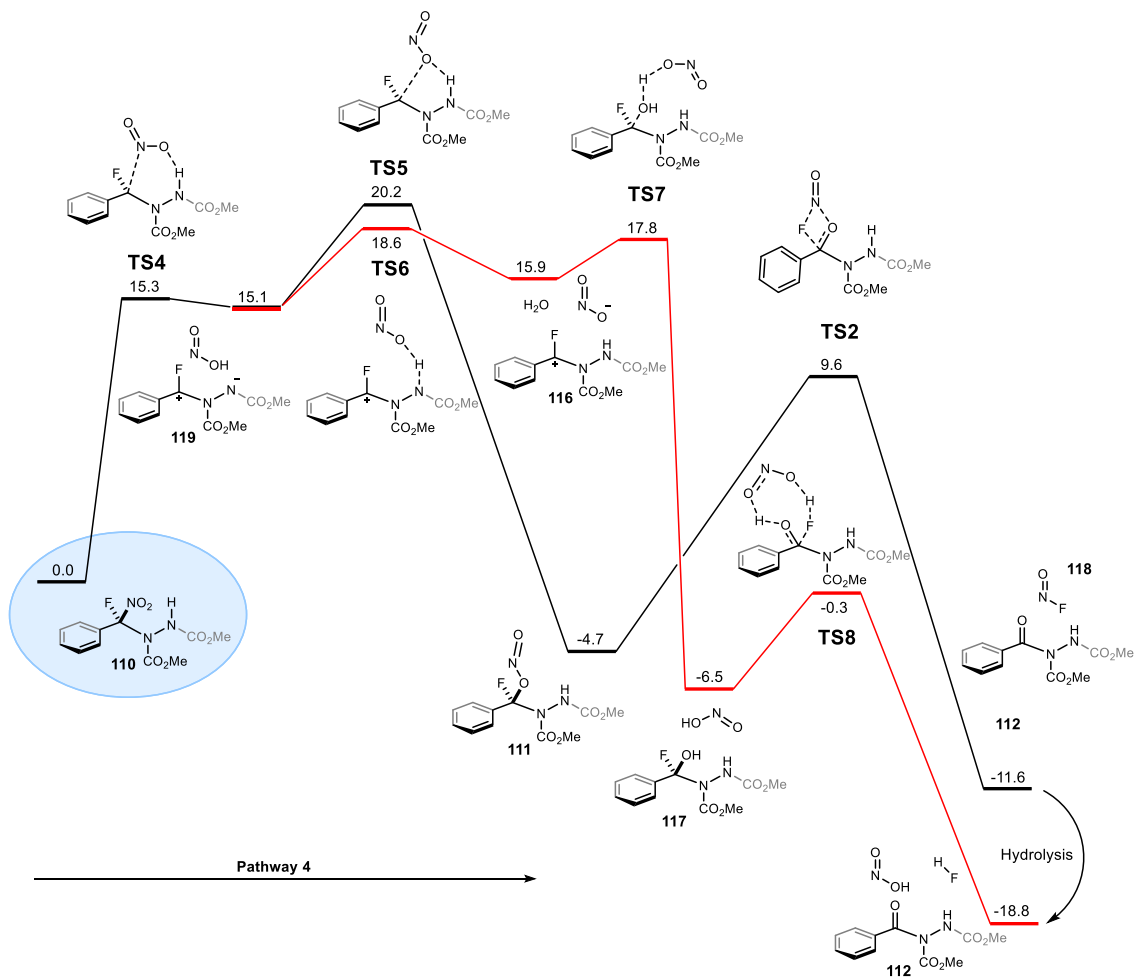


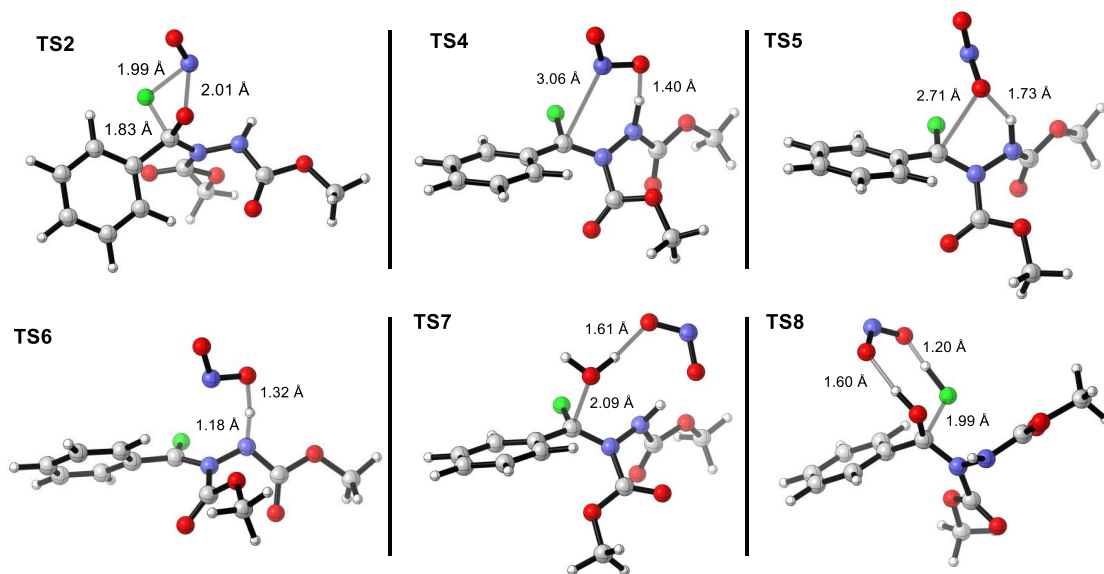
Figure 15. Energy profile corresponding to stepwise nitro to nitrite isomerization pathway leading to amide from formation of nitrite ester (black line) or water capture (red line). Calculated relative free energies at 298 K (kcal mol⁻¹) include single-point energy corrections at the IEFPCM(DMSO)/uB3LYP/6-311++G(2d,2p)//IEFPCM(DMSO)/uB3LYP/6-31G(d) level



Turning first to Pathway 1, concerted nitro to nitrite isomerization proceeds by transition state **TS1** displaying elongated bond breaking C···N and bond making C···O distances of 2.78 Å and 2.80 Å associated with a sizable Gibbs free energy of activation (ΔG^\ddagger) of 31.3 kcal mol⁻¹ (Figure 5). The resulting nitrite ester intermediate **111** undergoes fluoride loss coupled with N···O bond breakage at a distance of 2.01 Å via **TS2** with an activation barrier of 14.3 kcal mol⁻¹,

providing F–N=O (**118**) and amide product **112**. The large barrier of 1,2-migration (**TS1**),

Figure 16. Transition states associated with Figure 15



associated with a theoretical half-life ($t_{1/2}$) of ~ 172 hours, suggests that this pathway is not operative under the reaction conditions.

Heterolytic C–F bond cleavage Pathway 2 involving rate determining **TS3** with a C \cdots F bond breaking distance of 2.27 Å linked to proton transfer, was deemed unfavorable as well, owing to an activation barrier of 33.4 kcal mol⁻¹. Homolytic C–NO₂ bond cleavage, *viz.* Pathway 3, was next considered, yet a transition state for this transformation proved elusive. As a recourse, we turned to bond dissociation energy as an approximation of the activation energy for homolytic bond cleavage;^{152,153} which is a metric previously used for comparing concerted nitro to nitrite

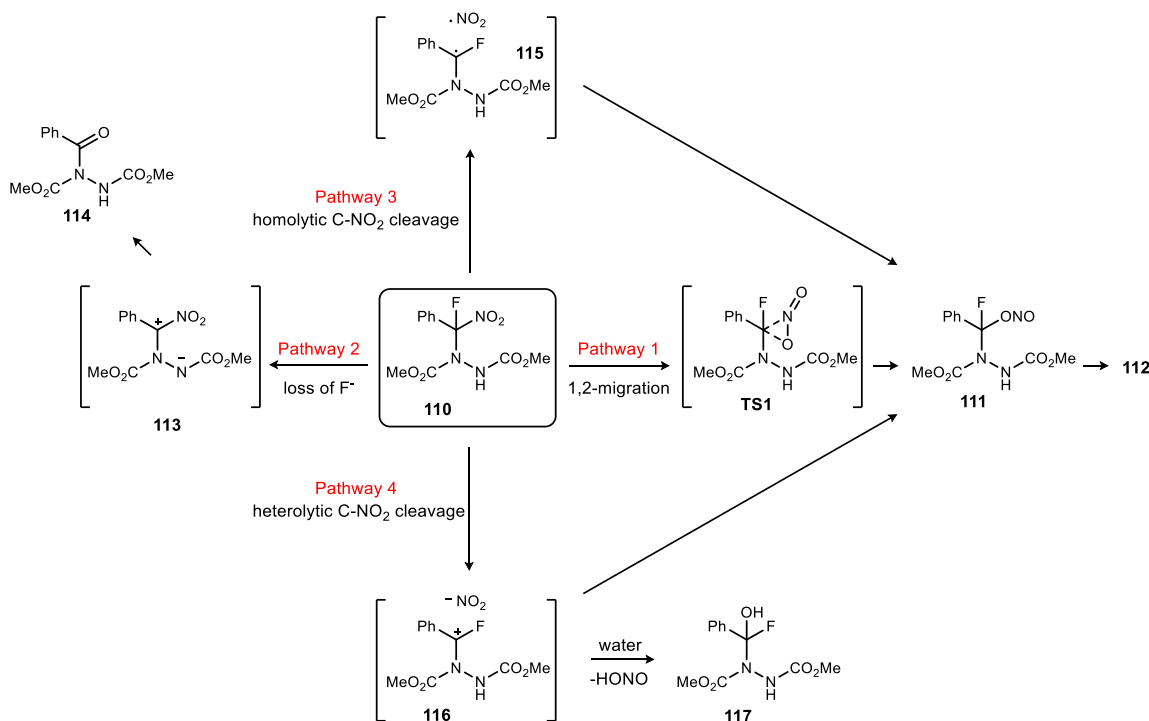
¹⁵² Liu, C.; Zhang, Y.; Huang, X. *Fuel Process. Technol.* **2014**, *123*, 159.

¹⁵³ Wang, M.; Liu, C.; Xu, X.; Li, Q. *Chem. Phys. Lett.* **2016**, *654*, 41.

isomerization to bond homolysis/recombination.^{112,115,116,117,149,150} The large 32.9 kcal mol⁻¹ computed dissociation energy of the C–NO₂ bond of **110** by Pathway 3 was similar in magnitude to the unfavorable energetics of Pathways 1 and 2. This suggested that Pathways 1-3 are unlikely under the reaction conditions.

As a last option, stepwise nitro to nitrite isomerization Pathway 4 was explored, initiating with ionization of **110** to 1,3-dipolarophile **119** by **TS4** (Figure 16) having an activation barrier of

Scheme 36. Representative pathways that were explored using computational methods



15.3 kcal mol⁻¹, putting it substantially below concerted nitro to nitrite isomerization, defluorination, or homolytic bond cleavage (Figure 14 and Figure 15). Elongated bond breaking C···N distance of 3.06 Å, as well as, O···H and N···H distances of 1.40 Å and 1.14 Å are the salient geometric features of this first-order saddle point. Nitrite ester (**111**) formation via **TS5** (black line) or water capture by proton transfer **TS6** initially affording benzylic cation **116** (red

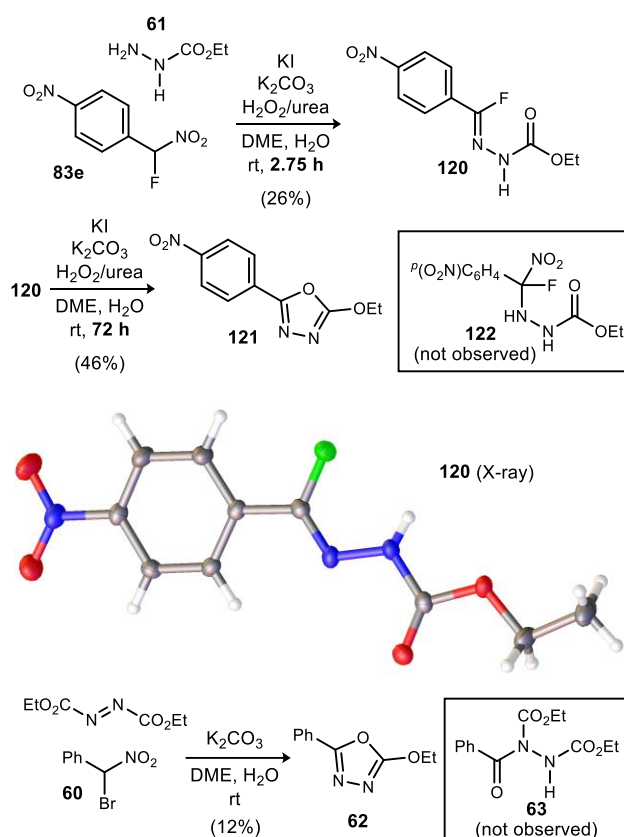
line), are both energetically feasible and consistent with labeling studies. The former, **TS5** with a C···O bond forming distance of 2.71 Å and activation barrier of 5.1 kcal mol⁻¹ being slightly more endergonic than **TS6** with an activation barrier of 3.5 kcal mol⁻¹.

Nitrite ester intermediate **111** then undergoes fluoride loss coupled with N···O bond breakage measuring 2.01 Å by **TS2** having an activation barrier of 14.3 kcal mol⁻¹ to provide an overall exergonic calculated pathway yielding F-N=O (**118**) that subsequently undergoes hydrolysis to afford HF, nitrous acid, and amide product **112** (See SI for hydrolysis of F-N=O). Competitive amide forming process propagating from benzylic cation **116** involves low barrier water addition transition state **TS7** displaying a C···O forming bond of 2.09 Å. The resulting intermediate **117** then undergoes nitrous acid assisted fluoride loss by **TS8** to afford amide product **112**, providing a mechanistic scenario consistent with the role of water in our amide carbonyl oxygen ¹⁸O-labeling studies.

2.3.8 Application of Fluoro Nitroalkanes to Study Diverted UmAS

The calculations reveal clearly that the carbamate *N*-H is positioned well to affect the energies along the pathway from nitroalkane to amide. Although this functionality is not typically present in UmAS to amides, it is present in the intermediate hypothesized for diverted UmAS.^{89,120} In order to probe this possible connection further, **83e** was selected for attempts to isolate

Scheme 37. The nitro-nitrite isomerization and possible pathways contributing to partial ¹⁸O-label loss



intermediates in diverted UmAS for oxadiazole synthesis.

Using the standard conditions for that reaction, a 26% yield of a crystalline compound exhibiting all of the spectroscopic properties consistent with **120** was observed (Scheme 37). In addition to that evidence, X-ray analysis was performed on a single crystal grown from heptane/

dichloromethane (Scheme 37). The tetrahedral intermediate believed to be operable in this reaction (**122**) was not observed, however the observation of **120** establishes the loss of nitrite (NO_2^-) *prior to* elimination of fluoride. A key difference in the use of hydrazide (**61**) is the lack of an acyl group at electrophilic nitrogen. A TI' here (eg. **122**) would have a more electron-donating nitrogen substituent, and is therefore more electronically similar to those in standard UmAS. The intermediate **120** was resubjected to the reaction conditions, leading to the formation of oxadiazole **62** in 46% yield. This establishes the fluoro hydrazone as a potential intermediate along the pathway to heterocycle.

A series of experiments (not shown) revealed that potassium carbonate is the minimum reagent needed for this conversion (**120**→**121**). α -Halo hydrazones are known precursors to oxadiazoles.¹⁵⁴ Were bromine to replace fluorine here, it is unclear whether bromine or NO_2 would leave first. There are several examples of elimination from 1,1-bromo-nitro species without clear preference for either to leave.^{155,156,157,158,159} Finally, although low yielding for oxadiazole (**62**), α -bromo phenylnitromethane (**60**) and DEAD react without evidence for the amide (**63**), an example that further highlights the interplay between the halogen substituent and its effect on pathways from the TI'. Moreover, the demonstration that an imide (e.g. **63**) is not an intermediate to oxadiazole⁸⁹ excludes a traditional active ester intermediate.

¹⁵⁴ Lv, L.-P.; Zhou, X.-F.; Shi, H.-B.; Gao, J.-R.; Hu, W.-X. *J. Chem. Res.* **2014**, *38*, 368.

¹⁵⁵ Hartshorn, M.; Martyn, R.; Vaughan, J.; Wright, G. *Aust. J. Chem.* **1983**, *36*, 839.

¹⁵⁶ John, J.; Thomas, J.; Parekh, N.; Dehaen, W. *Eur. J. Org. Chem.* **2015**, *2015*, 4922.

¹⁵⁷ Thomas, J.; John, J.; Parekh, N.; Dehaen, W. *Angew. Chem. Int. Ed.* **2014**, *53*, 10155.

¹⁵⁸ Campbell, M. M.; Cosford, N.; Zongli, L.; Sainsbury, M. *Tetrahedron* **1987**, *43*, 1117.

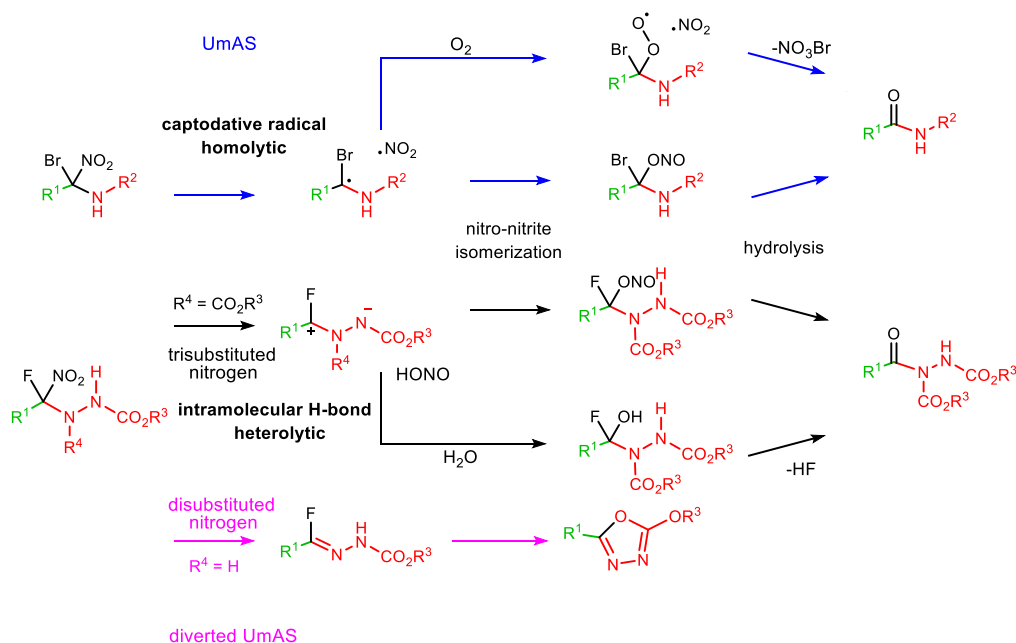
¹⁵⁹ Piltan, M.; Kalantari, S. *J. Heterocycl. Chem.* **2017**, *54*, 301.

2.3.9 Conclusions

This work set out to provide concrete evidence for an unprecedented functional motif, a halo-amino-nitroalkane, serving as an intermediate in UmAS. Spectroscopic and crystallographic observations of a model system have clearly validated that the HANA functional group can form when an α -halo nitronate engages with an electrophilic nitrogen. The HANA in this work also readily converts to an imide (amide analogue) helping to tie the model system in this work to UmAS. With the umpolung nature of UmAS firmly established, future reaction development can be undertaken with confidence in both fundamental underlying concepts as well as crucial epimerization-avoiding polarity.

Taking further advantage of the opportunity this model systems provided led us to perform

Scheme 38. Unified hypothesis for HANA collapse pathways and factors determining outcome



^{18}O labeling, kinetics, byproduct analysis, radical probing, and computational studies. The culmination of these experiments has provided unrivaled mechanistic information in the UmAS field and points to a polar TI collapse in the model system. Although heterolytic in the model

system rather than homolytic, nitro to nitrite isomerization is common to both the model system and UmAS. The origin of the heterolytic nature of the model system collapse was determined to be a consequence of an intramolecular hydrogen bond coincidentally applicable to diverted UmAS.

Probing diverted UmAS with the model system indicates exactly where and why the intermediates are “diverted” away from amide formation and towards heterocycles. These studies provide the most complete platform for judicious further development of UmAS and diverted UmAS. In summary, this work informs a unified hypothesis for reactions involving HANAs (Scheme 38). In UmAS (Scheme 38, blue arrows) the electron rich amine substituent without the option for intramolecular H-bond assisted elimination gives rise to homolytic C-NO₂ bond cleavage and associated aerobic and anaerobic pathways towards amide. In contrast, when a six membered hydrogen bond system can form heterolytic pathways dominate. For trisubstituted, electron-deficient amine substituents (Scheme 38, black arrows) this leads to azoamide ylide formation with pathways to imide through recombination or water attack. When the amine substituent is only disubstituted and not electron-poor (as in diverted UmAS, Scheme 38, purple arrows) intramolecular cyclization ultimately generating oxadiazole is possible.

Chapter 3. New Applications for HANAs

3.1 Introduction

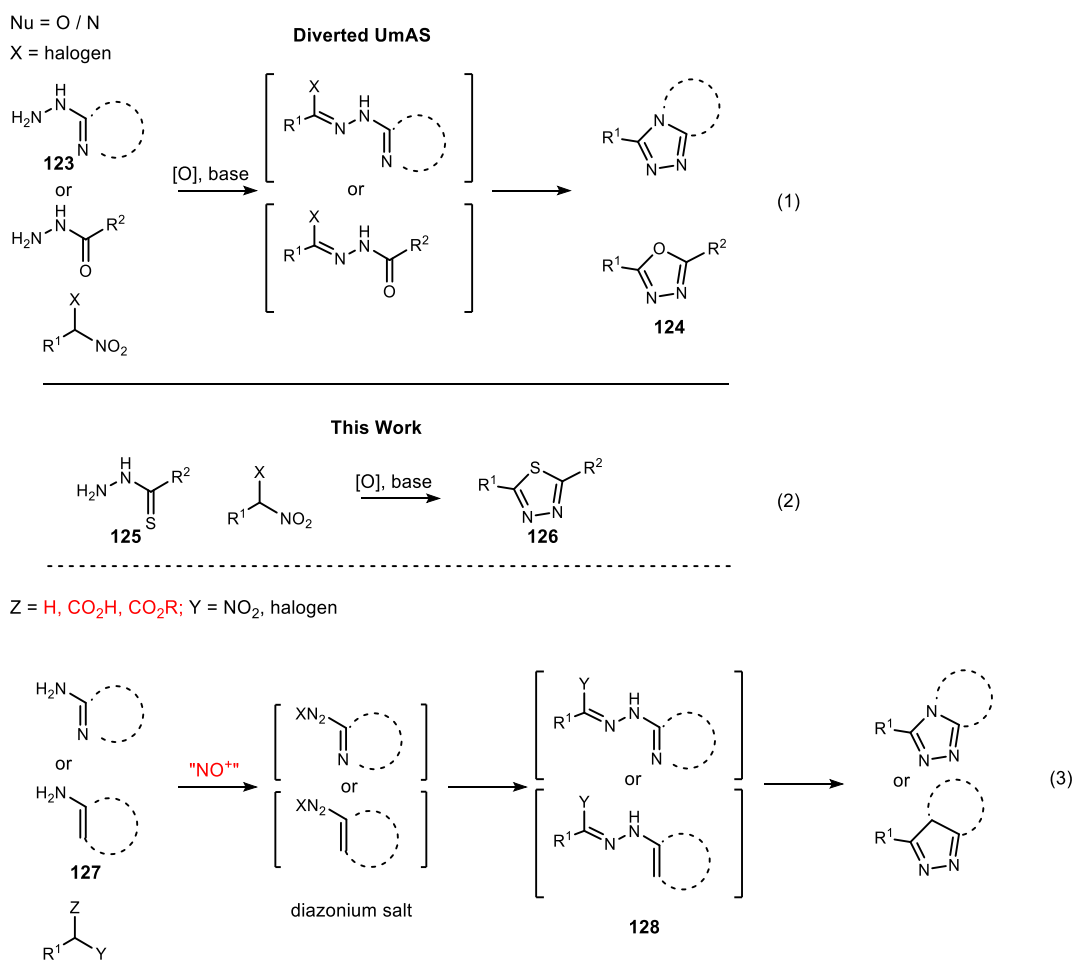
When considering any reaction, a solid mechanistic understanding is crucial for further development. Such an understanding allows scientists to predict benefits and limitations while producing useful modifications in an efficient and hypothesis-driven manner. The observation of HANAs in a variety of environments leading to several structurally disparate products establishes this motif as a dynamic functional group ripe for further exploration and reaction development.^{32,86,89,120} The mechanistic detail outlined in Chapter 2 serves as a solid basis for these efforts. Reaction development focused on two main areas: umpolung heterocycle access and umpolung *N*-aryl amide synthesis.

3.2 Expansion of Umpolung Heterocycle Access

3.2.1 Umpolung Heterocycle Access

With our confidence in the umpolung nature and mechanistic steps of diverted UmAS solidified,¹⁶⁰ we shifted focus to natural expansions of the chemistry. Thiadiazoles (**126**) are a valuable class of molecules and one that could, in theory, be accessed through a relatively small

Scheme 39. General scheme for diverted UmAS alongside proposed expansions



¹⁶⁰ Crocker, M. S.; Foy, H.; Tokumaru, K.; Dudding, T.; Pink, M.; Johnston, J. N. *Chem* **2019**, 5, 1248.

modification of the established oxadiazole synthesis (Scheme 39, eq 1-2). There are many routes to thiadiazoles, but in parallel to the case of oxadiazoles, the majority leverage acylated thiohydrazides by dehydrative cyclization or through the condensation of a thiohydrazide onto an aldehyde followed by oxidative cyclization.¹⁶¹ Exceptions include the conversion of oxadiazoles into thiadiazoles¹⁶² (although typical preparations of oxadiazoles are similarly limited) and the reaction between a hydrazoneyl halide and a thiocarbazine.¹⁶³ If diverted UmAS could be applied to 1,3,4-thiadiazole synthesis, then the benefits of the UmAS approach could be brought to this heterocycle as well.

Thiadiazoles, especially of the 1,3,4-variety (which is the connectivity obtained in diverted UmAS), are included in several clinical compounds and have been demonstrated to have biological activity in a large variety of areas.¹⁶⁴ In addition to involving, with few exceptions, harsh dehydrative conditions, many of the established methods are not general with respect to substituents at the carbons of the thiadiazole. While diverted UmAS demands that one substituent (**124**, R¹) be a carbon (though both alkyl and aryl are tolerated) there is significant flexibility in the other substituent (**124**, R²; oxygen, nitrogen, aryl and alkyl are all demonstrated). Clearly, development in the field is warranted; particularly if it produces a mild system for the construction of a range of substituted thiadiazoles. This work represents the first attempt at umpolung thiadiazole synthesis.

¹⁶¹ Hu, Y.; Li, C.-Y.; Wang, X.-M.; Yang, Y.-H.; Zhu, H.-L. *Chem. Rev.* **2014**, *114*, 5572.

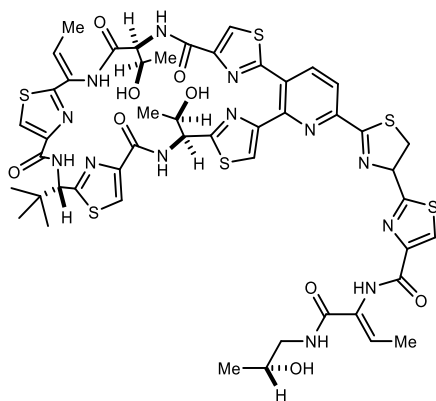
¹⁶² Padmavathi, V.; Reddy, S. N.; Reddy, G. D.; Padmaja, A. *Eur. J. Med. Chem.* **2010**, *45*, 4246.

¹⁶³ Sayed, A. R. *Tetrahedron Lett.* **2010**, *51*, 4490.

¹⁶⁴ Jain, A. K.; Sharma, S.; Vaidya, A.; Ravichandran, V.; Agrawal, R. K. *Chem. Biol. Drug Des.* **2013**, *81*, 557.

In perhaps a more ambitious leap for the chemistry, another five membered aromatic

Figure 17. Example thiazole-containing antibiotic (thiocillin I)



heterocycle that could be accessed using UmAS is the thiazole. Thiazoles are even better represented in medicinal chemistry and natural products than are thiadiazoles.¹⁶⁵ One of the more well known examples is the class of antibiotic natural products with members such as micrococcin P1, LFF571, E2270 A, and thiocillin I (Figure 17) among others.^{166,167,168,169} These antibiotics are typically macrocyclic, peptide-derived compounds with several thiazoles, all qualities that underscore the importance of the umpolung approach. In biological molecules, the thiazole ring is intimately associated with the cysteine residue. Not surprisingly, there are a vast number of natural products that contain the motif. Synthetic and medicinal chemists have taken note and developed a wide array of biologically active synthetic compounds including many drugs containing the

¹⁶⁵ T Chhabria, M.; Patel, S.; Modi, P.; S Brahmkshatriya, P. *Curr. Top. Med. Chem.* **2016**, *16*, 2841.

¹⁶⁶ Selva, E.; Beretta, G.; Montanini, N.; Saddler, G.; Gastaldo, L.; Ferrari, P.; Lorenzetti, R.; Landini, P.; Ripamonti, F.; Goldstein, B. *J. Antibiot.* **1991**, *44*, 693.

¹⁶⁷ Ciufolini, M. A.; Lefranc, D. *Nat. Prod. Rep.* **2010**, *27*, 330.

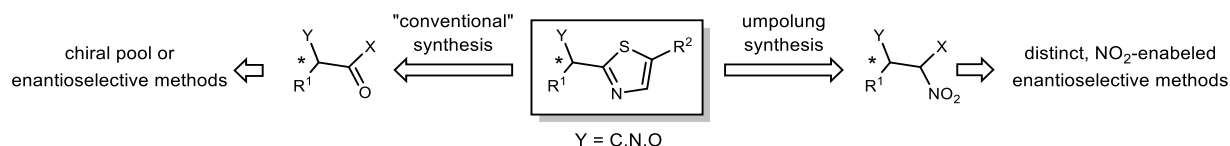
¹⁶⁸ Aulakh, V. S.; Ciufolini, M. A. *J. Am. Chem. Soc.* **2011**, *133*, 5900.

¹⁶⁹ LaMarche, M. J.; Leeds, J. A.; Amaral, A.; Brewer, J. T.; Bushell, S. M.; Deng, G.; Dewhurst, J. M.; Ding, J.; Dzik-Fox, J.; Gamber, G. *J. Med. Chem.* **2012**, *55*, 2376.

group.¹⁶⁵ Stemming from this natural inspiration, synthesis of the heterocycle very frequently draws on the biomimetic approach to synthesis. Indeed, thiazoles are often generated via cyclization of a peptide bearing a cysteine residue.¹⁷⁰ Intrinsic to this approach is a separate amide coupling as well as an oxidation step.

The drawbacks of common amide syntheses aside, this approach is inefficient with respect to linear synthetic steps. Another common approach is to buy the heterocycle and incorporate it in the molecule via coupling. Once again, however, extra steps are usually introduced in order to then functionalize the monosubstituted ring. Also significant for the synthesis of thiazole natural products is the substitution reaction between a thioamide or thiourea and an α -halo ketone followed by dehydrative cyclization (Hantzsch synthesis). Bringing the reagents in with that oxidation state excludes the need for a separate oxidation step. An umpolung approach to the heterocycle still stands to contribute unique advantages. Namely, due to the ease with which enantioenriched α -bromo nitroalkanes can be prepared, giving quick access to α -oxy or amino thiazoles (a common feature in peptide-like thiazole compounds) in high enantiomeric excess (Scheme 40).

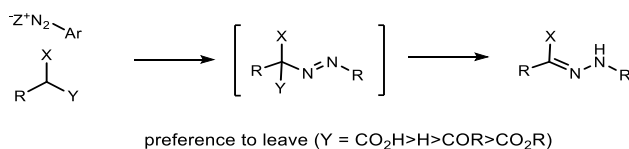
Scheme 40. Thiazole access from conventional methods and umpolung methods



¹⁷⁰ Dekić, B. R.; Radulović, N. S.; Dekić, V. S.; Vukićević, R. D.; Palić, R. M. *Molecules* **2010**, *15*, 2246.

Additionally, the recent progress in applying HANAs to cyclization reactions^{89,120} and the new mechanistic insight implicating an α -halo hydrazone as an intermediate for these cyclizations caught our attention (Scheme 39, eq 1). An attractive possibility was generating a diazoate or diazonium salt to produce cyclization products from more accessible starting materials (Scheme 39, eq 3). Ideally, this objective would simultaneously expand the scope of the chemistry to include previously inaccessible motifs such as indazoles. While this modified synthesis would not strictly involve a HANA, the concept and downstream intermediates are highly analogous and will therefore be discussed in this section. An initial motivation for this methodology was the mechanistic information that an orthogonal access to activated hydrazones could contribute. Synthesis of an α -nitro hydrazone (**128**, Y = NO₂), for example, could help clarify whether diverted UmAS involves an α -halo or α -nitro hydrazone or if both are viable. Upon further consideration, another major motivation became apparent. Aniline starting materials (**127**) are much more readily available than are aryl hydrazines (**123**, which are often synthesized in two steps from the aniline) and the direct use of unhalogenated nitroalkanes (Scheme 41, Y = H; X = NO₂) also saves one synthesis step.

Scheme 41. Azo to hydrazone rearrangement



There has been relatively little recent work regarding carbon nucleophile addition into diazonium electrophiles, but the reaction is well precedented.¹⁷¹ The carbon nucleophile is very flexible and can be a ketone,^{172,173,174,175,176} an ester,¹⁷⁷ a β -keto acid or ester (including the Japp-Klingemann reaction),^{178,179,180} a malonic acid or ester,^{181,182,183,184,185} a nitrile,^{186,187,188} a saturated or unsaturated hydrocarbon,^{189,190,191} or, encouragingly, a nitroalkane.^{192,193,194} In nearly every example in which the resulting azo compounds can rearrange to hydrazines that transformation is favored (Scheme 41). The driving force for hydrazine formation is so strong that the reaction is spontaneous with not only α -hydrogen azo compounds, but also α -carboxyl (through

¹⁷¹ Parmerter, S. M. In *Organic Reactions*; John Wiley & Sons, Inc., Ed.; John Wiley & Sons, Inc.: Hoboken, NJ, USA, 2011; pp 1–142.

¹⁷² Bamberger, E.; Wulz, P. *Berichte der deutschen chemischen Gesellschaft* **1891**, 24, 2055.

¹⁷³ Keneford, J. R.; Simpson, J. C. E. *J. Chem. Soc.* **1947**, 917.

¹⁷⁴ Chattaway, F.; Lye, R. *Journal of the Chemical Society (Resumed)* **1933**, 480.

¹⁷⁵ Favrel, Bull. Soc. Chim. France, **1927**, 4, 1494.

¹⁷⁶ Wislicenus and Hentrich, *Ann.*, **1924**, 9.

¹⁷⁷ Borsche, W.; Diacont, K. *Ann.* **1934**, 510, 287.

¹⁷⁸ Bamberger, E.; Wheelwright, E. W. *J. Prakt. Chem.* **1902**, 123.

¹⁷⁹ Bamberger, E.; Lorenzen, J. *Ber. Dtsch. Chem. Ges.* **1892**, 3539.

¹⁸⁰ Japp, F. R.; Klingemann, F. *Ber. Dtsch. Chem. Ges.* **1888**, 549.

¹⁸¹ Leonard, N. J.; Boyd, S. N.; Herbrandson, H. F. *J. Org. Chem.* **1947**, 47.

¹⁸² Hantzsch, A.; Thompson, K. J. *Ber. Dtsch. Chem. Ges.* **1905**, 2266.

¹⁸³ Pechmann, H. *Ber. Dtsch. Chem. Ges.* **1892**, 3175.

¹⁸⁴ Fusco, R.; Romani, R. *Gazz. Chim. Ital.* **1946**, 76, 419.

¹⁸⁵ Walker, T. K. *J. Chem. Soc., Trans.* **1923**, 2775.

¹⁸⁶ Pschorr, R.; Hoppe, G. *Ber. Dtsch. Chem. Ges.* **1910**, 43, 2543.

¹⁸⁷ Kruckeberg, *J. prakt. Chem.*, **1894**, 321.

¹⁸⁸ Feofilaktov and Onishchenko, *J. Gen. Chem. U.S.S.R.*, **1939**, 325.

¹⁸⁹ Proter and Peterson, *Org. Syntheses*, Coll. Vol. III, 660.

¹⁹⁰ Richter, V. *Ber. Dtsch. Chem. Ges.* **1883**, 677.

¹⁹¹ Widman, O. *Ber. Dtsch. Chem. Ges.* **1884**, 722.

¹⁹² Ponzi, *Gazz. Chim. Ital.*, **1909**, 535.

¹⁹³ Jones, E. C. S.; Kenner, J. *J. Chem. Soc.* **1930**, 919.

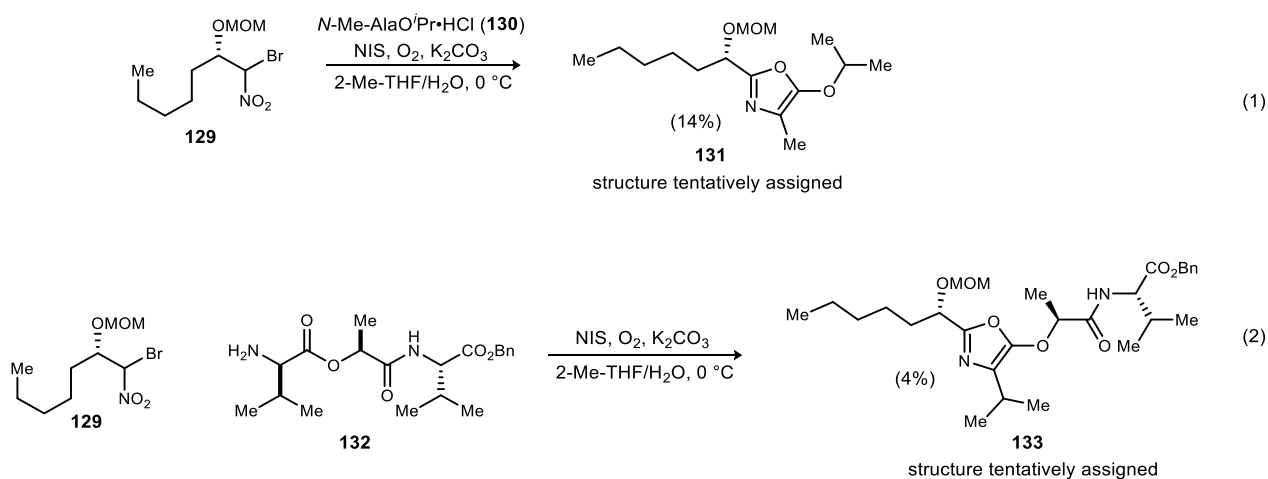
¹⁹⁴ Shestakova, T.; Khalymbadza, I.; Deev, S.; Eltsov, O.; Rusinov, V.; Shenkarev, Z.; Arseniev, A.; Chupakhin, O. *Russ. Chem. Bull.* **2011**, 60, 729.

decarboxylation) and even α -keto, ester, and aldehyde azo's. The preference for a group to leave in order to establish the C=N double bond qualitatively follows the order $\text{CO}_2\text{H} > \text{H} > \text{COR} > \text{CO}_2\text{R}$.

3.2.2 Investigation of an Unexpected Product from Standard UmAS Applied to an *N*-Methyl α -Amino Ester

In the context of the work described herein as well as the recently reported heterocycle synthesis, it is accurate to say that the mechanistic understanding as well as the synthetic utility of

Scheme 42. Suspected oxazole formation in UmAS



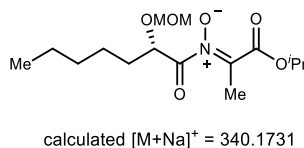
UmAS-type reactions is growing.^{89,120} One driving factor of this development has been the careful analysis of by-products which led to the development of the diverted UmAS heterocycle synthesis and could have mechanistic implications. With those factors in mind, the observation of an interesting minor product from certain UmAS reactions performed by Suzanne Batiste (Scheme 42) was further investigated. In her work Dr. Batiste tentatively assigned the product from Scheme 42, eq 1 as an oxazole (**131**) based on missing methyl and methine peaks by ^1H NMR, both corresponding to the *N*-methyl α -amino ester acceptor (**130**).

To begin work in this area, eq 1 in Scheme 42 was reproduced in my hands and gave the same product, albeit in lower yield. Attempts were made to favor this product both to make further analysis easier and start early-stage development of another diverted-UmAS heterocycle synthesis if the product was indeed an oxazole. To favor the reaction with presumed intramolecular steps, a lower concentration was used, but yield was essentially unaffected. Additionally, degassing to limit O₂ exposure and changing the halogen also failed to favor the oxazole product. Because nucleophilic alkylation of the *N*-Me carbon could be the limiting step towards oxazole formation, a hydrazone workup was also investigated but failed to improve yield.

At this point in the investigations, HRMS data was obtained and scrutiny of that data showed that the product of interest was not the expected oxazole ($M_{\text{oxazole}} + \text{Na} = 308.1832$) but rather a compound with observed $M_{\text{unknown}} + \text{Na} = 340.1736$. Low resolution mass spectrometry at the time of the original isolation gave a mass of 340 which was attributed to a methanol adduct ($M_{\text{oxazole}} + M_{\text{methanol}} + \text{Na} = 340.2094$). The higher resolution obtained in this work unambiguously rules out the methanol adduct possibility despite the matching nominal mass.

A structure fully consistent with the mass and NMR data discussed to this point is the

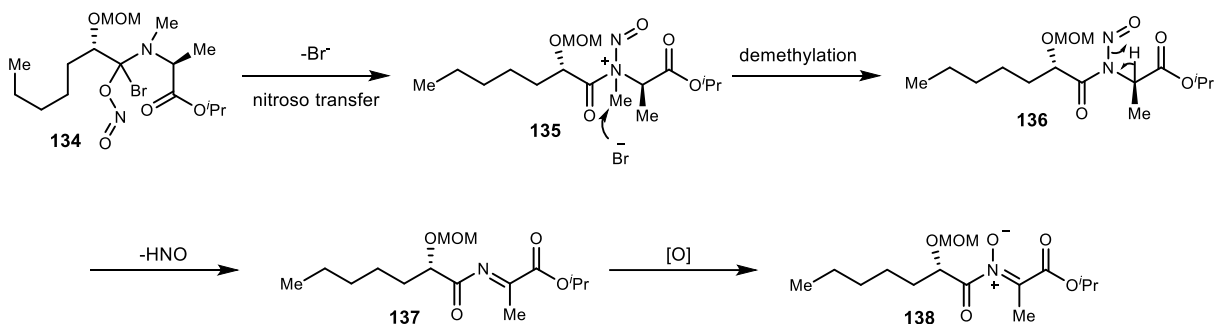
Figure 18. Nitron product initially assigned as oxazole



nitron shown in Figure 18. Key aspects of the NMR data include a methyl singlet at 3.40 ppm, whose deshielded behavior suggests an allylic nature. The disappearance of an alanine methine is also rationalized by the nitron. Three deshielded carbons at 169.4, 162.6, and 157.9 ppm are also

consistent with the amide, ester, and imine carbons in the proposed nitrone. This type of acyl-nitrone is known in literature but has not received widespread usage.^{195,196}

Scheme 43. Possible mechanism leading to nitrone product



An assessment of the possible pathways leading to this product suggests that the mechanism diverges from that of UmAS after the nitro-nitrite isomerization. In UmAS we hypothesize that the intermediate nitrite ester is hydrolyzed to give the amide product, but the nitrone can be envisioned to result from intramolecular redox processes leading to tetra substituted nitrogen intermediates. In the potential mechanism in Scheme 43, *N*-demethylation and elimination of the alanine hydrogen are enabled by the higher degree of substitution at nitrogen. The proposed pathway involves intramolecular nitroso transfer (**134**→**135**) followed by demethylation (**135**→**136**) and HNO elimination to give an imine (**137**). Further oxidation gives the nitrone product (**138**). The initial nitroso transfer step can be compared to observations of UmAS⁴⁴ and to work in Chapter 2, but those are intermolecular and 1,4 transfers respectively while this would be a 1,3 transfer. Ultimately, this proposal invokes a tetra substituted nitrogen to justify a strange dealkylation, but the final oxidation step remains to be well explained.

¹⁹⁵ Sukhorukov, A. Y. *Adv. Synth. Catal.* **2020**, 362, 724.

¹⁹⁶ Baldwin, S. W.; Young, B. G.; McPhail, A. T. *Tetrahedron Lett.* **1998**, 39, 6819.

Further attempts to explore this unusual reactivity could involve application of *N*-Me valine derivatives or other amines which would give highly sterically congested nitrite esters. Alternatively, anhydrous conditions could be applied to further encourage non-hydrolysis pathways. Presently, the very low yields, apparent substrate dependence, and lack of clear application for the products would need to be addressed for meaningful development of this reaction. An appreciation for the factors favoring nitrene formation over *N*-Me amide formation could, however, lead to optimization of *N*-Me substrates in UmAS.

3.2.3 Attempted Umpolung Synthesis of Indazoles and Triazoles from Diazonium Salts

With activated hydrazones implicated as the intermediate paramount to cyclization in diverted UmAS, we wanted to commit effort to forming such a species from an aniline and either a nitroalkane or an alkyl halide with an α substituent able to activate the compound and be removed by azo to hydrazone isomerization. Our initial studies with α -halo carboxylic acids and esters were not promising, leading us to believe that halide may be removed preferentially to the carboxylic acid or ester substituents in the azo/hydrazone isomerization (Scheme 41) leading to unproductive pathways. We consequently continued our studies with nitroalkane and *para*-anisidine (Table 8, entry 1). The reaction was promising in that, despite incomplete conversion of nitroalkane, a new product with NMR characteristic of α -NO₂ hydrazone (4 doublets in the aromatic region and an N-H peak by ¹H NMR) was formed. Attempts to isolate this new product led to partial decomposition and sitting was found to lead to conversion to what is assumed to be the corresponding hydrazide through hydrolysis. Other conditions were found to be quite effective at generating reasonably clean hydrazone (Table 8, entry 2), but attempts to elucidate structure

through PMP deprotection using CTAN or cyclization through heating were unsuccessful. Both

Table 8. A survey of conditions targeting α -NO₂ hydrazones

$\text{R-CH}_2\text{-NO}_2 + \text{H}_2\text{N-Ar} \xrightarrow{\text{conditions}} \text{R-CH=N-NH-Ar}$
 hydrazone

entry	R	Ar	diazotisation reagents	order	outcome
1	4-ClC ₆ H ₄	4-OMeC ₆ H ₄	HCl/NaNO ₂	diazotization, NA addition, basify	SM + unstable product
2	4-ClC ₆ H ₄	4-OMeC ₆ H ₄	HNO ₃ /KNO ₂	diazotization, preformed nitronate addition	mostly unstable product
3	4-ClC ₆ H ₄	Ph	HNO ₃ /KNO ₂	diazotization, preformed nitronate addition	low conversion
4 ^a	4-ClC ₆ H ₄	Ph	HNO ₃ /KNO ₂	diazotization, preformed nitronate addition	confirmed hydrazone (150)
5 ^b	4-ClC ₆ H ₄ or Et	2-pyridyl or 2-thiazole	HNO ₃ /KNO ₂	diazotization, preformed nitronate addition	recovered NA amine decomposition
6	Et	2-pyridyl	acetic acid/tertbutyl nitrite	aryl amine added last	no reaction
7 ^c	4-ClC ₆ H ₄	2-pyridyl	NaOEt/isobutyl nitrite	diazotization, NA addition	recovered NA amine decomposition
8 ^c	Et	2-pyridyl	^t BuLi/isobutyl nitrite	diazotization, NA addition	amine decomposition
9	Et	2-pyridyl	NOBF ₄	diazotization, preformed nitronate addition	amine decomposition and some reaction with MeCN
10	Et	3-OMeC ₆ H ₄	tertbutyl nitrite or HBF ₄ /isoamyl nitrite	aryl amine added last	decomposition and SM
11	Et	4-OHC ₆ H ₄	^t Bu nitrite	aryl amine added last	decomposition

^a Both the diazotization and nitronate formation were performed in an H₂O/MeCN mixture. ^b Multiple acidic diazotization conditions were attempted; some NA was recovered when non-volatile nitroalkanes were used. ^c Several condition changes including time, temperature, and solvent and additives led to similar results.

reaction conditions led primarily to the already-mentioned hydrolysis product. We reasoned that a change in electronics may increase the stability of the presumed hydrazone and allow for proper characterization of products.

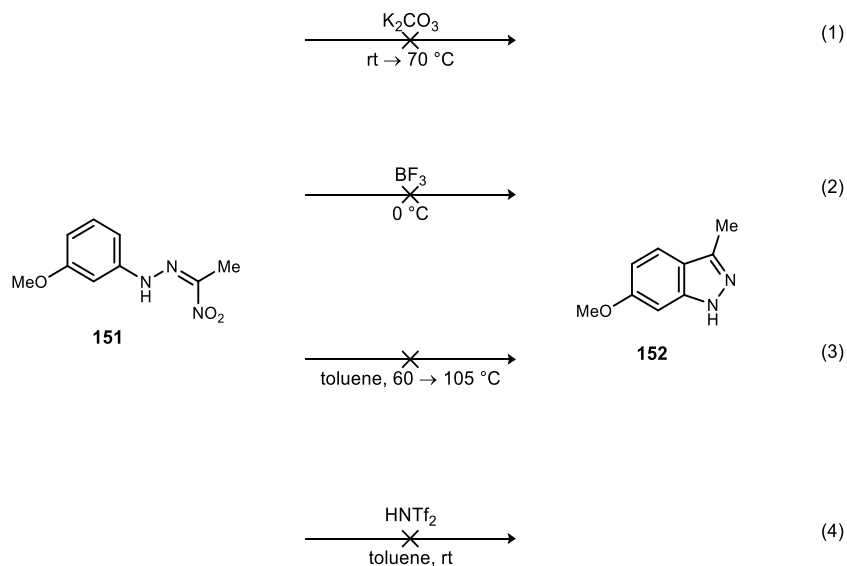
It was unfortunately the case that most substrates required re-optimization of conditions, but once suitable conditions were found, we were excited to see that applying aniline in the reactions in place of anisidine led to cleaner conversion to a product that was better suited to purification and characterization (Table 8, entries 3 and 4). Attempts to directly observe cyclized products or to convert the hydrazone to an indazole through heating, however, remained unsuccessful. It was still undetermined, however, if the failure to generate indazole was a consequence of the ambitious jump to a carbon nucleophile (in contrast to oxygen and nitrogen nucleophiles used in diverted UmAS) or of the activating group on the hydrazone, an NO₂ in this case and either an NO₂ or a halogen in diverted UmAS. To further probe this question we set a closer analogy to diverted UmAS by applying 2-amino pyridine and 2-amino thiazole as substrates.

Again, the reaction proved to be sensitive to substrate changes and simple diazotization conditions failed to give conversion (Table 8, entries 5-6). This is a known issue for electron deficient heterocycles, and these substrates frequently require basic conditions and involve a diazoate intermediate.¹⁹⁷ Applying such conditions, however, did not lead to the hydrazone or fused triazole despite optimization attempts (Table 8, entries 7-8). Nitrosonium tetrafluoroborate used as the nitrosylation reagent gave similar consumption of amine without evidence for productive reactivity. A small amount of the acetamide derived from reaction with solvent was observed (Table 8, entry 9). Even when conditions similar to those in Table 8, entry 8 were

¹⁹⁷ El-Safty, S. A.; Prabhakaran, D.; Ismail, A. A.; Matsunaga, H.; Mizukami, F. *Adv. Funct. Mater.* **2007**, *17*, 3731.

employed to give isolated diazoate used in many subsequent reactions with nitroalkanes or

Scheme 44. Conditions applied to hydrazone cyclization



performed nitronates under a variety of conditions, no benzotriazole was observed.

Another substrate modification that could aid in the cyclization step is adding electron donating groups at the three position of the aniline. Unfortunately, when *meta*-anisidine or 3-amino phenol were used with alkyl nitrite diazotization and 1-nitro propane, no traces of azo, hydrazone, or indazole were observed (Table 8, entries 10-11). Applying the conditions from Table 8, entry 4 to the *meta*-anisidine substrate with nitroethane gave isolable hydrazone product **151**, but attempts to elicit cyclization to the indazole (**152**) failed (Scheme 44).

The total lack of evidence for the formation of cyclized products here could suggest that diverted UmAS doesn't involve an α -nitro hydrazone, but rather, it involves an α -halo hydrazone and the halogen is necessary for product formation. As the hydrazone wasn't directly observed in the highly-analogous 2-pyridyl cases, it cannot be fully ruled out that the lack of productive reactivity in this work is a result of a failure to form an adduct between the diazonium salt and

nitroalkane. The successful formation of the hydrazone in the similar cases using aniline do indicate, though, that the blame does lie in the cyclization step. In any case it is clear that the established hydrazide/oxidant/halonitroalkane system remains the most effective for the umpolung synthesis of triazoles and that indazoles are not accessible via α -nitro hydrazones.

3.2.4 Attempted Umpolung Synthesis of Thiadiazoles and Thiazoles

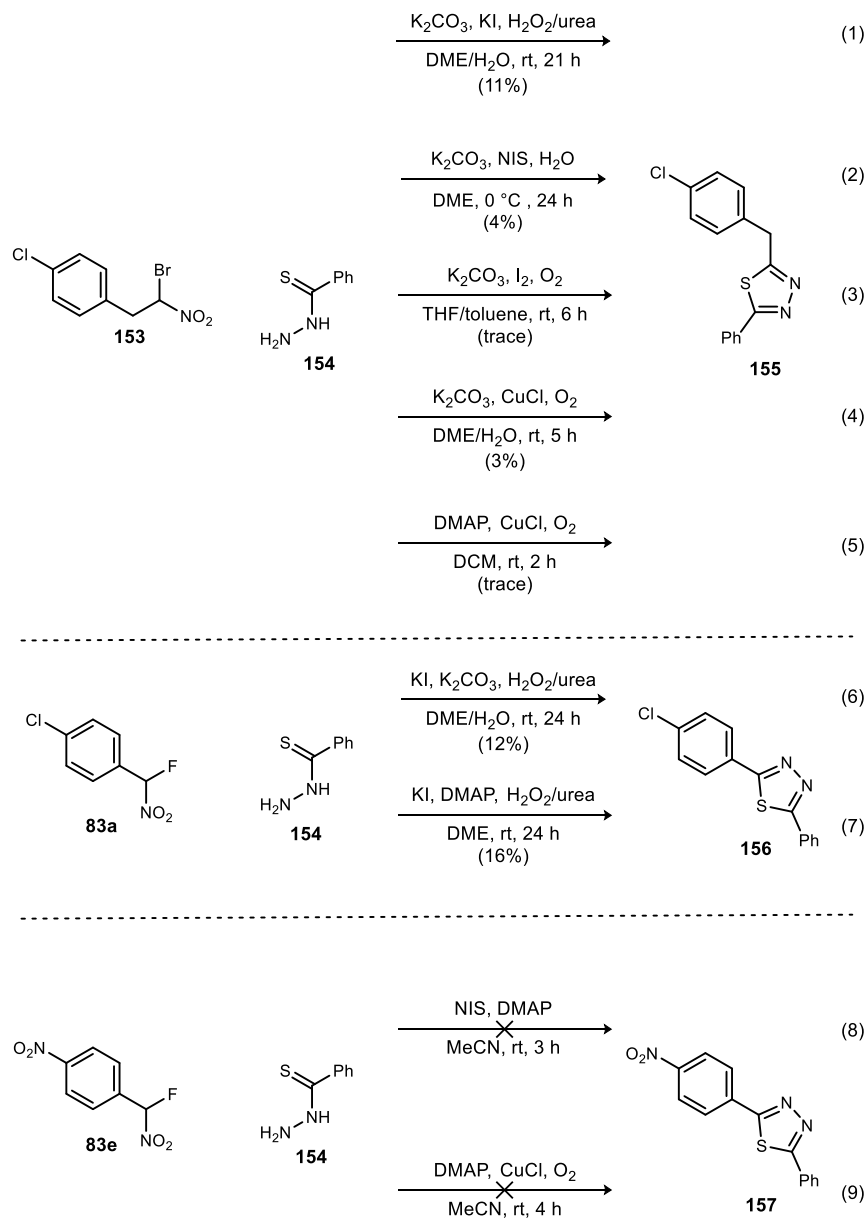
Investigating thiadiazoles first required preparation of a thiohydrazide. For initial investigations thiohydrazide **154** was chosen and synthesized in three steps from bromobenzene using reported procedures.^{198,199} With **154** in hand, we were able to test the standard diverted UmAS conditions¹²⁰ with this substrate (Scheme 45, eq 1). We were pleased to see that the established conditions were transferable (albeit low yielding) for thiadiazole synthesis. Attempts to perturb relative rates and favor the productive mechanism by altering temperature or H₂O₂/urea addition rate were unsuccessful in increasing yield. The low yield was assumed at this point to be a consequence of the more oxidatively labile thiohydrazide so other oxidant systems were applied. Other conditions optimized for amide formation³² gave a lower yield (Scheme 45, eq 2). This is not surprising and actually somewhat validating of our hypothesis because UmAS conditions are more harshly oxidizing than those of diverted UmAS. Similarly, conditions more closely resembling those developed by the Hayashi group⁴⁴ for amide formation gave only trace yield in this reaction starting from a bromonitroalkane (Scheme 45, eq 3) or nitroalkane (not shown).

¹⁹⁸ Wu, D.-Q.; Li, Z.-Y.; Li, C.; Fan, J.-J.; Lu, B.; Chang, C.; Cheng, S.-X.; Zhang, X.-Z.; Zhuo, R.-X. *Pharm. Res.* **2010**, *27*, 187.

¹⁹⁹ Singh, N. K.; Singh, S. B.; Shrivastav, A. *Met Based Drugs* **2002**, *9*, 109.

A common unidentified byproduct observed in these reactions was clearly thiohydrazide-

Scheme 45. Thiadiazole synthesis using diverted UmAS conditions



derived. Cu(I)/O₂ is a known system for oxidizing hydrazides²⁰⁰ so those procedures were adapted

²⁰⁰ Kim, M. H.; Kim, J. *J. Org. Chem.* **2018**, *83*, 1673.

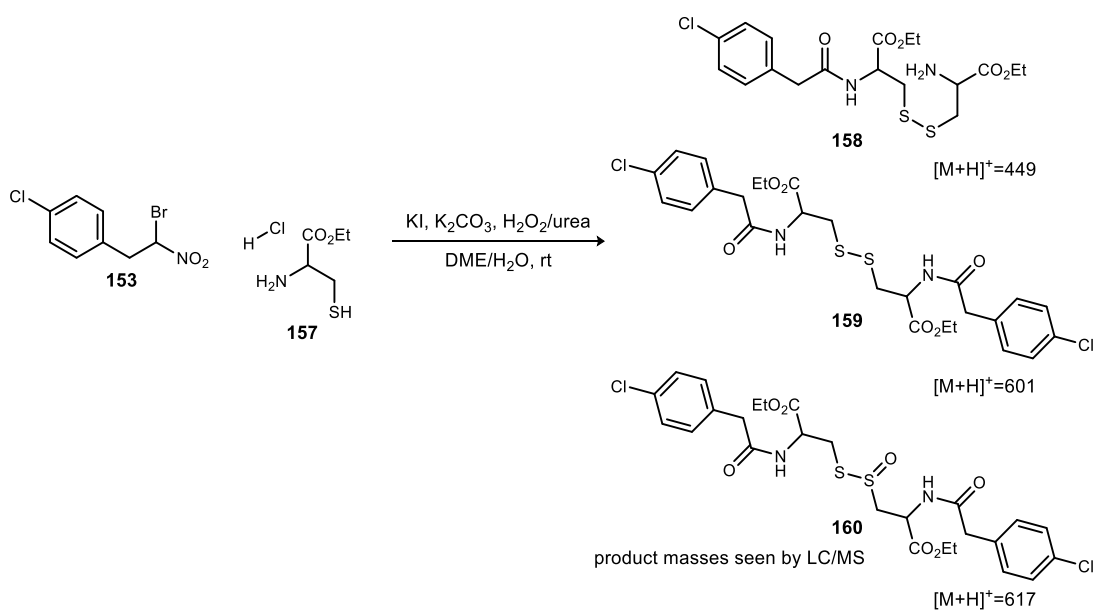
to diverted UmAS, but gave similarly poor yields (Scheme 45, eq 4). Changing the base to a weaker homogeneous base, and the solvent to dichloromethane in order to better represent the hydrazone oxidation conditions,²⁰⁰ all but eliminated productive reactivity (Scheme 45, eq 5). Using a fluoro nitroalkane with either K₂CO₃ or DMAP gave minor improvements to yield, but it is unclear if the increase is a consequence of the different halogen or of the different substrate structure (Scheme 45, eqs 6-7). Interestingly, a much more acidic fluoro nitroalkane known to give complete nitronate formation in minutes did not produce thiadiazole under the conditions in Scheme 45, eqs 8-9. This indicates that nitronate availability is not a limiting factor in this reaction. The consistently low yields under a variety of conditions spurred us to set this reaction aside for the time being.

Moving forward to thiazole synthesis, efforts were concentrated on using cysteine derivatives as the amine component. Beginning with H-cysteine-OEt·HCl (**157**) and a standard bromo nitroalkane (**153**) and applying the standard diverted UmAS conditions¹²⁰ led to no cyclized product, and instead gave disulfides, UmAS products, and oxidized forms of those products (**158-160**) as determined by LC-MS (Scheme 46). Similar results were observed when using a simple fluoro nitroalkane. When considering the results in Scheme 46 and the oxidative conditions used in all UmAS-related conditions, it seemed likely that disulfide formation is fast and difficult to avoid in this system. It was not yet apparent if disulfide formation precluded any productive route to thiazole. To test this we prepared H-cystine-OEt·2HCl²⁰¹ and used it as a substrate with standard bromo nitroalkane **153** and both UmAS³² and diverted UmAS¹²⁰ conditions. Diverted UmAS conditions again led to only UmAS products and several oxidized versions thereof. UmAS

²⁰¹ Benoiton, L. *Can. J. Chem.* **1968**, *46*, 1549.

conditions gave primarily decomposition of both reaction components. While testing the effect of

Scheme 46. Attempted diverted UmAS synthesis of thiazoles



limiting oxidant amount and identity, UmAS conditions using degassed solvents and inert atmospheres did not lead to more productive reaction outcomes. While these efforts are by no means exhaustive, they failed to present a tangible platform for continued investigations.

3.2.5 Conclusions

Important clarification of the identity of an UmAS byproduct was made. Because the compound was not an oxazole, we did not commit significant effort to an optimization campaign. The assignment of the product as a nitron in addition to the limited investigations reported in this work allows for some mechanistic speculation. Further experiments could give a less ambiguous assignment of mechanistic pathways and, possibly, inform the optimization of the relevant UmAS reaction for the amide product.

The successful preparation of an α -NO₂ hydrazone shows that simple nitronates are viable nucleophiles for single addition into diazonium salts. The absence of any reactivity of the α -NO₂

hydrazones to heterocycles precludes the advancement of the desired method, but is further evidence that the activated hydrazone in diverted UmAS has α -halo (not α -NO₂) substitution. Consequently, further efforts toward indazole and triazole synthesis from diazonium salts could focus on alkyl halides with an α -substituent that acidifies the position and can be eliminated in an azo to hydrazine rearrangement (Scheme 41, X = halogen; Y = CO₂H for example). Additionally, the observation of diacyl hydrazines as the major fate of α -NO₂ hydrazones could be further developed as a one-pot route to that motif from anilines and nitroalkanes.

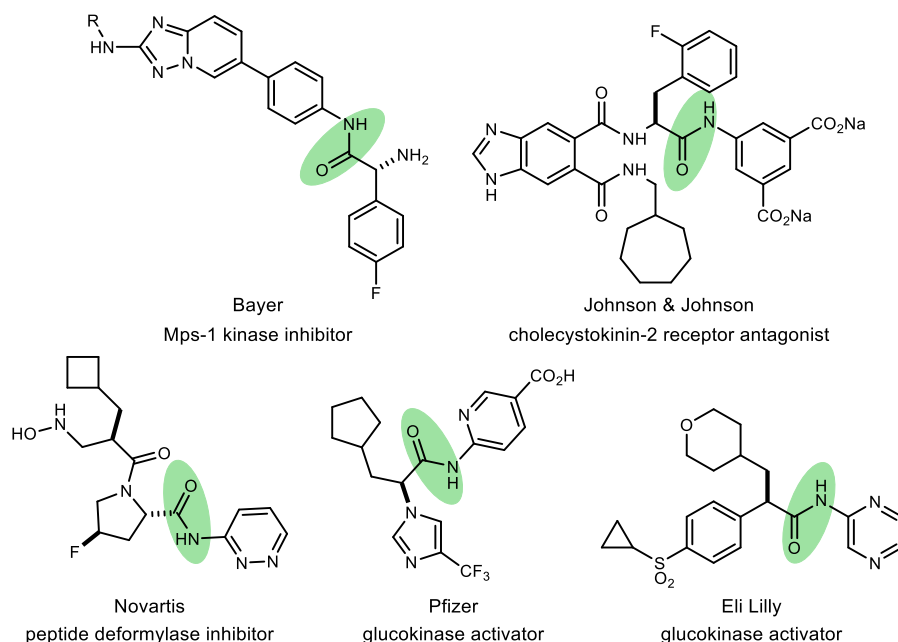
Thiadiazoles can be synthesized using diverted UmAS conditions, but only in low yields. This finding and the observation that thiazoles are not accessible from β -amino thiols using common UmAS conditions share a likely explanation. The oxidative conditions needed for UmAS are incompatible with many sulfur-containing functional groups. The best path towards an umpolung synthesis of sulfur-containing heterocycles is likely a completely different reaction platform with milder nitrogen activation.

3.3 Umpolung Synthesis of *N*-Aryl Amides

3.3.1 *N*-Aryl Amides

Amides bearing aryl substituents at nitrogen are a well-represented subclass. For example, of the 62 small molecule amides represented in the top 200 pharmaceutical products by retail sales in 2016 (as compiled by the Njardarson group) more than a third contain *N*-aryl amides. Aryl substituents are also favored by medicinal chemists for their value in structure-activity relationship

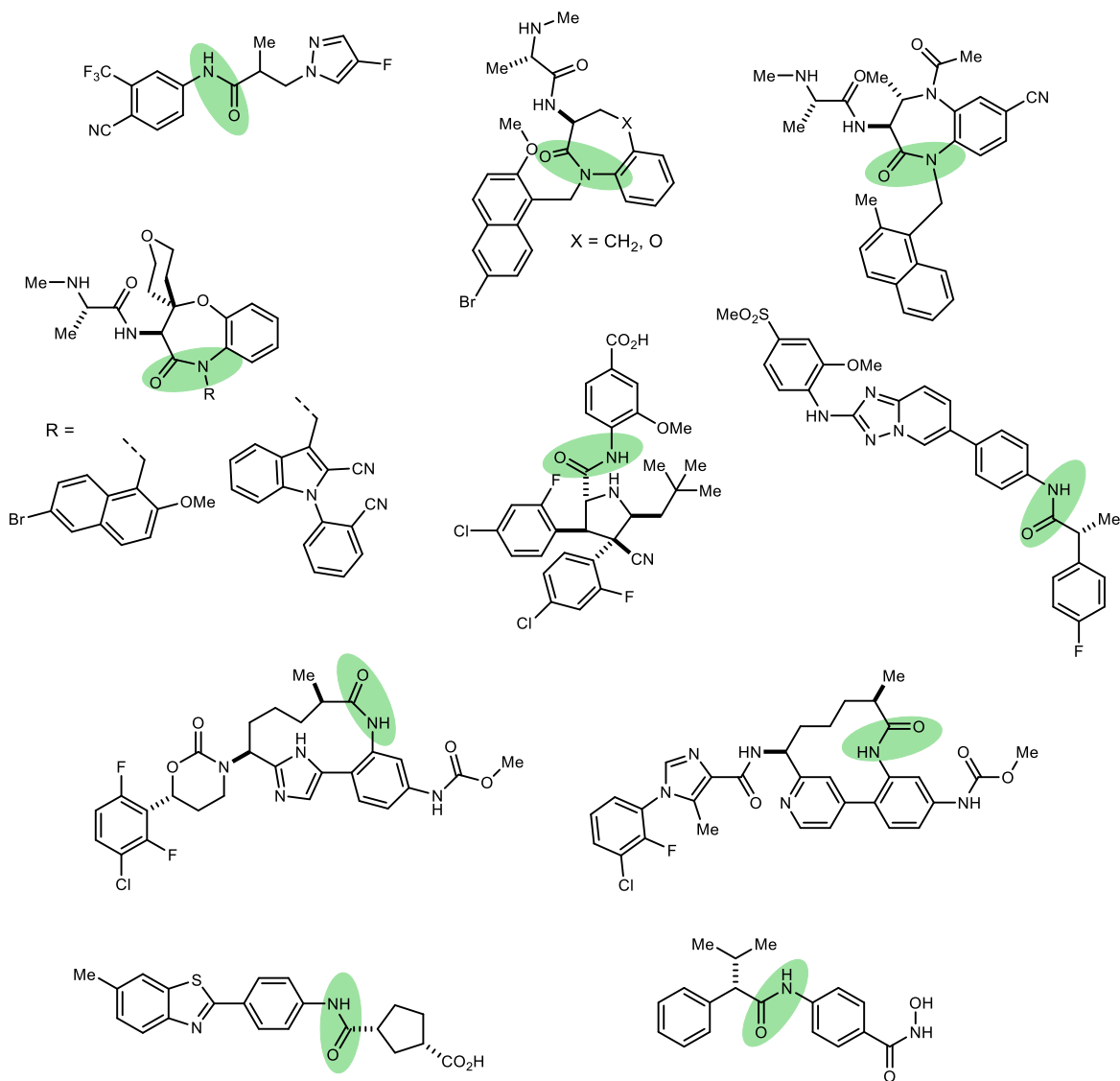
Figure 19. Examples of α -stereocenter containing *N*-aryl amides of pharmaceutical relevance – difficult couplings



screens. Specific examples of drug-like molecules synthesized on large scale where conventional

amide synthesis was troublesome can be seen in Figure 19.^{202,203,204,205,206} Even limiting a search

Figure 20. Examples of α -stereocenter containing *N*-aryl amides of pharmaceutical relevance²¹⁴



to *N*-aryl amides appearing in *J. Med. Chem.* articles published in 2020, and only considering molecules with stereocenters α to the amide while eliminating examples with natural amino-acid substitution, gives a large number of molecules (examples can be seen in Figure 20).^{207,208,209,210,211,212,213}

Despite the prevalence of the *N*-aryl amide motif, many of the most effective methods for the production of *N*-alkyl amides from alkyl amines are much less effective or require much harsher conditions when applied to aryl amines.²¹⁵ The standard conditions for UmAS have been found to be unsuited to aryl amines. There have been many previous attempts within the group to find suitable modifications to the conditions, but only low yields have ever been achieved, and, prior to this work, this remained a major need unaddressed by the approach. The application of UmAS to *N*-aryl amides will represent the first umpolung approach to that motif and will bring it under the umbrella of positive features of UmAS discussed at length in the previous chapter. Many of the incentives to use UmAS over traditional amide synthesis are amplified when considering *N*-aryl amides due to the lower performance of aryl amines in traditional coupling reactions. With

²⁰² Ormerod, D.; Willemsens, B.; Mermans, R.; Langens, J.; Winderickx, G.; Kalindjian, S. B.; Buck, I. M.; McDonald, I. M. *Org. Process Res. Dev.* **2005**, *9*, 499.

²⁰³ Magnus, N. A.; Braden, T. M.; Buser, J. Y.; DeBaillie, A. C.; Heath, P. C.; Ley, C. P.; Remacle, J. R.; Varie, D. L.; Wilson, T. M. *Org. Process Res. Dev.* **2012**, *16*, 830.

²⁰⁴ Dunetz, J. R.; Berliner, M. A.; Xiang, Y.; Houck, T. L.; Salingue, F. H.; Chao, W.; Yuandong, C.; Shenghua, W.; Huang, Y.; Farrand, D. *Org. Process Res. Dev.* **2012**, *16*, 1635.

²⁰⁵ Liu, Y.; Prashad, M.; Ciszewski, L.; Vargas, K.; Repič, O.; Blacklock, T. J. *Org. Process Res. Dev.* **2008**, *12*, 183.

²⁰⁶ Wengner, A. M.; Siemeister, G. Patent WO2014198645 (A1), 2014.

²⁰⁷ He, Y.; Hwang, D.-J.; Ponnusamy, S.; Thiyagarajan, T.; Mohler, M. L.; Narayanan, R.; Miller, D. D. *J. Med. Chem.* **2020**.

²⁰⁸ Blaquiere, N.; Villemure, E.; Staben, S. T. *J. Med. Chem.* **2020**.

²⁰⁹ Schulze, V. K.; Klar, U.; Kosemund, D.; Wengner, A. M.; Siemeister, G.; Stöckigt, D.; Neuhaus, R.; Lienau, P.; Bader, B.; Prechtel, S. *J. Med. Chem.* **2020**.

²¹⁰ Yang, W.; Wang, Y.; Lai, A.; Clark, C. G.; Corte, J. R.; Fang, T.; Gilligan, P. J.; Jeon, Y.; Pabbisetty, K. B.; Rampulla, R. A. *J. Med. Chem.* **2020**, *63*, 7226.

²¹¹ Corte, J. R.; Pinto, D. J.; Fang, T.; Osuna, H.; Yang, W.; Wang, Y.; Lai, A.; Clark, C. G.; Sun, J.-H.; Rampulla, R. *J. Med. Chem.* **2020**, *63*, 784.

²¹² Qiu, Y.; Huang, L.; Fu, J.; Han, C.; Fang, J.; Liao, P.; Chen, Z.; Mo, Y.; Sun, P.; Liao, D. *J. Med. Chem.* **2020**, *63*, 3665.

²¹³ Tng, J.; Lim, J.; Wu, K.-C.; Lucke, A. J.; Xu, W.; Reid, R. C.; Fairlie, D. P. *J. Med. Chem.* **2020**, *63*, 5956.

²¹⁴ *J. Med. Chem.* **2020**

²¹⁵ Xie, S.; Zhang, Y.; Ramström, O.; Yan, M. *Chem. Sci.* **2016**, *7*, 713.

that consideration in mind, it is particularly important to bring that functional group into the scope of UmAS.

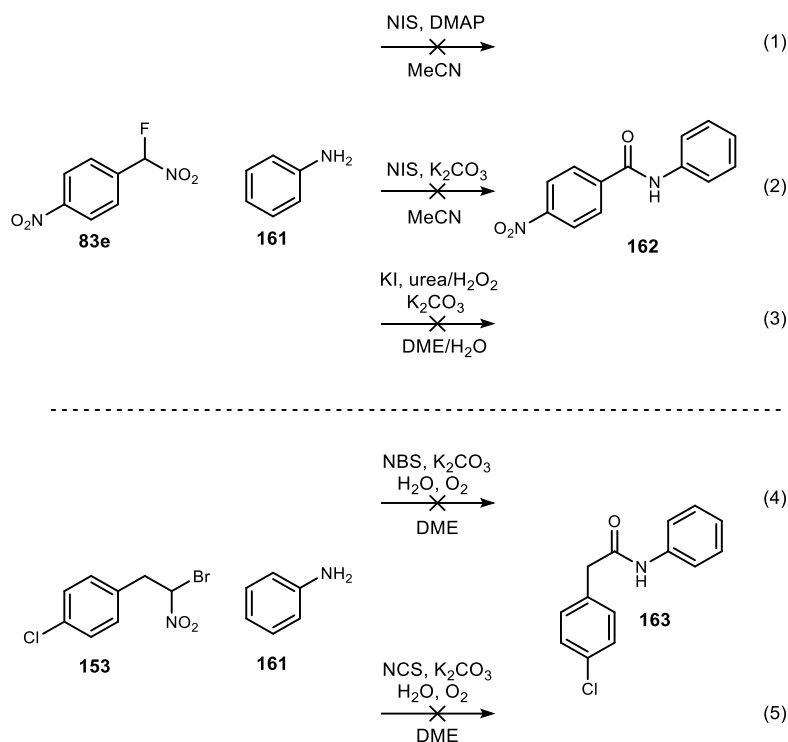
3.3.2 Reaction Discovery

It has long been the observation within the Johnston group that aryl amines are not viable substrates for UmAS. Considering the factors that prevent *N*-aryl amide synthesis using UmAS led to two hypotheses. We envisioned that 1) the oxidative conditions could be leading to unwanted oxidation at the electron-rich aryl ring (a known transformation of aniline derivatives in the presence of halogen)²¹⁶ or 2) the halamine electrophile was not forming due to the low nucleophilicity of the amine. In either case a different source for the nitrogen electrophile seemed prudent. It was the expectation that this modification could allow for an umpolung route to *N*-aryl amides in a way analogous to UmAS.

²¹⁶ Hodgson, H. H.; Marsden, E. *J. Chem. Soc.* **1937**, 1365.

Before changing electrophile outright, the direct application of aryl amines to newer UmAS conditions was explored. This was done first in the hope that the better nucleophile (fluoronitroalkane **83e**) of the conditions developed above in Chapter 2 or the milder oxidant system (urea hydrogen peroxide and potassium iodide) of diverted UmAS would aid in productive reactivity when applied to aryl amine substrates and, second, as a control confirming the general observation in the group that standard UmAS conditions are non-effective for the synthesis of *N*-aryl amides. Sadly, but not unexpectedly, application of DMAP or K_2CO_3 mediated addition of

Scheme 47. UmAS conditions unsuccessfully applied to aryl amines



fluoronitroalkanes (**83e**) to aniline (**161**) activated with NIS or KI/urea hydrogen peroxide gave no conversion to desired product (Scheme 47, eqs 1-3). Standard UmAS conditions between bromonitroalkane **153** and aniline activated with other halonium sources such as NBS or NCS were also unsuccessful (Scheme 47, eqs 4-5).

The direct activation of aniline derivatives in otherwise UmAS-like conditions remained the most attractive and intuitive means of forming *N*-aryl amides in an umpolung fashion. Given the incompatibility of halenium reagents in this system, we were moved to consider *N*-Se species as potential nitrogen electrophiles. Electrophilic selenium reagents do not have the same reported potential for aromatic ring oxidation as do halenium reagents, so *N* activation with these reagents could give the desired product without side reactivity. Electrophilic selenium reagents are used primarily for selenations and alkene activation chemistry.^{217,218} In those contexts, *N*-Se species are known and it was our hope to apply them as nitrogen electrophiles in this work.²¹⁹

Using UmAS-like conditions with a bromonitroalkane (**153**), 4-F aniline (**164**), and a small panel of selenium reagents excitingly gave some yield of amide product **165** (Scheme 48, entries 1-3). Diphenyl diselenide and its 4-Cl analogue gave better results than the phthalimide derived reagent. A few bases were also screened (Scheme 48, entries 4-7) and the stronger potassium hydroxide gave improved yield while the weaker DMAP gave little to no product. Not shown, a large number of redox-active metals were investigated as catalytic additives and all gave equivalent or lower yields to the unaltered conditions. Those complexes tried were selected based on their common usage in redox processes and are Ni(acac)₂, NiCl₂, Mn(OAc)₃, CuCl, CuCl₂, Cu(OAc)₂, CuI, Fe(OAc)₂, FeBr₂, and FeCl₃. The very low yields (<20%) that persisted after limited optimization efforts encouraged us to explore other reagent systems altogether.

²¹⁷ Wessjohann, L. A.; Sinks, U. *J. Prakt. Chem.* **1998**, *340*, 189.

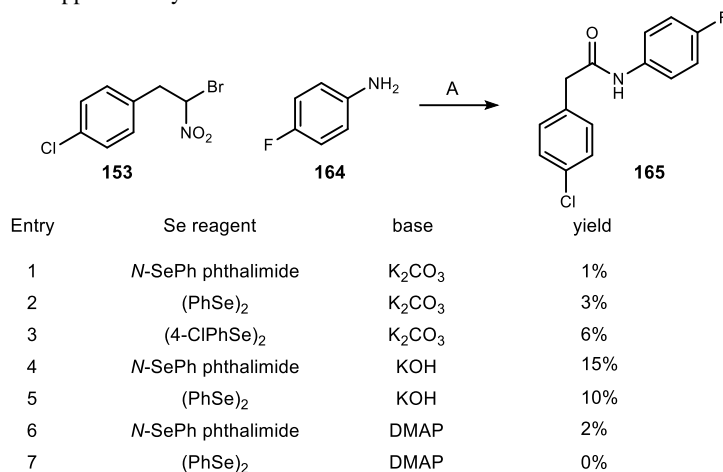
²¹⁸ Shao, L.; Li, Y.; Lu, J.; Jiang, X. *Org. Chem. Front.* **2019**, *6*, 2999.

²¹⁹ Dr. Ryan Yoder and Dr. Roozbah Yousefi investigate aniline activation with selenium reagents with some UmAS reactions giving very low yields of the *N*-aryl amide products

3.3.2.1 Hydroxylamine Precursors to Electrophilic N

With confirmation that UmAS conditions already in our arsenal or small modifications thereof would not be sufficient in advancing the desired scope expansion, we moved forward with developing a new methodology. A number of promising electrophilic aminations of carbon

Scheme 48. UmAS conditions applied to aryl amines with Se activation



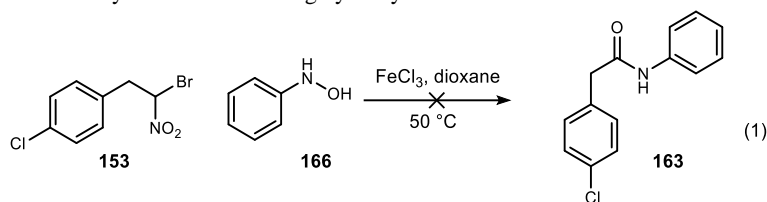
A) 4-F aniline (1.2 equiv), Se reagent (1 equiv), bromo nitroalkane (1 equiv), and water (5 equiv) were dissolved in dimethoxy ethane (100 mM) and brought to -20 °C. Base (2 equiv) was added and the reaction was stirred for 20 h.

nucleophiles, especially enolates, exist and serve as potential starting points for the desired halo nitroalkane amination that is the first step towards *N*-aryl amide synthesis. The Srivastava group has reported an iron catalyzed amination of β -keto esters starting from aryl hydroxylamines.²²⁰ The application of those conditions to bromo nitroalkane pronucleophile **153** with and without base gave only recovered bromo nitroalkane and decomposition of hydroxyl amine **166** (Scheme 49, eq 1). Use of slow addition of the hydroxylamine to circumvent the decomposition of that reagent prior to the formation of any active nucleophile did not change the course of the reaction. Since a nitroso species is proposed to be an intermediate in Srivastava's reaction, we also explored

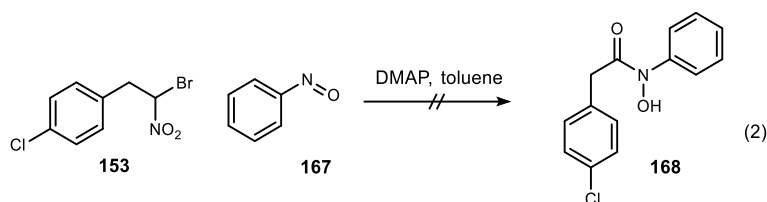
²²⁰ Murru, S.; Lott, C. S.; Fronczek, F. R.; Srivastava, R. S. *Org. Lett.* **2015**, *17*, 2122.

the competency of that electrophile (**167**) for TI formation with a bromo nitroalkane, but we found

Scheme 49. Exploration of Fe catalyzed amination using hydroxylamine



modifications: added KOH; slow hydroxylamine addition

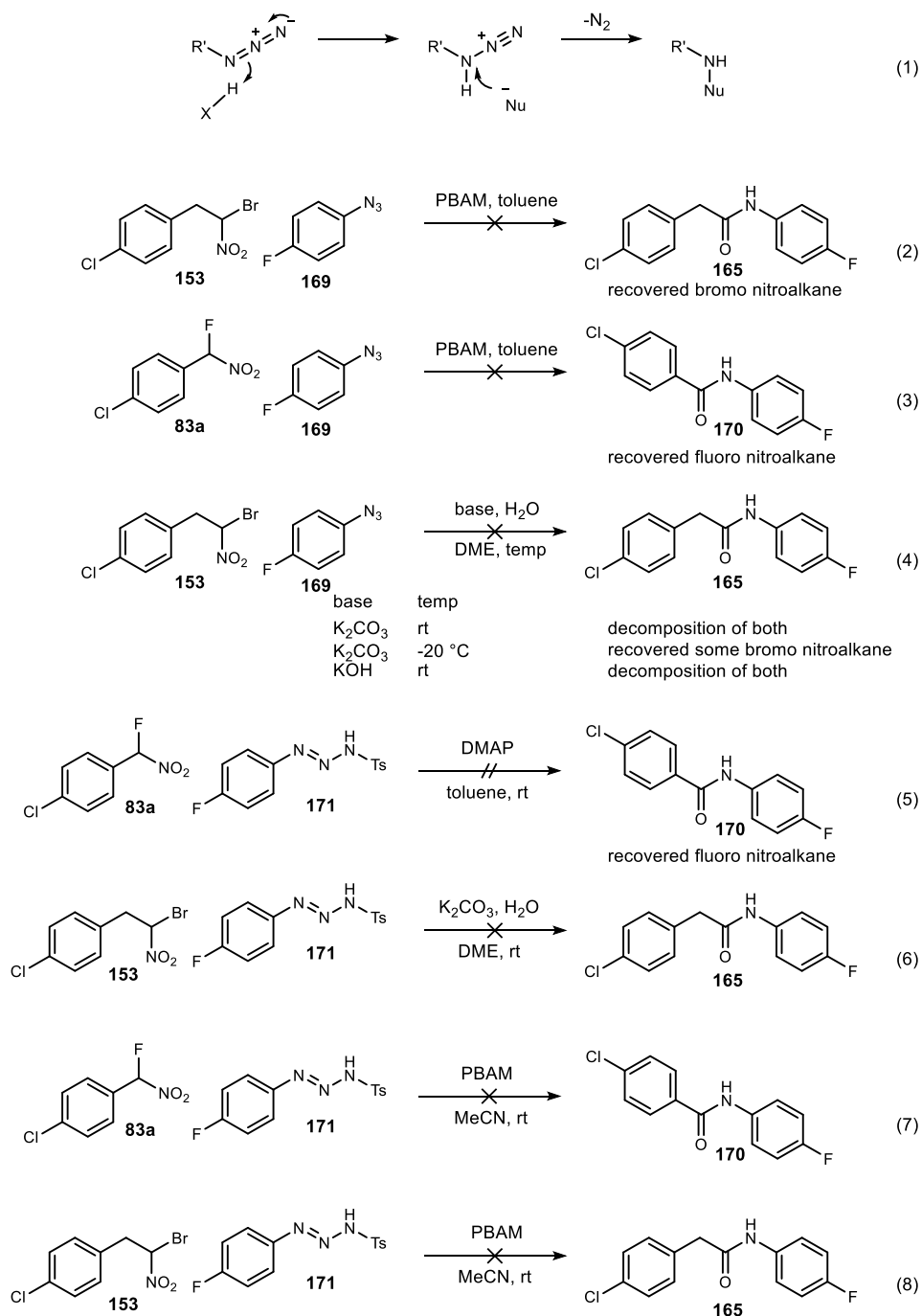


this combination did not give the amide (**163**) or hydroxamic acid (**168**) and primarily starting materials were recovered (Scheme 49, eq 2).

Azides are another potential source of electrophilic nitrogen. While their typical mode of reactivity is electrophilic at the terminal nitrogen, it was our hope that, through proper hydrogen bond activation, the aryl amine nitrogen could be attacked by a nitronate to give the desired C-N bond with the loss of N_2 . Since BAM catalysts are frequently useful in mediating nitroalkane additions^{18,20,29,30,32,33,34,35} that require chiral acid/base activation we wanted to test their competency in the desired nitroalkane amination. Scheme 50, eq1 lays out the potential productive pathway and shows results of selected examples. Unfortunately, neither BAM catalysis (Scheme 50, eqs 2-3) or simple basic conditions (Scheme 50, eq 4) led to any products expected to be derived from C-N bond formation. Another potential route to amide with intermediates similar to those in Scheme 50 eq 1 is the use of a sufficiently activated triazene. The triazene **171** was reacted with standard bromo and fluoro nitroalkanes (**153** and **83a**) under basic conditions, but gave no indication of C-N bond formation (Scheme 50, eqs 5-8).

Always on the lookout for reactions involving C-N bond formation between a carbon

Scheme 50. Hypothesis and results of attempted nitronate addition into internal azide nitrogen



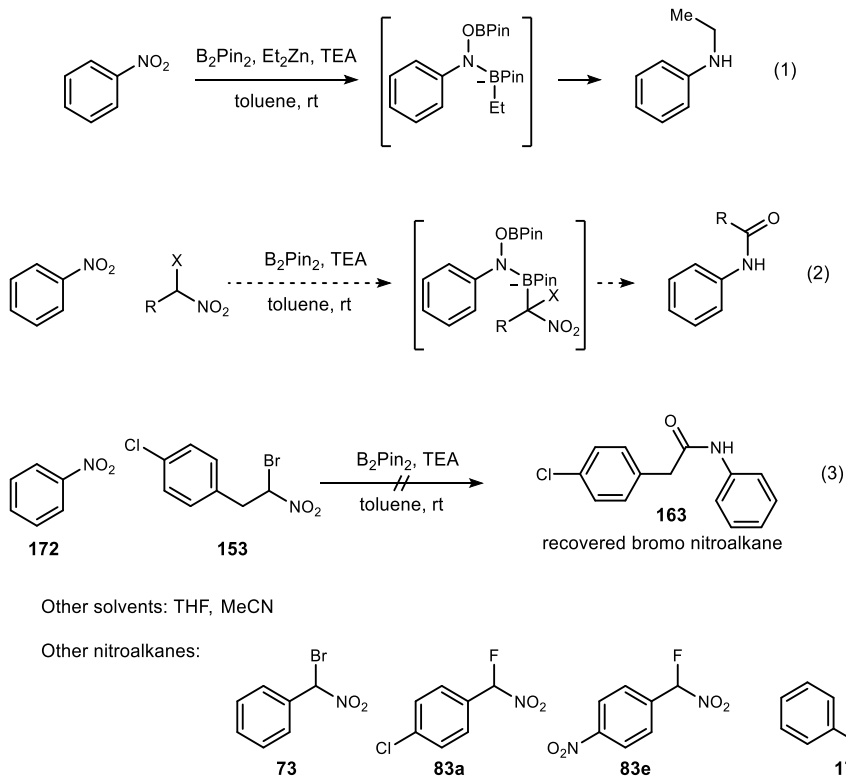
nucleophile and a nitrogen electrophile, we became aware of a new zincate amination reaction

enabled by the *in situ* partial reduction of nitroarenes (Scheme 51, eq 1).²²¹ We hoped that suitable conditions would allow for the nucleophile to be replaced with an α -halo nitroalkane. This substitution would generate a HANA upon rearrangement which could collapse to the *N*-aryl amide (Scheme 51, eq 2). Sadly, α -halo nitroalkanes (**153**, **73**, **83a**, **83e**, or **173**) did not react under the reported reaction conditions (Scheme 51, eq 3), and we suspect this is due to the vast difference in nucleophilicity between the nitronate and the zincate. Increasing the temperature to 50 °C gave some recovered bromonitroalkane as well as signs of decomposition. Other solvents and pronucleophiles showed varying degrees of conversion but never to the amide product (Scheme 51).

²²¹ Rauser, M.; Ascheberg, C.; Niggemann, M. *Angew. Chem.* **2017**, *129*, 11728.

We had limited ourselves, to this point, to approaches that would deliver the nitrogen

Scheme 51. Zincate amination via nitroarene partial reduction and its proposed adaptation to nitroalkanes



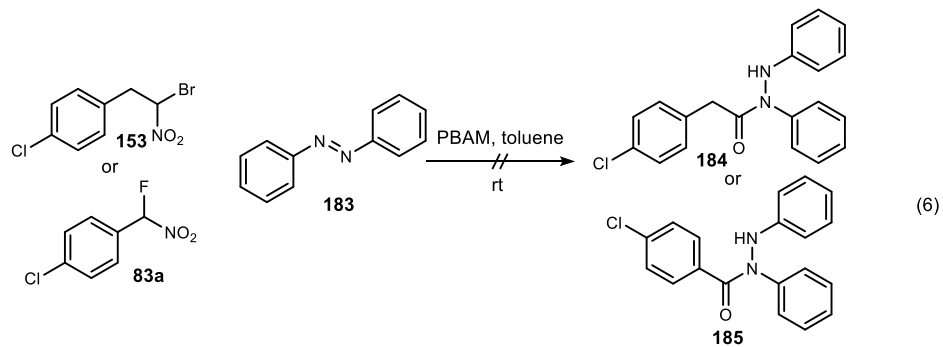
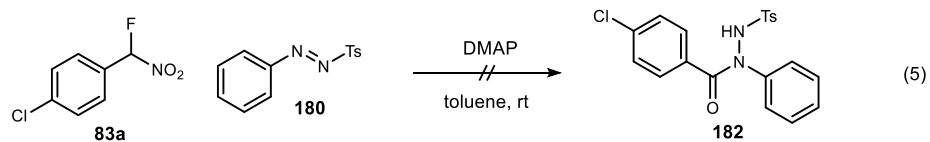
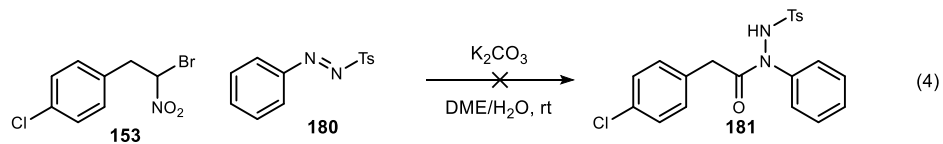
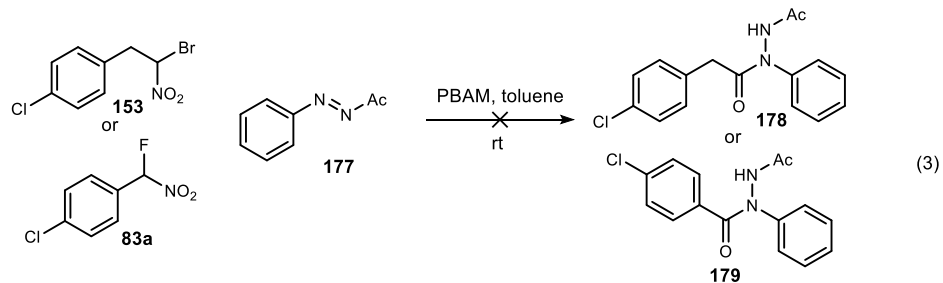
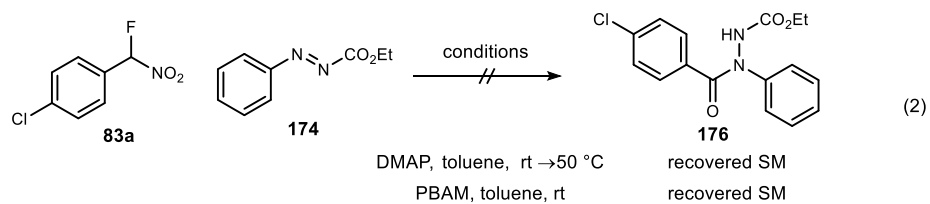
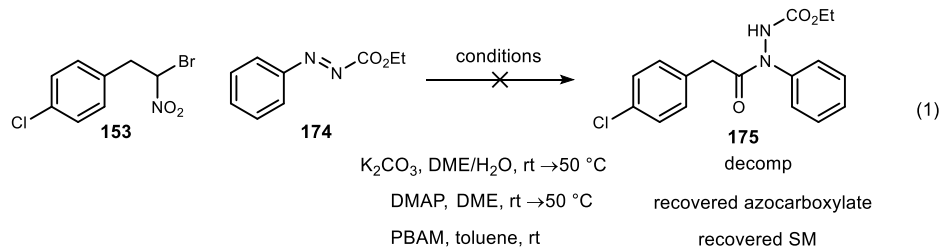
electrophile at the proper oxidation state. Due to the difficulty of arriving at a suitable electrophile with that restraint, we also considered electrophiles that could give *N*-aryl amide derivatives with a higher oxidation state at nitrogen. Inspired by the success seen with azodicarboxylates in the work in Chapter 2 as well as Ying's success with nitroso electrophiles,²²² various aryl azo compounds with electron withdrawing groups were explored. Most analogous to the DEAD electrophile in Chapter 2 is phenyl ethylazocarboxylate (**174**), but this nucleophile was

²²² Wong, F. T.; Patra, P. K.; Seayad, J.; Zhang, Y.; Ying, J. Y. *Org. Lett.* **2008**, *10*, 2333.

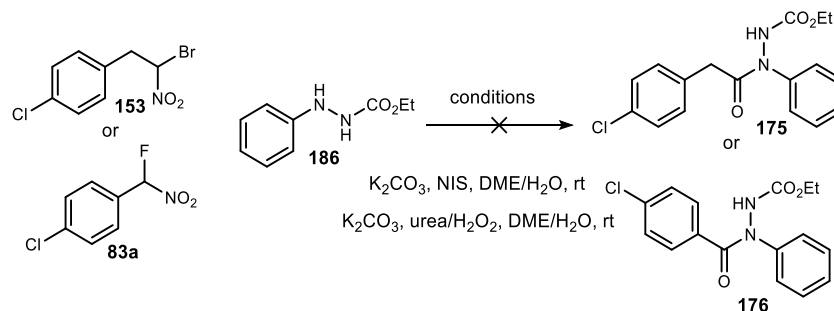
insufficiently electrophilic to undergo bond formation under conditions known to produce α -bromo or α -fluoro nitronates (Scheme 52, eqs 1-2).

Similarly, a phenyl azo compound activated with an acetyl group (**177**) led to decomposition when paired with a fluoro or bromo nitroalkane (**83a** or **153**) under basic conditions (Scheme 52, eq 3). An aryl azo compound activated with a tosyl group (**180**) had similar behavior to the azo carboxylate. Reaction with bromo nitroalkane **153** using K_2CO_3 as base led to decomposition while fluoro nitroalkane **83a** and DMAP returned starting materials (Scheme 52, eqs 4 and 5). Unsurprisingly, azobenzene (**183**) showed no reactivity when exposed to bromo or fluoro nitroalkanes in the presence of PBAM (Scheme 52, eq 6). Finally, an *in situ* oxidation of a hydrazide under UmAS or diverted UmAS conditions did not give better results than using the preformed azocarboxylate (Scheme 53).

Scheme 52. Other nitrogen electrophiles tried in *N*-aryl amide synthesis



Scheme 53. *In situ* hydrazone activation

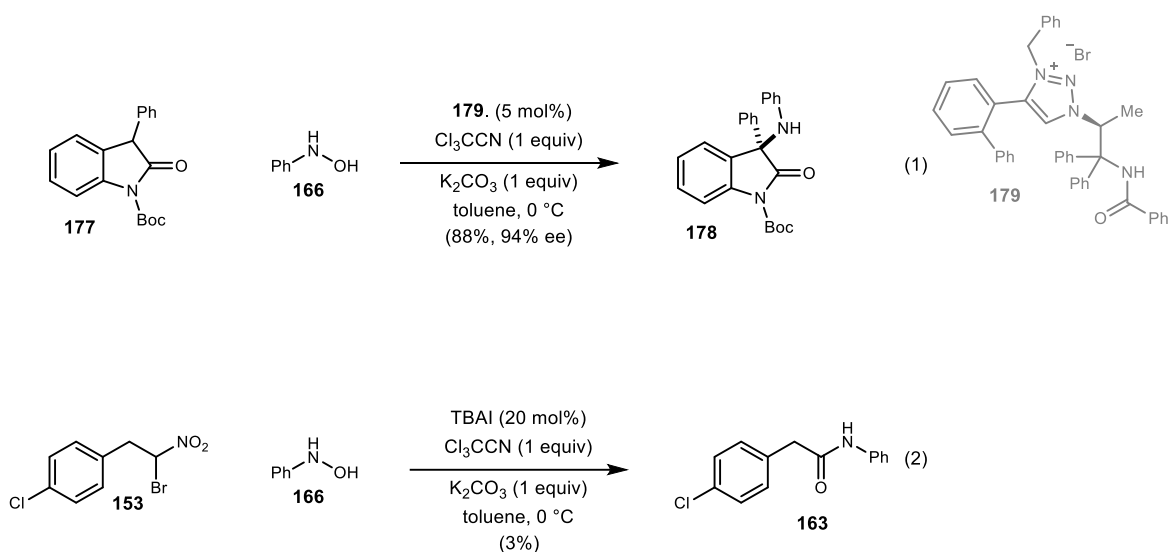


The failure of more conventional electrophiles as partners for nitronates led us to reevaluate the electrophilic amination literature in search of effective reagents. Recent work by the Ooi group using hydroxylamines as enolate aminating reagents caught our attention.²²³ This reaction is related to the Srivastava group's work (above) but activates the hydroxylamine (**166**) as a trichloroacetimidate rather than with an iron catalyst (Scheme 54, eq 1). Applying similar conditions to bromo nitroalkane pronucleophile **153** led to a low yield of desired amide product **168** (Scheme 54, eq 2).

Early efforts to increase yield included screening metals in a way similar to the selenation work above, screening solvents including the DME/H₂O solvent system often employed in UmAS, modifying K_2CO_3 particle size, excluding water, excluding O₂, increasing temperature, and purifying TBAI prior to use. None of these modifications led to any significant increase in the production of amide product, so we began looking into the factors that could impart such different outcomes when switching from the enolate to nitronate nucleophile.

²²³ Ohmatsu, K.; Ando, Y.; Nakashima, T.; Ooi, T. *Chem* **2016**, *1*, 802.

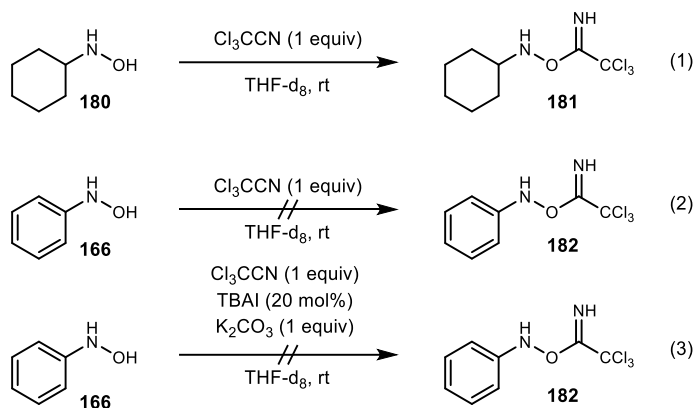
Scheme 54. Ooi amination of enolates and its application to amide formation



3.3.3 Reaction Optimization

NMR studies of the hydroxylamines following the procedure in the Ooi paper²²³ corroborated their observation that an alkyl hydroxylamine (**180**) is rapidly consumed to produce a trichloroacetimidate (**181**) when in the presence of trichloro acetonitrile (Scheme 55, eq 1).

Scheme 55. NMR studies of trichloroacetimidate formation



Interestingly, when applying those conditions to an *N*-aryl hydroxylamine (**166**) no such reaction was observed (Scheme 55, eq 2). Because aryl and alkyl hydroxylamines are successful in Ooi's

reaction we considered that perhaps, under the full reaction conditions, the base or phase transfer catalyst was taking part in encouraging trichloroacetimidate formation in the more difficult *N*-aryl cases. Scheme 55, eq 3 was performed in hopes of observing the trichloroacetimidate (**182**) and confirming our hypothesis. The lack of any indication of trichloroacetimidate (**182**) formation in this case suggested that either Ooi's reaction can still proceed even if the hydroxylamine-trichloroacetimidate reaction is in equilibrium and lies heavily towards starting materials or that the TBAI we are using in place of chiral triazolium catalyst **179** is not achieving the same function.

To explore the source of the limitations our simplified conditions are encountering, we elected to use PBAM as an additive to the conditions in Scheme 54, eq 2. We hoped PBAM would provide hydrogen bond donors and acceptors to serve the same purpose as Ooi's triazolium catalyst (**179**). Sadly, no improvement to the reaction was observed with 5 mol % of PBAM. These results encouraged us to prepare Ooi's triazolium catalyst (**179**) both in the pursuit of this reaction as well as an addition to the group's catalyst library.

3.3.3.1 Use of a Ritter Reaction to Improve Access to Ooi's Triazolium Salt

The intermediate **183** was prepared in 10 steps (all >1 g scale) according to literature procedures^{224, 225, 226, 227, 228, 229} leaving only a three step azide formation/reduction/acylation sequence²³⁰ before final benzylation to afford the catalyst. Initial attempts at the S_N1 step to install

²²⁴ Islam, M. A.; Zhang, Y.; Wang, Y.; McAlpine, S. R. *MedChemComm* **2015**, 6, 300.

²²⁵ Uraguchi, D.; Sakaki, S.; Ooi, T. *J. Am. Chem. Soc.* **2007**, 129, 12392.

²²⁶ Goddard-Borger, E. D.; Stick, R. V. *Org. Lett.* **2007**, 9, 3797.

²²⁷ Zhu, Y.-Q.; Dong, L. *J. Org. Chem.* **2015**, 80, 9973.

²²⁸ {Hossain, 2014 #295}

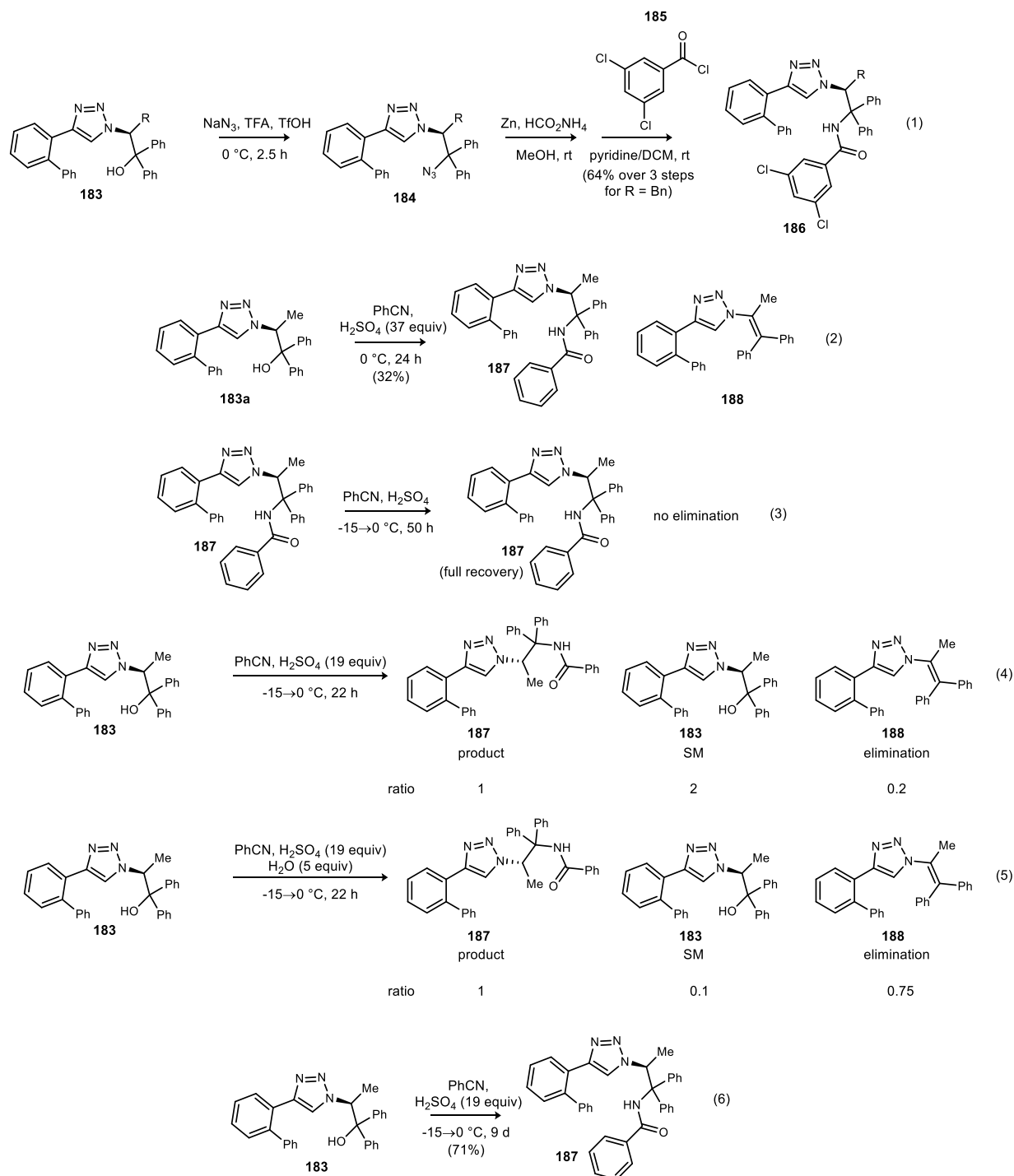
²²⁹ Juwarker, H.; Lenhardt, J. M.; Pham, D. M.; Craig, S. L. *Angew. Chem. Int. Ed.* **2008**, 47, 3740.

²³⁰ Ohmatsu, K.; Kiyokawa, M.; Ooi, T. *J. Am. Chem. Soc.* **2011**, 133, 1307.

the azide (Scheme 56, eq 1) exhibited low conversion and almost no identifiable product. Rather than dedicate much effort to diagnosing and resolving this issue, another approach, a Ritter reaction, was considered. An initial Ritter reaction gave low (32%) yield (Scheme 56, eq 2), and running the reaction at room temperature or for lower reaction times gave worse outcomes. Other acids such as HNO₃ or HClO₄ gave no conversion and TfOH gave only an elimination product assigned tentatively as **188** on the basis of proton NMR. Because this elimination product seemed to be the only major competing pathway, its minimization became a focus.

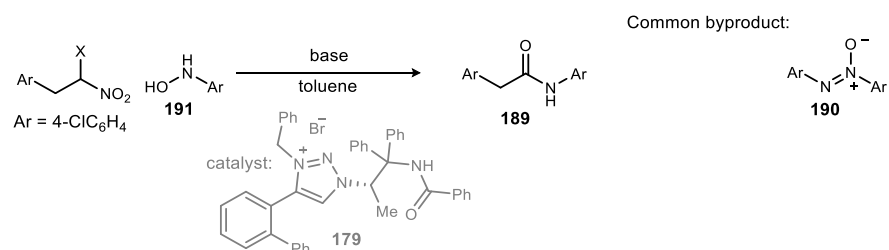
Re-subjection of the product (**187**) to the reaction conditions resulted in no degradation or elimination (Scheme 56, eq 3) so we believe that the elimination happens prior to product

Scheme 56. Ending sequence for the synthesis of Ooi's triazolium catalyst



formation. Lowering the temperature during the slow addition of acid gave better results, and while higher concentration seemed unimpactful, using fewer equivalents of acid resulted in slower overall rate but less elimination. Reactivity could be substantially increased by the addition of water; however, this reactivity came at the price of sharply increased elimination (Scheme 56, eqs 4 and 5). Combining a lower acid amount with added water gave only the disadvantages of each set of conditions and resulted in low reactivity and high elimination. Doing the acid addition at as low a temperature as possible was found to be the final adjustment necessary to make this reaction quite efficient (although below ~ -15 °C, viscosity/freezing became an issue). Concentration did not seem to be impactful on the final conditions, so the original concentration was used, ultimately resulting in completion of the desired transformation with 71% yield (Scheme 56, eq 6). This represents a modest increase in yield compared to a similar transformation reported by Ooi, but is operationally much more simple owing to the single step replacing three in the reported synthesis. A noted disadvantage of the approach reported here is the use of benzonitrile as solvent which is non-optimal for the installation of more substituted aryl groups.

Table 9. Early optimization of the hydroxylamine *N*-aryl amide synthesis



entry	X	base	Temp (°C)	additive/modification	Yield (%)
1	Br	K ₂ CO ₃	60	179 (0.05 equiv), Cl ₃ CCN (1 equiv)	3
2	Br	K ₂ CO ₃	60		16
3	Br	K ₂ CO ₃	60	NIS (1 equiv)	trace
4	Br	K ₂ CO ₃	60	H ₂ O (5 equiv)	15
5	Br	Na ₂ CO ₃	60		0
6	Br	NaHCO ₃	60		0
7	Br	KOH	60		13
8	Br	TEA or DMAP	60		1
9	Br	PBAM	60		0
10	Br	TMG	60		16
11	Br	Cs ₂ CO ₃	60		30
12	Br	CsOH	60		4
13	Br	none	60		0
14	Br	Cs ₂ CO ₃	60	isopentyl nitrite	15
15	Br	Cs ₂ CO ₃	60	O ₂	30
16	Br	Cs ₂ CO ₃	60	dark	26
17	Br	Cs ₂ CO ₃	rt		33
18	Br	Cs ₂ CO ₃	rt	TBAB (1 equiv)	21
19	Br	Cs ₂ CO ₃	rt	Selectfluor (1 equiv)	27
20	Br	Cs ₂ CO ₃	rt	NCS (1 equiv)	26
21	Br	Cs ₂ CO ₃	rt	CO ₂	0
22	Br	Cs ₂ CO ₃	rt	NaHSO ₃ (1 equiv)	29
23	Br	Cs ₂ CO ₃	rt	N ₂ H ₄ ·H ₂ O (1 equiv)	15
24	Cl	Cs ₂ CO ₃	60		43
25	F	Cs ₂ CO ₃	60		46
26 ^b	F	Cs ₂ CO ₃	rt		64

^aGeneral procedure: nitroalkane (1 equiv., 0.1 M), hydroxylamine (1.5 equiv.), and base (2 equiv) were sparged with Ar for ~2 min. The reaction was stirred overnight. ^b0.05 M. ^c3 equiv. base.

3.3.3.2 Use of Ooi's Triazolium Salt in Nitronate Amination

With the catalyst in hand, experiments applying it to the desired amidation could commence. Disappointingly, when the Ooi conditions were attempted with the Ooi catalyst **179** (instead of TBAI) (Table 9, entry 1) similar results were observed (using either the shown bromonitroalkane or fluoronitroalkane **83a**). This was a discouraging result, but it turned out to be the surprise we needed to set us down a productive line of study. The information we had gained to this point was that catalyst identity seems not to matter in the reaction, the hydroxylamine is not significantly forming a trichloroacetimidate, and despite these circumstances, some amide is forming. Reevaluating our view of what is occurring in this reaction made us consider if the catalyst and trichloroacetonitrile are even serving a purpose. Excitingly, leaving out the catalyst and activator in a control reaction led to a significant jump in yield from 3% to 16% (Table 9, entry 2).

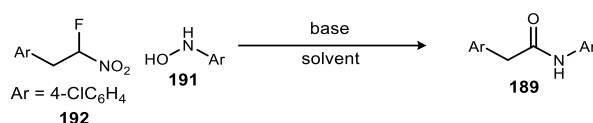
Additives including NIS (to activate the hydroxylamine) or water (to solubilize the base) had negative or little impact on the reaction respectively (Table 9, entries 3-4). Screening a number of organic and inorganic bases led to another notable increase in yield (Table 9, entries 5-13), but starting material was still being observed even after overnight heating at 60 °C. Based on past observations of UmAS and similar reactions, we considered that a nitrosylation reagent, an oxidant, or light exclusion could all have impacts on reactive intermediates, but none of these modifications to the standard conditions were helpful for amide formation (Table 9, entries 14-16). In fact, isopentyl nitrite was detrimental, an observation that highlights the major byproduct from these reactions. Azoxy (**190**) formation from hydroxyl amine oxidation/dimerization was consistently observed and tracked to give insights into reaction outcome. Significant effort was

also committed to applying the azoxy species as a substrate, but this structure is highly unreactive even under very forcing conditions.

Surprisingly, a drop in temperature to 20 °C (rt) gave similar to marginally improved yields of amide product (Table 9, entry 17). Another round of additives included TBAB (to serve as a phase transfer catalyst), Selectfluor or NCS (to activate the hydroxylamine or form a dihalo nitroalkane), CO₂ (to activate the hydroxylamine or a reactive intermediate as a carbonate), sodium bisulfite (to reduce an intermediate at too high of an oxidation state if nitroso species are at play), and hydrazine (to serve as a nucleophile in collapsing electrophilic intermediates) all failed to improve yield (Table 9, entries 18-23), but only CO₂ and N₂H₄ were significantly detrimental. Next the low reactivity was hypothesized to be a consequence of an insufficiently nucleophilic nitronate. This rationale plus the consistent observation of debrominated nitroalkane as a byproduct encouraged us to explore other halogens for the halo-nitroalkane (Table 9, entries 24-25). Both chloro and fluoro-nitroalkanes led to higher reactivity and better yield with fluorine being the optimal α -substituent. With this reagent system, full conversion could be observed after one day at room temperature. Dilution (Table 9, entry 26) was next discovered to increase the yield to 64%. These conditions gave a synthetically useful 64% yield for this test substrate combination and were very exciting, but we still sought further improvement. Namely, reactions at this point still exhibited incomplete conversion of the fluoronitroalkane and significant amounts of the azoxy byproduct.

A screen of redox active transition metal catalysts (RhCl₂, Pd(OAc)₂, RuCl₃, CuSO₄, CuBr₂, Cu(OAc)₂, CuI, AgOAc, NiCl₂, SnCl₂, Fe(BF₄)₂, FeBr₂, CoCl₂, Zn(ClO₄)₂, Mg(OAc)₂, and Cs₂Cr₂O₇) did not improve yields, so another optimization phase commenced. First, further dilution (Table 10, entry 2) gave no additional increase to yield, so other reaction parameters became the focus. Stirring (Table 10, entry 3), hydroxylamine equivalents (Table 10, entries 4-5), and temperature (Table 10, entries 6-7) were explored but found to be already optimal. Additives such as 4 Å mol sieves and trichloroacetonitrile (Table 10, entries 8-9) were also unhelpful.

Table 10. Final optimization of the hydroxylamine *N*-aryl amide synthesis



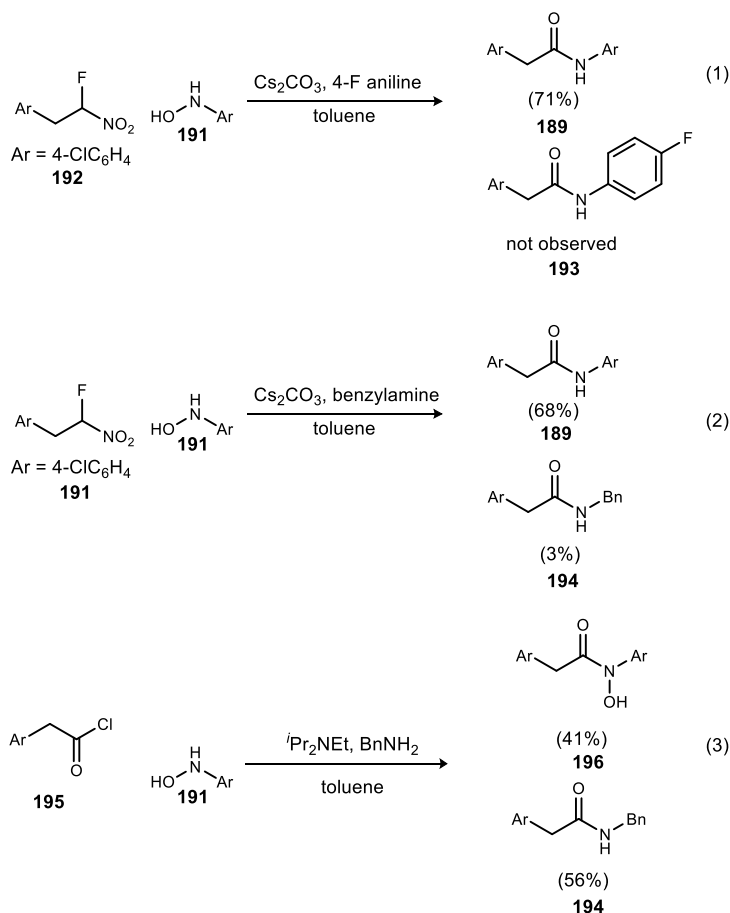
entry	solvent	base	temp (°C)	additive/modification	yield (%)
1	toluene	Cs ₂ CO ₃	rt		64
2 ^b	toluene	Cs ₂ CO ₃	rt		61
3	toluene	Cs ₂ CO ₃	rt	larger vial (better stirring)	60
4	toluene	Cs ₂ CO ₃	rt	3 equiv of hydroxylamine	62
5	toluene	Cs ₂ CO ₃	rt	hydroxylamine limiting reagent	49
6	toluene	Cs ₂ CO ₃	0		41
7	toluene	Cs ₂ CO ₃	150	5 min reaction time	24
8	toluene	Cs ₂ CO ₃	rt	4 Å mol sieves	44
9	toluene	Cs ₂ CO ₃	rt	Cl ₃ CCN (1 equiv)	23
10	MeCN	Cs ₂ CO ₃	rt		62
11	DME	Cs ₂ CO ₃	rt		29
12	MeCN	Cs ₂ CO ₃	rt	hydroxylamine added over 2 h	39
13	toluene	TMG	rt		38
14	toluene	Cs ₂ CO ₃	rt	18-crown-6 (2 equiv)	23
15	toluene	K ₂ CO ₃	rt		24
16	MeCN	K ₂ CO ₃	rt		56
17	toluene	K ₂ CO ₃	60		31
18	toluene	K ₂ CO ₃	rt	Cs ₂ CO ₃ (1 equiv)	73
19	toluene	K ₂ CO ₃	rt	Na ₂ SO ₄ (5 equiv), Cs ₂ CO ₃ (1 equiv)	71
20	xylenes	K ₂ CO ₃	rt	Cs ₂ CO ₃ (1 equiv)	75
21^c	toluene	Cs₂CO₃	rt		78

^aGeneral procedure: nitroalkane (1 equiv., 0.05 M), hydroxylamine (1.5 equiv.), and base (2 equiv) were sparged with Ar for ~2 min. The reaction was stirred overnight. ^b0.025 M. ^c3 equiv. base.

Screening other solvents showed acetonitrile to be competent but DME to be quite detrimental (Table 10, entries 10-11). Testing addition rate of hydroxylamine using MeCN as the reaction solvent in order to arrive at optimal concentrations of the hydroxylamine solution showed that the yield was negatively impacted relative to the control reaction (Table 10, entry 12). Other bases (focusing on those that gave the best results in the original Table 9 screen) were also not well tolerated (Table 10, entries 13-15), but K_2CO_3 in particular seemed to be mostly an issue of conversion. We attempted to address that issue using MeCN as solvent or higher temperatures to better solubilize the base, but while both modifications increased conversion, yields were still lower than when using Cs_2CO_3 (Table 10, entries 16-17). We also considered a mixture of K_2CO_3 and Cs_2CO_3 in order to maintain some base solubility but with a slower overall rate of deprotonation (Table 10, entry 18). Yield of amide increased with this combination, but did not significantly change when adding drying reagent or using xylenes as solvent (Table 10, entries 19-20). Ultimately, it was discovered that the source of the increased yield was simply the additional equivalent of base, so the final optimized conditions used 3 equivalents of Cs_2CO_3 (Table 10, entry 21).

3.3.4 Mechanistic Insights

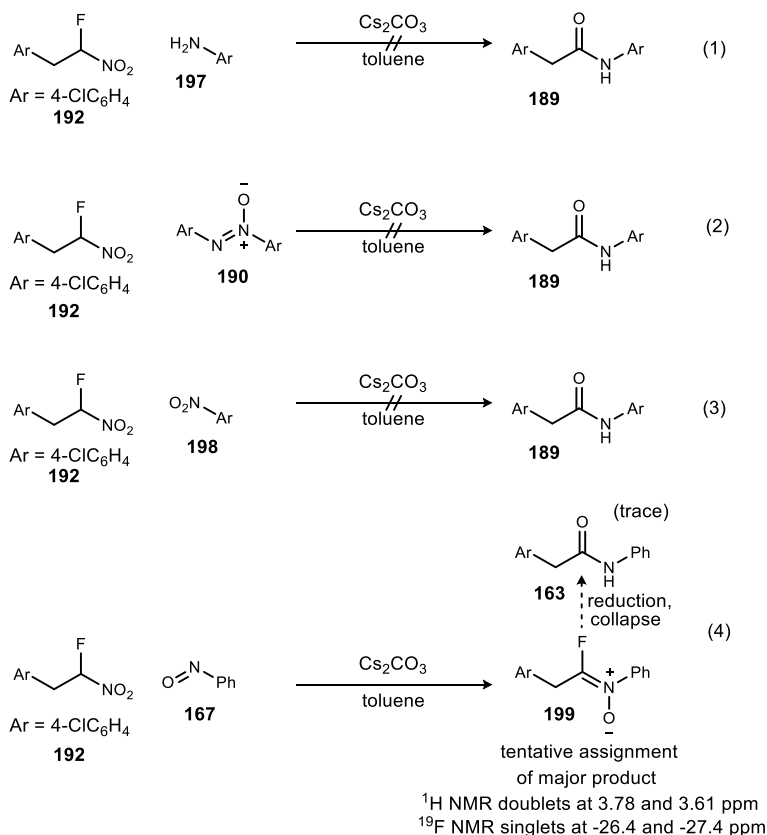
The most striking aspect of the optimized conditions is the lack of an activator for the hydroxylamine. While this finding leads to a significantly simpler and more accessible experimental setup it does beg the question whether this reaction is proceeding with the reversal of polarity that gives UmAS its name. If not, then an active ester or similar species could be at play and the epimerization-avoiding aspect of UmAS may be lost. To test this, competition reactions were devised where the hydroxylamine was forced to compete with a comparable nucleophile (4-fluoroaniline) or a significantly better nucleophile (benzylamine) (Scheme 57, eqs 1-2). These experiments showed no aniline-derived amide and only trace benzyl amine-derived **194**. Experiments probing the umpolung nature of this amination



amide despite significant conversion to the hydroxylamine derived amide. A contrasting result can be observed when the aryl hydroxylamine and benzylamine are reacted with an acyl chloride (Scheme 57, eq 3). Clearly, in that context the benzylamine is the more nucleophilic. These experiments support the umpolung paradigm, and the trace amide formed from benzylamine can be explained on the basis of minor competing mechanisms or the formation of oxidizing species that enable standard UmAS reactivity. Although suggestive of an umpolung mechanism, the competition experiments do not explain how that is possible given both reactants appear to be nucleophiles.

To further probe this conundrum, the reaction outcomes of a panel of potential nucleophiles

Scheme 58. Experiments probing various nitrogen sources in the amidation

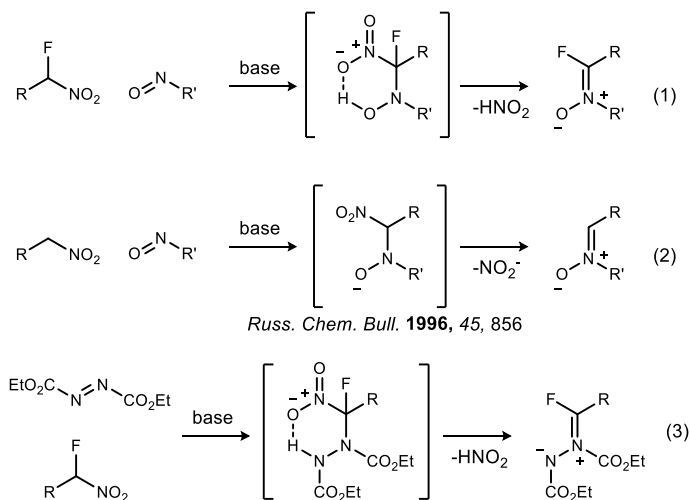


and electrophiles were compared to gain insights about which may be on-pathway to amide.

Starting with 4-Cl aniline (a potential reduction product of the hydroxylamine), no formation of an amide (Scheme 58, eq 1) occurred, suggesting it is not operative in this chemistry. The same result was also observed with the azoxy species known to form under the reaction conditions when using hydroxylamine, as well as the nitroarene (Scheme 58, eqs 2-3). A nitroso arene (an electrophile), however, gave a trace amount of the amide product alongside an unstable fluorine-containing compound as the major component in the crude mixture (Scheme 58, eq 4).

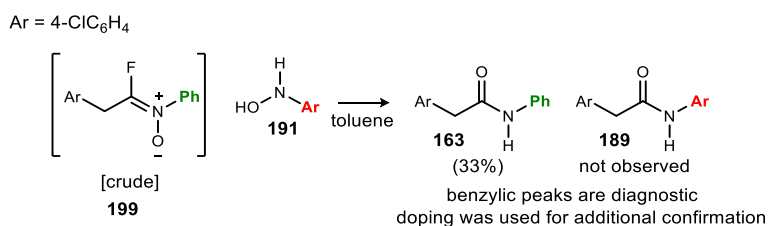
Unfortunately, isolation and derivation attempts on this and other analogues were unsuccessful; however, NMR of crude mixtures reveals a set of doublets at 3.78 and 3.61 ppm by ^1H NMR and a set of singlets at -26.4 and -27.4 ppm by ^{19}F NMR. Each set has ~1:0.3 ratio by integration, and non-decoupled ^{19}F experiments show that the fluorine is coupled to the ^1H doublets. The best explanation for the extremely deshielded fluorine coupled to a benzylic methylene is E and Z isomers of an α -fluoro nitron. This motif has been postulated

Scheme 59. Additional justification for α -fluoro nitron assignment



previously^{231,232} and other α -heteroatom nitrones are known,^{233,234} but we are unable to find any NMR data that may be useful for assignment through analogy. While attempts at structural confirmation by independent synthesis or derivatization were also unsuccessful, such a structure would be the direct result of HNO₂ elimination from the HANA this reagent combination is expected to give (Scheme 59, eq 1). Formation of nitrones in this way is well established (Scheme 59, eq 2).²³⁵

Previous work on UmAS also suggests that this elimination would be the favored pathway based on analogy to HANAs derived from azodicarboxylate electrophiles (Scheme 59, eq 3). An α -fluoro imine would also be consistent with the data described above, but it is not the favored theory because of relative water stability of the compound observed, and the lack of a reducing agent during its production. Analogy aside, we considered that the HANA in this work could proceed to amide through a radical. As will later be shown in the substrate scope (Table 11) several fluoro nitroalkanes with functionality set up to intramolecularly trap a radical were investigated **Scheme 60**. Crossover experiment demonstrating aryl group origin in amide product



²³¹ Sarantakis, D.; Sutherland, J.; Tortorella, C.; Tortorella, V. *ChemComm* **1966**, 105.

²³² Zhang, X. *J. Mol. Struct.* **2011**, *1002*, 121.

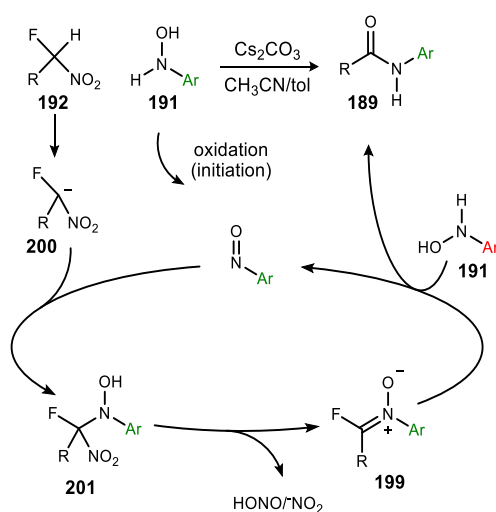
²³³ Voinov, M. A.; Shevelev, T. G.; Rybalova, T. V.; Gatilov, Y. V.; Pervukhina, N. V.; Burdukov, A. B.; Grigor'ev, I. A. *Organometallics* **2007**, *26*, 1607.

²³⁴ Voinov, M. A.; Grigor'ev, I. A. *Tetrahedron Lett.* **2002**, *43*, 2445.

²³⁵ Lyapkalo, I.; Ioffe, S.; Strelenko, Y. A.; Tartakovsky, V. *Russ. Chem. Bull.* **1996**, *45*, 856.

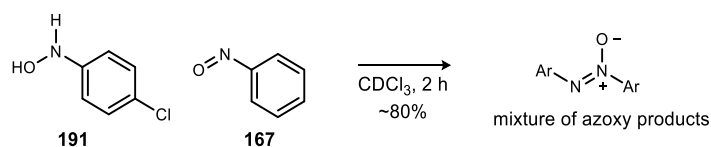
with no evidence for radical formation. TEMPO was also investigated as an exogenous radical trap, but an immediate quenching of the orange color upon exposure to the hydroxylamine and large quantity of azoxy found in the crude reaction mixture suggest the TEMPO immediately oxidized the hydroxylamine and consequently cannot serve as a radical trap.

Experiments to probe transformations of this presumed intermediate (**199**) demonstrate that it converts to amide under a number of conditions including exposure to water and heat, silica gel, **Scheme 61**. Partial mechanistic hypothesis



or hydroxylamine (Scheme 60). The competency of hydroxylamine in transforming the species to amide further supports its identity as an intermediate in the reaction conditions and forms the basis of the mechanistic hypothesis in Scheme 61. With a nitrosoarene acting as the electrophile in the reaction conditions, the question of polarity is addressed, but another question is raised. With the nitrogen electrophile at that oxidation state, a reduction must occur to generate an amide. This will be elaborated on below, but we suspect hydroxylamine serves as the reductant. This circumstance

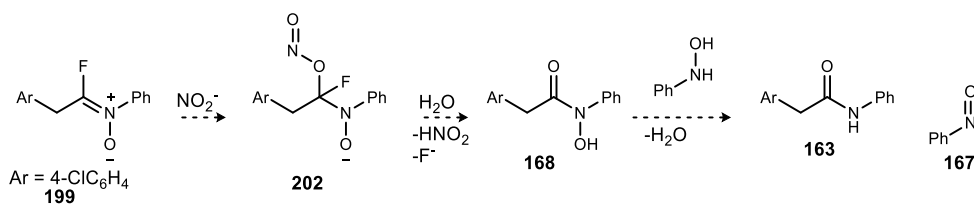
Scheme 62. Azoxy formation from hydroxylamine and nitroso compounds



leads to a truly fascinating triple role of hydroxylamine in the reaction as a pro-electrophile for the nitronate, nucleophile for the nitrone, and reducing agent to give amide and nitroso electrophile. The synergistic roles of the aryl hydroxylamine and nitroso arene are particularly unexpected given that NMR experiments mixing these species shows they quickly combine to form an azoxy compound which is a dead-end in this chemistry (Scheme 62). Here, the success of the amidation pathway is dependent on the competitive rate of azoxy formation.

As discussed above, it seems likely that, under the optimized reaction conditions, hydroxylamine is acting on the intermediate to generate the amide and regenerate the nitroso arene. Consequently, we were curious whether the aryl ring in the product was carried forward from the original nitroso upon which the halo nitroalkane acted (Scheme 61, in green) or if its origin is actually the hydroxylamine (Scheme 61, in red) that converts the intermediate to product. This question was answered using a crossover experiment. Tentatively assigned α -fluoro nitrone was prepared from nitrosobenzene. As a crude reaction mixture, this was converted to amide using *N*-(4-chlorophenyl)hydroxylamine (Scheme 60). A single amide was produced in this crossover reaction and its identity was confirmed as the unchlorinated one via sequential spiking with separately prepared authentic samples of both possible amides. This shows unambiguously that the aryl group in the α -fluoro nitrone carries forward to the product. Furthermore, the essential role of the aryl hydroxylamine in *N*-aryl amide production is documented.

Scheme 63. UmAS analogy mechanism for α -fluoro nitrone to amide conversion



Two possibilities remained likely regarding the mechanism of this new amidation. First, we considered that the reaction was proceeding from the α -fluoro nitrone to amide in a manner highly analogous to UmAS (nitro-nitrite isomerization then hydrolysis of the nitrite ester with loss of F^- and HNO_2 in Scheme 63). This would generate the hydroxamic acid which, in theory could be reduced by hydroxylamine to give amide and nitroso arene. While this reduction is not reported, the present work suggests *N*-aryl hydroxylamines are viable reductants (Scheme 62, Scheme 60), and *N*-aryl hydroxamic acids have been shown to be quite susceptible to reduction to the corresponding amides. Specifically, light or nucleophiles such as hydrazine can elicit reduction.^{236,237} This option fails to explain why significant conversion to hydroxamic acid is not observed when only preformed nitroso arene is used in the reaction. Another possibility is that the mechanism is fundamentally distinct from UmAS's after HANA formation. ^{18}O Labeling experiments clearly indicate that this is the case. Oxygen labeling has been consistently useful in studies of HANA behavior.^{88,160} The functional group has proven to be rather dynamic; offering many pathways to be exploited based on its environment. The main modes of reactivity can be summarized as 1) radical where homolytic loss of $\cdot NO_2$ leads to a carbon radical that is captured by $\cdot ONO$ or O_2 ,^{32, 88} or 2) polar where loss of HNO_2 (or $\cdot X$) precedes attack by $\cdot ONO$, water, or an intramolecular nucleophile.^{160,89,120} The polar mechanism seems to predominate only when an intramolecular, six-membered hydrogen bond system aids in HNO_2 elimination. Experimental evidence for the intermediacy of an α -fluoro nitrone, the lack of evidence for a radical pathway,

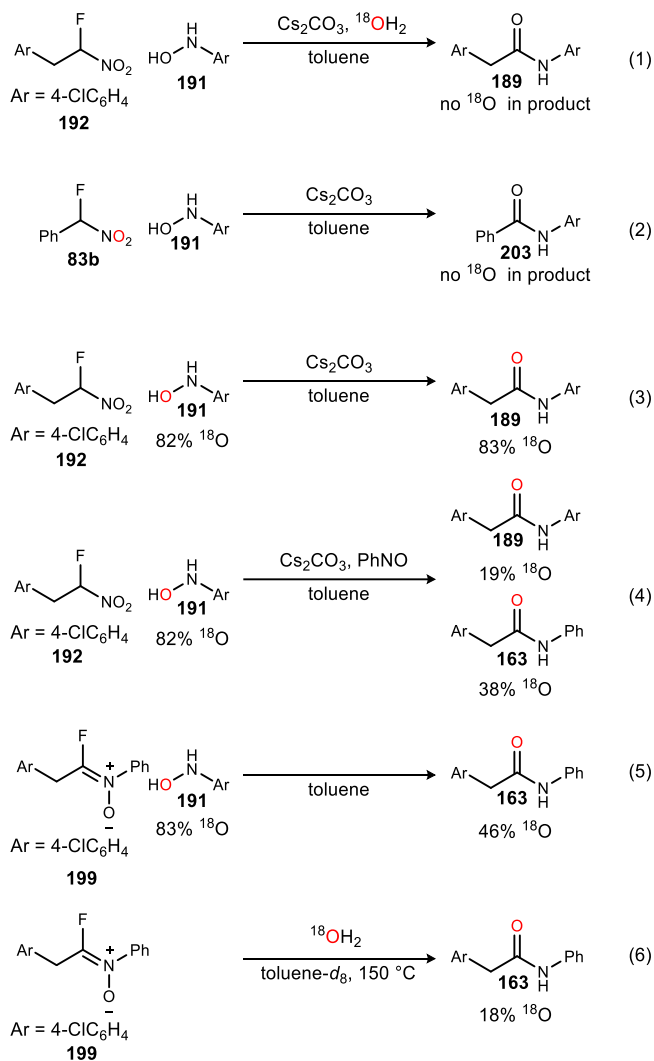
²³⁶ Robinson, C. H.; Gnoj, O.; Mitchell, A.; Wayne, E.; Townley, P.; Kabasakalian, P.; Oliveto, E. P.; Barton, D. H. *R. J. Am. Chem. Soc.* **1961**, 83, 1771.

²³⁷ Lipczynska-Kochany, E.; Iwamura, H.; Kochany, J. *Monatsh. Chem.* **1987**, 118, 1345.

and the opportunity for H-bond assisted elimination all indicate that this system follows a polar pathway.

Accordingly, water and the nitro group of the halo nitroalkane were examined as sources of the amide oxygen. Interestingly, when H_2^{18}O was added to the system, or when ^{18}O -labeled nitroalkane was used, no ^{18}O was incorporated into the product (Scheme 64, eq 1-2). The only

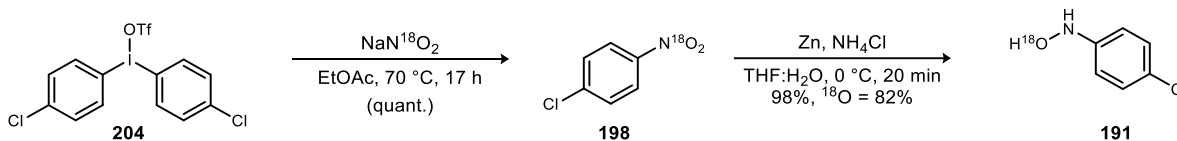
Scheme 64. ^{18}O labeling experiments



other oxygen containing-molecules in the reaction are those in the carbonate base and hydroxylamine (molecular oxygen should be minimal). Hydroxylamine seemed a more likely

candidate, and indeed, using an ^{18}O -labeled hydroxylamine led to amide product with high incorporation of the heavy isotope (Scheme 64, eq 3). The synthesis of ^{18}O labeled *N*-phenyl hydroxylamine (from ^{18}O nitrobenzene) has been reported previously,^{238,239} but those methods give a low degree of incorporation of the ^{18}O isotope, rely on reactions run in ^{18}O water, and are otherwise time consuming and tedious. A noted improvement can be achieved by using iodonium salts and labeled sodium nitrite (Scheme 65).²⁴⁰ To the best of our knowledge this work is the first application of these reactions for the preparation of ^{18}O -labeled materials, and the 98% yield over two steps, efficient use of labeled $\text{NaN}^{18}\text{O}_2$, and high (82%) degree of ^{18}O incorporation make this

Scheme 65. New route to ^{18}O labeled hydroxylamine



an attractive method.²⁴¹

With the source of amide oxygen confirmed, a number of targeted experiments tie the labeling studies (Scheme 64) to the above work with the presumed α -fluoro nitron (199). Assuming the assignment of the α -fluoro nitron (199) is correct, the most intuitive assessment of the mechanism would be oxaziridine formation followed by opening and reduction (Scheme 66, pathway 1). This agrees with ^{18}O -labeling experiments to this point, but no evidence for the

²³⁸ Nakamura, I.; Owada, M.; Jo, T.; Terada, M. *Org. Lett.* **2017**, *19*, 2194.

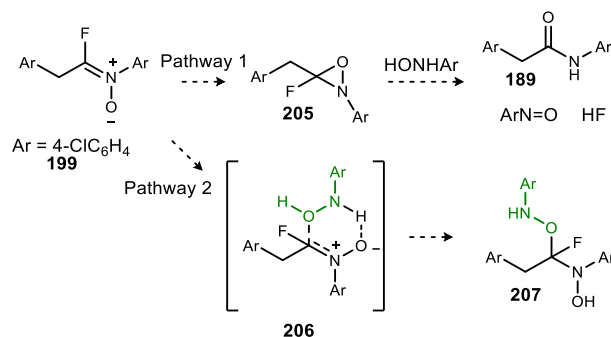
²³⁹ Rajendran, G.; Santini, R. E.; Van Etten, R. L. *J. Am. Chem. Soc.* **1987**, *109*, 4357.

²⁴⁰ Reitti, M.; Villo, P.; Olofsson, B. *Angew. Chem.* **2016**, *128*, 9074.

²⁴¹ We are grateful to Eric Huseman and Steve Townsend for providing iodonium salts used to ensure this route was worth pursuing.

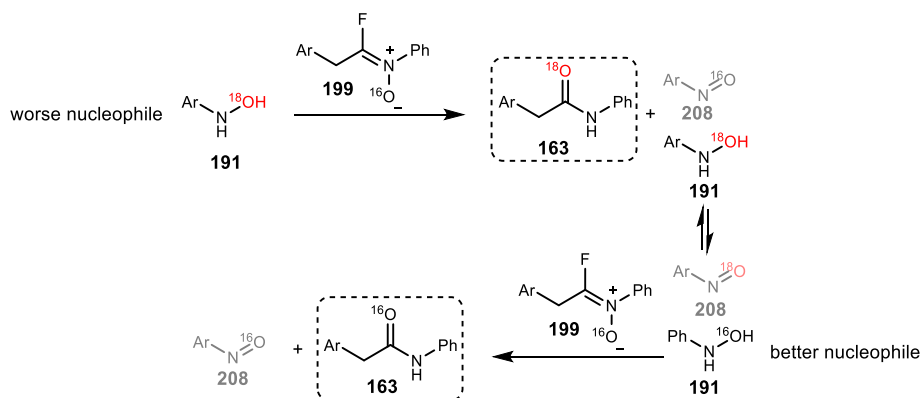
oxaziridine has been obtained when **199** is isolated in the absence of hydroxylamine. Furthermore,

Scheme 66. Possible mechanisms for α -F nitron collapse



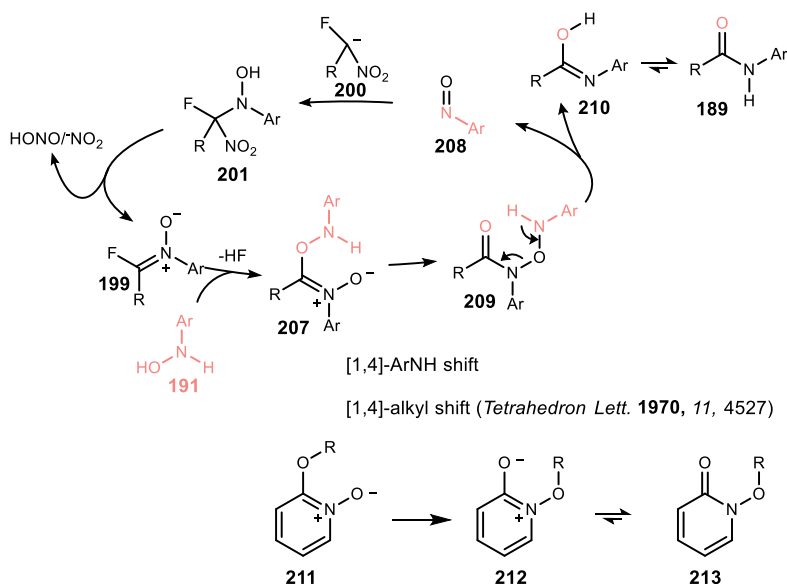
a crossover reaction adding unlabeled nitroso to the standard conditions using ¹⁸O-labeled hydroxylamine led to ¹⁸O in both amide products (Scheme 64, reaction 4). This is at odds with any mechanism involving intramolecular transfer of oxygen from N to C because these pathways would deliver the aryl group and oxygen to the same molecule and show no scrambling. This line of thinking only holds, however, if there is no oxygen scrambling prior to C-N bond formation. The control experiment in this case (mixing unlabeled nitroso and labeled hydroxylamine) gave some indication that oxygen scrambling is possible in that the labeling of the hydroxylamine fell slightly, but the drop was small and the other species were not observed in the mass spectrum so this could not be confirmed.

Scheme 67. ¹⁸O-labeling in preformed nitron collapse



Gratifyingly, more solid evidence for intermolecular delivery of oxygen occurring post C-N bond formation could be acquired by using preformed α -fluoro nitron in labeling studies. Subjecting unlabeled **199** to ^{18}O labeled hydroxylamine led to product with significant incorporation (Scheme 64, reaction 5). The incomplete labeling (46%) observed in the product might seem unexpected, but one must remember that, as the reaction proceeds, unlabeled nitroso is being generated (Scheme 67). This nitroso will be in fast redox equilibrium with the labeled hydroxylamine, so ^{16}O will be fed into the system. Even still, one could suspect high (~83%) labeling at the onset of the reaction with roughly halved (~42%) labeling at the end of the reaction to give amide with time-averaged labeling of ~63%. This doesn't account for the fact that the generated ^{16}O species (*N*-phenylhydroxylamine) is a better nucleophile than the ^{18}O labeled *N*-(4-chlorophenyl)hydroxylamine. Considering qualitatively the effect of the electron withdrawing halogen or quantitative parameters such as Hammett constants, a labeling of 46% seems reasonable.

Scheme 68. Detailed mechanistic hypothesis



It is also interesting to note that, under forcing conditions, water can serve as the source of amide oxygen when starting from the nitron (Scheme 64, eq 6). This result suggests that in the absence of hydroxylamine and under forcing conditions other nucleophiles can attack the nitron (199). This may explain why trace benzylamine-derived amide was observed in the competition reactions (Scheme 57, eq 2). With the growing body of mechanistic work in mind we came to favor nucleophilic attack of hydroxylamine at the nitron carbon (Scheme 66, pathway 2). It is curious that the α -fluoro nitron electrophile shows such a preference for hydroxylamine nucleophiles, but the answer to this behavior may lie in the principle of microscopic reversibility. In the way that a six-membered intramolecular H-bond system allows for HNO₂ elimination, the same may be true for nucleophilic attack (the reverse transformation). Hydroxylamines are uniquely situated among the potential nucleophiles to activate the nitron functionality with this hydrogen bonding (Scheme 66, pathway 2). Taken together, these experiments suggest the mechanistic proposal in Scheme 68. The exact steps between hydroxylamine attack of the α -fluoro nitron and product are difficult to study experimentally but one possibility is -NHAr transfer followed by loss of nitroso arene. Alkyl O to O transfer has been observed for ortho-alkoxy pyridine *N*-oxides (Scheme 68).²⁴²

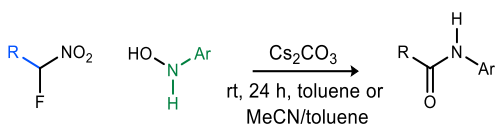
3.3.5 Reaction Scope and Application

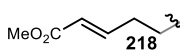
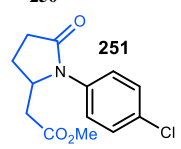
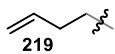

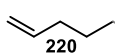
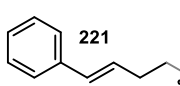
Throughout the mechanistic studies our goal remained to define the scope of the reaction using optimal reaction conditions. This ultimately led to an array of *N*-aryl amides prepared as

²⁴² Schöllkopf, U.; Hoppe, I. *Tetrahedron Lett.* **1970**, *11*, 4527.

shown in Table 11. The hydroxyl amine can contain electron donating (eg. **226**, **227**, **191**) or withdrawing groups (eg. **228**, **230**, **235**), as

Table 11. Reaction scope of umpolung *N*-aryl amide synthesis

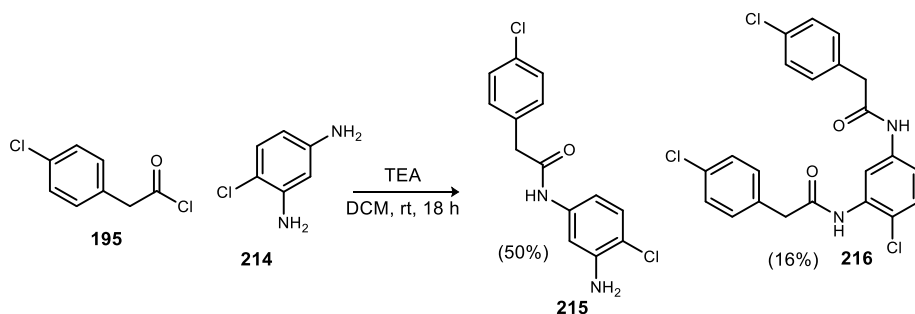


entry	solvent	R	Ar	product	yield (%)
1	toluene	4-Cl benzyl (192)	3-pyridyl-4-Cl (225)	237	76
2 ^b	toluene	4-Cl benzyl (192)	3-NH ₂ C ₆ H ₄ (226)	238	58
3	toluene	4-Cl benzyl (192)	4-OMeC ₆ H ₄ (227)	239	85
4	toluene	4-Cl benzyl (192)	3-CF ₃ C ₆ H ₄ (228)	240	65
5	toluene	4-Cl benzyl (192)	4-ClC ₆ H ₄ (191)	189	72 ^a
6	toluene	4-Cl benzyl (192)	Ph (166)	163	64
7	toluene	4-Cl benzyl (192)	6-benzothiazolyl (229)	241	37
8	toluene	4-Cl benzyl (192)	3,5-CO ₂ MeC ₆ H ₃ (230)	242	73
9	toluene	4-Cl benzyl (192)	2-pyridyl (231)	243	36
10	toluene	4-Cl benzyl (192)	2-pyridyl-4-CO ₂ Me (232)	244	36
11	toluene	4-Cl benzyl (192)	3-NH ₂ -4-ClC ₆ H ₃ (233)	215	55
12	toluene	4-Cl benzyl (192)	2-Cl-5-NH ₂ C ₆ H ₃ (234)	245	65
13	toluene	4-Cl benzyl (192)	4-CF ₃ C ₆ H ₄ (235)	246	62
14	toluene	4-Cl benzyl (192)	6-quinolinyl (236)	247	50
15	toluene/MeCN	4-FC ₆ H ₄ (83c)	4-ClC ₆ H ₄ (189)	248	71
16	toluene/MeCN	4-CF ₃ C ₆ H ₄ (83d)	4-ClC ₆ H ₄ (189)	249	66
17	toluene	CH ₂ CH ₂ Ph (217)	4-ClC ₆ H ₄ (189)	250	79
18	toluene	 218	4-ClC ₆ H ₄ (189)	 251	41
19	toluene	 219	4-ClC ₆ H ₄ (189)	252	76
20	xylenes	 105	4-ClC ₆ H ₄ (189)	253	76
21 ^c	toluene	 220	4-ClC ₆ H ₄ (189)	254	62
22 ^c	toluene	 221	4-ClC ₆ H ₄ (189)	255	76
23 ^c	toluene/MeCN	4-NO ₂ C ₆ H ₄ (83e)	4-ClC ₆ H ₄ (189)	256	60
24	toluene/MeCN	3-MeC ₆ H ₄ (222)	4-ClC ₆ H ₄ (189)	257	55
25	toluene/MeCN	2-FC ₆ H ₄ (223)	4-ClC ₆ H ₄ (189)	258	62
26	toluene	Et (224)	4-ClC ₆ H ₄ (189)	259	73

^a 85% on gram scale

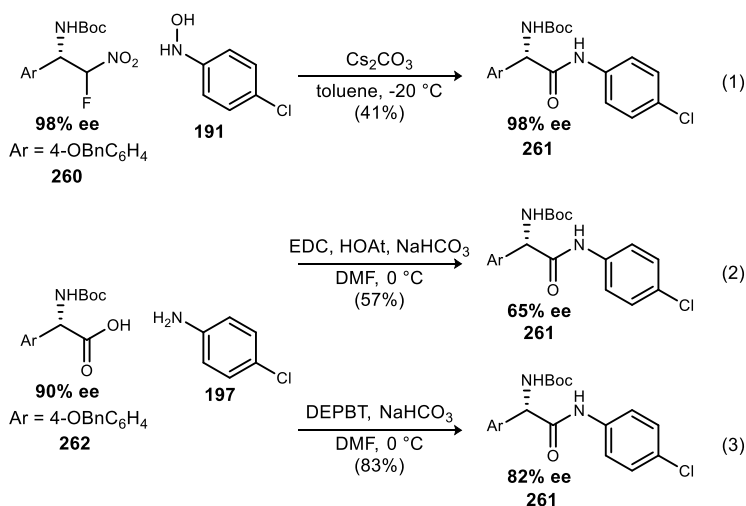
well as electron deficient heterocycles (eg. **236**, **225**). The reaction proceeded efficiently on gram scale (**189**) and the absence of coupling reagent by-products allows for simple trituration to afford clean product.

Scheme 69. A comparison of conventional amide synthesis to UmAS for regiospecific *N*-aryl amide formation



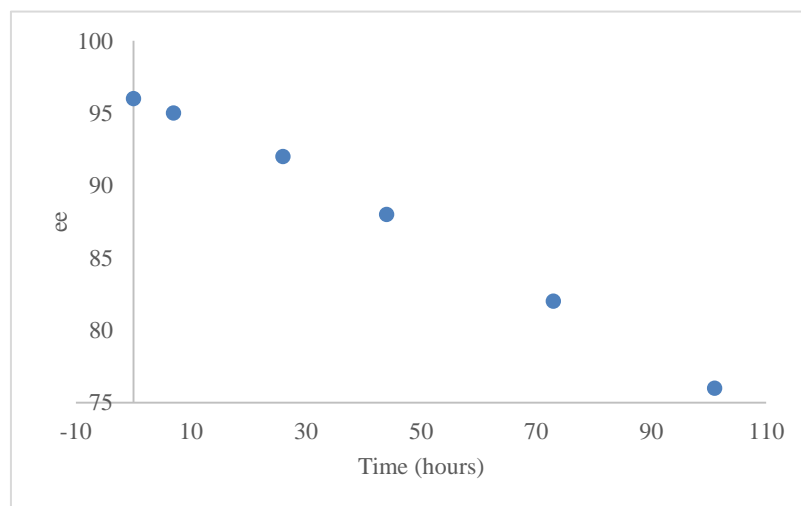
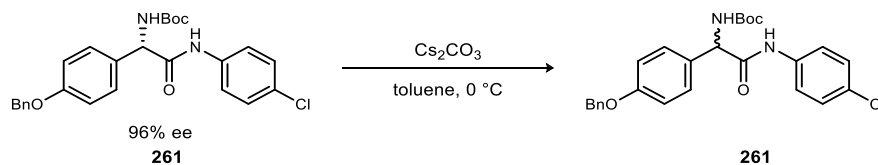
The ability to selectively acylate an *N*-aryl hydroxylamine in the presence of an unprotected amine underscores valuable orthogonality to standard amide synthesis. For example, both **215** and **245** can be prepared as a single regioisomer using this method (Table 11). In contrast, treatment of **214** with triethylamine and an acyl chloride (**195**) gives a mixture of mono and diacylated products (Scheme 69).

Scheme 70. Epimerization studies



The fluoro nitroalkane also has a general scope and may be aryl (eg. **83c**, **83d**, **222**, **223**) or alkyl (eg. **192**, **217**, **105**, **224**) and electron rich or electron-poor. Some reactions of cyclopropyl-substituted bromonitromethane are not stereospecific,⁴⁴ but **253** was obtained as a single diastereomer when starting from diastereopure fluoronitroalkane, suggesting a stereospecific reaction. This finding is complementary with our mechanistic studies, and serves as further evidence that a mechanism with radical intermediates is not operative.

Finally, the total stereoconservation observed in an α -amino amide substrate (**261**) is an exciting demonstration that the intermediates in this reaction do not suffer from the same proclivity for epimerization as do those in condensative amide synthesis (Scheme 70, eq 1). We selected an **Scheme 71**. Aryl glycine product epimerization



aryl glycine residue for several reasons. First, the presence of this motif in important natural

products^{243,244,245} underscores its relevance to complex molecule synthesis. Second, the ease of access of the requisite nitroalkanes using enantioselective methods⁶¹ highlights the value of the unique synthetic pathways opened by the umpolung approach. Finally, the difficulty in accessing the motif in an epimerization-free fashion through traditional amide synthesis provides a compelling justification for the development of new epimerization-free methods.^{246,247,248}

Our work not only shows complete stereoconservation in the reaction, but also suggests that the low temperatures employed to totally eliminate epimerization are only serving to prevent loss of enantioenrichment of the highly acidic product rather than any reaction intermediate. Epimerization studies on the product show that the final compound itself is so epimerization prone Cs_2CO_3 alone can erode its ee (Scheme 71). These results are particularly striking considering that the same amide was obtained from standard coupling with significant erosion of ee (Scheme 70, eqs 2-3). Because the product was independently shown to maintain enantioenrichment when resubjected to the standard coupling conditions, it follows that epimerization in these experiments is arising from active ester intermediates.

3.3.4.1 Synthesis of an Eli Lilly Glucokinase Activator

²⁴³ McCormick, M. H.; McGuire, J. M.; Pittenger, G. E.; Pittenger, R. C.; Stark, W. M. *Antibiotics annual* **1955**, 3, 606.

²⁴⁴ Townsend, C. A.; Brown, A. M. *J. Am. Chem. Soc.* **1983**, 105, 913.

²⁴⁵ Vértesy, L.; Aretz, W.; Knauf, M.; Markus, A.; Vogel, M.; Wink, J. *J. Antibiot.* **1999**, 52, 374.

²⁴⁶ Smith, G. G.; Sivakua, T. *J. Org. Chem.* **1983**, 48, 627.

²⁴⁷ Williams, R. M.; Hendrix, J. A. *Chem. Rev.* **1992**, 92, 889.

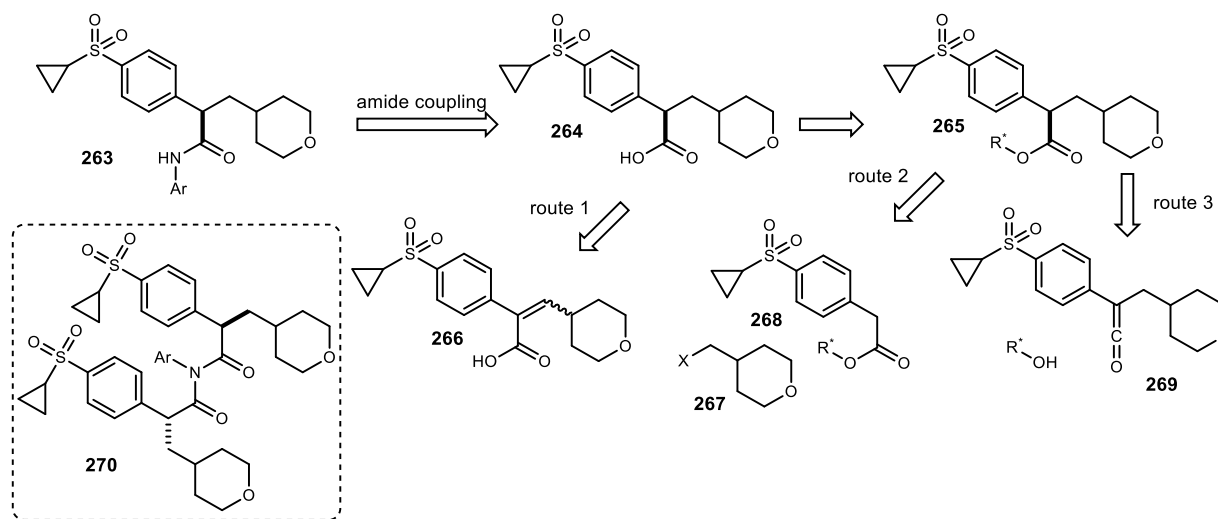
²⁴⁸ Al Toma, R. S.; Brieke, C.; Cryle, M. J.; Süßmuth, R. D. *Nat. Prod. Rep.* **2015**, 32, 1207.

As discussed throughout this document, the full value of UmAS and, by extension, the new methodology discussed in this chapter is clearest when considering synthetic pathways to molecules with a couple of structural features. The first feature is an epimerizable stereocenter located α to the amide being targeted. Epimerization-avoidance is a major advantage of the umpolung approach to amides. The substituents at the chiral center are also crucial. If chiral pool options are an impractical or inefficient source for the desired stereochemistry and enantioselective methods are to be employed, the umpolung approach allows for the leverage of the nitro group in an enantioselective transformation. Many molecules, especially those of significance in a pharmaceutical context, satisfy those criteria (see Figure 19 and Figure 20). A class of glucokinase activators patented by Eli Lilly²⁴⁹ caught our attention for its potential to spotlight umpolung *N*-aryl amide synthesis as well as an enantioselective methodology also being explored in the Johnston group.

²⁴⁹ Fyfe, M., C., T.; Proctor, M. J. Tricyclo Substituted Amides. WO2007051845A1, May 10, 2007.

The patent mentions that chiral separation, chiral auxiliaries, or high-pressure

Scheme 72. Retrosynthetic analysis of published routes to non-racemic Eli Lilly glucokinase inhibitors



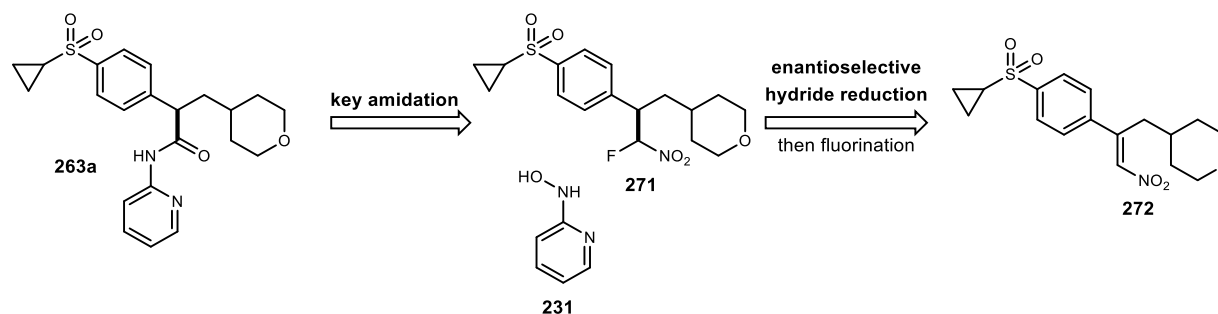
enantioselective hydrogenation using precious metals (Rh or Ru) can be employed to generate the enantioenriched carboxylic acid precursor **264** (Scheme 72, routes 1-2). More recently a ketene desymmetrization using a chiral alcohol in a stoichiometric amount has been reported (Scheme 72, route 3).^{250,251} An enantioselective, organocatalytic synthesis of this molecule would be a first and would have unique practical benefits compared to even the Rh/Ru hydrogenation which required additional manipulations to remove residual metal.²⁵¹ Additionally, the published conventional amide coupling required optimized and obscure conditions in order to eliminate epimerization.²⁰³ Furthermore, despite the effort put into optimizing conditions for the amide coupling, over acylation was observed to give undesired imide product **270**.

²⁵⁰ Yamagami, T.; Moriyama, N.; Kyuhara, M.; Moroda, A.; Uemura, T.; Matsumae, H.; Moritani, Y.; Inoue, I. *Org. Process Res. Dev.* **2014**, *18*, 437.

²⁵¹ DeBaillie, A. C.; Magnus, N. A.; Laurila, M. E.; Wepsiec, J. P.; Ruble, J. C.; Petkus, J. J.; Vaid, R. K.; Niemeier, J. K.; Mick, J. F.; Gunter, T. Z. *Org. Process Res. Dev.* **2012**, *16*, 1538.

We envisioned that final compound **263a** could be synthesized with an umpolung

Scheme 73. Retrosynthetic analysis for **263a**



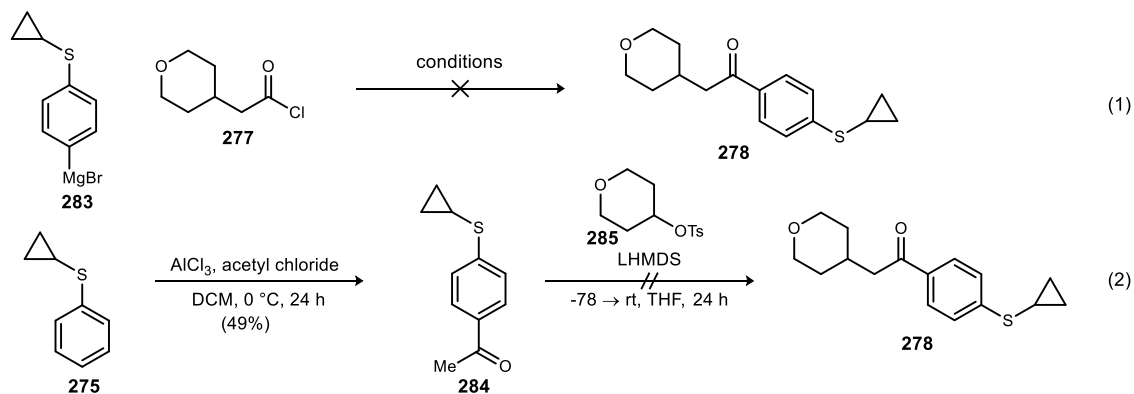
amidation (Scheme 73) to give not only stereoconservation but also exclusively mono-acylation. The nitro alkane partner (**271**) could be prepared from enantioselective, organocatalytic nitroalkene (**272**) reduction. This combination of steps should allow for mild conditions in the enantioselective step due to the nitro group's inherent reactivity and total retention of ee for the remainder of the sequence.

To start, synthesis of the Friedel-Crafts partners was straightforward and high-yielding, but the Friedel-Crafts reaction itself gave variable yield even after significant optimization (Scheme 74). Performing the acyl chloride (rather than forming it *in situ*) was important, as was order of addition and Lewis acid identity. Of several Lewis acids screened, a mixture of AlCl_3 and EtAlCl_2 gave the best results. The presence of $\text{Al}(\text{OH})_x$ species also seemed important as a new bottle gave lower yield. Due to the variability of the Friedel-Crafts, alternatives such as a Friedel Crafts with acetyl chloride followed by alkylation and a Grignard addition (Scheme 75, eqs 1-2) were explored but ultimately abandoned.

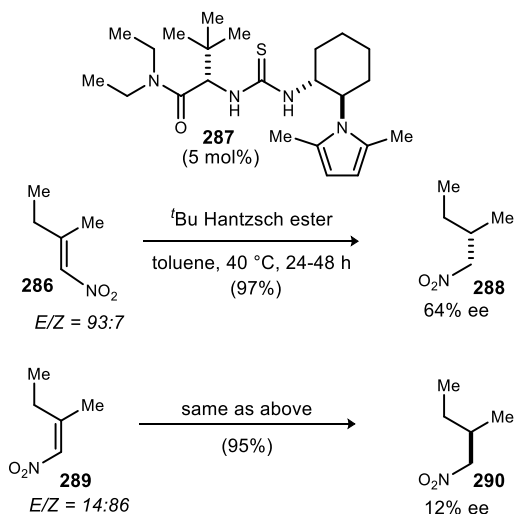
carefully controlled. Specifically, ample time (>12 h) must be allowed for ylide formation and the phosphonium salt must be finely ground. Otherwise no reactivity was observed.

The subsequent nitration (**280**→**272**) proved to be the largest hurdle in moving material forward. A satisfactory yield was obtained using an Fe(NO₃)₃/TEMPO system,²⁵² but other

Scheme 75. Attempted early-stage alternatives



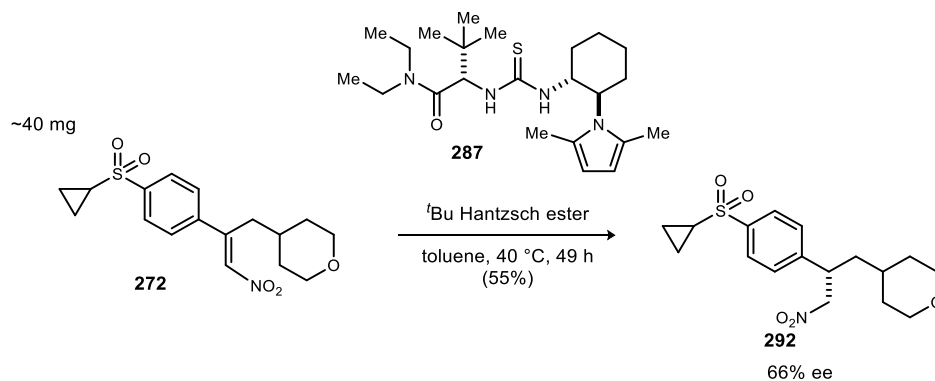
Scheme 76. Stereochemical outcome in List nitroalkene reduction as it relates to alkene geometry



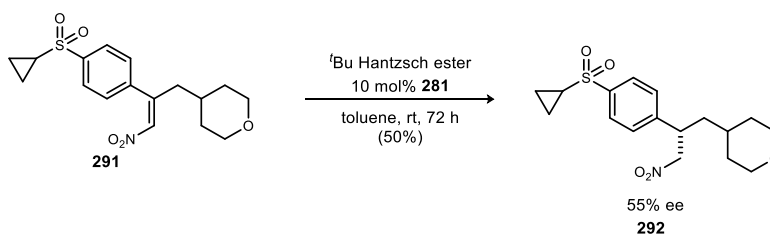
²⁵² Naveen, T.; Maity, S.; Sharma, U.; Maiti, D. *J. Org. Chem.* **2013**, *78*, 5949.

conditions²⁵³ were less ideal for this substrate. A reasonable (4:1) ratio of stereoisomers was obtained from the optimized conditions leading to a 54% yield of pure *E*-nitroalkene (**XX**) (assigned by NOE using both geometric isomers). The importance of the exclusion of *Z*-isomer was suspected based on work by the List group who showed it favors reduction from the opposite face when using a Jacobson-type thiourea catalyst (Scheme 76).⁸⁷

With the stage set for the enantioselective step, we first applied the List conditions (Scheme 77). The reaction applied to List's selection of substrates is primarily very enantioselective with ee's in the 90's in almost every example. However, the demonstrated substrates are structurally similar with few examples departing from 2-aryl-2-*n*-alkyl nitroalkanes. It was a setback to **Scheme 77**. Established organocatalytic enantioselective nitroalkene reduction



Scheme 78. *Z*-Nitroalkene reduction using catalyst **281**



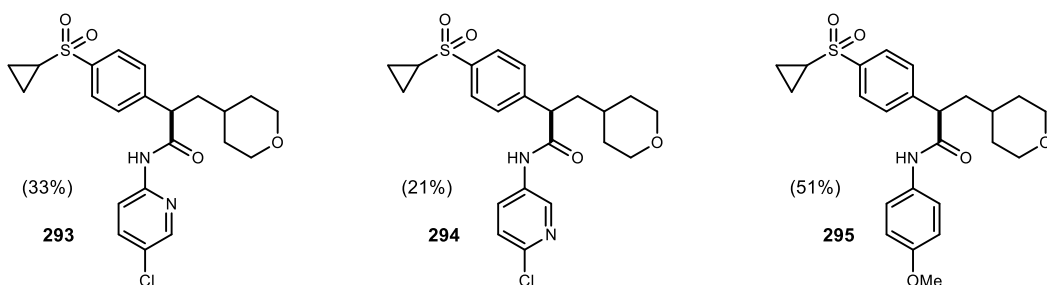
²⁵³ Yu, Y.-B.; Cheng, L.; Li, Y.-P.; Fu, Y.; Zhu, S.-F.; Zhou, Q.-L. *Chem. Commun.* **2016**, 52, 4812.

observe a low ee (66%) on this target relevant substrate. Excitingly, a catalyst scaffold in development by Zihang Deng for nitroalkene reduction gave markedly better results (Scheme 74). The optimized reaction used 1.65 equivalents of the Hantzsch ester added in two portions at room temperature. Despite the long reaction time (6d), the reaction was stirred at ambient temperature and delivered the desired molecule in 91% yield at 86% ee. Experiments were also performed using the *Z*-nitroalkene and this catalyst system confirming that it favors the formation of the undesired nitroalkane enantiomer and in low ee (Scheme 78).

The end game of the synthesis required a fluorination (which proceeded efficiently) and the amination developed in this chapter. This final amination (Scheme 74, **271**→**263a**) gave the patented molecule in 26% yield using cesium carbonate at low temperature. We were excited to obtain complete retention of stereochemistry when running the reaction at lowered temperature. Although the yield was low, it was in line with examples of 2-pyridyl hydroxylamines in the substrate scope (Table 11, **243** and **244**). Recall that low amide yields are usually reflective of a slow UmAS reaction, and this allows the azoxy formation to consume hydroxylamine. Also, considering that this highly polar component may be only sparingly soluble in toluene, toluene/acetonitrile mixtures were explored, but yields did not improve. To the first point, our observations of the hydroxylamine used in this reaction convince us that it is highly unstable, decomposing upon sitting at rt or concentration. To address this, a portion-wise addition of additional equivalents of hydroxylamine over two hours was implemented, but to no avail. Later NMR experiments indicated that a more spread-out addition timeframe may be beneficial. Dosing of additional hydroxylamine over three days or establishing an O₂ atmosphere to jump-start nitroso formation gave no improvement. Increasing temperature had a slight positive impact on yield, but at the expense of product ee. To further probe the generality of the reaction, a separate analogue

from the same patent as well as two previously unsynthesized analogues were prepared in low to moderate yield (Scheme 79).

Scheme 79. Other analogues in the Eli Lilly glucokinase activator series



3.3.6 Conclusions

An extensive search for a nitronate/*N*-aryl nitrogen electrophile combination which could give an *N*-aryl amide-producing HANA has led to the surprising combination of hydroxylamines and α -fluoro nitroalkanes. The conditions are exquisitely simple, using only a cheap carbonate base. The reaction is reasonably general, giving good yields for a broad scope of substrates. One exception is the 2-pyridiyl hydroxylamines necessary for the enantioselective synthesis of a Lilly lead compound. These were found to give more modest yields. Complete retention of α -stereocenters is achieved so long as the product is stable to carbonate base at low temperatures (a stark contrast to conventional methods).

Thorough mechanistic studies suggest a pathway involving a HANA but with a collapse that is fundamentally distinct from all previously reported reactions involving the intermediate. The proposed mechanism, in addition to being supported by ^{18}O labeling, intermediate observation, and control/crossover/competition experiments, is harmonious with descriptions of collapse-determining factors discussed in Chapter 2, and further establishes HANAs as a versatile

and valuable functional motif. In total the reaction has been demonstrated on ~30 substrates, including a gram-scale synthesis, and application to a pharmaceutically-relevant molecule.

References

- Adam, W.; Harrer, H. M.; Kita, F.; Korth, H.-G.; Nau, W. M. *J. Org. Chem.* **1997**, *62*, 1419.
- Adamo, C.; Barone, V. *J. Chem. Phys.* **1998**, *108*, 664.
- Adams, H.; Anderson, J. C.; Peace, S.; Pennell, A. M. *J. Org. Chem.* **1998**, *63*, 9932.
- Ağirbas, H.; Jackson, R. A. *Journal of the Chemical Society, Perkin Transactions 2* **1983**, 739.
- Al Toma, R. S.; Brieke, C.; Cryle, M. J.; Süßmuth, R. D. *Nat. Prod. Rep.* **2015**, *32*, 1207.
- Alfrey Jr, T.; Price, C. C. *Journal of Polymer Science* **1947**, *2*, 101.
- Amin, M. R.; Dekker, L.; Hibbert, D. B.; Ridd, J. H.; Sandall, J. P. B. *J. Chem. Soc., Chem. Commun.* **1986**, 658.
- Anderson, J. E.; Lehn, J. M. *Tetrahedron* **1968**, *24*, 123.
- Anderson, J. E.; Lehn, J. M. *Tetrahedron* **1968**, *24*, 137.
- Arai, T.; Matsumura, E. *Synlett* **2014**, *25*, 1776.
- Ashtekar, K. D.; Marzijarani, N. S.; Jaganathan, A.; Holmes, D.; Jackson, J. E.; Borhan, B. *J. Am. Chem. Soc.* **2014**, *136*, 13355.
- Aulakh, V. S.; Ciufolini, M. A. *J. Am. Chem. Soc.* **2011**, *133*, 5900.
- Azizi, K.; Heydari, A. *Synlett* **2018**, *29*, 189.
- Baldwin, S. W.; Young, B. G.; McPhail, A. T. *Tetrahedron Lett.* **1998**, *39*, 6819.
- Bamberger, E.; Lorenzen, J. *Ber. Dtsch. Chem. Ges.* **1892**, 3539.
- Bamberger, E.; Wheelwright, E. W. *J. Prakt. Chem.* **1902**, 123.
- Bamberger, E.; Wulz, P. *Berichte der deutschen chemischen Gesellschaft* **1891**, *24*, 2055.
- Banks, B. J.; Barrett, A. G. M.; Russell, M. A. *J. Chem. Soc., Chem. Commun.* **1984**, 670.
- Barrett, A. G. M.; Cheng, M. C.; Spilling, C. D.; Taylor, S. J. *J. Org. Chem.* **1989**, *54*, 992.
- Barrett, A. G. M.; Graboski, G. G.; Russell, M. A. *J. Org. Chem.* **1986**, *51*, 1012.

Barrett, A. G.; Cheng, M. C.; Spilling, C. D.; Taylor, S. J. *J. Org. Chem.* **1989**, *54*, 992.

Baum, K.; Archibald, T. G.; Tzeng, D.; Gilardi, R.; Flippen-Anderson, J. L.; George, C. *J. Org. Chem.* **1991**, *56*, 537.

Becke, A. D. *J. Chem. Phys.* **1993**, *98*, 5648.

Beenen, M. A.; Weix, D. J.; Ellman, J. A. *J. Am. Chem. Soc.* **2006**, *128*, 6304.

Benoiton, L. *Can. J. Chem.* **1968**, *46*, 1549.

Benson, S. W. *J. Chem. Educ.* **1965**, *42*, 502.

Bera, K.; Namboothiri, I. N. N. *J. Org. Chem.* **2015**, *80*, 1402.

Blaquiere, N.; Villemure, E.; Staben, S. T. *J. Med. Chem.* **2020**.

Blomquist, A. T.; Shelley, T. H. *J. Am. Chem. Soc.* **1948**, *70*, 147.

Bode Jeffrey, W.; Fox Ryan, M.; Baucom Kyle, D. *Angew. Chem. Int. Ed.* **2006**, *45*, 1248.

Böge, N.; Krüger, S.; Schröder, M.; Meier, C. *Synthesis* **2007**, *2007*, 3907.

Bøgevig, A. J. *Angew. Chem. Int. Ed* **2002**, *41*, 1790.

Bombek, S.; Požgan, F.; Kočevan, M.; Polanc, S. *J. Org. Chem.* **2004**, *69*, 2224.

Bordwell, F. G.; Bartmess, J. E. *J. Org. Chem.* **1978**, *43*, 3101.

Bordwell, F. G.; Satish, A. V. *J. Am. Chem. Soc.* **1994**, *116*, 8885.

Borsche, W.; Diacont, K. *Ann.* **1934**, *510*, 287.

Campbell, M. M.; Cosford, N.; Zongli, L.; Sainsbury, M. *Tetrahedron* **1987**, *43*, 1117.

Cancès, E.; Mennucci, B.; Tomasi, J. *J. Chem. Phys.* **1997**, *107*, 3032.

Carrieri, A.; Muraglia, M.; Corbo, F.; Pacifico, C. *Eur. J. Med. Chem.* **2009**, *44*, 1477.

Chan, W.-K.; Ho, C.-M.; Wong, M.-K.; Che, C.-M. *J. Am. Chem. Soc.* **2006**, *128*, 14796.

Chattaway, F.; Lye, R. *Journal of the Chemical Society (Resumed)* **1933**, 480.

Cho, S. H.; Yoo, E. J.; Bae, I.; Chang, S. *J. Am. Chem. Soc.* **2005**, *127*, 16046.

Chudasama, V.; Ahern, J. M.; Dhokia, D. V.; Fitzmaurice, R. J.; Caddick, S. *Chem. Commun.* **2011**, *47*, 3269.

Ciufolini, M. A.; Lefranc, D. *Nat. Prod. Rep.* **2010**, *27*, 330.

Constable, D. J.; Dunn, P. J.; Hayler, J. D.; Humphrey, G. R.; Leazer Jr, J. L.; Linderman, R. J.; Lorenz, K.; Manley, J.; Pearlman, B. A.; Wells, A. *Green Chem.* **2007**, *9*, 411.

Corte, J. R.; Pinto, D. J.; Fang, T.; Osuna, H.; Yang, W.; Wang, Y.; Lai, A.; Clark, C. G.; Sun, J.-H.; Rampulla, R. *J. Med. Chem.* **2020**, *63*, 784.

Cousin, S. F.; Kadeřávek, P.; Haddou, B.; Charlier, C.; Marquardsen, T.; Tyburn, J. M.; Bovier, P. A.; Engelke, F.; Maas, W.; Bodenhausen, G. *Angew. Chem. Int. Ed.* **2016**, *55*, 9886.

Creary, X. *Acc. Chem. Res.* **2006**, *39*, 761.

Crocker, M. S.; Foy, H.; Tokumaru, K.; Dudding, T.; Pink, M.; Johnston, J. N. *Chem* **2019**, *5*, 1248.

Davis, T. A.; Danneman, M. W.; Johnston, J. N. *Chem. Commun.* **2012**, *48*, 5578.

Davis, T. A.; Dobish, M. C.; Schwieter, K. E.; Chun, A. C.; Johnston, J. N. *Org. Synth.* **2012**, *89*, 380.

Davis, T. A.; Johnston, J. N. *Chem. Sci.* **2011**, *2*, 1076.

Davis, T. A.; Wilt, J. C.; Johnston, J. N. *J. Am. Chem. Soc.* **2010**, *132*, 2880.

Davis, T. *Org. Lett.* **2010**, *12*, 5744.

Dawson, P. E.; Muir, T. W.; Clark-Lewis, I.; Kent, S. B. *Science* **1994**, *266*, 776.

De Vleeschouwer, F.; Van Speybroeck, V.; Waroquier, M.; Geerlings, P.; De Proft, F. *Org. Lett.* **2007**, *9*, 2721.

Dean, J. A. *Lange's handbook of chemistry*; McGraw-Hill, 1992.

DeBaillie, A. C.; Magnus, N. A.; Laurila, M. E.; Wepsiec, J. P.; Ruble, J. C.; Petkus, J. J.; Vaid, R. K.; Niemeier, J. K.; Mick, J. F.; Gunter, T. Z. *Org. Process Res. Dev.* **2012**, *16*, 1538.

Dekić, B. R.; Radulović, N. S.; Dekić, V. S.; Vukićević, R. D.; Palić, R. M. *Molecules* **2010**, *15*, 2246.

Dennington, R.; Keith, T.; Millam, J. GaussView, version 5; Semichem Inc.: Shawnee Mission, KS, **2009**.

Dhotare, B. B.; Kumar, M.; Nayak, S. K. *J. Org. Chem.* **2018**, *83*, 10089.

Dieter, R. K. *Tetrahedron* **1999**, *55*, 4177.

Dong, X.; Zhou, X.; Jing, H.; Chen, J.; Liu, T.; Yang, B.; He, Q.; Hu, Y. *Eur. J. Med. Chem.* **2011**, *46*, 5949.

Dunetz, J. R.; Berliner, M. A.; Xiang, Y.; Houck, T. L.; Salingue, F. H.; Chao, W.; Yuandong, C.; Shenghua, W.; Huang, Y.; Farrand, D. *Org. Process Res. Dev.* **2012**, *16*, 1635.

Dunetz, J. R.; Magano, J.; Weisenburger, G. A. *Org. Process Res. Dev.* **2016**, *20*, 140.

Dust, J. M.; Arnold, D. R. *J. Am. Chem. Soc.* **1983**, *105*, 1221.

El-Safty, S. A.; Prabhakaran, D.; Ismail, A. A.; Matsunaga, H.; Mizukami, F. *Adv. Funct. Mater.* **2007**, *17*, 3731.

Engstrom, J. P.; Greene, F. D. *J. Org. Chem.* **1972**, *37*, 968.

Erdik, E. *Tetrahedron* **2004**, *60*, 8747.

Faisca Phillips, A. M.; Guedes da Silva, M. F. C.; Pombeiro, A. J. *Front. Chem.* **2020**, *8*, 30.

Famulok, M.; Boche, G. *Angew. Chem.* **1989**, *101*, 470.

Famulok, M.; Bosold, F.; Boche, G. *Tetrahedron Lett.* **1989**, *30*, 321.

Fauq, A. H.; Simpson, K.; Maharvi, G. M.; Golde, T.; Das, P. *Bioorg. Med. Chem. Lett.* **2007**, *17*, 6392.

Favrel, Bull. Soc. Chim. France, **1927**, *4*, 1494.

Feofilaktov and Onishchenko, *J. Gen. Chem. U.S.S.R.*, **1939**, 325.

Fini, F.; Sgarzani, V.; Pettersen, D.; Herrera, R. P.; Bernardi, L.; Ricci, A. *Angew. Chem. Int. Ed.* **2005**, *44*, 7975.

Fischer, D. F.; Xin, Z. q.; Peters, R. *Angew. Chem. Int. Ed.* **2007**, *46*, 7704.

Fischer, E.; Otto, E. *Ber. Deutsch. Chem. Ges* **1903**, *36*, 2106.

Fisher, T.; Meierhoefer, A. *J. Org. Chem.* **1978**, *43*, 224.

Franck, J.; Rabinowitsch, E. *Transactions of the Faraday Society* **1934**, *30*, 120.

Frisch, M. J.; Trucks, G. W.; Schlegel, H. B.; Scuseria, G. E.; Robb, M. A.; Cheeseman, J. R.; Scalmani, G.; Barone, V.; Mennucci, B.; Petersson, G. A.; Nakatsuji, H.; Caricato, M.; Li, X.; Hratchian, H. P.; Izmaylov, A. F.; Bloino, J.; Zheng, G.; Sonnenberg, J. L.; Hada, M.; Ehara, M.; Toyota, K.; Fukuda, R.; Hasegawa, J.; Ishida, M.; Nakajima, T.; Honda, Y.; Kitao, O.; Nakai, H.; Vreven, T.; Montgomery, J. A., Jr.; Peralta, J. E.; Ogliaro, F.; Bearpark, M.; Heyd, J. J.; Brothers, E.; Kudin, K. N.; Staroverov, V. N.; Kobayashi, R.; Normand, J.; Raghavachari, K.; Rendell, A.; Burant, J. C.; Iyengar, S. S.; Tomasi, J.; Cossi, M.; Rega, N.; Millam, J. M.; Klene, M.; Knox, J. E.; Cross, J. B.; Bakken, V.; Adamo, C.; Jaramillo, J.; Gomperts, R.; Stratmann, R. E.; Yazyev, O.; Austin, A. J.; Cammi, R.; Pomelli, C.; Ochterski, J. W.; Martin, R. L.; Morokuma, K.; Zakrzewski, V. G.; Voth, G. A.; Salvador, P.; Dannenberg, J. J.; Dapprich, S.; Daniels, A. D.; Farkas, O.; Foresman, J. B.; Ortiz, J. V.; Cioslowski, J.; Fox, D. J. Gaussian 09, revision D.01; Gaussian, Inc.: Wallingford, CT, **2013**.

Fusco, R.; Romani, R. *Gazz. Chim. Ital.* **1946**, *76*, 419.

Fyfe, M., C., T.; Proctor, M. J. Tricyclo Substituted Amides. WO2007051845A1, May 10, 2007.

Galletti, F.; Zheng, W.; Gopalakrishnan, M.; Rutledge, A.; Triggle, D. J. *Eur. J. Pharmacol.* **1991**, *195*, 125.

Goddard-Borger, E. D.; Stick, R. V. *Org. Lett.* **2007**, *9*, 3797.

Goodman, M.; McGahren, W. J. *J. Am. Chem. Soc.* **1966**, *88*, 3887.

Greene, F. D.; Berwick, M. A.; Stowell, J. C. *J. Am. Chem. Soc.* **1970**, *92*, 867.

Gunanathan, C.; Ben-David, Y.; Milstein, D. *Science* **2007**, *317*, 790.

Handa, S.; Gnanadesikan, V.; Matsunaga, S.; Shibasaki, M. *J. Am. Chem. Soc.* **2010**, *132*, 4925.

Hansch, C.; Leo, A.; Taft, R. *Chem. Rev.* **1991**, *91*, 165.

Hantzsch, A.; Thompson, K. J. *Ber. Dtsch. Chem. Ges.* **1905**, 2266.

Hartshorn, M.; Martyn, R.; Vaughan, J.; Wright, G. *Aust. J. Chem.* **1983**, *36*, 839.

Hartshorn, M.; Robinson, W.; Wright, G.; Cheng, L. *Aust. J. Chem.* **1989**, *42*, 1569.

He, C.; Chen, C.; Cheng, J.; Liu, C.; Liu, W.; Li, Q.; Lei, A. *Angew. Chem. Int. Ed.* **2008**, *47*, 6414.

He, Y.; Hwang, D.-J.; Ponnusamy, S.; Thiyagarajan, T.; Mohler, M. L.; Narayanan, R.; Miller, D. D. *J. Med. Chem.* **2020**.

Henry, L. *Bull. Cl. Sci., Acad. R. Belg.* **1896**, *32*, 33.

Hochstein, W.; Schöllkopf, U. *Ann.* **1978**, *1978*, 1823.

Hodgson, H. H.; Marsden, E. *J. Chem. Soc.* **1937**, 1365.

Howell, J. M.; Liu, W.; Young, A. J.; White, M. C. *J. Am. Chem. Soc.* **2014**, *136*, 5750.

Hu, Y.; Li, C.-Y.; Wang, X.-M.; Yang, Y.-H.; Zhu, H.-L. *Chem. Rev.* **2014**, *114*, 5572.

Hurd, C. D.; Strong, J. S. *J. Am. Chem. Soc.* **1950**, *72*, 4813.

Hynes, P. S.; Stuppel, P. A.; Dixon, D. J. *Org. Lett.* **2008**, *10*, 1389.

Islam, M. A.; Zhang, Y.; Wang, Y.; McAlpine, S. R. *MedChemComm* **2015**, *6*, 300.

Ito, R.; Migita, T.; Morikawa, N.; Simamura, O. *Tetrahedron* **1965**, *21*, 955.

Jaffé, H. H. *Chem. Rev.* **1953**, *53*, 191.

Jain, A. K.; Sharma, S.; Vaidya, A.; Ravichandran, V.; Agrawal, R. K. *Chem. Biol. Drug Des.* **2013**, *81*, 557.

Jakubec, P.; Cockfield, D. M.; Dixon, D. J. *J. Am. Chem. Soc.* **2009**, *131*, 16632.

Japp, F. R.; Klingemann, F. *Ber. Dtsch. Chem. Ges.* **1888**, 549.

Jiang, X.; Ji, G. *J. Org. Chem.* **1992**, *57*, 6051.

John, J.; Thomas, J.; Parekh, N.; Dehaen, W. *Eur. J. Org. Chem.* **2015**, *2015*, 4922.

Jones, E. C. S.; Kenner, J. *J. Chem. Soc.* **1930**, 919.

Juwarker, H.; Lenhardt, J. M.; Pham, D. M.; Craig, S. L. *Angew. Chem. Int. Ed.* **2008**, *47*, 3740.

Kamimura, A.; Gunjigake, Y.; Mitsudera, H.; Yokoyama, S. *Tetrahedron Lett.* **1998**, *39*, 7323.

Keneford, J. R.; Simpson, J. C. E. *J. Chem. Soc.* **1947**, 917.

Khrapkovskii, G.; Nikolaeva, E.; Chachkov, D.; Shamov, A. *Russ. J. Gen. Chem.* **2004**, *74*, 908.

Kim, M. H.; Kim, J. *J. Org. Chem.* **2018**, *83*, 1673.

Kobayashi, S.; Ishitani, H. *Chem. Rev.* **1999**, *99*, 1069.

Kovacic, P.; Lowery, M. K.; Field, K. W. *Chem. Rev.* **1970**, *70*, 639.

Kruckeberg, J. *prakt. Chem.*, **1894**, 321.

Kumaraswamy, G.; Pitchaiah, A. *Tetrahedron* **2011**, *67*, 2536.

LaMarche, M. J.; Leeds, J. A.; Amaral, A.; Brewer, J. T.; Bushell, S. M.; Deng, G.; Dewhurst, J. M.; Ding, J.; Dzink-Fox, J.; Gamber, G. *J. Med. Chem.* **2012**, *55*, 2376.

Lan, Q.; Wang, X.; He, R.; Ding, C.; Maruoka, K. *Tetrahedron Lett.* **2009**, *50*, 3280.

Lee, C.; Yang, W.; Parr, R. G. *Physical Review B* **1988**, *37*, 785.

Lee, E. C.; Fu, G. C. *J. Am. Chem. Soc.* **2007**, *129*, 12066.

Legault, C. Y. CYLview, version 1.0b; Université de Sherbrooke: Quebec, Canada, **2009**;
<http://www.cylview.org>.

Leigh, W. J.; Arnold, D. R.; Humphreys, R. W.; Wong, P. C. *Can. J. Chem.* **1980**, *58*, 2537.

Leighty, M. W.; Shen, B.; Johnston, J. N. *J. Am. Chem. Soc.* **2012**, *134*, 15233.

Leonard, N. J.; Boyd, S. N.; Herbrandson, H. F. *J. Org. Chem.* **1947**, 47.

Li, J.; Lear, M. J.; Kawamoto, Y.; Umemiya, S.; Wong, A. R.; Kwon, E.; Sato, I.; Hayashi, Y. *Angew. Chem. Int. Ed.* **2015**, *54*, 12986.

Li, J.; Lear, M. J.; Kwon, E.; Hayashi, Y. *Chem. Eur. J.* **2016**, *22*, 5538.

Lim, V. T.; Tsukanov, S. V.; Stephens, A. B.; Johnston, J. N. *Org. Synth.* **2016**, *93*, 88.

Lindsley, C.; Hallett, D.; Wolkenberg, S. Azetidine Glycine Transporter Inhibitors.
WO2005110983, November 25, 2005.

Lipczynska-Kochany, E.; Iwamura, H.; Kochany, J. *Monatsh. Chem.* **1987**, *118*, 1345.

Liu, C.; Zhang, Y.; Huang, X. *Fuel Process. Technol.* **2014**, *123*, 159.

Liu, H.; Gao, Z.-B.; Yao, Z.; Zheng, S.; Li, Y.; Zhu, W.; Tan, X.; Luo, X.; Shen, J.; Chen, K.; Hu, G.-Y.; Jiang, H. *J. Med. Chem.* **2007**, *50*, 83.

Liu, T.-Y.; Cui, H.-L.; Zhang, Y.; Jiang, K.; Du, W.; He, Z.-Q.; Chen, Y.-C. *Org. Lett.* **2007**, *9*, 3671.

Liu, Y.; Prashad, M.; Ciszewski, L.; Vargas, K.; Repič, O.; Blacklock, T. J. *Org. Process Res. Dev.* **2008**, *12*, 183.

Lorand, J. P.; Grant, R. W.; Samuel, P. A.; O'Connell, S. E. M.; Zaro, J.; Pilotte, J.; Wallace, R. W. *J. Org. Chem.* **1973**, *38*, 1813.

Lu, Z.; Chai, Y.; Wang, J.; Pan, Y.; Sun, C.; Zeng, S. *Rapid Commun. Mass Spectrom.* **2014**, *28*, 1641.

Lucet, D.; Le Gall, T.; Mioskowski, C. *Angew. Chem. Int. Ed.* **1998**, *37*, 2580.

Lv, L.-P.; Zhou, X.-F.; Shi, H.-B.; Gao, J.-R.; Hu, W.-X. *J. Chem. Res.* **2014**, *38*, 368.

Lyapkalo, I.; Ioffe, S.; Strelenko, Y. A.; Tartakovsky, V. *Russ. Chem. Bull.* **1996**, *45*, 856.

Magnus, N. A.; Braden, T. M.; Buser, J. Y.; DeBaillie, A. C.; Heath, P. C.; Ley, C. P.; Remacle, J. R.; Varie, D. L.; Wilson, T. M. *Org. Process Res. Dev.* **2012**, *16*, 830.

Mamone, M.; Morvan, E.; Milcent, T.; Ongeri, S.; Crousse, B. *J. Org. Chem.* **2015**, *80*, 1964.

Martin, N. J. A.; Ozores, L.; List, B. *J. Am. Chem. Soc.* **2007**, *129*, 8976.

McCormick, M. H.; McGuire, J. M.; Pittenger, G. E.; Pittenger, R. C.; Stark, W. M. *Antibiotics annual* **1955**, *3*, 606.

McGrath, N. A.; Brichacek, M.; Njardarson, J. T. *J. Chem. Educ.* **2010**, *87*, 1348.

Meyer, V.; Ambühl, G. *Berichte Dtsch. Chem. Ges.* **1875**, *8*, 1073

Mitsunobu, O.; Yamada, M. *Bull. Chem. Soc. Jpn.* **1967**, *40*, 2380.

Muizebelt, W. J.; Nivard, R. J. F. *Journal of the Chemical Society B: Physical Organic* **1968**, 913.

Murru, S.; Lott, C. S.; Fronczek, F. R.; Srivastava, R. S. *Org. Lett.* **2015**, *17*, 2122.

Najera, C.; Sansano, J. M. *Chem. Rev.* **2007**, *107*, 4584.

Nakamura, I.; Owada, M.; Jo, T.; Terada, M. *Org. Lett.* **2017**, *19*, 2194.

Naveen, T.; Maity, S.; Sharma, U.; Maiti, D. *J. Org. Chem.* **2013**, *78*, 5949.

Nguyen, M. T.; Le, H. T.; Hajgato, B.; Veszpremi, T.; Lin, M. *J. Phys. Chem. A* **2003**, *107*, 4286.

Nguyen, N. V.; Baum, K. *Tetrahedron Lett.* **1992**, *33*, 2949.

Nikolaeva, E.; Shamov, A.; Khrapkovskii, G. *Russ. J. Gen. Chem.* **2014**, *84*, 2076.

Nishiwaki, N.; Rahbek Knudsen, K.; Gothelf, K. V.; Jørgensen, K. A. *Angew. Chem. Int. Ed.* **2001**, *40*, 2992.

Noble, A.; Anderson, J. C. *Chem. Rev.* **2013**, *113*, 2887.

Noland, W. E. *Chem. Rev.* **1955**, *55*, 137.

Nordstrøm, L. U.; Vogt, H.; Madsen, R. *J. Am. Chem. Soc.* **2008**, *130*, 17672.

Nugent, B. M.; Yoder, R. A.; Johnston, J. N. *J. Am. Chem. Soc.* **2004**, *126*, 3418.

Ohmatsu, K.; Ando, Y.; Nakashima, T.; Ooi, T. *Chem* **2016**, *1*, 802.

Ohmatsu, K.; Kiyokawa, M.; Ooi, T. *J. Am. Chem. Soc.* **2011**, *133*, 1307.

Okamoto, Y.; Brown, H. C. *J. Org. Chem.* **1957**, *22*, 485.

Okino, T.; Nakamura, S.; Furukawa, T.; Takemoto, Y. *Org. Lett.* **2004**, *6*, 625.

Ono, N.; Kaji, A. *Synthesis* **1986**, 1986, 693.

Ono, N.; Tamura, R.; Tanikaga, R.; Kaji, A. *J. Chem. Soc., Chem. Commun.* **1981**, *0*, 71.

Ormerod, D.; Willemsens, B.; Mermans, R.; Langens, J.; Winderickx, G.; Kalindjian, S. B.; Buck, I. M.; McDonald, I. M. *Org. Process Res. Dev.* **2005**, *9*, 499.

Owens, A. P.; Williams, B. J.; Harrison, T.; Swain, C. J.; Baker, R.; Sadowski, S.; Cascieri, M. A. *Bioorg. Med. Chem. Lett.* **1995**, *5*, 2761.

Padmavathi, V.; Reddy, S. N.; Reddy, G. D.; Padmaja, A. *Eur. J. Med. Chem.* **2010**, *45*, 4246.

Palomo, C.; Oiarbide, M.; Laso, A.; López, R. *J. Am. Chem. Soc.* **2005**, *127*, 17622.

Pan, C.; Cheng, J.; Wu, H.; Ding, J.; Liu, M. *Synth. Commun* **2009**, *39*, 2082.

Pangborn, A. B.; Giardello, M. A.; Grubbs, R. H.; Rosen, R. K.; Timmers F. J. *Organometallics* **1996**, *15*, 1518

Park, K. K.; Lee, C. W.; Choi, S. Y. *J. Chem. Soc., Perkin Trans. 1* **1992**, 601.

Parmerter, S. M. In *Organic Reactions*; John Wiley & Sons, Inc., Ed.; John Wiley & Sons, Inc.: Hoboken, NJ, USA, 2011; pp 1–142.

Pechmann, H. *Ber. Dtsch. Chem. Ges.* **1892**, 3175.

Perdew, J. P.; Burke, K.; Ernzerhof, M. *Phys. Rev. Lett.* **1996**, *77*, 3865.

Piltan, M.; Kalantari, S. *J. Heterocycl. Chem.* **2017**, *54*, 301.

Pirisino, C. G. E. *Archivio Bimestrale di Scienze Mediche e Naturali* **1977**, *55*, 307.

Ponzi, *Gazz. Chim. Ital.*, **1909**, 535.

Process for Preparing the Antiviral Agent [1s-(1alpha, 3 Alpha, 4 Beta)]-2-Amino-1,9-Dihydro-9-[4-Hydroxy-3-(hydroxymethyl)-2-Methylenecyclo. WO2004052310 (A2), June 24, 2004.

Proter and Peterson, *Org. Syntheses*, Coll. Vol. III, 660.

Pschorr, R.; Hoppe, G. *Ber. Dtsch. Chem. Ges.* **1910**, *43*, 2543.

Qiu, Y.; Huang, L.; Fu, J.; Han, C.; Fang, J.; Liao, P.; Chen, Z.; Mo, Y.; Sun, P.; Liao, D. *J. Med. Chem.* **2020**, *63*, 3665.

Rajendran, G.; Santini, R. E.; Van Etten, R. L. *J. Am. Chem. Soc.* **1987**, *109*, 4357.

Rausser, M.; Ascheberg, C.; Niggemann, M. *Angew. Chem.* **2017**, *129*, 11728.

Reddy, K. L.; Sharpless, K. B. *J. Am. Chem. Soc.* **1998**, *120*, 1207.

Reitti, M.; Villo, P.; Olofsson, B. *Angew. Chem.* **2016**, *128*, 9074.

Richter, V. *Ber. Dtsch. Chem. Ges.* **1883**, 677.

Robinson, C. H.; Gnoj, O.; Mitchell, A.; Wayne, E.; Townley, P.; Kabasakalian, P.; Oliveto, E. P.; Barton, D. H. R. *J. Am. Chem. Soc.* **1961**, *83*, 1771.

Sakurai, H.; Hayashi, S.-i.; Hosomi, A. *Bull. Chem. Soc. Jpn.* **1971**, *44*, 1945.

Sarantakis, D.; Sutherland, J.; Tortorella, C.; Tortorella, V. *ChemComm* **1966**, 105.

Saxon, E.; Armstrong, J. I.; Bertozzi, C. R. *Org. Lett.* **2000**, 2, 2141.

Saxon, R. P.; Yoshimine, M. *Can. J. Chem.* **1992**, 70, 572.

Sayed, A. R. *Tetrahedron Lett.* **2010**, 51, 4490.

Schöllkopf, U.; Hoppe, I. *Tetrahedron Lett.* **1970**, 11, 4527.

Schulze, V. K.; Klar, U.; Kosemund, D.; Wengner, A. M.; Siemeister, G.; Stöckigt, D.; Neuhaus, R.; Lienau, P.; Bader, B.; Precht, S. *J. Med. Chem.* **2020**.

Schwieter, K. E.; Johnston, J. N. *ACS Catalysis* **2015**, 5, 6559.

Schwieter, K. E.; Johnston, J. N. *Chem. Sci.* **2015**, 6, 2590.

Schwieter, K. E.; Johnston, J. N. *J. Am. Chem. Soc.* **2016**, 138, 14160.

Schwieter, K. E.; Shen, B.; Shackleford, J. P.; Leighty, M. W.; Johnston, J. N. *Org. Lett.* **2014**, 16, 4714.

Seebach, D. *Angew. Chem. Int. Ed.* **1979**, 18, 239.

Selva, E.; Beretta, G.; Montanini, N.; Sandler, G.; Gastaldo, L.; Ferrari, P.; Lorenzetti, R.; Landini, P.; Ripamonti, F.; Goldstein, B. *J. Antibiot.* **1991**, 44, 693.

Senkus, M. *J. Am. Chem. Soc.* **1946**, 68, 1611.

Senter, T. J.; O'Reilly, M. C.; Chong, K. M.; Sulikowski, G. A.; Lindsley, C. W. *Tetrahedron Lett.* **2015**, 56, 1276.

Seo, Y.; Kim, H.; Chae, D. W.; Kim, Y. G. *Tetrahedron: Asymmetry* **2014**, 25, 625.

Seo, Y.; Lee, S.; Kim, Y. G. *Applied Chemistry for Engineering* **2015**, 26, 111.

Shackleford, J. P.; Shen, B.; Johnston, J. N. *Proc. Natl. Acad. Sci. U. S. A.* **2012**, 109, 44.

Shamsabadi, A.; Ren, J.; Chudasama, V. *RSC Adv.* **2017**, 7, 27608.

Shang, G.; Yang, Q.; Zhang, X. *Angew. Chem. Int. Ed.* **2006**, 45, 6360.

Shao, L.; Li, Y.; Lu, J.; Jiang, X. *Org. Chem. Front.* **2019**, 6, 2999.

Sheldrick, G. (2008). A short history of shelx. *Acta Crystallographica Section A* 64, 112-122.

Shen, B. PhD. Dissertation, Vanderbilt University, 2010

Shen, B.; Johnston, J. N. *Org. Lett.* **2008**, *10*, 4397.

Shen, B.; Makley, D. M.; Johnston, J. N. *Nature*. **2010**, *465*, 1027.

Shestakova, T.; Khalymbadzha, I.; Deev, S.; Eltsov, O.; Rusinov, V.; Shenkarev, Z.; Arseniev, A.; Chupakhin, O. *Russ. Chem. Bull.* **2011**, *60*, 729.

Singh, A.; Johnston, J. N. *J. Am. Chem. Soc.* **2008**, *130*, 5866.

Singh, A.; Yoder, R. A.; Shen, B.; Johnston, J. N. *J. Am. Chem. Soc.* **2007**, *129*, 3466.

Singh, N. K.; Singh, S. B.; Shrivastav, A. *Met Based Drugs* **2002**, *9*, 109.

Smith, G. G.; Sivakua, T. *J. Org. Chem.* **1983**, *48*, 627.

Soto, J.; Arenas, J. F.; Otero, J. C.; Pelaez, D. *J. Phys. Chem. A* **2006**, *110*, 8221.

Spivack, K. J.; Walker, J. V.; Sanford, M. J.; Rupert, B. R.; Ehle, A. R.; Tocyloski, J. M.; Jahn, A. N.; Shaak, L. M.; Obiany, O.; Usher, K. M. *J. Org. Chem.* **2017**, *82*, 1301.

Stephens, P. J.; Devlin, F. J.; Chabalowski, C. F.; Frisch, M. J. *J. Phys. Chem.* **1994**, *98*, 11623.

Stoner, E. J.; Hart, A. C. *Encyclopedia of Reagents for Organic Synthesis* **2001**.

Streitwieser, A.; Perrin, C. *J. Am. Chem. Soc.* **1964**, *86*, 4938.

Sukhorukov, A. Y. *Adv. Synth. Catal.* **2020**, *362*, 724.

Sweeney, J. B. *Chem. Soc. Rev.* **2009**, *38*, 1027.

T Chhabria, M.; Patel, S.; Modi, P.; S Brahmkshatriya, P. *Curr. Top. Med. Chem.* **2016**, *16*, 2841.

Thakkalapally, A.; Benin, V. *Tetrahedron* **2005**, *61*, 4939.

Thomas, J.; John, J.; Parekh, N.; Dehaen, W. *Angew. Chem. Int. Ed.* **2014**, *53*, 10155.

Tng, J.; Lim, J.; Wu, K.-C.; Lucke, A. J.; Xu, W.; Reid, R. C.; Fairlie, D. P. *J. Med. Chem.* **2020**, *63*, 5956.

Tokumaru, K.; Bera, K.; Johnston, J. N. *Synthesis* **2017**, *49*, 4670.

Tokumaru, K.; Johnston, J. N. *Chem. Sci.* **2017**, *8*, 3187.

Townsend, C. A.; Brown, A. M. *J. Am. Chem. Soc.* **1983**, *105*, 913.

Tsuritani, N.; Yamada, K.-i.; Yoshikawa, N.; Shibasaki, M. *Chem. Lett.* **2002**, *31*, 276.

Tvaroška, I.; Bleha, T. In *Adv. Carbohydr. Chem. Biochem.*; Elsevier: 1989; Vol. 47, p 45.

Uraguchi, D.; Kinoshita, N.; Nakashima, D.; Ooi, T. *Chem. Sci.* **2012**, *3*, 3161.

Uraguchi, D.; Sakaki, S.; Ooi, T. *J. Am. Chem. Soc.* **2007**, *129*, 12392.

Vasudevan, N.; Routholla, G.; TejaIlla, G.; Reddy, D. S. *Tetrahedron* **2020**, 131262.

Vértesy, L.; Aretz, W.; Knauf, M.; Markus, A.; Vogel, M.; Wink, J. *J. Antibiot.* **1999**, *52*, 374.

Viehe, H. G.; Janousek, Z.; Merenyi, R.; Stella, L. *Acc. Chem. Res.* **1985**, *18*, 148.

Vishe, M.; Johnston, J. N. *Chem. Sci.* **2019**, *10*, 1138.

Voinov, M. A.; Grigor'ev, I. A. *Tetrahedron Lett.* **2002**, *43*, 2445.

Voinov, M. A.; Shevelev, T. G.; Rybalova, T. V.; Gatilov, Y. V.; Pervukhina, N. V.; Burdukov, A. B.; Grigor'ev, I. A. *Organometallics* **2007**, *26*, 1607.

Wade, P. A.; Hinney, H. R.; Amin, N. V.; Vail, P. D.; Morrow, S. D.; Hardinger, S. A.; Saft, M. *S. J. Org. Chem.* **1981**, *46*, 765.

Walker, T. K. *J. Chem. Soc., Trans.* **1923**, 2775.

Wang, M.; Liu, C.; Xu, X.; Li, Q. *Chem. Phys. Lett.* **2016**, *654*, 41.

Wang, S.-P.; Cheung, C. W.; Ma, J.-A. *J. Org. Chem.* **2019**, *84*, 13922.

Ward, H. R. *Acc. Chem. Res.* **1972**, *5*, 18.

Wells, P. R. *Chem. Rev.* **1963**, *63*, 171.

Weng, J.; Li, Y.-B.; Wang, R.-B.; Li, F.-Q.; Liu, C.; Chan, A. S. C.; Lu, G. *J. Org. Chem.* **2010**, *75*, 3125.

Wengner, A. M.; Siemeister, G. Patent WO2014198645 (A1), 2014.

Wessjohann, L. A.; Sinks, U. *J. Prakt. Chem.* **1998**, *340*, 189.

Widman, O. *Ber. Dtsch. Chem. Ges.* **1884**, 722.

Williams, R. M.; Hendrix, J. A. *Chem. Rev.* **1992**, *92*, 889.

Wilt, J. C.; Pink, M.; Johnston, J. N. *Chem. Commun.* **2008**, 4177.

Wislicenus and Hentrich, *Ann.*, **1924**, 9.

Wong, F. T.; Patra, P. K.; Seayad, J.; Zhang, Y.; Ying, J. Y. *Org. Lett.* **2008**, *10*, 2333.

Wu, D.-Q.; Li, Z.-Y.; Li, C.; Fan, J.-J.; Lu, B.; Chang, C.; Cheng, S.-X.; Zhang, X.-Z.; Zhuo, R.-X. *Pharm. Res.* **2010**, *27*, 187.

Wu, L.; Yang, X.; Yan, F. *Bull. Chem. Soc. Ethiop.* **2011**, 25.

Xie, H.; Zhang, Y.; Zhang, S.; Chen, X.; Wang, W. *Angew. Chem. Int. Ed.* **2011**, *50*, 11773.

Xie, S.; Zhang, Y.; Ramström, O.; Yan, M. *Chem. Sci.* **2016**, *7*, 713.

Xu, M.-L.; Huang, W. *Synth. Commun.* **2014**, *44*, 3435.

Xu, X.; Furukawa, T.; Okino, T.; Miyabe, H.; Takemoto, Y. *Chem. Eur. J.* **2006**, *12*, 466.

Yadav, J.; Reddy, B. S.; Kumar, G. M.; Madan, C. *Synlett* **2001**, *2001*, 1781.

Yamada, K.-i.; Harwood, S. J.; Gröger, H.; Shibasaki, M. *Angew. Chem. Int. Ed.* **1999**, *38*, 3504.

Yamagami, T.; Moriyama, N.; Kyuhara, M.; Moroda, A.; Uemura, T.; Matsumae, H.; Moritani, Y.; Inoue, I. *Org. Process Res. Dev.* **2014**, *18*, 437.

Yamamoto, T. *Bull. Chem. Soc. Jpn.* **1967**, *40*, 642.

Yang, D.; Fan, M.; Zhu, H.; Guo, Y.; Guo, J. *Synthesis* **2013**, *45*, 1325.

Yang, W.; Wang, Y.; Lai, A.; Clark, C. G.; Corte, J. R.; Fang, T.; Gilligan, P. J.; Jeon, Y.; Pabbisetty, K. B.; Rampulla, R. A. *J. Med. Chem.* **2020**, *63*, 7226.

Yim, W.-L.; Liu, Z.-f. *J. Am. Chem. Soc.* **2001**, *123*, 2243.

Yoo, W.-J.; Li, C.-J. *J. Am. Chem. Soc.* **2006**, *128*, 13064.

Yoon, T. P.; Jacobsen, E. N. *Angew. Chem. Int. Ed.* **2005**, *44*, 466.

Yu, Y.-B.; Cheng, L.; Li, Y.-P.; Fu, Y.; Zhu, S.-F.; Zhou, Q.-L. *Chem. Commun.* **2016**, *52*, 4812.

Zhang, C.; Wang, Q. *Macromol. Rapid Commun.* **2011**, *32*, 1180.

Zhang, C.; Wang, X.; Zhou, M. *J. Comput. Chem.* **2011**, *32*, 1760.

Zhang, H.-B.; Wang, Y.; Gu, Y.; Xu, P.-F. *RSC Adv.* **2014**, *4*, 27796.

Zhang, X. *J. Mol. Struct.* **2011**, *1002*, 121.

Zhang, Y.; Reynolds, N. T.; Manju, K.; Rovis, T. *J. Am. Chem. Soc.* **2002**, *124*, 9720.

Zhao, W.; Guizzetti, S.; Schwindeman, J. A.; Daniels, D. S. B.; Douglas, J. J.; Petit, S.; Knight, J. *Org. Process Res. Dev.* **2020**, *24*, 115.

Zhao, Y.; Truhlar, D. G. *Acc. Chem. Res.* **2008**, *41*, 157.

Zhao, Y.; Truhlar, D. G. *Theor. Chem. Acc.* **2008**, *120*, 215.

Zhu, Y.-Q.; Dong, L. *J. Org. Chem.* **2015**, *80*, 9973.

Zuend, S. J.; Coughlin, M. P.; Lalonde, M. P.; Jacobsen, E. N. *Nature* **2009**, *461*, 968.

Appendix A: Experimental

Solvents and reagents were commercial grade and used as received unless otherwise noted. Dry solvents were acquired from an MBRAUN MB-SPS solvent system.²⁵⁴ All reactions were carried out in glassware that had been flamed-dried under vacuum. Prior to concentration, organic phases resulting from workup were dried with anhydrous magnesium sulfate. Water used in reactions was deionized.

Flash column chromatography was performed with silica gel from Sorbent Technologies with a diameter of 40-63 μm and a porosity of 60 \AA . Thin layer chromatography utilized 250 μm silica gel immobilized on glass. Compound spots were visualized using UV light or an appropriate stain if noted.

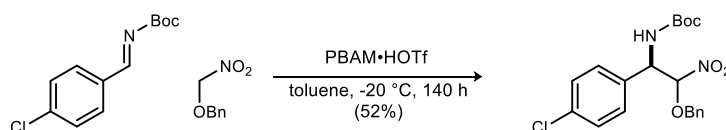
IR (neat films on NaCl) was acquired on a Nicolet Avatar 360 spectrophotometer in transmission mode and reported in wavenumbers. Nuclear magnetic resonance spectra were collected from a Bruker DRX-500 (500 MHz), Bruker AV-400 (400 MHz), or Bruker AV II-600 (600 MHz), and chemical shifts were calibrated to residual solvent peaks. Mass spectrometry was performed by the Indiana University Mass Spectrometry Facility on a high resolution Thermo Electron Corporation MAT 95XP-Trap or a Thermo Orbitrap by use of chemical ionization (CI), electron impact ionization (EI), or electro-spray ionization (ESI) or in-house on a Thermo Orbitrap by use of chemical ionization (CI) or electro-spray ionization (ESI). Optical rotations were determined

²⁵⁴ Pangborn, A. B.; Giardello, M. A.; Grubbs, R. H.; Rosen, R. K.; Timmers F. J. *Organometallics* **1996**, *15*, 1518

by polarimetry on a Perkin Elmer-341 instrument. An Agilent 1100 series Chiral HPLC equipped with the indicated ChiralPak column was used to measure enantiopurity.

General Procedure for Aza-Henry Reactions

The appropriate nitroalkane (1 equiv.) was dissolved in dry toluene (100 mM) in a 2 dram vial equipped with a stir bar. This solution was cooled in a freezer to the indicated temperature, then imine (1 equiv.) and catalyst (0.2 equiv.) were added. The solution was stirred for the indicated time before filtration through a silica plug (EtOAc) and concentration in vacuo. Flash column chromatography on silica gel was performed as described.



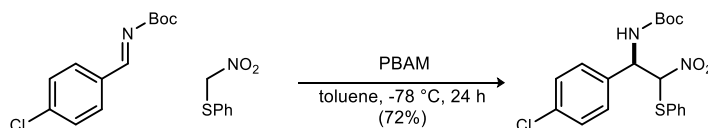
***tert*-Butyl ((1*R*)-2-(benzyloxy)-1-(4-chlorophenyl)-2-nitroethyl)carbamate (19).**

Benzyloxy nitromethane (33.4 mg, 200 μ mol)²⁵⁵ was dissolved in dry toluene (2 mL) in a 2 dram vial equipped with a stir bar. This solution was cooled in a -20 °C freezer, and then *tert*-butyl (*E*)-(4-chlorobenzylidene)carbamate (48.0 mg, 200 μ mol)⁸⁴ and PBAM·HOTf (26.3 mg, 40.0 μ mol)²⁵⁶ were added. The solution was stirred for 140 h before it was filtered through a silica plug (EtOAc) and concentrated to provide a 9:1 mixture of diastereomers. The residue was subjected to silica gel chromatography (5-10% ethyl acetate in hexanes) to provide the product as a white solid (42.2 mg, 52%). The diastereomers were determined to be 98/86% ee by chiral HPLC analysis (Chiralpak

²⁵⁵ Barrett, A. G.; Cheng, M. C.; Spilling, C. D.; Taylor, S. J. *J. Org. Chem.* **1989**, *54*, 992.

²⁵⁶ Davis, T. A.; Dobish, M. C.; Schwieter, K. E.; Chun, A. C.; Johnston, J. N. *Org. Synth.* **2012**, *89*, 380.

OJ-H, 6% EtOH/hexanes, 1.0 mL/min, t_r (d_{1e1}, major, major) = 15.9 min, t_r (d_{2e1}, minor, minor) = 19.2 min, t_r (d_{1e2}, major, minor) = 20.7 min, t_r (d_{2e2}, minor, major) = 26.7 min).²⁵⁷ $[\alpha]_D^{20}$ -41.5 (*c* 0.77, CHCl₃); mp 105-109 °C; R_f = 0.13 (10% EtOAc/hexanes); IR (film) 3422, 3335, 2976, 2930, 1708, 1561, 1496, 1364, 1248, 1165, 1092, 1013, 834, 748 cm⁻¹; ¹H NMR (400 MHz, CDCl₃) δ 7.39-7.18 (m, 16H), 7.02 (d, *J* = 7.0 Hz, 2H), 5.53 (br d, *J* = 6.4 Hz, 1H), 5.53 (br d, *J* = 7.0 Hz, 1H), 5.46 (br d, *J* = 6.7 Hz, 1H), 5.33 (br s, 1H), 5.26 (br s, 1H), 5.17 (br d, *J* = 7.0 Hz, 1H), 4.95 (d, *J* = 11.8 Hz, 1H), 4.91 (d, *J* = 11.6 Hz, 1H), 4.54 (d, *J* = 11.7 Hz, 1H), 4.41 (d, *J* = 11.5 Hz, 1H), 1.39 (s, 18H); ¹³C NMR (100 MHz, CDCl₃) ppm 154.7, 154.6, 135.3, 134.9, 134.4 (2C), 134.0 (2C), 129.5, 129.11, 129.08, 129.01 (2C), 128.97, 128.8, 128.7, 128.6, 128.2, 107.9, 107.7, 80.8 (2C) 74.3 (2C), 56.3, 55.9, 28.3 (2C); HRMS (ESI): Exact mass calcd for C₂₀H₂₃ClN₂NaO₅ [M+Na]⁺ 429.1193, found 429.1180.

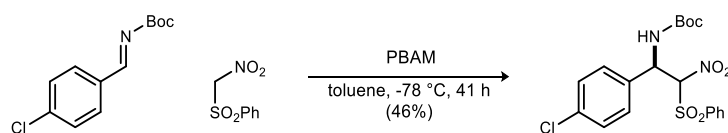


***tert*-Butyl (1-(4-chlorophenyl)-2-nitro-2-(phenylthio)ethyl)carbamate (22).** Thiophenyl nitromethane (33.8 mg, 200 μ mol)²⁵⁸ was dissolved in dry toluene (2 mL) in a 2-dram vial equipped with a stir bar. This solution was cooled (-78 °C), and then *tert*-butyl (*E*)-(4-chlorobenzylidene)carbamate (48.0 mg, 200 μ mol)⁸⁴ and PBAM (20.3 mg, 40.0 μ mol)²⁵⁶ were added. The solution was stirred for 24 h, filtered through a silica plug (EtOAc), and concentrated

²⁵⁷ The major enantiomer for each diastereomer was assigned as having an R configuration at the carbamate-substituted carbon on the basis of analogy to BAM catalyzed aza-Henry reactions in literature.³³

²⁵⁸ Barrett, A. G. M.; Graboski, G. G.; Russell, M. A. *J. Org. Chem.* **1986**, *51*, 1012.

to provide a 1.7:1 mixture of diastereomers. The residue was subjected to silica gel chromatography (7-10% ethyl acetate in hexanes) to provide the product as a white solid (58.7 mg, 72%). The diastereomers were each 95% ee by chiral HPLC analysis (Chiralpak IA, 15% EtOH/hexanes, 1.0 mL/min, t_r (d_{1e1} , minor, major) = 6.1 min, t_r (d_{2e1} , major, minor) = 7.1 min, t_r (d_{1e2} , minor, minor) = 8.9 min, t_r (d_{2e2} , major, major) = 11.7 min). Mp 126-130 °C; R_f = 0.21 (10% EtOAc/hexanes); IR (film) 3334, 2922, 1702, 1554, 1493, 1359, 1250, 1164 cm^{-1} ; ^1H NMR (400 MHz, CDCl_3) δ 7.46-7.21 (m, 18H), 5.99 (br d, J = 9.2 Hz, 1H), 5.83 (br s, 1H), 5.83 (br s, 1H), 5.53 (br s, 1H), 5.39 (br s, 1H), 5.37 (br s, 1H), 1.47 (s, 9H), 1.45 (s, 9H); ^{13}C NMR (100 MHz, CDCl_3) ppm 155.0, 154.7, 135.0, 134.9, 134.8 (2C), 133.9 (2C), 130.5, 130.2, 130.1, 129.94, 129.88, 129.82, 129.32, 129.26, 128.7, 128.0, 97.8 (2C), 81.2, 81.1, 56.4, 56.0, 28.38, 28.37; HRMS (CI): Exact mass calcd for $\text{C}_{19}\text{H}_{21}\text{ClN}_2\text{O}_4\text{S}$ $[\text{M}]^+$ 408.0905, found 408.0905.

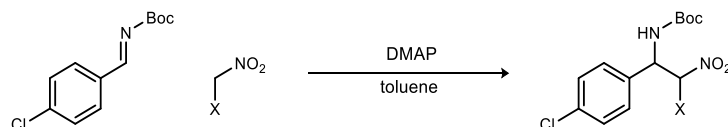


***tert*-Butyl ((1*R*)-1-(4-chlorophenyl)-2-nitro-2-(phenylsulfonyl)ethyl)carbamate (23).**

Phenylsulfonyl nitromethane (20.1 mg, 100 μmol)²⁵⁹ was dissolved in dry toluene (1 mL) in a 2-dram vial equipped with a stir bar. This solution was cooled ($-78\text{ }^\circ\text{C}$) then the imine (24.0 mg, 100 μmol) and PBAM (10.2 mg, 20.0 μmol) were added. The solution was stirred for 41 h and then filtered through a silica plug (EtOAc), and concentrated to provide a 1.2:1 mixture of diastereomers. The residue was subjected to silica gel chromatography (0-1% methanol in

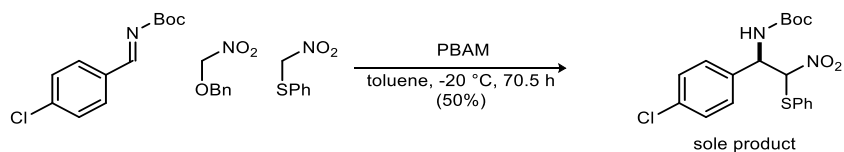
²⁵⁹ Wade, P. A.; Hinney, H. R.; Amin, N. V.; Vail, P. D.; Morrow, S. D.; Hardinger, S. A.; Saft, M. S. *J. Org. Chem.* **1981**, *46*, 765.

dichloromethane with 0.5% acetic acid) to provide the product as a white solid (20.4 mg, 46%). Through conversion to compound **24** with reported conditions,²⁶ the combined ee of the diastereomers was determined to be 78% by chiral HPLC analysis (Chiralpak AD-H, 8% IPA/hexanes, 1.0 mL/min, t_r (e₁, minor) = 13.3 min, t_r (e₂, major) = 16.8 min). Mp 147-154 °C; R_f = 0.27 (1% MeOH/dichloromethane with one drop of acetic acid); IR (film) 3378, 2924, 1699, 1565, 1498, 1346, 1248, 1158, 1085 cm^{-1} ; ^1H NMR (400 MHz, $\text{DMSO}-d_6$) δ 7.97-7.85 (m, 4H), 7.81-7.74 (m, 3H), 7.58-7.50 (m, 5H), 7.43-7.35 (m, 8H), 6.69 (d, J = 10.5 Hz, 1H), 6.51 (d, J = 10.9 Hz, 1H), 5.48 (dd, J = 9.8, 9.8 Hz, 1H), 5.24 (dd, J = 10.2, 10.2 Hz, 1H), 1.36 (s, 9H), 1.30 (s, 9H); ^{13}C NMR (100 MHz, $\text{DMSO}-d_6$) ppm 154.0, 153.6, 136.0, 135.4 (2C), 135.0, 134.9, 134.0, 133.7, 133.6, 130.4, 129.8, 129.7 (2C), 129.6, 128.9, 128.8, 128.5, 102.4, 102.0, 79.4 (2C), 53.8 (2C), 28.0, 27.9; HRMS (ESI): Exact mass calcd for $\text{C}_{19}\text{H}_{21}\text{ClN}_2\text{NaO}_6\text{S}$ $[\text{M}+\text{Na}]^+$ 463.0706, found 463.0719.



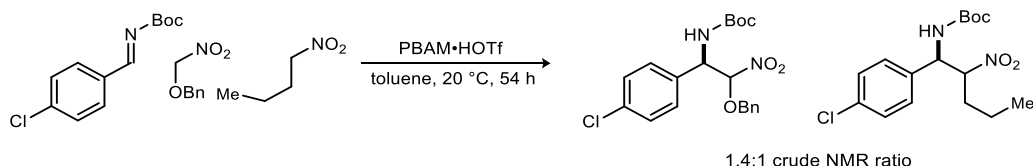
General Procedure for Aza-Henry Reactions to Prepare Racemic Standards

Racemates were prepared according to the general procedure for aza-Henry reactions using DMAP as catalyst. The temperature and time for **19** was rt for 4 days and that for **22** and **23** was $-78\text{ }^\circ\text{C}$ for 24 h.



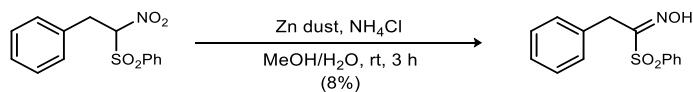
Competition Reaction Between α -OBn and α -SPh Nitromethane

The reaction was run according to “General Procedure for Aza-Henry Reactions” with 1 equiv. of each nitroalkane. The crude residue was subjected to silica gel chromatography (5-10% ethyl acetate in hexanes) to provide exclusively the α -thiophenyl nitromethane-derived product.



Competition Reaction Between α -OBn Nitromethane and Nitrobutane

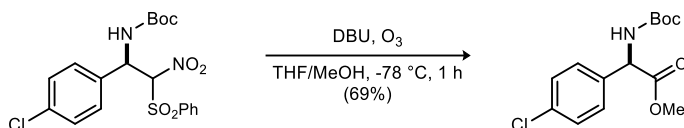
The reaction was run according to “General Procedure for Aza-Henry Reactions” with 1 equiv. of each nitroalkane. The crude reaction mixture showed a 1.4:1 mixture of products favoring the benzyloxy nitromethane derived product.



Example α -Nitrosulfone Reduction Leading to Oxime (E)-2-phenyl-1-(phenylsulfonyl)ethan-1-one (S1)

As adapted from a literature procedure,⁵⁶ the nitroalkane (29.1 mg, 100 μ mol) in a MeOH/satd aq NH_4Cl mixture (3 mL of 4:1 (v/v) mixture) was charged into a vial with a stir bar. Freshly-activated zinc dust (65.1 mg, 1.00 mmol) was added-portion wise over 15 min and the reaction was stirred for an additional 3 hours. The resulting suspension was diluted with ethyl acetate, filtered, washed with water and brine, dried, and concentrated. The residue was purified using flash chromatography on silica gel (10-20% ethyl acetate in hexanes) to provide the product as a white

solid (2.2 mg, 8%). Mp 112-115 °C; $R_f = 0.38$ (40% EtOAc/hexanes); IR (film) 3305, 3062, 2919, 2854, 1633, 1593, 1492, 1447, 1310, 1151, 1078, 994, 717, 687 cm^{-1} ; ^1H NMR (400 MHz, CDCl_3) δ 8.58 (br s, 1H), 7.78 (dd, $J = 8.1, 0.9$ Hz, 2H), 7.58 (tt, $J = 7.5, 1.3$ Hz, 1H), 7.44 (t, $J = 7.9$ Hz, 2H), 7.22-7.17 (m, 5H), 4.08 (s, 2H); ^{13}C NMR (100 MHz, CDCl_3) ppm 161.2, 138.2, 134.1, 133.8, 129.4, 129.2, 129.0, 128.7, 127.2, 30.9; HRMS (ESI): Exact mass calcd for $\text{C}_{14}\text{H}_{13}\text{NNaO}_3\text{S}$ $[\text{M}+\text{Na}]^+$ 298.0514, found 298.0519.

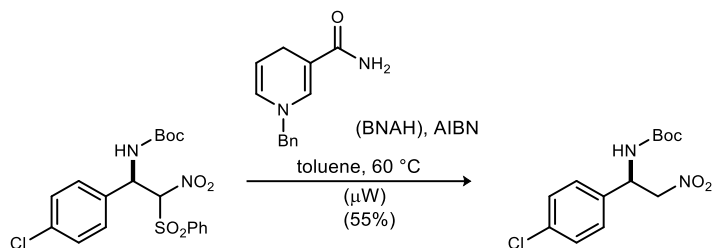


Ozonolysis of **23** for ee Determination

As adapted from a literature procedure,³⁸ the nitroalkane (20.4 mg, 46.4 μmol) and DBU (21 μL , 139 μmol) in a MeOH/THF mixture (2 mL of 3:1 (v/v) mixture) were charged into a vial with a stirbar. The solution was brought to -78 °C followed by 1 hour of O₃ exposure (bubbling through the solution). Excess O₃ was purged using a stream of O₂ and the reaction was then quenched with acetic acid (200 μL) and allowed to warm slowly to room temperature. The resulting solution was concentrated, dissolved in ethyl acetate, washed with satd aq NH_4Cl , dried, and concentrated. The residue was purified using flash chromatography on silica gel (0-10% ethyl acetate in hexanes) to provide the ester (9.6 mg, 69%).²⁶⁰ The material was determined to be 68% ee by chiral HPLC

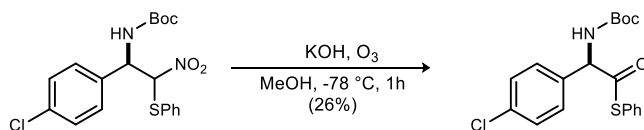
²⁶⁰ Arai, T.; Matsumura, E. *Synlett* **2014**, 25, 1776.

analysis (Chiralpak OZ-H, 4% EtOH/hexanes, 1.0 mL/min, t_r (e₁, minor) = 6.2 min, t_r (e₂, major) = 8.1 min).



Desulfonylation of 23 for ee Determination

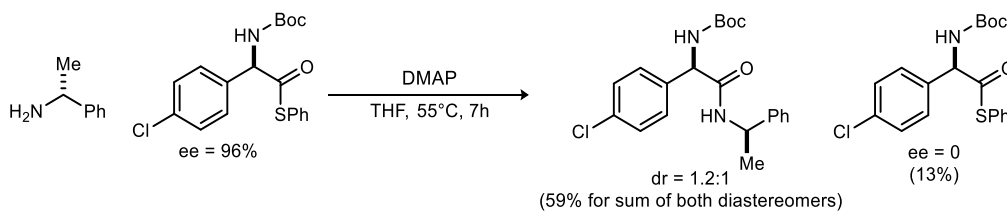
As adapted from a literature procedure,³⁸ the nitroalkane (24.8mg, 56.0 μmol), *N*-benzylnicotinamide (34.9 mg, 165 μmol), and AIBN (1.9 mg, 11.2 μmol) in toluene (750 μL) were charged into a microwave vial with a stirbar. The solution was brought to 60 °C by microwave irradiation followed by 47 min of stirring. The resulting solution was diluted with ethyl acetate and water, extracted with ethyl acetate, dried, and concentrated. The residue was purified using flash chromatography on silica gel (20-50% ethyl acetate in hexanes) to provide the nitro alkane (9.3 mg, 55%).²⁷ The material's ee was determined by chiral HPLC analysis (Chiralpak AD-H, 8% IPA/hexanes, 1.0 mL/min, t_r (e₁, minor) = 13.3 min, t_r (e₂, major) = 16.8 min).



S-Phenyl (R)-2-((tert-butoxycarbonyl)amino)-2-(4-chlorophenyl)ethanethioate (69).

As adapted from a literature procedure,⁶⁰ *tert*-butyl (1-(4-chlorophenyl)-2-nitro-2-(phenylthio)ethyl)carbamate (50.0 mg, 122 μmol) was added to a stirred solution of potassium hydroxide (7.5 mg, 134 μmmol) and methanol (1.2 mL) in a 2-dram vial at 0 °C. Slight warming

was necessary to completely dissolve the nitro compound, and once dissolution was achieved, the reaction was returned to 0 °C. Stirring was continued for 30 minutes, and methanol (3 mL) was used to dilute the reaction. The mixture was cooled to -78 °C and ozone was introduced using a sparging tube. Once a blue color was observed (~5 min), the reaction was purged with oxygen, and dimethyl sulfide (100 μL) was added before the reaction was allowed to slowly warm to room temperature. The resulting solution was concentrated, dissolved in water, and extracted with dichloromethane. The combined organic layers were washed with water, dried, and concentrated. The residue was subjected to silica gel chromatography (0-10% ethyl acetate in hexanes) to provide the product as a white solid (11.9 mg, 26%). The product was determined to be 95% ee by chiral HPLC analysis (Chiralpak IA, 5% IPA/hexanes, 1.0 mL/min, t_r (e₁, major) = 15.0 min, t_r (e₂, minor) = 16.3 min). $[\alpha]_D^{20}$ -110.1 (*c* 1.04, CHCl₃); Mp 140-142 °C; R_f = 0.22 (10% EtOAc/hexanes); IR (film) 3327, 3063, 2969, 2920, 2853, 1702, 1489, 1365, 1250, 1164, 1090, 1019, 745 cm⁻¹; ¹H NMR (400 MHz, CDCl₃) δ 7.41-7.33 (m, 9H), 5.58 (br d, *J* = 6.0 Hz, 1H), 5.51 (br d, *J* = 6.1 Hz, 1H), 1.45 (s, 9H); ¹³C NMR (100 MHz, CDCl₃) ppm 196.7, 154.8, 135.1, 135.0, 134.7, 129.9, 129.4, 129.1, 128.2, 126.7, 80.9, 63.9, 28.4; HRMS (ESI): Exact mass calcd for C₁₉H₂₀ClNNaO₃S [M+Na]⁺ 400.0750, found 400.0761.

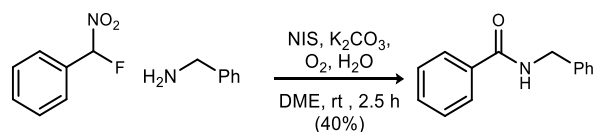


Conventional Amide Synthesis from Thioester

The active ester (1 equiv.) in THF (~0.1 M) and a catalytic amount of DMAP was loaded into a vial equipped with a stirbar. (*R*)-(+)- α -methyl benzylamine (2.0 equiv.) was added. The vial was brought to 55 °C and stirred for 7 h (TLC). The resulting solution was concentrated under vacuum, and purification was carried out using flash chromatography on silica gel (0-10% ethyl acetate in hexanes) to provide the product as a 1.2:1 mixture of diastereomers. The recovered thioester was determined to be 0% ee by chiral HPLC analysis (Chiralpak IA, 5% IPA/hexanes, 1.0 mL/min, t_r (e_1 , major) = 15.0 min, t_r (e_2 , minor) = 16.3 min).

General Procedure for UmAS Reactions

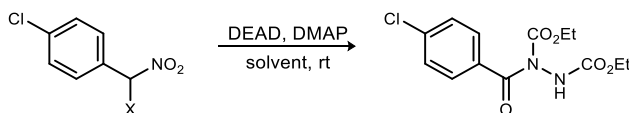
The nitroalkane (1 equiv.) in DME (0.1 M) and water (5 equiv.) was loaded into a vial equipped with a stirbar. K_2CO_3 (1 equiv.), NIS (1 equiv.) and then amine (1.2 equiv.) were added. The vial was fitted with an O_2 balloon, brought to the indicated temperature, and stirred overnight. The resulting solution was diluted with dichloromethane and washed with $Na_2S_2O_3$. The combined organic layers were concentrated under vacuum, and purification was carried out using flash chromatography on silica gel.



Use of Fluoronitroalkane in UmAS

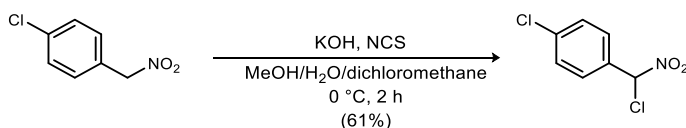
The nitroalkane (15.5 mg, 100 μ mol) was dissolved in DME (1 mL), and then water (9 μ L, 500 μ mol), K_2CO_3 (13.8 mg, 100 μ mol), and NIS (22.5 mg, 100 μ mol) were added. After 1.5 h, amine

was added (21.8 μL , 200 μmol), the reaction was fitted with an O_2 balloon and stirring was continued for 30 min. The reaction was then diluted with dichloromethane, washed with $\text{Na}_2\text{S}_2\text{O}_3$, dried, and concentrated under vacuum. Column chromatography (SiO_2 , 10-15% ethyl acetate in hexanes) gave the amide (10.7 mg, 40%).²⁶¹



General Procedure for Halogen Screening in the Tetrahedral Intermediate (TI') Synthesis

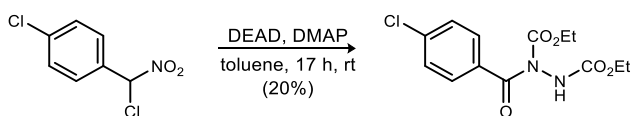
The α -halo nitroalkane (1.0 equiv) was dissolved in solvent (0.1 M). DEAD (1.1 equiv) was then added, followed by DMAP (0.22 equiv), and the reaction mixture was stirred at room temperature. The reaction mixture was filtered through a silica plug with dichloromethane and ethyl acetate before drying and concentration. The crude product was purified by prep-HPLC. Following prep-HPLC, the fractions were diluted with ethyl acetate and the organic phase was washed with satd aq NaHCO_3 and brine before drying and concentration.



1-Chloro-4-(chloro(nitro)methyl)benzene (77c). Prepared by mixing 1-chloro-4-(nitromethyl)benzene (32.8 mg, 190.7 μmol) with a 1:3 (v/v) mixture of methanol:water (500 μL).

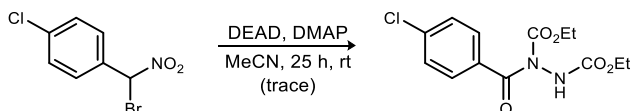
²⁶¹ Nordstrøm, L. U.; Vogt, H.; Madsen, R. *J. Am. Chem. Soc.* **2008**, *130*, 17672.

This solution was then brought to 0 °C and KOH (12.6 mg of 85% solid, 191 μmol) was added. After the solution appeared homogeneous (~1 h), dichloromethane at -78 °C (1.25 mL) was added, followed immediately by NCS (24.9 mg, 231 μmol). The reaction appeared complete by TLC after 30 additional minutes. The mixture was diluted with H₂O and dichloromethane, the phases were separated, and the aqueous phase was extracted with dichloromethane. The organic layers were dried and concentrated, and the residue was purified by column chromatography (2% diethyl ether in hexanes) to afford the desired compound as a colorless oil (23.9 mg, 61%); *R_f* = 0.59 (20% ethyl acetate in hexanes); IR (film) 2922, 1572, 1490, 1349, 1236, 1093, 880, 824, 754 cm⁻¹; ¹H NMR (400 MHz, CDCl₃) δ 7.59 (d, *J* = 8.8 Hz, 2H), 7.44, (d, *J* = 8.8 Hz, 2H), 6.74 (s, 1H); ¹³C NMR (100 MHz, CDCl₃) ppm 138.1, 131.1, 129.7, 129.2, 91.6; HRMS (ESI): Exact mass calcd for C₇H₄Cl₂NO₂ [M-H]⁻ 203.9625, found 203.9625.



Chloro Nitroalkane in the Tetrahedral Intermediate (TI') Synthesis

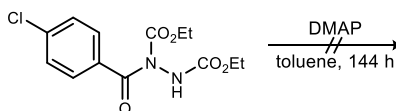
The amide (**79a**, characterized below in general procedure for tetrahedral intermediate conversion) was obtained in 20% isolated yield according to the general procedure for halogen screening in tetrahedral intermediate synthesis. The reaction time was 17 h in toluene.



Bromo Nitroalkane in the Tetrahedral Intermediate (TI') Synthesis

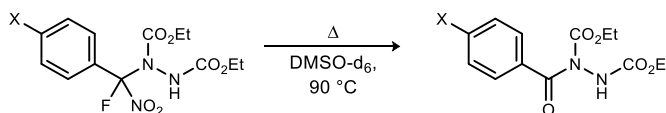
Evidence for formation of trace amounts of the amide (**79a**) was obtained by crude NMR of material from the general procedure for halogen screening in the tetrahedral intermediate synthesis.

The reaction time was 25 h in acetonitrile.



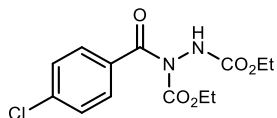
Evaluation of Imide Stability

The imide **79a** (9.3 mg, 30 μ mol) was dissolved in toluene (500 μ L). To this solution was added DMAP (700 μ g, 6 μ mol), and the reaction was stirred at room temperature for 144 h. The reaction mixture was filtered through a silica plug with dichloromethane and EtOAc before drying and concentration. The reaction mixture showed the imide largely intact.



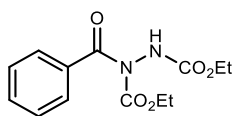
General Procedure for Tetrahedral Intermediate Conversion

The tetrahedral intermediate was dissolved in DMSO- d_6 and the solution was transferred to a J-Young NMR tube. The tube was placed into an oil bath at 90 $^{\circ}$ C. The crude product was purified by prep-HPLC. For prep-HPLC, the fractions were extracted with ethyl acetate, and the combined organic phase was washed with satd aq NaHCO_3 and brine before drying and concentration.



Diethyl 1-(4-chlorobenzoyl)hydrazine-1,2-dicarboxylate (79a).²⁶²

Prepared from **85a** (20.5 mg, 56.3 μmol) according to the general procedure for tetrahedral intermediate conversion. The reaction reached full conversion within 4.5 h. Preparatory HPLC (0-95% MeCN in H₂O) afforded the desired compound as a colorless oil (9.6 mg, 54%). $R_f = 0.38$ (40% EtOAc/hexanes); IR (film) 3309, 2983, 1735, 1592, 1494, 1382, 1250, 1075, 841, 760 cm^{-1} ; ¹H NMR (600 MHz, CDCl₃) δ 7.65 (br d, $J = 6.1$ Hz, 2H), 7.40 (d, $J = 9.0$ Hz, 2H), 6.94 (br s, 1H), 4.25 (q, $J = 7.2$ Hz, 2H), 4.19 (q, $J = 7.2$ Hz, 2H), 1.31 (t, $J = 6.5$ Hz, 3H), 1.14 (t, $J = 6.5$ Hz, 3H); ¹³C NMR (150 MHz, CDCl₃) ppm 170.2, 155.7, 153.4, 138.6, 133.2, 129.8, 128.7, 64.3, 63.0, 14.5, 14.0; HRMS (ESI): Exact mass calcd for C₁₃H₁₅ClN₂NaO₅ [M+Na]⁺ 337.0567, found 337.0565.

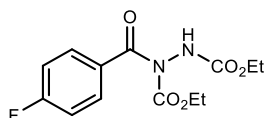


Diethyl 1-benzoylhydrazine-1,2-dicarboxylate (79b).²⁶² Prepared from

85b (25.8 mg, 78.4 μmol) according to the general procedure for tetrahedral intermediate conversion. The DMSO-*d*₆ used was from an ampule, and the solution was subjected to three freeze-pump-thaw cycles prior to heating. Also prior to heating but after degassing, water (2.8 μL , 160 μmol) and dibromomethane (3.0 μL , 42.7 μmol) were added. The reaction reached full conversion within 2 h. Preparatory HPLC (0-95% MeCN in H₂O) afforded the desired compound as a colorless oil (9.2 mg, 42%). $R_f = 0.11$ (20% EtOAc/hexanes); IR (film) 3311, 2985,

²⁶² At the time that the analytical data for this compound was collected the compound was unknown in literature. Prior to our publication, however, the compound was synthesized and published with associated characterization data (ref. Azizi, K.; Heydari, A. *Synlett* **2018**, 29, 189.). With the exception of physical nature, there is general agreement between collected data.

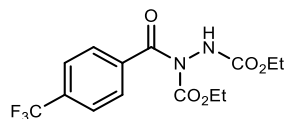
1735, 1499, 1376, 1250, 1063 cm^{-1} ; ^1H NMR (600 MHz, CDCl_3) δ 7.69 (br d, $J = 6.3$ Hz, 2H), 7.52 (t, $J = 7.4$ Hz, 1H), 7.42 (dd, $J = 7.6$ Hz, 7.6, 2H), 7.02 (br s, 1H), 4.25 (q, $J = 7.1$ Hz, 2H), 4.15 (br q, $J = 7.1$ Hz, 2H), 1.30 (br t, $J = 7.1$ Hz, 3H), 1.07 (br t, $J = 6.8$ Hz, 3H); ^{13}C NMR (150 MHz, CDCl_3) ppm 171.1, 155.7, 153.6, 134.9, 132.2, 128.3 (2C), 64.1, 62.9, 14.5, 13.9; HRMS (ESI): Exact mass calcd for $\text{C}_{13}\text{H}_{16}\text{N}_2\text{NaO}_5$ $[\text{M}+\text{Na}]^+$ 303.0962, found 303.0954.



Diethyl 1-(4-fluorobenzoyl)hydrazine-1,2-dicarboxylate (79c).

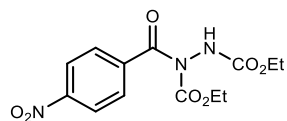
Prepared from **85c** (21.1 mg, 60.9 μmol) according to the general procedure for tetrahedral intermediate conversion. The $\text{DMSO}-d_6$ used was from an ampule, and the solution was subjected to three freeze-pump-thaw cycles prior to heating. Also, dibromomethane (2.00 μL , 28.5 μmol) was added prior to degassing. The reaction reached full conversion within 150 min. Preparatory HPLC (0-95% MeCN in H_2O) afforded the desired compound as a colorless oil (9.5 mg, 45%). $R_f = 0.12$ (20% EtOAc/hexanes); IR (film) 3309, 2983, 1731, 1602, 1498, 1244, 1063 cm^{-1} ; ^1H NMR (400 MHz, CDCl_3) δ 7.74 (br s, 2H), 7.11 (dd, $J = 8.8$, 8.8 Hz, 2H), 6.93 (br s, 1H), 4.25 (q, $J = 7.1$ Hz, 2H), 4.18 (q, $J = 7.1$ Hz, 2H), 1.31 (br t, $J = 7.0$ Hz, 3H), 1.14 (br t, $J = 7.0$ Hz, 3H); ^{13}C NMR (100 MHz, CDCl_3) ppm 165.3 (d, $^1J_{\text{CF}} = 253.6$ Hz), 153.5, 131.1 (d, $^3J_{\text{CF}} = 9.2$ Hz), 115.6 (d, $^2J_{\text{CF}} = 22.2$ Hz), 64.3, 63.0, 14.5, 14.0 [two quaternary carbons (the amide and one carbamate) were not observed due to insufficient signal to noise]; ^{19}F NMR (376 MHz, CDCl_3) δ

-106.0; HRMS (ESI): Exact mass calcd for C₁₃H₁₆FN₂O₅ [M+H]⁺ 299.1038, found 299.1040. The data here is consistent with that previously reported.^{263,264,265}



Diethyl 1-(4-(trifluoromethyl)benzoyl)hydrazine-1,2-dicarboxylate (79d). Prepared from **85d** (24.0 mg, 60.5 μmol)

according to the general procedure for tetrahedral intermediate conversion. The DMSO-*d*₆ used was from an ampule, and the solution was subjected to three freeze-pump-thaw cycles prior to heating. Also prior to heating but after degassing, water (2.20 μL, 121 μmol) and dibromomethane (3.00 μL, 42.7 μmol) were added. The reaction reached full conversion within 950 min. Preparatory HPLC (0-95% MeCN in H₂O) afforded the desired compound as a colorless oil (9.5 mg, 45%). R_f = 0.14 (20% EtOAc/hexanes); IR (film) 3311, 2989, 1738, 1501, 1391, 1255, 1138, 1065, 856, 768 cm⁻¹; ¹H NMR (400 MHz, CDCl₃) δ 7.77 (br d, *J* = 6.8 Hz, 2H), 7.69 (br d, *J* = 8.1 Hz, 2H), 6.98 (br s, 1H), 4.26 (q, *J* = 7.1 Hz, 2H), 4.18 (q, *J* = 7.1 Hz, 2H), 1.31 (br t, *J* = 7.0 Hz, 3H), 1.11 (br t, *J* = 6.8 Hz, 3H); ¹³C NMR (100 MHz, CDCl₃) ppm 170.0, 155.6, 153.2, 138.5, 133.5 (q, ²*J*_{CF} = 33.8 Hz), 128.4, 125.4 (q, ³*J*_{CF} = 3.6 Hz), 123.7 (q, ¹*J*_{CF} = 272.5 Hz), 64.5, 63.1, 14.5, 13.9; ¹⁹F NMR (376 MHz, CDCl₃) δ -63.1; HRMS (ESI): Exact mass calcd for C₁₄H₁₆F₃N₂O₅ [M+H]⁺ 349.1006, found 349.1007.



Diethyl 1-(4-nitrobenzoyl)hydrazine-1,2-dicarboxylate (79e).

Prepared from **85e** (38.6 mg, 103 μmol) according to the general

²⁶³ Chudasama, V.; Ahern, J. M.; Dhokia, D. V.; Fitzmaurice, R. J.; Caddick, S. *Chem. Commun.* **2011**, 47, 3269.

²⁶⁴ Shamsabadi, A.; Ren, J.; Chudasama, V. *RSC Adv.* **2017**, 7, 27608.

²⁶⁵ Zhang, H.-B.; Wang, Y.; Gu, Y.; Xu, P.-F. *RSC Adv.* **2014**, 4, 27796.

procedure for tetrahedral intermediate conversion. The DMSO-*d*₆ used was from an ampule, and the solution was subjected to three freeze-pump-thaw cycles prior to heating. Also prior to heating but after degassing, water (4.10 μ L, 226 μ mol) was added. The reaction reached full conversion within 2240 min. Preparatory HPLC (0-95% MeCN in H₂O) afforded the desired compound as a colorless oil (9.0 mg, 28%). R_f = 0.35 (40% EtOAc/hexanes); IR (film) 3318, 2988, 1738, 1605, 1521, 1355, 1254, 1064, 857, 719 cm^{-1} ; ¹H NMR (600 MHz, CDCl₃) δ 8.28 (d, J = 8.7 Hz, 2H), 7.81 (br d, J = 6.8 Hz, 2H), 7.01 (br s, 1H), 4.27 (q, J = 7.1 Hz, 2H), 4.20 (br q, J = 7.1 Hz, 2H), 1.32 (br t, J = 6.9 Hz, 3H), 1.16 (br t, J = 6.7 Hz, 3H); ¹³C NMR (150 MHz, CDCl₃) ppm 169.4, 155.6, 153.0, 149.5, 140.9, 128.8, 123.6, 64.7, 63.2, 14.5, 14.0; HRMS (ESI): Exact mass calcd for C₁₃H₁₅N₃NaO₇ [M+Na]⁺ 348.0808, found 348.0818.

Conversion of (-)-85e

(-)-85e (12.7 mg, 34.0 μ mol, 74% ee) was converted to imide according to the general procedure for tetrahedral intermediate conversion. Small aliquots of the reaction were taken at 20, 140, and 1400 min (<1% conversion, <1% conversion, and 68% conversion respectively), purified by prep-TLC to recover unreacted starting material, and found to have no loss in enantiopurity by chiral HPLC.

TI' Conversion in the Presence of TEMPO

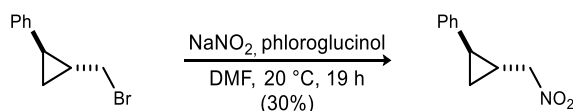
HANA 85a (28.5 mg, 78.5 μ mol) and TEMPO (12.2 mg, 78.5 μ mol) were used for this experiment which was run according to the general procedure for tetrahedral intermediate conversion, with the exceptions that the reaction was performed in toluene (1 mL), the temperature was 20 °C for 1 h, 50 °C for 1 h, 70 °C for 2 h, and 90 °C for 1 h, and purification was accomplished with flash

column chromatography (SiO₂, 0-20% ethyl acetate in hexanes). The only major products were recovered starting TI' (10.1 mg, 35%) and imide **79a** (11.2 mg, 42%).

Chemically Induced Dynamic Nuclear Polarization (CIDNP) Experiment

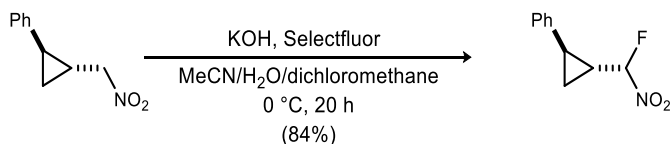
HANA **85a** (127.7 mg, 350.8 μmol) was dissolved in DMSO-*d*₆ (1 g) from an ampule and transferred to a J-Young NMR tube. The solution was subjected to three freeze-pump-thaw cycles prior to the addition of water (12.6 μL, 700 μmol) and α,α,α-trifluorotoluene (2.5 μL, 20.4 μmol). The NMR tube was added to an instrument with a temperature-controlled probe and the temperature was slowly ramped from 20 °C to 100 °C with frequent ¹H and ¹⁹F NMR scans. No CIDNP effects (enhancement or inversion of peaks) were observed.

Cyclopropane Radical Probe Experiments



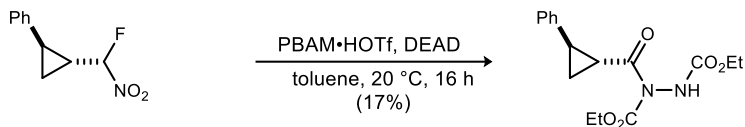
(*trans*-2-(Nitromethyl)cyclopropyl)benzene (S2). Prepared by adding a mixture of the bromide ((*trans*-2-(bromomethyl)cyclopropyl)benzene) and an impurity ((1-bromobut-3-en-1-yl)benzene) (1.7294 g of a 2.5:1 mixture of bromide to impurity, 5.85 mmol of bromide) to a solution of sodium nitrite (1.0336 g, 14.981 mmol) and phloroglucinol dihydrate (1.5184 g, 9.3647 mmol) in DMF (40 mL). The reaction was stirred for 19 h at room temperature before it was poured into ice water, extracted with diethyl ether, and washed with water. The resulting organic phase was dried and concentrated. Column chromatography (SiO₂, 2-5% ethyl acetate in hexanes) afforded the desired compound as a yellow oil (315.3 mg, 30%). R_f = 0.54 (20% EtOAc/hexanes); IR (film) 3027, 1552, 1375, 1153, 1088, 880, 756, 699 cm⁻¹; ¹H NMR (400 MHz, CDCl₃) δ 7.30 -

7.27 (m, 2H), 7.22 -7.18 (m, 1H), 7.13-7.10 (m, 2H), 4.40 (dd, $J = 13.2, 7.6$ Hz, 1H), 4.37 (dd, $J = 13.2, 7.6$ Hz, 1H), 2.05 (ddd, $J = 9.6, 5.0, 5.0$ Hz, 1H), 1.79 (dddd, $J = 8.4, 7.6, 7.6, 5.3, 4.5$ Hz, 1H), 1.22 (ddd, $J = 8.4, 5.7, 5.7$ Hz, 1H), 1.10 (ddd, $J = 9.1, 5.5, 5.5$ Hz, 1H); ^{13}C NMR (100 MHz, CDCl_3) ppm 140.4, 128.4, 126.23, 126.19, 79.3, 22.4, 19.4, 13.8; HRMS (ESI): Exact mass calcd for $\text{C}_{10}\text{H}_{10}\text{NO}_2$ $[\text{M}-\text{H}]^-$ 176.0717, found 176.0719.



(*trans*-2-((*R*)-Fluoro(nitro)methyl)cyclopropyl)benzene (103). Prepared from **S2** (79.0 mg, 4463 μmol) by dissolving in acetonitrile (350 μL) and water (700 μL). The solution was brought to 0 °C and KOH (33.8 mg, 514 μmol) was added and the reaction was stirred for an hour. Dichloromethane (1.3 mL) at -78 °C and selectfluor (207.8 mg, 586.8 μmol) were quickly added and the reaction was stirred vigorously as it warmed to 0 °C. The reaction was stirred between 0 and 10 °C for 19 h. Diethyl ether was added before 10 additional minutes of stirring, then the reaction was diluted with water and the phases were separated. The aqueous phase was extracted with diethyl ether and then the combined organic layers were dried and concentrated to afford a 1:1.5 mixture of diastereomers of the desired compound as a colorless oil (72.9 mg, 84%). $R_f = 0.19$ and 0.06 (5% $\text{Et}_2\text{O}/\text{hexanes}$); IR (film) 3036, 2931, 1574, 1480, 1367, 1175, 1105, 758, 691 cm^{-1} ; ^1H NMR (400 MHz, CDCl_3 , major diastereomer) δ 7.30-7.24 (m, 2H), 7.24-7.18 (m, 1H), 7.11-7.06 (m, 2H), 5.66 (dd, $^2J_{\text{H-F}} = 50.4$ Hz, $J = 5.7$ Hz, 1H), 2.41-2.32 (m, 1H), 1.79-1.91 (m, 1H), 1.43-1.33 (m, 1H), 1.30-1.18 (m, 1H); ^{13}C NMR (100 MHz, CDCl_3 , major diastereomer) ppm 138.9, 128.8, 127.0, 126.5, 111.1 (d, $^1J_{\text{C-F}} = 239.2$ Hz), 23.7 (d, $^2J_{\text{C-F}} = 22.7$ Hz), 20.8 (d, $^3J_{\text{C-F}} =$

5.5 Hz), 11.4; ^{19}F NMR (376 MHz, CDCl_3 , major diastereomer) δ -148.2; HRMS (CI): Exact mass calcd for $\text{C}_{10}\text{H}_{10}\text{FNO}_2$ $[\text{M}]^+$ 195.0690, found 195.0687.



Diethyl 1-(*trans*-2-phenylcyclopropane-1-carbonyl)hydrazine-1,2-dicarboxylate

(104). Prepared from **103** (19.5 mg, 100 μmol) by dissolving in toluene (1 mL) and adding PBAM·HOTf (13.1 mg, 20.0 μmol) and DEAD (50.0 μL of 40 wt% in toluene solution, 110 μmol).

This reaction was stirred for 16 hours at room temperature and then filtered through a silica plug (ethyl acetate), dried, and concentrated. Preparatory HPLC (0-95% MeCN in H_2O) afforded the title compound as a pale yellow oil (5.5 mg, 17%). No other diastereomer was observed (^1H NMR).

R_f = 0.16 (20% EtOAc/hexanes); IR (film) 3310, 2988, 1738, 1497, 1389, 1243, 1071, 762 cm^{-1} ;

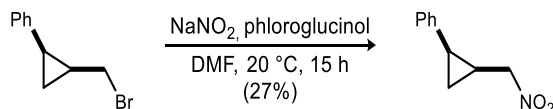
^1H NMR (400 MHz, CDCl_3) δ 7.31-7.26 (m, 2H), 7.23-7.18 (m, 1H), 7.16-7.12 (m, 2H), 6.69 (br s, 1H), 4.29 (q, J = 7.1 Hz, 2H), 4.22 (q, J = 7.1 Hz, 2H), 3.16 (br ddd, J = 7.5, 3.8, 3.8 Hz, 1H),

2.65 (ddd, J = 9.1, 6.4, 4.3 Hz, 1H), 1.77 (ddd, J = 9.1, 4.6, 4.6 Hz, 1H), 1.46 (ddd, J = 8.1, 6.5,

4.3 Hz, 1H), 1.32-1.24 (m, 6H); ^{13}C NMR (150 MHz, CDCl_3) ppm 173.4, 155.6, 153.5, 140.0,

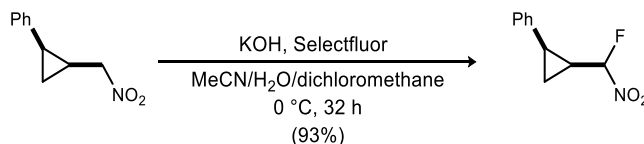
128.6, 126.8, 126.6, 64.2, 62.8, 29.2, 25.4, 19.2, 14.5, 14.2; HRMS (APCI): Exact mass calcd for

$\text{C}_{16}\text{H}_{21}\text{N}_2\text{O}_5$ $[\text{M}+\text{H}]^+$ 321.1445, found 321.1449.



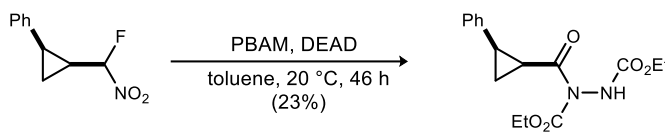
(*cis*-2-(Nitromethyl)cyclopropyl)benzene (S3). Prepared by adding a 1:0.15 mixture of the bromide ((*cis*-2-(bromomethyl)cyclopropyl)benzene) and impurity ((1-bromobut-3-en-1-

yl)benzene) (0.500 g, 2.06 mmol of bromide) to a solution of sodium nitrite (298.8 mg, 4.331 mmol) and phloroglucinol dihydrate (439.0 mg, 2.708 mmol) in DMF (12 mL). The reaction was stirred for 15 h at room temperature before diluting with ice water, extracting with diethyl ether, and washing with water. The resulting organic phase was dried and concentrated. Column chromatography (SiO₂, 2-5% ethyl acetate in hexanes) afforded the desired compound as a light yellow oil (108.3 mg, 27%). R_f = 0.17 (5% Et₂O/hexanes); IR (film) 3031, 1551, 1377, 1228, 1039, 839, 762, 706 cm⁻¹; ¹H NMR (400 MHz, CDCl₃) δ 7.34-7.28 (m, 2H), 7.27-7.23 (m, 1H), 7.23-7.18 (m, 2H), 4.10 (dd, *J* = 14.1, 7.6 Hz, 1H), 3.93 (dd, *J* = 14.1, 7.8 Hz, 1H), 2.50 (ddd, *J* = 8.3, 8.3, 6.8 Hz, 1H), 1.86 (dddd, *J* = 8.1, 8.1, 8.1, 8.1, 5.6 Hz, 1H), 1.26 (ddd, *J* = 8.4, 8.4, 5.9 Hz, 1H), 1.10 (ddd, *J* = 5.9, 5.9, 5.9 Hz, 1H); ¹³C NMR (100 MHz, CDCl₃) ppm 136.4, 129.2, 128.7, 127.1, 76.1, 21.5, 15.6, 8.5; HRMS (CI): Exact mass calcd for C₁₀H₁₁NO₂ [M]⁺ 177.0784, found 177.0786.



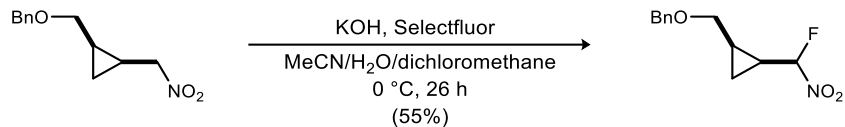
(*cis*-2-(Fluoro(nitro)methyl)cyclopropyl)benzene (105). Prepared from **S3** (71.7 mg, 405 μmol) by dissolving in acetonitrile (300 μL) and water (600 μL). The solution was chilled to 0 °C, KOH (30.7 mg, 466 μmol) was added, and the reaction was stirred for an hour. Selectfluor (188.5 mg, 532.1 μmol) in dichloromethane (1.2 mL) at -78 °C was added quickly, and the reaction was stirred vigorously as it warmed to 0 °C. The reaction was stirred at that temperature for 31 h. Diethyl ether was added before 10 additional minutes of stirring then the reaction was diluted with water and the phases were separated. The aqueous phase was extracted with diethyl ether, and the combined organic layers were dried and concentrated to afford a 1:1.5 mixture of diastereomers

of the desired compound as a colorless oil (73.7 mg, 93%). $R_f = 0.61$ (20% EtOAc/hexanes); IR (film) 3039, 2926, 1573, 1371, 1176, 1097, 975, 846, 767, 703 cm^{-1} ; ^1H NMR (400 MHz, CDCl_3 , major diastereomer) δ 7.40-7.27 (m, 5H), 4.94 (dd, $^2J_{\text{H-F}} = 50.7$ Hz, $J = 8.4$ Hz, 1H), 2.69-2.60 (m, 1H), 1.93-1.80 (m, 1H), 1.45 (ddd, $J = 6.2, 6.2, 6.2$ Hz, 1H), 1.42-1.34 (m, 1H); ^{13}C NMR (100 MHz, CDCl_3 , major diastereomer) ppm 134.9, 129.1, 128.8, 127.6, 111.5 (d, $^1J_{\text{C-F}} = 235.8$ Hz), 21.8 (d, $^3J_{\text{C-F}} = 7.0$ Hz), 24.2 (d, $^2J_{\text{C-F}} = 24.2$ Hz), 7.1 (d, $^4J_{\text{C-F}} = 2.6$ Hz); ^{19}F NMR (376 MHz, CDCl_3 , major diastereomer) δ -142.2; HRMS (CI): Exact mass calcd for $\text{C}_{10}\text{H}_{10}\text{FNO}_2$ $[\text{M}]^+$ 195.0690, found 195.0689.

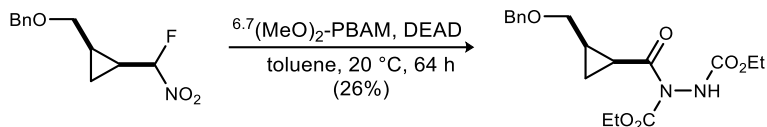


Diethyl 1-(*cis*-2-phenylcyclopropane-1-carbonyl)hydrazine-1,2-dicarboxylate (**106**).

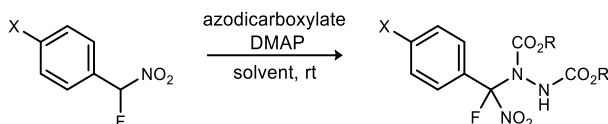
Prepared from **105** (19.5 mg, 100 μmol) by dissolving in toluene (1 mL) and adding PBAM (10.4 mg, 20.0 μmol) and DEAD (17.2 μL , 110 μmol). This reaction was stirred for 45.5 hours at room temperature before it was filtered through a silica plug (ethyl acetate), dried, and concentrated. Preparatory HPLC (0-95% MeCN in H_2O) afforded the title compound as a yellow oil (7.2 mg, 23%). No other diastereomer was observed (^1H NMR). $R_f = 0.14$ (20% EtOAc/hexanes); IR (film) 3319, 2985, 1735, 1377, 1325, 1242, 1032, 765 cm^{-1} ; ^1H NMR (400 MHz, CDCl_3) δ 7.20-7.15 (m, 1H), 7.26-7.20 (m, 4H), 6.45 (br s, 1H), 4.31 (q, $J = 7.1$ Hz, 2H), 4.15 (br s, 2H), 3.16 (br s, 1H), 2.80 (ddd, $J = 8.5, 8.5, 8.5$ Hz, 1H), 1.96 (br ddd, $J = 6.0, 6.0, 6.0$ Hz, 1H), 1.44 (ddd, $J = 7.9, 7.9, 5.1$ Hz, 1H), 1.34 (t, $J = 7.1$ Hz, 3H), 1.23 (br t, $J = 5.4$ Hz, 3H); ^{13}C NMR (100 MHz, CDCl_3) ppm 170.5 (br s), 155.5, 153.4, 136.1, 129.3, 128.2, 126.9, 63.9, 62.6, 27.9, 25.2 (br s), 14.4, 14.3, 12.5 (br s); HRMS (APCI): Exact mass calcd for $\text{C}_{16}\text{H}_{21}\text{N}_2\text{O}_5$ $[\text{M}+\text{H}]^+$ 321.1445, found 321.1449.



(((*cis*-2-(Fluoro(nitro)methyl)cyclopropyl)methoxy)methyl)benzene (107). Prepared from (((2-(nitromethyl)cyclopropyl)methoxy)methyl)benzene (38.9 mg, 176 μmol) by dissolving in acetonitrile (130 μL) and water (260 μL). The solution was chilled to 0 $^\circ\text{C}$ and KOH (13.3 mg, 203 μmol) was added and the reaction was stirred for 45 minutes. Dichloromethane (522 μL) at -78 $^\circ\text{C}$ and selectfluor (81.9 mg, 232 μmol) were quickly added and the reaction was stirred vigorously as it warmed to 0 $^\circ\text{C}$. The reaction was stirred at that temperature for 25 h. Diethyl ether was added before 10 additional minutes of stirring then the reaction was diluted with water and the phases were separated. The aqueous phase was extracted with diethyl ether and then the combined organic layer was dried and concentrated to afford a 1:1.9 mixture of diastereomers of desired compound. Column chromatography (SiO_2 , 5-15% Et_2O in hexanes) followed by preparatory HPLC (0-95% MeCN in H_2O) gave a clean 1:1.8 mixture of diastereomers as a colorless oil (23.0 mg, 55%). $R_f = 0.42$ (20% EtOAc /hexanes); IR (film) 3029, 2868, 1572, 1457, 1369, 1094, 745, 699 cm^{-1} ; ^1H NMR (600 MHz, CDCl_3 , major diastereomer) δ 7.39-7.34 (m, 2H), 7.34-7.29 (m, 3H), 5.86 (dd, $^2J_{\text{HF}} = 50.3$ Hz, $J = 7.8$ Hz, 1H), 4.55 (d, $J = 11.3$ Hz, 1H), 4.49 (d, $J = 11.6$ Hz, 1H), 3.85 (dd, $J = 10.0, 3.8$ Hz, 1H), 3.73-3.68 (m, 1H), 1.64-1.45 (m, 2H), 1.12-0.98 (m, 2H); ^{13}C NMR (150 MHz, CDCl_3 , major diastereomer) ppm 137.8, 128.6, 128.0, 127.9, 111.5 (d, $^1J_{\text{C-F}} = 236.0$ Hz), 73.2, 67.2, 18.1 (d, $^2J_{\text{C-F}} = 24.7$ Hz), 16.6 (d, $^3J_{\text{C-F}} = 5.9$ Hz), 6.7; ^{19}F NMR (376 MHz, CDCl_3 , major diastereomer) δ -139.7; HRMS (ESI): Exact mass calcd for $\text{C}_{12}\text{H}_{14}\text{FNNO}_3$ $[\text{M}+\text{Na}]^+$ 262.0850, found 262.0850.



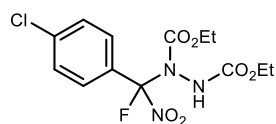
Diethyl 1-(*cis*-2-((Benzyloxy)methyl)cyclopropane-1-carbonyl)hydrazine-1,2-dicarboxylate (108). Prepared from **107** (11.5 mg, 48.1 μmol) by dissolving in toluene (500 μL) and adding $6,7\text{-}(\text{MeO})_2\text{-PBAM}$ (5.6 mg, 9.6 μmol) and DEAD (8.3 μL , 53 μmol). The solution was stirred for 64 hours at room temperature before it was filtered through a silica plug (ethyl acetate), dried, and concentrated. Preparatory HPLC (0-95% MeCN in H_2O) afforded the title compound as a colorless oil (4.5 mg, 26%). No other diastereomer was observed (^1H NMR). $R_f = 0.17$ (20% EtOAc/hexanes); IR (film) 3323, 2923, 1740, 1374, 1238, 1065 cm^{-1} ; ^1H NMR (400 MHz, toluene- d_8) δ 7.09-7.04 (m, 1H), 7.15 (t, $J = 7.5$ Hz, 2H), 7.27-7.19 (m, 2H), 7.30 (br s, 1H), 4.26 (br s, 2H), 3.94 (q, $J = 6.9$ Hz, 2H), 3.90 (q, $J = 6.8$ Hz, 2H), 3.58 (dd, $J = 10.4, 5.6$ Hz, 1H), 3.37 (dd, $J = 9.6, 9.6$ Hz, 1H), 1.51 (br dddd, $J = 8.3, 8.3, 8.3, 8.3$ Hz, 1H), 1.31 (br s, 1H), 1.23 (ddd, $J = 6.2, 6.2, 4.7$ Hz, 1H), 0.96 (t, $J = 7.1$ Hz, 3H), 0.91 (t, $J = 7.1$ Hz, 3H), 0.69 (ddd, $J = 7.8, 7.8, 4.7$ Hz, 1H); ^{13}C NMR (150 MHz, toluene- d_8) ppm 171.4 (br s), 155.5, 153.6, 139.4, 128.3, 127.9, 127.5 (br s), 72.6, 68.6, 63.3, 62.0, 30.3, 22.5, 14.4, 14.1, 12.0 (br s); HRMS (ESI): Exact mass calcd for $\text{C}_{18}\text{H}_{24}\text{N}_2\text{NaO}_6$ $[\text{M}+\text{Na}]^+$ 387.1527, found 387.1531.



General procedure for Tetrahedral Intermediate Synthesis

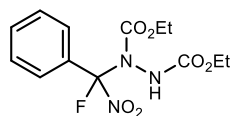
The α -fluoro nitroalkane (1.0 equiv) was dissolved in solvent (0.1 M). To this solution was added the azodicarboxylate and DMAP (0.2 equiv), and the reaction was stirred at room temperature.

The reaction mixture was filtered through a silica plug with dichloromethane and EtOAc before drying and concentration. The crude product was purified by prep-HPLC. For prep-HPLC, the fractions were diluted with ethyl acetate and the organic phase was washed with satd aq NaHCO₃ and brine before drying and concentration.



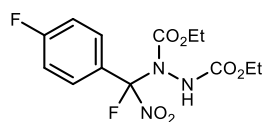
Diethyl 1-((4-chlorophenyl)fluoro(nitro)methyl)hydrazine-1,2-dicarboxylate (85a). Prepared from 1-chloro-4-

(fluoro(nitro)methyl)benzene (38.0 mg, 200 μ mol) and DEAD (35.2 μ L, 220 μ mol) in toluene according to the general procedure for tetrahedral intermediate synthesis. Full conversion was reached after 4.5 h. Preparatory HPLC (0-95% MeCN in H₂O) afforded the desired compound as a colorless oil (51.6 mg, 71%); R_f = 0.57 (40% EtOAc/hexanes); IR (film) 3310, 2989, 1749, 1590, 1497, 1379, 1283, 1087, 1026, 773 cm^{-1} ; ¹H NMR (400 MHz, DMSO-*d*₆, major conformer) δ 10.20 (d, ⁴ J_{HF} = 6.7 Hz, 1H), 7.74-7.53 (m, 4H), 4.33-3.87 (m, 4H), 1.22-0.99 (m, 6H); ¹³C NMR (100 MHz, DMSO-*d*₆, major conformer) ppm 155.5, 152.7, 137.0, 128.9 (br s), 128.1 (d, ³ J_{CF} = 7.8 Hz), 127.7 (d, ² J_{CF} = 25.5 Hz), 119.4 (d, ¹ J_{CF} = 264.6 Hz), 64.2, 61.6, 14.1, 13.9; ¹⁹F NMR (376 MHz, DMSO-*d*₆, major conformer) δ -103.1; HRMS (ESI): Exact mass calcd for C₁₃H₁₄ClFN₃O₆ [M-H]⁻ 362.0555, found 362.0542. The complexity observed in the NMR is in line with literature precedence for hindered hydrazine derivatives and has been attributed to a combination of hindered carbamate C-N bond rotation and hindered N-N bond rotation.^{105,106} Further confirmation by variable temperature NMR is not conclusive, as the material converts slowly to imide at 90 °C, prior to coalescence.



Diethyl 1-(fluoro(nitro)(phenyl)methyl)hydrazine-1,2-dicarboxylate (85b). Prepared from (fluoro(nitro)methyl)benzene (15.5 mg,

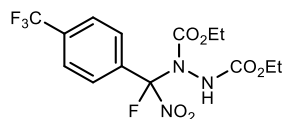
100 μmol) and DEAD (50.0 μL of 40 wt% in toluene solution, 110 μmol) in toluene according to the general procedure for tetrahedral intermediate synthesis. The reaction reached full conversion within 24 h. Preparatory HPLC (0-95% MeCN in H_2O) afforded the desired compound as a colorless oil (20.7 mg, 63%); $R_f = 0.17$ (20% EtOAc/hexanes); IR (film) 3306, 2989, 2925, 1746, 1586, 1510, 1284, 1075, 1037, 738 cm^{-1} ; ^1H NMR (600 MHz, CDCl_3) δ 7.79-7.40 (m, 5H), 6.73-6.33 (m, 1H), 4.35-3.97 (m, 4H), 1.29 (t, $J = 7.1$, 3H), 1.09 (t, $J = 6.7$ Hz, 3H); ^{13}C NMR (150 MHz, CDCl_3 , major conformer) ppm 155.2, 153.0, 131.8, 129.6 (d, $^2J_{\text{CF}} = 24.5$ Hz), 128.8, 126.2 (d, $^3J_{\text{CF}} = 7.1$ Hz), 120.2 (d, $^1J_{\text{CF}} = 264.4$ Hz), 64.9, 62.8, 14.3, 14.1; ^{19}F NMR (376 MHz, CDCl_3 , major conformer) δ -101.2; HRMS (ESI): Exact mass calcd for $\text{C}_{13}\text{H}_{16}\text{ClFN}_3\text{O}_6$ [$\text{M}+\text{Cl}$] $^-$ 364.0717, found 364.0708.



Diethyl 1-(fluoro(4-fluorophenyl)(nitro)methyl)hydrazine-1,2-dicarboxylate (85c). Prepared from 1-fluoro-4-

(fluoro(nitro)methyl)benzene (34.6 mg, 200 μmol) and DEAD (35.2 μL , 220 μmol) in toluene according to the general procedure for tetrahedral intermediate synthesis. The reaction was complete after 30 h. Preparatory HPLC (0-95% MeCN in H_2O) afforded the desired compound as a colorless oil (34.3 mg, 49%); $R_f = 0.21$ (20% EtOAc/hexanes); IR (film) 3306, 2990, 1746, 1592, 1509, 1250, 1078, 784 cm^{-1} ; ^1H NMR (600 MHz, CDCl_3 , major conformer) δ 7.64-7.63 (m, 2H), 7.13-7.11 (m, 2H), 6.75 (d, $J = 6.0$ Hz, 1H), 4.33-4.02 (m, 4H), 1.28 (t, $J = 7.1$ Hz, 3H), 1.13 (t, $J = 6.6$ Hz, 3H); ^{13}C NMR (150 MHz, CDCl_3 , major conformer) ppm 165.5, 163.8, 154.1 (d, $^1J_{\text{CF}} = 375.3$ Hz), 128.8 (dd, $^3J_{\text{CF}} = 7.8$, 7.8 Hz), 125.6 (d, $^2J_{\text{CF}} = 25.6$ Hz), 119.7 (d, $^1J_{\text{CF}} = 263.7$ Hz), 116.1 (d, $^2J_{\text{CF}} = 22.2$ Hz), 65.0, 63.0, 14.3, 14.0; ^{19}F NMR (376 MHz, CDCl_3 , major conformer) δ

-100.5, -107.5; HRMS (ESI): Exact mass calcd for C₁₃H₁₄F₂N₃O₆ [M-H]⁻ 346.0856, found 346.0847.

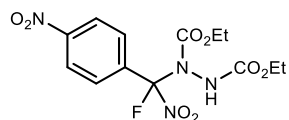


Diethyl

1-(fluoro(nitro)(4-

(trifluoromethyl)phenyl)methyl)hydrazine-1,2-dicarboxylate

(85d). Prepared from 1-(fluoro(nitro)methyl)-4-(trifluoromethyl)benzene (44.6 mg, 200 μmol) and DEAD (35.2 μL, 220 μmol) in toluene according to the general procedure for tetrahedral intermediate synthesis. The reaction was complete within 1.5 h. Preparatory HPLC (0-95% MeCN in H₂O) afforded the desired compound as a colorless oil (30.4 mg, 77%); R_f = 0.25 (20% EtOAc/hexanes); IR (film) 3304, 2992, 1747, 1592, 1507, 1306, 1151, 787 cm⁻¹; ¹H NMR (400 MHz, DMSO-*d*₆, major conformer) δ 10.24 (d, *J* = 6.7 Hz, 1H), 7.95-7.85 (m, 4H), 4.28-3.90 (m, 4H), 1.19 (t, *J* = 7.1 Hz, 3H), 0.97 (t, *J* = 7.1 Hz, 3H); ¹³C NMR (100 MHz, DMSO-*d*₆, major conformer) ppm 155.4, 152.6, 132.8 (d, ²*J*_{CF} = 24.7 Hz), 132.1 (q, ²*J*_{CF} = 32.0 Hz), 127.3 (d, ³*J*_{CF} = 7.9 Hz), 125.9, 123.5 (q, ¹*J*_{CF} = 272.4 Hz), 119.2 (d, ¹*J*_{CF} = 267.0 Hz), 64.3, 61.6, 14.1, 13.9; ¹⁹F NMR (376 MHz, CDCl₃, major conformer) δ -63.2, -101.1; HRMS (ESI): Exact mass calcd for C₁₄H₁₄F₄N₃O₆ [M-H]⁻ 396.0824, found 396.0824.

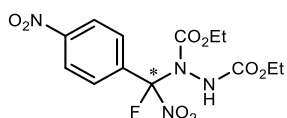


Diethyl 1-(fluoro(nitro)(4-nitrophenyl)methyl)hydrazine-1,2-

dicarboxylate (85e). Prepared from 1-(fluoro(nitro)methyl)-4-

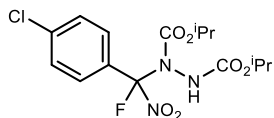
nitrobenzene (40.0 mg, 200 μmol) and DEAD (35.2 μL, 220 μmol) in acetonitrile according to the general procedure for tetrahedral intermediate synthesis. The reaction reached full conversion within 30 min. Preparatory HPLC (0-95% MeCN in H₂O) afforded the desired compound as a colorless oil (51.6 mg, 71%); R_f = 0.17 (20% EtOAc/hexanes); IR (film) 3310, 2990, 1749, 1593, 1525, 1288, 1082, 737 cm⁻¹; ¹H NMR (600 MHz, CDCl₃, major conformer) δ 8.63 (d, *J* = 8.8 Hz,

2H), 8.22 (br d, $J = 8.2$ Hz, 2H), 7.26 (d, $^4J_{\text{FH}} = 7.1$ Hz, 1H), 4.69-4.31 (m, 4H), 1.62 (t, $J = 7.2$ Hz, 3H), 1.47 (br t, $J = 6.9$ Hz, 3H); ^{13}C NMR (150 MHz, CDCl_3 , major conformer) ppm 155.5, 152.6, 149.9, 135.7 (d, $^2J_{\text{CF}} = 25.8$ Hz), 127.9 (d, $^3J_{\text{CF}} = 6.5$ Hz), 123.9, 119.0 (d, $^1J_{\text{CF}} = 264.3$ Hz), 65.3, 63.3, 14.2, 14.0; ^{19}F NMR (376 MHz, CDCl_3 , major conformer) δ -100.9; HRMS (ESI): Exact mass calcd for $\text{C}_{13}\text{H}_{15}\text{FN}_4\text{NaO}_8$ $[\text{M}+\text{Na}]^+$ 397.0771, found 397.0773.



(-)-Diethyl 1-(fluoro(nitro)(4-nitrophenyl)methyl)hydrazine-1,2-dicarboxylate ((-)-85e). Prepared from 1-(fluoro(nitro)methyl)-4-

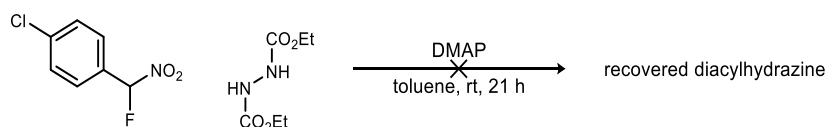
nitrobenzene (10.0 mg, 50.0 μmol) and DEAD (8.8 μL , 55 μmol) in toluene according to the general procedure for tetrahedral intermediate synthesis with the exceptions that the catalyst was PBAM·HNTf₂ and the temperature was -78 °C. The reaction reached full conversion within 3 days. Preparatory HPLC (0-95% MeCN in H₂O) afforded the desired compound (12.7 mg, 68%) matching all characterization data for **32e**. The e.e. was determined by chiral HPLC analysis (Chiralpak IA, 10% EtOH/hexanes, 1.0 mL/min, t_r (e₁, minor) = 15.2 min, t_r (e₂, major) = 18.1 min to be 74%. $[\alpha]_D^{20}$ -8.7 (c 1.13, CHCl_3) for a separately prepared sample of 78% ee.



Diisopropyl 1-((4-chlorophenyl)fluoro(nitro)methyl)hydrazine-1,2-dicarboxylate (88). Prepared from 1-chloro-4-

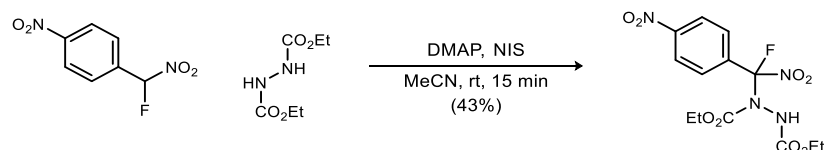
(fluoro(nitro)methyl)benzene (38.0 mg, 200 μmol) and DIAD (39.0 μL , 200 μmol) in toluene according to the general procedure for tetrahedral intermediate synthesis. The reaction reached full conversion within 6 h. Preparatory HPLC (0-95% MeCN in H₂O) afforded the desired compound as a colorless amorphous solid (20.5 mg, 29%); $R_f = 0.57$ (40% EtOAc/hexanes); IR (film) 3311, 2984, 1743, 1588, 1496, 1373, 1274, 1099, 975, 791 cm^{-1} ; ^1H NMR (600 MHz, CDCl_3 , major conformer) δ 7.58 (d, $J = 7.7$ Hz, 2H), 7.41 (d, $J = 8.6$ Hz, 2H), 6.59 (d, $J = 5.9$ Hz, 1H), 5.07-4.77

(m, 2H), 1.30 (d, $J = 6.1$ Hz, 6H), 1.25 (d, $J = 5.8$ Hz, 6H); ^{13}C NMR (150 MHz, CDCl_3 , major conformer) ppm 155.0, 152.4, 138.2, 129.1 (br s), 128.4 (d, $^2J_{\text{CF}} = 24.6$ Hz), 127.9 (d, $^3J_{\text{CF}} = 6.7$ Hz), 119.8 (d, $^1J_{\text{CF}} = 264.6$ Hz), 74.0, 71.1, 22.0-21.5 (m, 4C); ^{19}F NMR (376 MHz, CDCl_3 , major conformer) δ -100.8; HRMS (ESI): Exact mass calcd for $\text{C}_{15}\text{H}_{18}\text{ClFN}_3\text{O}_6$ $[\text{M-H}]^-$ 390.0868, found 390.0868.



Control Reaction with Diacyl Hydrazine

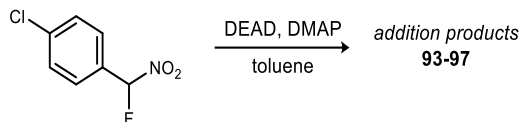
The α -fluoro nitroalkane (38.2 mg, 200 μmol) was dissolved in toluene (2 mL). To this solution was added the diacyl hydrazine (35.2 mg, 200 μmol) and DMAP (4.8 mg, 40 μmol), and the reaction was stirred at room temperature for 21 h. The reaction mixture was filtered through a silica plug with dichloromethane and EtOAc before drying and concentration. The crude material showed no conversion to imide or HANA.



Control Reaction with Diacyl Hydrazine and Oxidant

The diacyl hydrazine (21.1 mg, 120 μmol), NIS (27.0 mg, 120 μmol), and DMAP (14.4 mg, 120 μmol) were dissolved in acetonitrile (1 mL). α -Fluoro nitroalkane (20.0 mg, 100 μmol) was added dropwise as a solution in acetonitrile (1 mL), and the reaction was stirred at room temperature for 15 min. The reaction mixture was filtered through a silica plug with dichloromethane and EtOAc

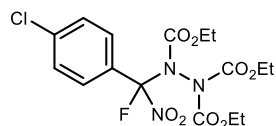
before drying and concentration. Preparatory HPLC (0-95% MeCN in H₂O) afforded the TI' (16.2 mg, 43%).



General Procedure for Preparation of Tetrahedral Intermediate Synthesis

Byproducts

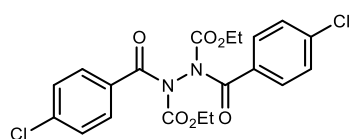
1-Chloro-4-(fluoro(nitro)methyl)benzene (1.0 equiv) was dissolved in toluene (0.1 M). DEAD and DMAP (0.2 equiv) were added, and the reaction was stirred. The reaction mixture was filtered through a silica plug with dichloromethane and ethyl acetate before drying and concentration.



Diethyl 1-(4-chlorobenzoyl)hydrazine-1,2-dicarboxylate (93).

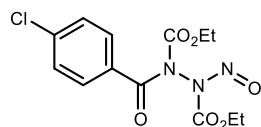
Prepared from fluoro nitroalkane (114.0 mg, 600 μ mol) and DEAD (105 μ L, 660 μ mol) according to the general procedure for preparation of tetrahedral intermediate synthesis byproducts. The reaction was stopped after 15 h at rt. Preparatory HPLC (0-95% MeCN in H₂O) afforded the product as a colorless oil (8.1 mg, 4%). $R_f = 0.23$ (20% EtOAc/hexanes); IR (film) 2986, 1766, 1592, 1470, 1264, 1101, 1020, 774 cm^{-1} ; ^1H NMR (600 MHz, CDCl_3) δ 7.59 (br d, $J = 7.8$ Hz, 2H), 7.39 (d, $J = 8.7$ Hz, 2H), 4.39-4.27 (m, 4H), 4.27-4.17 (m, 2H), 1.42-1.36 (m, 3H), 1.31-1.23 (m, 6H); ^{13}C NMR (150 MHz, CDCl_3 , one conformation) ppm 151.2-150.7 (m, 3C), 138.8, 129.3, 127.3 (d, $^2J_{\text{HF}} = 28.4$ Hz), 127.2 (d, $^3J_{\text{HF}} = 7.6$ Hz), 117.9 (d, $^1J_{\text{HF}} = 266.0$ Hz), 64.8, 64.7 (2C), 14.2-13.7 (m, 3C); ^{19}F NMR (376 MHz, CDCl_3 , major conformation) δ -103.5; HRMS (ESI): Exact mass calcd for $\text{C}_{16}\text{H}_{19}\text{ClFN}_3\text{NaO}_8$ $[\text{M}+\text{Na}]^+$ 458.0742, found 458.0741.

This compound appears to exist as two conformational isomers by NMR spectroscopy, slightly favoring one. Specifically, two distinct fluorine resonances are observed (-100.59, -103.53 ppm), alongside two distinct ^{13}C doublets for the sp^3 -hybridized carbon (118.5 ($^1J_{\text{CF}} = 265.3$ Hz), 117.9 ($^1J_{\text{CF}} = 266.0$)). The ester carbonyls appear as six peaks in the range 151.2-150.7. We speculate that the imide bond (cis-, trans-imide) or the N-N bond results in the isomers due to restricted rotation (see discussion for **32a**).



Diethyl 1,2-bis(4-chlorobenzoyl)hydrazine-1,2-dicarboxylate (94). Prepared from fluoro nitroalkane (76.0 mg,

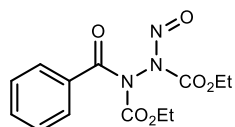
400 μmol) and DEAD (64.0 μL , 440 μmol) according to the general procedure for preparation of tetrahedral intermediate synthesis byproducts. The reaction was stopped after 69 h at rt. The residue was subjected to silica gel chromatography (10-20% ethyl acetate in hexanes) to give the product as a colorless oil (5.6 mg, 6%). $R_f = 0.69$ (40% ethyl acetate in hexanes); IR (film) 2922, 2855, 1759, 1710, 1590, 1473, 1373, 1241 cm^{-1} ; ^1H NMR (600 MHz, CDCl_3) δ 7.67 (d, $J = 8.4$ Hz, 2H), 7.43 (d, $J = 8.5$ Hz, 2H), 4.21 (q, $J = 7.1$ Hz, 2H), 1.14 (t, $J = 7.1$ Hz, 3H); ^{13}C NMR (150 MHz, CDCl_3) δ 168.1, 152.1, 138.7, 132.6, 129.7, 128.6, 64.5, 13.8; HRMS (ESI): Exact mass calcd for $\text{C}_{20}\text{H}_{18}\text{Cl}_2\text{N}_2\text{NaO}_6$ [$\text{M}+\text{Na}$] $^+$ 475.0440, found 475.0406.



Diethyl 1-(4-chlorobenzoyl)-2-nitrosohydrazine-1,2-dicarboxylate (95a). Prepared from fluoro nitroalkane (76.0 mg, 400

μmol) and DEAD (64.0 μL , 400 μmol) according to the general procedure for preparation of tetrahedral intermediate synthesis byproducts. The reaction was stopped after 162.5 h at rt under an oxygen atmosphere. Column chromatography (SiO_2 , 6-15% ethyl acetate in hexanes) afforded the product as a colorless oil (12.0 mg, 10%). $R_f = 0.66$ (40% EtOAc/hexanes); IR (film) 2987,

2926, 1768, 1574, 1469, 1382, 1228, 1091, 1008, 831 cm^{-1} ; ^1H NMR (600 MHz, CDCl_3) δ 7.65 (d, $J = 8.5$ Hz, 2H), 7.43 (d, $J = 8.4$ Hz, 2H), 4.62 (q, $J = 7.1$ Hz, 2H), 4.13 (d, $J = 7.1$ Hz, 2H), 1.49 (t, $J = 7.1$ Hz, 3H), 1.09 (t, $J = 7.1$ Hz, 3H); ^{13}C NMR (150 MHz, CDCl_3) ppm 166.3, 151.1, 150.2, 139.4, 131.7, 130.0, 128.8, 65.9, 64.9, 14.4, 13.9; HRMS (ESI): Exact mass calcd for $\text{C}_{13}\text{H}_{14}\text{ClN}_3\text{NaO}_6$ $[\text{M}+\text{Na}]^+$ 366.0469, found 366.0465.

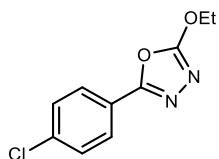


Diethyl 1-benzoyl-2-nitrosohydrazine-1,2-dicarboxylate (95b).

Prepared from **85b** (13.3 mg, 21.5 μmol) according to the general procedure for tetrahedral intermediate conversion with the substitution of toluene- d_8 for DMSO- d_6 . Prior to heating, dibromomethane (1.50 μL , 21.4 μmol) was added. The reaction reached full conversion within 40 min to give an NMR yield of 70%. Or, from **79b** by adapted literature procedure²⁶⁶ in which **79b** (18.5 mg, 66.1 μmol) was dissolved in acetonitrile (1 mL) in a flame-dried vial with a stirbar. To that solution was added pyridine (10.6 μL , 132 μmol) before it was brought to -20 $^\circ\text{C}$. NOBF_4 (15.5 mg, 132 μmol) was added and the reaction was allowed to warm to 0 $^\circ\text{C}$ while stirring under a nitrogen atmosphere. The reaction was stopped after an hour by passing it through a silica plug with 20% ethyl acetate in hexanes. Preparatory HPLC (0-95% MeCN in H_2O) afforded the desired compound as a light yellow oil (11.7 mg, 57%). $R_f = 0.40$ (20% EtOAc/hexanes); IR (film) 2924, 1766, 1717, 1554, 1454, 1375, 1303, 1206, 1085, 1008, 892, 826 cm^{-1} ; ^1H NMR (600 MHz, CDCl_3) δ 7.70 (d, $J = 7.1$ Hz, 2H), 7.57 (t, $J = 7.5$ Hz, 1H), 7.80 (dd, $J = 7.8$ Hz, 7.8, 2H), 4.62 (q, $J = 7.1$ Hz, 2H), 4.11 (br q, $J = 7.1$ Hz, 2H), 1.49 (t, $J = 7.1$ Hz, 3H), 1.04 (t, $J = 7.1$ Hz,

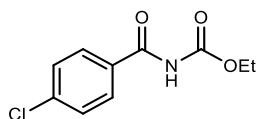
²⁶⁶Thakkalapally, A.; Benin, V. *Tetrahedron* **2005**, *61*, 4939.

3H); ^{13}C NMR (150 MHz, CDCl_3) ppm 167.2, 151.2, 150.4, 133.4, 132.9, 128.5, 128.4, 65.8, 64.7, 14.4, 13.8; HRMS (ESI): Exact mass calcd for $\text{C}_{13}\text{H}_{15}\text{N}_3\text{NaO}_6$ $[\text{M}+\text{Na}]^+$, 332.0853, found 332.0854.



Diethyl 1-(4-chlorobenzoyl)hydrazine-1,2-dicarboxylate (96).

Prepared from fluoro nitroalkane (76.0 mg, 400 μmol) and DEAD (64.0 μL , 400 μmol) according to the general procedure for preparation of tetrahedral intermediate synthesis byproducts. The reaction was stopped after 55 h at 45 $^\circ\text{C}$. Preparatory HPLC (0-95% MeCN in H_2O) afforded the product with some impurities. Prep-TLC then yielded the clean product as a white solid (2.0 mg, 2%). Mp 109-111 $^\circ\text{C}$; R_f = 0.45 (40% EtOAc/hexanes); IR (film) 2922, 1606, 1413, 1281, 1088, 836, 730 cm^{-1} ; ^1H NMR (400 MHz, CDCl_3) δ 7.87 (d, J = 8.4 Hz, 2H), 7.45 (d, J = 8.4 Hz, 2H), 4.61 (q, J = 7.1 Hz, 2H), 1.52 (t, J = 7.2 Hz, 3H); ^{13}C NMR (150 MHz, CDCl_3) ppm 165.9, 159.8, 137.5, 129.5, 127.5, 122.8, 69.5, 14.5; HRMS (ESI): Exact mass calcd for $\text{C}_{10}\text{H}_9\text{ClN}_2\text{NaO}_2$ $[\text{M}+\text{Na}]^+$ 225.0431, found 225.0437.



Diethyl 1-(4-chlorobenzoyl)hydrazine-1,2-dicarboxylate (97)²⁶⁷.

Prepared from fluoro nitroalkane (76.0 mg, 400 μmol) and DEAD (64.0 μL , 400 μmol) according to the general procedure for preparation of tetrahedral intermediate synthesis byproducts. The reaction was stopped after 55 h at 45 $^\circ\text{C}$. Preparatory HPLC (0-95% MeCN in H_2O) afforded the product as a white solid (0.9 mg, 1%). Mp 116-118 $^\circ\text{C}$; R_f = 0.25 (40% EtOAc/hexanes); IR (film) 3283, 2926, 1762, 1509, 1200, 1029 cm^{-1} ; ^1H NMR (600 MHz, CDCl_3)

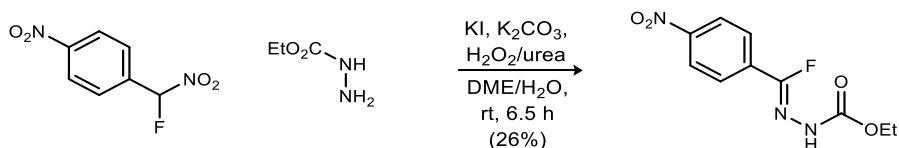
²⁶⁷ Wu, L.; Yang, X.; Yan, F. *Bull. Chem. Soc. Ethiop.* **2011**, 25.

δ 7.94 (br s, 1H), 7.76 (d, $J = 8.6$ Hz, 2H), 7.46 (d, $J = 8.6$ Hz, 2H), 4.31 (q, $J = 7.1$ Hz, 2H), 1.35 (t, $J = 7.1$ Hz, 3H); ^{13}C NMR (150 MHz, CDCl_3) ppm 164.1, 151.0, 139.6, 131.5, 129.4, 129.2, 62.8, 14.4; HRMS (ESI): Exact mass calcd for $\text{C}_{10}\text{H}_{10}\text{ClNO}_3$ $[\text{M}]^+$ 250.0247, found 250.0241.



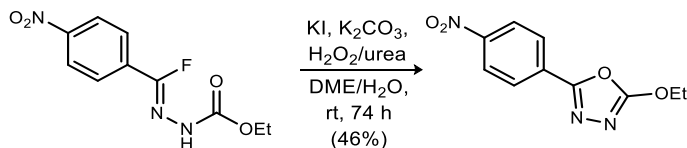
Conversion of **95a** in the Presence of $^{18}\text{OH}_2$

HANA **95a** (1.2 mg, 3.5 μmol) was subjected to the general procedure for tetrahedral intermediate conversion with $^{18}\text{OH}_2$ (1 μL , 50 μmol) added to the reaction prior to heating. The reaction was stopped after 10 h. Preparatory HPLC (0-95% MeCN in H_2O) afforded imide (<1 mg) with negligible ^{18}O incorporation as determined by high resolution mass spectrometry.



Ethyl (Z)-2-(fluoro(4-nitrophenyl)methylene)hydrazine-1-carboxylate (120). As adapted from literature procedure⁸⁹, the fluoro nitroalkane (40.0 mg, 200 μmol), hydrazide (25.0 mg, 240 μmol), potassium iodide (66.4 mg, 400 μmol), and potassium carbonate (55.2 mg, 400 μmol) were stirred in 1,2-dimethoxyethane (2.0 mL) while a solution of urea-hydrogen peroxide in 4:1 1,2-dimethoxyethane:water (0.400 mL of a 0.50 M solution, 200 μmol) was added over two hours by syringe pump. The solution was stirred for an additional 4.5 h after addition was complete then quenched with satd aq sodium thiosulfate. The crude mixture was then extracted with ethyl acetate, washed with brine, dried over sodium sulfate, and concentrated. Preparatory HPLC (0-

95% MeCN in H₂O) afforded the product as a white solid (11.6 mg, 26%). Mp 139-140 °C; R_f = 0.14 (20% EtOAc/hexanes); IR (film) 3250, 2925, 1732, 1600, 1525, 1338, 1240, 1078, 856 cm⁻¹; ¹H NMR (600 MHz, CDCl₃) δ 8.32 (br s, 1H), 8.26 (d, *J* = 7.8 Hz, 2H), 8.01 (d, *J* = 8.0 Hz, 2H), 4.32 (q, *J* = 7.0 Hz, 2H), 1.35 (t, *J* = 6.8 Hz, 3H); ¹³C NMR (150 MHz, CDCl₃) ppm 152.9 (br), 149.3, 142.8 (br d, ¹J_{CF} = 314.6 Hz), 132.7 (d, ²J_{CF} = 34.5 Hz), 127.2 (d, ³J_{CF} = 4.1 Hz), 124.0, 62.8, 14.6; ¹⁹F NMR (376 MHz, CDCl₃) δ -74.9 (br); HRMS (CI): Exact mass calcd for C₁₀H₁₁FN₃O₄ [M+H]⁺ 256.0728, found 256.0723.²⁶⁸



2-Ethoxy-5-(4-nitrophenyl)-1,3,4-oxadiazole (121). The acyl hydrazone (15.0 mg, 58.8 μmol), potassium iodide (66.4 mg, 400 μmol), and potassium carbonate (55.2 mg, 400 μmol) were stirred in 1,2-dimethoxyethane (580 μL) while a solution of urea-hydrogen peroxide in 4:1 1,2-dimethoxyethane:water (116 μL of a 0.50 M solution, 58 μmol) was added over one and a half hours in portions. The solution was stirred for an additional 72 h after addition was complete, and then quenched with satd aq sodium thiosulfate. The crude mixture was then extracted with ethyl acetate, washed with brine, dried over sodium sulfate, and concentrated. Column chromatography (SiO₂, 40% ethyl acetate in hexanes) afforded the product as a white solid (6.3 mg, 46%). Mp 145-147 °C; R_f = 0.42 (40% EtOAc/hexanes); IR (film) 2926, 1599, 1519, 1459, 907, 730 cm⁻¹; ¹H

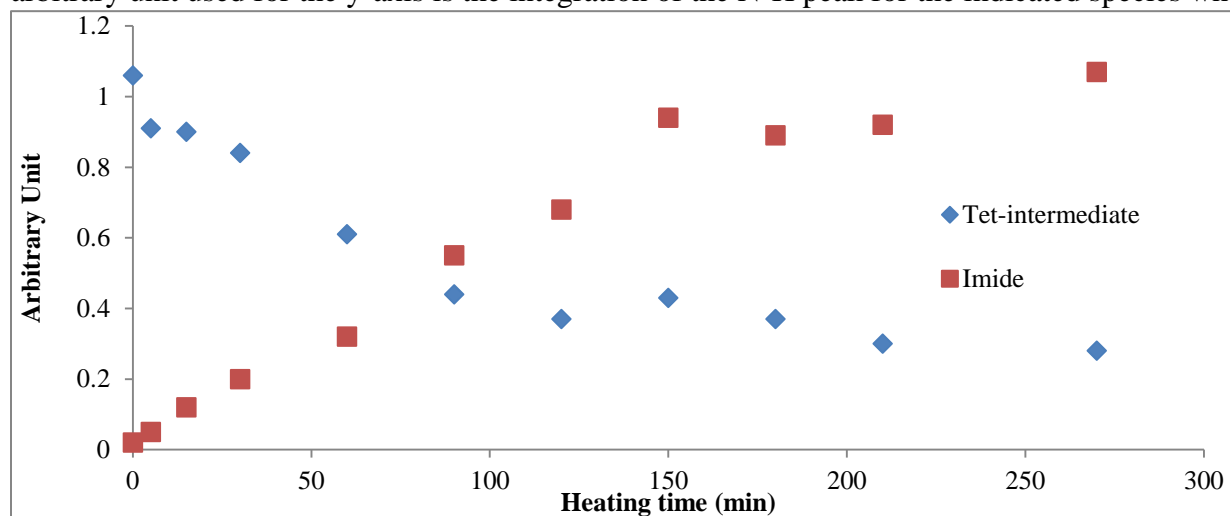
²⁶⁸ The critical ¹⁹F and ¹³C peaks are quite close in value to related α-fluoro hydrazones in literature (Mamone, M.; Morvan, E.; Milcent, T.; Ongeri, S.; Crousse, B. *J. Org. Chem.* **2015**, *80*, 1964.)

NMR (600 MHz, CDCl₃) δ 8.34 (d, $J = 8.9$ Hz, 2H), 8.13 (d, $J = 8.9$ Hz, 2H), 4.66 (q, $J = 7.1$ Hz, 2H), 1.55 (t, $J = 7.1$ Hz, 3H); ¹³C NMR (150 MHz, CDCl₃) ppm 166.4, 158.9, 149.3, 129.8, 127.0, 124.5, 70.0, 14.5; HRMS (CI): Exact mass calcd for C₁₀H₁₀N₃O₄ [M+H]⁺ 236.0666, found 236.0660.

Tetrahedral Intermediate NMR Conversion Experiments

Conversion of 85a in Wet Oxygenated Solvent

85a (20.5 mg, 56.3 μmol) was converted to imide according to the general procedure for tetrahedral intermediate conversion. The $\text{DMSO-}d_6$ used was not from an ampule and therefore quite wet. No degassing was performed, so molecular oxygen was present in the reaction. The data collected from the ^1H NMR taken at various time points is graphically displayed below. The arbitrary unit used for the y-axis is the integration of the N-H peak for the indicated species when

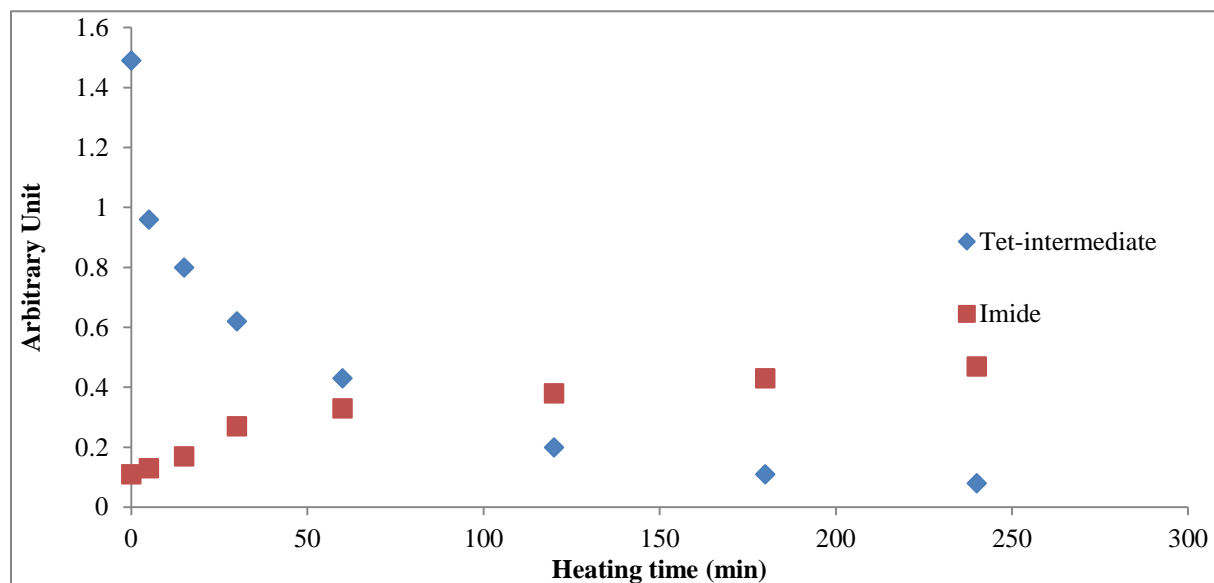


residual DMSO as internal standard is calibrated to a quantity of one.

Conversion of 85a in Dry Oxygenated Solvent

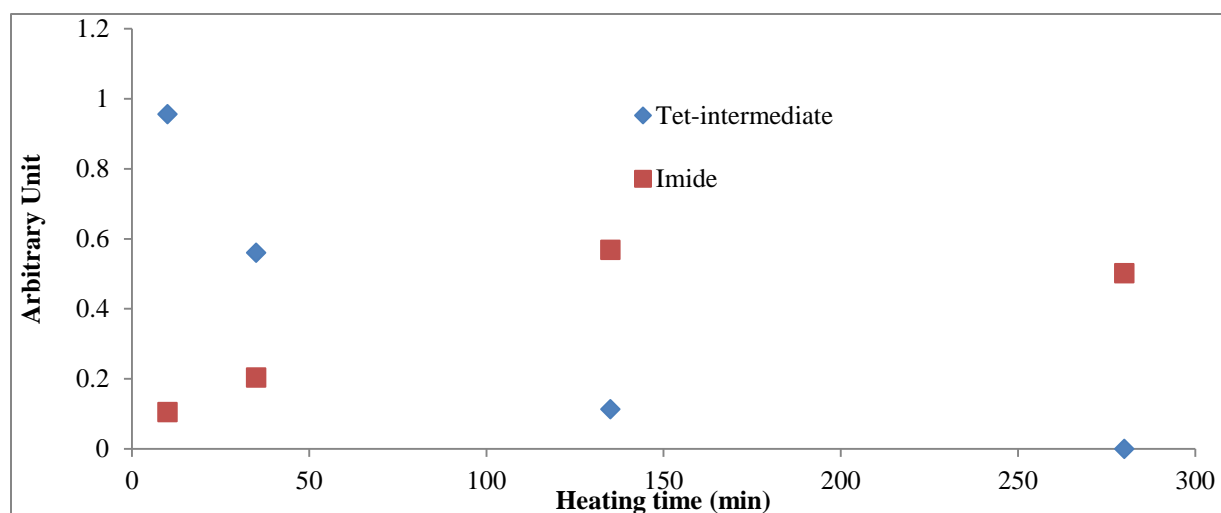
85a (21.8 mg, 59.9 μmol) was converted to imide according to the general procedure for tetrahedral intermediate conversion. The $\text{DMSO-}d_6$ used was from an ampule. Prior to heating, the solution was subjected to three freeze-pump-thaw cycles (the last of which was refilled using O_2). The data collected from the ^1H NMR taken at various time points is graphically displayed below.

The arbitrary unit used for the y-axis is the integration of the N-H peak for the indicated species when residual DMSO as internal standard is calibrated to a quantity of one.



Conversion of 85a in Dry Degassed Solvent

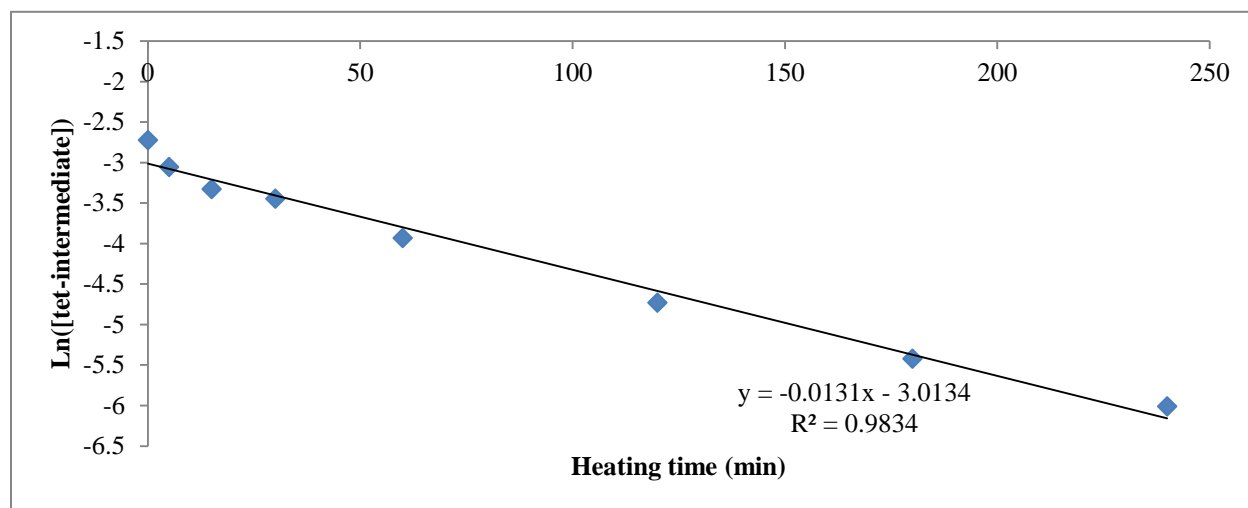
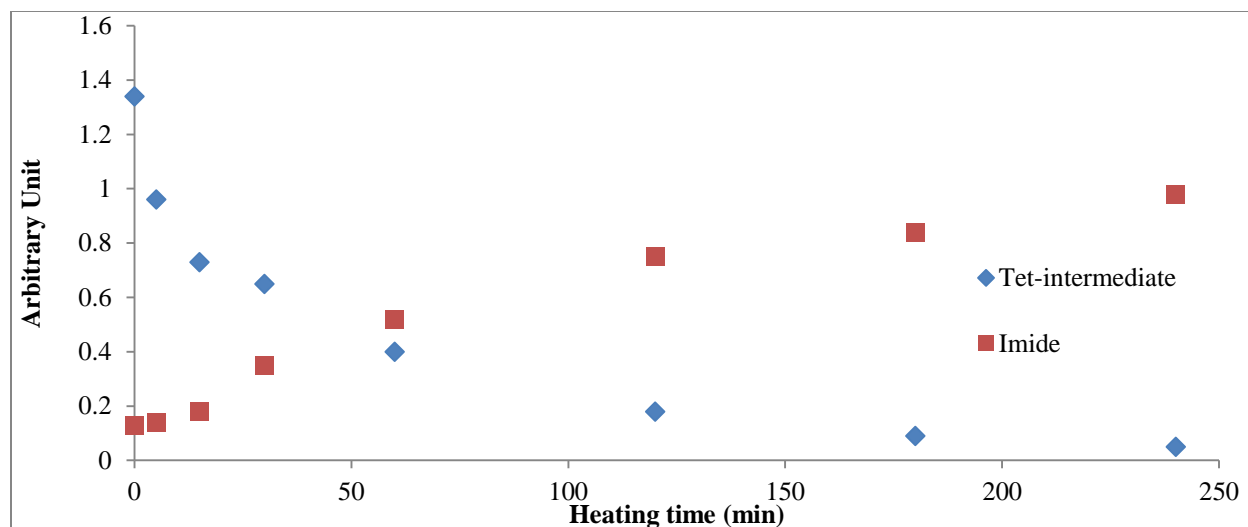
85a (<25.8 mg, 70.8 μmol) was converted to imide according to the general procedure for tetrahedral intermediate conversion. The $\text{DMSO-}d_6$ used was from an ampule. Prior to heating, the solution was subjected to three freeze-pump-thaw cycles. The data collected from the ^1H NMR taken at various time points is graphically displayed below. The arbitrary unit used for the y-axis



is the integration of the N-H peak for the indicated species when residual DMSO as internal standard is calibrated to a quantity of one.

Conversion of 85a in Degassed Solvent

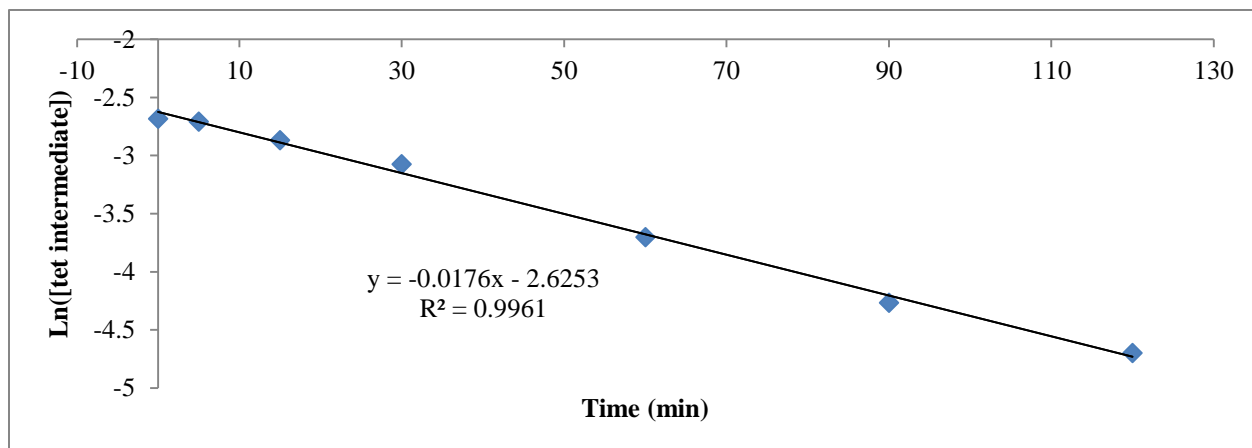
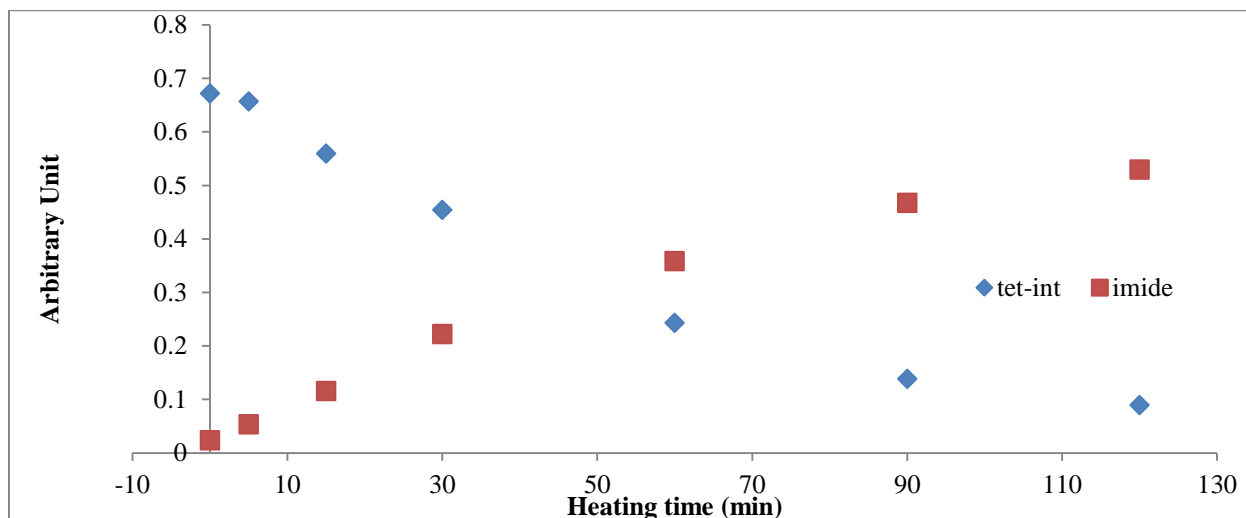
85a (21.8 mg, 59.9 μmol) was converted to imide according to the general procedure for tetrahedral intermediate conversion. The DMSO- d_6 used was from an ampule. Prior to heating, the solution was subjected to three freeze-pump-thaw cycles. After degassing, H_2^{18}O (2.2 μL , 120 μmol) was added. The data collected from the ^1H NMR taken at various time points is graphically displayed below. The arbitrary unit used for the y-axis is the integration of the N-H peak for the indicated species when residual DMSO as internal standard is calibrated to a quantity of one. The data was used to derive kinetic data and that graph is also shown. SI II contains an overlay of the raw NMR spectra.



Conversion of 85b in Degassed Solvent

85b (25.8 mg, 78.4 μmol) was converted to imide according to the general procedure for tetrahedral intermediate conversion. The $\text{DMSO-}d_6$ used was from an ampule. Prior to heating, the solution was subjected to three freeze-pump-thaw cycles. After degassing, H_2O (2.80 μL , 157 μmol) and dibromomethane (3.00 μL , 42.7 μmol) were added. The data collected from the ^1H NMR taken at various time points is graphically displayed below. The arbitrary unit used for the y-axis is the integration of the N-H peak for the indicated species when dibromomethane as internal

standard is calibrated to an integration of one. The data was used to derive kinetic data and that graph is also shown. SI II contains an overlay of the raw NMR spectra.

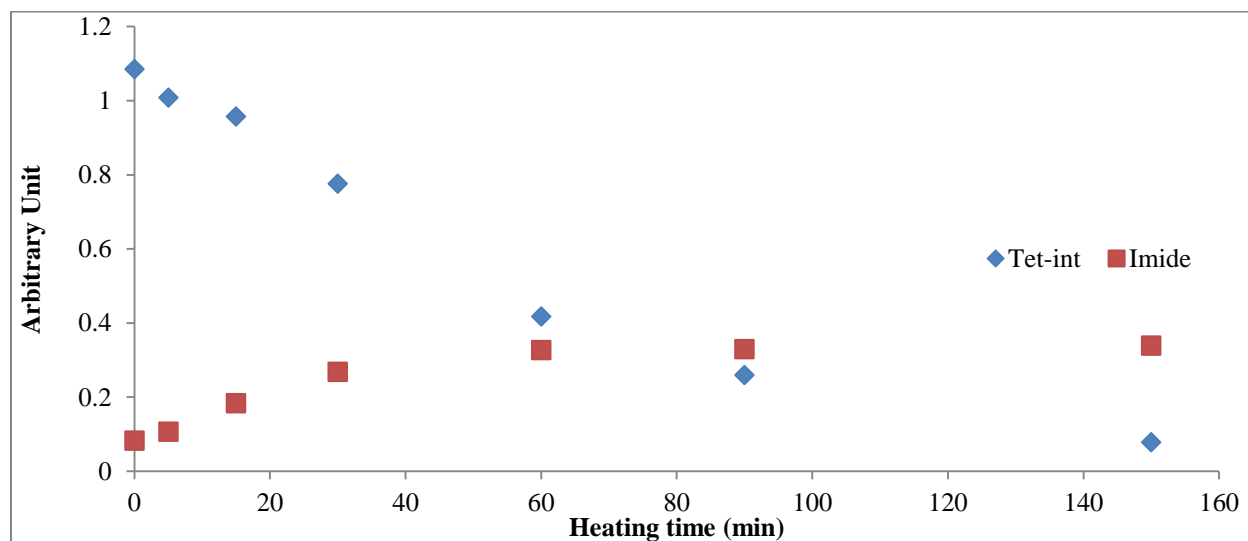


General Procedure for 85c Conversion Comparison Experiments: Sample Preparation

Compound **85c** (63.4 mg, 183 μmol) was brought into a glovebox and dissolved in 2 ampules of $\text{DMSO-}d_6$ (1.82 mL). Dibromomethane (6 μL , 85.4 μmol) was added and the solution was partitioned evenly into 3 J-Young tubes.

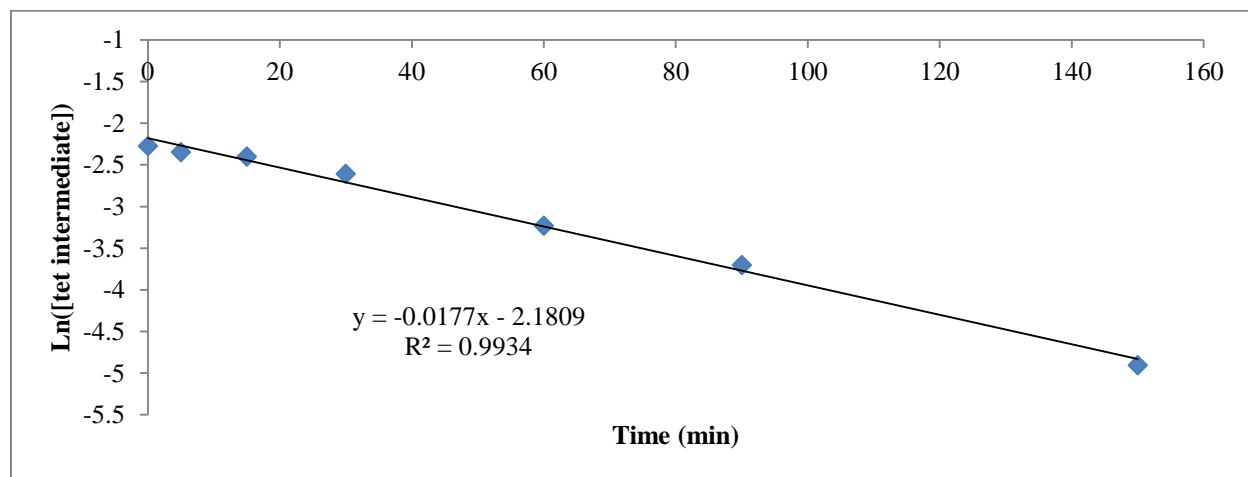
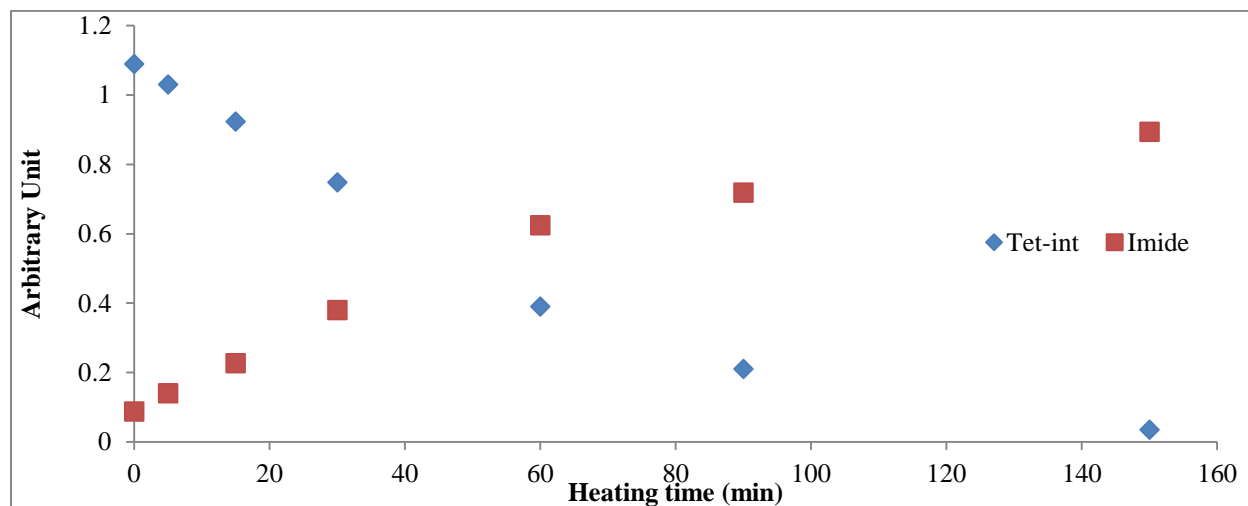
Conversion of 85c in Dry Degassed Solvent

One tube prepared as described above was removed from the glovebox, subjected to three freeze-pump-thaw cycles, refilled with N_2 and heated in a 90 $^\circ\text{C}$ oil bath. The data collected from the ^1H NMR taken at various time points is graphically displayed below. The arbitrary unit used for the y-axis is the integration of the N-H peak for the indicated species when dibromomethane as internal standard is calibrated to a quantity of one. SI II contains an overlay of the raw NMR spectra. For **32c** conversion kinetics plot see “Conversion of 32c in degassed solvent” section.



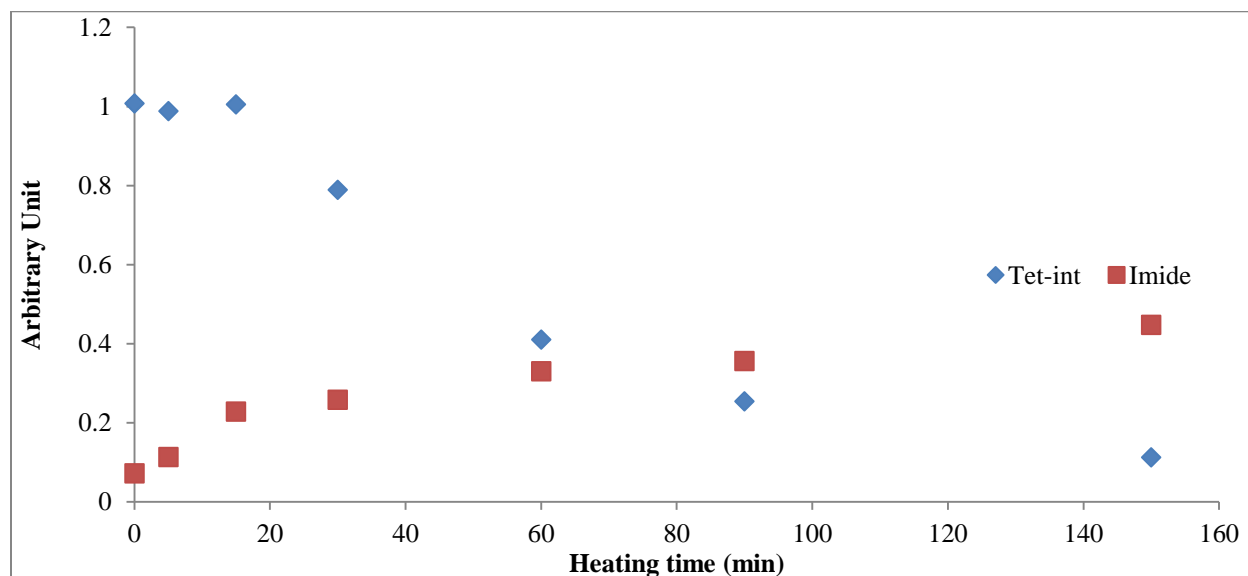
Conversion of 85c in Degassed Solvent

One tube prepared as described above had water (2.2 μL , 122 μmol) added to it, and was then removed from the glovebox, subjected to three freeze-pump-thaw cycles, refilled with N_2 and heated in a 90 $^\circ\text{C}$ oil bath. The data collected from the ^1H NMR taken at various time points is graphically displayed below. The arbitrary unit used for the y-axis is the integration of the N-H peak for the indicated species when dibromomethane as internal standard is calibrated to a quantity of one. The data was used to derive kinetic data and that graph is also shown. SI II contains an overlay of the raw NMR spectra.



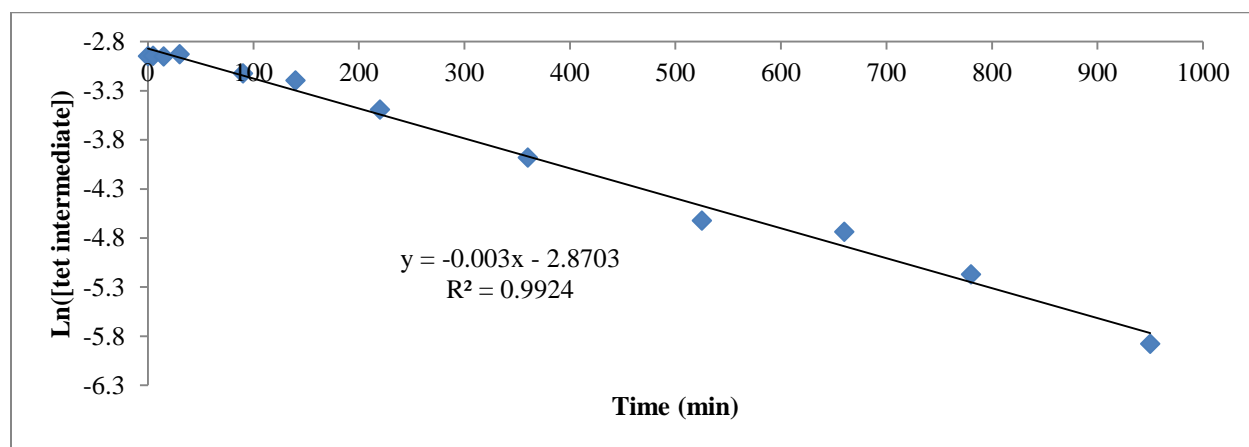
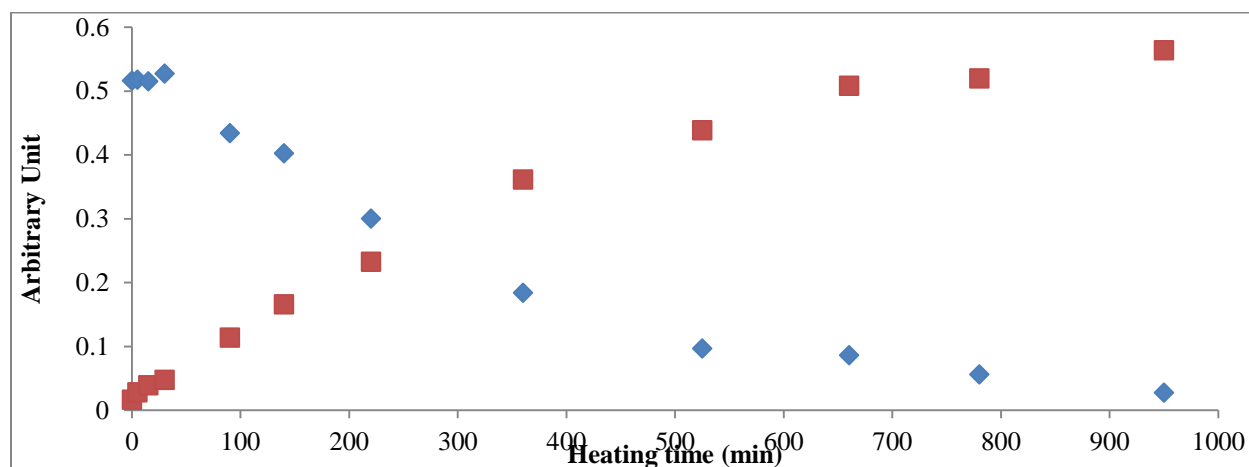
Conversion of **85c** in Dry Oxygenated Solvent

One tube prepared as described above was removed from the glovebox, subjected to three freeze-pump-thaw cycles, refilled with O₂, shaken, and heated in a 90 °C oil bath. The data collected from the ¹H NMR taken at various time points is graphically displayed below. The arbitrary unit used for the y-axis is the integration of the N-H peak for the indicated species when dibromomethane as internal standard is calibrated to a quantity of one. SI II contains an overlay of the raw NMR spectra. For **85c** conversion kinetics plot see “Conversion of **85c** in degassed solvent” section.



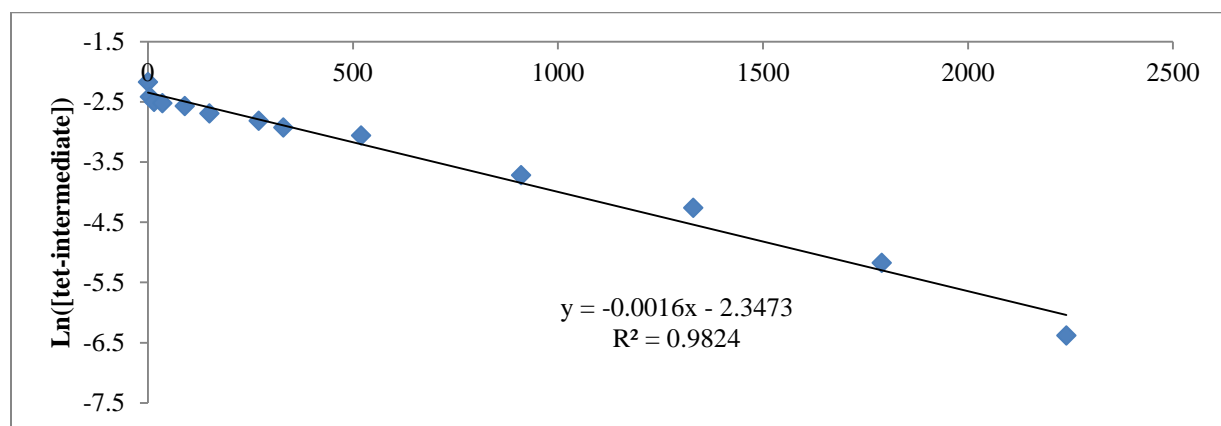
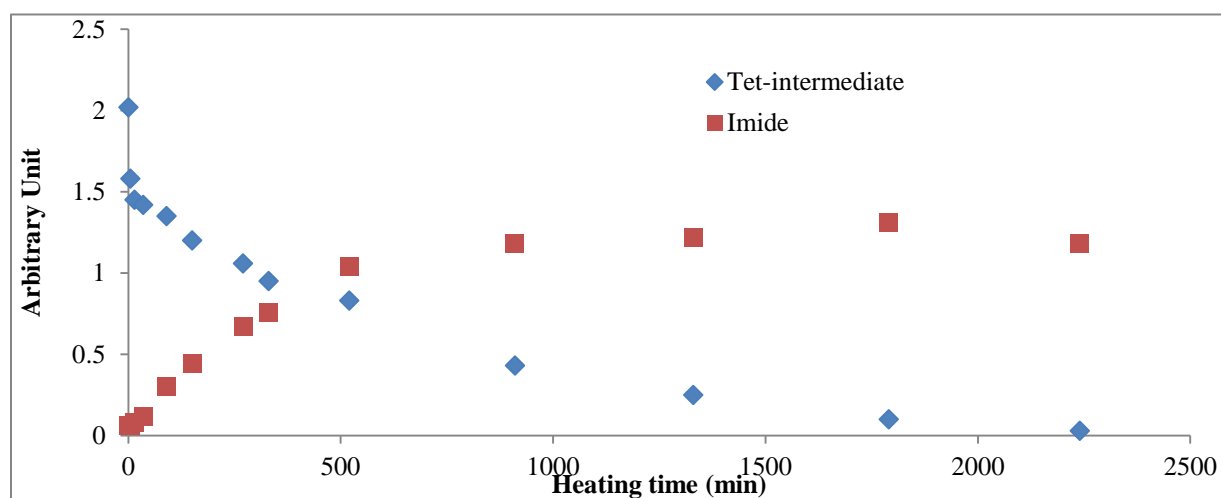
Conversion of 85d in Degassed Solvent

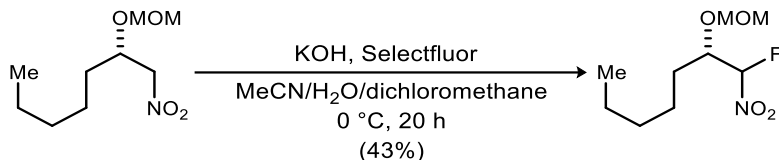
85d (24.0 mg, 60.5 μmol) was converted to imide according to the general procedure for tetrahedral intermediate conversion. The $\text{DMSO-}d_6$ used was from an ampule. Prior to heating, the solution was subjected to three freeze-pump-thaw cycles. After degassing, H_2O (2.20 μL , 121 μmol) and dibromomethane (3.00 μL , 42.7 μmol) were added. The data collected from the ^1H NMR taken at various time points is graphically displayed below. The arbitrary unit used for the y-axis is the integration of the N-H peak for the indicated species when dibromomethane as internal standard is calibrated to an integration of one. The data was used to derive kinetic data and that graph is also shown. SI II contains an overlay of the raw NMR spectra.



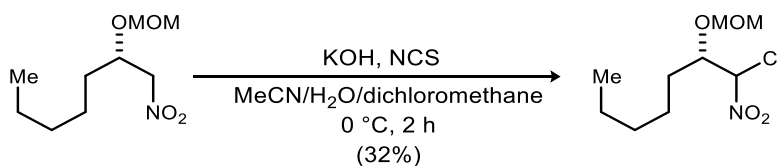
Conversion of 85e in Degassed Solvent

85e (38.6 mg, 103 μmol) was converted to imide according to the general procedure for tetrahedral intermediate conversion. The $\text{DMSO-}d_6$ used was from an ampule. Prior to heating, the solution was subjected to three freeze-pump-thaw cycles. After degassing, H_2O (4.10 μL , 226 μmol) was added. The data collected from the ^1H NMR taken at various time points is graphically displayed below. The arbitrary unit used for the y-axis is the integration of the N-H peak for the indicated species when residual DMSO as internal standard is calibrated to a quantity of one. The data was used to derive kinetic data and that graph is also shown. SI II contains an overlay of the raw NMR spectra.





(2S)-1-Fluoro-2-(methoxymethoxy)-1-nitroheptane (S4). Prepared from (S)-2-(methoxymethoxy)-1-nitroheptane (102.5 mg, 500.0 μmol) by dissolving in acetonitrile (400 μL) and water (800 μL). The solution was chilled to 0 $^{\circ}\text{C}$ and KOH (37.9 mg, 575 μmol) was added and the reaction was stirred for 1 hour. Dichloromethane (1.4 mL) at -78 $^{\circ}\text{C}$ and selectfluor (221.3 mg, 625.0 μmol) were quickly added and the reaction was stirred vigorously as it warmed to 0 $^{\circ}\text{C}$. The reaction was stirred at that temperature for 19 h. Diethyl ether was added before 10 additional minutes of stirring then the reaction was diluted with water and the phases were separated. The aq phase was extracted with diethyl ether, and then the combined organic layers were dried and concentrated to afford a 1:1.5 mixture of diastereomers of desired compound. The residue was purified by column chromatography (SiO_2 , 2-5% diethyl ether in hexanes) to afford a 1:1.4 mixture of diastereomers of the desired compound as a colorless oil (48.0 mg, 43%). $R_f = 0.47$ (10% Et_2O /hexanes); IR (film) 2942, 1578, 1459, 1362, 1138, 1031 cm^{-1} ; ^1H NMR (400 MHz, CDCl_3 , major diastereomer) δ 5.91 (dd, $^2J_{\text{HF}} = 50.3$ Hz, $J = 3.0$ Hz, 1H), 4.73 (d, $J = 7.1$ Hz, 1H), 4.71 (d, $J = 7.1$ Hz, 1H), 4.09 (ddt, $^3J_{\text{HF}} = 17.8$ Hz, $J = 8.5, 3.4$ Hz, 1H), 3.39 (s, 3H), 1.76-1.19 (m, 8H), 0.93-0.84 (m, 3H); ^{13}C NMR (100 MHz, CDCl_3 , major diastereomer) ppm 110.9 (d, $^1J_{\text{CF}} = 243.6$ Hz), 97.4, 77.3 ($^2J_{\text{CF}} = 20.6$ Hz), 56.3, 31.6, 28.9 ($^3J_{\text{CF}} = 3.9$), 24.6, 22.5, 14.0; HRMS (CI): Exact mass calcd for $\text{C}_9\text{H}_{17}\text{FNO}_4$ $[\text{M}-\text{H}]^-$ 222.1136, found 222.1130.

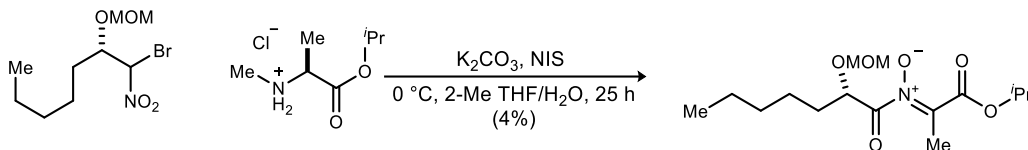


(2S)-1-Chloro-2-(methoxymethoxy)-1-nitroheptane (S5). Prepared from (S)-2-(methoxymethoxy)-1-nitroheptane (102.5 mg of 87% ee material, 500 μ mol) by dissolving in acetonitrile (400 μ L) and water (800 μ L). The solution was chilled to 0 °C and KOH (37.9 mg, 575 μ mol) was added and the reaction was stirred for 1 hour. Dichloromethane (1.4 mL) at -78 °C and NCS (66.8 mg, 500 μ mol) were quickly added and the reaction was stirred vigorously as it warmed to 0 °C. The reaction was stirred at that temperature for 1 h. Diethyl ether was added before 10 additional minutes of stirring, and then the reaction was diluted with water and the phases were separated. The aq phase was extracted with diethyl ether, and then the combined organic layers were dried and concentrated to afford a 5.5:1 mixture of diastereomers of the desired compound. The residue was purified by column chromatography (SiO₂, 2-5% diethyl ether in hexanes) to afford a 1:1 mixture of diastereomers of desired compound as a colorless oil (37.8 mg, 32%).²⁶⁹ R_f = 0.13 (2% Et₂O/hexanes, KMnO₄ stain); IR (film) 2940, 1572, 1458, 1357, 1235, 1136, 1030, 920, 736 cm⁻¹; ¹H NMR (400 MHz, CDCl₃, major diastereomer²⁷⁰) δ 5.89 (d, J = 7.0 Hz, 1H), 4.66 (d, J = 5.7 Hz, 1H), 4.63 (d, J = 7.2 Hz, 1H), 4.21 (td, J = 6.8, 3.7 Hz, 1H), 3.36 (s, 3H), 1.79-1.59 (m, 2H), 1.48-1.24 (m, 6H), 0.93-0.85 (m, 3H); ¹³C NMR (100 MHz, CDCl₃, both diastereomers) ppm 97.4, 97.0, 93.5, 92.1, 79.5, 79.2, 56.52, 56.49, 31.7, 31.6, 31.0, 29.7, 24.9, 23.6, 22.5 (2C), 14.04, 14.03; HRMS (CI): Exact mass calcd for C₉H₁₈ClNO₄ [M]⁺ 238.0841, found 238.0833.²⁷¹

²⁶⁹ Change in dr upon purification can be attributed to the exclusion of some chromatography fraction containing the major diastereomer in the interest of purity.

²⁷⁰ Major diastereomer is assigned as that which was major prior to purification.

²⁷¹ Ee is assumed to be conserved in this reaction (87%), but optical rotation nor chiral HPLC traces were collected for this compound.



Isopropyl (*S*)-2-((2-(methoxymethoxy)heptanoyl)imino)propanoate *N*-oxide (**138**).

Prepared from the nitroalkane (74.8 mg, 263 μmol) and the amine (71.9 mg, 395 μmol) according to the General Procedure for UmAS Reactions. The only deviation from those conditions was the solvent choice and use of additional K_2CO_3 (3 equiv total). The residue was purified by column chromatography (SiO_2 , 10% ethyl acetate in hexanes) to afford the desired compound as a colorless oil (3.0 mg, 4%). $R_f = 0.14$ (10% EtOAc/hexanes); IR (film) 2931, 1785, 1725, 1454, 1310, 1167, 1099, 1030, 924 cm^{-1} ; ^1H NMR (600 MHz, CDCl_3) δ 5.18 (sep, $J = 6.3$ Hz, 1H), 4.73 (d, $J = 7.0$ Hz, 1H), 4.69 (d, $J = 7.0$ Hz, 1H), 4.30 (dd, $J = 7.0, 5.8$ Hz, 1H), 3.40 (s, 3H), 2.21 (s, 3H), 1.85-1.81 (m, 2H), 1.52-1.42 (m, 2H), 1.36 (d, 6H), 1.34-1.29 (m 4H), 0.89 (br t, $J = 7.0$ Hz, 3H); ^{13}C NMR (150 MHz, CDCl_3) ppm 169.4, 162.6, 157.9, 96.4, 74.7, 71.1, 56.3, 33.1, 31.5, 25.0, 22.6, 21.8, 14.1, 13.4; HRMS (ESI): Exact mass calcd for $\text{C}_{15}\text{H}_{27}\text{NNaO}_6$ $[\text{M}+\text{Na}]^+$ 340.1731, found 340.1736.

Procedure for HCl/ NaNO_2 Diazotization

As adapted from literature²⁷², *para*-anisidine (30.8 g, 250 μmol) was added to a 0 $^\circ\text{C}$ aqueous HCl solution (9 M, 273 μL). After 10 min, a solution of sodium nitrite (18.2 mg, 263 μmol) in water (227 μL) was added dropwise followed by water (~ 200 μL) to wash solids down the sides of the

²⁷² Cousin, S. F.; Kadeřávek, P.; Haddou, B.; Charlier, C.; Marquardsen, T.; Tyburn, J. M.; Bovier, P. A.; Engelke, F.; Maas, W.; Bodenhausen, G. *Angew. Chem. Int. Ed.* **2016**, *55*, 9886.

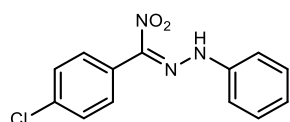
vial and the mixture was stirred for 30 minutes. Dimethoxy ethane (~500 μL) then nitroalkane (45.3 mg, 263 μmol) was added dropwise followed by the dropwise addition of an aqueous solution of sodium hydroxide (5 M) until the reaction was just basic. The resulting mixture was stirred for 1.5 h. The heterogeneous reaction mixture was then filtered to remove precipitate and extracted three times with diethyl ether. The organic layers were combined and dried over anhydrous MgSO_4 . The volatile components were removed leading to a red solid containing suspected hydrazone. Column chromatography (SiO_2 , 5% ethyl acetate in hexanes) afforded the desired compound with several minor impurities as a red solid (5.9 mg, 8%). $R_f = 0.26$ (10% EtOAc/hexanes); $^1\text{H NMR}$ (400 MHz, CDCl_3) δ 7.65 (d, $J = 8.7$ Hz, 2H), 7.41 (d, $J = 8.7$ Hz, 2H), 7.32 (d, $J = 9.0$, 2H), 6.95 (d, $J = 9.0$, 2H), 3.83 (s, 3H). Upon sitting overnight in the NMR tube this material had fully converted to what is assumed to be the corresponding hydrazide resulting from hydrolysis. The product is tentatively assigned as the hydrazide on the basis of $^1\text{H NMR}$ analysis. $^1\text{H NMR}$ (400 MHz, CDCl_3) δ 8.09 (d, $J = 8.7$ Hz, 2H), 8.02 (d, $J = 9.1$ Hz, 2H), 7.50 (d, $J = 8.7$, 2H), 7.05 (d, $J = 9.0$, 2H), 3.93 (s, 3H).

General Procedure for $\text{HNO}_3/\text{KNO}_2$ Diazotization

As adapted from literature²⁷³, aryl amine was added to a solution of HNO_3 (250 mM). Upon complete dissolution, the solution was brought to 0 $^\circ\text{C}$ and a solution of potassium nitrite (22.4 mg, 263 μmol) was added dropwise and the mixture was stirred. Simultaneously, nitroalkane was added to solvent at 0 $^\circ\text{C}$ with potassium hydroxide (17.3 mg of 85% solid, 263 μmol) and the

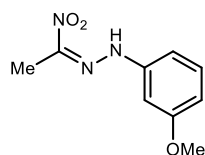
²⁷³ Meyer, V.; Ambühl, G. *Berichte Dtsch. Chem. Ges.* **1875**, 8, 1073

mixture was stirred vigorously until no oil was observed (complete nitronate formation). The diazonium salt solution was quickly transferred to the nitronate solution followed by stirring at 0 °C. The reaction mixture was extracted three times with diethyl ether. The organic layers were combined, dried over anhydrous MgSO₄, and the volatile components were removed.



1-((4-Chlorophenyl)(nitro)methylene)-2-phenylhydrazine (S6).

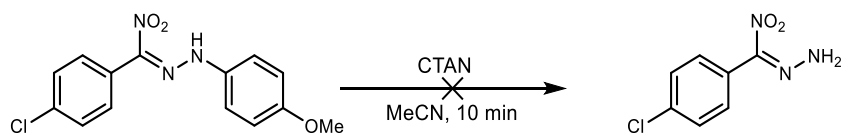
Prepared from 1-chloro-4-(nitromethyl)benzene (43.1 mg, 250 μmol) and aniline (24 μL, 263 μmol) according to the General Procedure for HNO₃/KNO₂ Diazotization. The HNO₃ solution was aqueous (2 mL). The potassium nitrite solution was aqueous (500 μL). The diazotization time was 10 min. The nitronate solvent was water (2 mL). The nitronate and diazonium salt were allowed to react for 5 minutes. Recrystallization from ethanol/water afforded the desired compound as an orange solid (64.0 mg, 93%). Mp 124-125 °C; R_f = 0.56 (20% EtOAc/hexanes); IR (film) 3223, 1556, 1485, 1403, 1305, 1184, 1094, 974, 895, 819, 682 cm⁻¹; ¹H NMR (600 MHz, CDCl₃) δ 7.65 (d, *J* = 8.7 Hz, 2H), 7.42-7.39 (m, 4H), 7.36 (d, *J* = 7.6 Hz, 2H), 7.17 (t, *J* = 7.3 Hz, 1H); ¹³C NMR (150 MHz, CDCl₃) ppm 141.5, 135.4, 134.3, 130.3, 129.8, 129.2, 128.6, 125.3, 115.6; HRMS (CI): Exact mass calcd for C₁₃H₁₀ClN₃O₂ [M]⁺ 275.0456, found 275.0449.



1-(3-Methoxyphenyl)-2-(1-nitroethylidene)hydrazine (151).

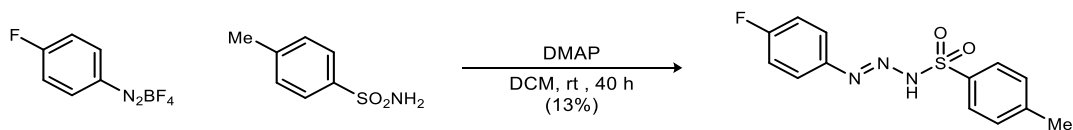
Prepared from nitroethane (19.6 μL, 275 μmol) and *meta*-anisidine (29.4 μL, 263 μmol) according to the General procedure for HNO₃/KNO₂ diazotization. The HNO₃ solution was in 1:1 MeCN:H₂O (2.1 mL). The potassium nitrite solution was aqueous (500 μL). The diazotization time was 1 hour. The nitronate solvent was 4:1 MeCN:H₂O (1.25 mL). The nitronate and diazonium salt were allowed to react for 4 hours. Column chromatography (SiO₂,

15% ethyl acetate in hexanes) afforded the desired compound as an orange solid (30.9 mg, 56%). Mp 112-114 °C; $R_f = 0.34$ (20% EtOAc/hexanes); IR (film) 3260, 2931, 1591, 1487, 1421, 1305, 1196, 1142, 1044, 859, 772 cm^{-1} ; ^1H NMR (400 MHz, CDCl_3) δ 12.22 (s, 1H), 7.25 (t, $J = 8.2$ Hz, 1H), 6.89 (t, $J = 2.2$ Hz, 1H), 6.81 (dd, $J = 7.9, 1.6$ Hz, 1H), 6.65 (dd, $J = 8.2, 2.2$ Hz, 1H), 3.83 (s, 3H), 2.43 (s, 3H); ^{13}C NMR (100 MHz, CDCl_3) ppm 161.0, 143.1, 132.8, 130.5, 110.2, 107.8, 100.6, 55.5, 18.2; HRMS (ESI): Exact mass calcd for $\text{C}_9\text{H}_{10}\text{N}_3\text{O}_3$ $[\text{M}-\text{H}]^-$ 208.0728, found 208.0729.



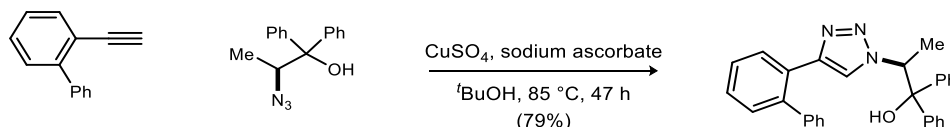
CTAN Deprotection of S6

As adapted from literature²⁷⁴, the suspected hydrazone from Table 8, entry 2 (28.8 mg, 94.1 μmol) in MeCN (1 mL) was added dropwise to an aqueous (2 mL) solution of CTAN (187.7 mg, 188.2 μmol). This mixture was stirred for 10 min before being diluted with water and diethyl ether. The phases were separated, the aqueous phase was extracted with diethyl ether, and the combined organic phases were dried with MgSO_4 and concentrated. The crude material contained no signs of deprotected hydrazone by crude NMR.



²⁷⁴ Fischer, D. F.; Xin, Z. q.; Peters, R. *Angew. Chem. Int. Ed.* **2007**, *46*, 7704.

(E)-1-(4-Fluorophenyl)-3-tosyltriazen-1-ene (171). Prepared from the diazonium salt (210.0 mg, 1.000 mmol) and sulfonamide (171.0 mg, 1.000 mmol) by suspending in DCM (10 mL). The suspension was stirred at room temperature for 26 hours with no change in appearance or TLC at which point DMAP (121.0 mg, 1 mmol) was added. The resulting bright orange suspension was stirred for 40 hours before filtration to remove solids and concentration of the filtrate. The residue was purified by column chromatography (SiO₂, 5% ethyl acetate in hexanes) to afford the desired compound as an orange-brown solid (37.4 mg, 13%). Mp 97-100 °C; R_f = 0.49 (20% EtOAc/hexanes); IR (film) 3416, 2922, 1590, 1493, 1410, 1339, 1229, 1161, 1087, 848, 811, 719, 664 cm⁻¹; ¹H NMR (400 MHz, CDCl₃) δ 7.89-7.79 (m, 4H), 7.39 (d, *J* = 8.6 Hz, 2H), 7.17 (dd, ³*J*_{HF} = 8.4 Hz, *J* = 8.4 Hz, 2H), 2.47 (s, 3H); ¹³C NMR (100 MHz, CDCl₃) ppm 166.7 (d, ¹*J*_{CF} = 258.7 Hz), 146.2, 145.81, 145.78, 130.5, 130.0, 127.2 (d, ³*J*_{CF} = 9.8 Hz), 116.9 (d, ²*J*_{CF} = 23.2 Hz), 21.9; ¹⁹F NMR (376 MHz, CDCl₃) δ -101.9; HRMS could not be obtained for this compound. Comparison to the other reasonable product of this reaction (the known *N*-aryl sulfonamide, *N*-(4-fluorophenyl)-4-methylbenzenesulfonamide) rules out that structure.²⁷⁵

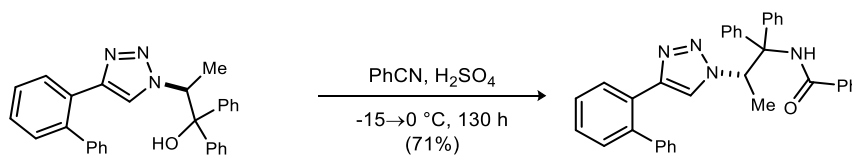


(S)-2-(4-([1,1'-Biphenyl]-2-yl)-1H-1,2,3-triazol-1-yl)-1,1-diphenylpropan-1-ol (183).

Prepared according to a modified literature procedure.²³⁰ The alkyne (51.5 mg, 289 μmol) and azide (94.2 mg, 289 μmol) were dissolved in tert-butanol (3.1 mL). CuSO₄·5H₂O (22.1 mg, 89.1

²⁷⁵ Pan, C.; Cheng, J.; Wu, H.; Ding, J.; Liu, M. *Synth. Commun* **2009**, *39*, 2082.

μmol) and sodium ascorbate (35.0 mg, 178.2 μmol) were added and the reaction was stirred at 85 $^{\circ}\text{C}$ for 47 hours. The reaction was diluted with water and ethyl acetate, the phases were separated, and the aqueous phase was extracted with ethyl acetate. The combined organic phases were dried and concentrated. The residue was purified by column chromatography (SiO_2 , 10% ethyl acetate in hexanes) to afford the desired compound as a white solid (98.9 mg, 79%). $[\alpha]_D^{20} -52.5$ (c 1.13, CHCl_3); Mp 155-156 $^{\circ}\text{C}$; $R_f = 0.40$ (20% EtOAc/hexanes); IR (film) 3400, 3059, 1449, 1358, 1179, 1027, 821, 759, 701 cm^{-1} ; ^1H NMR (400 MHz, CDCl_3) δ 8.04 (d, $J = 7.7$ Hz, 1H), 7.51 (d, $J = 7.4$ Hz, 2H), 7.44-7.08 (m, 16H), 6.48 (s, 1H), 5.34 (q, $J = 6.8$ Hz, 1H), 4.45 (s, 1H), 1.39 (d, $J = 6.8$ Hz, 3H); ^{13}C NMR (100 MHz, CDCl_3) ppm 145.5, 144.7, 143.6, 141.8, 140.2, 130.3, 129.4, 128.9, 128.5 (3C), 128.3, 128.1, 127.9, 127.4, 127.2, 127.1, 125.6, 125.2, 123.3, 79.7, 62.9, 17.1; HRMS (ESI): Exact mass calcd for $\text{C}_{29}\text{H}_{26}\text{N}_3\text{O}$ $[\text{M}+\text{H}]^+$ 432.2070, found 432.2059.



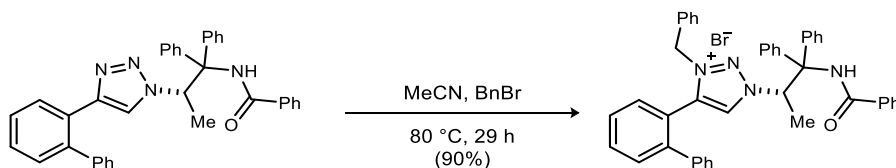
(S)-N-(2-(4-([1,1'-Biphenyl]-2-yl)-1H-1,2,3-triazol-1-yl)-1,1-

diphenylpropyl)benzamide (187). Prepared according to a modified literature procedure.²⁷⁶

The alcohol (1.5 g, 3.5 mmol) was dissolved in benzonitrile (14 mL, 140 mmol). The solution was brought to -15 $^{\circ}\text{C}$ in a brine/ice bath, and then conc. H_2SO_4 (3.5 mL, 64 mmol) was added dropwise over 30 minutes by syringe pump. After the addition was complete, the reaction was allowed to warm to 0 $^{\circ}\text{C}$ in a reaction freezer, and it was stirred at that temperature for 217 hours. The reaction

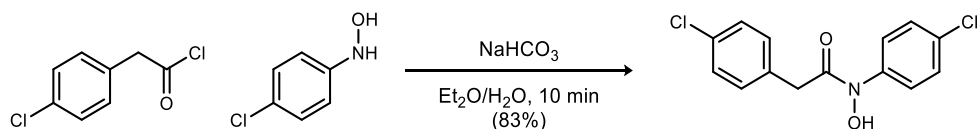
²⁷⁶ Dhotare, B. B.; Kumar, M.; Nayak, S. K. *J. Org. Chem.* **2018**, 83, 10089.

was quenched by the dropwise addition of cold H₂O, followed by cold 5 M aq NaOH until basic. The mixture was extracted with ethyl acetate and the combined organic layers were dried and concentrated. The dichloromethane soluble portion of the residue was purified by column chromatography (SiO₂, 15-25% ethyl acetate in hexanes) to afford the desired compound as an amorphous white solid (1.3355 g, 71%). $[\alpha]_D^{20} +96.4$ (*c* 1.28, CHCl₃); *R*_f = 0.21 (20% EtOAc/hexanes); IR (film) 3374, 3060, 1676, 1528, 1288, 911, 710 cm⁻¹; ¹H NMR (400 MHz, CDCl₃) δ 8.15 (s, 1H), 8.05 (d, *J* = 7.7 Hz, 1H), 7.84 (d, *J* = 7.4 Hz, 2H), 7.56 (d, *J* = 7.7 Hz, 2H), 7.53 (t, *J* = 7.4 Hz, 1H), 7.47-7.44 (m, 3H), 7.39 (t, *J* = 7.4 Hz, 1H), 7.36-7.26 (m, 7H), 7.24-7.20 (m, 3H), 7.09 (d, *J* = 7.7 Hz, 2H), 7.06 (dd, *J* = 7.4, 1.7 Hz, 2H), 5.82 (q, *J* = 7.0 Hz, 1H), 5.63 (s, 1H), 1.36 (d, *J* = 7.1 Hz, 3H); ¹³C NMR (100 MHz, CDCl₃) ppm 165.5, 145.8, 141.6, 140.5, 140.0, 135.5, 134.4, 131.8, 130.3, 129.1, 129.0, 128.8 (3C), 128.4 (2C), 128.1, 128.02, 127.98, 127.83, 127.76 (2C), 127.2 (2C), 122.4, 67.9, 63.3, 16.2; HRMS (ESI): Exact mass calcd for C₃₆H₃₁N₄O [M+H]⁺ 535.2492, found 535.2486.



(S)-4-([1,1'-Biphenyl]-2-yl)-1-(1-benzamido-1,1-diphenylpropan-2-yl)-3-phenethyl-1H-1,2,3-triazol-3-ium bromide (179). Prepared according to a modified literature procedure.²⁷⁶ The triazole (1.3330 g, 2.4916 mmol) and benzyl bromide (876 μL, 7.42 mmol) were dissolved in acetonitrile (20 mL) in a microwave vial. The solution was brought to 80 °C and stirred for 29 hours. The reaction was concentrated and the residue was triturated with ethyl acetate/satd aq sodium bromide. The filtrate was washed twice with satd aq sodium bromide and

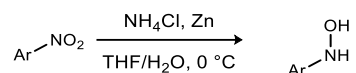
once with water before drying and concentration. The resulting solid was triturated again with ethyl acetate, and the solids from both triturations were combined to afford the desired compound as an amorphous white solid (1.4 g, 90%). $[\alpha]_D^{20} +6.7$ (c 0.36, CHCl_3); $R_f = 0.09$ (5% MeOH/EtOAc); IR (film) 3267, 3054, 2928, 1673, 1484, 1278, 1146, 753, 704 cm^{-1} ; ^1H NMR (600 MHz, CDCl_3) δ 10.19 (br s, 1H), 8.66 (br s, 1H), 8.22 (d, $J = 7.4$ Hz, 2H), 7.88 (br d, $J = 7.3$ Hz, 3H), 7.66 (td, $J = 7.6, 0.9$ Hz, 1H), 7.47-7.40 (m, 5H), 7.38-7.34 (m, 3H), 7.31-7.25 (m, 2H), 7.23-7.16 (m, 4H), 7.03-7.00 (m, 4H), 6.93 (d, $J = 7.2$ Hz, 2H), 6.90 (br s, 2H), 6.58 (d, $J = 7.4$ Hz, 2H), 4.88 (d, $J = 14.5$ Hz, 1H), 4.85 (d, $J = 14.6$ Hz, 1H), 1.65 (d, $J = 6.9$ Hz, 3H); ^{13}C NMR (150 MHz, CDCl_3) ppm 167.5, 143.0, 140.4, 139.9, 138.6, 135.4, 133.7, 132.9, 132.4, 132.00, 131.96, 131.1, 130.2, 129.9, 129.4, 129.2, 129.0, 128.9, 128.83, 128.80, 128.59, 128.56, 128.48, 128.4, 128.3, 127.9, 127.6, 127.2, 120.3, 69.4, 65.9, 55.3, 15.8; HRMS (ESI): Exact mass calcd for $\text{C}_{43}\text{H}_{37}\text{N}_4\text{O}$ $[\text{M}-\text{Br}]^+$ 625.2962, found 625.2945.



N,2-bis(4-Chlorophenyl)-N-hydroxyacetamide (196). Prepared according to a modified literature procedure.²⁷⁷ A vial was charged with NaHCO_3 (16.8 mg, 200 μmol), the hydroxylamine (28.8 mg, 200 μmol), diethyl ether (1 mL), and water (1 mL). Vigorous stirring was established and the active ester (29 μL , 200 μmol) was added. The reaction was stirred at rt for 10 minutes. The phases were separated and the aqueous phase was extracted twice with diethyl ether. The

²⁷⁷ Fauq, A. H.; Simpson, K.; Maharvi, G. M.; Golde, T.; Das, P. *Bioorg. Med. Chem. Lett.* **2007**, *17*, 6392.

combined organic phases were dried and concentrated to afford the desired compound as a white solid (49.1 mg, 83%). Mp 126-128 °C; $R_f = 0.20$ (20% EtOAc/hexanes); IR (film) 3198, 2912, 1627, 1484, 1372, 1283, 1079, 808 cm^{-1} ; ^1H NMR (400 MHz, $\text{DMSO-}d_6$) δ 10.85 (s, 1H), 7.67 (d, $J = 8.7$ Hz, 2H), 7.42 (d, $J = 8.8$ Hz, 2H), 7.38 (d, $J = 8.2$ Hz, 2H), 7.30 (d, $J = 8.1$ Hz, 2H), 3.95 (s, 2H); ^{13}C NMR (100 MHz, $\text{DMSO-}d_6$) ppm 170.2, 140.5, 134.3, 131.6, 131.2, 128.3 (2C), 128.1, 121.5, 39.6; HRMS (ESI): Exact mass calcd for $\text{C}_{14}\text{H}_{12}\text{Cl}_2\text{NO}_2$ $[\text{M}+\text{H}]^+$ 296.0240, found 296.0237. The azanyl ester (resulting from hydroxylamine O addition to the acyl chloride) can be ruled out on the basis of the IR carbonyl stretch (1627 cm^{-1}) which is close to similar hydroxamic acids²⁷⁸ ($\sim 1640\text{-}1620 \text{ cm}^{-1}$) and not azanyl esters ($\sim 1760\text{-}1740 \text{ cm}^{-1}$).^{279,280}



General Procedure for *N*-Aryl Hydroxylamine Synthesis

Hydroxylamines were prepared by mixing the nitroarene and ammonium chloride (13 equiv.) in a 2:1 (v:v) mixture of tetrahydrofuran:water (200 mM with respect to nitroarene). This solution was cooled to 0 °C in an ice bath and sparged with argon for 5 minutes before the addition of zinc powder (7.5 equiv.).²⁸¹ The reaction was stirred until thin layer chromatography indicated

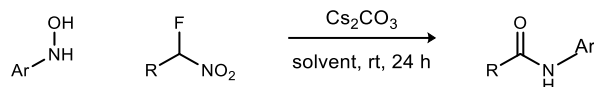
²⁷⁸ Böge, N.; Krüger, S.; Schröder, M.; Meier, C. *Synthesis* **2007**, 2007, 3907.

²⁷⁹ Famulok, M.; Bosold, F.; Boche, G. *Tetrahedron Lett.* **1989**, 30, 321.

²⁸⁰ Famulok, M.; Boche, G. *Angew. Chem.* **1989**, 101, 470.

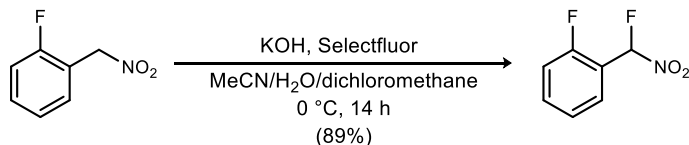
²⁸¹ Zinc powder was activated by washing with dilute aq HCl and stored for up to a year in an airtight container without loss of reactivity.

complete conversion.²⁸² The reaction was filtered through Celite using argon-sparged solvent and concentrated.



General Procedure for Umpolung *N*-Aryl Amide Synthesis

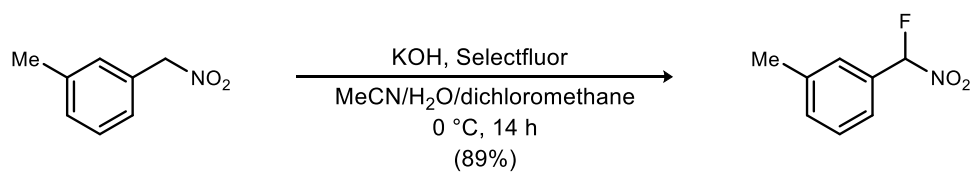
Amides were prepared by mixing Cs_2CO_3 (97.8 mg, 300 μmol), aryl hydroxylamine (150 μmol), fluoronitroalkane (100 μmol), and solvent (2 mL) in a microwave vial. Solvent was toluene or, in cases of aryl fluoronitroalkanes or low hydroxylamine solubility, a 1:1 (v:v) mixture of toluene and acetonitrile. The vial was sealed and the solution was sparged with Ar for ~2 min and stirred at room temperature for 24 hours. The reaction was stopped by filtration through a pad of SiO_2 (ethyl acetate) and concentration.



1-Fluoro-2-(fluoro(nitro)methyl)benzene (223). Prepared by dissolving 1-fluoro-2-(nitromethyl)benzene (289.4 mg, 1.867 mmol) in a 1:2 (v:v) mixture of acetonitrile and water (6 mL). This solution was cooled to 0 °C and potassium hydroxide (123.2 mg of 85% solid, 1.867 mmol) was added. The reaction was stirred for 2.5 h at which time it appeared homogeneous and was further cooled to the freezing point of the solution (~-20 °C). At that temperature

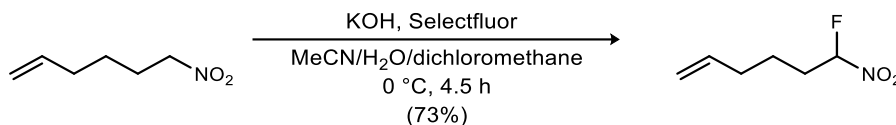
²⁸² Over reduction can result if reaction is not stopped soon after nitroarene consumption.

dichloromethane pre-cooled to $-78\text{ }^{\circ}\text{C}$ (6 mL) and Selectfluor (991.4 mg, 2.801 mmol) were added quickly. The solution was placed into a $0\text{ }^{\circ}\text{C}$ freezer and the reaction was allowed to proceed for 14 h. The reaction was diluted with diethyl ether (6 mL) and the layers were separated. The aqueous phase was extracted two additional times with diethyl ether. The combined organics were dried and concentrated to give the product as a colorless oil (286.8 mg, 89%). $R_f = 0.53$ (20% EtOAc/hexanes); IR (film) 2925, 1581, 1367 cm^{-1} ; ^1H NMR (400 MHz, CDCl_3) δ 7.59-7.52 (m, 2H), 7.28 (dd, $J = 7.5, 7.5$ Hz, 1H), 7.21 (dd, $J = 9.1, 9.1$ Hz, 1H), 6.89 (d, $^2J_{\text{HF}} = 47.9$ Hz, 1H); ^{13}C NMR (100 MHz, CDCl_3) ppm 160.8 (dd, $^1J_{\text{CF}} = 253.3$ Hz, $^3J_{\text{CF}} = 5.6$ Hz), 134.2 (dd, $^3J_{\text{CF}} = 8.5, 1.5$ Hz), 127 (dd, $^4J_{\text{CF}} = 5.4, 1.4$ Hz), 125.1 (d, $^3J_{\text{CF}} = 3.7$ Hz), 118.5 (dd, $^2J_{\text{CF}} = 22.0, 12.6$ Hz), 116.5 (d, $^2J_{\text{CF}} = 20.4$ Hz), 104.6 (dd, $^1J_{\text{CF}} = 236.7$ Hz, $^3J_{\text{CF}} = 3.3$ Hz); ^{19}F NMR (376 MHz, CDCl_3) δ -117.4, -141.3; HRMS (ESI): Exact mass calcd for $\text{C}_7\text{H}_5\text{F}_2$ $[\text{M}-\text{NO}_2]^+$ 127.0359, found 127.0357.



1-(Fluoro(nitro)methyl)-3-methylbenzene (222). Prepared by dissolving 1-methyl-3-(nitromethyl)benzene (330.0 mg, 2.205 mmol) in a 1:2 (v:v) mixture of acetonitrile and water (6 mL). This solution was cooled to $0\text{ }^{\circ}\text{C}$ and potassium hydroxide (145.5 mg of 85% solid, 2.205 mmol) was added. The reaction was stirred for 2.5 h at which time it appeared homogeneous and was further cooled to the freezing point of the solution ($\sim -20\text{ }^{\circ}\text{C}$). At that temperature dichloromethane pre-cooled to $-78\text{ }^{\circ}\text{C}$ (6 mL) and Selectfluor (1.1709 g, 3.3075 mmol) were added quickly. The solution was placed into a $0\text{ }^{\circ}\text{C}$ freezer and the reaction was allowed to proceed for 14 h. The reaction was diluted with diethyl ether (6 mL) and the layers were separated. The

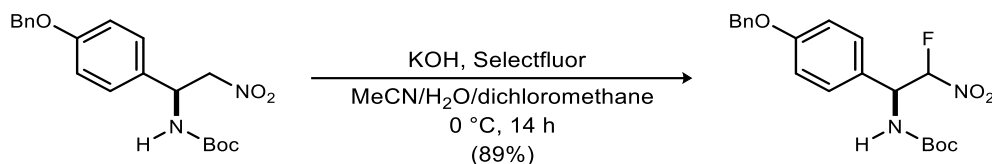
aqueous phase was extracted two additional times with diethyl ether. The combined organics were dried and concentrated to give the product as a yellow oil (281.0 mg, 75%). $R_f = 0.59$ (20% EtOAc/hexanes); IR (film) 2926, 1575, 1371, 1281, 1167, 113, 739 cm^{-1} ; ^1H NMR (400 MHz, CDCl_3) δ 7.42-7.41 (m, 2H), 7.38-7.33 (m, 2H), 6.56 (d, $^2J_{\text{HF}} = 48.8$ Hz, 1H), 2.40 (s, 3H); ^{13}C NMR (100 MHz, CDCl_3) ppm 139.4, 132.9, 130.3 (d, $^2J_{\text{CF}} = 20.9$ Hz), 129.2, 127.1 (d, $^3J_{\text{CF}} = 6.1$ Hz), 123.8 (d, $^3J_{\text{CF}} = 6.3$ Hz), 110.3 ($^1J_{\text{CF}} = 239.5$ Hz), 21.4; ^{19}F NMR (376 MHz, CDCl_3) δ -139.4; HRMS (ESI): Exact mass calcd for $\text{C}_8\text{H}_8\text{F} [\text{M}-\text{NO}_2]^+$ 123.0610, found 123.0609.



6-Fluoro-6-nitrohex-1-ene (220).²⁸³ 6-nitrohex-1-ene (1.2 g, 9.3 mmol), was dissolved in a 2:1 water:acetonitrile solution (21 mL) and brought to 0 °C. KOH (600 mg, 9.3 mmol) was added and the reaction was stirred for 1 hour. The solution was cooled until it became a slurry, and dichloromethane (32 mL) that had been cooled to -78 °C with Selectfluor (5.26 g, 14.9 mmol) was added. The reaction was stirred for 3.5 hours at 0 °C. Diethyl ether (30 mL) was added before 10 additional minutes of stirring. The mixture was filtered through celite, and the phases were separated. The aq phase was extracted three times with 1:1 dichloromethane:hexanes, and the combined organics were dried and concentrated. Column chromatography (SiO_2 , 2-5% diethyl ether in hexanes) afforded the desired compound as a pale yellow oil (997 mg, 73%). $R_f = 0.6$ (20% EtOAc/hexanes); IR (film) 2933, 1573, 1131, 918 cm^{-1} ; ^1H NMR (400 MHz, CDCl_3) δ

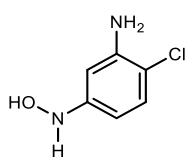
²⁸³ Reaction performed by Dr. Jade Bing; characterization data collected in the course of this work.

5.88-5.70 (m, 2H), 5.08-5.02 (m, 2H), 2.26-2.06 (m, 4H), 1.69-1.49 (m, 2H); ^{13}C NMR (100 MHz, CDCl_3) ppm 136.9, 116.3, 111.2 (d, $^1J_{\text{CF}} = 239.1$ Hz), 32.7, 32.6 (d, $^2J_{\text{CF}} = 19.5$ Hz), 22.0 (d, $^3J_{\text{CF}} = 2.9$ Hz); ^{19}F NMR (376 MHz, CDCl_3) δ -146.8; HRMS (EI): Exact mass calcd for $\text{C}_6\text{H}_9\text{FNO}_2$ $[\text{M}-\text{H}]^+$ 146.0612, found 146.0607.



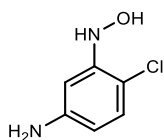
***tert*-Butyl ((1*S*)-1-(4-(benzyloxy)phenyl)-2-fluoro-2-nitroethyl)carbamate (260).** Prepared by dissolving *tert*-butyl (*S*)-1-(4-(benzyloxy)phenyl)-2-nitroethylcarbamate (113.1 mg, 304.0 μmol) in a 1:1 (v:v) mixture of acetonitrile and water (2 mL). This solution was cooled to 0 $^\circ\text{C}$ and potassium hydroxide (20.1 mg of 85% solid, 304 μmol) was added. The reaction was stirred for 2.5 h at which time it appeared homogeneous and was further cooled to the freezing point of the solution (\sim -20 $^\circ\text{C}$). At that temperature dichloromethane pre-cooled to -78 $^\circ\text{C}$ (2 mL) and Selectfluor (161.4 mg, 455.9 μmol) were added quickly. The solution was placed into a 0 $^\circ\text{C}$ freezer and the reaction allowed to proceed for 14 h. The reaction was diluted with diethyl ether (2 mL) and the layers were separated. The aqueous phase was extracted two additional times with diethyl ether. The combined organics were dried and concentrated and the residue was purified by column chromatography (SiO_2 , 10-20% ethyl acetate in hexanes) to afford the desired compound as a colorless solid (65.3 mg, 55%) (1:1.5 mixture of diastereomers). The e.e. was determined by chiral HPLC analysis (Chiralpak AD, 10% IPA/hexanes, 0.6 mL/min) t_r (d_{1e1} , minor/minor) = 27.5 min, t_r (d_{1e1} , major/major) = 31.2 min, t_r (d_{1e1} , major/minor) = 33.4 min, t_r (d_{1e1} , minor/major) = 38.1 min to be 99%. Mp 115-116 $^\circ\text{C}$; R_f = 0.19 (10% EtOAc/hexanes); IR (film) 3331, 2979, 1708, 1576, 1508, 1372, 1245, 1166, 1022 cm^{-1} ; ^1H NMR (600 MHz, CDCl_3 , major diastereomer) δ

7.43-7.38 (m, 4H), 7.35-7.32 (m, 1H), 7.25 (d, $J = 8.6$ Hz, 2H), 7.00 (d, $J = 8.7$ Hz, 2H), 5.96 (d, $^2J_{\text{HF}} = 48.8$ Hz, 1H), 5.55 (dd, $^3J_{\text{HF}} = 22.3$, $J = 8.8$ Hz, 1H), 5.35 (br s, 1H), 5.07 (s, 2H), 1.43 (s, 9H); ^{13}C NMR (150 MHz, CDCl_3 , major diastereomer) ppm 159.8, 159.5, 154.6, 136.6 (d, $^3J_{\text{CF}} = 6.0$ Hz), 129.4, 128.8, 128.3, 127.6, 115.7, 110.2 (d, $^1J_{\text{CF}} = 244.5$ Hz), 81.3, 70.2, 55.6 (d, $^2J_{\text{CF}} = 18.2$ Hz), 28.4; ^{19}F NMR (376 MHz, CDCl_3 , major diastereomer) δ -156.9; HRMS (ESI): Exact mass calcd for $\text{C}_{20}\text{H}_{23}\text{O}_5\text{N}_2\text{NaF}$ $[\text{M}+\text{Na}]^+$ 413.1483, found 413.1482.



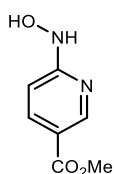
2-Chloro-5-(hydroxyamino)aniline (233). Prepared according to the general procedure for *N*-aryl hydroxylamine synthesis from 2-chloro-5-nitroaniline (346.0 mg, 2.000 mmol). Full conversion was observed at 15 minutes. The

soluble portion of the resulting black residue was purified by column chromatography (SiO_2 , 0-2% methanol in dichloromethane). The insoluble material was further triturated with dichloromethane and forced through a silica plug (2% methanol in dichloromethane). Upon concentration, the material combined from the column and plug afforded the desired compound as a brown solid (65.6 mg, 21%). Mp 70 °C (decomposition); $R_f = 0.25$ (40% EtOAc/hexanes); IR (film) 3428, 3277, 2921, 1618, 1459, 1020, 965, 851, 812 cm^{-1} ; ^1H NMR (400 MHz, $\text{DMSO}-d_6$) δ 8.18 (d, $J = 1.6$ Hz, 1H), 8.09 (s, 1H), 6.91 (d, $J = 8.5$ Hz, 1H), 6.34 (d, $J = 2.2$ Hz, 1H), 6.03 (dd, $J = 8.5, 2.3$ Hz, 1H), 5.11 (br s, 2H); ^{13}C NMR (100 MHz, $\text{DMSO}-d_6$) ppm 151.8, 144.5, 128.5, 107.8, 102.7, 99.7; HRMS (ESI): Exact mass calcd for $\text{C}_6\text{H}_8\text{ClN}_2\text{O}$ $[\text{M}+\text{H}]^+$ 159.0320, found 159.0325.

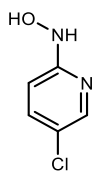


4-Chloro-3-(hydroxyamino)aniline (234). Prepared according to the general procedure for *N*-aryl hydroxylamine synthesis from 4-chloro-3-nitroaniline (34.6 mg, 200 μmol). Full conversion was observed at 10 min. The soluble portion of

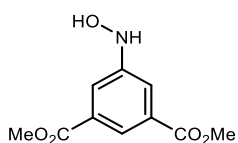
the resulting residue was purified by a SiO₂ plug (diethyl ether) to afford the desired compound as a light orange-brown solid (25.9 mg, 81%). Mp 70 °C (decomposition); R_f = 0.26 (40% EtOAc/hexanes); IR (film) 3283, 3185, 2839, 1605, 1479, 799 cm⁻¹; ¹H NMR (400 MHz, DMSO-*d*₆) δ 8.34 (d, *J* = 1.7 Hz, 1H), 7.75 (s, 1H), 6.82 (d, *J* = 8.4 Hz, 1H), 6.46 (d, *J* = 2.5 Hz, 1H), 6.00 (dd, *J* = 8.4, 2.6 Hz, 1H), 5.07 (br s, 2H); ¹³C NMR (100 MHz, DMSO-*d*₆) ppm 148.4, 147.8, 128.7, 106.2, 103.9, 100.3; HRMS (ESI): Exact mass calcd for C₆H₈ClN₂O [M+H]⁺ 159.0320, found 159.0322.



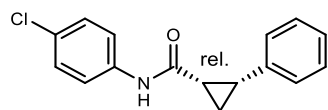
Methyl 6-(hydroxyamino)nicotinate (232). Prepared according to the general procedure for *N*-aryl hydroxylamine synthesis from methyl 6-nitronicotinate (182.0 mg, 1.000 mmol). Full conversion was observed at 5 minutes. The reaction was filtered through filter paper, rather than Celite, using argon-sparged diethyl ether and water. The filtrate was washed with 0.1 N aq ethylenediamine tetraacetic acid·2Na (EDTA·2Na), and the aqueous phase was extracted with diethyl ether, dichloromethane, and ethyl acetate. The combined organic layers were washed twice with the EDTA·2Na solution and brine before they were dried and concentrated. The resulting residue was purified by column chromatography (SiO₂, 2.5-5% methanol in dichloromethane) to afford the desired compound as a yellow solid (49.2 mg, 29%). Mp 111-114 °C; R_f = 0.09 (2.5% MeOH/dichloromethane); IR (film) 3292, 2918, 1709, 1606, 1438, 1286, 1121 cm⁻¹; ¹H NMR (400 MHz, DMSO-*d*₆) δ 9.71 (br s, 1H), 9.02 (br s, 1H), 8.59 (br s, 1H), 8.02 (br d, *J* = 7.0 Hz, 1H), 6.79 (br d, *J* = 7.3 Hz, 1H), 3.78 (br s, 3H); ¹³C NMR (100 MHz, DMSO-*d*₆) ppm 165.5, 165.0, 150.1, 138.4, 115.4, 104.7, 51.5; HRMS (ESI): Exact mass calcd for C₇H₉N₂O₃ [M+H]⁺ 169.0608, found 169.0612.



N-(5-Chloropyridin-2-yl)hydroxylamine (S7). Prepared according to the general procedure for *N*-aryl hydroxylamine synthesis from 5-chloro-2-nitropyridine (317.0 mg, 2.000 mmol). Full conversion was observed at 5 minutes. The filter cake was washed with EtOAc, and the filtrate was washed with 0.1 N aq ethylenediamine tetraacetic acid·2Na (EDTA·2Na). The resulting organic phase was dried and concentrated to give a red/orange solid. Trituration with toluene afforded the desired compound as a cream-colored solid (61.5 mg, 21%). Mp 80 °C (decomposition); R_f = 0.34 (40% EtOAc/hexanes); IR (film) 3200, 2917, 1480, 1384 cm^{-1} ; ^1H NMR (600 MHz, DMSO- d_6) δ 8.93 (s, 1H), 8.72 (d, J = 1.3 Hz, 1H), 8.07 (d, J = 2.3 Hz, 1H), 7.67 (dd, J = 8.8, 2.4 Hz, 1H), 6.84 (d, J = 8.9 Hz, 1H); ^{13}C NMR (150 MHz, DMSO- d_6) ppm 162.0, 145.4, 137.3, 120.4, 108.0; HRMS (EI): Exact mass calcd for $\text{C}_5\text{H}_5\text{ClN}_2\text{O}$ $[\text{M}]^+$ 144.0085, found 144.0084.

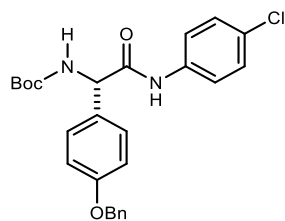


Dimethyl 5-(hydroxyamino)isophthalate (230). Prepared according to the general procedure for *N*-aryl hydroxylamine synthesis from dimethyl 5-nitroisophthalate (239.0 mg, 1.000 mmol). Full conversion was observed at 5 minutes. The resulting residue was purified by trituration (dichloromethane) to afforded the desired compound as a colorless solid (89.2 mg, 40%). Mp 135 °C (decomposition); R_f = 0.06 (20% EtOAc/hexanes); IR (film) 3351, 3304, 2957, 1721, 1700, 1653, 1635, 1596, 1559, 1540, 1521, 1507, 1489, 1440, 1398, 1353 cm^{-1} ; ^1H NMR (400 MHz, DMSO- d_6) δ 8.81 (d, J = 1.4 Hz, 1H), 8.71 (d, J = 2.0 Hz, 1H), 7.89 (t, J = 1.4 Hz, 1H), 7.64 (d, J = 1.4 Hz, 2H), 3.86 (s, 6H); ^{13}C NMR (100 MHz, DMSO- d_6) ppm 165.7, 152.8, 130.5, 120.1, 117.1, 52.3; HRMS (ESI): Exact mass calcd for $\text{C}_{10}\text{H}_{10}\text{NO}_5$ $[\text{M}-\text{H}]^-$ 224.0564, found 224.0556.



***N*-(4-Chlorophenyl)-2-phenylcyclopropane-1-carboxamide (253).**

Prepared by mixing Cs_2CO_3 (32.6 mg, 100 μmol), *N*-(4-chlorophenyl)hydroxylamine (1 mL of 75 mM solution in toluene, 75 μmol), and ((*trans*)-2-(fluoro(nitro)methyl)cyclopropyl)benzene (9.8 mg, 50 μmol) in a microwave vial. This solution was sparged with Ar for ~2 min and stirred at room temperature for 16 hours. The reaction was stopped by filtration through a pad of SiO_2 and then concentrated. The residue was purified by column chromatography (SiO_2 , 15-20% ethyl acetate in hexanes) to afford the desired compound as a colorless solid (16.1 mg, 76%). Mp 198-200 °C; R_f = 0.25 (20% EtOAc/hexanes); IR (film) 3237, 3178, 3053, 2920, 2852, 1656, 1598, 1535, 1490, 1402, 1297, 1252, 1188, 1088, 827 cm^{-1} ; ^1H NMR (600 MHz, CDCl_3) δ 7.30-7.28 (m, 4H), 7.22-7.20 (m, 1H), 7.16 (s, 4H), 7.01 (s, 1H), 2.59 (ddd, J = 8.5, 8.5, 8.5 Hz, 1H), 2.05 (ddd, J = 8.5, 8.5, 5.6 Hz, 1H), 1.79 (ddd, J = 5.9, 5.9, 5.9 Hz, 1H), 1.41 (ddd, J = 8.3, 8.3, 5.3 Hz, 1H); ^{13}C NMR (150 MHz, CDCl_3) ppm 168.0, 136.5, 136.4, 129.2, 129.0 (2C), 128.4, 127.1, 121.0, 25.6, 24.8, 11.0; HRMS (ESI): Exact mass calcd for $\text{C}_{16}\text{H}_{15}\text{ClNO}$ $[\text{M}+\text{H}]^+$ 272.0837, found 272.0844.



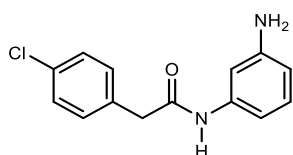
***tert*-Butyl (*S*)-(1-(4-(benzyloxy)phenyl)-2-((4-chlorophenyl)amino)-2-**

oxoethyl)carbamate (261). Prepared by mixing Cs_2CO_3 (48.8 mg, 150 μmol), *N*-(4-chlorophenyl)hydroxylamine (10.8 mg, 75 μmol), *tert*-butyl

((*1S*)-1-(4-(benzyloxy)phenyl)-2-fluoro-2-nitroethyl)carbamate (19.5

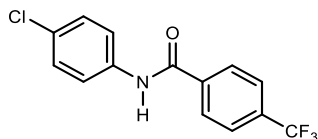
mg, 50 μmol , 98% e.e.), and toluene (1 mL) in a microwave vial. The vial was sealed and the solution was sparged with Ar for ~2 min and stirred at -20 °C for 24 hours. The reaction was stopped by filtration through a pad of SiO_2 . Concentration of the filtered reaction mixture gave a residue with 41% yield by ^1H NMR. Preparatory TLC of a small aliquot of the residue gave clean material for e.e. determination. The e.e. was determined to be 98% by chiral HPLC analysis

(Chiralpak IA, 20% IPA/hexanes, 1.0 mL/min): t_r (e₁, major) = 21.4 min, t_r (e₂, minor) = 38.6 min. Column chromatography (SiO₂, 20% ethyl acetate in hexanes) of a separate sample afforded the desired compound as a colorless oil (13.1 mg, 56%). $[\alpha]_D^{20} +80.1$ (*c* 1.53, CHCl₃) for a separately prepared sample of 88% ee. $R_f = 0.20$ (20% EtOAc/hexanes); IR (film) 3309, 2927, 1675, 1606, 1503, 1369, 1244, 1169, 1021, 827, 734 cm⁻¹; ¹H NMR (600 MHz, CDCl₃) δ 8.25 (br s, 1H), 7.41-7.31 (m, 9H), 7.20-7.17 (m, 2H), 6.95-6.93 (m, 2H), 5.80-5.74 (m, 1H), 5.36 (br s, 1H), 5.03-5.02 (m, 2H), 1.43 (s, 9H); ¹³C NMR (150 MHz, CDCl₃) ppm 169.1, 159.2, 155.8, 136.8, 136.3, 129.6, 129.5, 128.9, 128.84, 128.76, 128.2, 127.6, 121.2, 115.6, 80.8, 70.2, 58.8, 28.5; HRMS (ESI): Exact mass calcd for C₂₆H₂₇ClKN₂O₄ [M+K]⁺ 505.1316, found 505.1291.



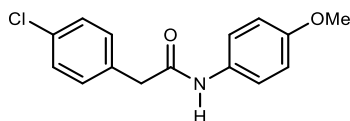
***N*-(3-Aminophenyl)-2-(4-chlorophenyl)acetamide (238).** Prepared

according to the general procedure for umpolung *N*-aryl amide synthesis from 3-(hydroxyamino)aniline (18.6 mg, 150 μ mol delivered as a solution in acetonitrile due to instability of the compound in its neat form) and 1-chloro-4-(2-fluoro-2-nitroethyl)benzene (20.4 mg, 100 μ mol) in a 1:1 mixture of toluene and acetonitrile. Concentration of the filtered reaction mixture (58% yield by ¹H NMR) preceded preparatory HPLC purification (0-95% MeCN in H₂O) afforded the desired compound as a colorless solid (3.9 mg, 15%). Mp 140 °C (decomposition); $R_f = 0.14$ (40% EtOAc/hexanes); IR (film) 3300, 2920, 1658, 1494, 1445, 1195 cm⁻¹; ¹H NMR (600 MHz, DMSO-*d*₆) δ 9.83 (s, 1H), 7.38 (d, *J* = 8.5 Hz, 2H), 7.33 (d, *J* = 8.4 Hz, 2H), 6.90-6.88 (m, 2H), 6.67 (d, *J* = 7.8 Hz, 1H), 6.24 (dd, *J* = 7.9, 1.2 Hz, 1H), 5.03 (s, 2H), 3.59 (s, 2H); ¹³C NMR (150 MHz, DMSO-*d*₆) ppm 168.3, 149.0, 139.7, 135.2, 131.2, 130.9, 128.9, 128.2, 109.3, 107.0, 104.8, 42.5; HRMS (ESI): Exact mass calcd for C₁₄H₁₄ClN₂O [M+H]⁺ 261.0789, found 261.0788.



***N*-(4-Chlorophenyl)-4-(trifluoromethyl)benzamide (249).** ²⁸⁴

Prepared according to the general procedure for umpolung *N*-aryl amide synthesis from 1-(fluoro(nitro)methyl)-4-(trifluoromethyl)benzene (22.3 mg, 100 μ mol) and *N*-(4-chlorophenyl)hydroxylamine (21.6 mg, 150 μ mol) in a 1:1 mixture of toluene and acetonitrile. Concentration of the filtered reaction mixture provided a solid (66% yield by ¹H NMR). Trituration with 20% dichloromethane in hexanes afforded the desired compound as a colorless solid (15.3 mg, 55%). Mp 182-183 °C; R_f = 0.53 (20% EtOAc/hexanes); IR (film) 3313, 1653, 1517, 1331, 1134, 826 cm^{-1} ; ¹H NMR (600 MHz, CDCl₃) δ 7.96 (d, J = 8.1 Hz, 2H), 7.88 (s, 1H), 7.75 (d, J = 8.2 Hz, 2H), 7.59 (d, J = 8.7 Hz, 2H), 7.35 (d, J = 8.8 Hz, 2H); ¹³C NMR (150 MHz, CDCl₃) ppm 164.6, 138.0, 136.2, 133.9 (q, ² J_{CF} = 33.9 Hz), 130.3, 129.4, 127.7, 126.1 (q, ³ J_{CF} = 3.3 Hz), 123.7 (q, ¹ J_{CF} = 272.7 Hz), 121.7; ¹⁹F NMR (376 MHz, CDCl₃) δ -63.0; HRMS (ESI): Exact mass calcd for C₁₄H₈ClF₃NO [M-H]⁻ 298.0252, found 298.0241.



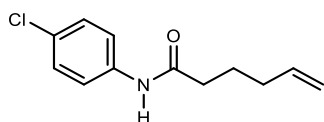
2-(4-Chlorophenyl)-*N*-(4-methoxyphenyl)acetamide (239). ²⁸⁵

Prepared according to the general procedure for umpolung *N*-aryl amide synthesis from 1-chloro-4-(2-fluoro-2-nitroethyl)benzene (20.4 mg, 100 μ mol) and *N*-(4-methoxyphenyl)hydroxylamine (20.9 mg, 150 μ mol) in toluene. Concentration of the filtered reaction mixture provided a solid (85% yield by ¹H NMR). Trituration with dichloromethane in hexanes afforded the desired compound as a cream-colored solid (10.6 mg, 38%). Mp 181-182 °C;

²⁸⁴ Partial characterization data previously reported: Wang, S.-P.; Cheung, C. W.; Ma, J.-A. *J. Org. Chem.* **2019**, *84*, 13922.

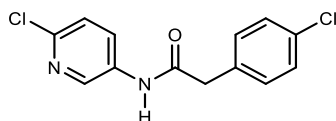
²⁸⁵ Partial characterization data previously reported: Vasudevan, N.; Routholla, G.; TejaIlla, G.; Reddy, D. S. *Tetrahedron* **2020**, 131262.

$R_f = 0.14$ (20% EtOAc/hexanes); IR (film) 3278, 3135, 3076, 2961, 1649, 1510, 1411, 1310, 1254, 1179, 1104, 1030, 828, 737 cm^{-1} ; $^1\text{H NMR}$ (400 MHz, $\text{DMSO-}d_6$) δ 10.02 (s, 1H), 7.48 (d, $J = 8.3$ Hz, 2H), 7.39 (d, $J = 8.0$ Hz, 2H), 7.33 (d, $J = 8.0$ Hz, 2H), 6.86 (d, $J = 8.4$ Hz, 2H), 3.71 (s, 3H), 3.60 (s, 2H); $^{13}\text{C NMR}$ (100 MHz, $\text{DMSO-}d_6$) ppm 168.1, 155.2, 135.1, 132.2, 131.2, 131.0, 128.2, 120.6, 113.8, 55.1, 42.3; HRMS (ESI): Exact mass calcd for $\text{C}_{15}\text{H}_{15}\text{ClNO}_2$ $[\text{M}+\text{H}]^+$ 276.0786, found 276.0796.



***N*-(4-Chlorophenyl)hex-5-enamide (254)**. Prepared according to the

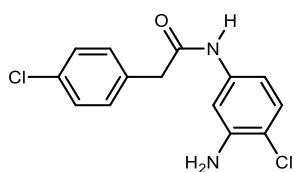
general procedure for umpolung *N*-aryl amide synthesis from 6-fluoro-6-nitrohex-1-ene (14.7 mg, 100 μmol) and *N*-(4-chlorophenyl)hydroxylamine (21.6 mg, 150 μmol) in toluene. Concentration of the filtered reaction mixture provided a solid (62% yield by $^1\text{H NMR}$). Column chromatography (SiO_2 , 50-100% dichloromethane in hexanes) afforded the desired compound as a colorless solid (9.6 mg, 43%). Mp 65-67 $^\circ\text{C}$; $R_f = 0.39$ (dichloromethane); IR (film) 3289, 2926, 1656, 1593, 1528, 1398, 1094, 914, 823 cm^{-1} ; $^1\text{H NMR}$ (400 MHz, CDCl_3) δ 7.46 (d, $J = 8.6$ Hz, 2H), 7.27 (d, $J = 8.5$ Hz, 2H), 7.24 (br s, 1H), 5.80 (ddt, $J = 17.3, 10.2, 6.5$ Hz, 1H), 5.05 (d, $J = 17.1$ Hz, 1H), 5.02 (d, $J = 10.2$ Hz, 1H), 2.35 (t, $J = 7.5$ Hz, 2H), 2.15 (dt, $J = 7.0, 7.0$ Hz, 2H), 1.83 (tt, $J = 7.5, 7.5$ Hz, 2H); $^{13}\text{C NMR}$ (100 MHz, CDCl_3) ppm 171.3, 137.8, 136.6, 129.3, 129.1, 121.1, 115.7, 36.9, 33.2, 24.6; HRMS (ESI): Exact mass calcd for $\text{C}_{12}\text{H}_{15}\text{ClNO}$ $[\text{M}+\text{H}]^+$ 224.0837, found 224.0848.



2-(4-chlorophenyl)-*N*-(6-chloropyridin-3-yl)acetamide (237).

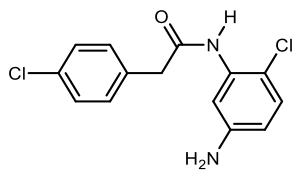
Prepared according to the general procedure for umpolung *N*-aryl amide synthesis from 1-chloro-4-(2-fluoro-2-nitroethyl)benzene (20.4 mg, 100 μmol) and *N*-(6-chloropyridin-3-yl)hydroxylamine (21.8 mg, 150 μmol) in a 1:1 mixture of toluene and

acetonitrile. Concentration of the filtered reaction mixture provided an oil (76% yield by ^1H NMR). Column chromatography (SiO_2 , 30-40% ethyl acetate in hexanes) afforded the desired compound as a yellow oil (9.0 mg, 32%). $R_f = 0.27$ (40% EtOAc/hexanes); IR (film) 3254, 3094, 1674, 1594, 1530, 1464, 1370, 1288, 1106, 1019, 830 cm^{-1} ; ^1H NMR (400 MHz, $\text{DMSO-}d_6$) δ 10.54 (s, 1H), 8.59 (d, $J = 2.6$ Hz, 1H), 8.07 (dd, $J = 8.7, 2.8$ Hz, 1H), 7.46 (d, $J = 8.7$ Hz, 1H), 7.39 (d, $J = 8.5$ Hz, 2H), 7.34 (d, $J = 8.5$ Hz, 2H), 3.70 (s, 2H); ^{13}C NMR (100 MHz, $\text{DMSO-}d_6$) ppm 169.4, 143.6, 140.3, 135.3, 134.4, 131.4, 131.1, 129.7, 128.2, 124.2, 42.1; HRMS (ESI): Exact mass calcd for $\text{C}_{13}\text{H}_{11}\text{Cl}_2\text{N}_2\text{O}$ $[\text{M}+\text{H}]^+$ 281.0243, found 281.0257.



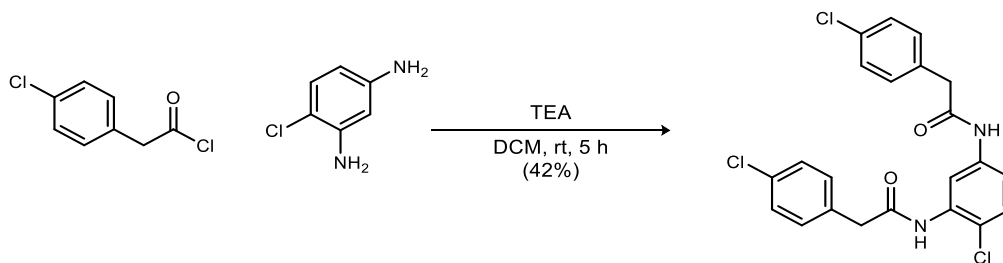
***N*-(3-Amino-4-chlorophenyl)-2-(4-chlorophenyl)acetamide (215).**

Prepared according to the general procedure for umpolung *N*-aryl amide synthesis from 1-chloro-4-(2-fluoro-2-nitroethyl)benzene (20.4 mg, 100 μmol) and 2-chloro-5-(hydroxyamino)aniline (23.9 mg, 150 μmol) in a 1:1 mixture of toluene and acetonitrile. Concentration of the filtered reaction mixture provided a solid (55% yield by ^1H NMR). The solid was suspended in dichloromethane, followed by filtration and washing of the solid (dichloromethane) to afford the desired compound as a cream-colored solid (11.1 mg, 38%). Mp 180 $^\circ\text{C}$ (decomposition); $R_f = 0.31$ (1% methanol in dichloromethane); IR (film) 3282, 3060, 1667, 1615, 1546, 1484, 1418, 1340, 1240, 1112, 868, 798, 736 cm^{-1} ; ^1H NMR (400 MHz, acetone- d_6) δ 9.20 (br s, 1H), 7.37 (d, $J = 8.6$ Hz, 2H), 7.33 (d, $J = 8.5$ Hz, 2H), 7.33 (d, $J = 2.3$ Hz, 1H), 7.07 (d, $J = 8.6$ Hz, 1H), 6.78 (dd, $J = 8.6, 2.2$ Hz, 1H), 4.91 (br s, 2H), 3.66 (s, 2H); ^{13}C NMR (100 MHz, acetone- d_6) ppm 168.3, 144.5, 138.9, 134.8, 131.9, 130.8, 128.8, 128.1, 112.3, 108.8, 106.1, 42.8; HRMS (ESI): Exact mass calcd for $\text{C}_{14}\text{H}_{13}\text{Cl}_2\text{N}_2\text{O}$ $[\text{M}+\text{H}]^+$ 295.0399, found 295.0404.



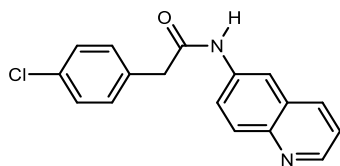
***N*-(5-Amino-2-chlorophenyl)-2-(4-chlorophenyl)acetamide (245).**

Prepared according to the general procedure for umpolung *N*-aryl amide synthesis from 1-chloro-4-(2-fluoro-2-nitroethyl)benzene (20.4 mg, 100 μ mol) and 4-chloro-3-(hydroxyamino)aniline (23.9 mg, 150 μ mol) in a 1:1 mixture of toluene and acetonitrile. Concentration of the filtered reaction mixture provided a solid (65% yield by ^1H NMR). Column chromatography (30-40% ethyl acetate in hexanes) afford the desired compound as a pale orange solid (12.4 mg, 42%). Mp 110 $^{\circ}\text{C}$ (decomposition); $R_f = 0.26$ (40% EtOAc/hexanes); IR (film) 3238, 2920, 1657, 1528, 1444 cm^{-1} ; ^1H NMR (400 MHz, DMSO- d_6) δ 9.36 (br s, 1H), 7.38 (br s, 4H), 7.04 (d, $J = 8.5$ Hz, 1H), 6.93 (br s, 1H), 6.36 (d, $J = 7.9$ Hz, 1H), 5.26 (br s, 2H), 3.69 (br s, 2H); ^{13}C NMR (100 MHz, DMSO- d_6) ppm 168.7, 148.1, 135.0, 134.7, 131.3, 131.0, 129.2, 128.2, 112.1, 111.9, 111.0, 41.9; HRMS (ESI): Exact mass calcd for $\text{C}_{14}\text{H}_{13}\text{Cl}_2\text{N}_2\text{O}$ $[\text{M}+\text{H}]^+$ 295.0399, found 295.0403.



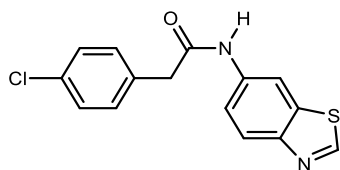
***N,N'*-(4-Chloro-1,3-phenylene)bis(2-(4-chlorophenyl)acetamide) (216).** In a 2-dram vial, the acyl chloride (58.6 μL , 400 μmol), the diamine (14.3 mg, 100 μmol), and triethyl amine (62.4 μL , 440 μmol) were dissolved in dichloromethane (2 mL). The reaction was stirred at room temperature for 5 hours. The reaction was quenched with 1 M aq hydrogen chloride and extracted three times with ethyl acetate. The combined organics were dried and concentrated, and the residue was purified by column chromatography (SiO_2 , 30% ethyl acetate in hexanes) to afford the desired

product as a colorless solid (18.9 mg, 42%). Mp 195-198 °C; R_f = 0.34 (40% EtOAc/hexanes); IR (film) 3296, 2922, 1665, 1602, 1530, 1416, 1091 cm^{-1} ; ^1H NMR (400 MHz, $\text{DMSO-}d_6$) δ 10.31 (s, 1H), 9.68 (s, 1H), 7.92 (s, 1H), 7.51 (d, J = 8.6 Hz, 1H), 7.40-7.31 (m, 9H), 3.73 (s, 2H), 3.62 (s, 2H); ^{13}C NMR (100 MHz, $\text{DMSO-}d_6$) ppm 169.1, 168.9, 138.2, 134.9, 134.75, 134.73, 131.34, 131.32, 131.04, 131.01, 129.4, 128.24, 128.22, 120.2, 116.9, 116.5, 42.4, 41.7; HRMS (ESI): Exact mass calcd for $\text{C}_{22}\text{H}_{18}\text{Cl}_3\text{N}_2\text{O}_2$ $[\text{M}+\text{H}]^+$ 447.0428, found 447.0438.



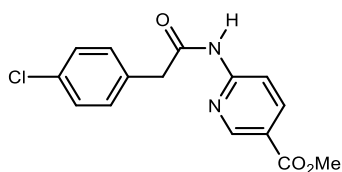
2-(4-chlorophenyl)-N-(quinolin-6-yl)acetamide (247). Prepared according to the general procedure for umpolung *N*-aryl amide synthesis from 1-chloro-4-(2-fluoro-2-nitroethyl)benzene (20.4 mg,

100 μmol) and *N*-(quinolin-6-yl)hydroxylamine (24.0 mg, 150 μmol) in a 1:1 mixture of toluene and acetonitrile. Concentration of the filtered reaction mixture provided a solid (47% yield by ^1H NMR). Column chromatography (SiO_2 , 40-50% ethyl acetate in hexanes) could afford the desired compound as a ~12:1 mixture of product to 6-aminoquinoline. Preparatory HPLC (0-95% MeCN in H_2O) afforded the desired compound as a colorless solid (4.4 mg, 15%). Mp 187-189 °C; R_f = 0.09 (2% methanol in dichloromethane); IR (film) 3263, 2920, 1659, 1536, 1087, 813 cm^{-1} ; ^1H NMR (400 MHz, $\text{DMSO-}d_6$) δ 10.51 (br s, 1H), 8.77 (dd, J = 4.1, 1.5 Hz, 1H), 8.36 (d, J = 1.7 Hz, 1H), 8.06 (d, J = 8.1 Hz, 1H), 7.97 (d, J = 9.1 Hz, 1H), 7.80 (dd, J = 9.0, 2.1 Hz, 1H), 7.46 (dd, J = 8.3, 4.2 Hz, 1H), 7.40 (s, 4H), 3.73 (s, 2H); ^{13}C NMR (100 MHz, $\text{DMSO-}d_6$) ppm 169.2, 149.0, 144.7, 137.0, 135.5, 134.8, 131.3, 131.1, 129.5, 128.3, 128.2, 123.2, 121.8, 115.0, 42.4; HRMS (ESI): Exact mass calcd for $\text{C}_{17}\text{H}_{14}\text{ClN}_2\text{O}$ $[\text{M}+\text{H}]^+$ 297.0789, found 297.0787.



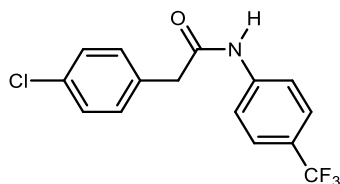
***N*-(Benzo[d]thiazol-6-yl)-2-(4-chlorophenyl)acetamide (241).** Prepared according to the general procedure for umpolung *N*-aryl

amide synthesis from 1-chloro-4-(2-fluoro-2-nitroethyl)benzene (20.4 mg, 100 μmol) and *N*-(benzo[d]thiazol-6-yl)hydroxylamine (24.9 mg, 150 μmol) in a 1:1 mixture of toluene and acetonitrile. Concentration of the filtered reaction mixture provided a solid (35% yield by ^1H NMR). Trituration (dichloromethane) afforded the desired compound as a cream colored solid (1.1 mg, 4%). Mp 213-215 $^{\circ}\text{C}$; $R_f = 0.20$ (40% EtOAc/hexanes); IR (film) 3448, 2922, 1658, 1472, 1396, 1259, 1090 cm^{-1} ; ^1H NMR (400 MHz, $\text{DMSO-}d_6$) δ 10.46 (s, 1H), 9.25 (s, 1H), 8.53 (d, $J = 1.4$ Hz, 1H), 8.01 (d, $J = 8.8$ Hz, 1H), 7.59 (dd, $J = 8.8, 1.8$ Hz, 1H), 7.40 (d, $J = 8.7$ Hz, 2H), 7.37 (d, $J = 8.9$ Hz, 2H), 3.71 (s, 2H); ^{13}C NMR (100 MHz, $\text{DMSO-}d_6$) ppm 169.0, 154.7, 149.1, 136.8, 134.8, 134.2, 131.3, 131.0, 128.2, 123.0, 118.7, 111.6, 42.4; HRMS (ESI): Exact mass calcd for $\text{C}_{15}\text{H}_{12}\text{ClN}_2\text{OS}$ $[\text{M}+\text{H}]^+$ 303.0353, found 303.0358.



Methyl 6-(2-(4-chlorophenyl)acetamido)nicotinate (244).

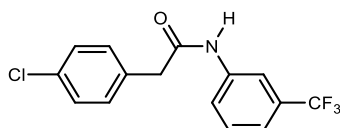
Prepared according to the general procedure for umpolung *N*-aryl amide synthesis from 1-chloro-4-(2-fluoro-2-nitroethyl)benzene (11.2 mg, 55 μmol) and methyl 6-(hydroxyamino)nicotinate (13.9 mg, 82.5 μmol) in toluene. Concentration of the filtered reaction mixture and column chromatography (SiO_2 , 20-40% ethyl acetate in hexanes) afforded the desired compound as a yellow-brown oil (6.0 mg, 36%). $R_f = 0.40$ (40% EtOAc/hexanes); IR (film) 3306, 2923, 2855, 1717, 1591, 1525, 1439, 1284, 1291, 1121, 1020, 778 cm^{-1} ; ^1H NMR (400 MHz, $\text{DMSO-}d_6$) δ 11.16 (s, 1H), 8.85 (d, $J = 1.9$ Hz, 1H), 8.27 (dd, $J = 8.9, 2.3$ Hz, 1H), 8.17 (d, $J = 8.8$ Hz, 1H), 7.39 (d, $J = 8.7$ Hz, 2H), 7.36 (d, $J = 8.6$ Hz, 2H), 3.85 (s, 3H), 3.78 (s, 2H); ^{13}C NMR (100 MHz, $\text{DMSO-}d_6$) ppm 170.3, 164.8, 155.1, 149.5, 139.3, 134.4, 131.4, 131.1, 128.3, 120.9, 112.5, 52.1, 42.1; HRMS (ESI): Exact mass calcd for $\text{C}_{15}\text{H}_{14}\text{ClN}_2\text{O}_3$ $[\text{M}+\text{H}]^+$ 305.0687, found 305.0689.



2-(4-Chlorophenyl)-N-(4-(trifluoromethyl)phenyl)acetamide

(246).²⁸⁶ Prepared according to the general procedure for umpolung

N-aryl amide synthesis from 1-chloro-4-(2-fluoro-2-nitroethyl)benzene (20.4 mg, 100 μ mol) and *N*-(4-(trifluoromethyl)phenyl)hydroxylamine (26.6 mg, 150 μ mol) in toluene. Concentration of the filtered reaction mixture gave a solid (62% yield by ¹H NMR). Trituration (1:1 dichloromethane:hexanes) afforded the desired compound as a colorless solid (6.9 mg, 22%). Mp 164-165 °C; R_f = 0.46 (dichloromethane); IR (film) 3277, 3137, 1669, 1606, 1542, 1494, 1408, 1323, 1260, 1158, 1117, 1068, 1017, 834 cm^{-1} ; ¹H NMR (600 MHz, DMSO-*d*₆) δ 10.53 (s, 1H), 7.80 (d, J = 8.6 Hz, 2H), 7.67 (d, J = 8.6 Hz, 2H), 7.39 (d, J = 8.5 Hz, 2H), 7.35 (d, J = 8.5 Hz, 2H), 3.70 (s, 2H); ¹³C NMR (150 MHz, DMSO-*d*₆) ppm 169.4, 142.7, 134.5, 131.4, 131.1, 128.3, 126.1 (q, ³ J_{CF} = 3.8 Hz), 124.4 (q, ¹ J_{CF} = 271.7 Hz), 123.3 (q, ² J_{CF} = 31.8 Hz), 119.0, 42.4; ¹⁹F NMR (376 MHz, DMSO-*d*₆) δ -60.3; HRMS (ESI): Exact mass calcd for C₁₅H₁₀ClF₃NO [M-H]⁻ 312.0408, found 312.0403.



2-(4-Chlorophenyl)-N-(3-(trifluoromethyl)phenyl)acetamide

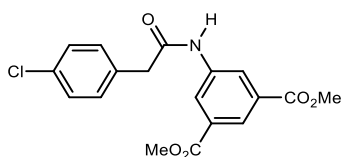
(240).²⁸⁷ Prepared according to the general procedure for umpolung

N-aryl amide synthesis from 1-chloro-4-(2-fluoro-2-nitroethyl)benzene (20.4 mg, 100 μ mol) and *N*-(3-(trifluoromethyl)phenyl)hydroxylamine (26.6 mg, 150 μ mol) in toluene. Concentration of the filtered reaction mixture gave a solid (65% yield by ¹H NMR). Column chromatography (SiO₂,

²⁸⁶ Partial characterization data previously reported: Lu, Z.; Chai, Y.; Wang, J.; Pan, Y.; Sun, C.; Zeng, S. *Rapid Commun. Mass Spectrom.* **2014**, *28*, 1641.

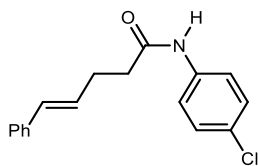
²⁸⁷ Partial characterization data previously reported: Pirisino, C. G. E. *Archivio Bimestrale di Scienze Mediche e Naturali* **1977**, *55*, 307.

100% dichloromethane) afforded the desired compound as a colorless solid (20.5 mg, 65%). Mp 112-113 °C; $R_f = 0.34$ (dichloromethane); IR (film) 3278, 2920, 1665, 1604, 1558, 1491, 1445, 1334, 1127 cm^{-1} ; $^1\text{H NMR}$ (400 MHz, $\text{DMSO-}d_6$) δ 10.51 (s, 1H), 8.09 (s, 1H), 7.77 (d, $J = 8.3$ Hz, 1H), 7.54 (dd, $J = 8.0, 8.0$ Hz, 1H), 7.40-7.34 (m, 5H), 3.69 (s, 2H); $^{13}\text{C NMR}$ (100 MHz, $\text{DMSO-}d_6$) ppm 169.3, 139.8, 134.5, 131.4, 131.1, 130.0, 129.4 (q, $^2J_{\text{CF}} = 31.5$ Hz), 128.2, 124.1 (q, $^1J_{\text{CF}} = 272.2$ Hz), 122.6, 119.6 (q, $^3J_{\text{CF}} = 3.6$ Hz), 115.1 (q, $^3J_{\text{CF}} = 3.9$ Hz), 42.4; $^{19}\text{F NMR}$ (376 MHz, $\text{DMSO-}d_6$) δ -61.4; HRMS (ESI): Exact mass calcd for $\text{C}_{15}\text{H}_{10}\text{ClF}_3\text{NO}$ $[\text{M-H}]^-$ 312.0408, found 312.0396.



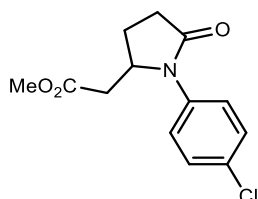
Dimethyl 5-(2-(4-chlorophenyl)acetamido)isophthalate (242).

Prepared according to the general procedure for umpolung *N*-aryl amide synthesis from 1-chloro-4-(2-fluoro-2-nitroethyl)benzene (20.4 mg, 100 μmol) and dimethyl 5-(hydroxyamino)isophthalate (33.8 mg, 150 μmol) in a 1:1 mixture of toluene and acetonitrile. Concentration of the filtered reaction mixture gave a solid (73% yield by $^1\text{H NMR}$). Column chromatography (SiO_2 , 0-0.5% methanol in dichloromethane) afforded the desired compound as a cream-colored solid (22.8 mg, 63%). Mp 190-191 °C; $R_f = 0.12$ (20% EtOAc/hexanes); IR (film) 3274, 2953, 1725, 1606, 1563, 1493, 1438, 1345, 1247, 1092, 1008, 906, 797, 757, 721 cm^{-1} ; $^1\text{H NMR}$ (400 MHz, $\text{DMSO-}d_6$) δ 10.63 (s, 1H), 8.48 (s, 2H), 8.14 (s, 1H), 7.39 (d, $J = 8.8$ Hz, 2H), 7.36 (d, $J = 8.5$ Hz, 2H), 3.88 (s, 6H), 3.69 (s, 2H); $^{13}\text{C NMR}$ (100 MHz, $\text{DMSO-}d_6$) ppm 169.4, 165.2, 140.0, 134.4, 131.4, 131.1, 130.7, 128.2, 124.0, 123.5, 52.5, 42.4; HRMS (ESI): Exact mass calcd for $\text{C}_{18}\text{H}_{17}\text{ClNO}_5$ $[\text{M+H}]^+$ 362.0790, found 362.0801.



(*E*)-*N*-(4-Chlorophenyl)-5-phenylpent-4-enamide (255). Prepared according to the general procedure for umpolung *N*-aryl amide synthesis

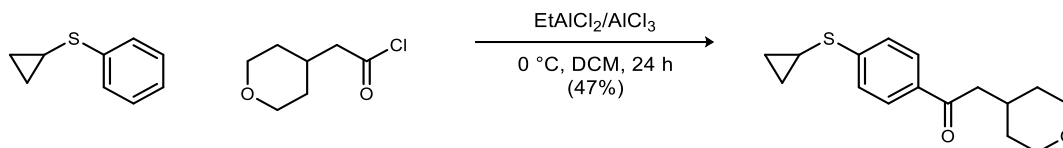
from (*E*)-(5-fluoro-5-nitropent-1-en-1-yl)benzene (20.9 mg, 100 μ mol) and *N*-(4-chlorophenyl)hydroxylamine (21.6 mg, 150 μ mol) in toluene. Concentration of the filtered reaction mixture gave a solid (59% yield by ^1H NMR). Trituration (5% dichloromethane in hexanes) afforded the desired compound as a pale-yellow solid (10.6 mg). Column chromatography of the soluble portion (SiO_2 , 20% ethyl acetate in hexanes) afforded additional desired compound as a pale-yellow solid (3.5 mg, 49% combined). Mp 140 $^\circ\text{C}$ (decomposition); $R_f = 0.50$ (40% EtOAc/hexanes); IR (film) 3284, 3026, 2916, 1653, 1594, 1530, 1491, 1443, 1399, 1298, 1091, 1013, 965, 825, 741, 691 cm^{-1} ; ^1H NMR (400 MHz, CDCl_3) δ 7.45 (d, $J = 8.7$ Hz, 2H), 7.36-7.19 (m, 8H), 6.48 (d, $J = 15.8$ Hz, 1H), 6.24 (dt, $J = 15.7, 6.9$ Hz, 1H), 2.63 (dt, $J = 7.1, 7.1$ Hz, 2H), 2.52 (t, $J = 7.2$ Hz, 2H); ^{13}C NMR (100 MHz, CDCl_3) ppm 170.6, 137.3, 136.5, 131.6, 129.4, 129.1, 128.7, 128.4, 127.5, 126.2, 121.3, 37.4, 28.9; HRMS (ESI): Exact mass calcd for $\text{C}_{17}\text{H}_{16}\text{ClNNaO}$ $[\text{M}+\text{Na}]^+$ 308.0813, found 308.0814.



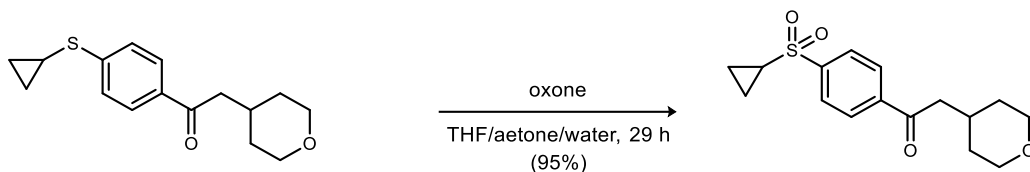
Methyl 2-(1-(4-chlorophenyl)-5-oxopyrrolidin-2-yl)acetate (251).

Prepared according to the general procedure for umpolung *N*-aryl amide synthesis from methyl (*E*)-6-fluoro-6-nitrohex-2-enoate (19.1 mg, 100 μ mol) and *N*-(4-chlorophenyl)hydroxylamine (21.6 mg, 150 μ mol) in toluene. Concentration of the filtered reaction mixture gave a solid (61% yield by ^1H NMR). Column chromatography of the soluble portion (SiO_2 , 30-40% ethyl acetate in hexanes) afforded desired compound as a colorless oil (11.1 mg, 41%). $R_f = 0.17$ (40% EtOAc/hexanes); IR (film) 2924, 1736, 1702, 1494, 1437, 1415, 1387, 1292, 1195, 1175, 1092, 1012, 830 cm^{-1} ; ^1H NMR (400 MHz, CDCl_3) δ 7.35 (s, 4H), 4.59 (dddd, $J = 8.3, 8.3, 4.4, 4.4$ Hz, 1H), 3.63 (s, 3H), 2.71-2.44 (m, 4H), 2.39 (dd, $J = 15.7, 9.1$ Hz, 1H), 1.96-1.88 (m, 1H); ^{13}C NMR (100 MHz, CDCl_3) ppm 174.1, 170.9, 135.7, 131.7, 129.4,

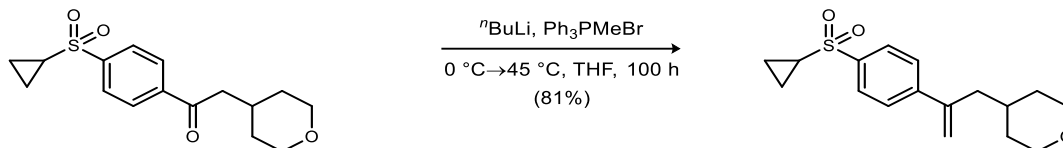
125.2, 56.5, 52.0, 38.3, 30.8, 24.5; HRMS (ESI): Exact mass calcd for C₁₃H₁₄ClNNaO₃ [M+Na]⁺ 290.0554, found 290.0557.



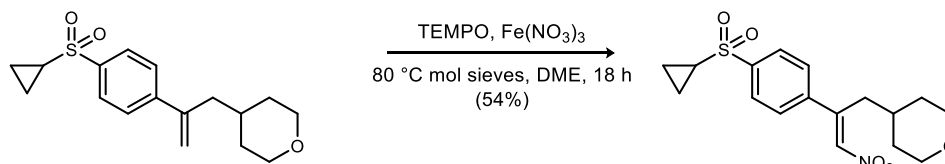
1-(4-(Cyclopropylthio)phenyl)-2-(tetrahydro-2H-pyran-4-yl)ethan-1-one (278). In a vial, the acyl chloride (1.2955 g, 7.9045 mmol) was dissolved in dichloromethane (18 mL). The solution was brought to 0 °C and ethyl aluminum dichloride (4.4 mL of 1.8 M solution in toluene, 7.9 mmol) and aluminum trichloride (1.0521 g, 7.9045 mmol) were added slowly. The arene (912.1 mg, 6.080 mmol) was added and the reaction was stirred at the same temperature for 24 hours. The reaction was quenched with satd aq sodium bicarbonate, extracted with dichloromethane, dried, and concentrated. Column chromatography (SiO₂, 20-30% ethyl acetate in hexanes) afforded the desired compound as a colorless solid (788.7 mg, 47%). Mp 63-66 °C; $R_f = 0.11$ (10% EtOAc/hexanes); IR (film) 2952, 2925, 2842, 1678, 1589, 1557, 1440, 1401, 1273, 1244, 1214, 1184, 1136, 1110, 1092, 1006, 971, 826, 813 cm⁻¹; ¹H NMR (400 MHz, CDCl₃) δ 7.85 (d, $J = 8.5$ Hz, 2H), 7.39 (d, $J = 8.5$ Hz, 2H), 3.93 (dd, $J = 11.1, 3.5$ Hz, 2H), 3.42 (ddd, $J = 11.8, 11.8, 1.7$ Hz, 2H), 2.84 (d, $J = 6.8$ Hz, 2H), 2.25-2.16 (m, 2H), 1.67 (dddd, $J = 12.9, 1.6, 1.6, 1.6$ Hz, 2H), 1.37 (dddd, $J = 12.3, 12.3, 12.3, 4.3$ Hz, 2H), 1.13 (ddd, $J = 6.9, 6.9, 5.2$ Hz, 2H), 0.70 (ddd, $J = 6.3, 4.6, 4.6$ Hz, 2H); ¹³C NMR (100 MHz, CDCl₃) ppm 198.4, 146.7, 133.7, 128.5, 125.3, 68.0, 45.2, 33.2, 21.6, 11.3, 8.7; HRMS (APCI): Exact mass calcd for C₁₆H₂₁O₂S [M+H]⁺ 277.1257, found 277.1259.



1-(4-(Cyclopropylsulfonyl)phenyl)-2-(tetrahydro-2H-pyran-4-yl)ethan-1-one (279). In a vial, the ketone (1.5425 g, 5.5895 mmol) was dissolved in tetrahydrofuran (5 mL) and acetone (2 mL). Oxone (2.5497 g, 16.767 mmol) in water (20 mL) was added in 4 mL aliquots, once per hour for 4 hours. Following the final addition of the Oxone solution, additional tetrahydrofuran (5 mL) and acetone (2 mL) were added to solubilize large aggregates of precipitate that formed. The reaction was stirred for 3 additional hours before the addition of another portion of Oxone (1.2749 mg, 8.384 mmol) in water (10 mL). Aggregates of precipitate were observed once again so tetrahydrofuran and acetone were added until only the free-flowing precipitate remained (~2 mL and 1 mL respectively). The reaction mixture was stirred for 21 additional hours, and then extracted with ethyl acetate. The extracts were dried, and concentrated to afford the desired compound as a pale-yellow solid (1.6340 g, 95%). Mp 112-114 °C; $R_f = 0.17$ (40% EtOAc/hexanes); IR (film) 2920, 2844, 1691, 1442, 1398, 1322, 1291, 1243, 1188, 1150, 1111, 1091, 1040, 1009, 973, 886, 830, 787, 733, 686, 650, 602, 572 cm^{-1} ; $^1\text{H NMR}$ (400 MHz, CDCl_3) δ 8.09 (d, $J = 8.3$ Hz, 2H), 7.99 (d, $J = 8.2$ Hz, 2H), 3.94 (dd, $J = 11.4, 3.8$ Hz, 2H), 3.43 (dd, $J = 11.7, 11.7$ Hz, 2H), 2.93 (d, $J = 6.7$ Hz, 2H), 2.47 (dddd, $J = 7.9, 7.9, 4.6, 4.6$ Hz, 1H), 2.26 (ddtt, $J = 10.9, 10.9, 10.7, 4.2$ Hz, 1H), 1.68 (d, $J = 12.7$ Hz, 2H), 1.43-1.33 (m, 4H), 1.06 (ddd, $J = 7.6, 7.6, 5.2$ Hz, 2H); $^{13}\text{C NMR}$ (100 MHz, CDCl_3) ppm 198.1, 144.6, 140.9, 128.9, 128.1, 67.9, 45.9, 33.1, 32.8, 31.3, 6.3; HRMS (ESI): Exact mass calcd for $\text{C}_{16}\text{H}_{19}\text{O}_4\text{S}$ $[\text{M}-\text{H}]^-$ 307.1010, found 307.0995.

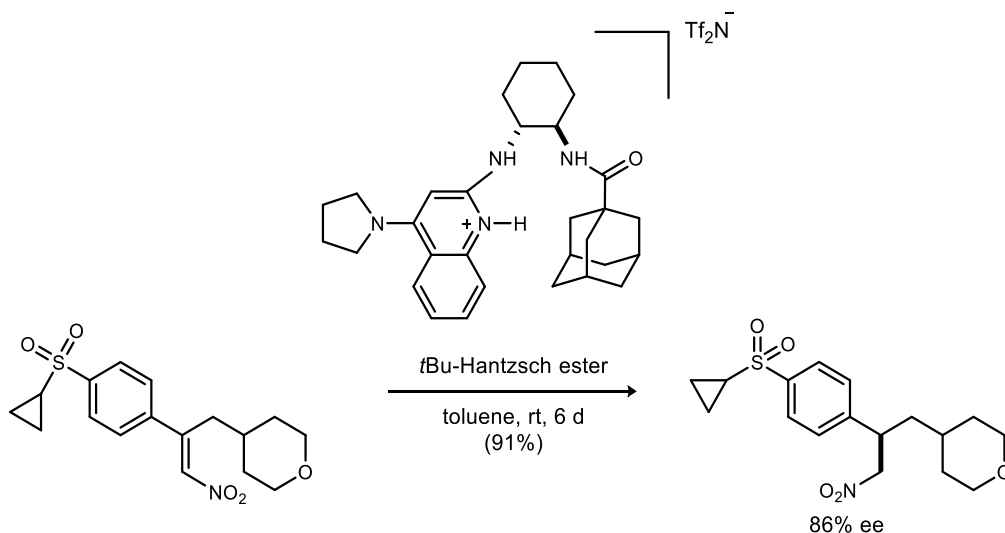


4-(2-(4-(Cyclopropylsulfonyl)phenyl)allyl)tetrahydro-2H-pyran (280). In a vial, freshly-ground triphenyl phosphonium bromide (507.7 mg, 1.4220 mmol) was dissolved in tetrahydrofuran (8 mL). The solution was cooled to 0 °C and ⁿBuLi (638 μL of 2.23 M solution in hexanes, 1.4220 mmol) was added slowly. After an hour of stirring at the same temperature, the reaction was allowed to warm to room temperature and stirred for 50 hours. The ketone (215.2 mg, 698.7 μmol) dissolved in tetrahydrofuran (8 mL) was added slowly, and the reaction was stirred at 45 °C for 50 hours. The reaction mixture was filtered through Celite and concentrated. Column chromatography (SiO₂, 40% ethyl acetate in hexanes) afforded the desired compound as a colorless solid (174.1 mg, 81%). Mp 120-121 °C; *R_f* = 0.31 (40% EtOAc/hexanes); IR (film) 2919, 2847, 1318, 1294, 1151, 1126, 1092, 886, 848, 703 cm⁻¹; ¹H NMR (400 MHz, CDCl₃) δ 7.85 (d, *J* = 8.4 Hz, 2H), 7.54 (d, *J* = 8.4 Hz, 2H), 5.40 (s, 1H), 5.19 (s, 1H), 3.90 (dd, *J* = 11.3, 3.8 Hz, 2H), 3.26 (ddd, *J* = 11.7, 11.7, 1.4 Hz, 2H), 2.51-2.44 (m, 3H), 1.56-1.46 (m, 3H), 1.36 (ddd, *J* = 6.7, 4.7, 4.7 Hz, 2H), 1.33-1.22 (m, 2H), 1.04 (ddd, *J* = 7.4, 7.4, 4.9 Hz, 2H); ¹³C NMR (100 MHz, CDCl₃) ppm 146.5, 145.0, 139.6, 127.9, 127.1, 117.1, 68.0, 42.9, 33.2, 33.03, 33.02, 6.1; HRMS (ESI): Exact mass calcd for C₁₇H₂₆NO₃S [M+NH₄]⁺ 324.1628, found 324.1623.



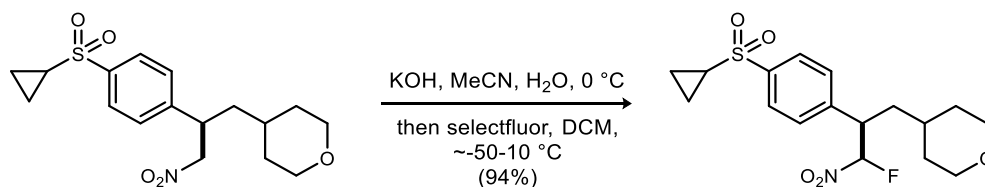
(E)-4-(2-(4-(Cyclopropylsulfonyl)phenyl)-3-nitroallyl)tetrahydro-2H-pyran (272). The styrene (137.1 mg, 448.0 μmol), TEMPO (13.6 mg, 88.2 μmol), Fe(NO₃)₃·9H₂O (361.8 mg, 895.9

μmol), 4 Å molecular sieves (135 mg), and dimethoxyethane (1.7 mL) were added to a vial. The mixture was warmed to 80 °C and stirred vigorously for 18 hours. The reaction was filtered through Celite with EtOAc, and the filtrate was concentrated. Column chromatography (SiO₂, 40% ethyl acetate in hexanes) afforded the desired compound as a pale yellow oil (85.4 mg, 54%). $R_f = 0.22$ (40% EtOAc/hexanes); IR (film) 3093, 2932, 2847, 1618, 1563, 1520, 1446, 1399, 1343, 1320, 1296, 1235, 1188, 1150, 1134, 1091, 1040, 1014, 984, 886, 831 cm⁻¹; ¹H NMR (400 MHz, CDCl₃) δ 7.95 (d, $J = 8.3$ Hz, 2H), 7.57 (d, $J = 8.3$ Hz, 2H), 7.20 (s, 1H), 3.85 (dd, $J = 11.2, 3.1$ Hz, 2H), 3.21 (td, $J = 11.6, 1.6$ Hz, 2H), 3.08 (d, $J = 7.1$ Hz, 2H), 2.49 (tt, $J = 8.1, 4.6$ Hz, 1H), 1.66-1.59 (m, 1H), 1.47 (d, $J = 12.9$ Hz, 2H), 1.40-1.31 (m, 4H), 1.07 (ddd, $J = 7.2, 7.2, 4.8$ Hz, 2H); ¹³C NMR (100 MHz, CDCl₃) ppm 150.1, 142.7, 142.3, 138.4, 128.5, 128.1, 67.6, 37.4, 34.7, 32.8 (2C), 6.2; HRMS (ESI): Exact mass calcd for C₁₇H₂₁ClNO₅S [M+Cl]⁻ 386.0834, found 386.0818.



(R)-4-(2-(4-(Cyclopropylsulfonyl)phenyl)-3-nitropropyl)tetrahydro-2H-pyran (282). The nitroalkene (376.5 mg, 961.3 μmol), catalyst (72.7 mg, 96.1 μmol), and *t*Bu-Hantzsch ester (326.3 mg, 1.057 mmol) were dissolved in toluene (3 mL). The reaction was stirred for 3 days, at which time TLC implied it had stalled. Taking aliquots for NMR at 3 and 4 days confirmed the reaction

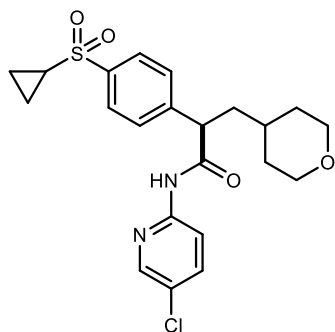
was stalled at partial conversion, so additional ^tBu-Hantzsch ester (163.2 mg, 528.5 μmol) was added at the 4-day mark. After a total of 6 days the reaction was concentrated. Column chromatography (SiO₂, 40% ethyl acetate in hexanes) afforded the desired compound as a colorless oil (307.4 mg, 91%). $[\alpha]_D^{20}$ -7.9 (*c* 1.18, CHCl₃) for a separately prepared sample of 87% ee. R_f = 0.14 (40% EtOAc/hexanes); IR (film) 2919, 2848, 1551, 1378, 1317, 1292, 1149, 1091, 886, 700 cm⁻¹; ¹H NMR (400 MHz, CDCl₃) δ 7.88 (d, *J* = 8.3 Hz, 2H), 7.40 (d, *J* = 8.3 Hz, 2H), 4.59 (dd, *J* = 11.5, 6.8 Hz, 1H), 4.54 (dd, *J* = 11.5, 8.6 Hz, 1H), 3.93-3.86 (m, 2H), 3.74-3.67 (m, 1H), 3.27-3.19 (m, 2H), 2.47 (dddd, *J* = 8.0, 8.0, 4.8, 4.8 Hz, 1H), 1.74 (ddd, *J* = 12.2, 12.2, 3.6 Hz, 1H), 1.66-1.55 (m, 2H), 1.45-1.41 (m, 1H), 1.38-1.33 (m, 2H), 1.32-1.21 (m, 3H), 1.09-1.03 (m, 2H); ¹³C NMR (100 MHz, CDCl₃) ppm 145.4, 140.5, 128.6, 128.5, 80.6, 67.7, 67.6, 41.0, 40.0, 33.5, 32.9, 32.2., 32.1, 6.2, 6.1; HRMS (ESI): Exact mass calcd for C₁₇H₂₇N₂O₅S [M+NH₄]⁺ 371.1635, found 371.1628.



4-((2*R*)-2-(4-(Cyclopropylsulfonyl)phenyl)-3-fluoro-3-nitropropyl)tetrahydro-2*H*-pyran

(**271**). The nitroalkane (307.4 mg, 870.4 μmol), was dissolved in a 2:1 water:acetonitrile solution (6 mL) and cooled to 0 °C. KOH (57.9 mg, 870.4 μmol) was added and the reaction was stirred for 27 hours. The solution was cooled until it became a slurry, and dichloromethane (6 mL) that had been cooled to -78 °C and Selectfluor (616.6 mg, 1.741 mmol) were added. The reaction was stirred for 15 hours at 0 °C. Diethyl ether (8 mL) was added before 10 additional minutes of stirring. The phases were separated, and the aq phase was extracted three times with diethyl ether.

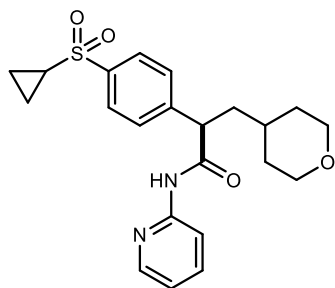
The combined organic layers were dried and concentrated to afford a 1:0.9 mixture of diastereomers of the desired compound as a colorless oil (303.0 mg, 94%). $R_f = 0.15$ and 0.18 (40% EtOAc/hexanes); IR (film) 2923, 2850, 1571, 1415, 1293, 1239, 1148, 1091, 1016, 886, 854, 705 cm^{-1} ; ^1H NMR (400 MHz, CDCl_3 , major diastereomer) δ 7.93 (d, $J = 8.3$ Hz, 2H), 7.47 (d, $J = 8.2$ Hz, 2H), 5.82 (dd, $^2J_{\text{HF}} = 50.1$ Hz, $J = 3.8$ Hz, 1H), 3.95-3.85 (m, 2H), 3.80-3.66 (m, 1H), 3.30-3.14 (m, 2H), 2.52-2.44 (m, 1H), 2.03-1.94 (m, 1H), 1.62-1.49 (m, 2H), 1.44-1.19 (m, 6H), 1.11-1.04 (m, 2H); ^{13}C NMR (100 MHz, CDCl_3 , both diastereomers) ppm 141.5, 141.3, 141.2, 139.8, 129.9, 129.6, 128.7, 128.4, 112.7 (d, $^1J_{\text{CF}} = 245.1$ Hz), 112.1 (d, $^1J_{\text{CF}} = 244.6$ Hz), 67.7 (2C), 67.55, 67.50, 45.7 (d, $^2J_{\text{CF}} = 41.7$ Hz), 45.5 (d, $^2J_{\text{CF}} = 41.0$ Hz), 37.6 (2C), 34.7 (d, $^3J_{\text{CF}} = 3.4$ Hz), 33.7, 33.5, 32.9 (2C), 32.1, 32.0, 31.8 (d, $^3J_{\text{CF}} = 2.2$ Hz), 6.23 (2C), 6.22 (2C); ^{19}F NMR (376 MHz, CDCl_3) δ -152.6 (major diastereomer), -154.7 (minor diastereomer); HRMS (ESI): Exact mass calcd for $\text{C}_{17}\text{H}_{26}\text{FN}_2\text{O}_5\text{S}$ $[\text{M}+\text{NH}_4]^+$ 389.1541, found 389.1535.



(R)-N-(5-Chloropyridin-2-yl)-2-(4-(cyclopropylsulfonyl)phenyl)-3-(tetrahydro-2H-pyran-4-yl)propanamide (293). Prepared

according to the general procedure for umpolung *N*-aryl amide synthesis from **271** (18.6 mg, 50 μmol) and *N*-(5-chloropyridin-2-yl)hydroxylamine (10.8 mg, 75 μmol) at half the standard scale in toluene. Concentration of the filtered reaction mixture gave a solid (33% yield by ^1H NMR). Column chromatography (SiO_2 , 40-50% ethyl acetate in hexanes with 0.1% triethyl amine) afforded the desired compound (4.4 mg) contaminated with one minor aromatic byproduct (~5:1 product:byproduct). Preparatory HPLC afforded the desired product as a colorless oil (1.3 mg, 6%). $[\alpha]_D^{20} -77$ (c 0.07, CHCl_3); $R_f = 0.14$ (40% EtOAc/hexanes); IR (film) 3315, 2919, 2849, 1694, 1574, 1518, 1459, 1376, 1292, 1110, 1091, 886, 836, 731, 692 cm^{-1} ; ^1H NMR (600 MHz,

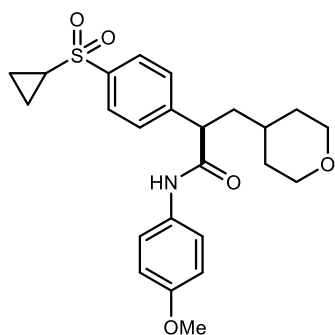
CDCl₃) δ 8.19-8.17 (m, 2H), 7.93 (br s, 1H), 7.89 (d, *J* = 8.3 Hz, 2H), 7.67 (dd, *J* = 9.0, 2.4 Hz, 1H), 7.55 (d, *J* = 8.3 Hz, 2H), 3.94-3.92 (m, 2H), 3.72 (dd, *J* = 7.5, 7.5 Hz, 1H), 3.30 (dddd, *J* = 11.7, 11.7, 6.4, 2.0 Hz, 2H), 2.46 (tt, *J* = 8.0, 4.8 Hz, 1H), 2.20 (ddd, *J* = 14.4, 7.2, 7.2 Hz, 1H), 1.81 (ddd, *J* = 13.9, 7.0, 7.0 Hz, 1H), 1.66-1.59 (m, 2H), 1.44 (dddddd, *J* = 11.1, 10.8, 7.3, 6.9, 3.5, 3.5 Hz, 1H), 1.39-1.31 (m, 4H), 1.07-1.02 (m, 2H); ¹³C NMR (150 MHz, CDCl₃) ppm 170.6, 149.3, 146.6, 144.8, 140.4, 138.3, 128.9, 128.6, 127.4, 114.8, 67.83, 67.80, 51.1, 40.6, 33.2, 33.0, 32.84, 32.78, 6.22, 6.20; HRMS (ESI): Exact mass calcd for C₂₂H₂₆ClN₂O₄S [M+H]⁺ 449.1296, found 449.1298.



(R)-2-(4-(Cyclopropylsulfonyl)phenyl)-N-(pyridin-2-yl)-3-(tetrahydro-2H-pyran-4-yl)propanamide (263a). Prepared according to the general procedure for umpolung *N*-aryl amide synthesis from **271** (18.6 mg, 50 μmol) and *N*-(pyridin-2-yl)hydroxylamine (8.3 mg, 75 μmol) at half the standard scale in

toluene. The reaction was run at -20 °C for 48 hours. Concentration of the filtered reaction mixture gave a solid (26% yield by ¹H NMR). Preparatory HPLC afforded the desired compound as a colorless oil (3.0 mg, 14%). *R_f* = 0.15 (60% EtOAc/hexanes); IR (film) 3320, 2919, 2849, 1693, 1577, 1595, 1525, 1433, 1294, 1147, 1091, 1016, 886, 780, 731, 692 cm⁻¹; ¹H NMR (600 MHz, CDCl₃) δ 8.23 (d, *J* = 4.9 Hz, 1H), 8.19 (d, *J* = 8.4 Hz, 1H), 8.00 (br s, 1H), 7.88 (d, *J* = 8.4 Hz, 2H), 7.71 (ddd, *J* = 8.6, 7.1, 1.8 Hz, 1H), 7.56 (d, *J* = 8.4 Hz, 2H), 7.05 (ddd, *J* = 7.3, 4.9, 0.9 Hz, 1H), 3.95-3.91 (m, 2H), 3.73 (dd, *J* = 7.4, 7.4 Hz, 1H), 3.30 (dddd, *J* = 11.8, 11.8, 6.2, 2.1 Hz, 2H), 2.45 (tt, *J* = 8.0, 4.8 Hz, 1H), 2.21 (ddd, *J* = 14.4, 7.2, 7.2 Hz, 1H), 1.80 (ddd, *J* = 14.1, 7.1, 7.1 Hz, 1H), 1.64 (ddd, *J* = 12.1, 3.0, 1.7 Hz, 1H), 1.60 (ddd, *J* = 13.1, 3.2, 1.7 Hz, 1H), 1.46 (dddddd, *J* = 11.2, 11.1, 7.5, 7.1, 3.4, 3.4 Hz, 1H), 1.38-1.32 (m, 4H), 1.05 (dd, *J* = 5.8, 2.3 Hz, 1H), 1.03

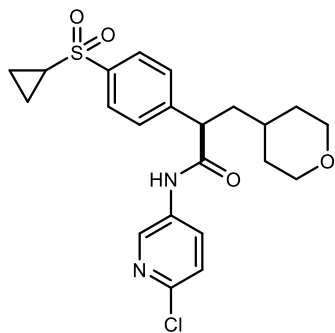
(dd, $J = 5.9, 2.3$ Hz, 1H); ^{13}C NMR (150 MHz, CDCl_3) ppm 170.7, 151.1, 147.9, 145.1, 140.2, 138.8, 128.9, 128.5, 120.4, 114.1, 67.9, 67.8, 51.2, 40.7, 33.2, 33.04, 32.89, 32.8, 6.22, 6.20; HRMS (ESI): Exact mass calcd for $\text{C}_{22}\text{H}_{27}\text{N}_2\text{O}_4\text{S}$ $[\text{M}+\text{H}]^+$ 415.1686, found 415.1689.



(R)-2-(4-(Cyclopropylsulfonyl)phenyl)-N-(4-methoxyphenyl)-3-(tetrahydro-2H-pyran-4-yl)propanamide (295). Prepared

according to the general procedure for umpolung *N*-aryl amide synthesis from **271** (18.6 mg, 50 μmol) and *N*-(4-methoxyphenyl)hydroxylamine (10.4 mg, 75 μmol) at half the

standard scale in toluene. Concentration of the filtered reaction mixture gave a solid (51% yield by ^1H NMR). Column chromatography (SiO_2 , 60-70% ethyl acetate in hexanes) afforded the desired compound as a red oil (11.1 mg, 50%). $R_f = 0.30$ (70% EtOAc/hexanes); IR (film) 3334, 2922, 2849, 1660, 1598, 1512, 1443, 1413, 1294, 1244, 1147, 1169, 1090, 1034, 886, 830, 758, 733 cm^{-1} ; ^1H NMR (600 MHz, CDCl_3) δ 7.84 (d, $J = 8.3$ Hz, 2H), 7.56 (d, $J = 8.3$ Hz, 2H), 7.37 (d, $J = 9.0$ Hz, 2H), 7.26 (s, 1H), 6.82 (d, $J = 9.0$ Hz, 2H), 3.94-3.89 (m, 2H), 3.77 (s, 3H), 3.68 (dd, $J = 7.6, 7.6$ Hz, 1H), 3.30 (dddd, $J = 11.1, 11.1, 11.1, 1.4$ Hz, 2H), 2.45 (tt, $J = 8.1, 4.4$ Hz, 1H), 2.19 (ddd, $J = 14.4, 7.2, 7.2$ Hz, 1H), 1.76 (ddd, $J = 13.9, 6.9, 6.9$ Hz, 1H), 1.66-1.59 (m, 2H), 1.48 (dddddd, $J = 11.1, 11.0, 7.0, 7.0, 3.5, 3.5$, 1H), 1.37-1.30 (m, 4H), 1.06-1.02 (m, 2H); ^{13}C NMR (150 MHz, CDCl_3) ppm 170.1, 156.8, 145.9, 139.8, 130.7, 128.8, 128.3, 121.9, 114.3, 67.88, 67.86, 55.6, 50.8, 41.0, 33.2, 33.0, 32.94, 32.87, 6.22, 6.17; HRMS (ESI): Exact mass calcd for $\text{C}_{24}\text{H}_{30}\text{NO}_5\text{S}$ $[\text{M}+\text{H}]^+$ 444.1839, found 444.1839.



(R)-N-(6-Chloropyridin-3-yl)-2-(4-(cyclopropylsulfonyl)phenyl)-

3-(tetrahydro-2H-pyran-4-yl)propanamide (294). Prepared

according to the general procedure for umpolung *N*-aryl amide synthesis from **271** (18.6 mg, 50 μ mol) and *N*-(6-chloropyridin-3-yl)hydroxylamine (10.8 mg, 75 μ mol) at half the standard scale in

toluene. Concentration of the filtered reaction mixture gave a solid (21% yield by ^1H NMR).

Column chromatography (SiO_2 , 60-70% ethyl acetate in hexanes) afforded an impure sample of

the desired product. Preparatory HPLC afforded the desired compound as a colorless oil (2.3 mg,

10%). $R_f = 0.14$ (70% EtOAc/hexanes); IR (film) 3329, 2923, 2851, 1694, 1595, 1528, 1464,

1370, 1288, 1147, 1106, 1017, 886, 831 cm^{-1} ; ^1H NMR (600 MHz, CDCl_3) δ 8.30 (d, $J = 2.7$ Hz,

1H), 8.13 (dd, $J = 8.7, 2.7$ Hz, 1H), 7.85 (d, $J = 8.3$ Hz, 2H), 7.57 (s, 1H), 7.54 (d, $J = 8.3$ Hz,

2H), 7.28 (d, $J = 8.7$ Hz, 1H), 3.95-3.90 (m, 2H), 3.74 (dd, $J = 7.5, 7.5$ Hz, 1H), 3.30 (dddd, $J =$

11.5, 11.5, 8.5, 2.1 Hz, 2H), 2.47 (tt, $J = 8.0, 4.8$ Hz, 1H), 2.19 (ddd, $J = 14.4, 7.2, 7.2$ Hz, 1H),

1.78 (ddd, $J = 13.9, 6.9, 6.9$ Hz, 1H), 1.61 (dd, $J = 14.4, 14.4$ Hz, 2H), 1.45 (dddddd, $J = 11.2,$

11.2, 7.1, 7.0, 3.1, 3.1 Hz, 1H), 1.38-1.31 (m, 4H), 1.07 (dd, $J = 5.3, 3.6$ Hz, 1H), 1.05 (dd, $J =$

5.6, 3.5 Hz, 1H); ^{13}C NMR (150 MHz, CDCl_3) ppm 170.7, 146.3, 145.0, 140.6, 140.0, 133.6,

130.2, 128.7, 128.4, 124.3, 67.70, 67.66, 50.6, 40.8, 33.0, 32.9, 32.71, 32.66, 6.12, 6.10; HRMS

(ESI): Exact mass calcd for $\text{C}_{22}\text{H}_{26}\text{ClN}_2\text{O}_4\text{S}$ $[\text{M}+\text{H}]^+$ 449.1296, found 449.1297.

X-ray of Single Crystal of **88**

A single crystal of pure **88** was grown by the vapor-diffusion method in diethyl ether under a heptane atmosphere. The structure was determined by X-ray crystallography.

Crystal data and structure refinement for 17011

Empirical formula C₁₅ H₁₉ Cl F N₃ O₆

Formula weight 391.78

Crystal color, shape, size colourless plate, 0.310 × 0.110 × 0.050 mm³

Temperature 173(2) K

Wavelength 0.71073 Å

Crystal system, space group Monoclinic, P2₁/c

Unit cell dimensions a = 18.5869(11) Å α = 90°.

b = 10.5454(6) Å β = 90.692(3)°.

c = 19.3234(11) Å γ = 90°.

Volume 3787.2(4) Å³

Z 8

Density (calculated) 1.374 Mg/m³

Absorption coefficient 0.247 mm⁻¹

F(000) 1632

Data collection

Diffractionmeter Kappa Apex II Duo, Bruker

Theta range for data collection 1.096 to 27.153°.

Index ranges $-23 \leq h \leq 23$, $-13 \leq k \leq 13$, $-24 \leq l \leq 22$

Reflections collected 30368

Independent reflections 8322 [$R_{\text{int}} = 0.0314$]

Observed Reflections 6648

Completeness to $\theta = 25.242^\circ$ 99.6 %

Solution and Refinement

Absorption correction Semi-empirical from equivalents

Max. and min. transmission 0.7455 and 0.6380

Solution Intrinsic methods

Refinement method Full-matrix least-squares on F^2

Weighting scheme $w = [\sigma^2 F_o^2 + AP^2 + BP]^{-1}$, with

$$P = (F_o^2 + 2 F_c^2)/3, A = 0.0467, B = 3.9903$$

Data / restraints / parameters 8322 / 255 / 522

Goodness-of-fit on F^2 1.045

Final R indices [$I > 2\sigma(I)$] $R_1 = 0.0542$, $wR_2 = 0.1291$

R indices (all data) $R_1 = 0.0705$, $wR_2 = 0.1384$

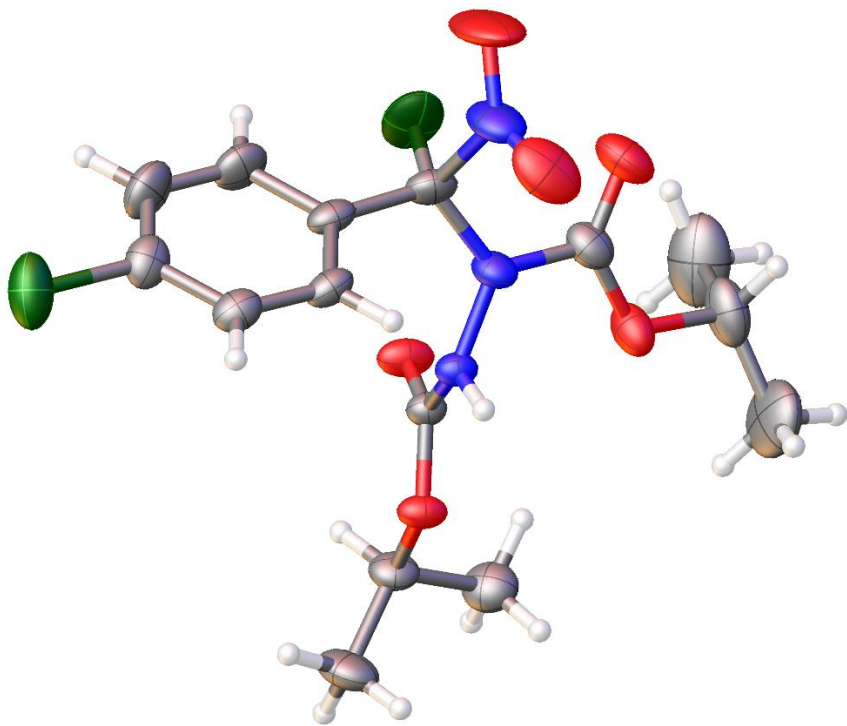
Largest diff. peak and hole 0.738 and $-0.562 \text{ e.}\text{\AA}^{-3}$

Structure solution and refinement.

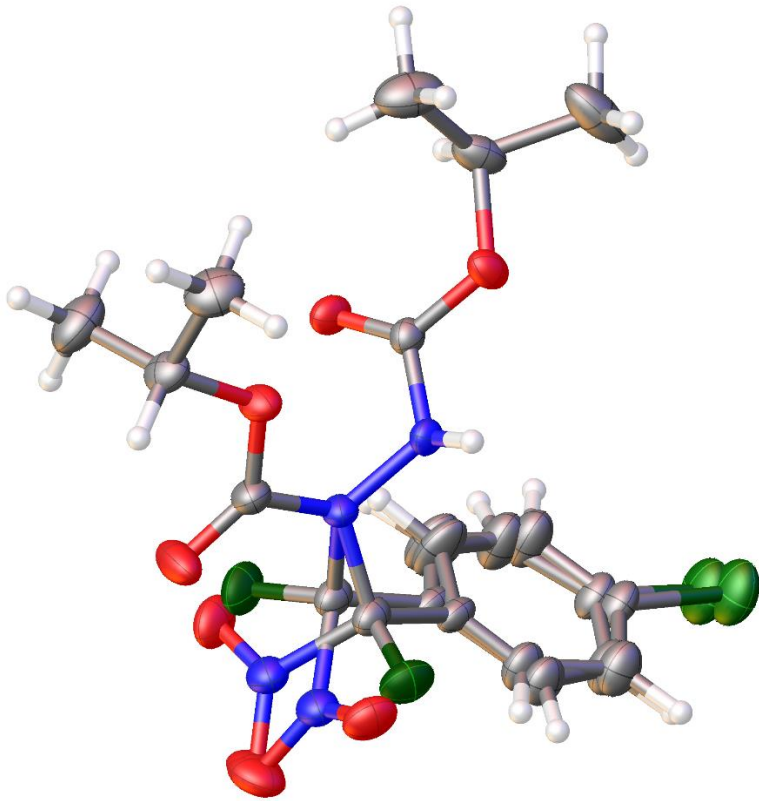
The centrosymmetric space group $P2_1/c$ was determined based on intensity statistics and systematic absences. The structure was solved and refined using the SHELX suite of programs.²⁸⁸ An intrinsic-methods solution was calculated, which provided most non-hydrogen atoms from the E-map. Full-matrix least squares / difference Fourier cycles were performed, which located the remaining non-hydrogen atoms. All non-hydrogen atoms were refined with anisotropic displacement parameters. The hydrogen atoms were placed in ideal positions and refined as riding atoms with relative isotropic displacement parameters with exception to those of N3a and N3b, which were freely refined. The structure was solved and refined using the Bruker SHELXTL Software Package, using the space group $P2_1/c$, with $Z = 8$. Disorder was refined of one of the two crystallographically independent molecules and set of restraints and constraints were applied. The final anisotropic full-matrix least-squares refinement on F^2 with 522 variables converged at $R1 = 5.42\%$, for the observed data and $wR2 = 13.84\%$ for all data. The goodness-of-fit was 1.045. The largest peak in the final difference electron density synthesis was $0.738 \text{ e}^-/\text{\AA}^3$ and the largest hole was $-0.562 \text{ e}^-/\text{\AA}^3$ with an RMS deviation of $0.052 \text{ e}^-/\text{\AA}^3$. On the basis of the final model, the calculated density was 1.374 g/cm^3 and $F(000)$, 1632 e^- . The structure is racemic.

Asymmetric unit.

²⁸⁸ Sheldrick, G. (2008). A short history of shelx. Acta Crystallographica Section A 64, 112-122.



Molecule A.



Molecule B.

X-ray of Single Crystal of 120

A single crystal of pure **120** was grown by the liquid-diffusion method in dichloromethane layered under heptane under a heptane atmosphere. The structure was determined by X-ray crystallography.

Crystal data and structure refinement for 17042

Empirical formula	C ₁₀ H ₁₀ F N ₃ O ₄	
Formula weight	255.21	
Crystal color, shape, size	colorless needle, 0.32 × 0.15 × 0.12 mm ³	
Temperature	173(2) K	
Wavelength	0.71073 Å	
Crystal system, space group	Monoclinic, P2 ₁ /c	
Unit cell dimensions	a = 15.5044(14) Å	α = 90°.
	b = 10.1356(10) Å	β = 90.114(7)°.
	c = 7.1599(7) Å	γ = 90°.
Volume	1125.15(19) Å ³	
Z	4	
Density (calculated)	1.507 Mg/m ³	
Absorption coefficient	0.129 mm ⁻¹	

F(000) 528

Data collection

Diffractionmeter APEX II Kappa Duo, Bruker

Theta range for data collection 1.313 to 30.121°.

Index ranges $-18 \leq h \leq 21$, $-14 \leq k \leq 10$, $-10 \leq l \leq 10$

Reflections collected 9731

Independent reflections 3268 [$R_{\text{int}} = 0.0404$]

Observed Reflections 2324

Completeness to $\theta = 25.242^\circ$ 99.7 %

Solution and Refinement

Absorption correction Semi-empirical from equivalents

Max. and min. transmission 0.7460 and 0.6524

Solution Intrinsic methods

Refinement method Full-matrix least-squares on F^2

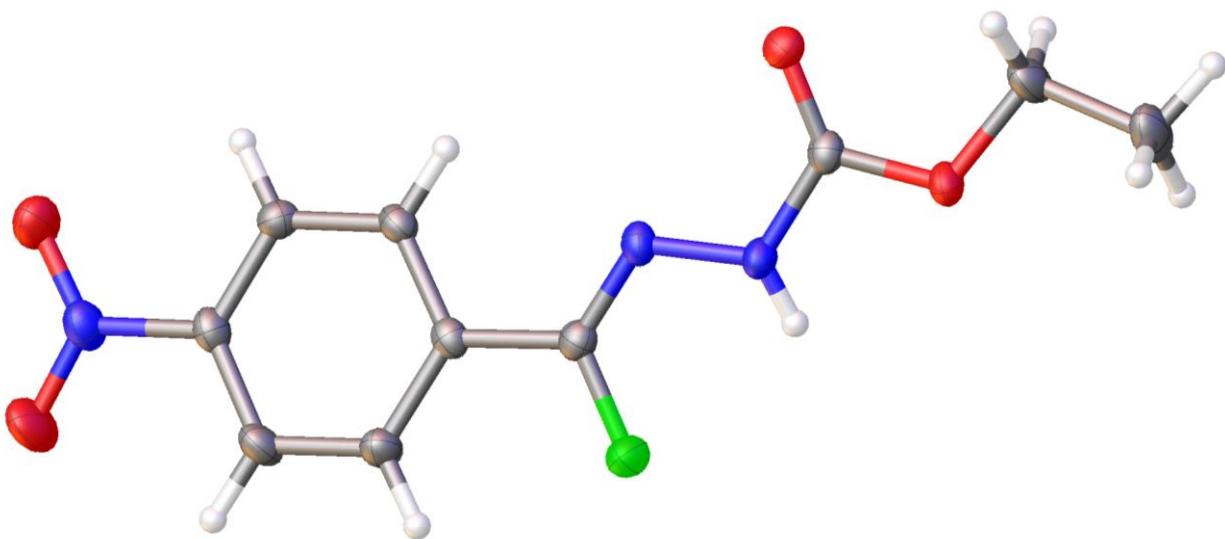
Weighting scheme $w = [\sigma^2 F_o^2 + AP^2]^{-1}$, with $P = (F_o^2 + 2 F_c^2)/3$, $A =$
0.0734

Data / restraints / parameters 3268 / 0 / 168

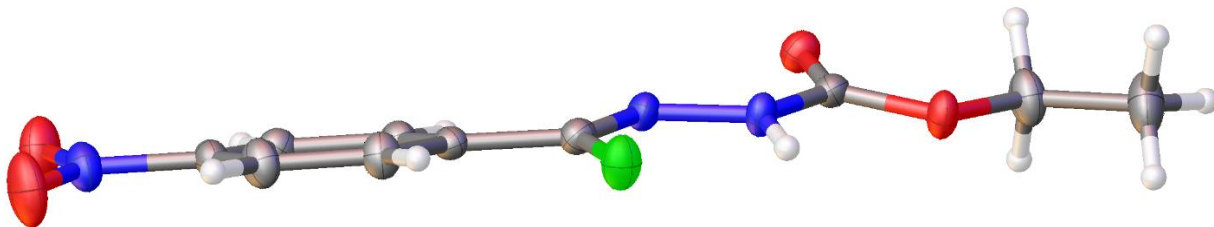
Goodness-of-fit on F^2	1.024
Final R indices [$I > 2\sigma(I)$]	R1 = 0.0461, wR2 = 0.1180
R indices (all data)	R1 = 0.0743, wR2 = 0.1307
Largest diff. peak and hole	0.297 and -0.234 e. \AA^{-3}

Structure solution and refinement

The space group $P2_1/c$ was determined based on intensity statistics and systematic absences. The structure was solved and refined using the SHELX suite of programs.²⁸⁸ An intrinsic-methods solution was calculated, which provided most non-hydrogen atoms from the E-map. Full-matrix least squares / difference Fourier cycles were performed, which located the remaining non-hydrogen atoms. All non-hydrogen atoms were refined with anisotropic displacement parameters. The hydrogen atoms were placed in ideal positions and refined as riding atoms with relative isotropic displacement parameters. The final anisotropic full-matrix least-squares refinement on F^2 with 168 variables converged at R1 = 4.61%, for the observed data and wR2 = 13.07% for all data. The goodness-of-fit was 1.024. The largest peak in the final difference electron density synthesis was 0.297 e $^{-}/\text{\AA}^3$ and the largest hole was -0.234 e $^{-}/\text{\AA}^3$ with an RMS deviation of 0.055 e $^{-}/\text{\AA}^3$. On the basis of the final model, the calculated density was 1.507 g/cm³ and F(000), 528 e $^{-}$. The remaining electron density is minuscule.



Formula unit.



Formula unit.

Computational Methods

All density functional theory (DFT) calculations were performed using Gaussian 09.²⁸⁹ Geometry optimizations and frequency calculations were performed at the uB3LYP^{290,291,292}/6-31G(d) level of theory. Normal vibrational mode analysis confirmed that optimized structures were minima (no imaginary frequency) or transition state structures (one imaginary frequency). Transition state structures were further verified by intrinsic reaction coordinate (IRC) calculations. uB3LYP/6-311++G(2d,2p) single points were computed on the uB3LYP/6-31G(d) optimized structures. For reference, single points were also calculated at the uM06-2X^{293, 294}/6-311++G(2d,2p), uPBEPBE²⁹⁵/6-311++G(2d,2p) and uMPW1PW91²⁹⁶/6-311++G(2d,2p) on uB3LYP/6-31G(d) optimized structures which provide trends qualitatively like those at the uB3LYP. Solvent effects

²⁸⁹ Frisch, M. J.; Trucks, G. W.; Schlegel, H. B.; Scuseria, G. E.; Robb, M. A.; Cheeseman, J. R.; Scalmani, G.; Barone, V.; Mennucci, B.; Petersson, G. A.; Nakatsuji, H.; Caricato, M.; Li, X.; Hratchian, H. P.; Izmaylov, A. F.; Bloino, J.; Zheng, G.; Sonnenberg, J. L.; Hada, M.; Ehara, M.; Toyota, K.; Fukuda, R.; Hasegawa, J.; Ishida, M.; Nakajima, T.; Honda, Y.; Kitao, O.; Nakai, H.; Vreven, T.; Montgomery, J. A., Jr.; Peralta, J. E.; Ogliaro, F.; Bearpark, M.; Heyd, J. J.; Brothers, E.; Kudin, K. N.; Staroverov, V. N.; Kobayashi, R.; Normand, J.; Raghavachari, K.; Rendell, A.; Burant, J. C.; Iyengar, S. S.; Tomasi, J.; Cossi, M.; Rega, N.; Millam, J. M.; Klene, M.; Knox, J. E.; Cross, J. B.; Bakken, V.; Adamo, C.; Jaramillo, J.; Gomperts, R.; Stratmann, R. E.; Yazyev, O.; Austin, A. J.; Cammi, R.; Pomelli, C.; Ochterski, J. W.; Martin, R. L.; Morokuma, K.; Zakrzewski, V. G.; Voth, G. A.; Salvador, P.; Dannenberg, J. J.; Dapprich, S.; Daniels, A. D.; Farkas, O.; Foresman, J. B.; Ortiz, J. V.; Cioslowski, J.; Fox, D. J. *Gaussian 09*, revision D.01; Gaussian, Inc.: Wallingford, CT, **2013**.

²⁹⁰ Lee, C.; Yang, W.; Parr, R. G. *Physical Review B* **1988**, *37*, 785.

²⁹¹ Becke, A. D. *J. Chem. Phys.* **1993**, *98*, 5648.

²⁹² Stephens, P. J.; Devlin, F. J.; Chabalowski, C. F.; Frisch, M. J. *J. Phys. Chem.* **1994**, *98*, 11623.

²⁹³ Zhao, Y.; Truhlar, D. G. *Theor. Chem. Acc.* **2008**, *120*, 215.

²⁹⁴ Zhao, Y.; Truhlar, D. G. *Acc. Chem. Res.* **2008**, *41*, 157.

²⁹⁵ Perdew, J. P.; Burke, K.; Ernzerhof, M. *Phys. Rev. Lett.* **1996**, *77*, 3865.

²⁹⁶ Adamo, C.; Barone, V. *J. Chem. Phys.* **1998**, *108*, 664.

were evaluated with the integral equation formalism polarizable continuum model (IEFPCM).²⁹⁷ All 3D rendering of optimized structures was generated by CYLview.²⁹⁸ GaussView²⁹⁹ was used to construct all initial structures used in our computations.

Single Point Energies, Enthalpy, and Entropy Data

Table 12. Single point energies, enthalpies and entropies for structures

Structure	Single Point Energy, E, (a.u.)	H (a.u.)	S (cal/mol*K)
110	-1142.11019784	-1141.471218	152.049
111	-1142.11586624	-1141.480442	154.231
118	-229.79519261	-229.692813	59.238
112	-912.32886824	-911.784158	140.289
113	-1142.06915855	-1141.413198	158.107
115	-936.89102049	-936.337593	142.706
119	-1142.08328008	-1141.440339	165.568
nitrogen dioxide	-205.14571863	-205.059498	58.765

²⁹⁷ Cancès, E.; Mennucci, B.; Tomasi, J. *J. Chem. Phys.* **1997**, *107*, 3032.

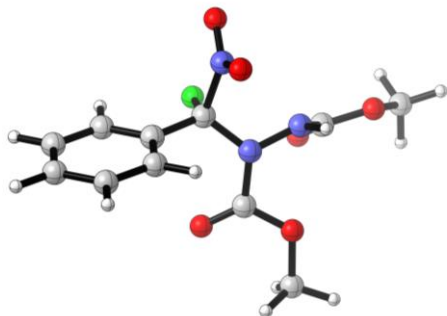
²⁹⁸ Legault, C. Y. CYLview, version 1.0b; Université de Sherbrooke: Quebec, Canada, **2009**; <http://www.cylview.org>.

²⁹⁹ Dennington, R.; Keith, T.; Millam, J. GaussView, version 5; Semichem Inc.: Shawnee Mission, KS, **2009**.

116	-1218.55451159	-1217.839720	174.238
117	-1218.59240042	-1217.885267	172.037
Nitrous Acid	-205.78274331	-205.675951	59.179
Hydrogen Fluoride	-100.49025303	-100.413313	41.547
H ₂ O	-76.46880216	-76.391288	45.147
TS1	-1142.05753903	-1141.407641	160.768
TS2	-1142.09155778	-1141.448207	155.674
TS3	-1142.05064132	-1141.401611	152.069
TS4	-1142.07957495	-1141.435904	160.031
TS5	-1142.07473929	-1141.428484	158.986
TS6	-1142.07737344	-1141.078770	157.598
TS7	-1218.55043252	-1217.840255	167.702
TS8	-1218.57677478	-1217.869045	166.233

Cartesian Coordinates

110



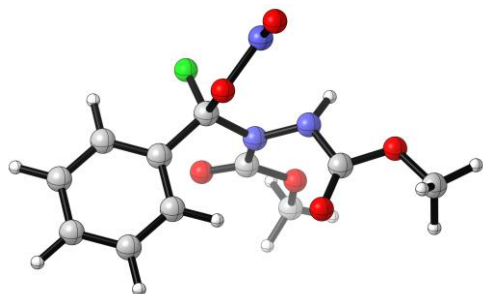
- Thermochemistry -

Zero-point correction=	0.242852 (Hartree/Particle)
Thermal correction to Energy=	0.263182
Thermal correction to Enthalpy=	0.264126
Thermal correction to Gibbs Free Energy=	0.191883
Sum of electronic and zero-point Energies=	-1141.492492
Sum of electronic and thermal Energies=	-1141.472162
Sum of electronic and thermal Enthalpies=	-1141.471218
Sum of electronic and thermal Free Energies=	-1141.543461

C	-4.18469100	-0.03332600	1.16503000
C	-4.68061100	0.54560100	-0.00426500
C	-2.84426100	-0.41217400	1.24703700
C	-1.99606800	-0.20189600	0.15484600
C	-2.49269300	0.37059000	-1.02341800
C	-3.83238300	0.74571000	-1.09734100
H	-4.21372000	1.19471800	-2.00961300
H	-4.83909000	-0.19249700	2.01687400
H	-5.72452600	0.83931500	-0.06572100
H	-1.83726400	0.51998500	-1.87431900
H	-2.45902100	-0.86086600	2.15508600
C	-0.56372000	-0.67158000	0.23159500
N	0.42752600	0.19700100	-0.33194700
N	1.61784400	-0.41380900	-0.70655100
C	0.43728600	1.56747400	0.01659700
O	-0.38984600	2.09071200	0.72990400
O	1.45939400	2.17972800	-0.58464900
C	1.59997700	3.58613700	-0.28200500

H	0.71040300	4.13073800	-0.60385100
H	2.47471100	3.91026600	-0.84334200
C	2.69991200	-0.34843000	0.16901500
H	1.81759900	-0.38219600	-1.70014000
O	2.62637900	-0.01151900	1.33255300
O	3.80321000	-0.74571400	-0.47816700
C	5.00833100	-0.78343600	0.31528400
H	4.89372300	-1.48462600	1.14465400
H	5.23926700	0.21186700	0.70081700
F	-0.23391100	-1.06048700	1.49590700
N	-0.46911900	-2.01355200	-0.61645300
O	-0.58724600	-1.90176500	-1.82829600
O	-0.34201700	-3.05182000	0.00652700
H	5.78836200	-1.12061800	-0.36578800
H	1.75553400	3.72581300	0.78960600

111



- Thermochemistry -

Zero-point correction= 0.240564 (Hartree/Particle)

Thermal correction to Energy= 0.261432

Thermal correction to Enthalpy= 0.262376

Thermal correction to Gibbs Free Energy= 0.189096

Sum of electronic and zero-point Energies= -1141.502255

Sum of electronic and thermal Energies= -1141.481386

Sum of electronic and thermal Enthalpies= -1141.480442

Sum of electronic and thermal Free Energies= -1141.553722

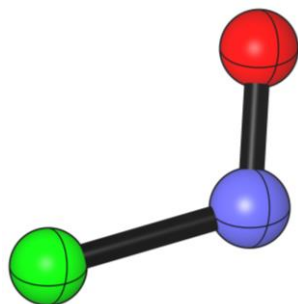
C 4.31508700 -0.11776600 0.39314800

C 4.13527000 0.15864300 1.75038400

C	3.21069300	-0.34407100	-0.42961600
C	1.92178800	-0.28532500	0.10699600
C	1.73661800	-0.01696500	1.46786500
C	2.84504400	0.20724200	2.28508600
H	2.70008800	0.42076700	3.34042400
H	5.31558100	-0.15639400	-0.02836800
H	4.99648100	0.33539600	2.38873700
H	0.73105100	0.02149300	1.87630700
H	3.34795900	-0.55584300	-1.48388200
C	0.71919600	-0.61671600	-0.75993500
N	-0.40964200	0.30981300	-0.58031000
N	-1.68517900	-0.19731700	-0.47106000
C	-0.21580800	1.67366000	-0.80416000
O	0.86359000	2.16738400	-1.06200400
O	-1.37239300	2.34332500	-0.68999500
C	-1.27691200	3.76903000	-0.89518900
H	-0.62113800	4.21630700	-0.14531000
H	-2.29470300	4.14047200	-0.78500700
C	-2.30304200	-0.17401600	0.77189700

H	-2.27921200	-0.11839000	-1.28959100
O	-1.73773000	0.01063700	1.83137600
O	-3.60933300	-0.43375700	0.60933000
C	-4.38211800	-0.51928500	1.82403500
H	-4.00684100	-1.32654400	2.45696100
H	-5.40079500	-0.72962700	1.50097100
F	1.07875300	-0.59621400	-2.10249300
N	-0.66135900	-2.49283200	-1.41892100
O	0.33517800	-1.91224700	-0.42262900
O	-0.96722600	-3.55480000	-1.06014300
H	-4.34049600	0.42668700	2.36819800
H	-0.89507300	3.98303200	-1.89550900

118



- Thermochemistry -

Zero-point correction= 0.007407 (Hartree/Particle)

Thermal correction to Energy= 0.010525

Thermal correction to Enthalpy= 0.011469

Thermal correction to Gibbs Free Energy= -0.016677

Sum of electronic and zero-point Energies= -229.696875

Sum of electronic and thermal Energies= -229.693757

Sum of electronic and thermal Enthalpies= -229.692813

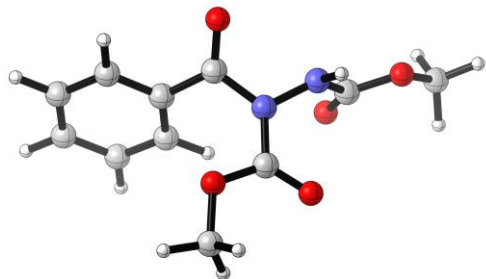
Sum of electronic and thermal Free Energies= -229.720959

F -0.96047800 -0.60267700 0.00000000

N 0.00000000 0.56263400 0.00000000

O 1.08053800 0.18570600 0.00000000

112



 - Thermochemistry -

Zero-point correction= 0.230211 (Hartree/Particle)

Thermal correction to Energy= 0.247904

Thermal correction to Enthalpy= 0.248848

Thermal correction to Gibbs Free Energy= 0.182192

Sum of electronic and zero-point Energies= -911.802795

Sum of electronic and thermal Energies= -911.785102

Sum of electronic and thermal Enthalpies= -911.784158

Sum of electronic and thermal Free Energies= -911.850814

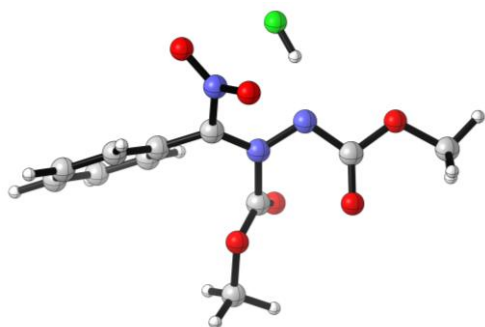
C 2.85435900 -0.77254800 -1.78543500

C 4.05452200 -1.03832200 -1.11987900

C	1.68094400	-0.57685300	-1.05927400
C	1.70486400	-0.66191600	0.34130000
C	2.90492400	-0.95643200	1.00462900
C	4.07895300	-1.12973900	0.27542100
H	5.01071000	-1.34086200	0.79187100
H	2.83231400	-0.72049000	-2.86998500
H	4.96922100	-1.18122200	-1.68829600
H	2.90690000	-1.03823900	2.08694900
H	0.74146000	-0.39554000	-1.57195200
C	0.45742700	-0.57007700	1.14348600
N	-0.58375500	0.28988800	0.65483700
N	-1.87765600	-0.12551000	0.90287800
C	-0.45065400	1.60640700	0.17101300
O	-1.39747000	2.25113100	-0.22964900
O	0.80813600	2.03727200	0.26419600
C	1.04917400	3.36931200	-0.24244600
H	0.45963200	4.09648500	0.31908200
H	0.79445200	3.42261000	-1.30276300
C	-2.60394400	-0.60083300	-0.17738900

O	-2.12676100	-0.95125300	-1.23906800
O	-3.90220900	-0.66108500	0.16290400
C	-4.77939300	-1.21577900	-0.83721800
H	-4.48691300	-2.24114800	-1.07441100
H	-4.75638900	-0.60696600	-1.74382800
H	-5.77261600	-1.19626700	-0.39029900
H	2.11424700	3.53984800	-0.09387600
H	-2.38176800	0.37572300	1.62592700
O	0.25475100	-1.24905200	2.13190800

113



- Thermochemistry -

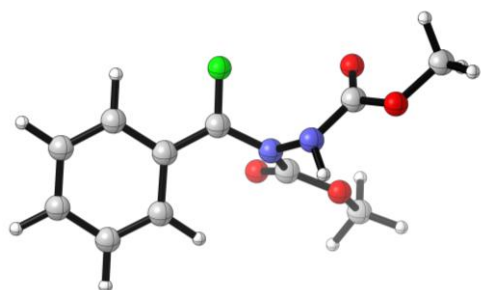
Zero-point correction=	0.238487 (Hartree/Particle)
Thermal correction to Energy=	0.259887
Thermal correction to Enthalpy=	0.260831
Thermal correction to Gibbs Free Energy=	0.185709
Sum of electronic and zero-point Energies=	-1141.435542
Sum of electronic and thermal Energies=	-1141.414142
Sum of electronic and thermal Enthalpies=	-1141.413198
Sum of electronic and thermal Free Energies=	-1141.488320

C	-4.24048400	-0.27159400	-0.73887200
C	-4.59278700	0.49964000	0.37472400
C	-2.92487600	-0.67891700	-0.91942900
C	-1.93809200	-0.29917100	0.01398900
C	-2.30103300	0.46591100	1.14111600
C	-3.62412100	0.86232000	1.31339600
H	-3.89953100	1.44127200	2.18903500
H	-4.99407500	-0.55497000	-1.46655300
H	-5.62428500	0.80855100	0.51399800
H	-1.56038200	0.71806200	1.89238800

H	-2.65717000	-1.27040700	-1.78883600
C	-0.55765600	-0.71460500	-0.17441000
N	0.50806000	0.01636200	0.06060100
N	1.70763200	-0.54324000	0.32080400
C	0.36698100	1.52218500	0.23951400
O	0.70508900	2.04540800	1.26142700
O	-0.19010300	2.01751300	-0.83642200
C	-0.42218800	3.45503900	-0.81636700
H	-1.09306700	3.70464400	0.00694700
H	-0.88011600	3.67675700	-1.77749700
C	2.77196000	0.23125600	-0.08629000
H	1.58274700	-1.91501600	1.18036600
O	2.70910800	1.28367700	-0.71443600
O	3.91211800	-0.35551900	0.31152100
C	5.12247600	0.33521800	-0.05203200
H	5.19600900	0.43215000	-1.13790000
H	5.93264100	-0.28412500	0.33116400
F	1.17179500	-2.68143000	1.61632700
N	-0.32954700	-2.10550500	-0.67127300

O	0.50670000	-2.26576900	-1.55105900
O	-1.06728700	-2.96765400	-0.21273700
H	0.53237200	3.97112100	-0.70586500
H	5.14960900	1.32658000	0.40650600

115



 - Thermochemistry -

Zero-point correction= 0.227779 (Hartree/Particle)

Thermal correction to Energy= 0.245762

Thermal correction to Enthalpy= 0.246706

Thermal correction to Gibbs Free Energy= 0.178902

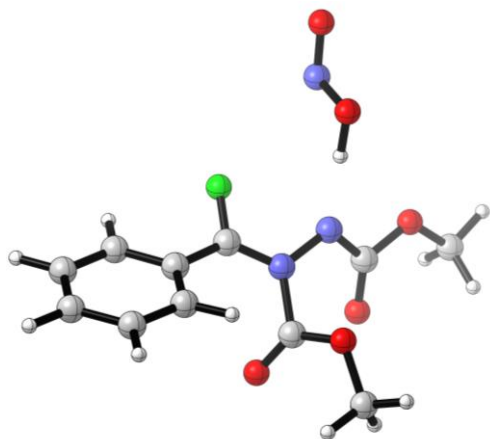
Sum of electronic and zero-point Energies= -936.356520

Sum of electronic and thermal Energies= -936.338537
Sum of electronic and thermal Enthalpies= -936.337593
Sum of electronic and thermal Free Energies= -936.405397

C	4.43502000	-1.10250200	-0.36320200
C	4.84954600	-0.12538300	0.55164800
C	3.09126400	-1.27156700	-0.65863500
C	2.10805700	-0.45361700	-0.03455700
C	2.54346900	0.53572700	0.89010600
C	3.89175700	0.68811100	1.17245000
H	4.20529100	1.44852000	1.88287100
H	5.17176100	-1.73615700	-0.84995400
H	5.90438100	0.00172100	0.77704900
H	1.81004100	1.16935900	1.37771700
H	2.77463700	-2.02663300	-1.36938100
C	0.74346700	-0.63005700	-0.33508000
N	-0.32124100	0.13075800	0.15021600
N	-1.32041100	-0.56609300	0.82546300
C	-0.56461100	1.42113400	-0.35392400

O	0.15833600	1.97914400	-1.14537600
O	-1.66085300	1.95078100	0.22227800
C	-2.00701300	3.26183200	-0.25719600
H	-1.18902400	3.96348100	-0.07716000
H	-2.89435900	3.54923600	0.30719200
C	-2.49828900	-0.85641600	0.14670700
H	-1.39915800	-0.36188600	1.81477200
O	-2.65901100	-0.77651300	-1.04869500
O	-3.41765600	-1.27217300	1.04642800
C	-4.67444900	-1.67034100	0.47637600
H	-4.53623700	-2.51249700	-0.20657100
H	-5.13035300	-0.83917300	-0.06761700
F	0.38009600	-1.63403200	-1.15774400
H	-5.29641800	-1.96235400	1.32296200
H	-2.22569100	3.22856600	-1.32718100

119



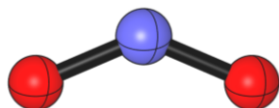
- Thermochemistry -

Zero-point correction=	0.238389 (Hartree/Particle)
Thermal correction to Energy=	0.260364
Thermal correction to Enthalpy=	0.261309
Thermal correction to Gibbs Free Energy=	0.182642
Sum of electronic and zero-point Energies=	-1141.463259
Sum of electronic and thermal Energies=	-1141.441283
Sum of electronic and thermal Enthalpies=	-1141.440339
Sum of electronic and thermal Free Energies=	-1141.519006

C	-4.41242400	1.32779700	-0.93182600
C	-5.01217500	0.53806100	0.05394400
C	-3.02864300	1.34466900	-1.06488900
C	-2.23594300	0.54641600	-0.21662600
C	-2.84202300	-0.23276900	0.78772200
C	-4.22606700	-0.23377900	0.91576200
H	-4.69167800	-0.82571200	1.69705000
H	-5.02338100	1.93238000	-1.59431800
H	-6.09283100	0.53282300	0.15919900
H	-2.23568500	-0.79827900	1.48692600
H	-2.55867400	1.95729500	-1.82632100
C	-0.79601400	0.60808800	-0.37061300
N	0.09928500	-0.31664300	-0.11742900
N	1.42044400	0.04442500	0.04575200
C	-0.31527200	-1.74650600	0.00416500
O	-1.05805700	-2.26326300	-0.78335700
O	0.20768100	-2.23452700	1.10911500
C	0.01917400	-3.66095700	1.30699800
H	0.49430800	-3.87766400	2.26133000

H	0.50758000	-4.20205700	0.49478300
C	2.26890500	-0.86252200	-0.51625900
O	1.96640600	-1.89092800	-1.12557200
O	3.54504700	-0.47159100	-0.29426800
C	4.55683100	-1.34220000	-0.82453000
H	4.46123300	-1.43269000	-1.90972200
H	4.49088000	-2.33497200	-0.37166300
F	-0.30467600	1.77164700	-0.75830700
N	2.33195700	3.23946900	0.33822200
O	2.67232600	4.30003400	0.78244200
O	2.19206700	2.30052000	1.32437900
H	5.50628200	-0.87238000	-0.56722300
H	-1.04607100	-3.89434900	1.33718400
H	1.90646200	1.46027800	0.82671500

Nitrogen dioxide



- Thermochemistry -

Zero-point correction= 0.008827 (Hartree/Particle)

Thermal correction to Energy= 0.011764

Thermal correction to Enthalpy= 0.012708

Thermal correction to Gibbs Free Energy= -0.015213

Sum of electronic and zero-point Energies= -205.063379

Sum of electronic and thermal Energies= -205.060442

Sum of electronic and thermal Enthalpies= -205.059498

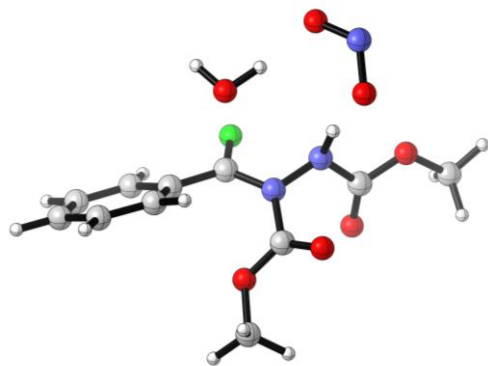
Sum of electronic and thermal Free Energies= -205.087419

N 0.00000000 0.32833100 0.00000000

O 1.10663400 -0.14384400 0.00000000

O -1.10663400 -0.14344500 0.00000000

116



 - Thermochemistry -

Zero-point correction= 0.263667 (Hartree/Particle)

Thermal correction to Energy= 0.288088

Thermal correction to Enthalpy= 0.289033

Thermal correction to Gibbs Free Energy= 0.206246

Sum of electronic and zero-point Energies= -1217.865086

Sum of electronic and thermal Energies= -1217.840664

Sum of electronic and thermal Enthalpies= -1217.839720

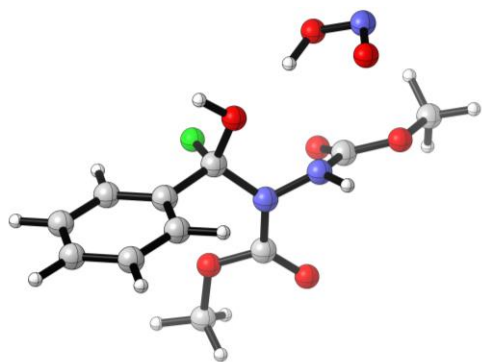
Sum of electronic and thermal Free Energies= -1217.922506

C 4.39174600 0.43111000 1.44901700

C	4.91589900	0.49780200	0.15521500
C	3.01588700	0.36375500	1.63813100
C	2.16194600	0.33431600	0.51747300
C	2.69219900	0.41504300	-0.78601000
C	4.06594000	0.49940800	-0.95860000
H	4.47875000	0.57833900	-1.95881600
H	5.05329000	0.43672600	2.30887000
H	5.99028600	0.56023900	0.01151200
H	2.02984100	0.46569000	-1.64223100
H	2.60166500	0.31309800	2.63861900
C	0.73883500	0.27639000	0.75319200
N	-0.19202800	-0.36280000	0.04531700
N	-1.51205300	-0.00944800	0.27602700
C	0.02540500	-1.40150200	-0.96617300
O	-0.78609600	-1.57738800	-1.83421500
O	1.12926700	-2.07159100	-0.71646500
C	1.46012700	-3.12137000	-1.66829800
H	0.66356800	-3.86628700	-1.67721400
H	2.39096600	-3.54666200	-1.30002800

C	-2.30865600	-1.03292400	0.76919800
O	-1.88446100	-2.10087900	1.17172400
O	-3.58761000	-0.64211800	0.75421200
C	-4.53371700	-1.59867600	1.27628500
H	-4.50609600	-2.51917700	0.68929700
H	-5.50587700	-1.11626200	1.18544200
F	0.31860300	0.76774200	1.89002200
H	-4.31182300	-1.81987100	2.32251800
H	1.59140000	-2.68907500	-2.66128300
H	-1.90971400	0.70529300	-0.39530000
O	-2.21212300	3.40958700	-0.42837700
O	-2.75904500	1.63949700	-1.50850300
N	-3.00432700	2.85111700	-1.23501500
H	-0.64618600	2.70532400	-0.33174900
O	0.30674300	2.40313100	-0.32510100
H	0.76427700	3.06885400	0.21308100

117



- Thermochemistry -

Zero-point correction= 0.266582 (Hartree/Particle)

Thermal correction to Energy= 0.290188

Thermal correction to Enthalpy= 0.291133

Thermal correction to Gibbs Free Energy= 0.209392

Sum of electronic and zero-point Energies= -1217.909817

Sum of electronic and thermal Energies= -1217.886211

Sum of electronic and thermal Enthalpies= -1217.885267

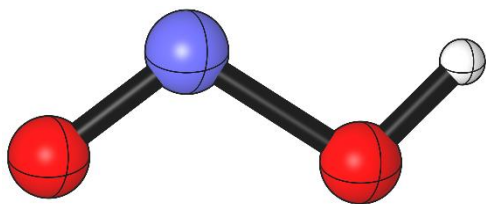
Sum of electronic and thermal Free Energies= -1217.967007

C -4.41919900 -0.95955900 0.85052700

C	-4.80442300	-1.21247600	-0.46739600
C	-3.08047200	-0.70699000	1.15580600
C	-2.12352400	-0.70657700	0.13756200
C	-2.50662000	-0.96908200	-1.18350500
C	-3.84538800	-1.21676600	-1.48431100
H	-4.13874100	-1.41452000	-2.51124900
H	-5.16023000	-0.95570200	1.64471500
H	-5.84719900	-1.40614500	-0.70245400
H	-1.75978900	-0.97610000	-1.97207700
H	-2.78070700	-0.50411600	2.17725900
C	-0.64640900	-0.53015300	0.45302800
N	0.02020300	0.48241300	-0.36007300
N	1.34301000	0.26039000	-0.68968400
C	-0.40680900	1.81746300	-0.45054300
O	0.20873900	2.65972000	-1.07178700
O	-1.55227900	2.01597500	0.20470800
C	-2.11406600	3.34115700	0.08892100
H	-1.42665600	4.07913200	0.50698100
H	-3.03852100	3.30774900	0.66351800

C	2.33393600	0.89530200	0.04475900
O	2.16896800	1.42597600	1.12417100
O	3.50025400	0.78168400	-0.61339800
C	4.65028500	1.31545400	0.07248300
H	4.51370800	2.38004600	0.27385200
H	5.48762700	1.15936200	-0.60653000
F	-0.49598300	-0.20583600	1.79956700
H	4.81399100	0.77968700	1.01032600
H	-2.31922500	3.57565900	-0.95757400
H	1.52496200	0.07838600	-1.66945200
O	2.73754700	-2.13797600	0.94170000
O	2.98268100	-2.69804600	-1.12682000
N	3.54470900	-2.57332700	-0.07651100
H	1.81859100	-1.99315800	0.57269500
O	0.04297600	-1.72210200	0.21816700
H	-0.51438300	-2.45257300	0.53985800

Nitrous Acid



 - Thermochemistry -

Zero-point correction= 0.020302 (Hartree/Particle)

Thermal correction to Energy= 0.023494

Thermal correction to Enthalpy= 0.024439

Thermal correction to Gibbs Free Energy= -0.003679

Sum of electronic and zero-point Energies= -205.680088

Sum of electronic and thermal Energies= -205.676896

Sum of electronic and thermal Enthalpies= -205.675951

Sum of electronic and thermal Free Energies= -205.704069

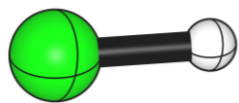
H 1.72652600 0.42476500 0.00001100

N -0.15990600 0.49170400 0.00000300

O 1.02969900 -0.26097000 0.00000300

O -1.10559700 -0.22236700 -0.00000600

Hydrogen Fluoride



- Thermochemistry -

Zero-point correction= 0.008981 (Hartree/Particle)

Thermal correction to Energy= 0.011342

Thermal correction to Enthalpy= 0.012286

Thermal correction to Gibbs Free Energy= -0.007454

Sum of electronic and zero-point Energies= -100.416618

Sum of electronic and thermal Energies= -100.414257

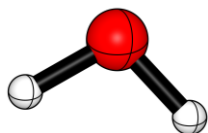
Sum of electronic and thermal Enthalpies= -100.413313

Sum of electronic and thermal Free Energies= -100.433054

F 0.00000000 0.00000000 0.09365900

H 0.00000000 0.00000000 -0.84292700

H₂O



- Thermochemistry -

Zero-point correction= 0.021130 (Hartree/Particle)

Thermal correction to Energy= 0.023964

Thermal correction to Enthalpy= 0.024909

Thermal correction to Gibbs Free Energy= 0.003457

Sum of electronic and zero-point Energies= -76.395066

Sum of electronic and thermal Energies= -76.392232

Sum of electronic and thermal Enthalpies= -76.391288

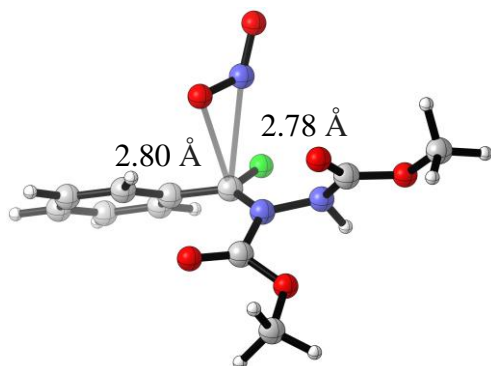
Sum of electronic and thermal Free Energies= -76.412739

O 0.00000000 0.00000000 0.12076500

H 0.00000000 0.75866600 -0.48306000

H 0.00000000 -0.75866600 -0.48306000

TS1



- Thermochemistry -

Zero-point correction= 0.238873 (Hartree/Particle)

Thermal correction to Energy= 0.260393

Thermal correction to Enthalpy= 0.261337

Thermal correction to Gibbs Free Energy= 0.184951

Sum of electronic and zero-point Energies= -1141.430105

Sum of electronic and thermal Energies= -1141.408585

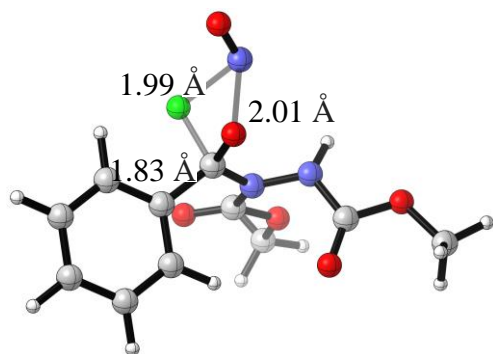
Sum of electronic and thermal Enthalpies= -1141.407641

Sum of electronic and thermal Free Energies= -1141.484027

C	-4.40367200	-0.00680000	1.20221200
C	-4.84291800	0.28035500	-0.09363900
C	-3.05102700	-0.20331200	1.44665700
C	-2.11805700	-0.06924600	0.39008100
C	-2.56896200	0.19922400	-0.91864400
C	-3.92750600	0.36999700	-1.14816400
H	-4.27804800	0.55929200	-2.15755500
H	-5.11393600	-0.08409700	2.01873300
H	-5.90261300	0.42010700	-0.28551300
H	-1.85953200	0.20644600	-1.72998400
H	-2.70912300	-0.42512000	2.45095400
C	-0.73436500	-0.28643600	0.75558600
N	0.37585300	0.41893600	0.49162000
N	1.54780500	-0.02154400	1.08909200
C	0.39617000	1.67039000	-0.26529700
O	-0.45490500	1.98292200	-1.05256700
O	1.46036600	2.35503300	0.10124800
C	1.65844600	3.61922600	-0.58924600
H	1.77128700	3.43592300	-1.65866800

H	2.57194400	4.02742800	-0.16284700
C	2.63735300	-0.24271900	0.24097400
H	1.72723400	0.35896100	2.01314500
O	2.57534200	-0.24538600	-0.96808600
O	3.71557400	-0.46267500	0.99649600
C	4.93780300	-0.72978100	0.27188200
H	4.82421300	-1.62810000	-0.33792400
H	5.69546100	-0.87938800	1.03924000
F	-0.56089800	-1.14491900	1.72552900
N	0.14116600	-2.46668200	-0.73833200
O	-0.34751400	-1.69886500	-1.62955300
O	0.54684800	-3.58171400	-1.14852000
H	0.80845800	4.27616800	-0.40083900
H	5.19368300	0.12177600	-0.36171500

TS2



- Thermochemistry -

Zero-point correction= 0.238770 (Hartree/Particle)

Thermal correction to Energy= 0.259766

Thermal correction to Enthalpy= 0.260710

Thermal correction to Gibbs Free Energy= 0.186744

Sum of electronic and zero-point Energies= -1141.470147

Sum of electronic and thermal Energies= -1141.449152

Sum of electronic and thermal Enthalpies= -1141.448207

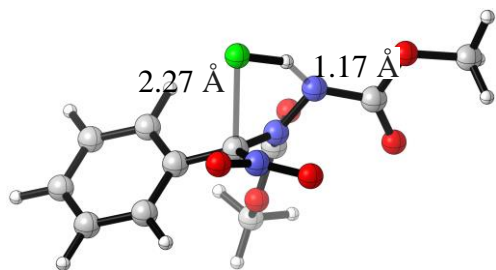
Sum of electronic and thermal Free Energies= -1141.522173

C 4.21715600 -0.48977900 -0.58984200

C	4.00702500	-1.74293800	-1.17419000
C	3.13157600	0.30184800	-0.21980600
C	1.82762100	-0.17004800	-0.41266100
C	1.61397300	-1.42111800	-1.00647800
C	2.70532800	-2.20355800	-1.38612100
H	2.53782000	-3.17235100	-1.84836100
H	5.22835400	-0.12883300	-0.42385700
H	4.85535300	-2.35575800	-1.46625000
H	0.59946600	-1.76553800	-1.18397900
H	3.27647900	1.27044900	0.24349000
C	0.65590900	0.72866000	-0.15508600
N	-0.52019200	0.11953100	0.39413000
N	-1.73836300	0.58563000	-0.05117600
C	-0.46866900	-0.74519000	1.49918200
O	0.55783500	-1.12431600	2.01986100
O	-1.70769100	-1.08485800	1.88400100
C	-1.77208400	-1.98498600	3.01068600
H	-1.27370400	-2.92668100	2.77133900
H	-2.83488900	-2.14638600	3.18496800

C	-2.43214600	-0.17987600	-0.96765100
H	-2.26277300	1.18752900	0.57257800
O	-1.96956100	-1.11732100	-1.58995300
O	-3.68042800	0.30475000	-1.08604700
C	-4.51243700	-0.35773900	-2.05848900
H	-4.07585200	-0.27109500	-3.05610400
H	-5.47051200	0.15895900	-2.01576200
F	1.19260800	1.66266800	1.33041200
N	0.11735800	3.09151000	0.46772900
O	0.48441700	1.70517300	-0.94765000
O	0.78715100	3.95906900	0.25116100
H	-4.63518700	-1.41205500	-1.80055200
H	-1.30293300	-1.53057300	3.88574800

TS3



- Thermochemistry -

Zero-point correction= 0.236367 (Hartree/Particle)

Thermal correction to Energy= 0.256864

Thermal correction to Enthalpy= 0.257808

Thermal correction to Gibbs Free Energy= 0.185555

Sum of electronic and zero-point Energies= -1141.423053

Sum of electronic and thermal Energies= -1141.402555

Sum of electronic and thermal Enthalpies= -1141.401611

Sum of electronic and thermal Free Energies= -1141.473864

C -4.16516900 -0.60956000 -0.62408000

C -4.54525900 0.13414200 0.49971200

C -2.82803000 -0.90936700 -0.84559500

C -1.85032800 -0.43407700 0.05648200

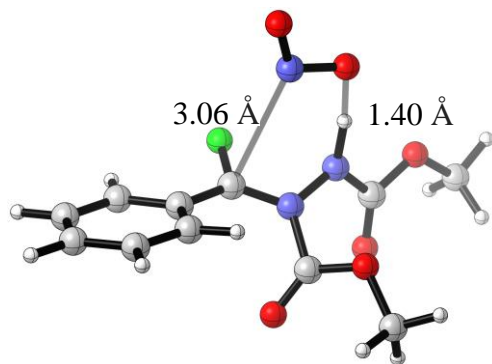
C -2.24203400 0.31136900 1.19276800

C -3.58453200 0.58750700 1.41045500

H	-3.88512800	1.14245900	2.29295100
H	-4.91608100	-0.95648300	-1.32614700
H	-5.59495900	0.35314400	0.67005100
H	-1.49377100	0.61648800	1.91677200
H	-2.53797300	-1.47793500	-1.72050100
C	-0.44394500	-0.68167300	-0.11755600
N	0.49825900	0.23240200	0.08554600
N	1.65966800	-0.21496600	0.67305700
C	0.28169400	1.68642000	0.05827200
O	0.82648400	2.41572200	0.84041800
O	-0.50957500	1.98667700	-0.95158200
C	-0.84952000	3.39307700	-1.08723700
H	-1.38040900	3.73030700	-0.19542100
H	-1.49028600	3.44208400	-1.96485800
C	2.83797700	0.14166000	0.05704600
H	1.28740100	-1.13540100	1.29603800
O	2.93726000	0.89083100	-0.90134400
O	3.86059000	-0.44175800	0.70471500
C	5.17097100	-0.12257500	0.19823100

H	5.26686200	-0.44176800	-0.84220400
H	5.86539100	-0.67377600	0.83128100
F	0.32637000	-1.86325500	1.65470300
N	-0.01629400	-1.96973000	-0.78644400
O	1.01333500	-1.93865800	-1.44739700
O	-0.77301600	-2.92190700	-0.68038300
H	0.06095400	3.97598800	-1.23276700
H	5.35766000	0.95143900	0.27096900

TS4



- Thermochemistry -

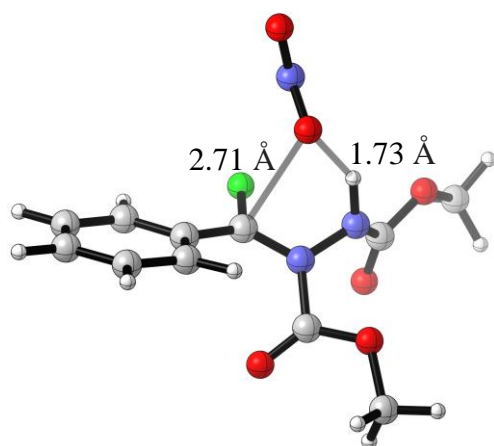
Zero-point correction=	0.235652 (Hartree/Particle)
Thermal correction to Energy=	0.257007
Thermal correction to Enthalpy=	0.257951
Thermal correction to Gibbs Free Energy=	0.181915
Sum of electronic and zero-point Energies=	-1141.458203
Sum of electronic and thermal Energies=	-1141.436848
Sum of electronic and thermal Enthalpies=	-1141.435904
Sum of electronic and thermal Free Energies=	-1141.511940

C	-4.35618200	-0.03386100	-1.38833000
C	-4.79612500	-0.56005100	-0.16928400
C	-3.01117400	0.25849400	-1.57271700
C	-2.09267900	-0.00559300	-0.53382500
C	-2.54236200	-0.52354900	0.69917100
C	-3.89191300	-0.79427000	0.87389800
H	-4.24443100	-1.17676700	1.82588700
H	-5.06264500	0.15204700	-2.19031700
H	-5.85002400	-0.77787100	-0.02585900
H	-1.85227800	-0.66610400	1.52301900

H	-2.66202400	0.66821200	-2.51373800
C	-0.71104300	0.33287600	-0.75065400
N	0.36404300	-0.21014700	-0.20370000
N	1.53106900	0.52984200	-0.19540900
C	0.35957100	-1.57804700	0.35695300
O	-0.30915800	-2.45508300	-0.11783800
O	1.16829600	-1.60921400	1.39106600
C	1.37738400	-2.92109700	1.98233300
H	0.42368000	-3.32794100	2.32075900
H	2.04882700	-2.74558900	2.81974100
C	2.63395200	-0.11076000	-0.70364600
H	1.48840800	1.47677500	0.43993200
O	2.62765400	-1.22969500	-1.19671600
O	3.70905400	0.67976500	-0.56574600
C	4.94884600	0.12710100	-1.05176600
H	4.87886300	-0.08581300	-2.12085400
H	5.19689400	-0.78797700	-0.50926300
F	-0.47330900	1.31840300	-1.57998700
N	-0.09839900	2.63816300	1.16387200

O	1.20484300	2.59597500	1.23632400
O	-0.61626200	3.54789600	1.81109100
H	5.69706200	0.89625300	-0.86447700
H	1.83539900	-3.58046900	1.24348100

TS5



- Thermochemistry -

Zero-point correction= 0.238732 (Hartree/Particle)

Thermal correction to Energy= 0.259925

Thermal correction to Enthalpy= 0.260869

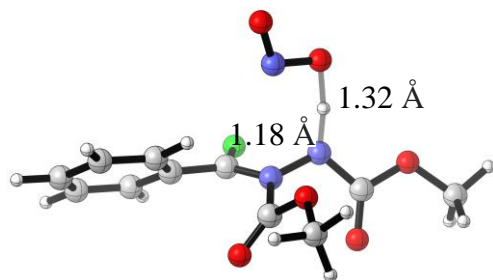
Thermal correction to Gibbs Free Energy= 0.185330
 Sum of electronic and zero-point Energies= -1141.450621
 Sum of electronic and thermal Energies= -1141.429428
 Sum of electronic and thermal Enthalpies= -1141.428484
 Sum of electronic and thermal Free Energies= -1141.504024

C	-4.13445800	-0.26913000	1.44120200
C	-4.69617200	0.39487800	0.34467400
C	-2.76203900	-0.46128600	1.50408900
C	-1.93946100	0.04185800	0.46938400
C	-2.51350200	0.70117000	-0.64183000
C	-3.88786700	0.86902100	-0.69747900
H	-4.33658100	1.35919100	-1.55478600
H	-4.76855900	-0.63771600	2.24032800
H	-5.77161000	0.53538600	0.29522000
H	-1.89204700	1.03386000	-1.46469200
H	-2.31624300	-0.97329300	2.34898000
C	-0.53407900	-0.20188600	0.54013900
N	0.46687600	0.49635800	-0.01083900

N	1.59634100	-0.22357500	-0.36524200
C	0.41855600	1.93040600	-0.23997900
O	-0.40419500	2.63207100	0.29035300
O	1.39926900	2.27699900	-1.04448000
C	1.52488000	3.70364700	-1.29023300
H	2.38214000	3.79692200	-1.95325200
H	1.69970800	4.22429000	-0.34751000
C	2.67706700	-0.16724700	0.50560100
O	2.78519500	0.63573700	1.41178500
O	3.57328100	-1.09096800	0.14230200
C	4.79232000	-1.11011400	0.91602300
H	4.57173300	-1.31808300	1.96508100
H	5.31076000	-0.15294300	0.82843300
F	-0.14423900	-1.21868600	1.27124900
N	-0.14940000	-3.07685900	-0.98947000
O	-0.74454200	-3.92486300	-1.67091200
O	-0.10160600	-1.89651100	-1.52797400
H	5.39086200	-1.91097800	0.48454600
H	0.61715100	4.07520200	-1.76787600

H 1.28342900 -1.08274900 -0.87499900

TS6



- Thermochemistry -

Zero-point correction= 0.238950 (Hartree/Particle)

Thermal correction to Energy= 0.259951

Thermal correction to Enthalpy= 0.260895

Thermal correction to Gibbs Free Energy= 0.186015

Sum of electronic and zero-point Energies= -1141.100714

Sum of electronic and thermal Energies= -1141.079714

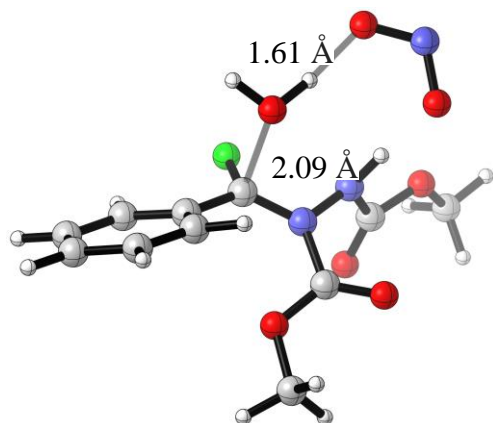
Sum of electronic and thermal Enthalpies= -1141.078770

Sum of electronic and thermal Free Energies= -1141.153649

C	-4.40634800	-1.20634400	-0.76351100
C	-4.78720700	-0.29463700	0.22156700
C	-3.07837300	-1.29210800	-1.15118300
C	-2.12926400	-0.47679600	-0.51725400
C	-2.51086200	0.45247100	0.46290900
C	-3.84583500	0.53996600	0.82430300
H	-4.15566300	1.26527700	1.56802200
H	-5.14651700	-1.84575000	-1.23119100
H	-5.83021300	-0.22410500	0.51248700
H	-1.77842100	1.13227300	0.88726400
H	-2.77182100	-1.99650300	-1.91651000
C	-0.75324400	-0.53515900	-0.94800500
N	0.31180300	-0.38681200	-0.20185400
N	1.49153100	0.00122900	-0.80752900
C	0.26409800	-0.58857700	1.25542400
O	-0.43428500	-1.42062700	1.75637000
O	1.08000200	0.26137200	1.81743400
C	1.24819900	0.10723900	3.24220100

H	0.28719200	0.23492600	3.74102900
H	1.94507600	0.88977200	3.53031600
C	2.55608100	-0.79398400	-0.45636000
H	1.53977000	1.17851700	-0.91232600
O	2.47739200	-1.82296800	0.19158800
O	3.67915200	-0.26584200	-0.93977500
C	4.87486200	-1.00148300	-0.65775300
H	4.82636700	-1.99338800	-1.11158300
H	5.02060500	-1.09618000	0.42004600
F	-0.53731300	-0.67619400	-2.21978300
N	0.23890500	2.65566700	-0.37388900
O	1.39068200	2.48743600	-0.94945800
O	-0.10955100	3.82165600	-0.28250600
H	5.68215300	-0.42140000	-1.10113800
H	1.66185400	-0.88002500	3.45126900

TS7



- Thermochemistry -

Zero-point correction= 0.263845 (Hartree/Particle)

Thermal correction to Energy= 0.286993

Thermal correction to Enthalpy= 0.287937

Thermal correction to Gibbs Free Energy= 0.208257

Sum of electronic and zero-point Energies= -1217.864348

Sum of electronic and thermal Energies= -1217.841199

Sum of electronic and thermal Enthalpies= -1217.840255

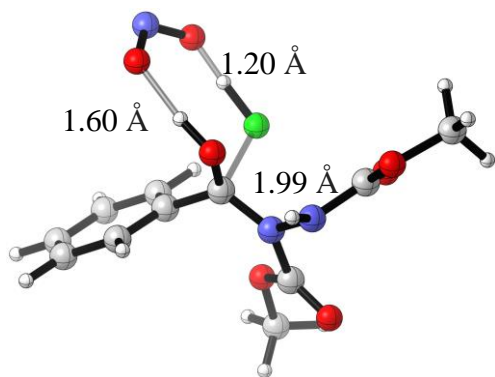
Sum of electronic and thermal Free Energies= -1217.919936

C 4.29323700 0.35084900 1.54362900

C	4.89459500	0.44641700	0.28737300
C	2.90476400	0.34048000	1.65281400
C	2.11760800	0.40132300	0.48990300
C	2.72378400	0.50967400	-0.77505600
C	4.10889600	0.53308300	-0.86886700
H	4.57969600	0.62802000	-1.84202300
H	4.90227500	0.29003900	2.43970300
H	5.97727900	0.46312900	0.20596900
H	2.11349100	0.61247500	-1.66494400
H	2.43416100	0.26999800	2.62673200
C	0.66563200	0.39705600	0.64915800
N	-0.22342900	-0.36127900	-0.02446400
N	-1.55739600	-0.04571900	0.16868000
C	0.04116500	-1.42262900	-0.98176700
O	-0.78976600	-1.72650300	-1.79761100
O	1.21275500	-1.98468600	-0.76250300
C	1.58100900	-3.04985000	-1.67966600
H	0.85613900	-3.86159700	-1.60539100
H	2.56586100	-3.37333900	-1.34967000

C	-2.33148200	-1.02932800	0.75891100
O	-1.89191700	-2.04148200	1.27223800
O	-3.62100100	-0.67082300	0.69086300
C	-4.55078300	-1.58703900	1.30416300
H	-4.49414200	-2.56579000	0.82279900
H	-5.53309300	-1.14226200	1.15059800
F	0.22469700	0.81384600	1.81848700
H	-4.33879600	-1.68729800	2.37095400
H	1.61718100	-2.66368000	-2.69941500
H	-1.96769500	0.63619900	-0.51443600
O	-2.05553000	3.34402500	-0.37195000
O	-2.75272400	1.72001500	-1.58681100
N	-2.91246500	2.90773900	-1.19785600
H	-0.65814500	2.55303300	-0.30511600
O	0.30588800	2.20835700	-0.32680400
H	0.82434400	2.87984200	0.15039400

TS8



- Thermochemistry -

Zero-point correction= 0.261753 (Hartree/Particle)

Thermal correction to Energy= 0.284446

Thermal correction to Enthalpy= 0.285391

Thermal correction to Gibbs Free Energy= 0.206408

Sum of electronic and zero-point Energies= -1217.892682

Sum of electronic and thermal Energies= -1217.869989

Sum of electronic and thermal Enthalpies= -1217.869045

Sum of electronic and thermal Free Energies= -1217.948027

C -3.67527700 -0.60398200 -0.78873000

C	-4.32090200	-0.84817100	0.42660400
C	-2.32157600	-0.27640300	-0.81693100
C	-1.60903600	-0.18792200	0.38384100
C	-2.25607200	-0.41783600	1.60801900
C	-3.60956400	-0.75605100	1.62366300
H	-4.10416600	-0.93975200	2.57261200
H	-4.22755400	-0.66701400	-1.72158200
H	-5.37604700	-1.10537400	0.43988600
H	-1.70635800	-0.33812300	2.54099500
H	-1.81261600	-0.08207300	-1.75014800
C	-0.16266400	0.19803600	0.49761100
N	0.85065100	-0.72493700	0.52927500
N	2.07555100	-0.32277600	1.02961300
C	0.84462900	-2.06923500	0.01734100
O	1.71710400	-2.85241100	0.29732600
O	-0.19306500	-2.27639000	-0.77284800
C	-0.32482600	-3.62177800	-1.29587200
H	-1.24243500	-3.60525500	-1.88054900
H	-0.39860500	-4.33573700	-0.47401300

C	3.03795000	0.12005700	0.13261400
O	3.00726900	-0.08168700	-1.06325500
O	4.01458900	0.73297000	0.81702800
C	5.14833900	1.15776400	0.03200700
H	4.83658600	1.88348900	-0.72212400
H	5.61757800	0.29858700	-0.45226500
F	0.08158500	1.01172400	-1.30272800
H	5.83299000	1.61668800	0.74386500
H	0.53480600	-3.85780300	-1.92510100
H	2.06386200	0.04599400	1.97209500
O	-1.18314200	2.98952300	-1.58448500
O	-1.54136000	3.18743300	0.53337600
N	-1.74632800	3.62132400	-0.61143400
H	-0.52828700	2.01314100	-1.35130500
O	0.12571300	1.27436000	1.17342200
H	-0.56600100	1.99517700	0.97448800

F-N=O + H₂O



- Thermochemistry -

Zero-point correction= 0.030758 (Hartree/Particle)

Thermal correction to Energy= 0.037777

Thermal correction to Enthalpy= 0.038721

Thermal correction to Gibbs Free Energy= -0.001513

Sum of electronic and zero-point Energies= -306.096829

Sum of electronic and thermal Energies= -306.089810

Sum of electronic and thermal Enthalpies= -306.088866

Sum of electronic and thermal Free Energies= -306.129100

N 1.05382100 -0.49458300 -0.01260500

O 2.13456600 -0.14977300 0.00849300

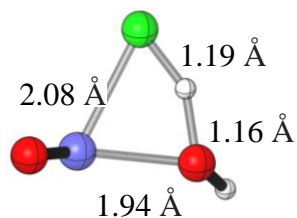
F 0.10549700 0.74385000 0.01042800

H -2.83062700 -0.33951400 0.83292600

O -2.60856100 -0.22809300 -0.10379500

H -1.70363300 0.12987000 -0.07613000

TS9



- Thermochemistry -

Zero-point correction= 0.029061 (Hartree/Particle)

Thermal correction to Energy= 0.033476

Thermal correction to Enthalpy= 0.034420

Thermal correction to Gibbs Free Energy= 0.002084

Sum of electronic and zero-point Energies= -306.077260

Sum of electronic and thermal Energies= -306.072845

Sum of electronic and thermal Enthalpies= -306.071901

Sum of electronic and thermal Free Energies= -306.104237

N -0.69015400 -0.00269000 0.50508000

O -1.48008900 -0.12531100 -0.27999000

F 0.98531200 -1.10066500 -0.03768700

H	1.03408700	1.55957500	0.65096900
O	0.70671300	1.16159600	-0.17706500
H	1.11618200	0.07495800	-0.19090800

Additional Structural Data

Table 13. Single point energies for structures. Geometry optimizations and frequency calculations were performed at the uB3LYP/6-31G(d) level of theory. Single point energies were calculated at the uB3LYP/6-311++G(2d,2p), uM06-2X/6-311++G(2d,2p), uPBEPBE/6-311++G(2d,2p) and uMPW1PW91/6-311++G(2d,2p) level of theory. Solvent effects were evaluated with the integral equation formalism polarizable continuum model (IEFPCM).

Structure	uB3LYP/6-311++G(2d,2p), E (a.u.)	uM06-2X/6-311++G(2d,2p), E (a.u.)	uPBEPBE/6-311++G(2d,2p), E (a.u.)	uMPW1PW91/6-311++G(2d,2p), E (a.u.)
110	-1142.11	-1141.68	-1140.86	-1141.82
111	-1142.12	-1141.69	-1140.87	-1141.82
118	-229.795	-229.702	-229.589	-229.73
112	-912.329	-911.974	-911.282	-912.09
113	-1142.07	-1141.63	-1140.83	-1141.77
115	-936.891	-936.526	-935.826	-936.65
119	-1142.08	-1141.64	-1140.84	-1141.78

nitrogen	-205.146	-205.056	-204.961	-205.088
dioxide				
116	-1218.55	-1218.08	-1217.22	-1218.23
117	-1218.59	-1218.13	-1217.26	-1218.27
Nitrous Acid	-205.783	-205.697	-205.588	-205.723
Hydrogen	-100.49	-100.451	-100.391	-100.463
Fluoride				
H₂O	-76.4688	-76.4309	-76.3827	-76.4449
TS1	-1142.06	-1141.62	-1140.81	-1141.75
TS2	-1142.09	-1141.65	-1140.85	-1141.79
TS3	-1142.05	-1141.6	-1140.81	-1141.75
TS4	-1142.08	-1141.64	-1140.83	-1141.78
TS5	-1142.07	-1141.63	-1140.83	-1141.77
TS6	-1142.08	-1141.64	-1140.83	-1141.78
TS7	-1218.55	-1218.08	-1217.22	-1218.23
TS8	-1218.58	-1218.11	-1217.25	-1218.25

Figure 21. Energy profiles corresponding to 1,2-migration and heterolytic C-F bond cleavage. Calculated relative free energies at 298 K (kcal mol^{-1}) include single-point energy corrections at the IEFPCM(DMSO)/uM06-2X/6-311++G(2d,2p)//IEFPCM(DMSO)/uB3LYP/6-31G(d) level. The inset scheme depicts homolytic C-N bond cleavage and associated bond dissociation energy (ΔH in kcal mol^{-1}).

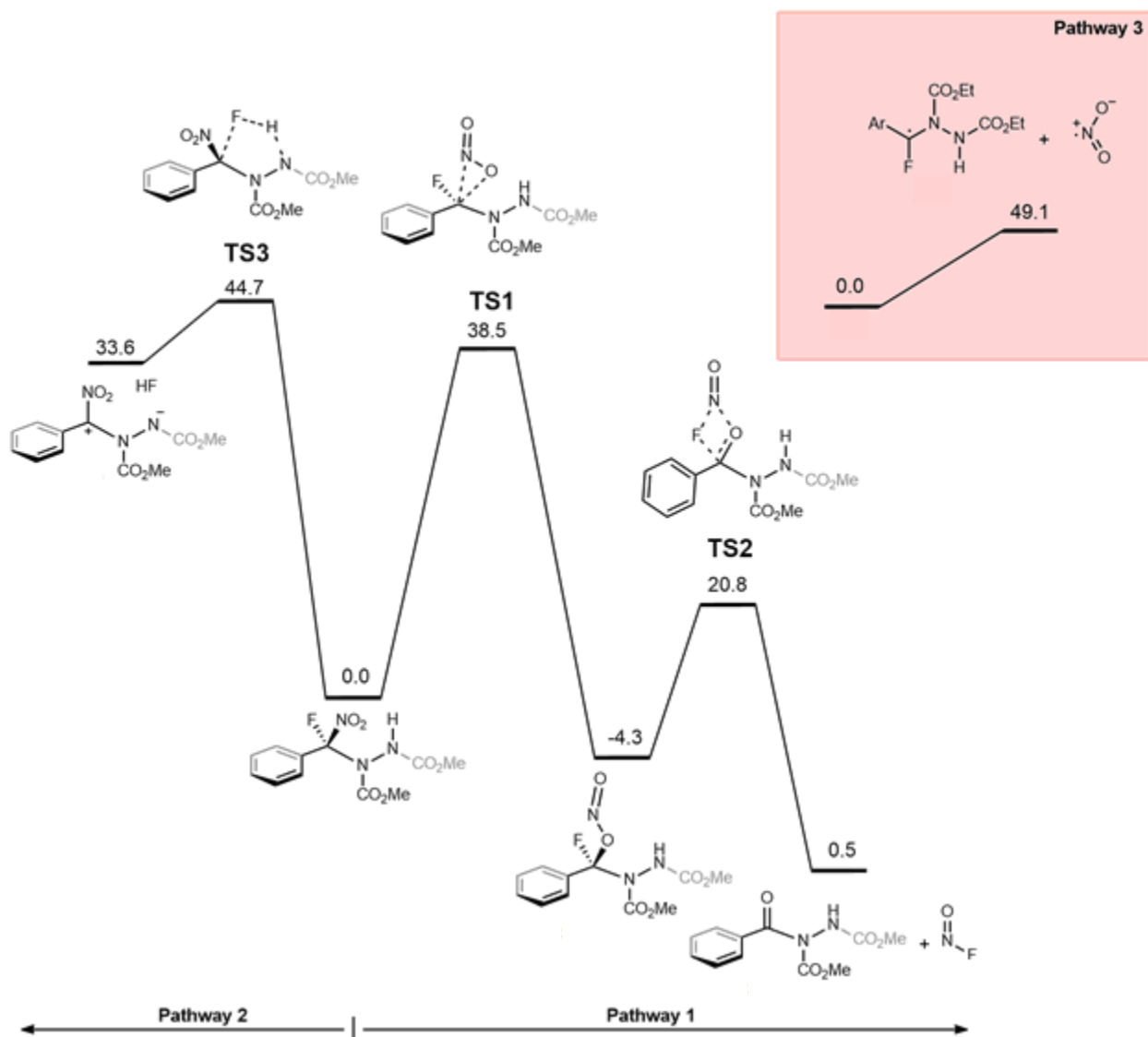


Figure 22. Energy profile corresponding to stepwise nitro to nitrite isomerization pathway leading to amide from formation of nitrite ester (black line) or water capture (red line). Calculated relative free energies at 298 K (kcal mol^{-1}) include single-point energy corrections at the IEFPCM(DMSO)/uM06-2X/6-311++G(2d,2p)//IEFPCM(DMSO)/uB3LYP/6-31G(d) level.

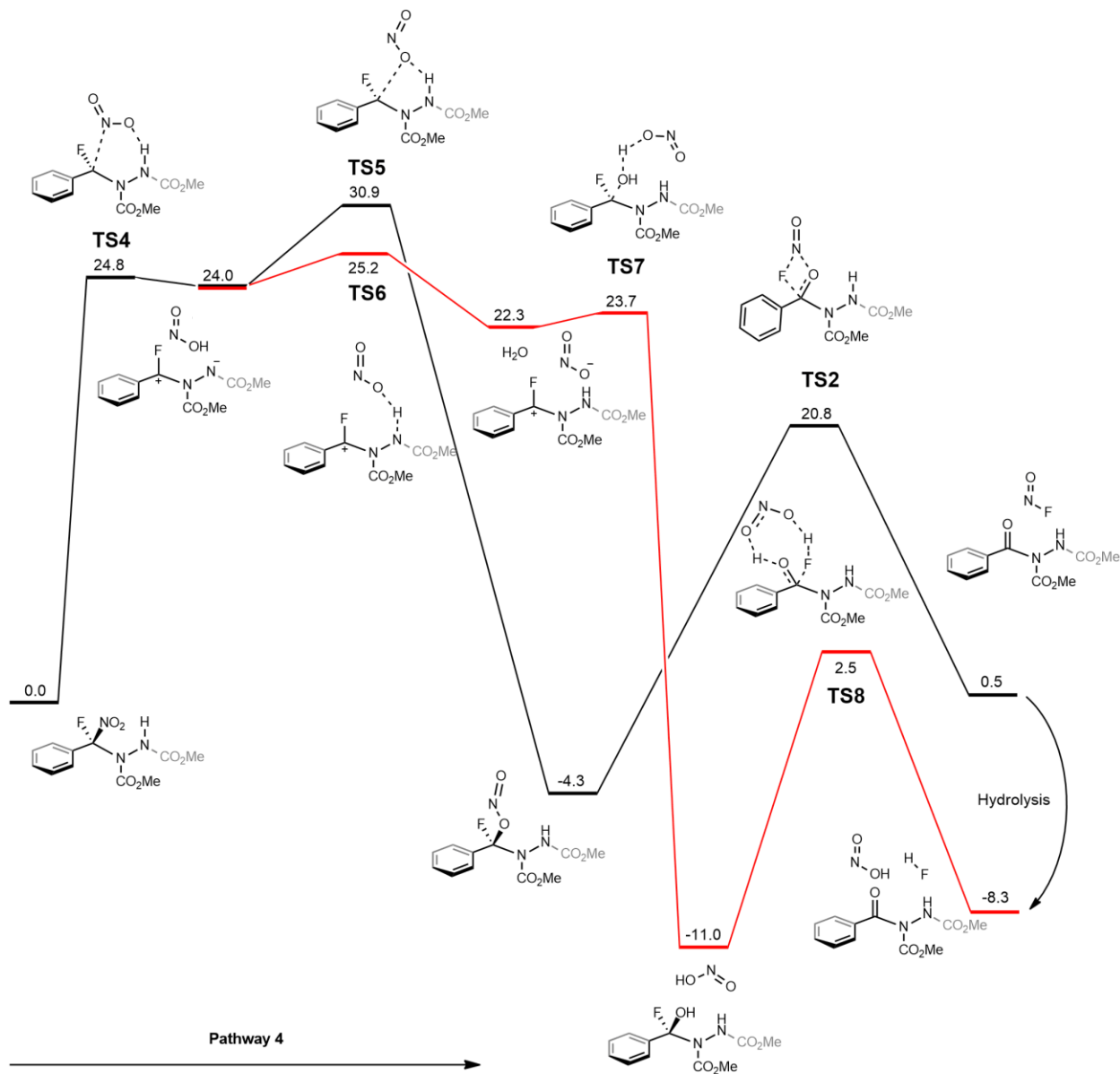


Figure 23. Energy profiles corresponding to 1,2-migration and heterolytic C-F bond cleavage. Calculated relative free energies at 298 K (kcal mol⁻¹) include single-point energy corrections at the IEFPCM(DMSO)/uPBEPBE/6-311++G(2d,2p)//IEFPCM(DMSO)/uB3LYP/6-31G(d) level. The inset scheme depicts homolytic C-N bond cleavage and associated bond dissociation energy (ΔH in kcal mol⁻¹).

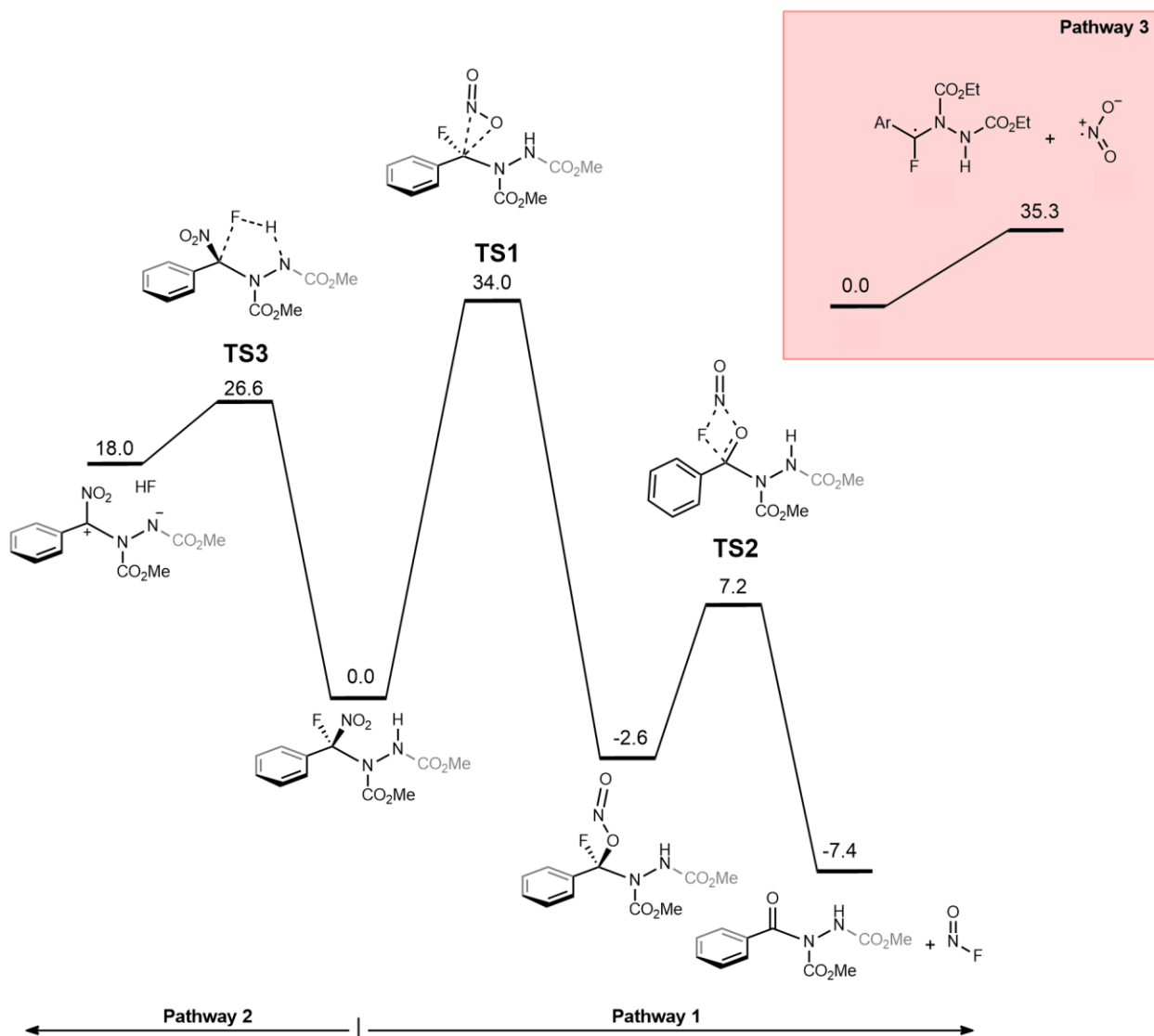


Figure 24. Energy profile corresponding to stepwise nitro to nitrite isomerization pathway leading to amide from formation of nitrite ester (black line) or water capture (red line). Calculated relative free energies at 298 K (kcal mol^{-1}) include single-point energy corrections at the IEFPCM(DMSO)/uPBEPBE/6-311++G(2d,2p)//IEFPCM(DMSO)/uB3LYP/6-31G(d) level.

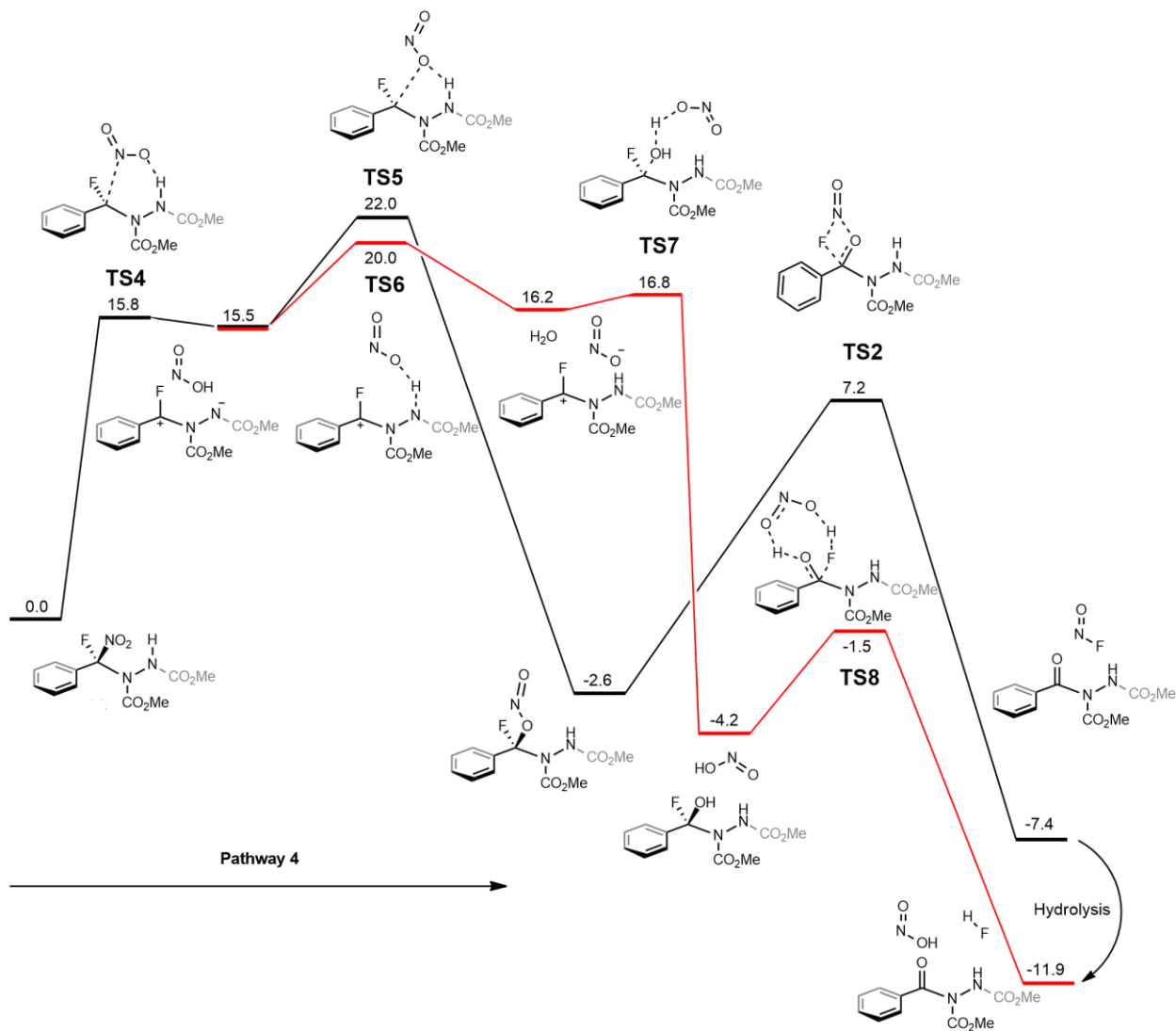


Figure 25. Energy profiles corresponding to 1,2-migration and heterolytic C-F bond cleavage. Calculated relative free energies at 298 K (kcal mol⁻¹) include single-point energy corrections at the IEFPCM(DMSO)/uMPW1PW91/6-311++G(2d,2p)//IEFPCM(DMSO)/uB3LYP/6-31G(d) level. The inset scheme depicts homolytic C-N bond cleavage and associated bond dissociation energy (ΔH in kcal mol⁻¹).

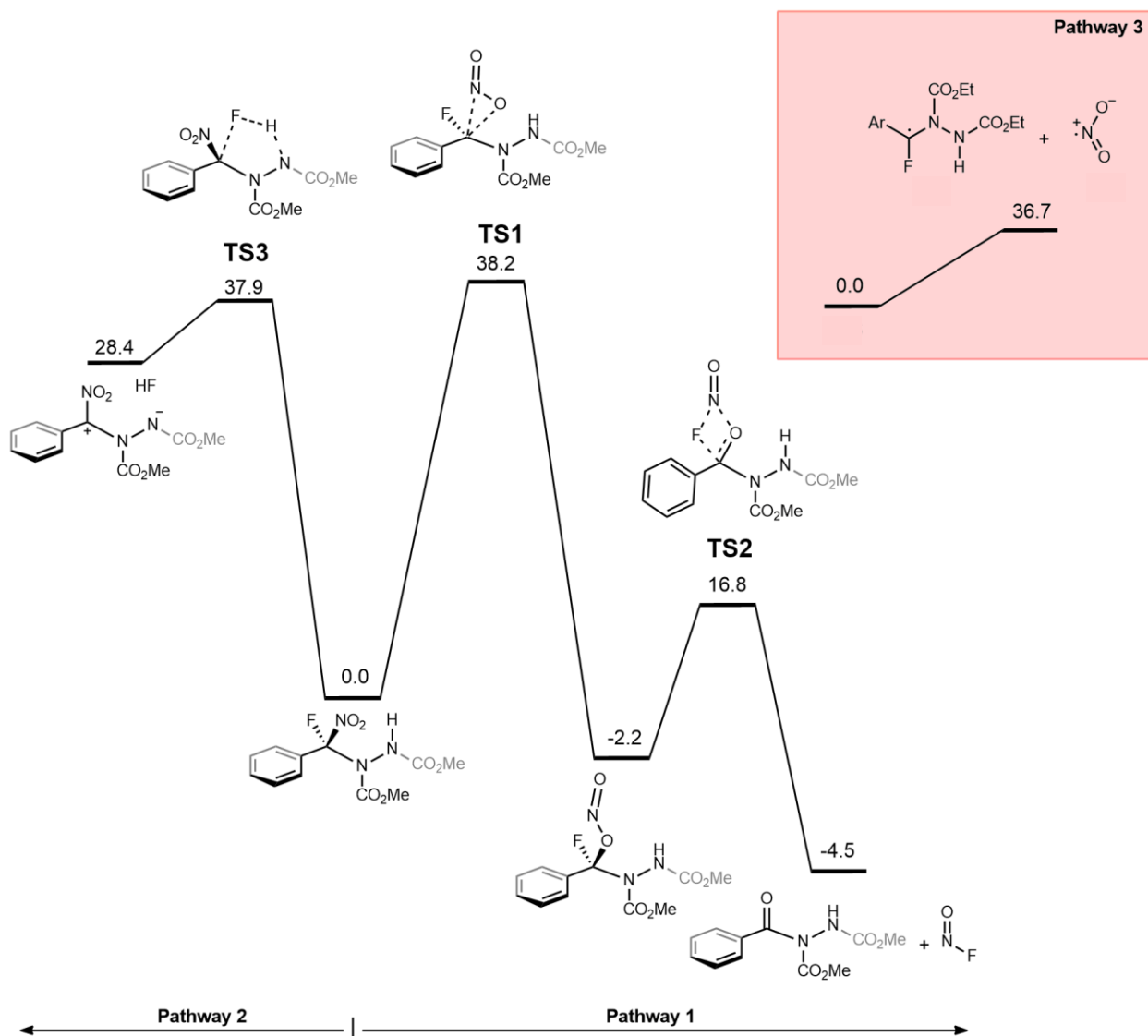
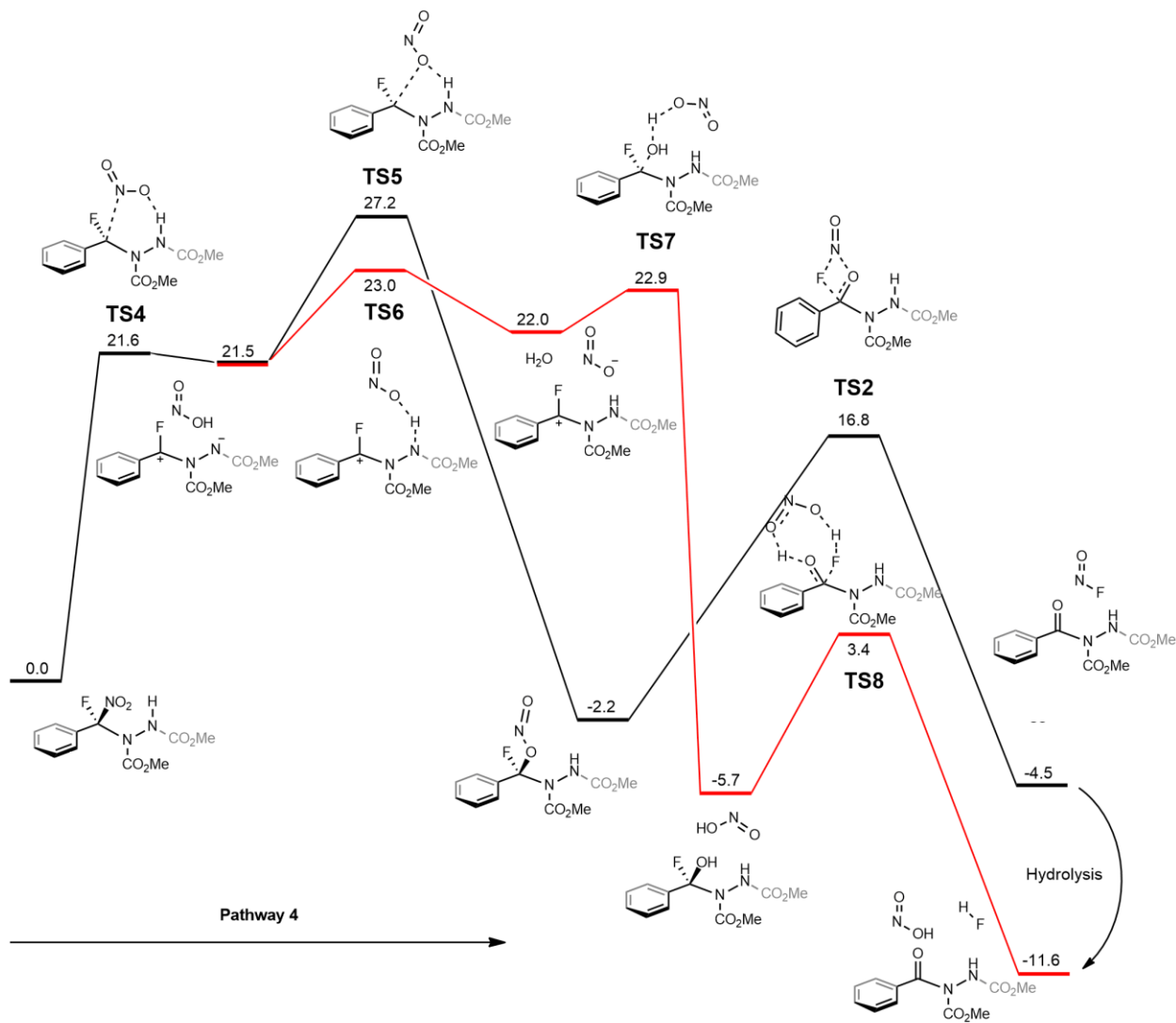


Figure 26. Energy profile corresponding to stepwise nitro to nitrite isomerization pathway leading to amide from formation of nitrite ester (black line) or water capture (red line). Calculated relative free energies at 298 K (kcal mol^{-1}) include single-point energy corrections at the IEFPCM(DMSO)/uMPW1PW91/6-311++G(2d,2p)//IEFPCM(DMSO)/uB3LYP/6-31G(d) level.



Hydrolysis of F-N=O

Table 14. Single point energies for the structures associated with the hydrolysis of F-N=O. Geometry optimizations and frequency calculations were performed at the uB3LYP/6-31G(d) level of theory. Single point energies were calculated at the uB3LYP/6-311++G(2d,2p), uM06-2X/6-311++G(2d,2p), uPBEPBE/6-311++G(2d,2p) and uMPW1PW91/6-311++G(2d,2p) level of theory. Solvent effects were evaluated with the integral equation formalism polarizable continuum model (IEFPCM).

Structure	uB3LYP/6- 311++G(2d,2p), E (a.u.)	uM06-2X/6- 311++G(2d,2p), E (a.u.)	uPBEPBE/6- 311++G(2d,2p), E (a.u.)	uMPW1PW91/6- 311++G(2d,2p), E (a.u.)
F-N=O + H₂O	-306.26850937	-306.13779515	-305.97677607	-306.17839835
TS9	-306.24974895	-306.11574633	-305.96642558	-306.15868064
Nitrous Acid + H₂O	-306.28003524	-306.15509522	-305.98698239	-306.19271870

Figure 27. Energy profile corresponding to hydrolysis of F-N=O. Calculated relative free energies at 298 K (kcal mol⁻¹) include single-point energy corrections at the IEFPCM(DMSO)/uB3LYP/6-311++G(2d,2p)//IEFPCM(DMSO)/uB3LYP/6-31G(d) level.

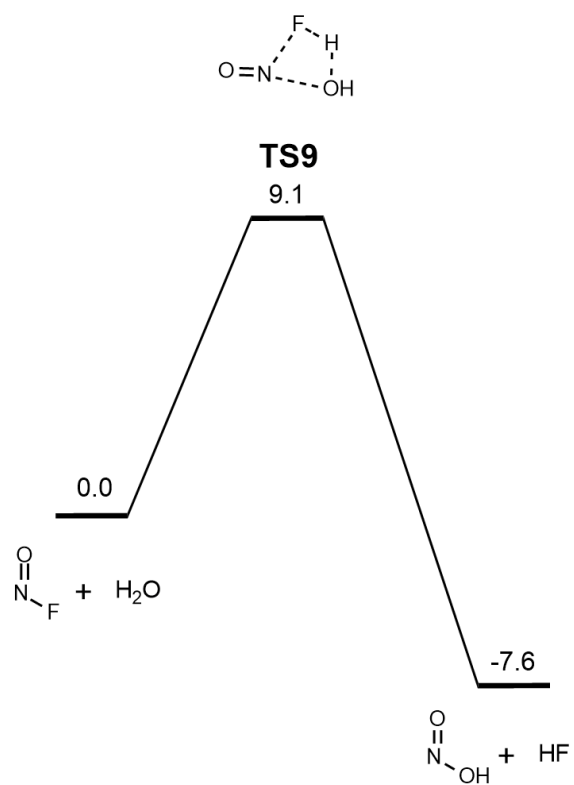


Figure 28. Energy profile corresponding to hydrolysis of F-N=O. Calculated relative free energies at 298 K (kcal mol⁻¹) include single-point energy corrections at the IEFPCM(DMSO)/uM06-2X/6-311++G(2d,2p)//IEFPCM(DMSO)/uB3LYP/6-31G(d) level.

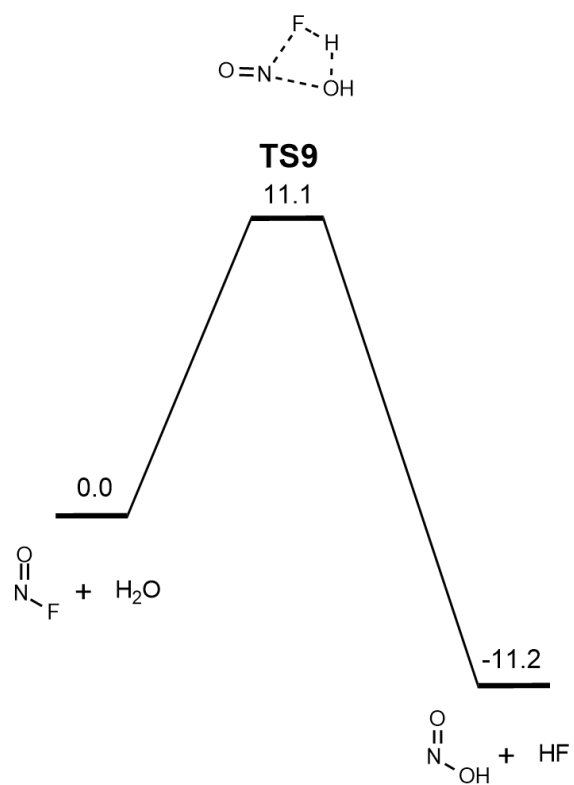


Figure 29. Energy profile corresponding to hydrolysis of F-N=O. Calculated relative free energies at 298 K (kcal mol⁻¹) include single-point energy corrections at the IEFPCM(DMSO)/uPBEPBE/6-311++G(2d,2p)//IEFPCM(DMSO)/uB3LYP/6-31G(d) level.

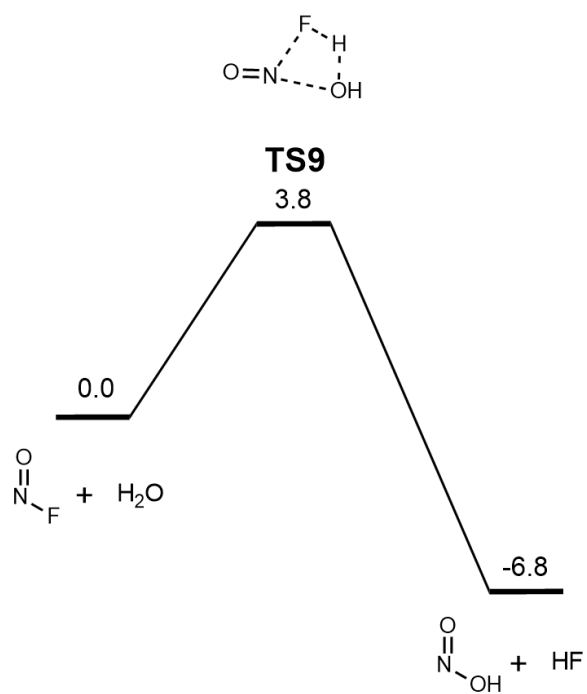
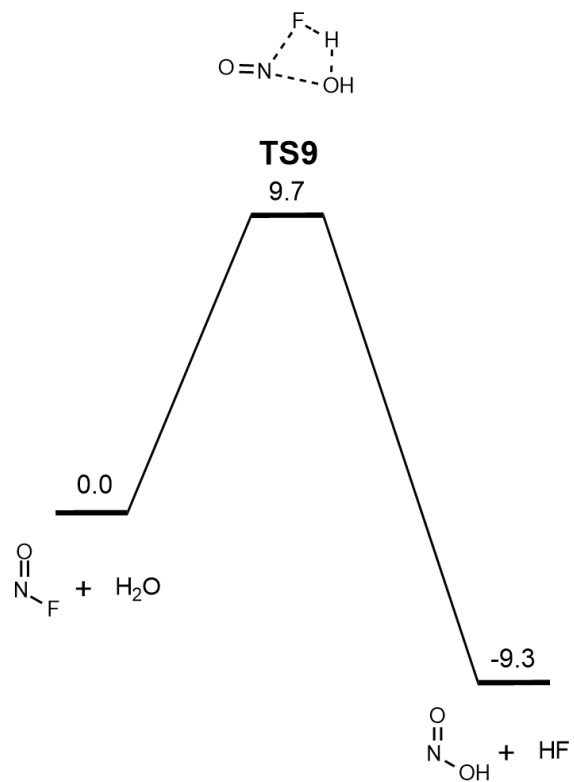


Figure 30. Energy profile corresponding to hydrolysis of F-N=O. Calculated relative free energies at 298 K (kcal mol⁻¹) include single-point energy corrections at the IEFPCM(DMSO)/uMPW1PW91/6-311++G(2d,2p)//IEFPCM(DMSO)/uB3LYP/6-31G(d) level.



Appendix B: Spectral Data and HPLC Traces

Figure 31. ^1H NMR (400 MHz, CDCl_3) of **19**

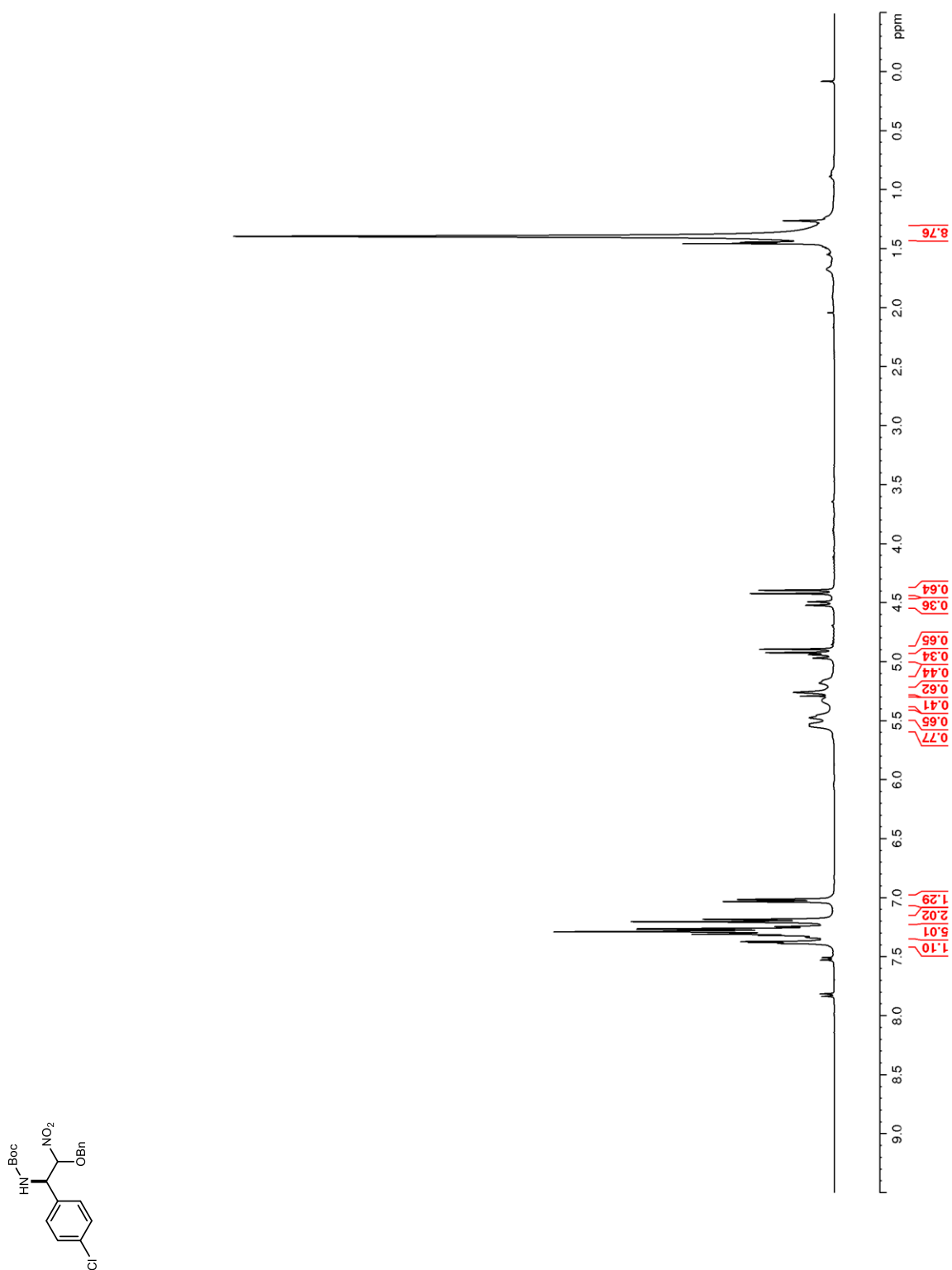


Figure 32. ^{13}C NMR (100 MHz, CDCl_3) of **19**

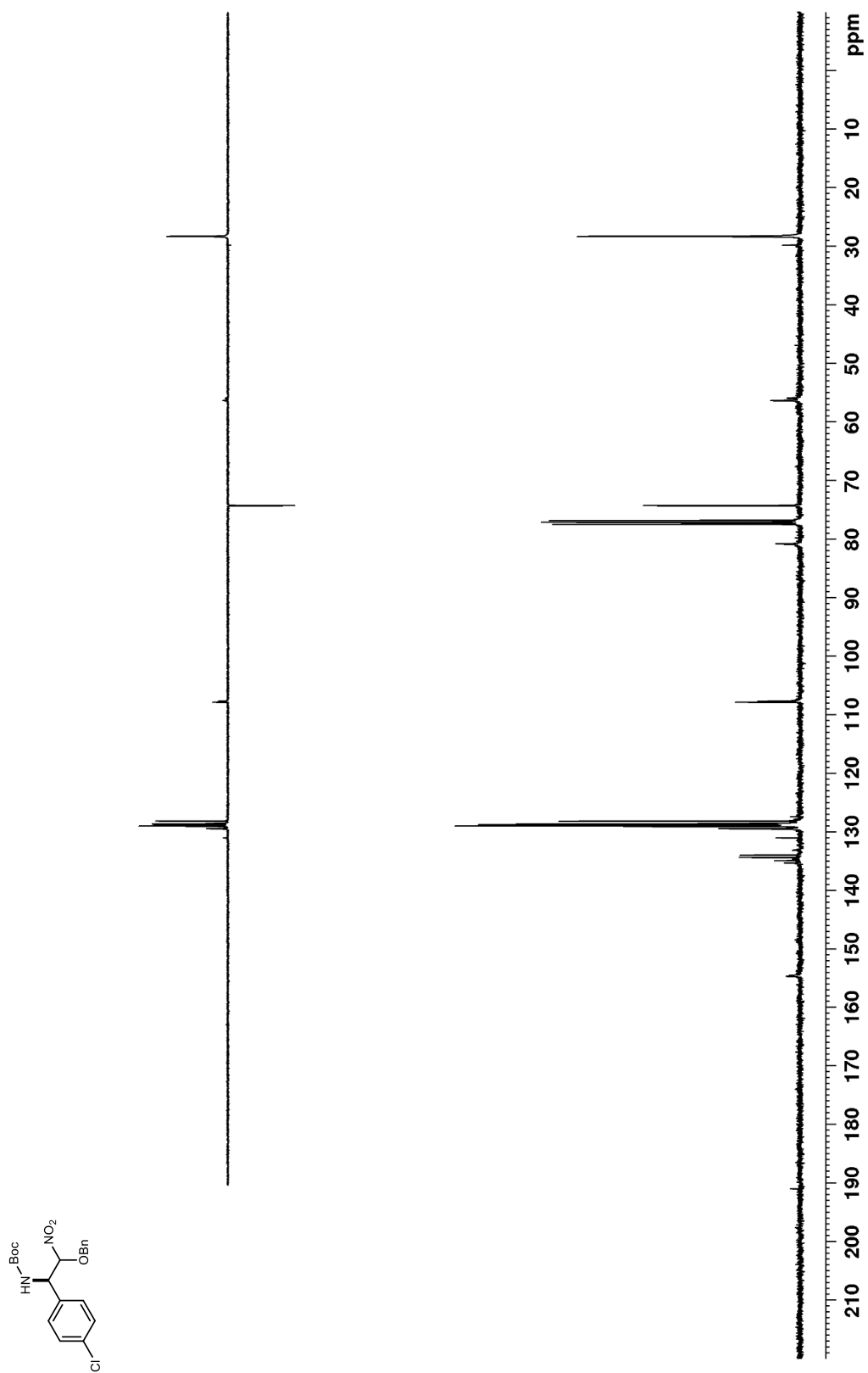


Figure 33. ^1H NMR (400 MHz, CDCl_3) of **22**

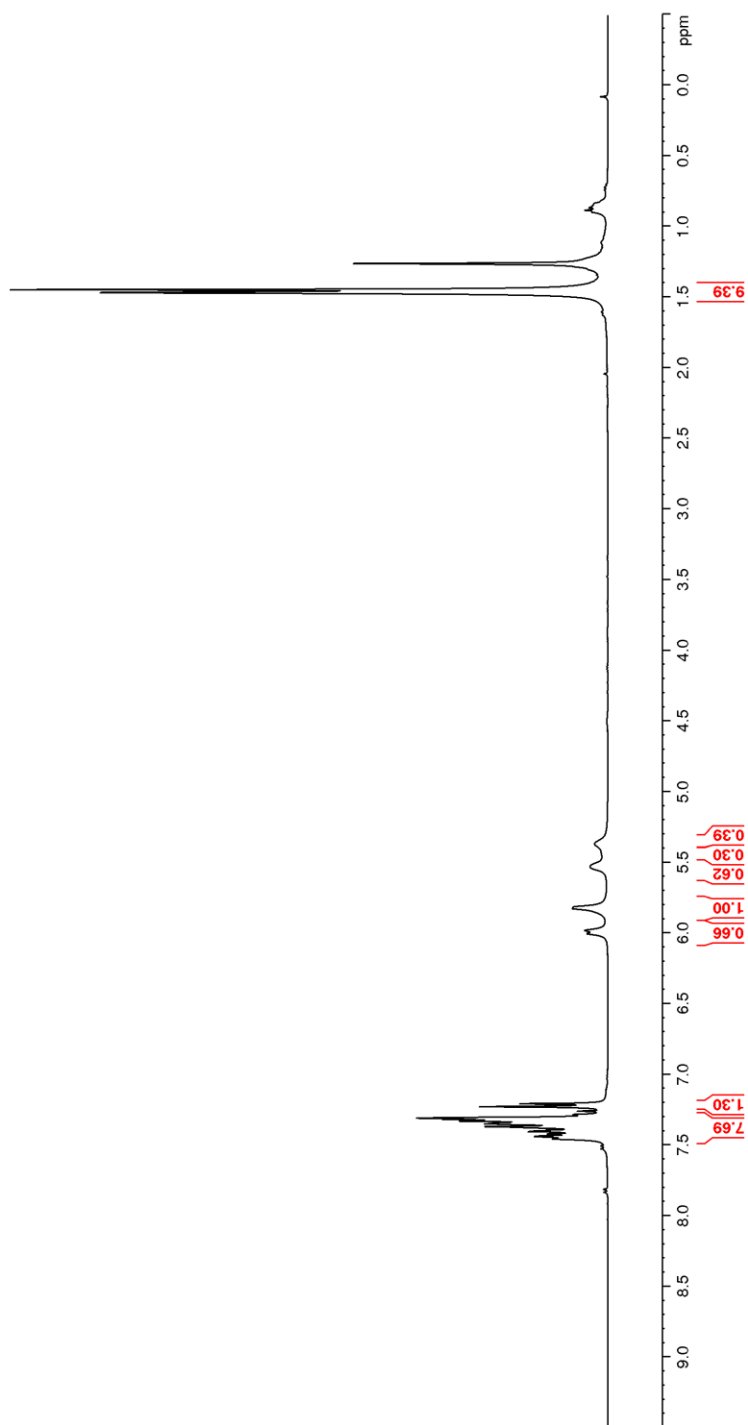
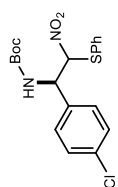


Figure 34. ^{13}C NMR (100 MHz, CDCl_3) of **22**

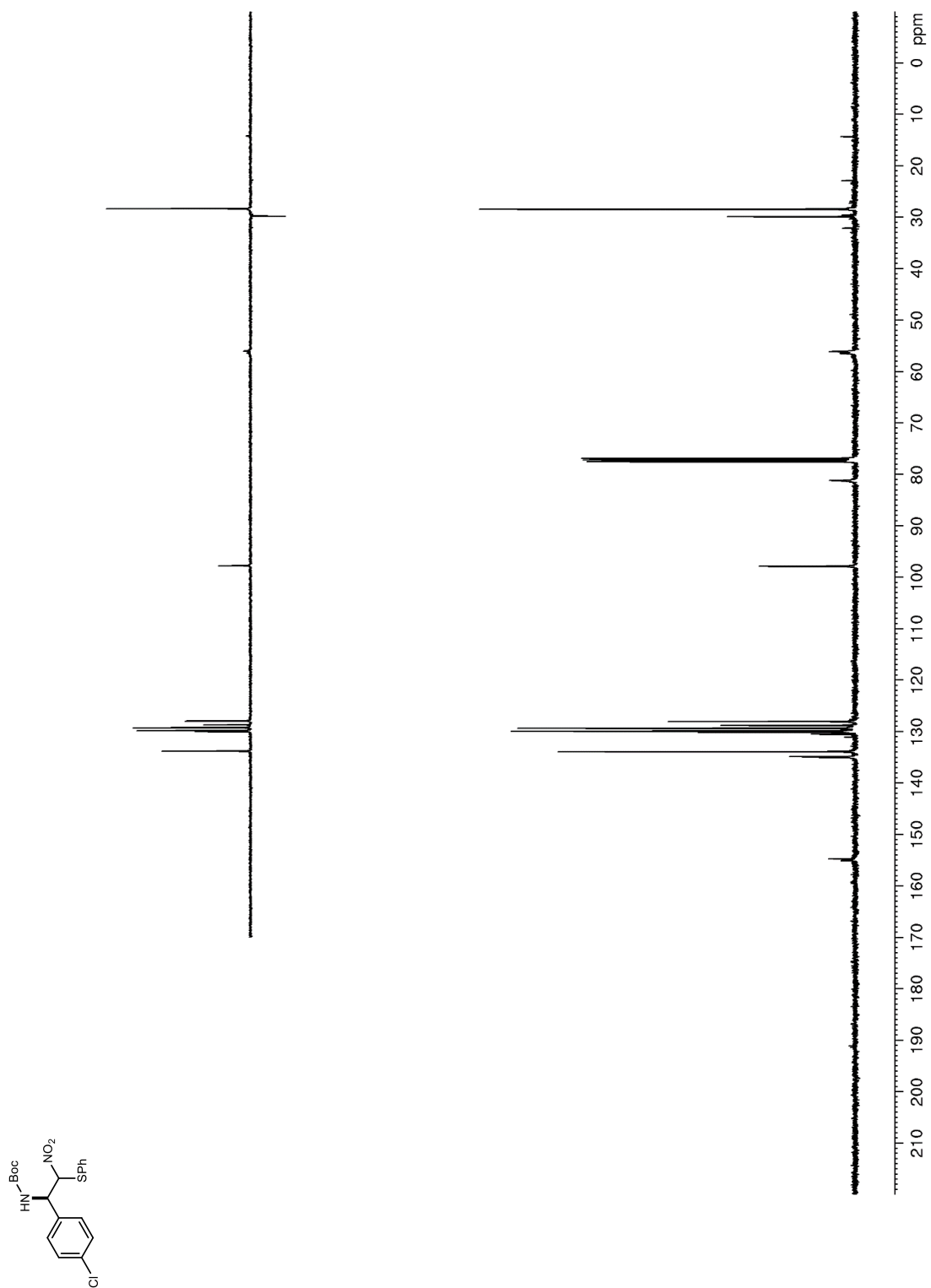


Figure 35. ^1H NMR (400 MHz, CDCl_3) of **23**

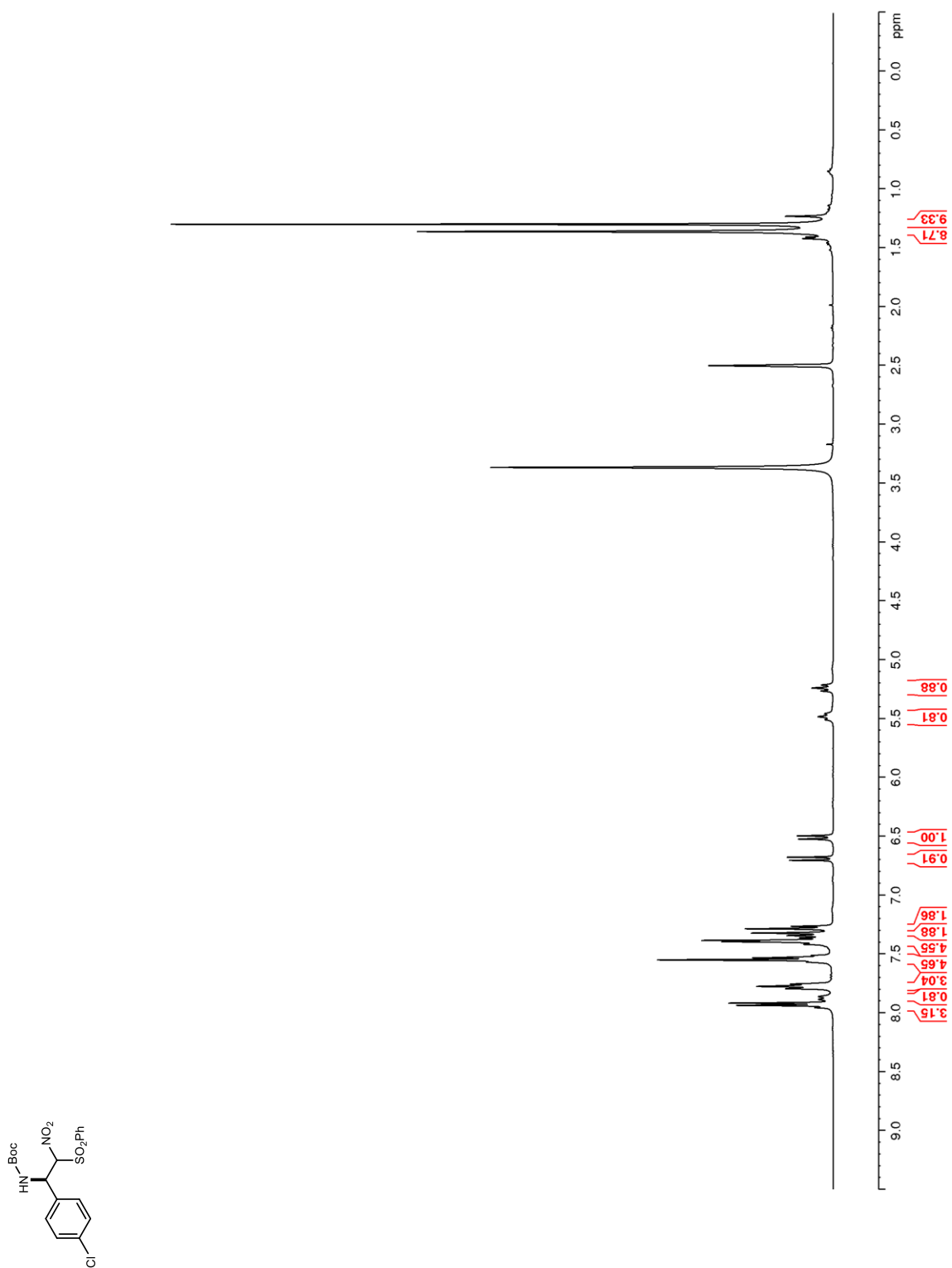


Figure 36. ^{13}C NMR (100 MHz, CDCl_3) of **23**

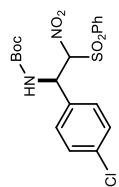
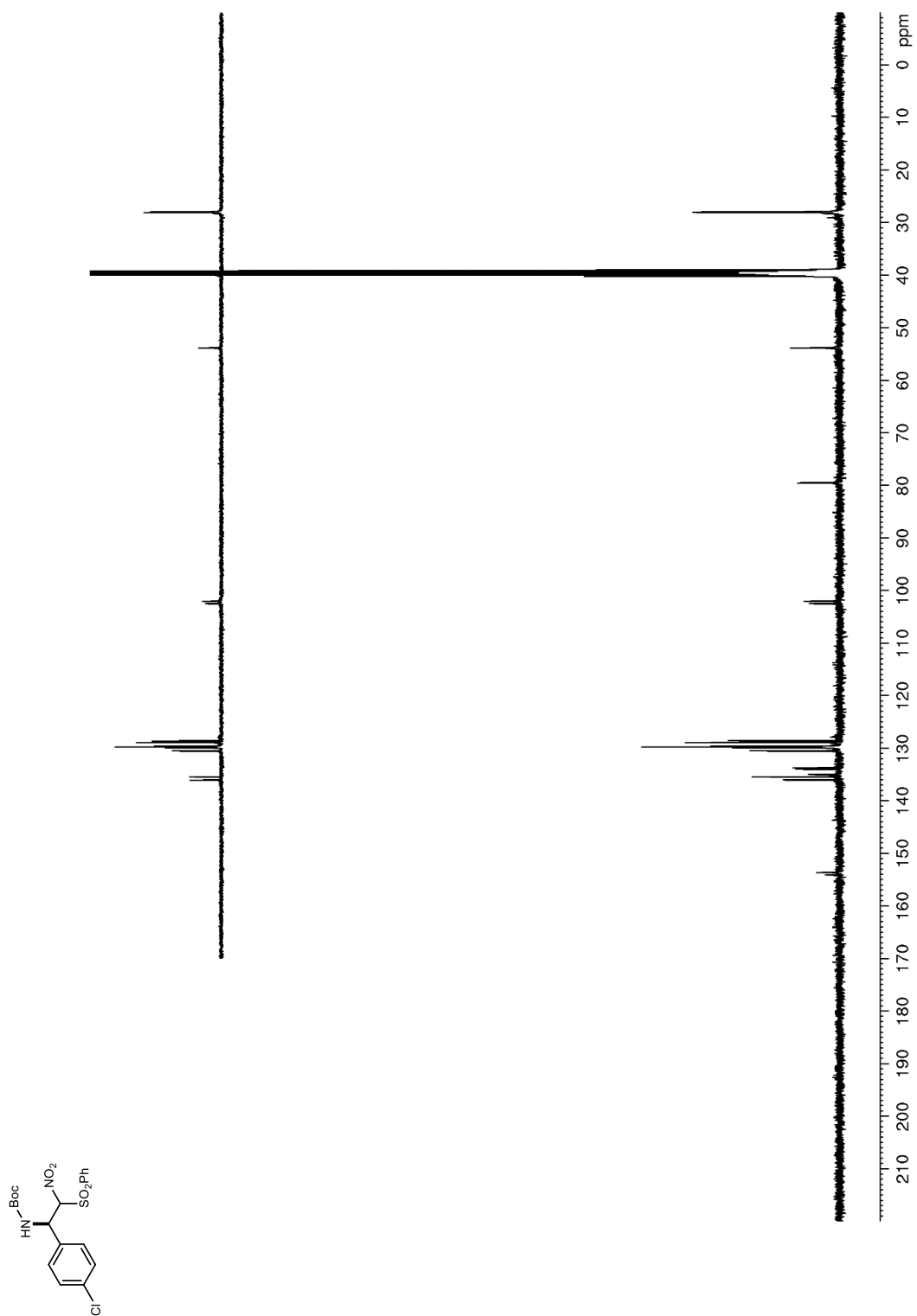


Figure 37. ^1H NMR (400 MHz, CDCl_3) of **69**

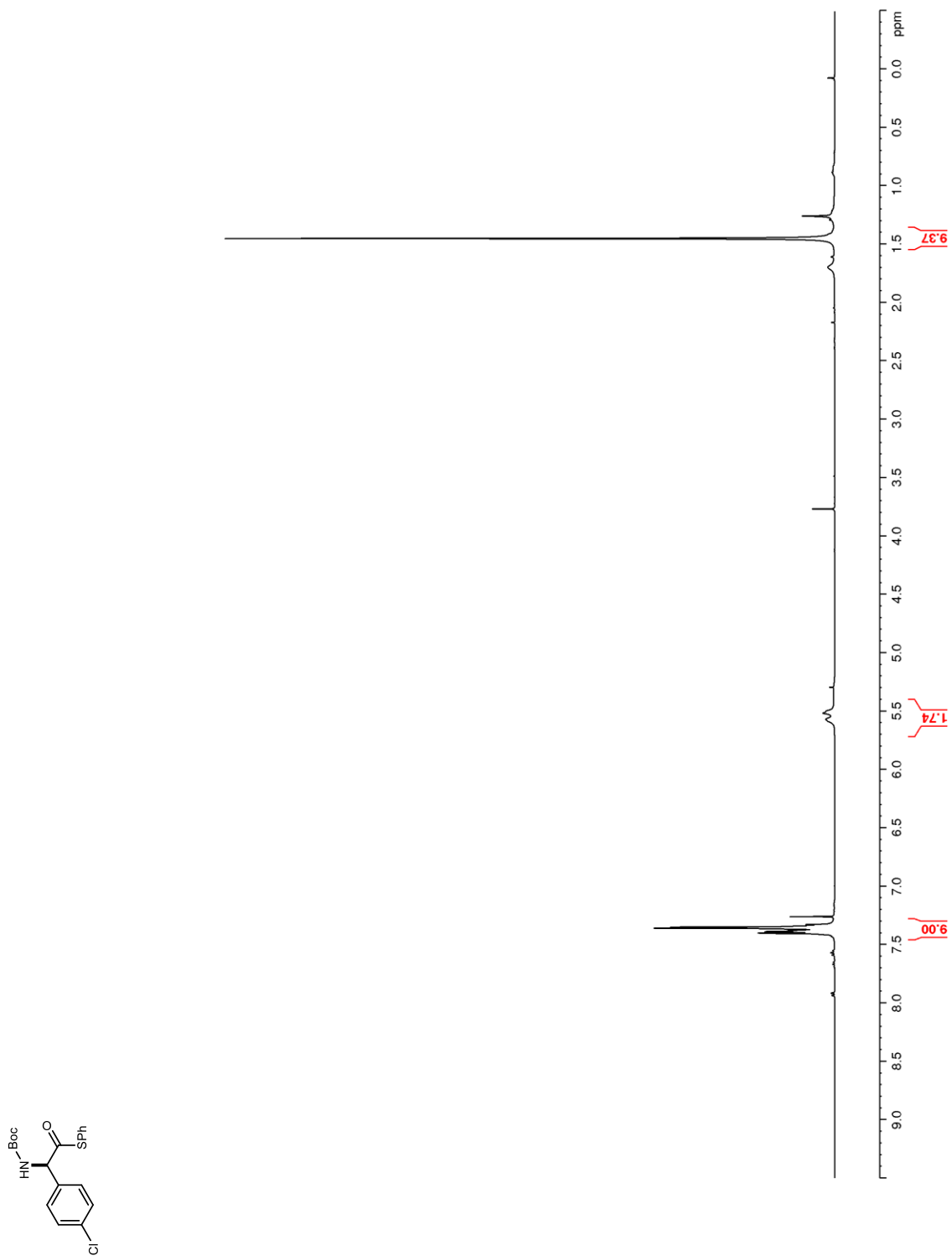


Figure 38. ^{13}C NMR (100 MHz, CDCl_3) of **69**

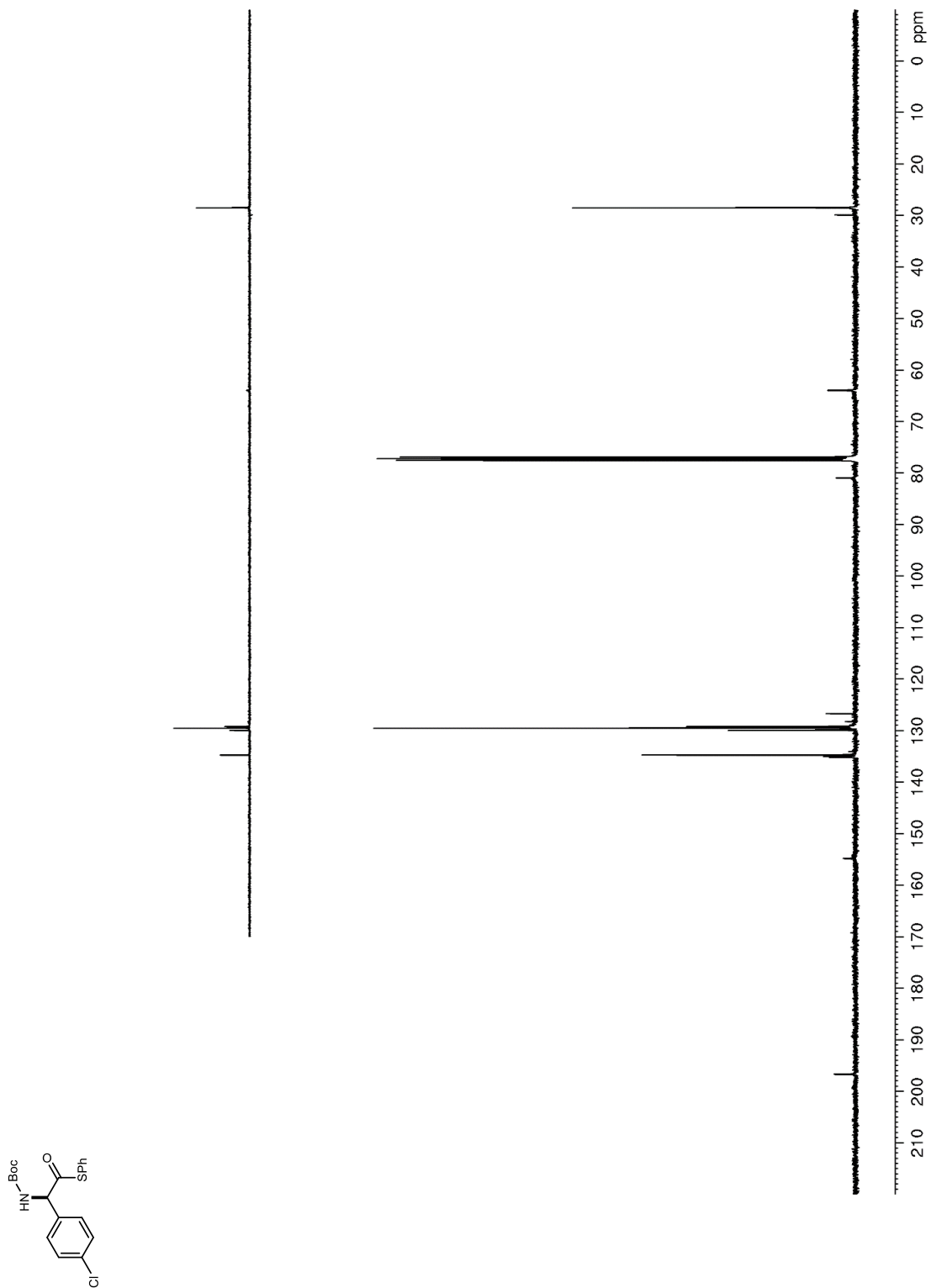


Figure 39. ^1H NMR (400 MHz, CDCl_3) of **77c**

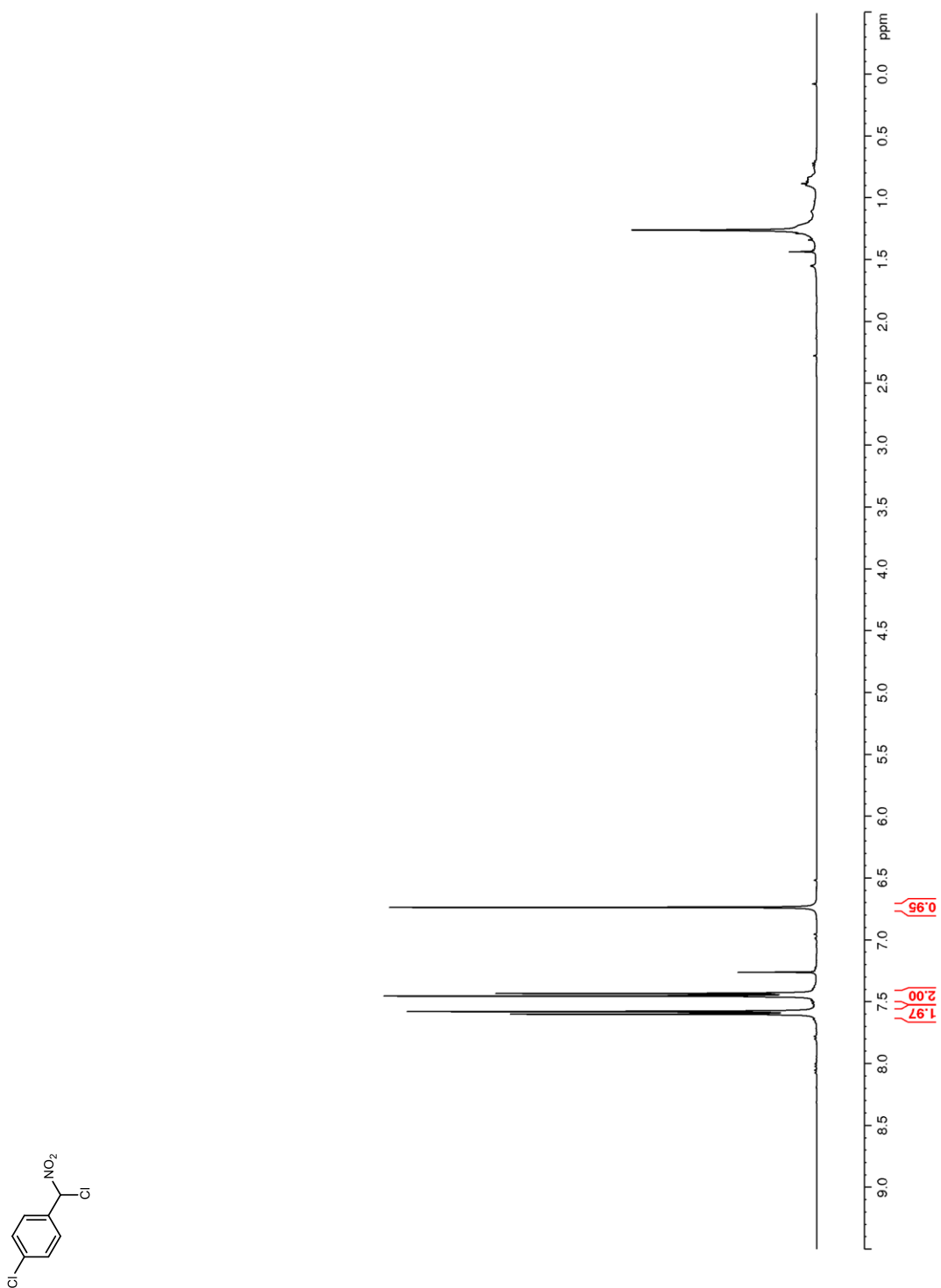


Figure 40. ^{13}C NMR (100 MHz, CDCl_3) of **77c**

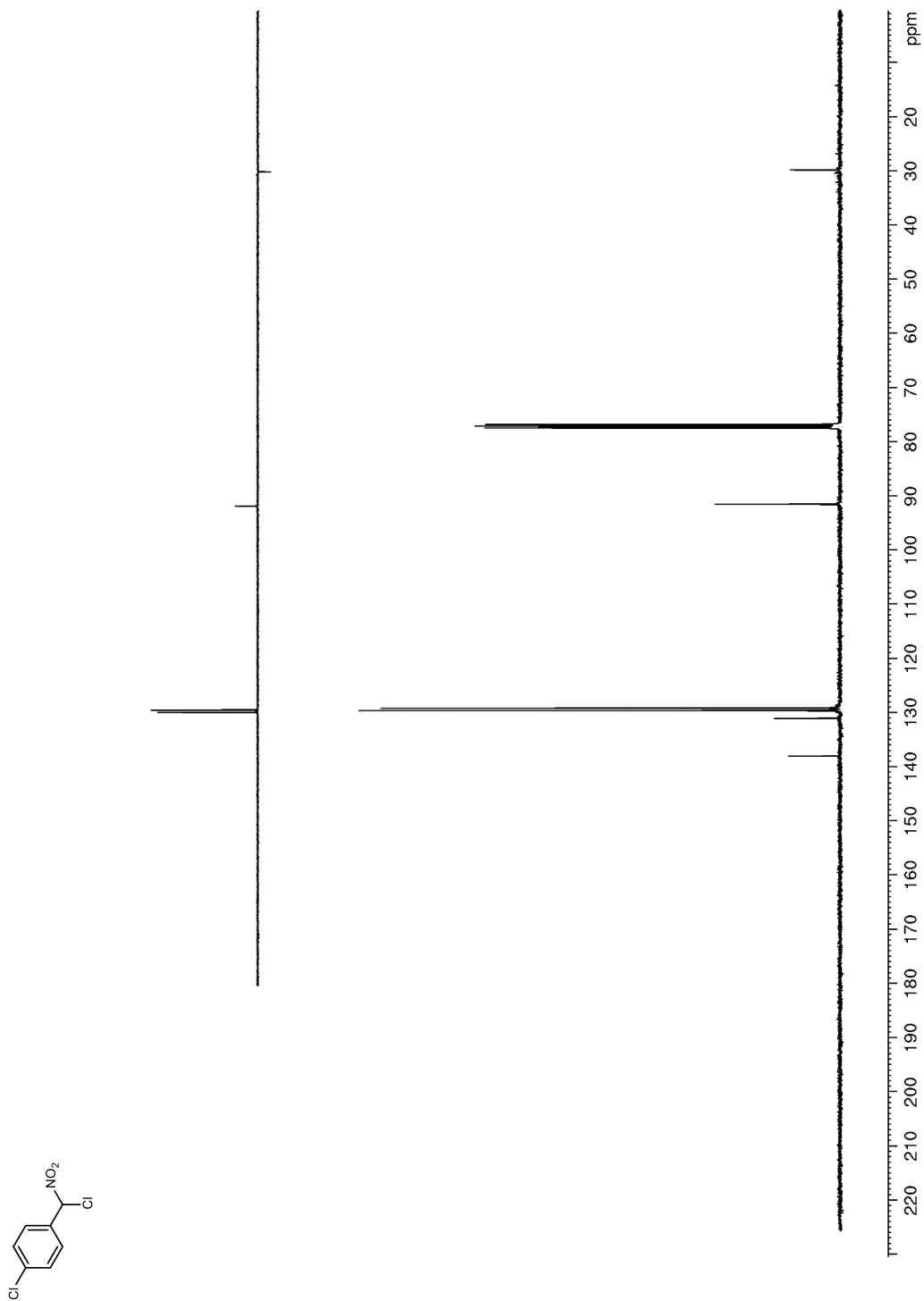


Figure 41. ^1H NMR (600 MHz, CDCl_3) of **79a**

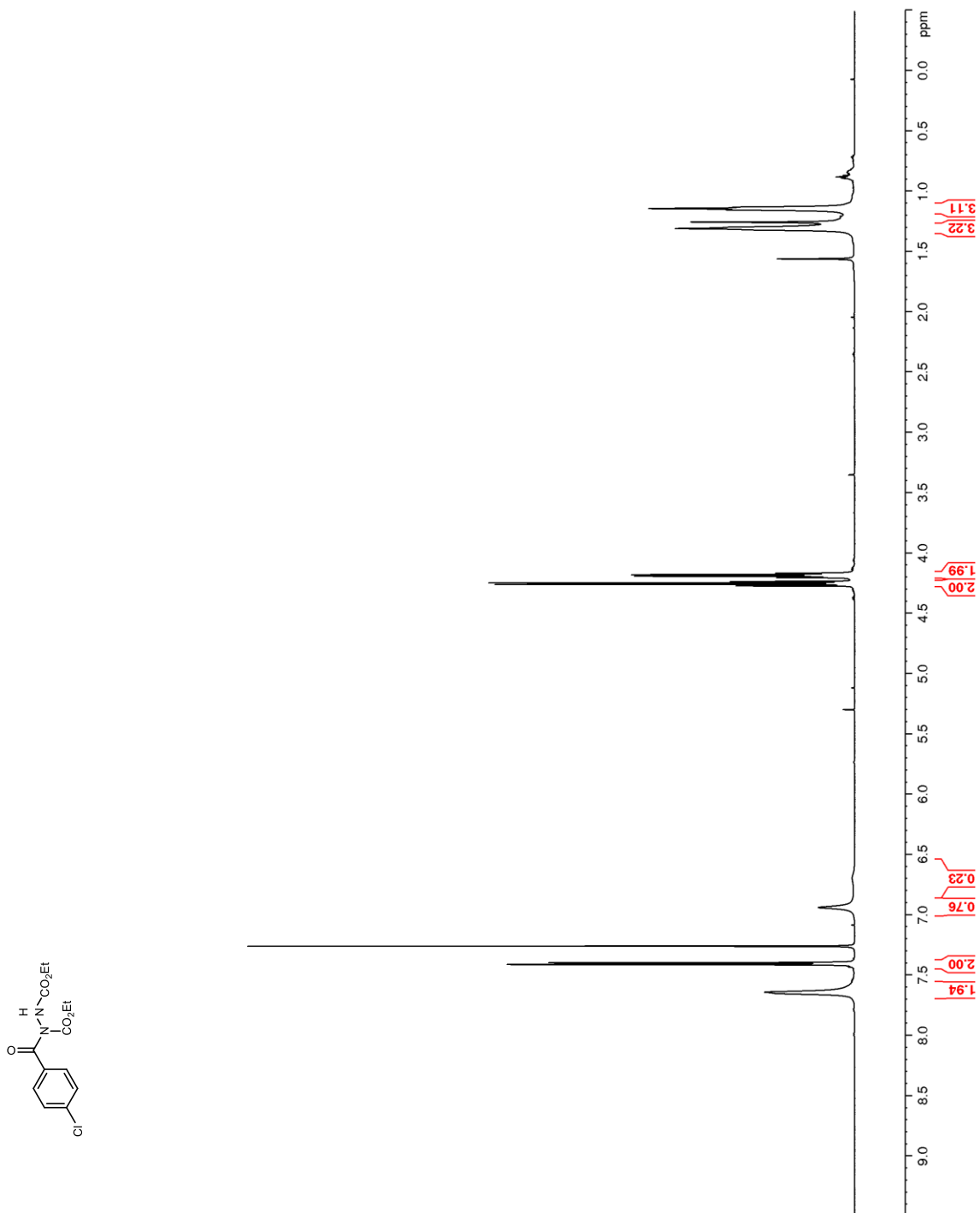


Figure 42. ^{13}C NMR (150 MHz, CDCl_3) of **79a**

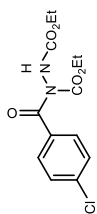
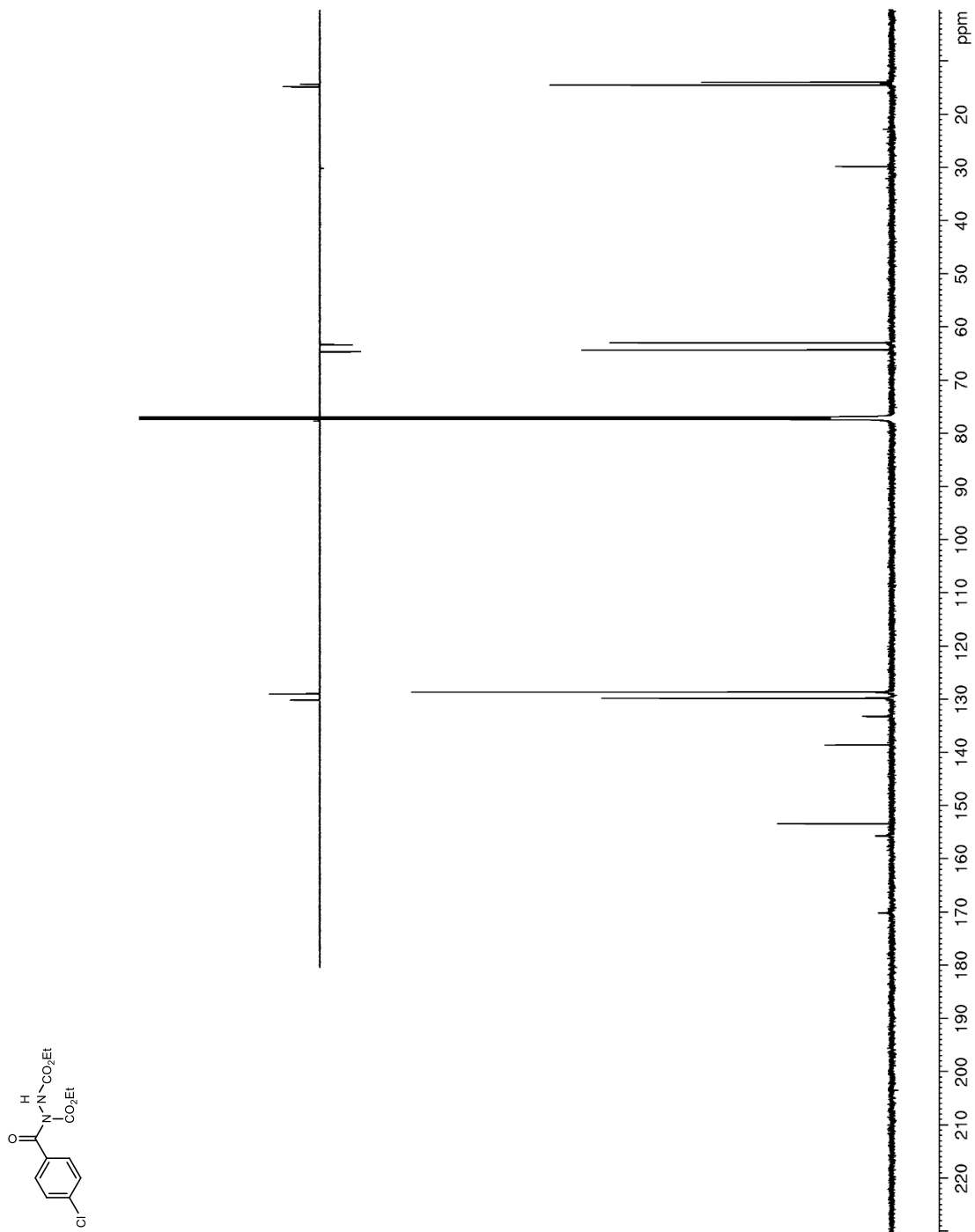


Figure 43. ^1H NMR (600 MHz, CDCl_3) of **79b**

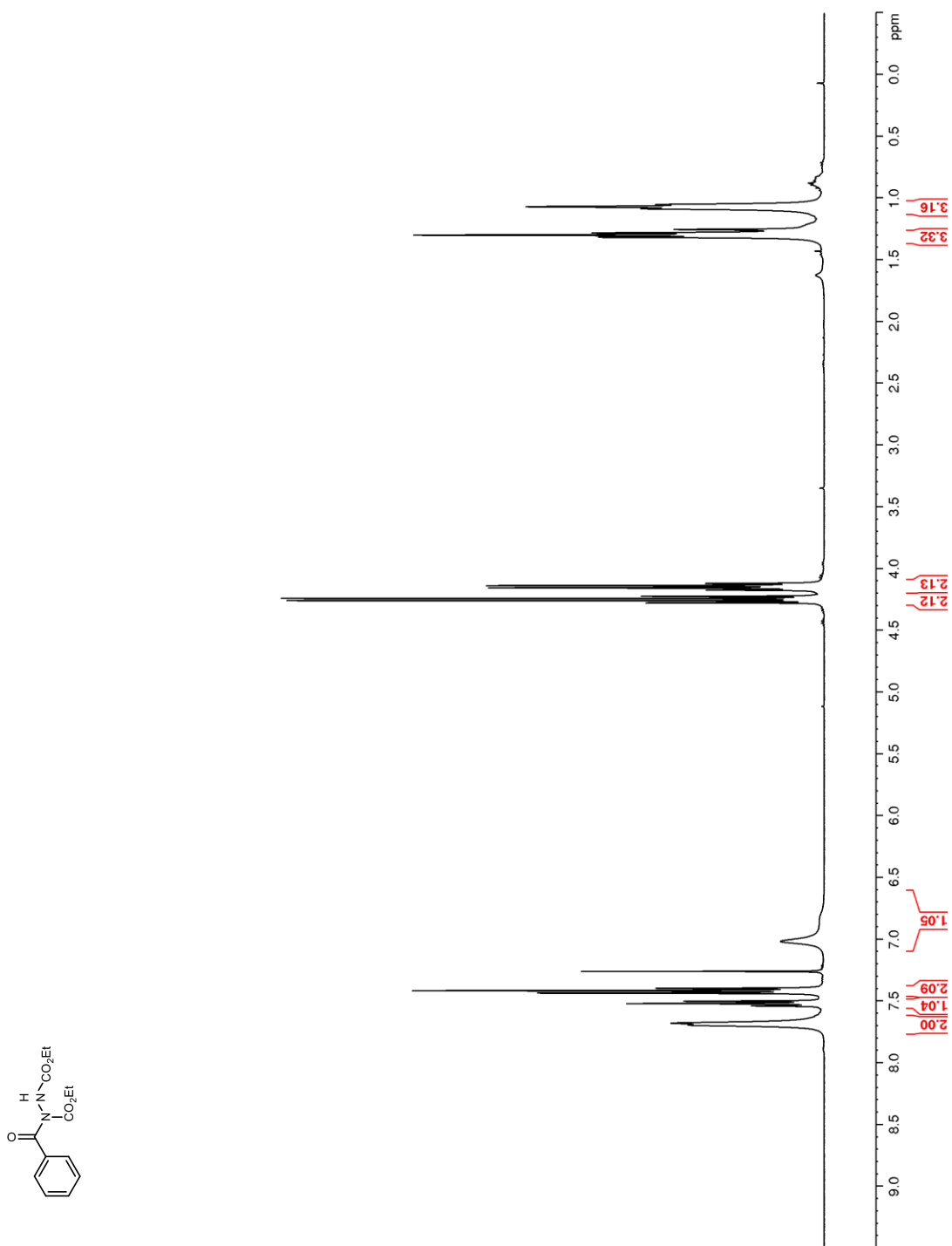


Figure 44. ^{13}C NMR (150 MHz, CDCl_3) of **79b**

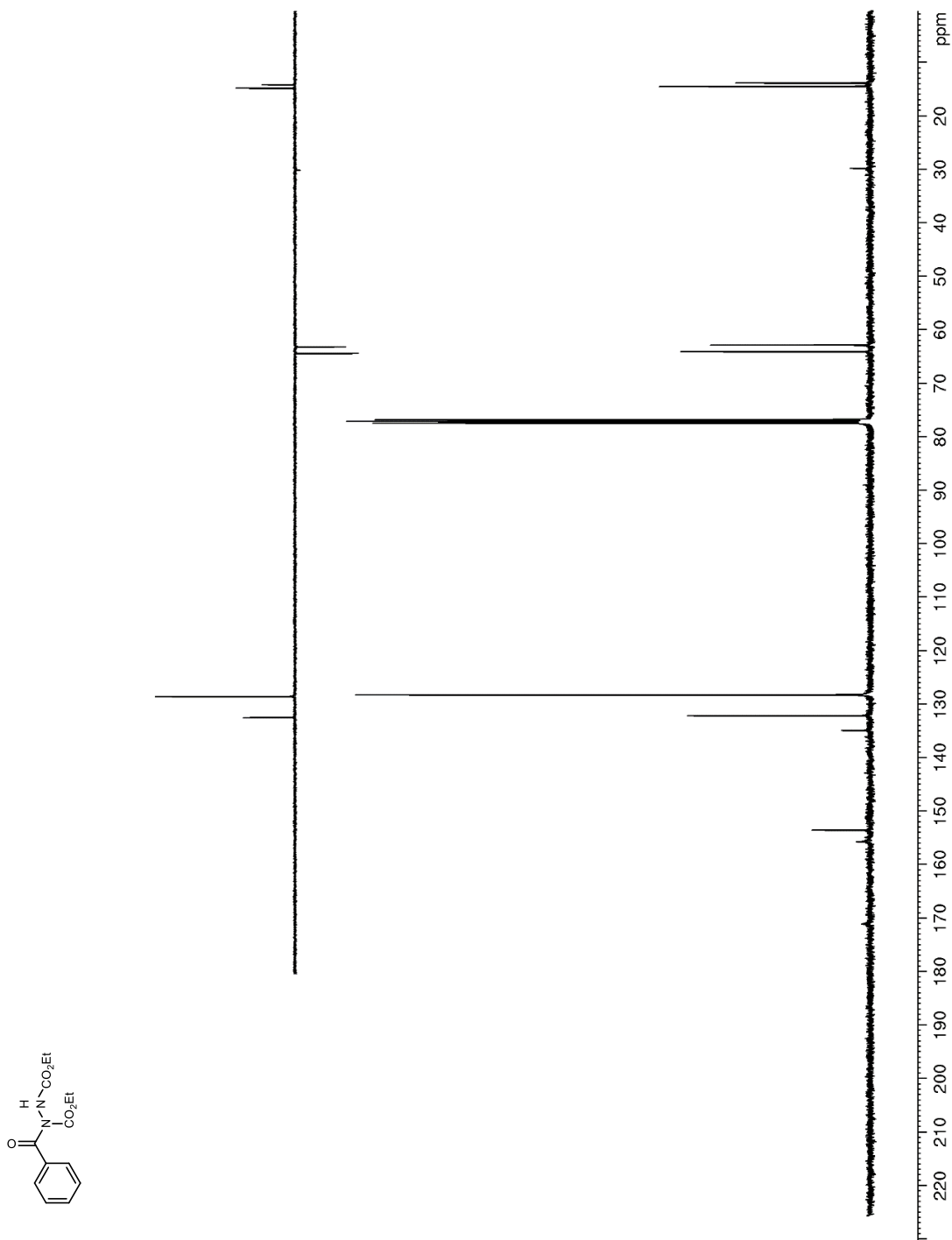


Figure 45. ^1H NMR (400 MHz, CDCl_3) of **79c**

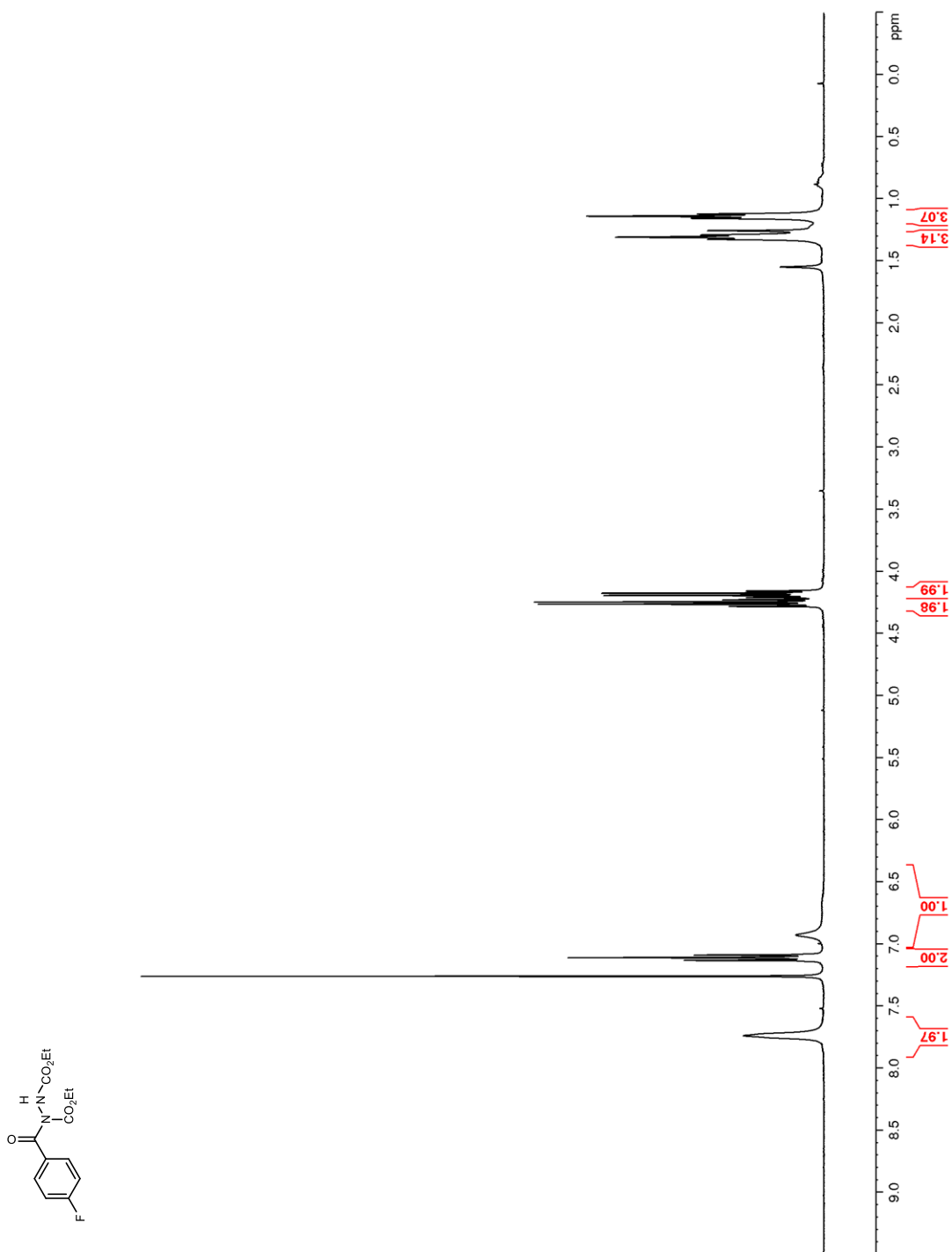


Figure 46. ^{13}C NMR (100 MHz, CDCl_3) of **79c**

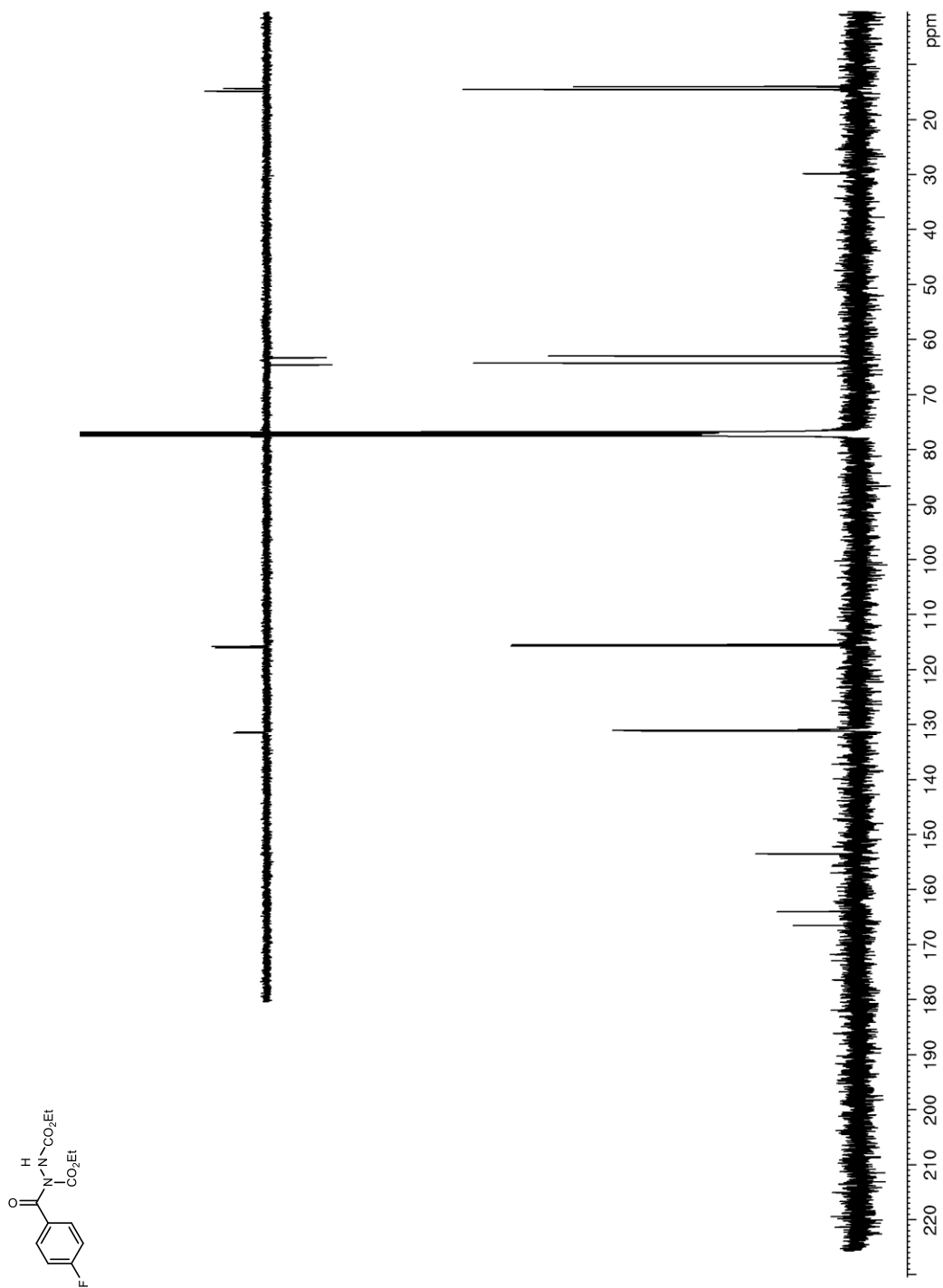


Figure 47. ^{19}F NMR (376 MHz, CDCl_3) of **79c**

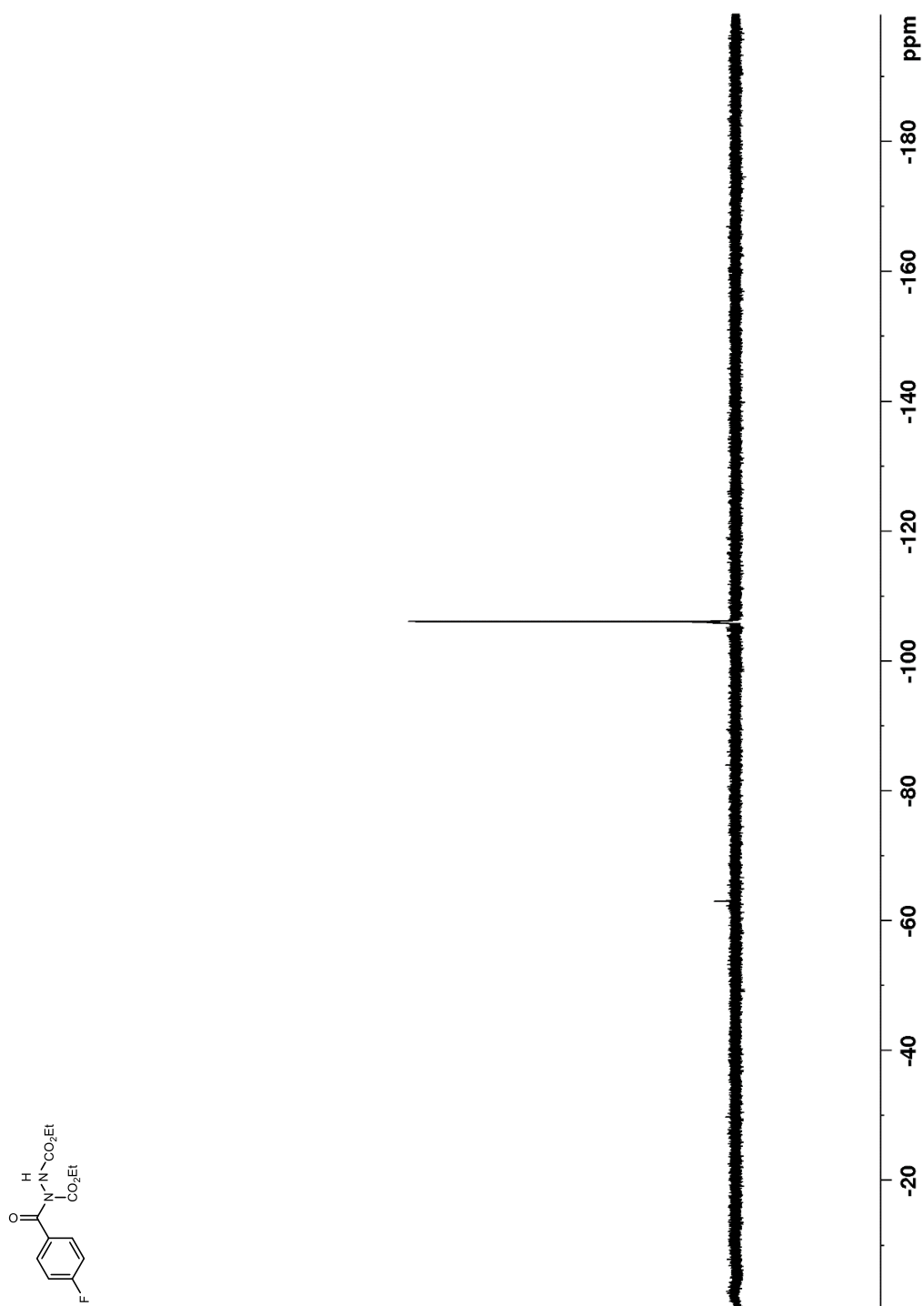


Figure 48. ^1H NMR (400 MHz, CDCl_3) of **79d**

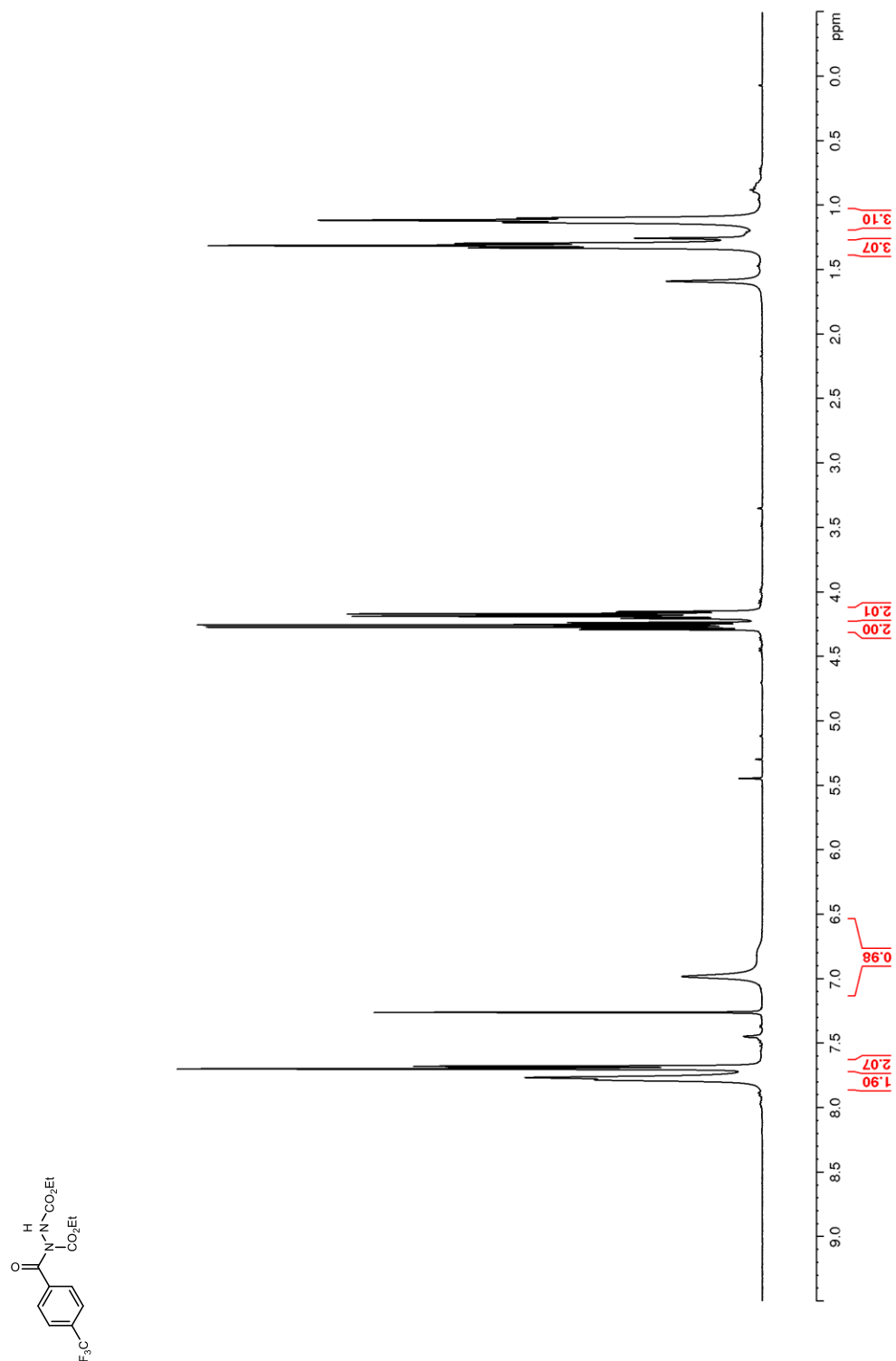


Figure 49. ^{13}C NMR (100 MHz, CDCl_3) of **79d**

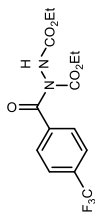
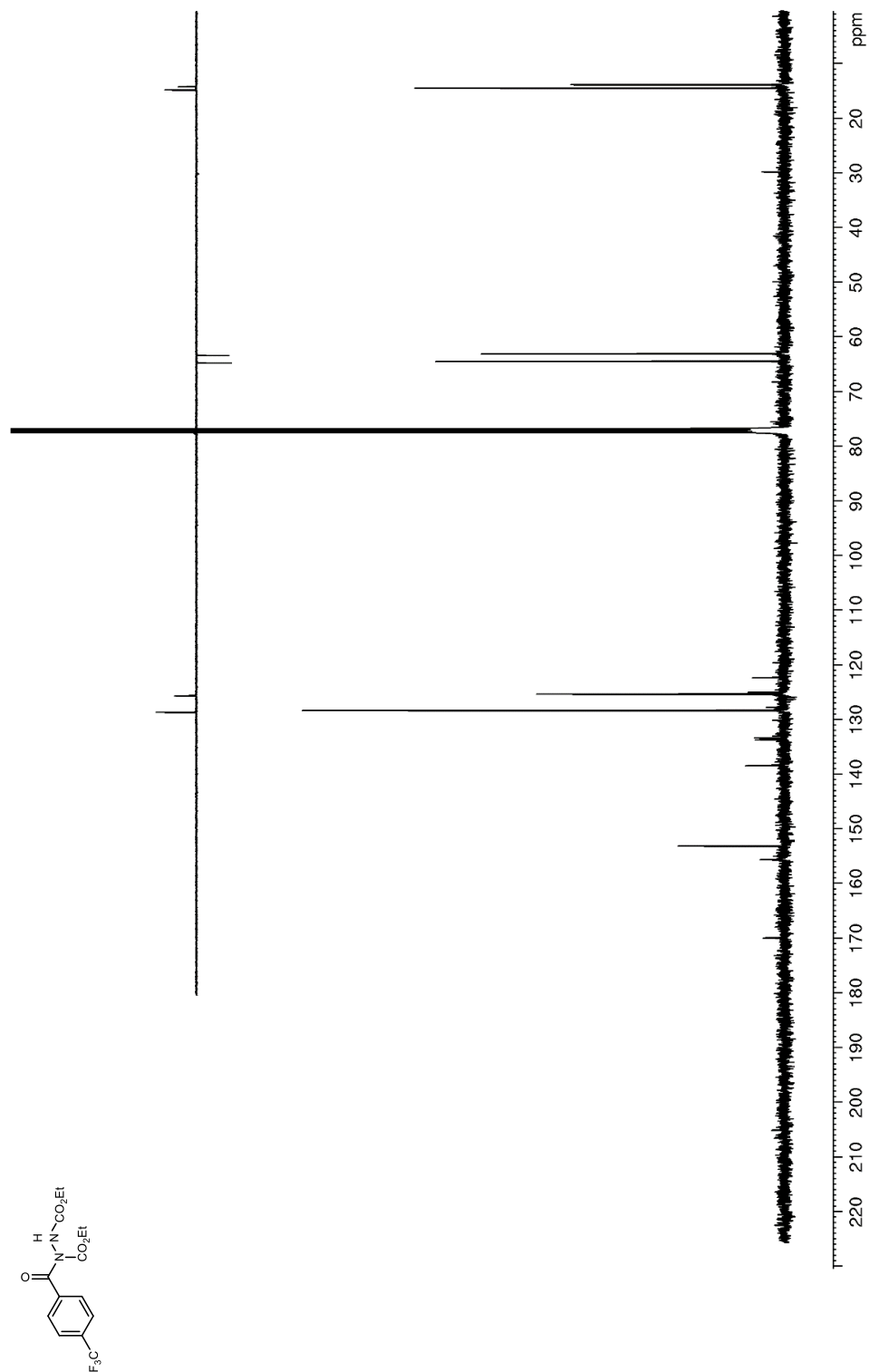


Figure 50. ^{19}F NMR (376 MHz, CDCl_3) of **79d**

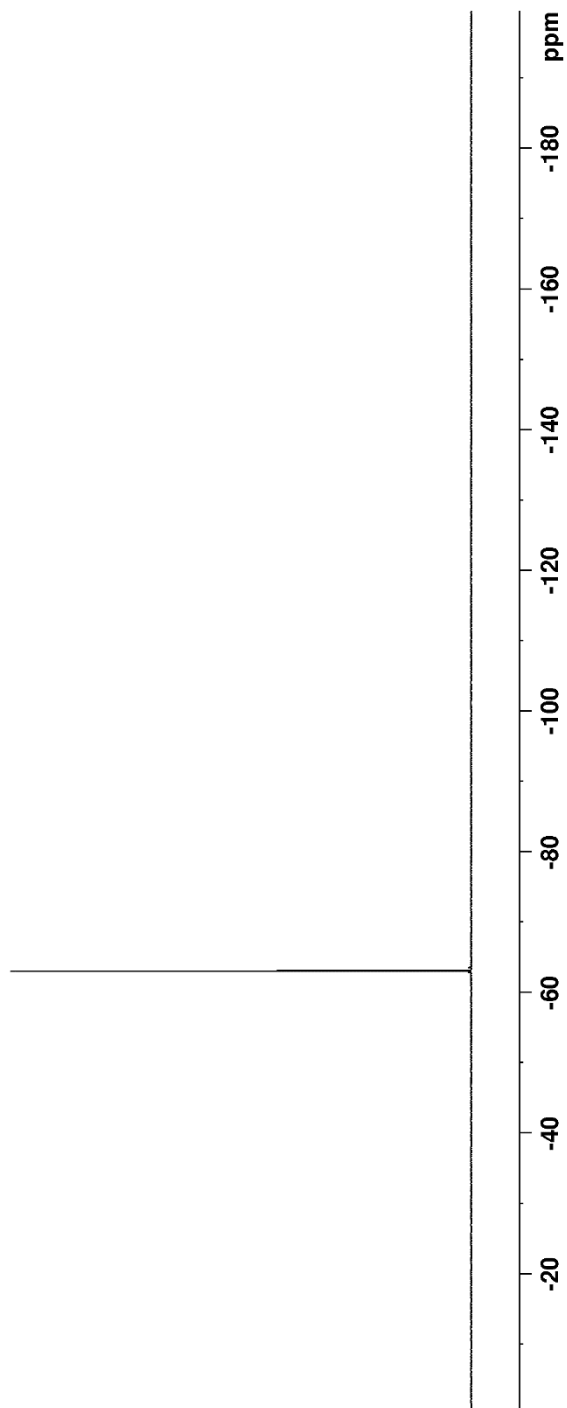
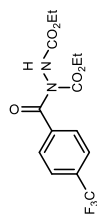


Figure 51. ^1H NMR (600 MHz, CDCl_3) of **79e**

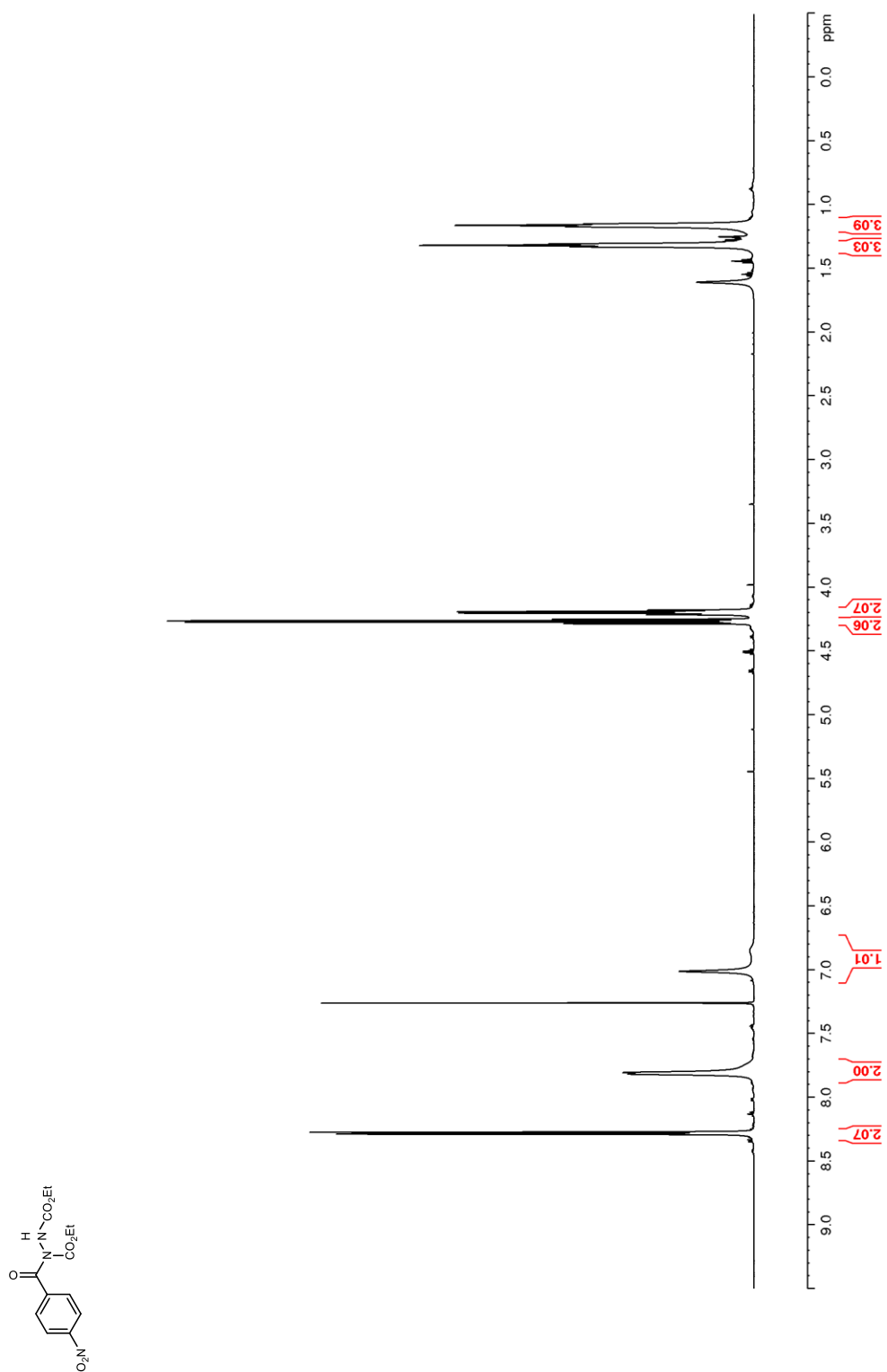


Figure 52. ^{13}C NMR (150 MHz, CDCl_3) of **79e**

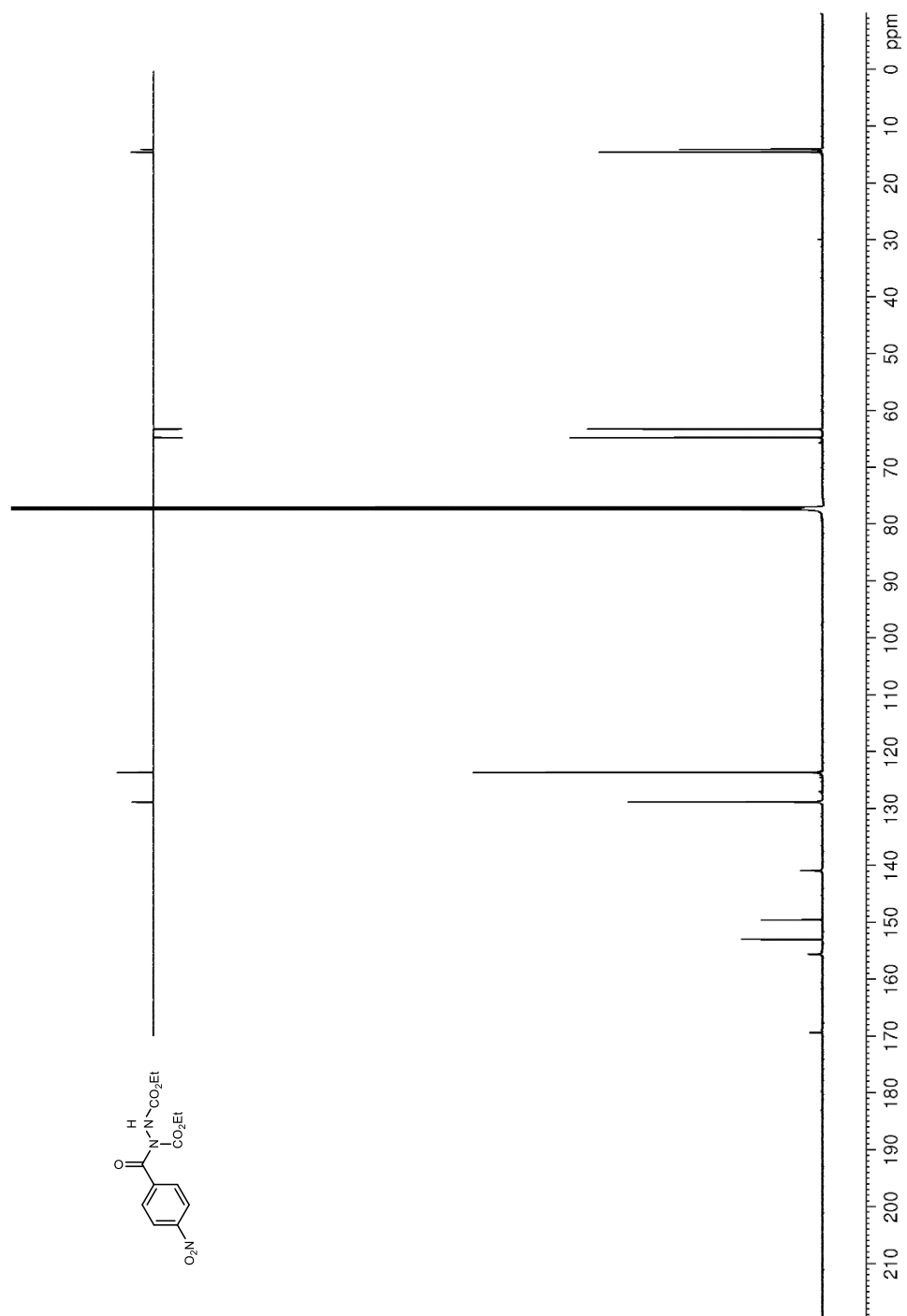


Figure 53. ^1H NMR (400 MHz, DMSO-d_6) of **85a**

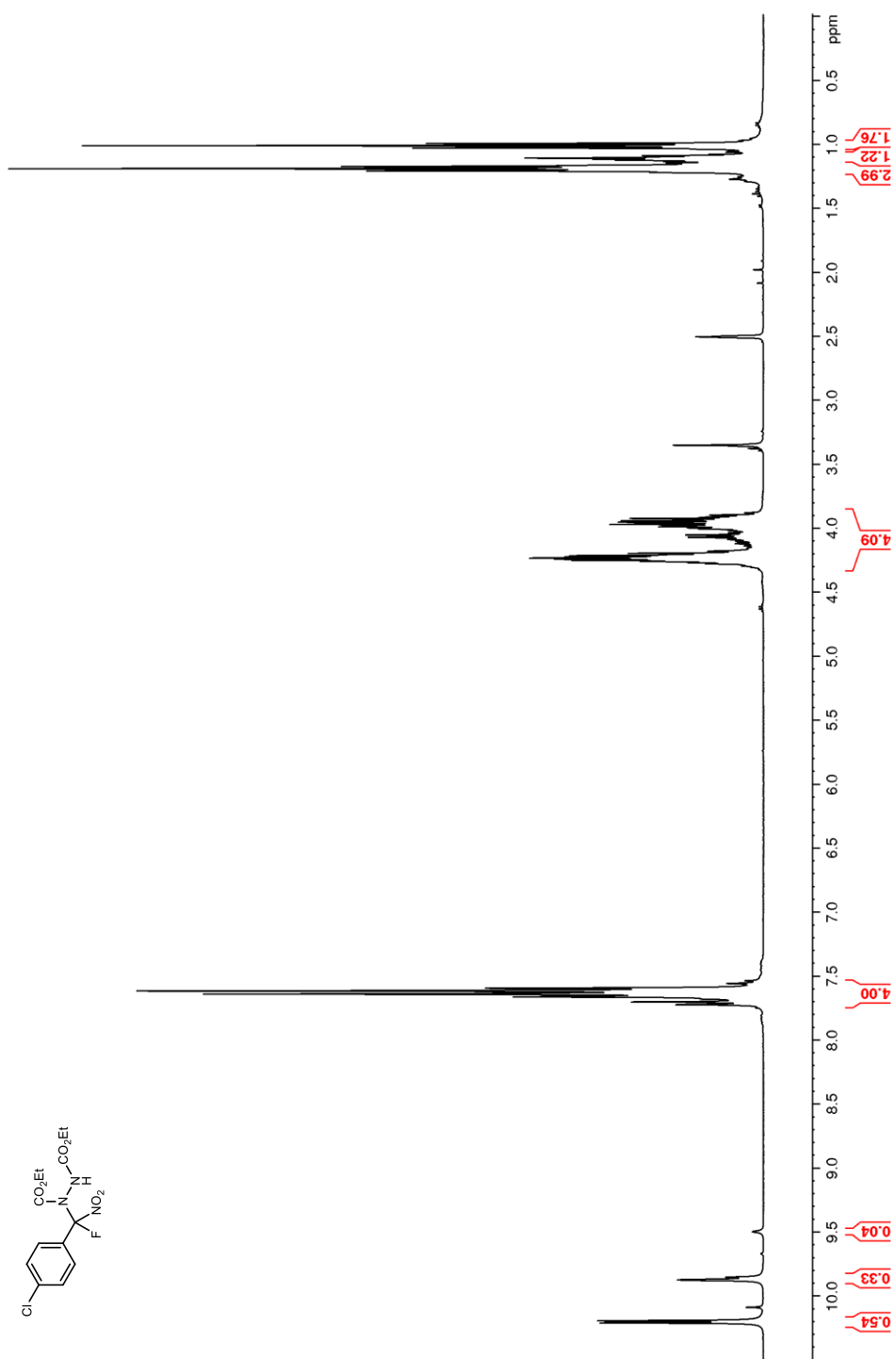


Figure 54. ^{13}C NMR (100 MHz, DMSO-d_6) of **85a**

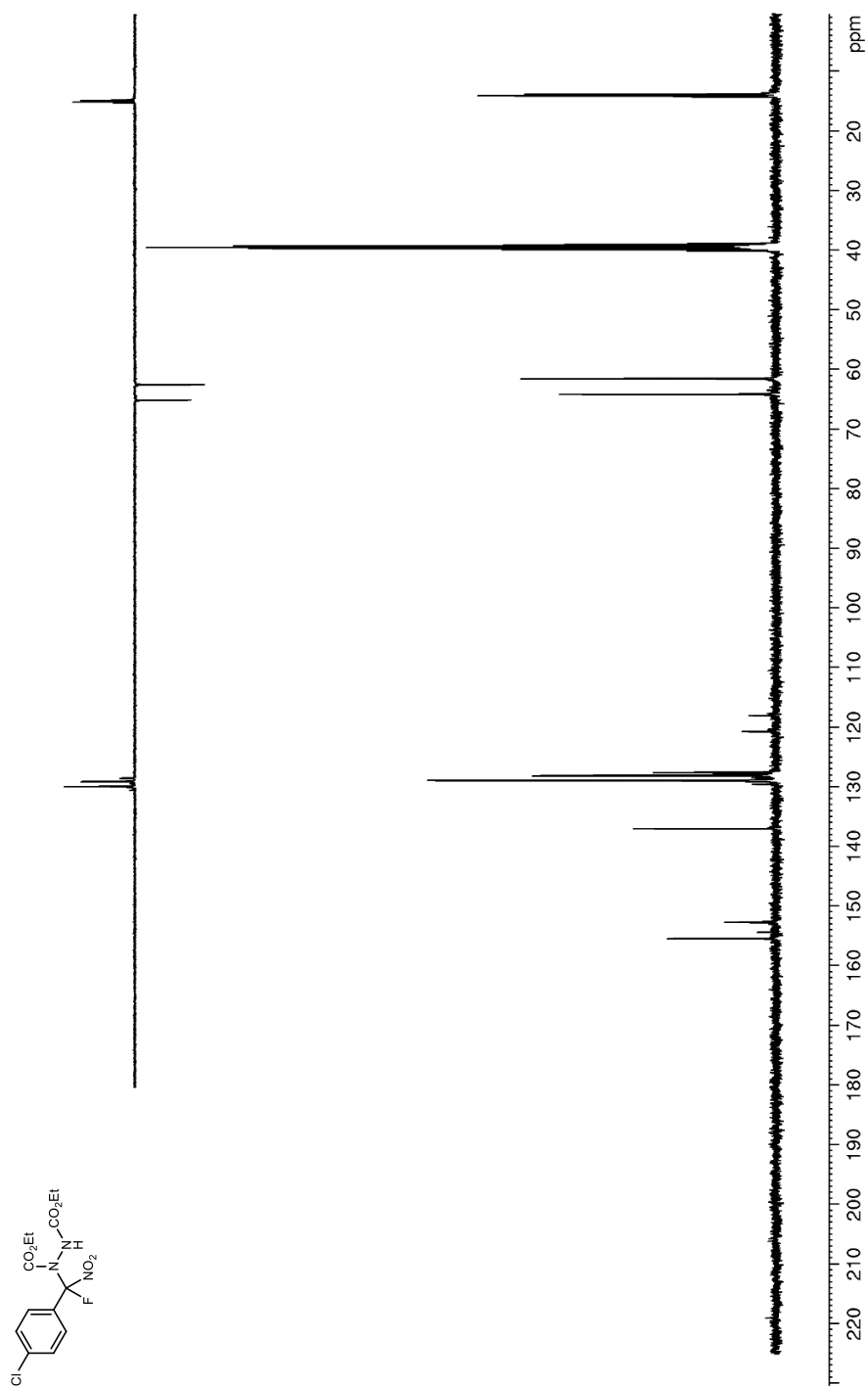


Figure 55. ^{19}F NMR (376 MHz, CDCl_3) of **85a**

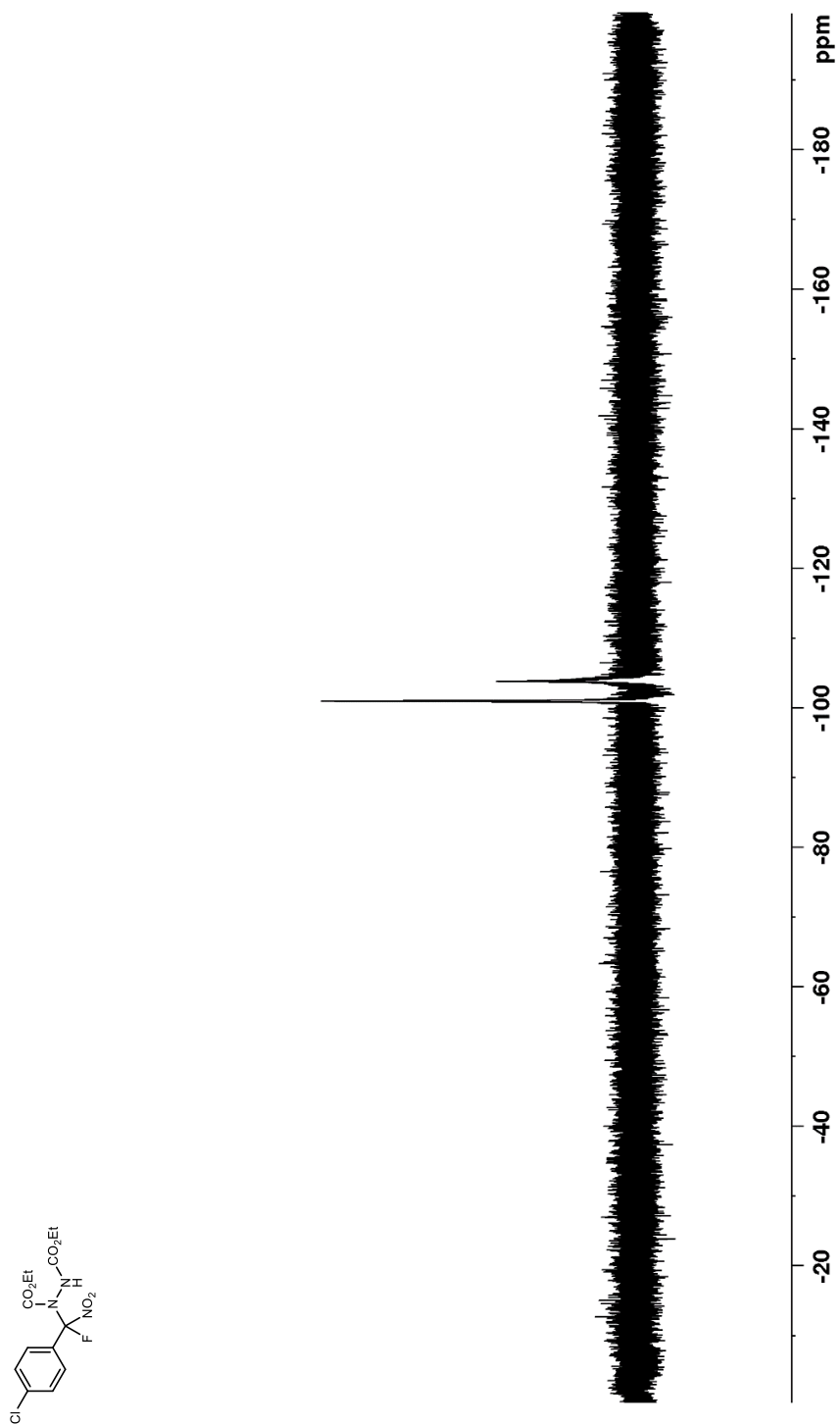


Figure 56. ^1H NMR (600 MHz, CDCl_3) of **85b**

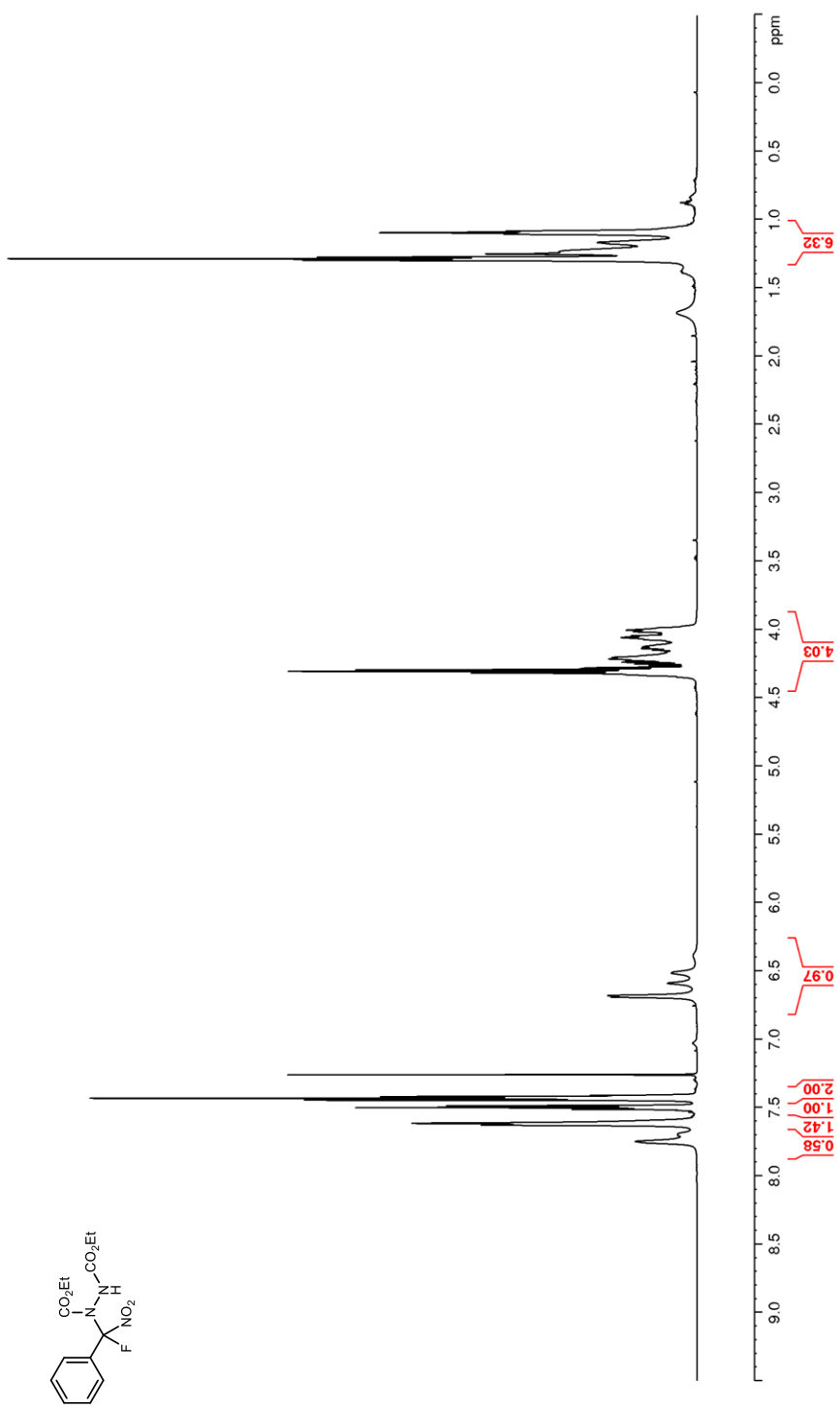


Figure 57. ^{13}C NMR (150 MHz, CDCl_3) of **85b**

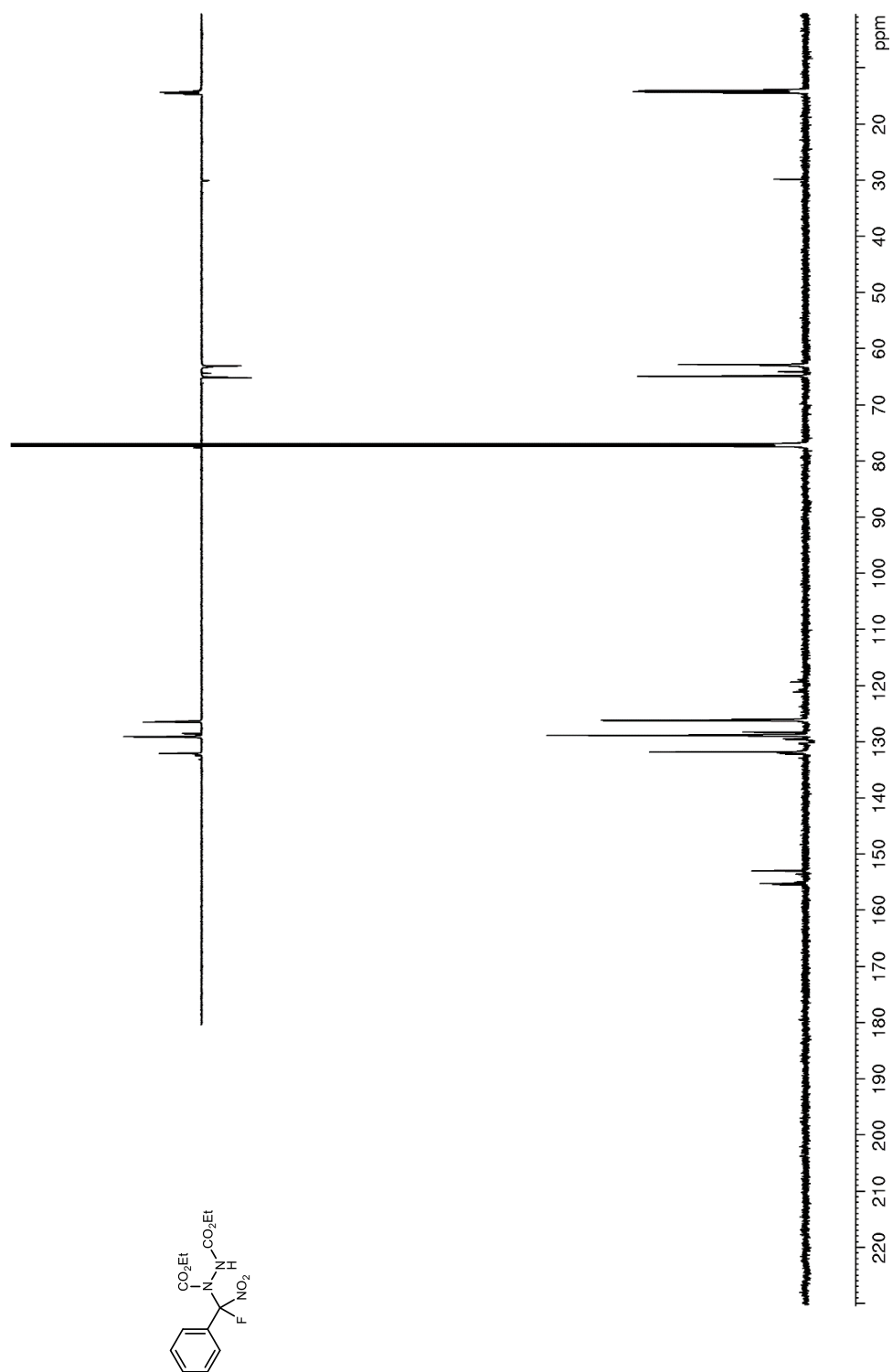


Figure 58. ^{19}F NMR (376 MHz, CDCl_3) of **85b**

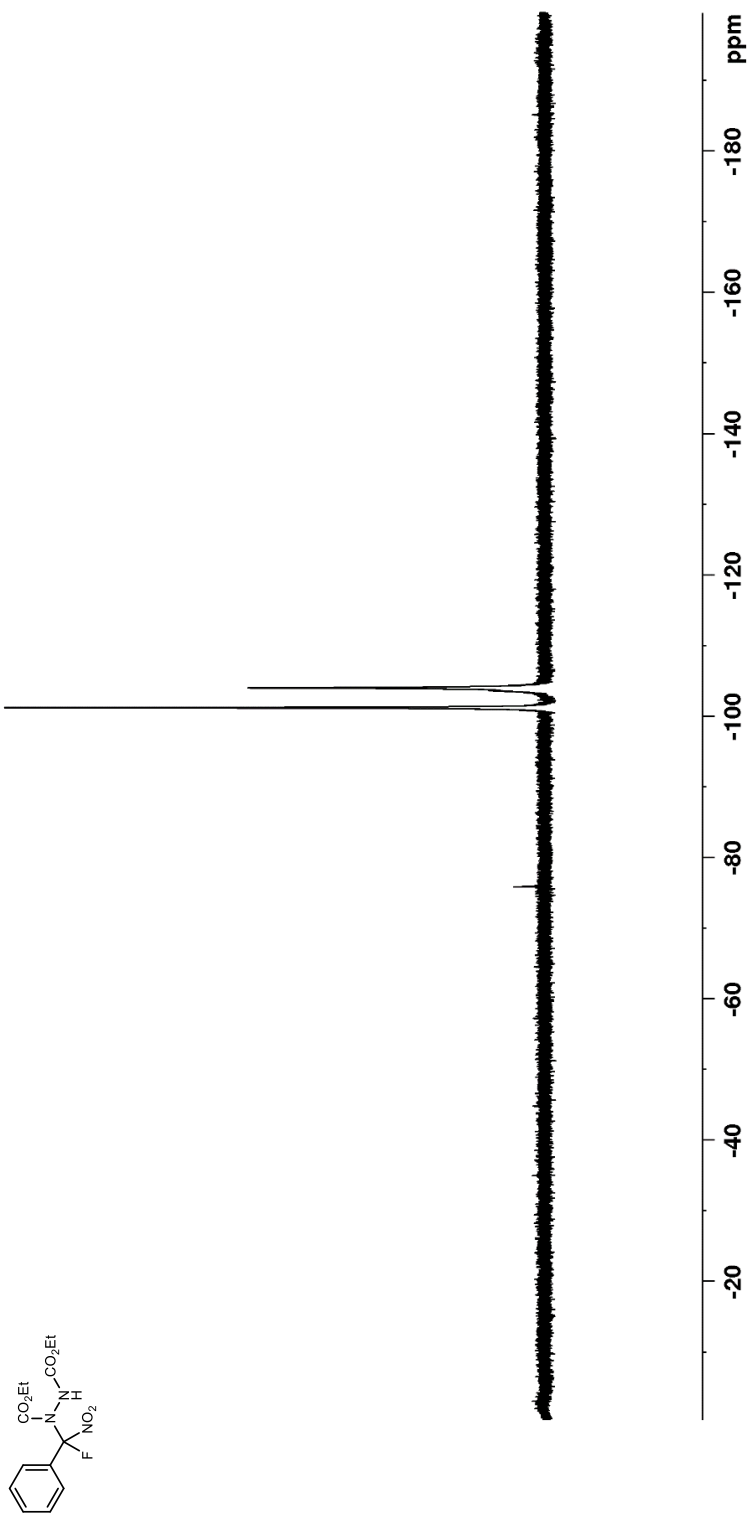


Figure 60. ^{13}C NMR (150 MHz, CDCl_3) of **85c**

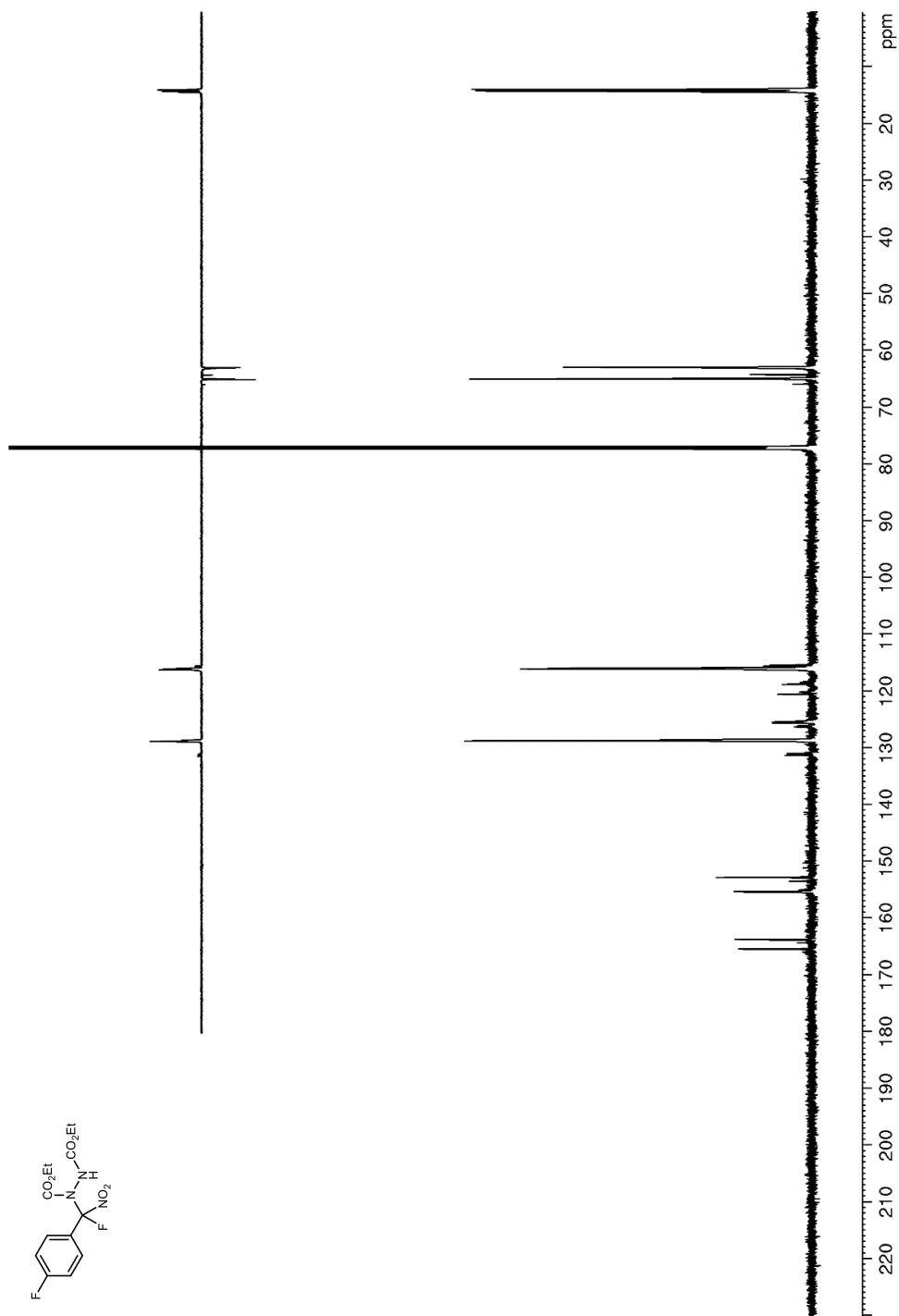


Figure 61. ^{19}F NMR (376 MHz, CDCl_3) of **85c**

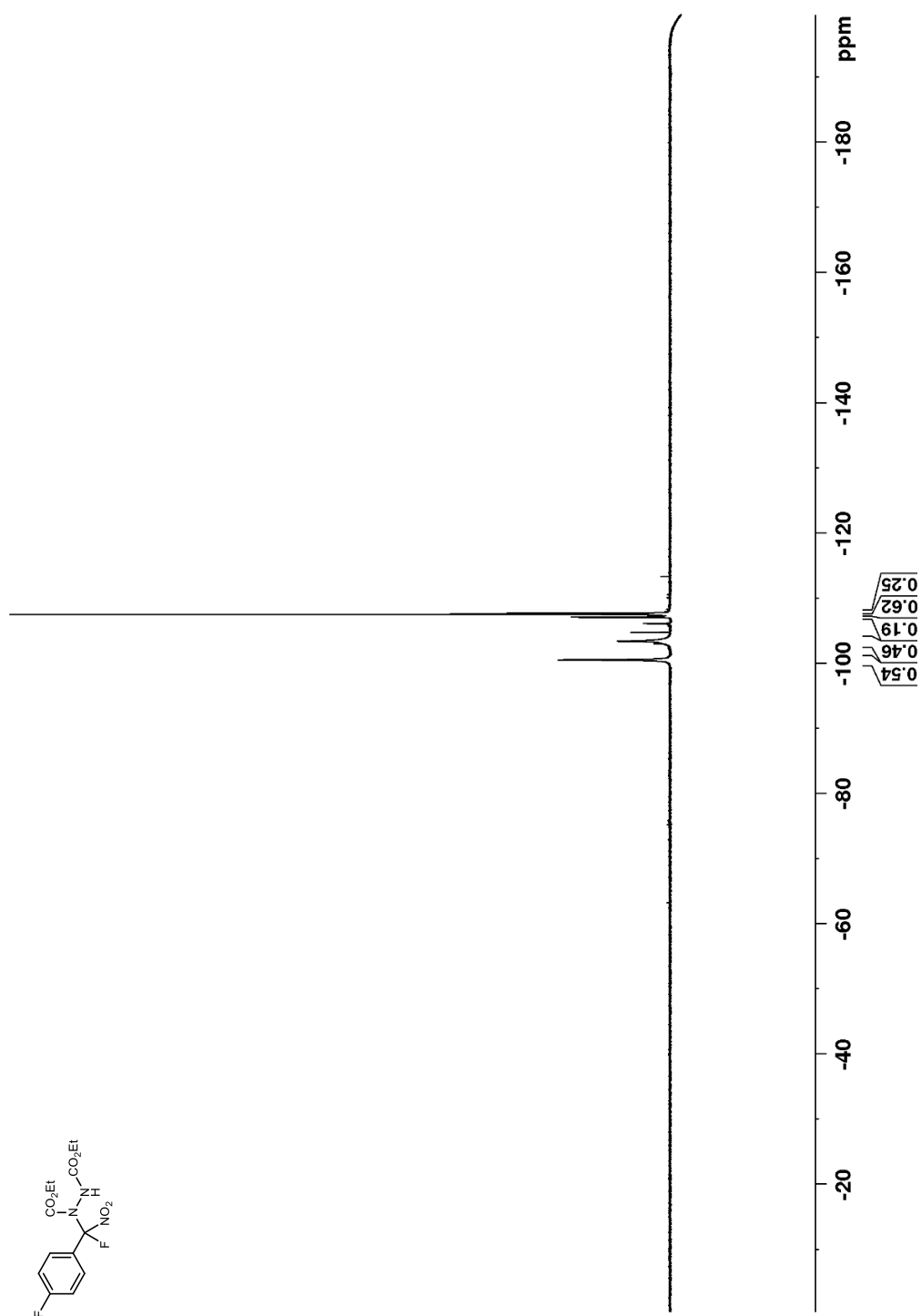


Figure 62. ^1H NMR (400 MHz, DMSO-d_6) of **85d**

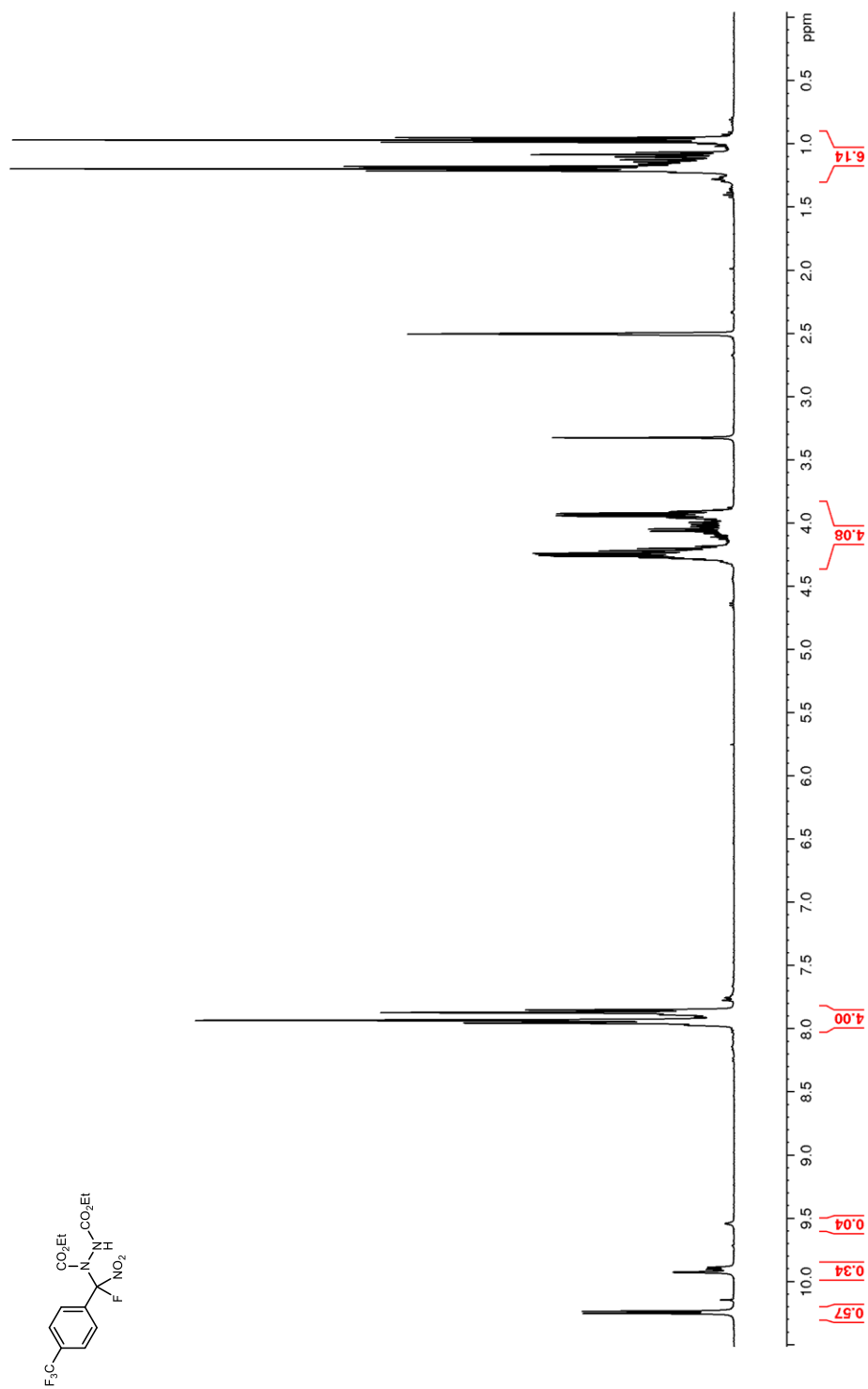


Figure 63. ^{13}C NMR (100 MHz, DMSO-d_6) of **85d**

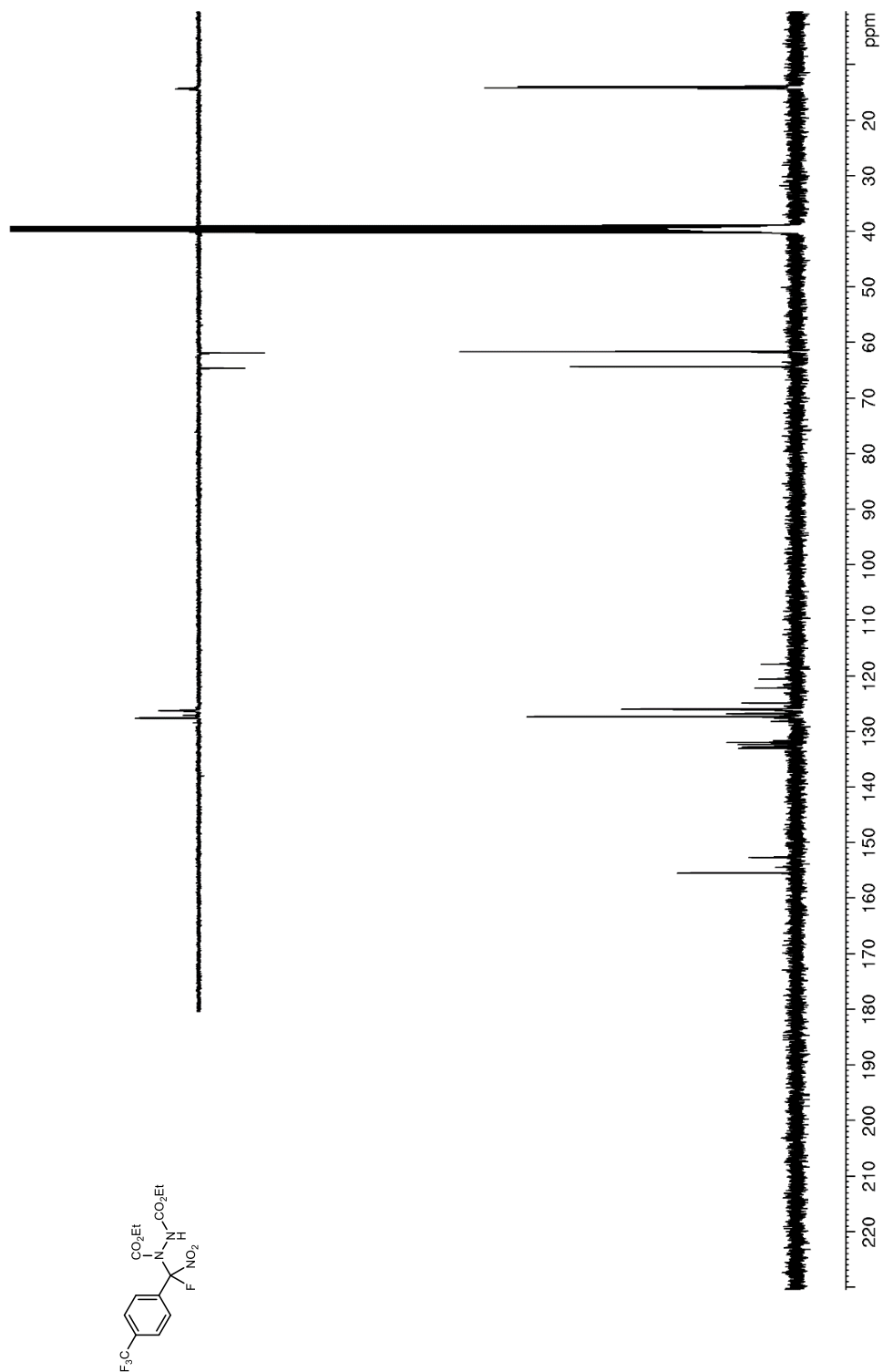


Figure 64. ^{19}F NMR (376 MHz, CDCl_3) of **85d**

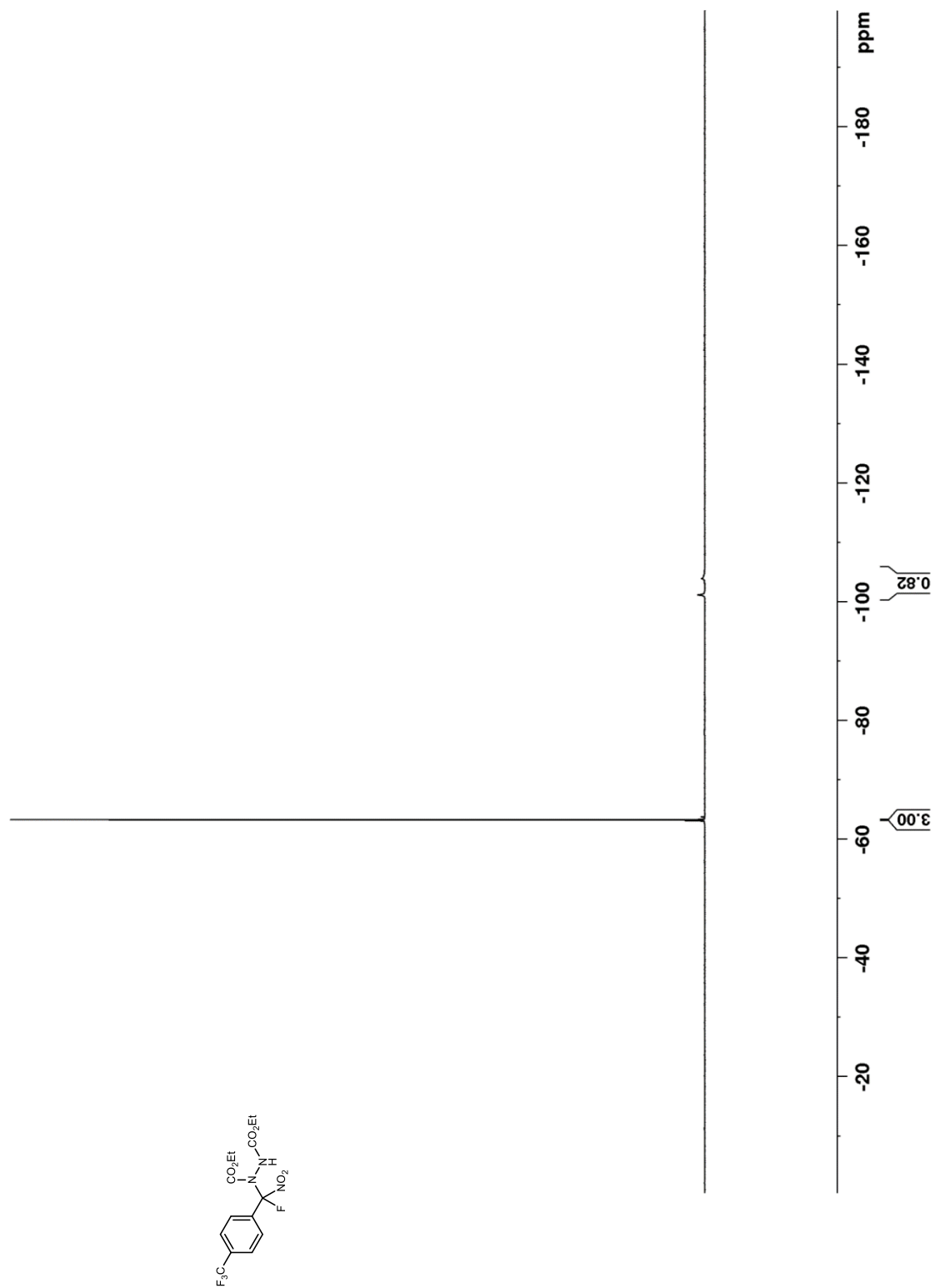


Figure 65. ^1H NMR (600 MHz, CDCl_3) of **85e**

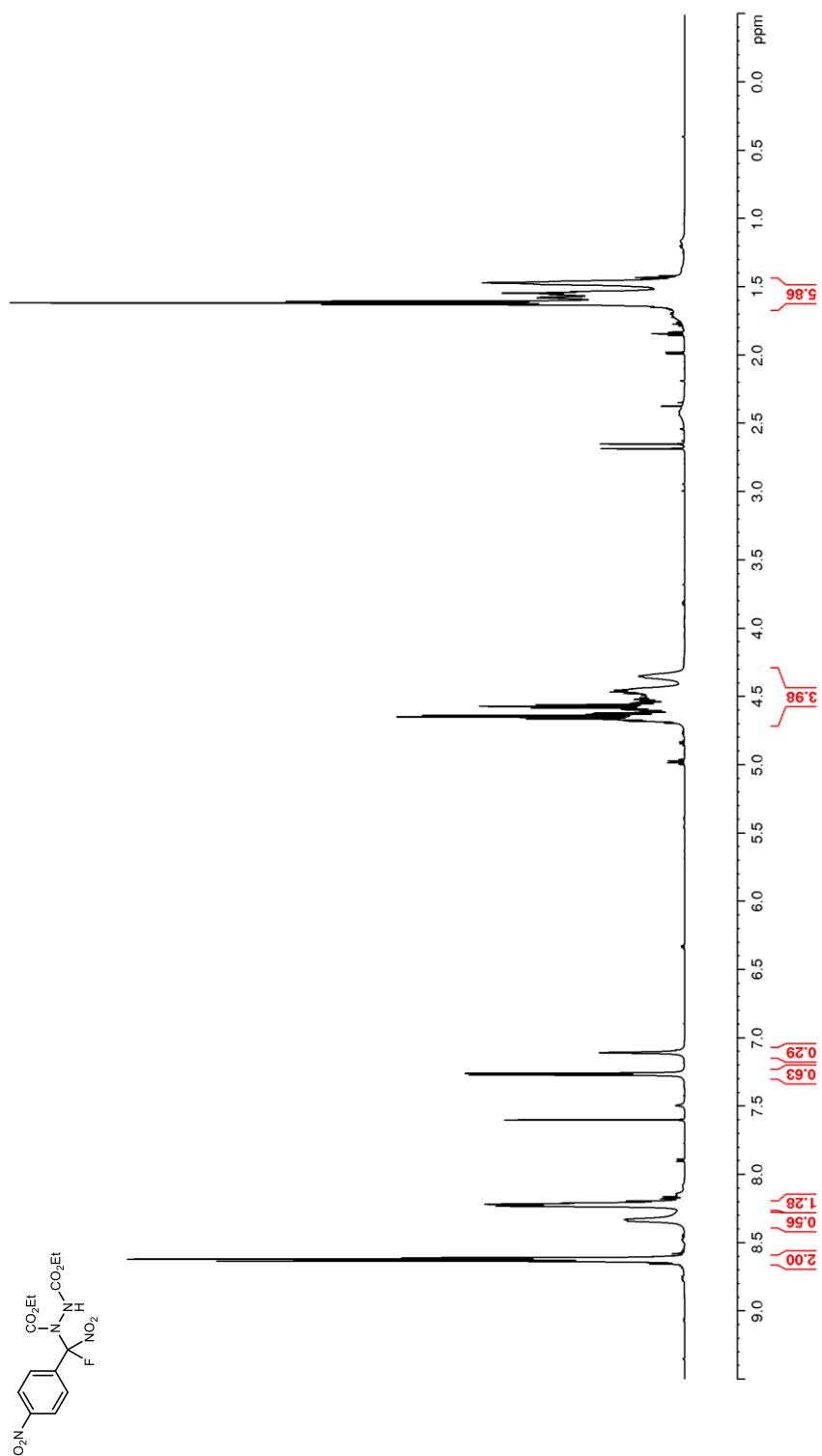


Figure 66. ^{13}C NMR (150 MHz, CDCl_3) of **85e**

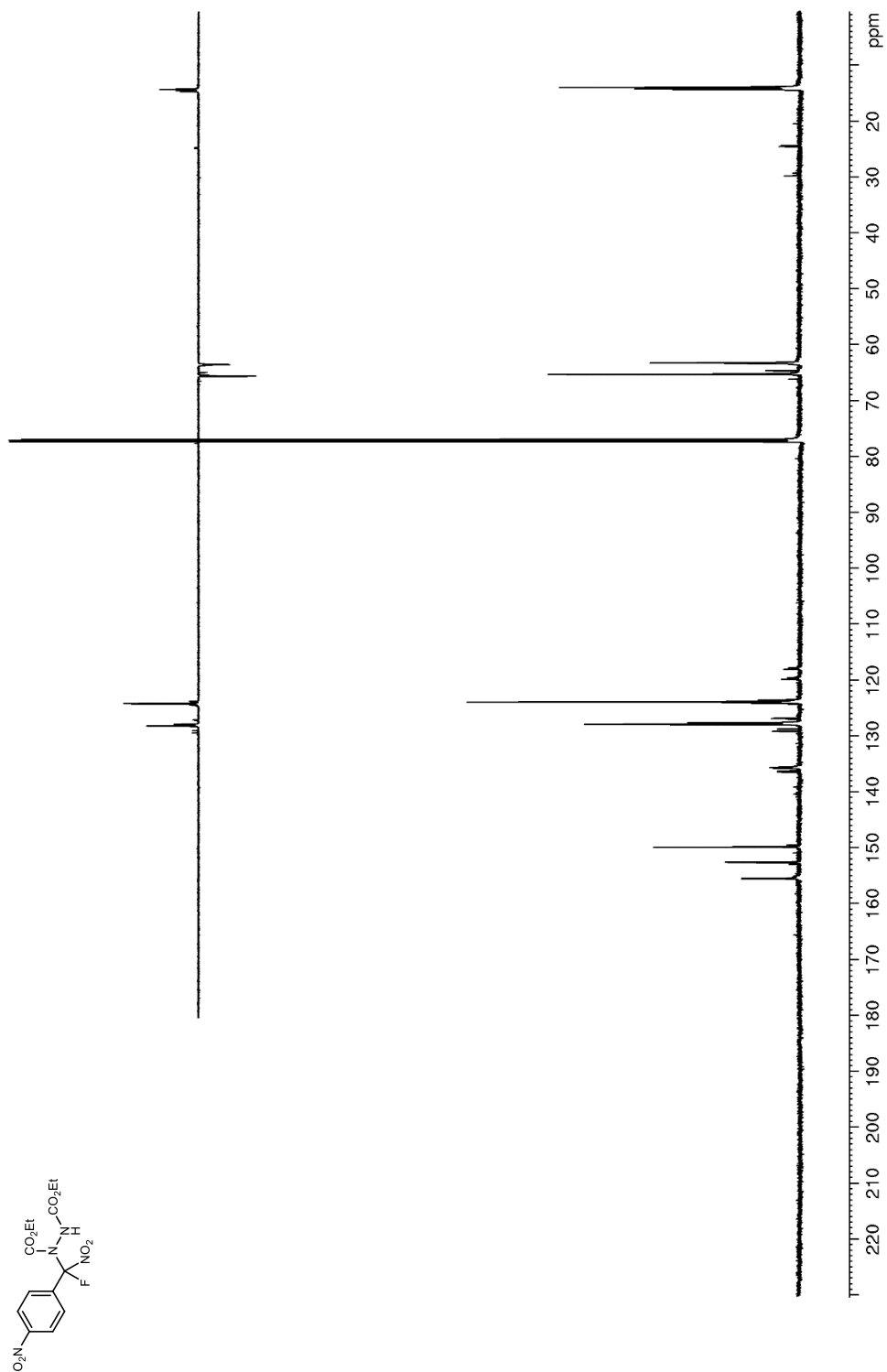


Figure 67. ^{19}F NMR (376 MHz, CDCl_3) of **85e**

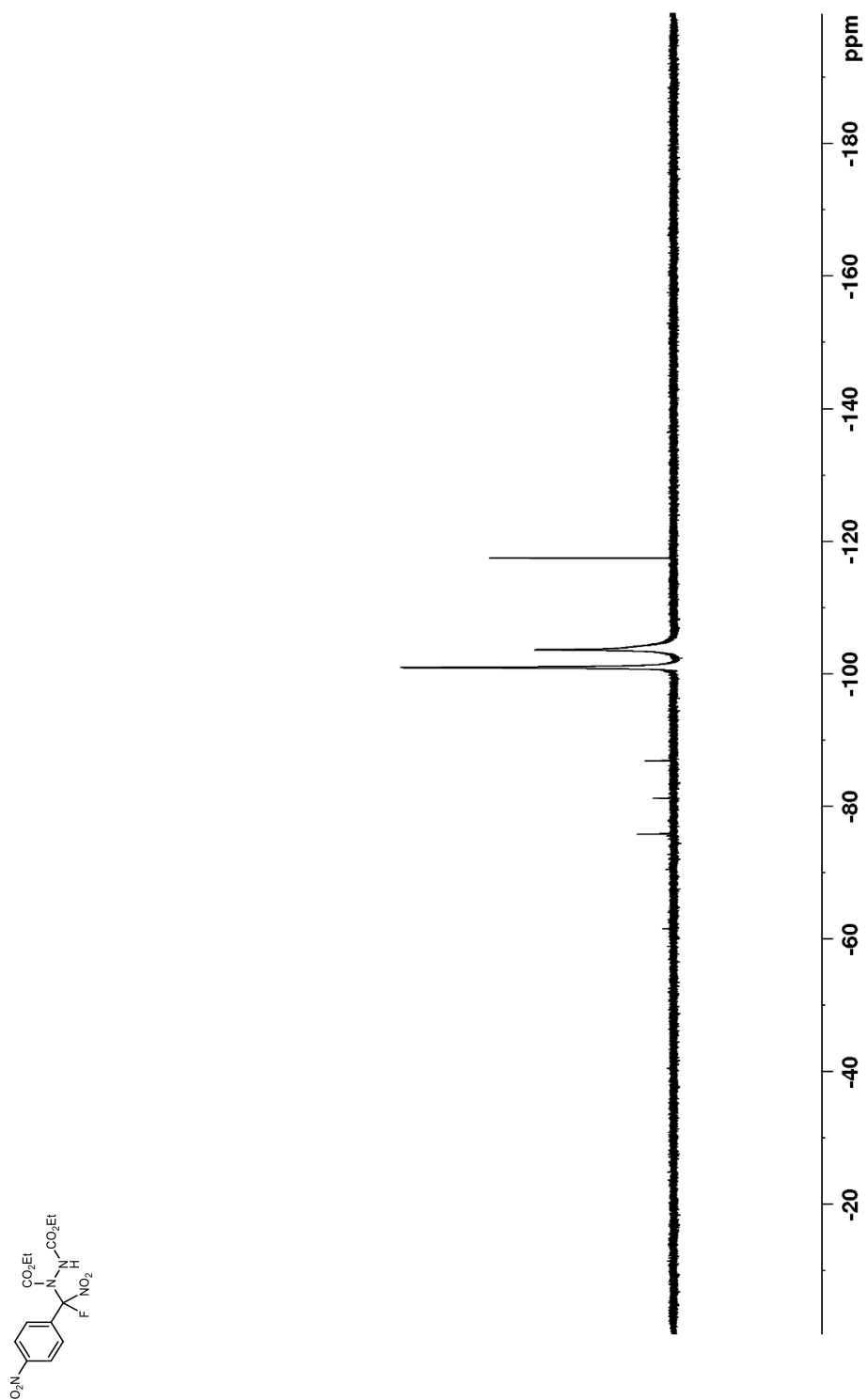


Figure 68. ^1H NMR (600 MHz, CDCl_3) of **88**

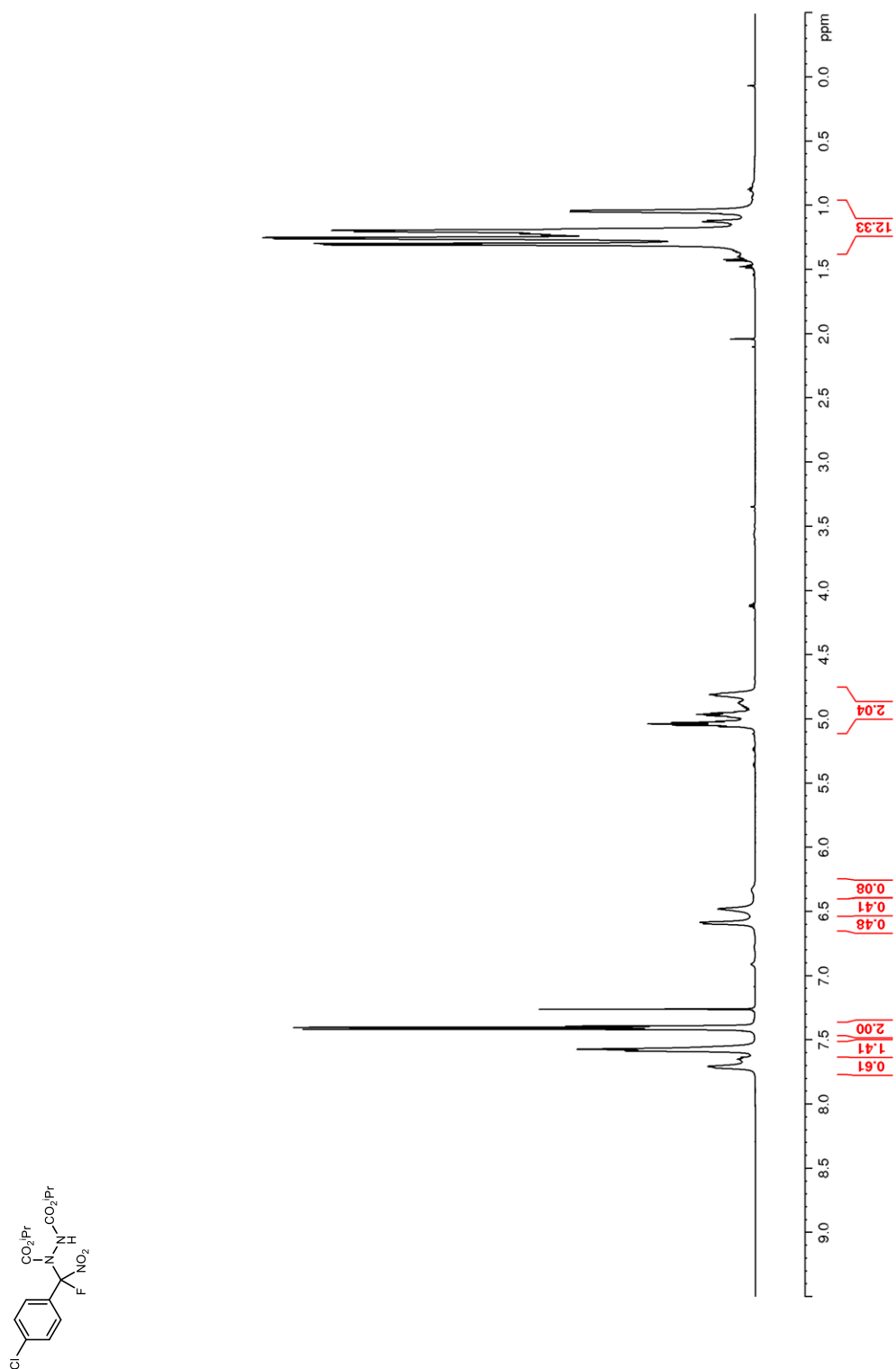


Figure 69. ^{13}C NMR (150 MHz, CDCl_3) of **88**

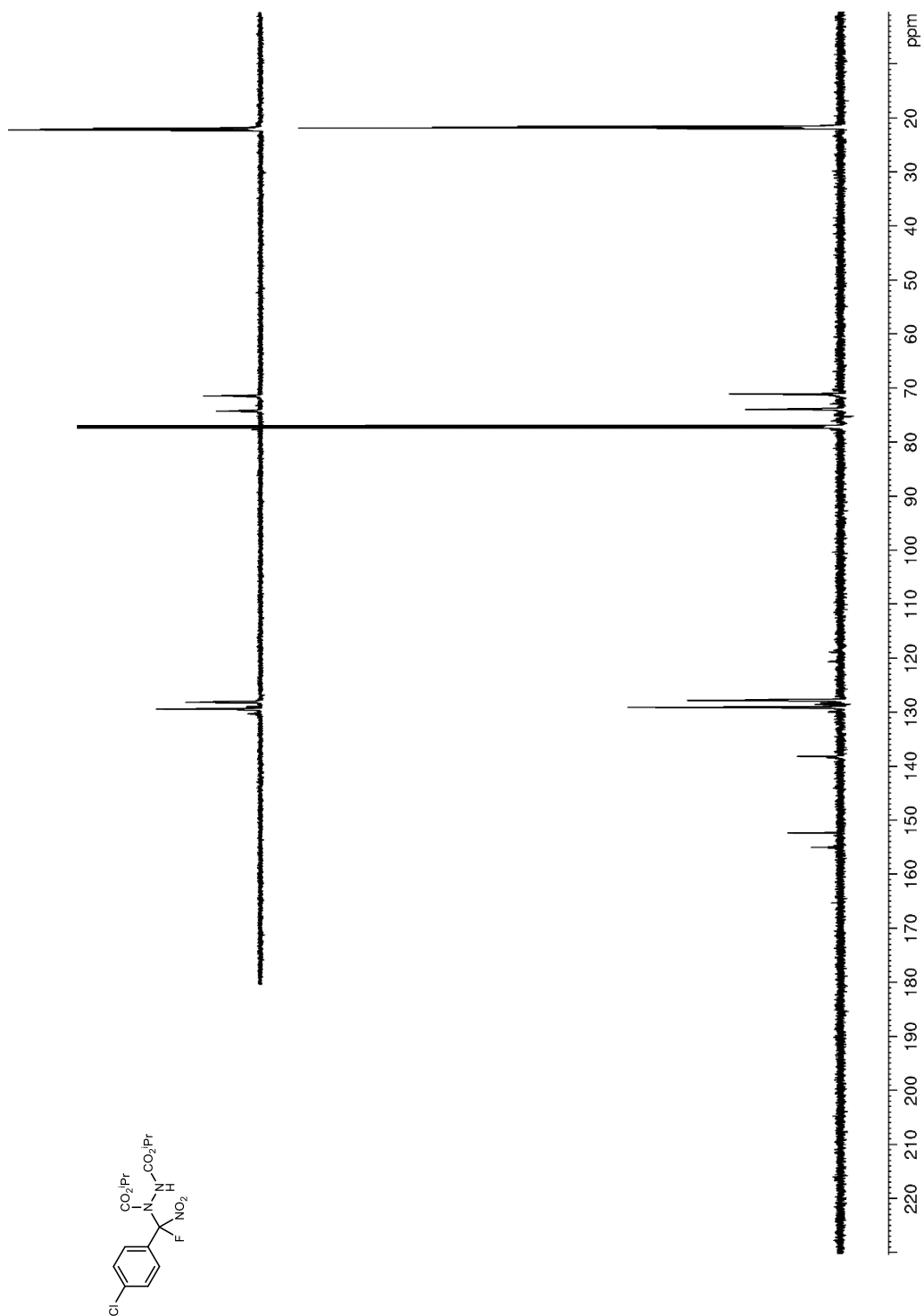


Figure 70. ^{19}F NMR (376 MHz, CDCl_3) of **88**

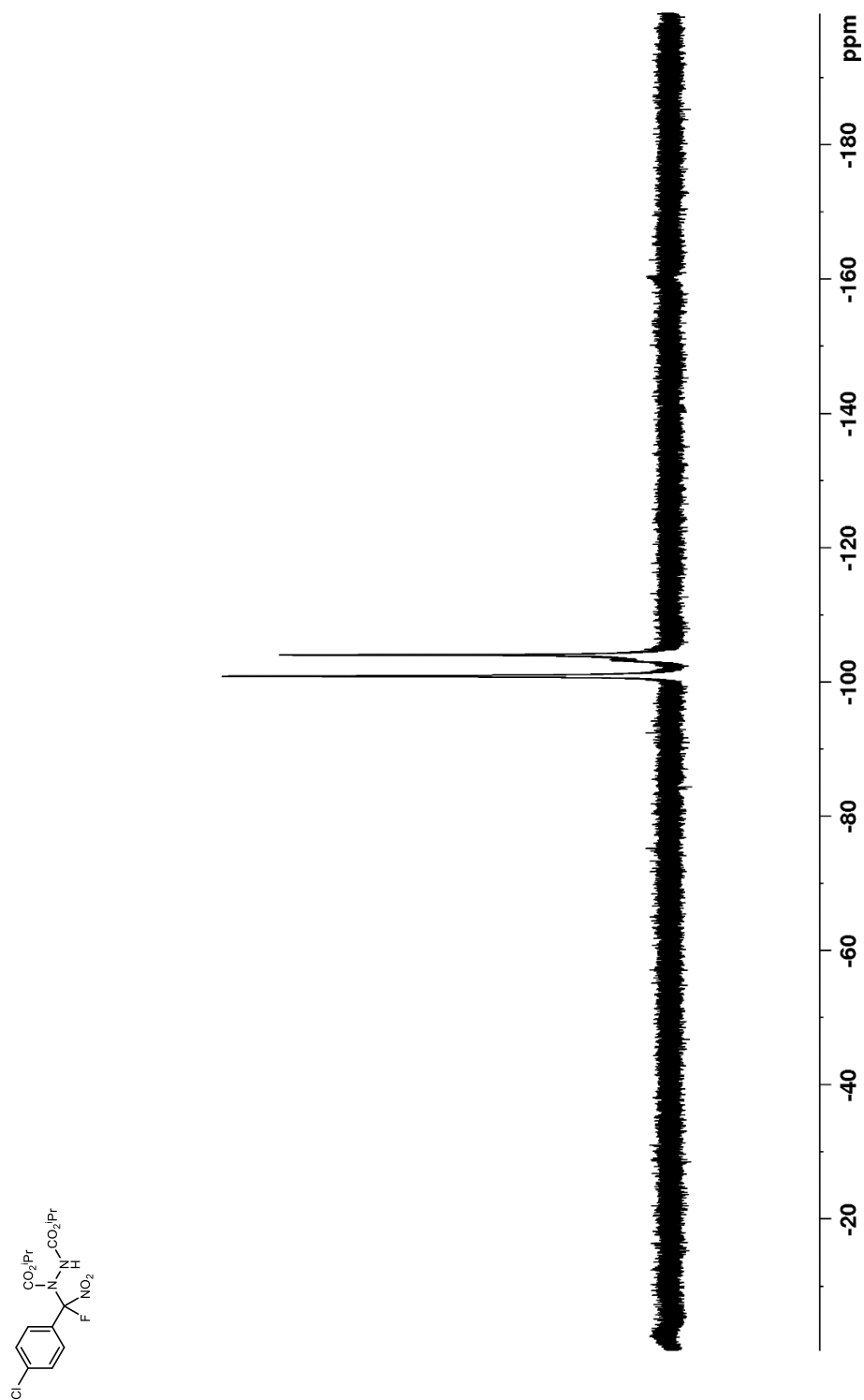


Figure 71. ^1H NMR (600 MHz, CDCl_3) of **93**

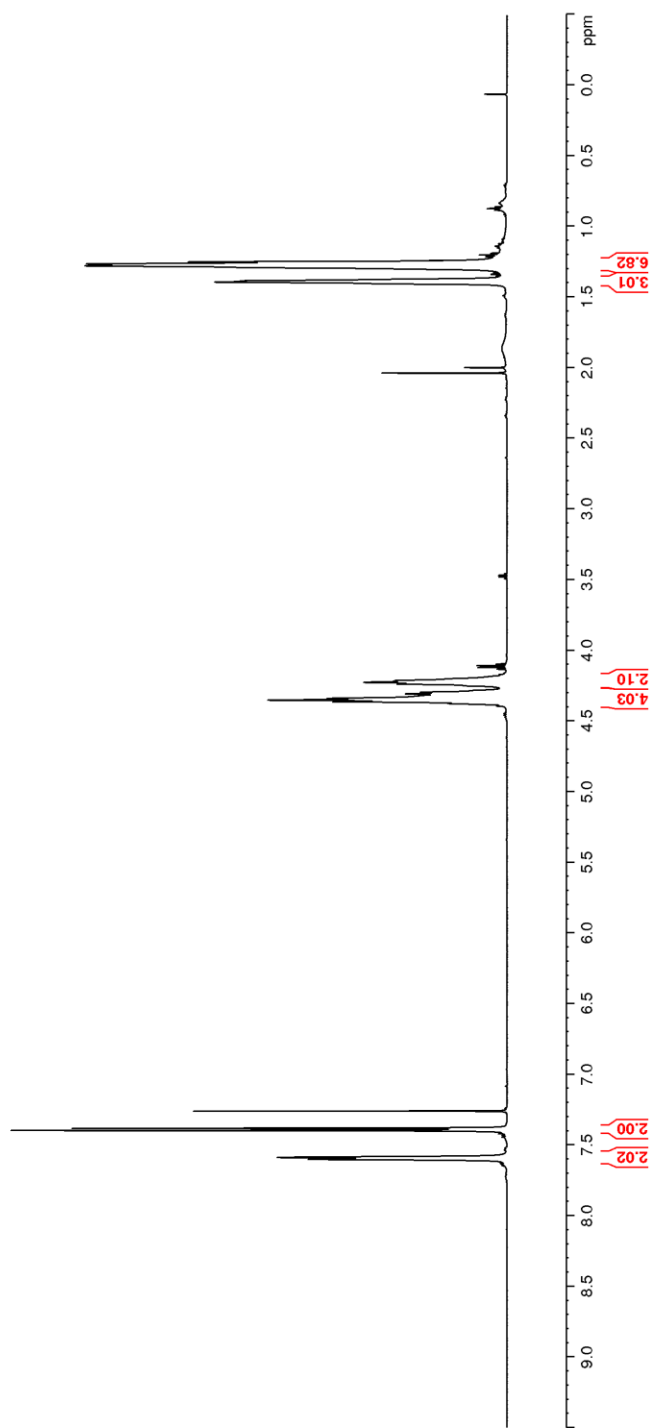
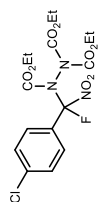


Figure 72. ^{13}C NMR (150 MHz, CDCl_3) of **93**

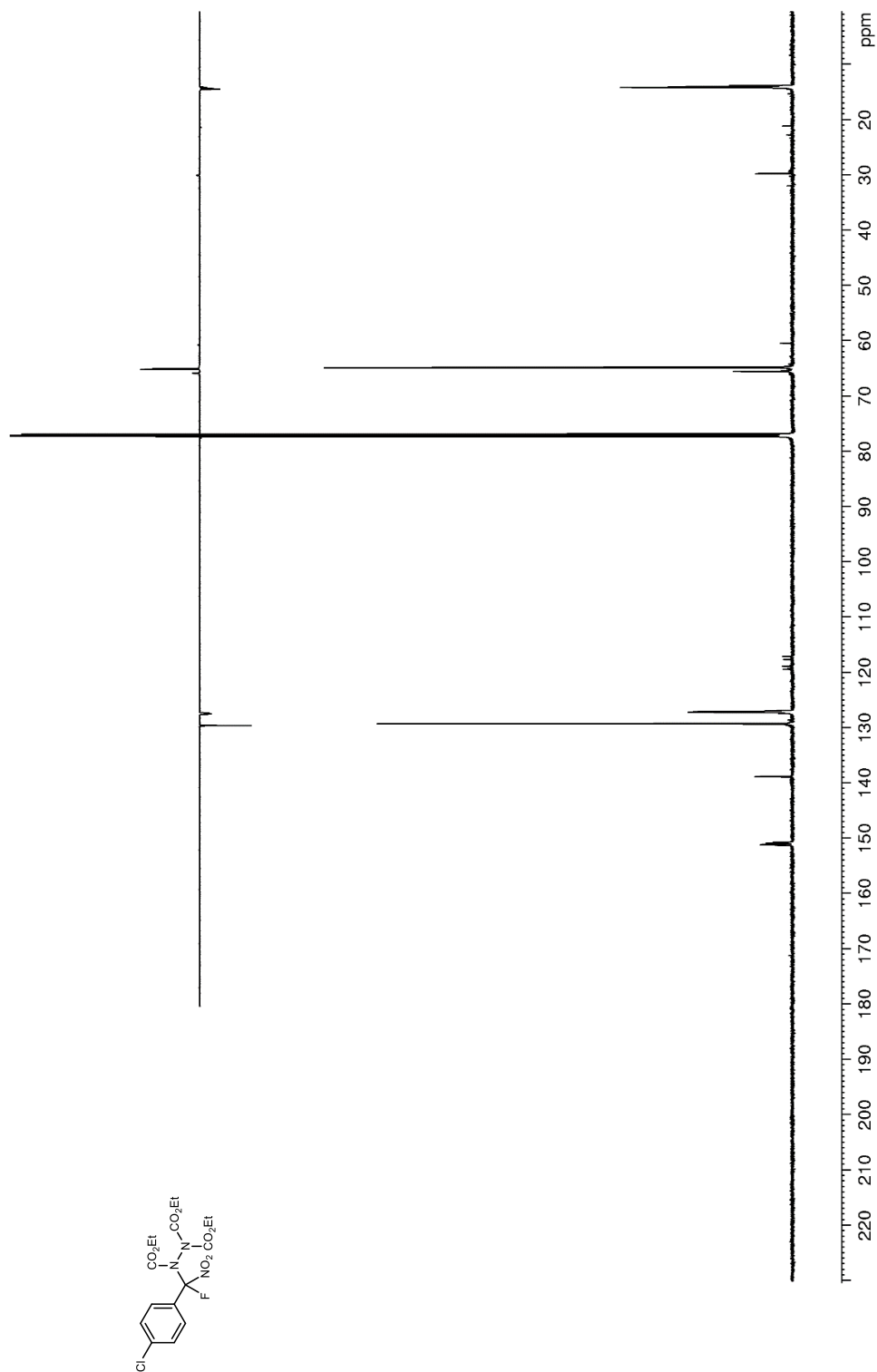


Figure 73. ^{19}F NMR (376 MHz, CDCl_3) of **93**

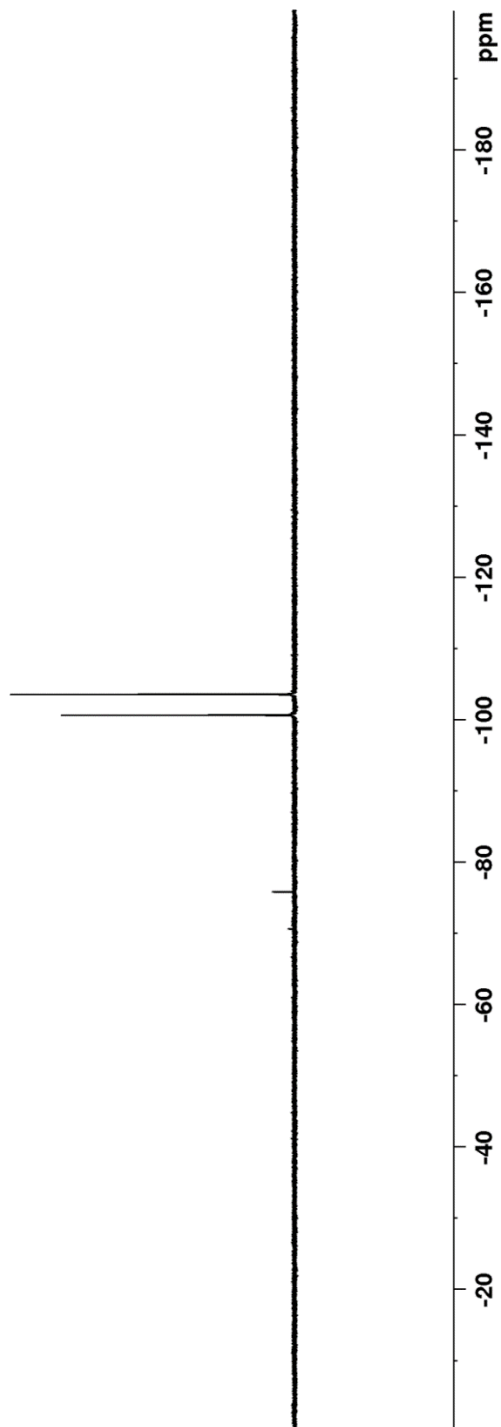
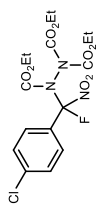


Figure 74. ^1H NMR (600 MHz, CDCl_3) of **94**

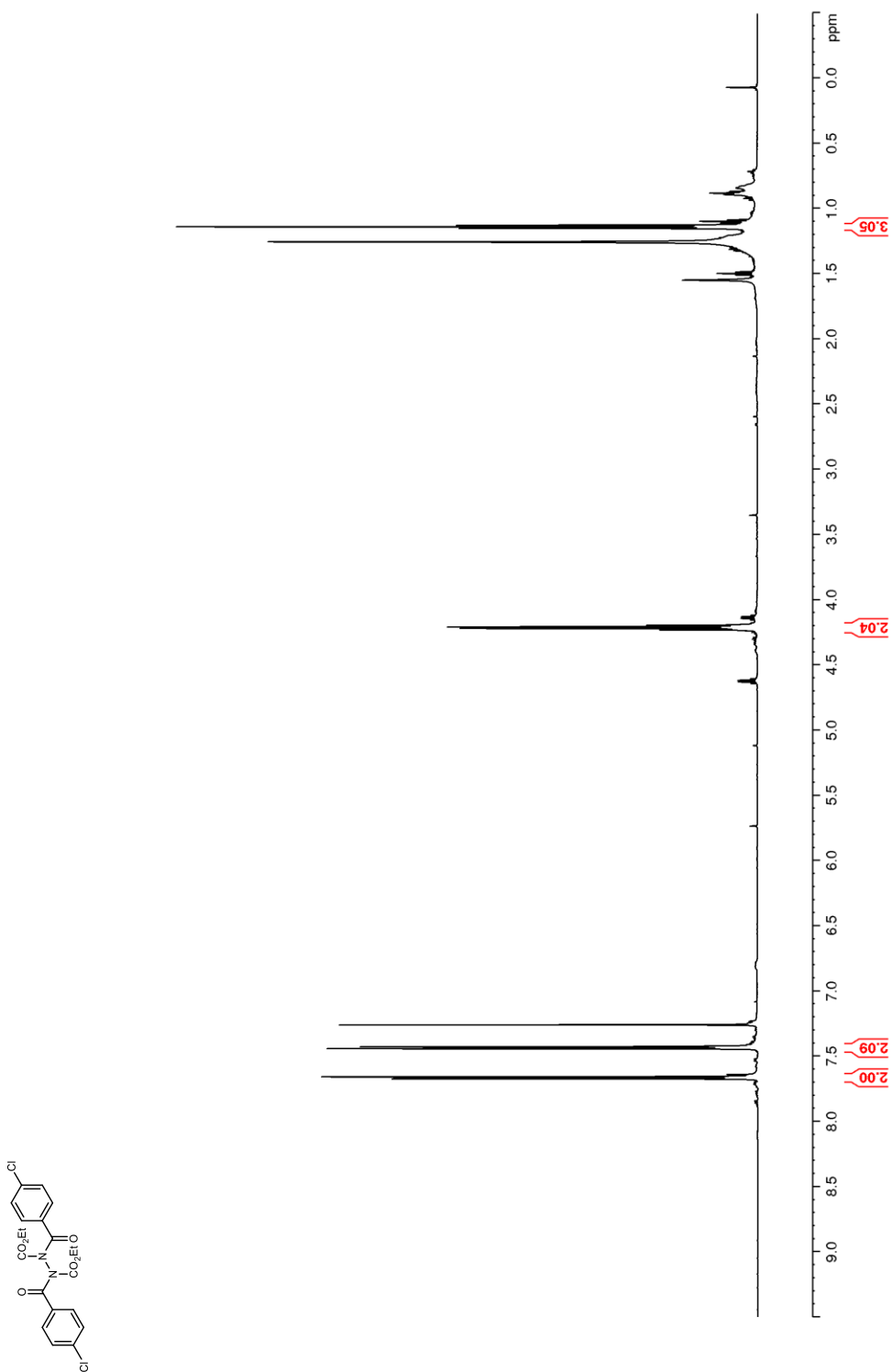


Figure 75. ^{13}C NMR (150 MHz, CDCl_3) of **94**

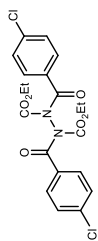
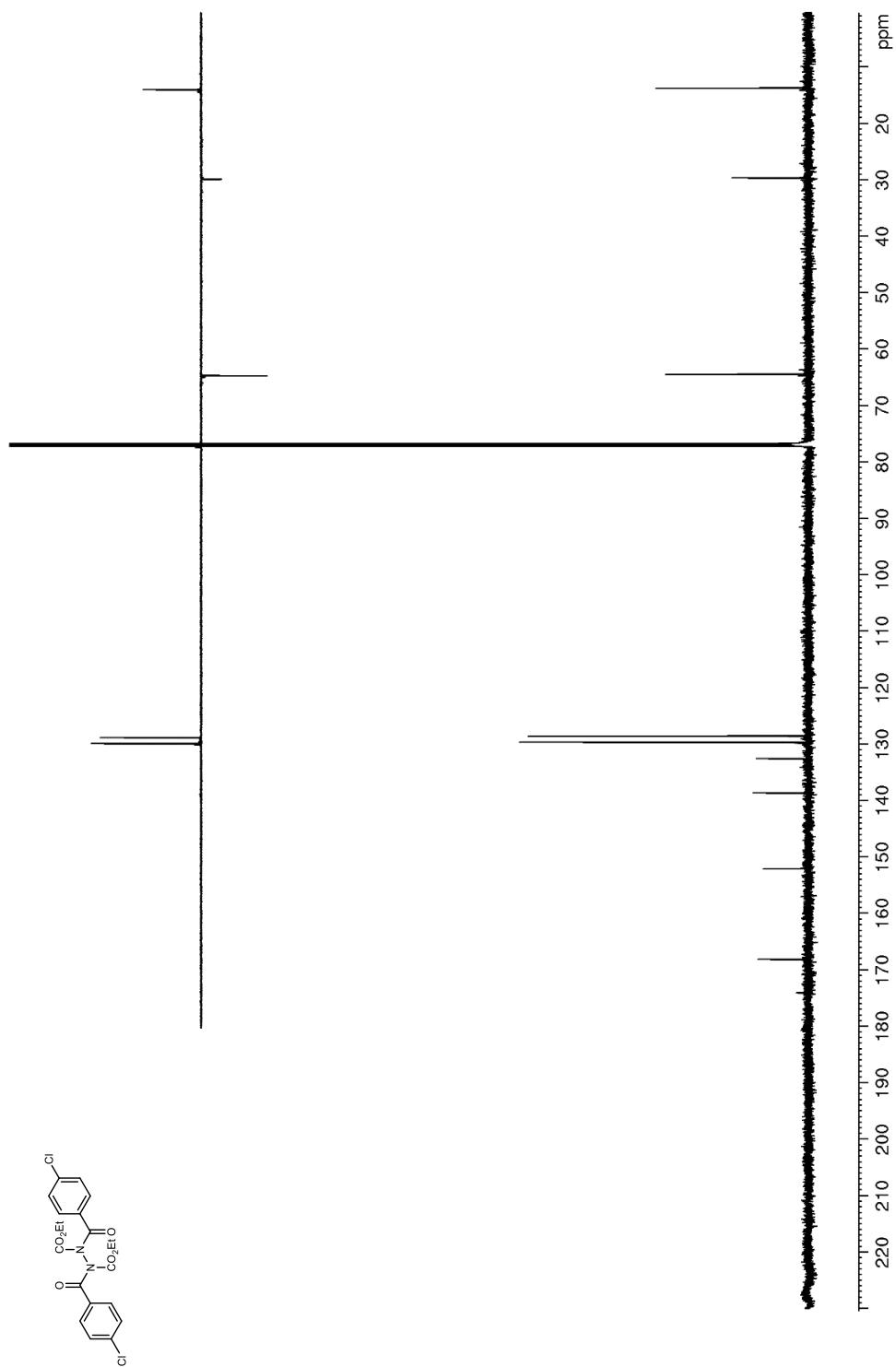


Figure 76. ^1H NMR (600 MHz, CDCl_3) of **95a**

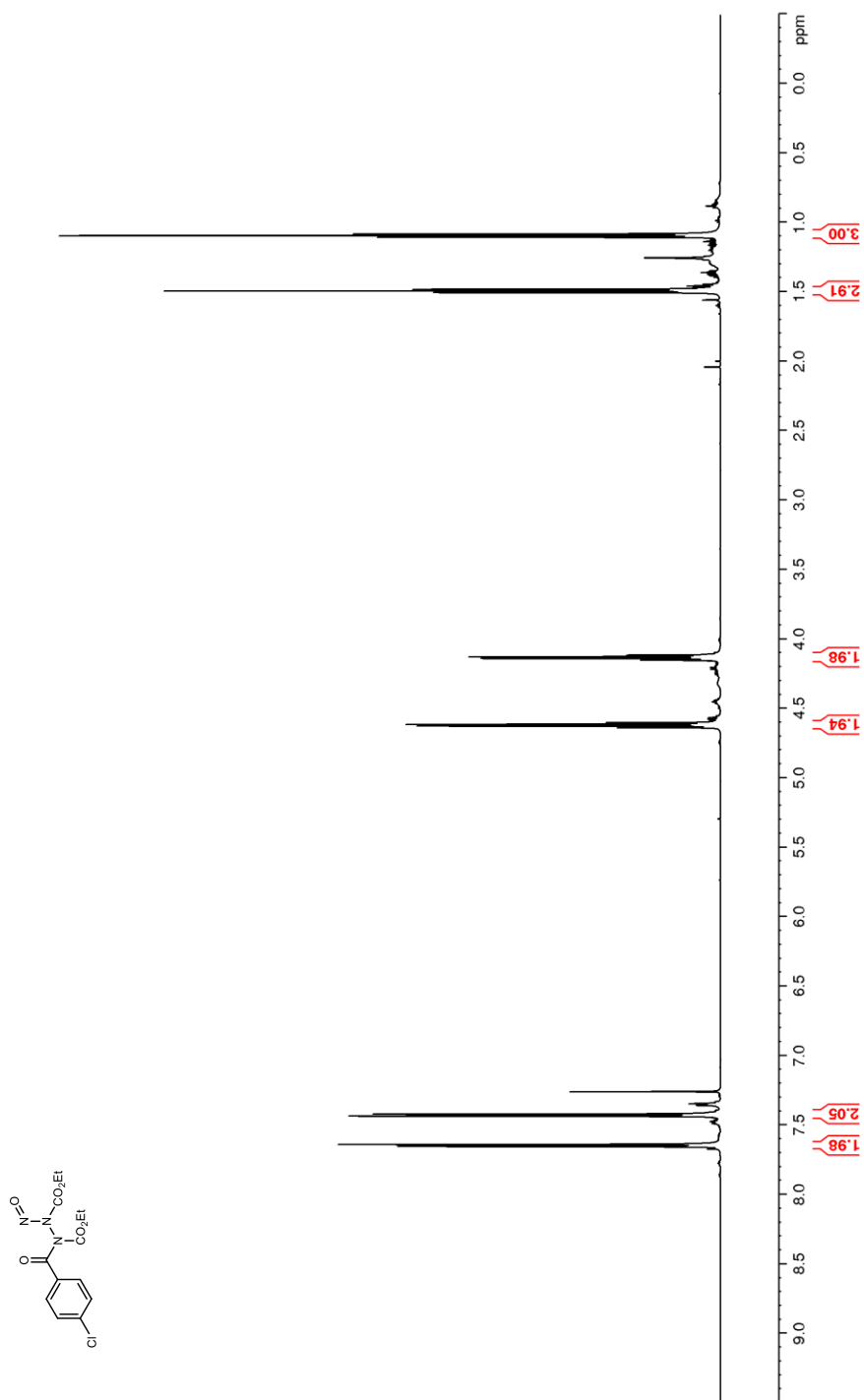


Figure 77. ^{13}C NMR (150 MHz, CDCl_3) of **95a**

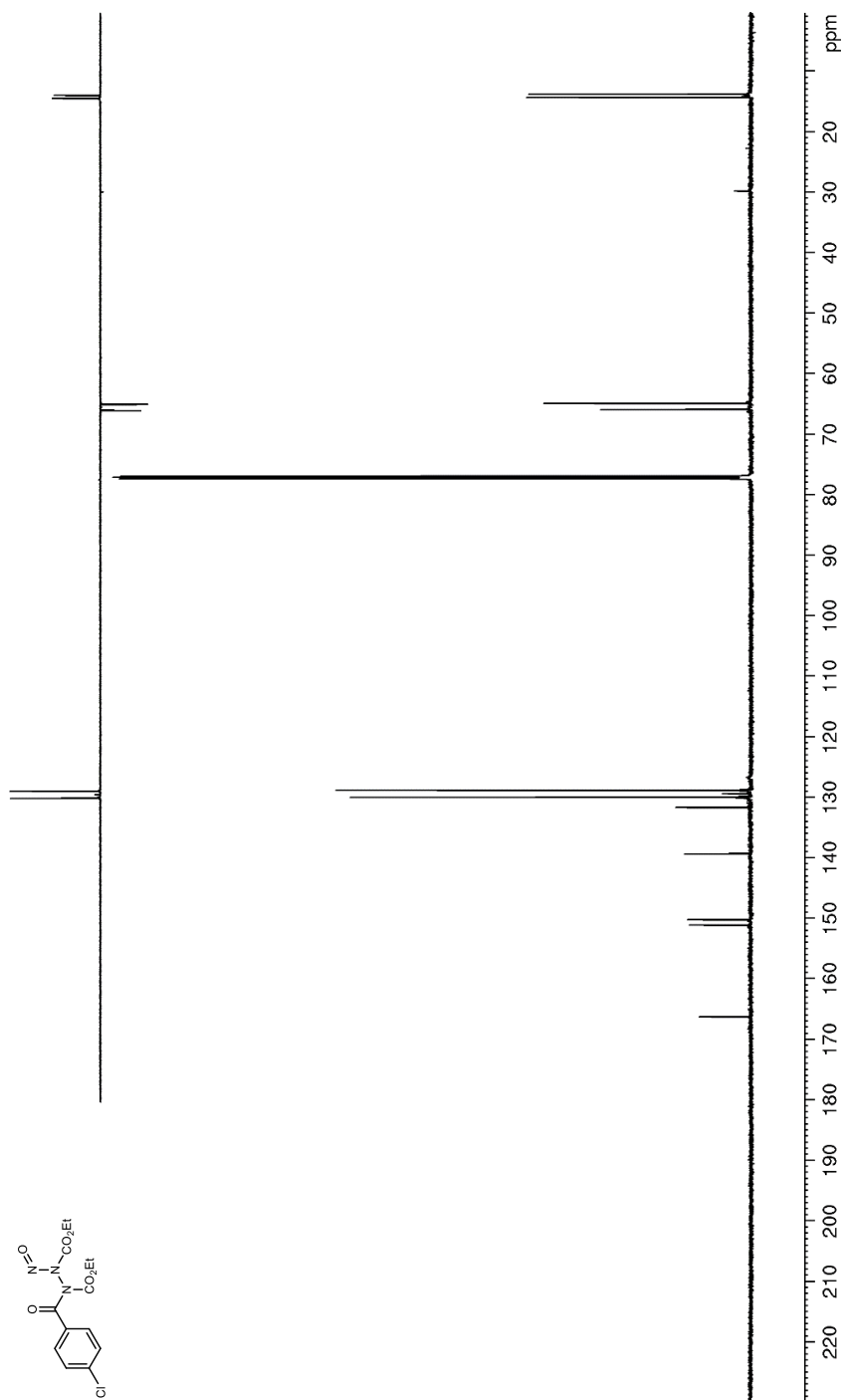


Figure 78. ^1H NMR (600 MHz, CDCl_3) of **95b**

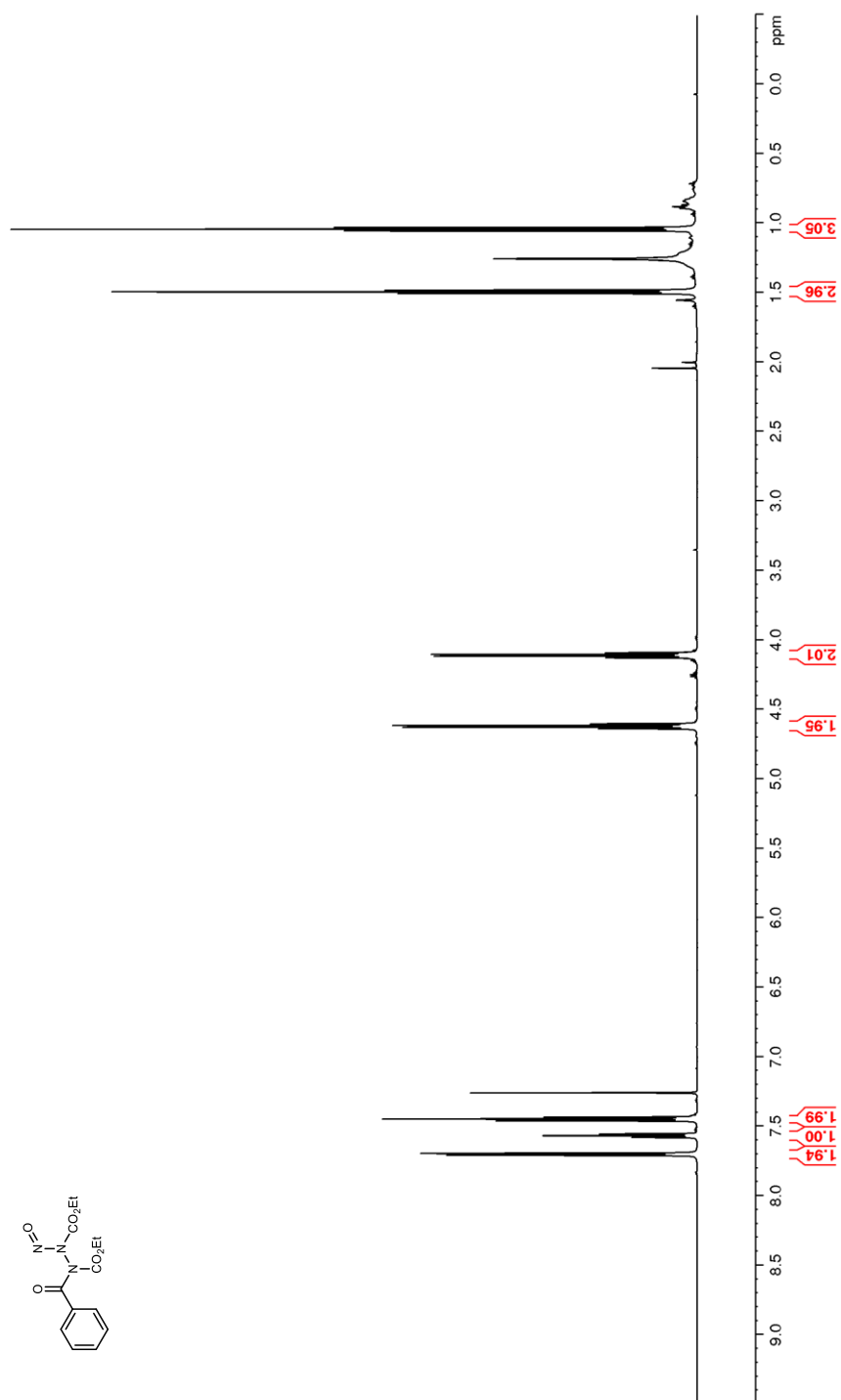


Figure 79. ^{13}C NMR (150 MHz, CDCl_3) of **95b**

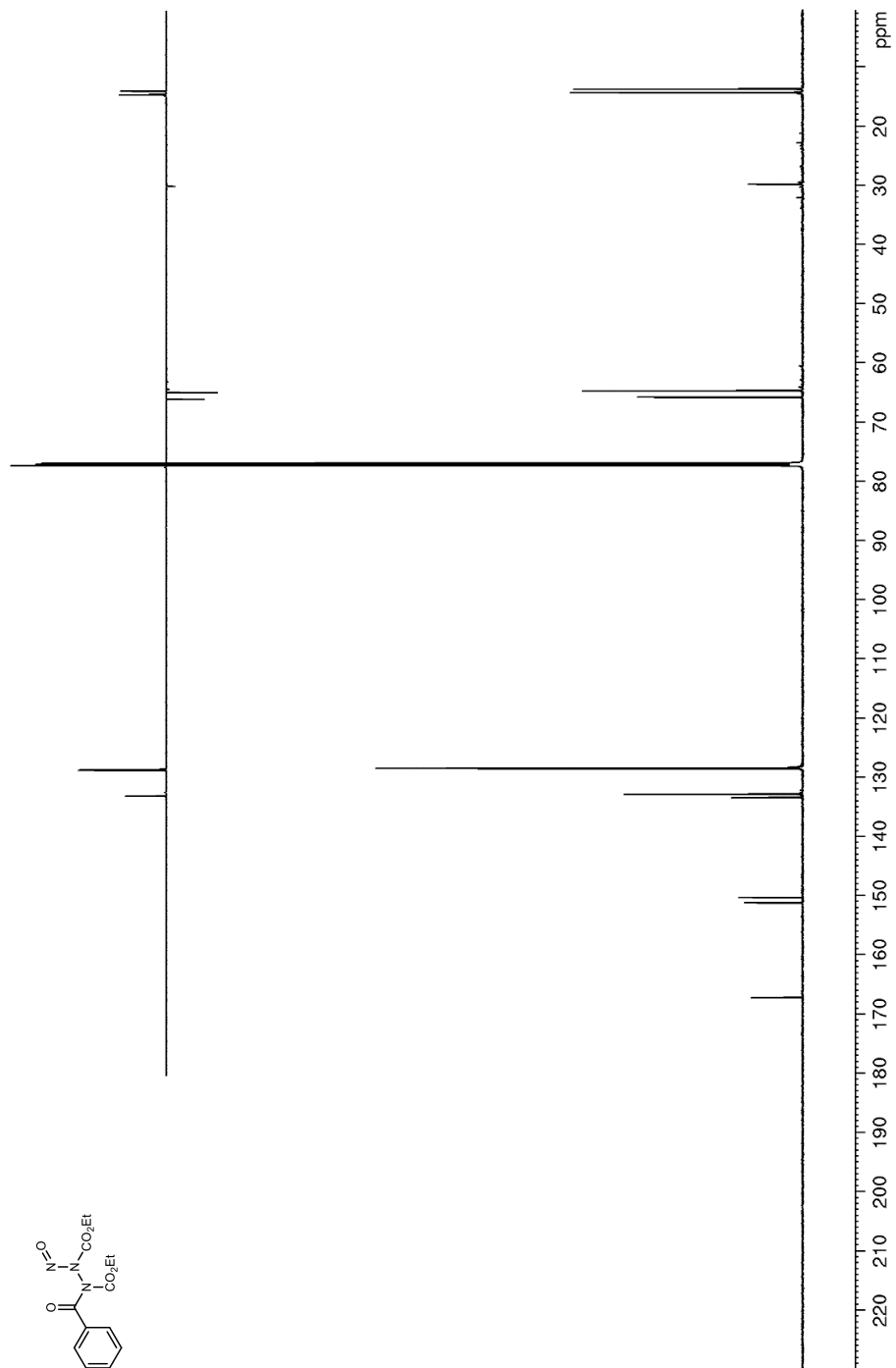


Figure 80. ^1H NMR (400 MHz, CDCl_3) of **96**

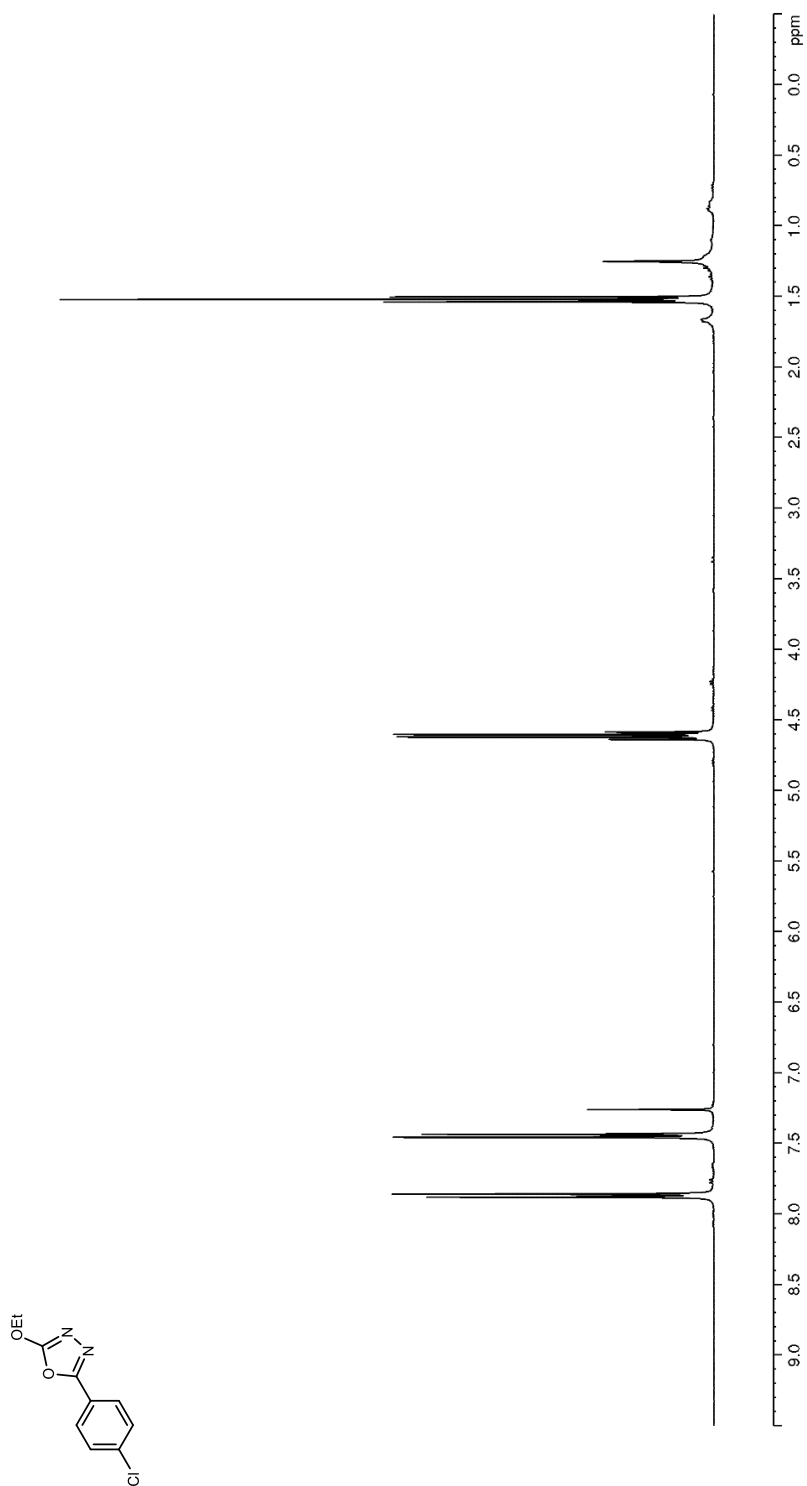


Figure 82. ^1H NMR (600 MHz, CDCl_3) of **97**

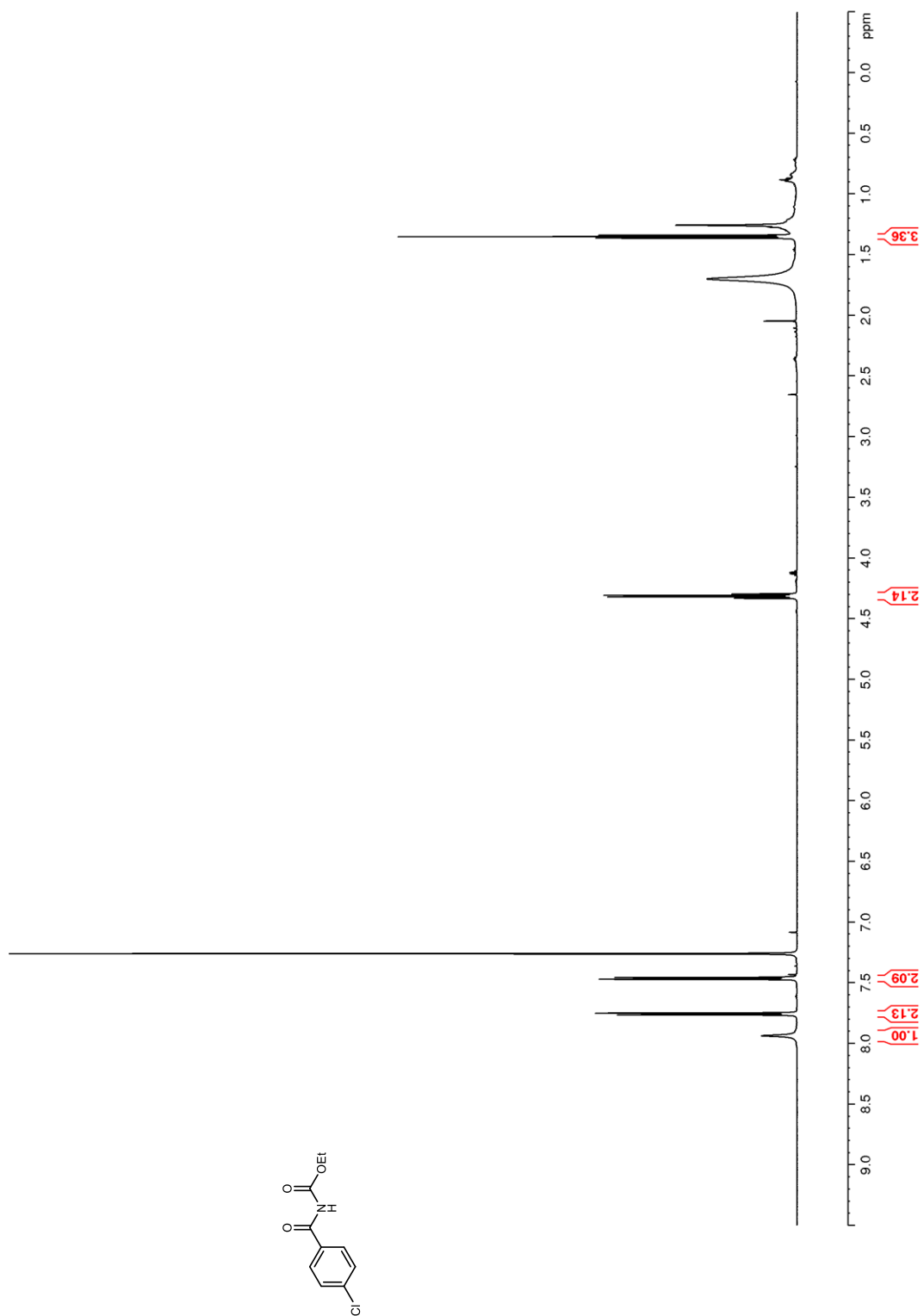
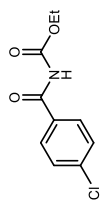
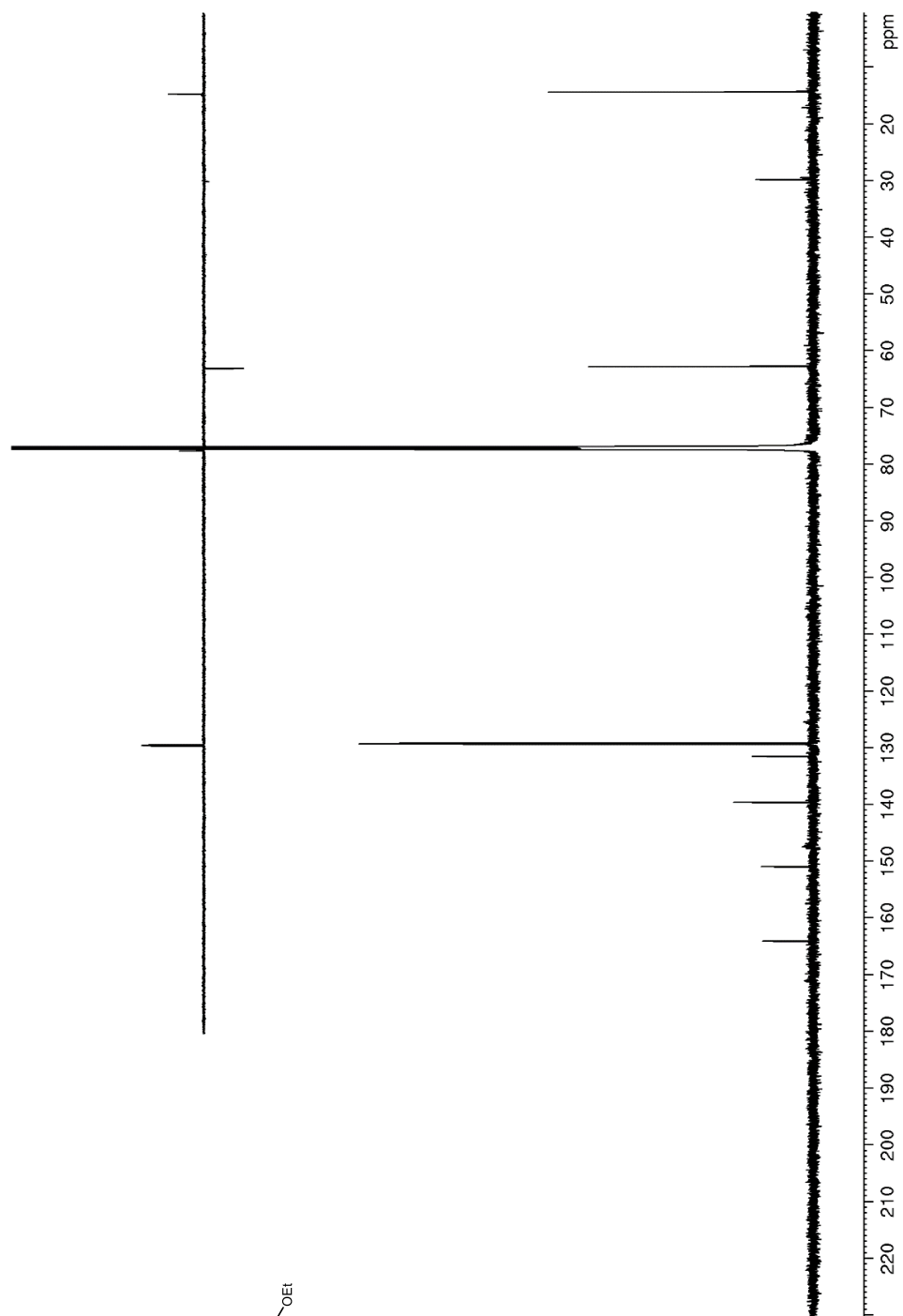


Figure 83. ^{13}C NMR (150 MHz, CDCl_3) of **97**



380

Figure 84. ^1H NMR (400 MHz, CDCl_3) of **103**

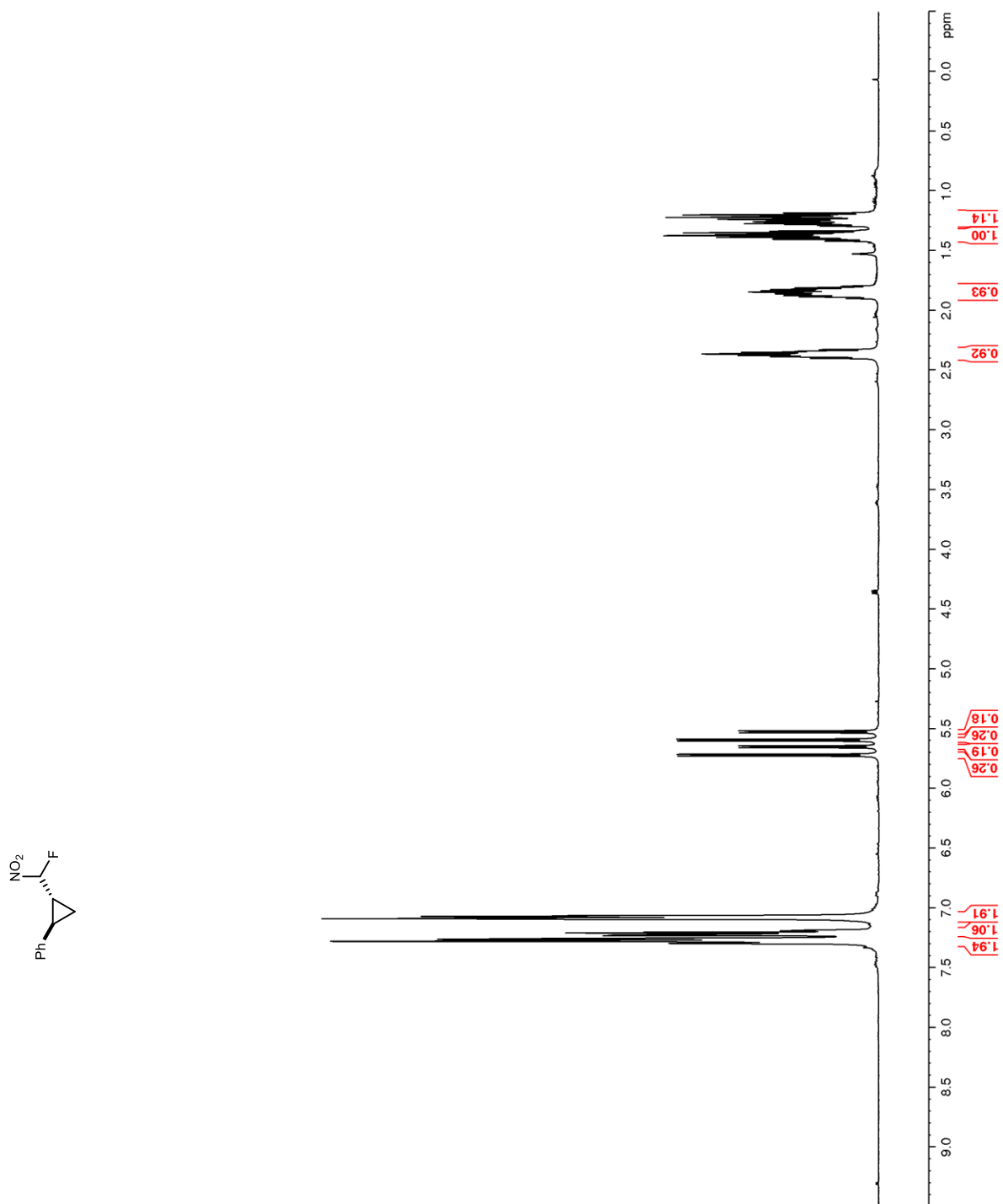


Figure 85. ^{13}C NMR (100 MHz, CDCl_3) of **103**

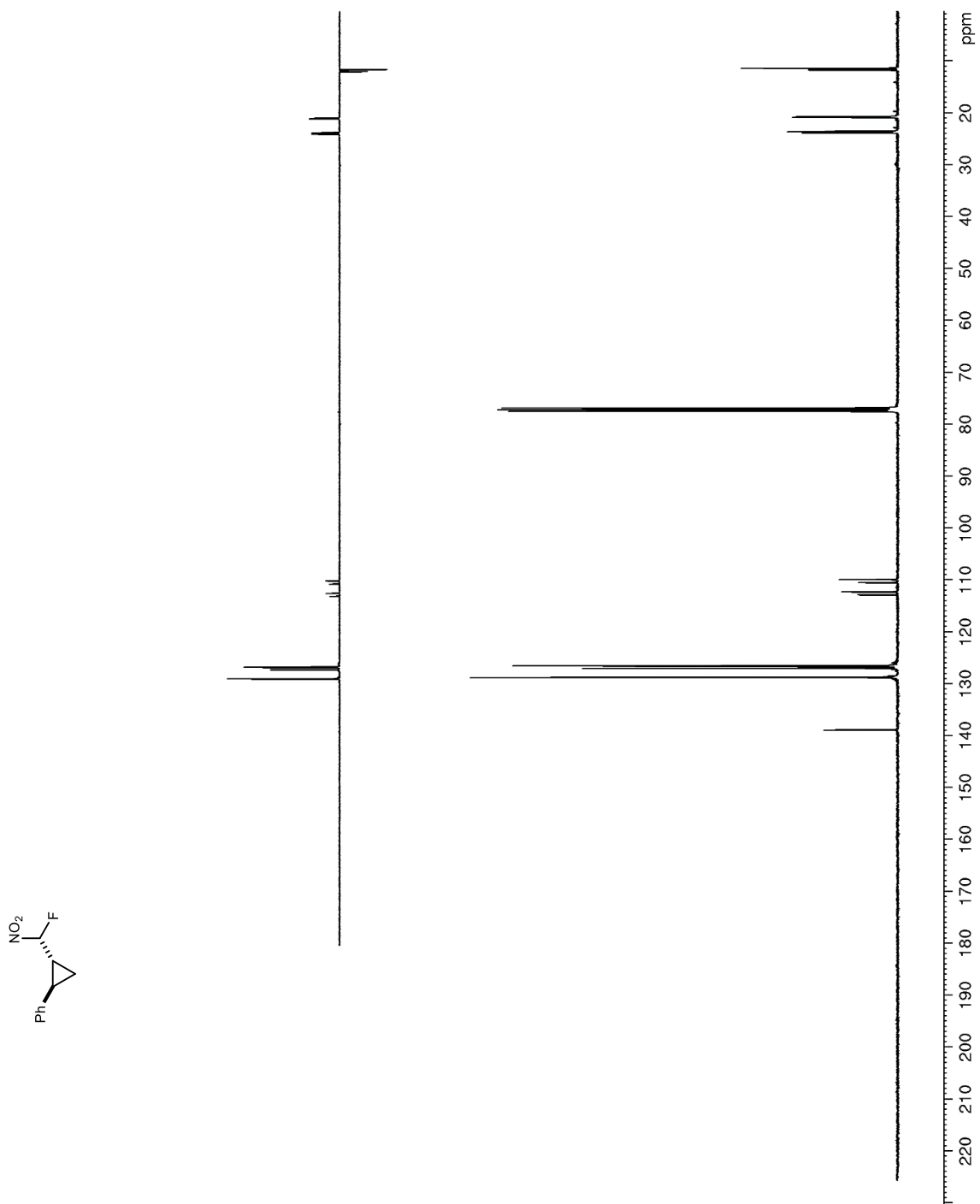


Figure 86. ^{19}F NMR (376 MHz, CDCl_3) of **103**

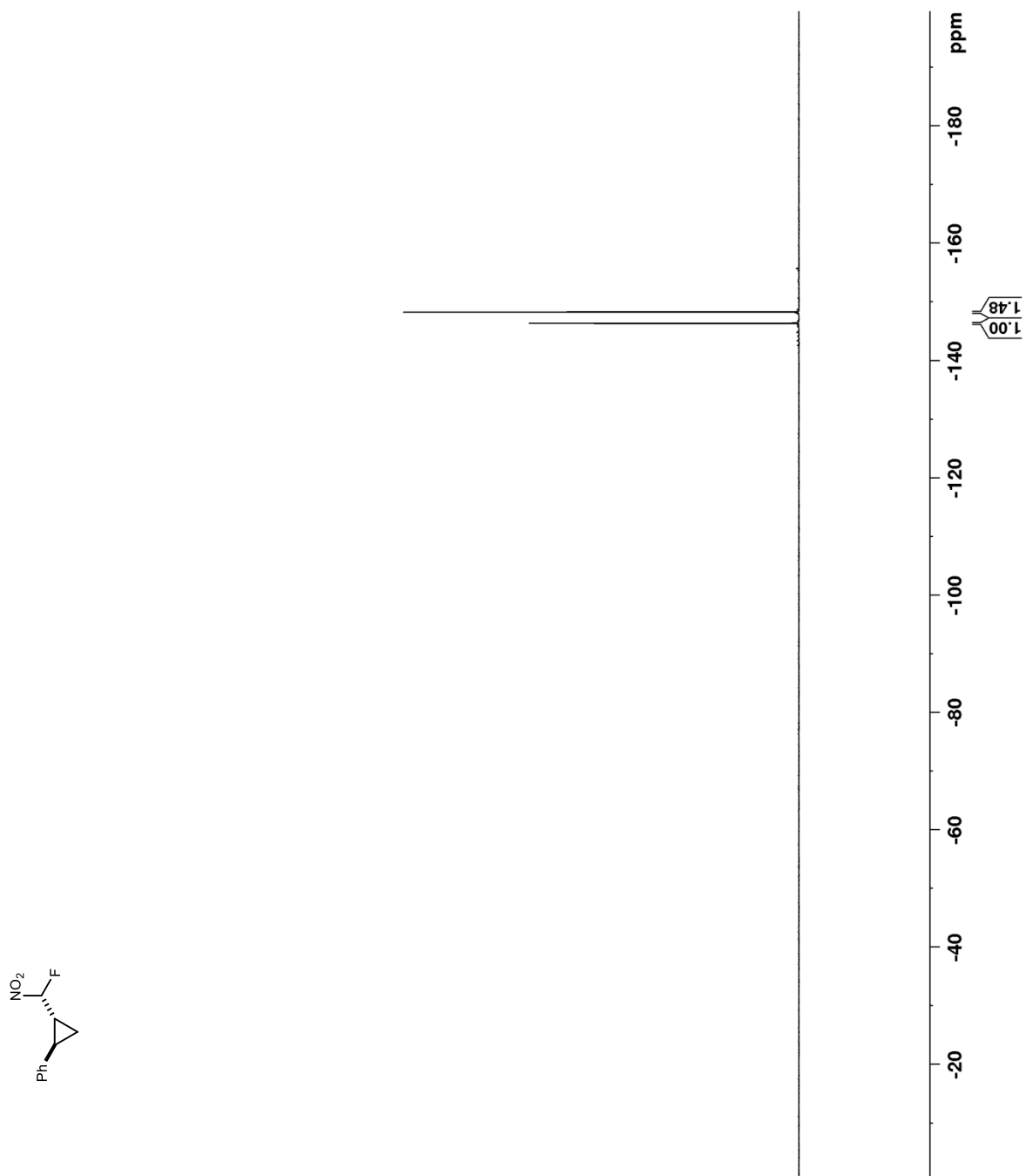


Figure 87. ^1H NMR (400 MHz, CDCl_3) of **104**

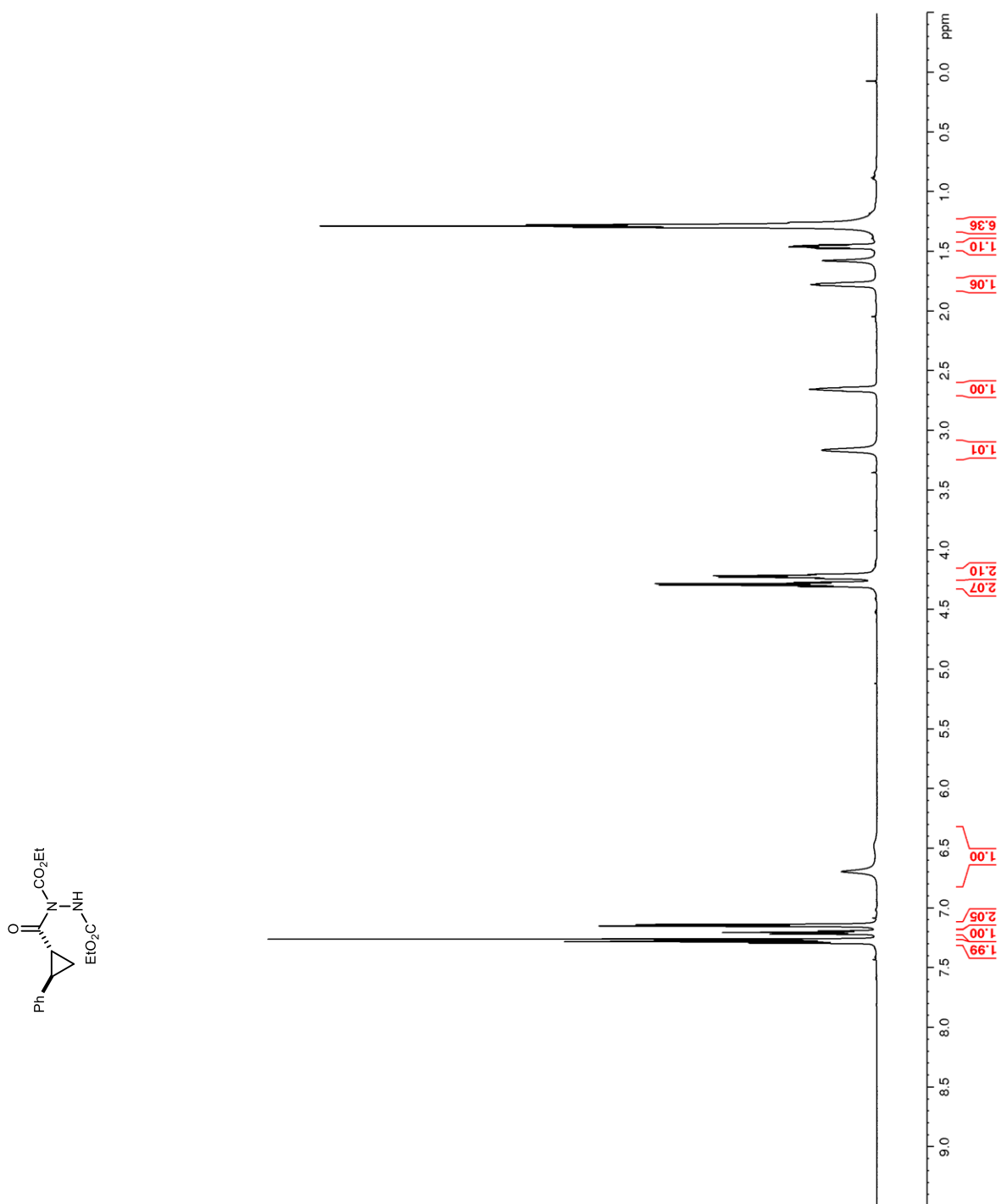


Figure 88. ^{13}C NMR (150 MHz, CDCl_3) of **104**

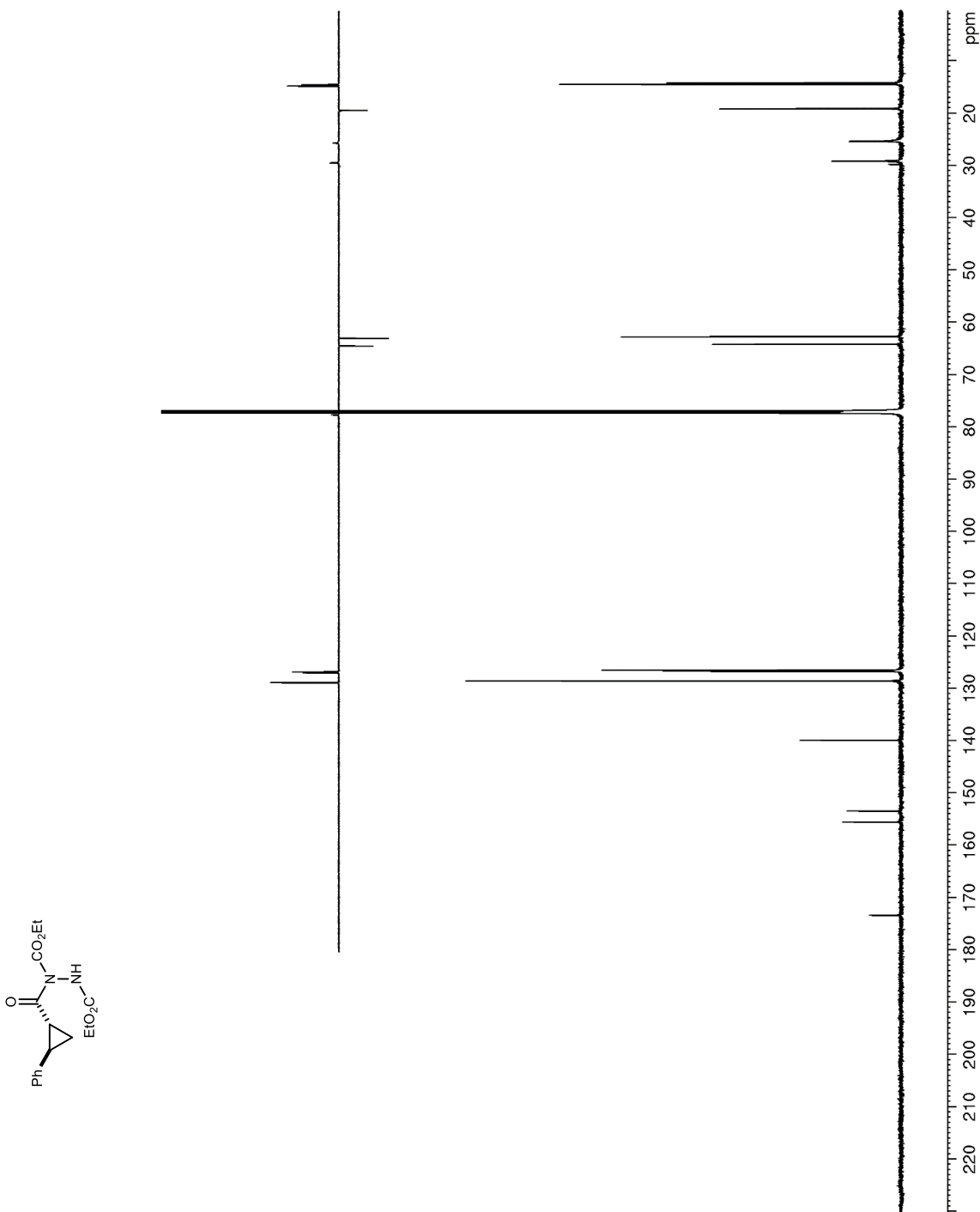


Figure 89. ^1H NMR (400 MHz, CDCl_3) of **105**

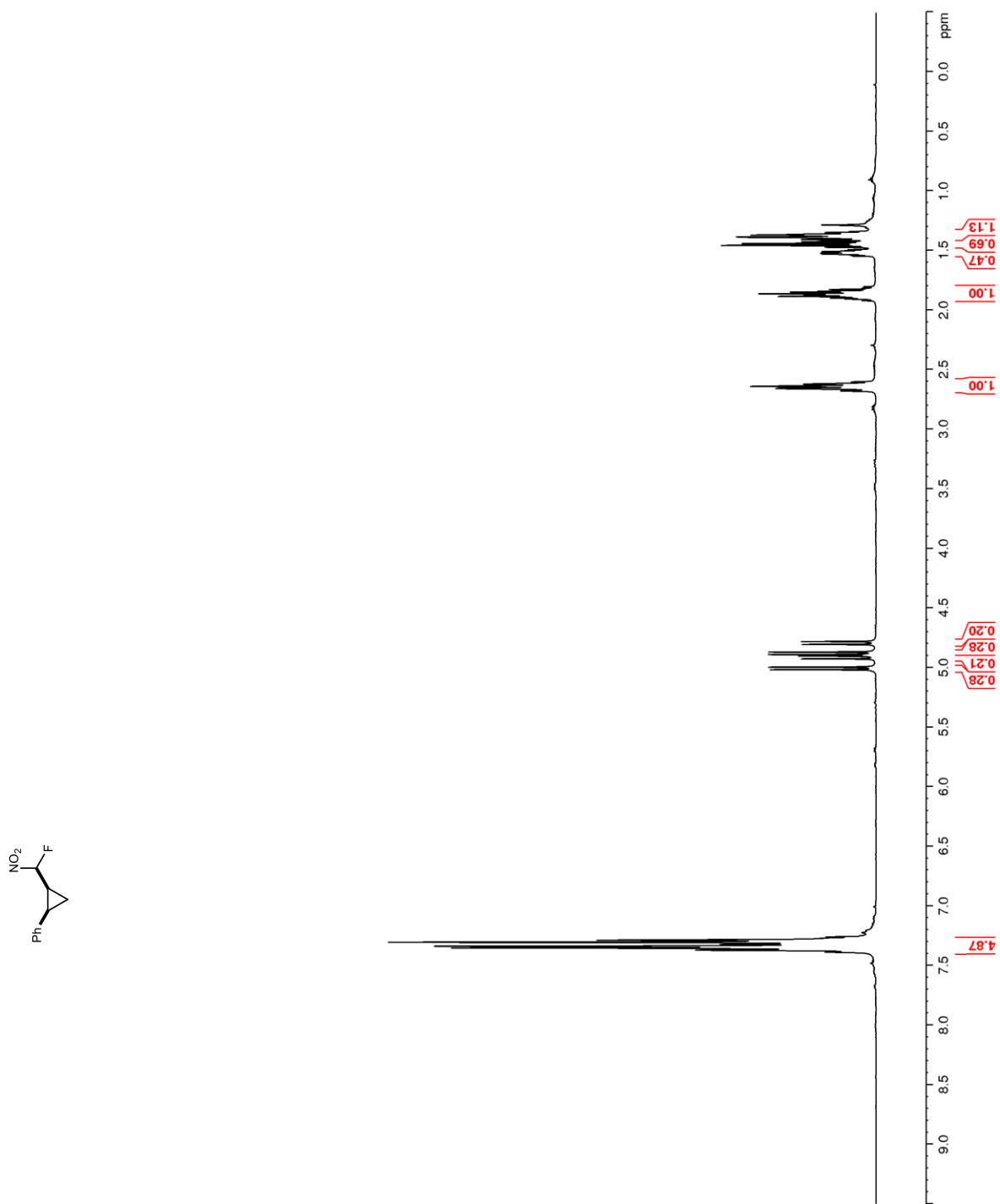


Figure 90. ^{13}C NMR (100 MHz, CDCl_3) of **105**

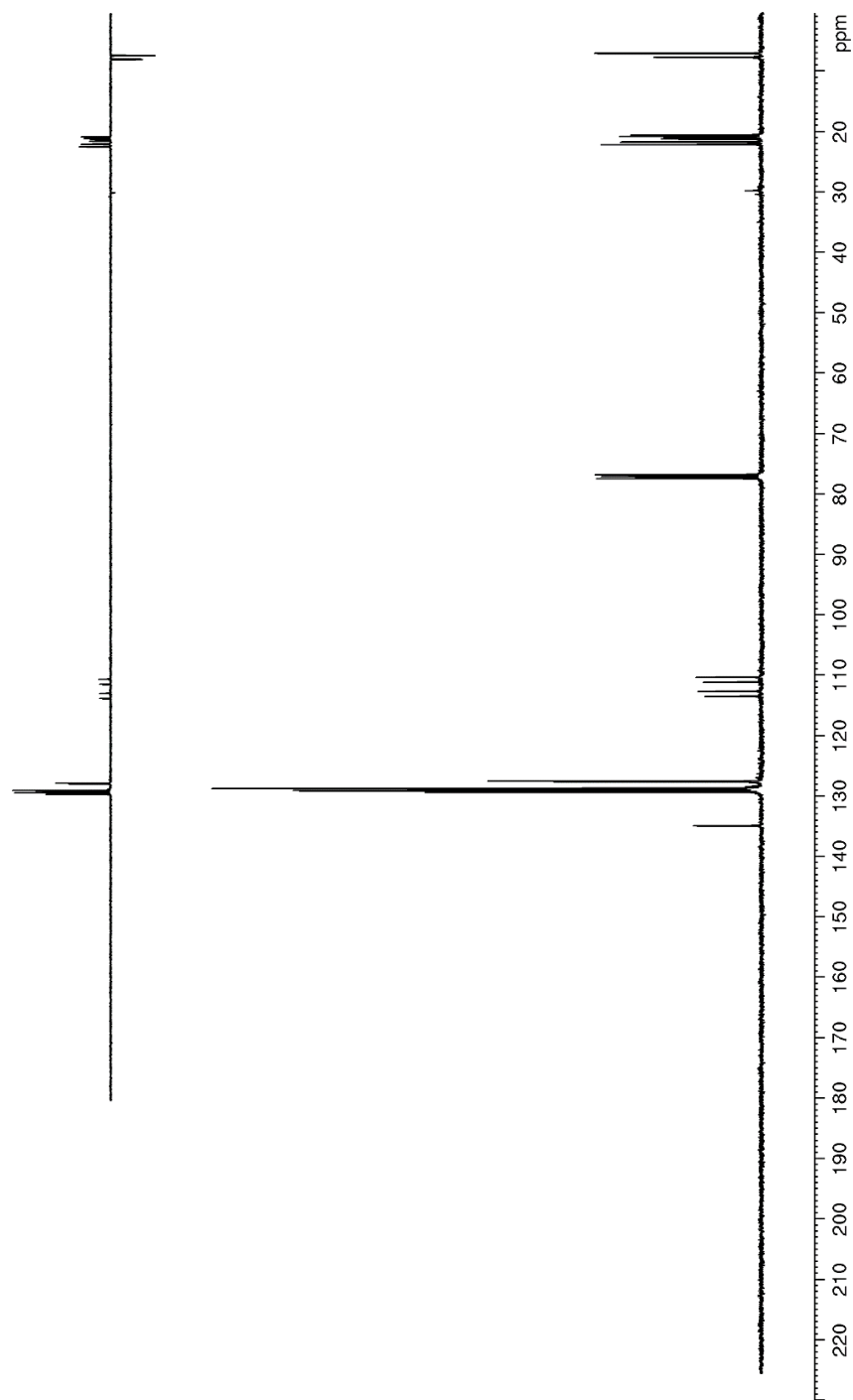
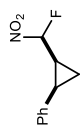


Figure 91. ^{19}F NMR (376 MHz, CDCl_3) of **105**

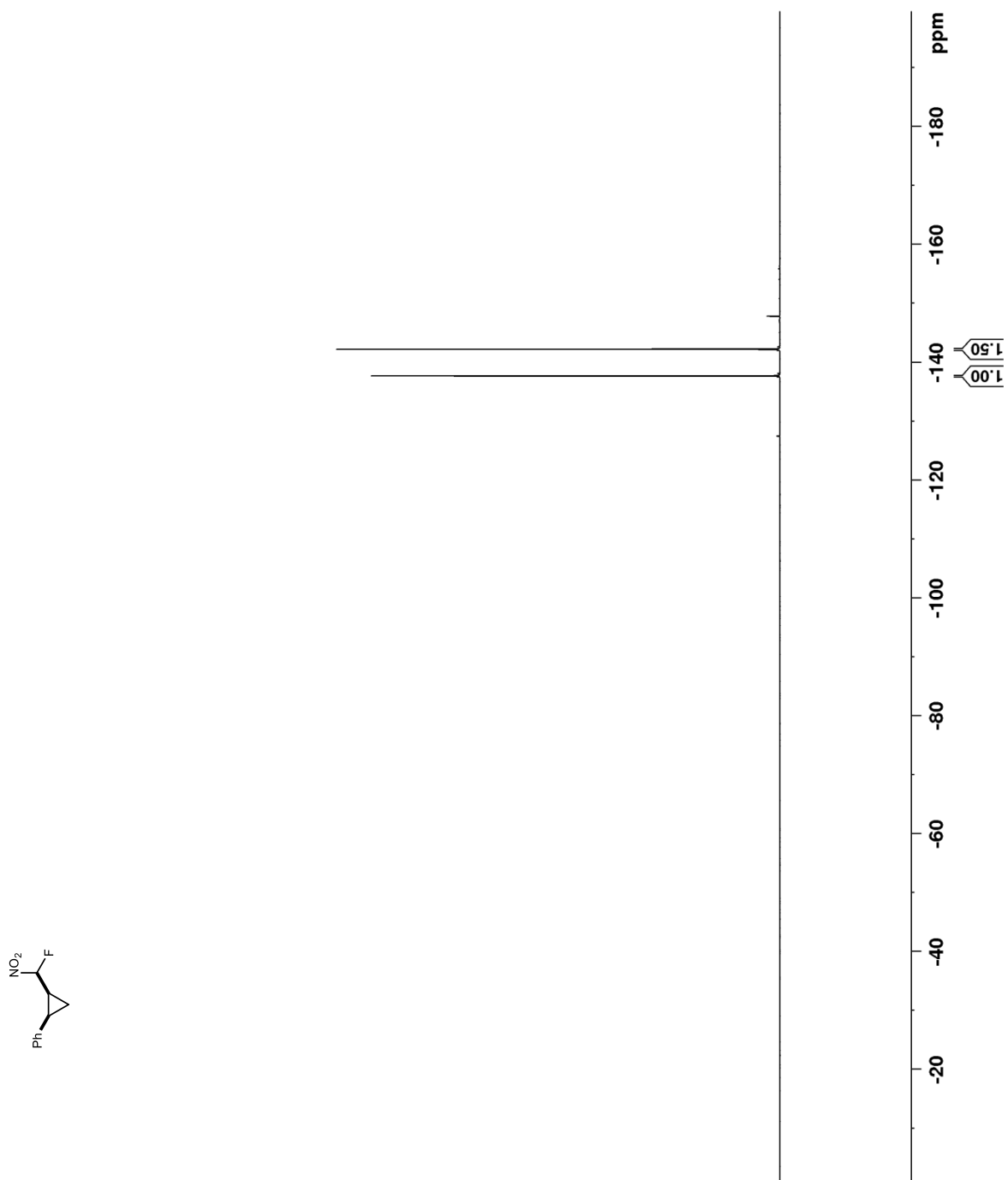


Figure 92. ^1H NMR (400 MHz, CDCl_3) of **106**

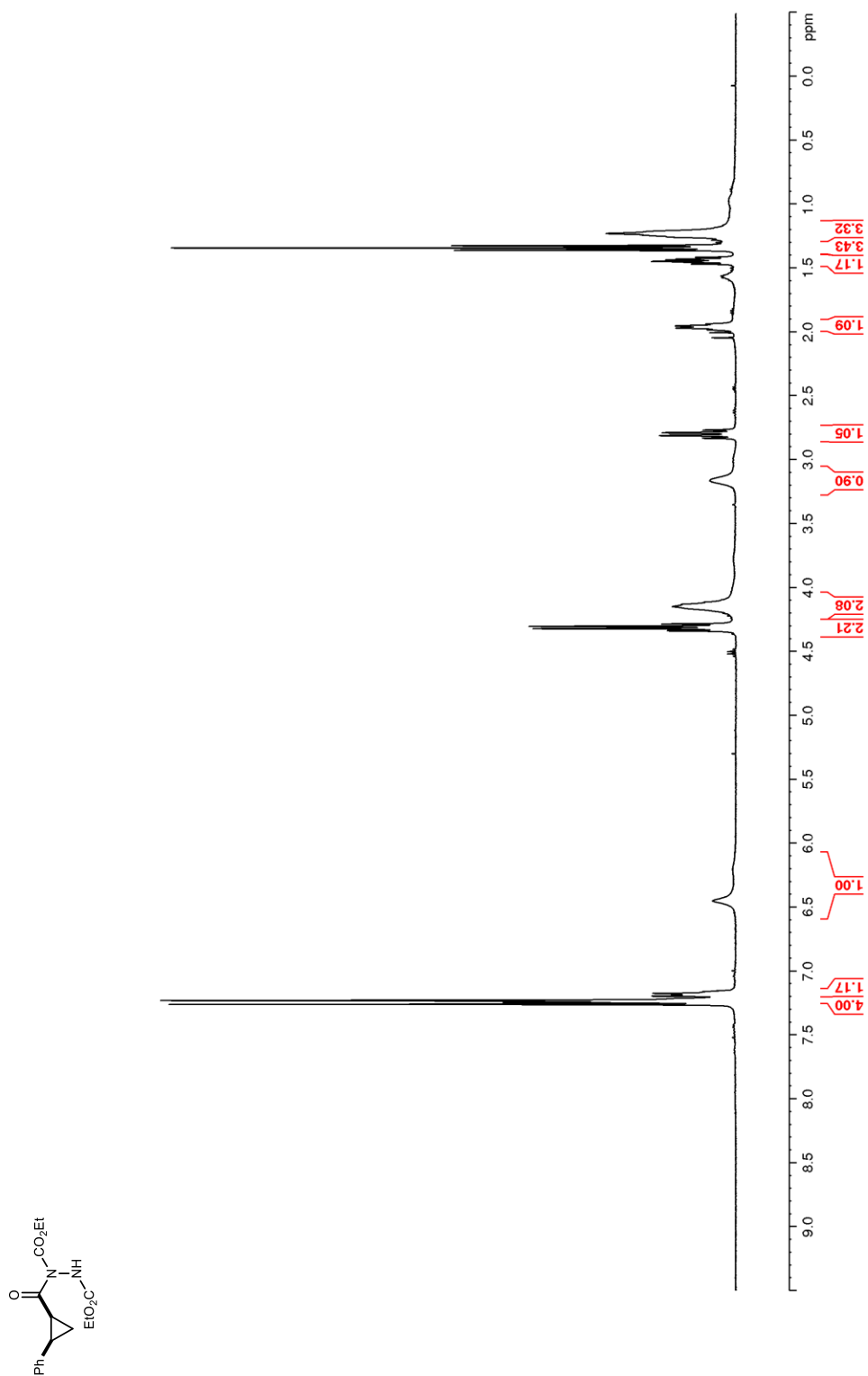


Figure 93. ^{13}C NMR (100 MHz, CDCl_3) of **106**

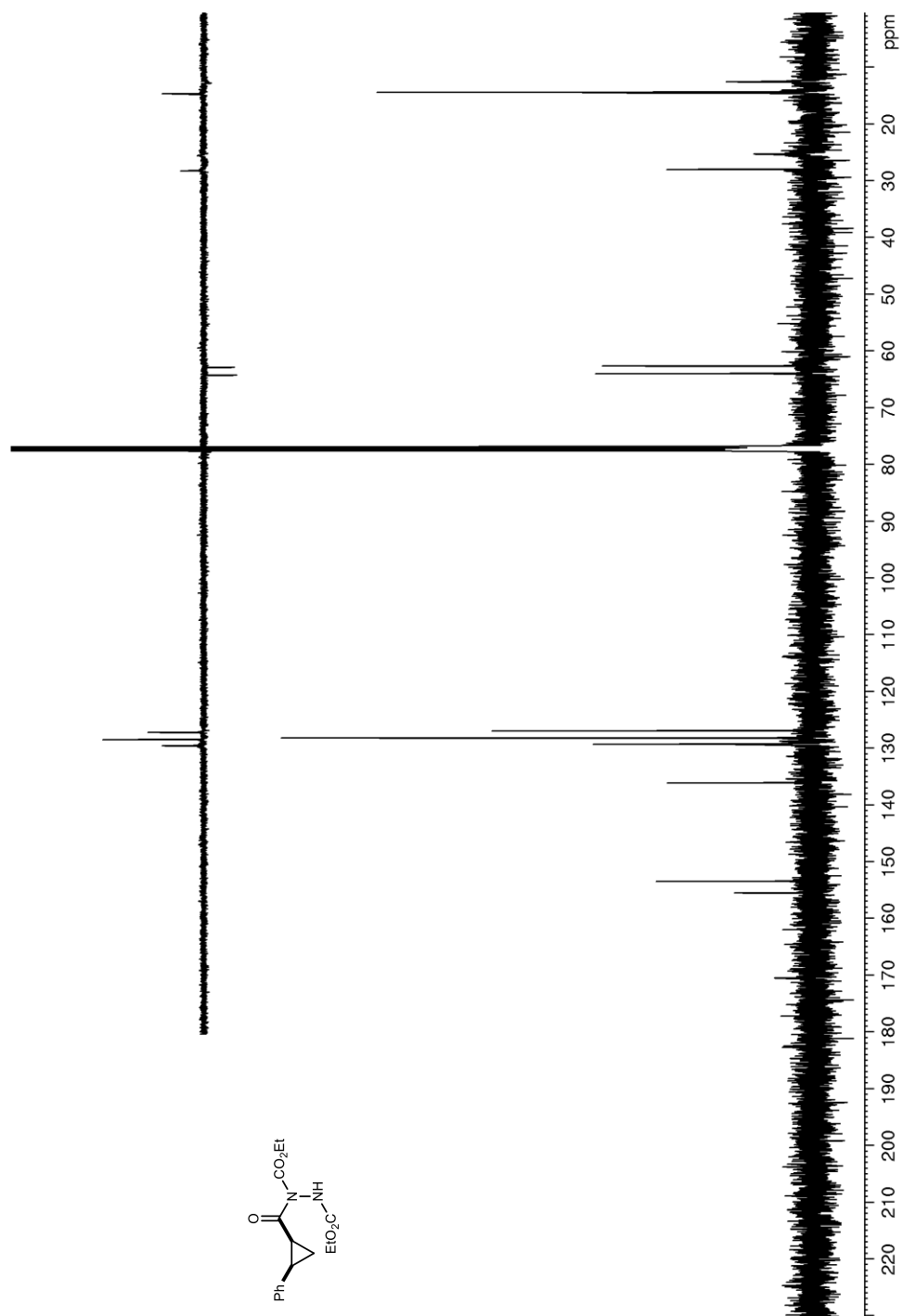


Figure 94. ^1H NMR (600 MHz, CDCl_3) of **107**

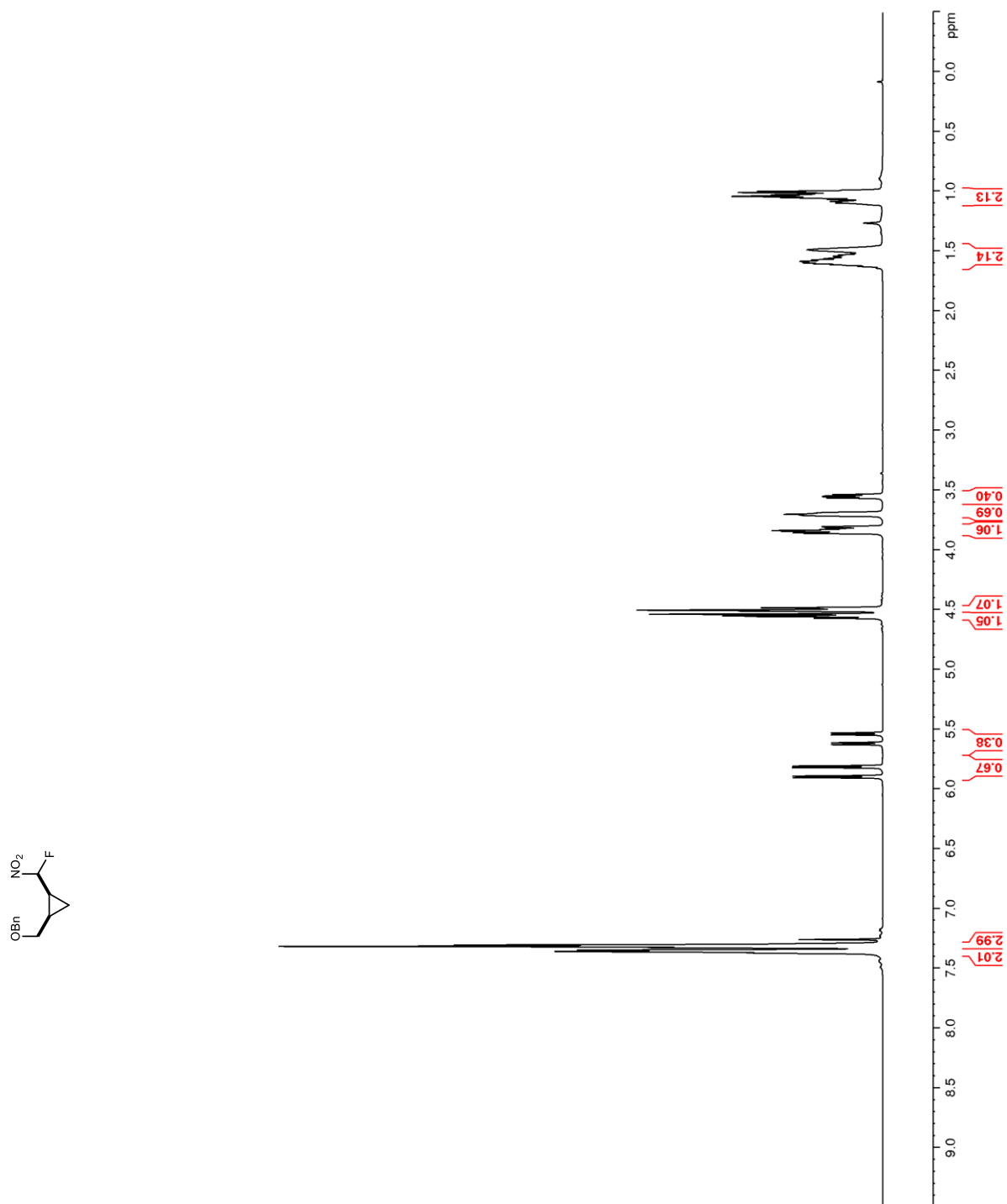


Figure 95. ^{13}C NMR (150 MHz, CDCl_3) of **107**

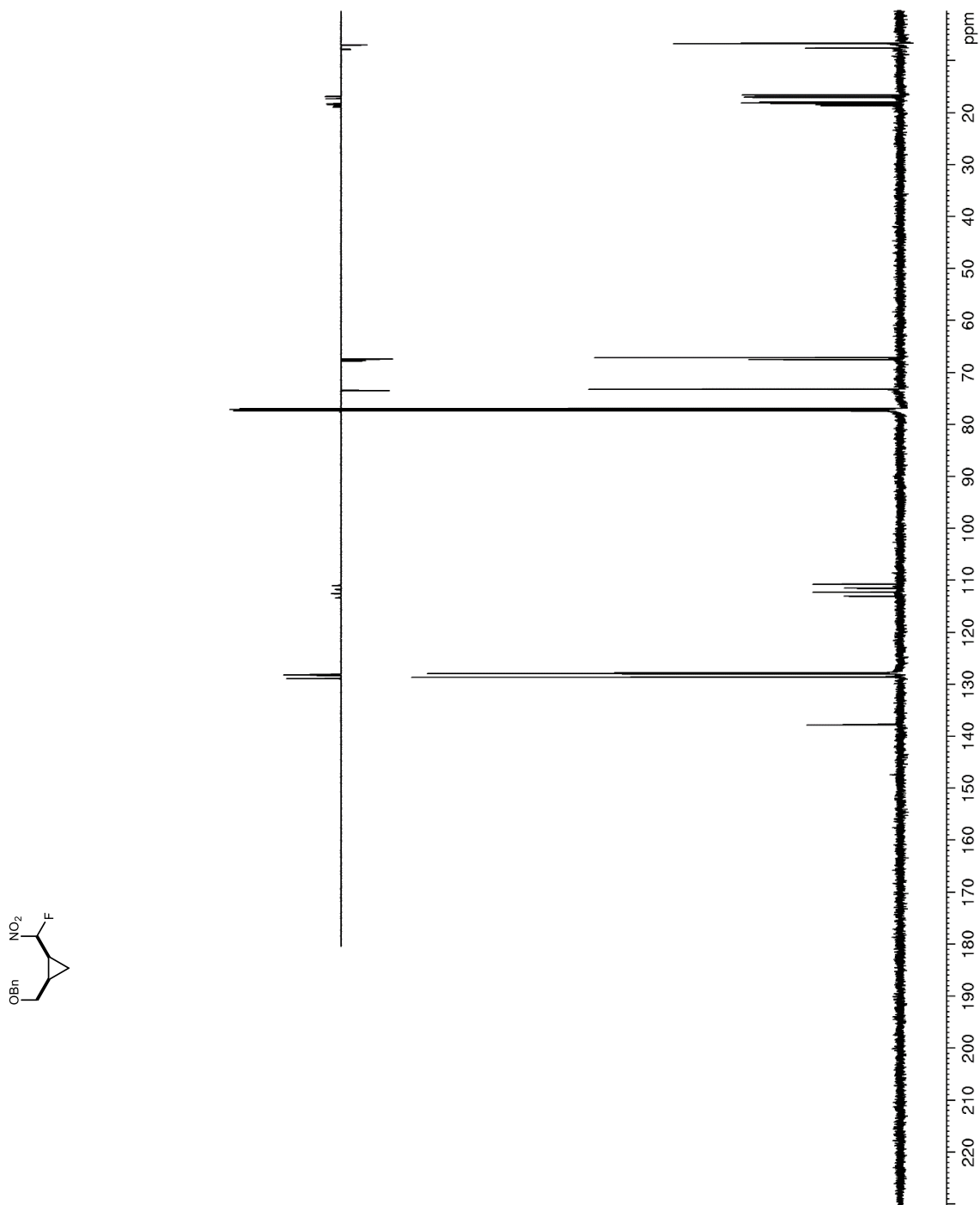


Figure 96. ^{19}F NMR (376 MHz, CDCl_3) of **107**

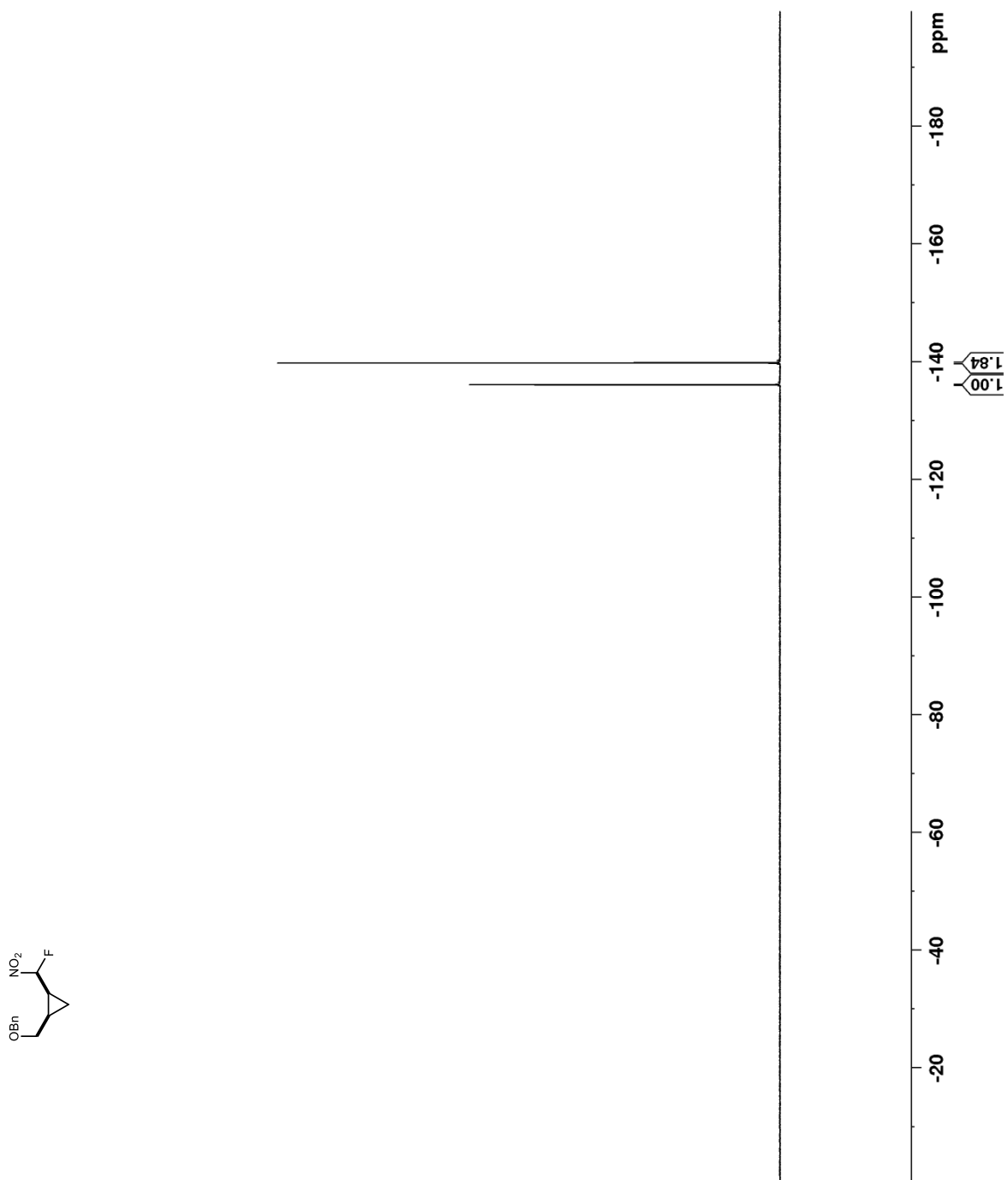


Figure 97. ^1H NMR (400 MHz, toluene- d_8) of **108**

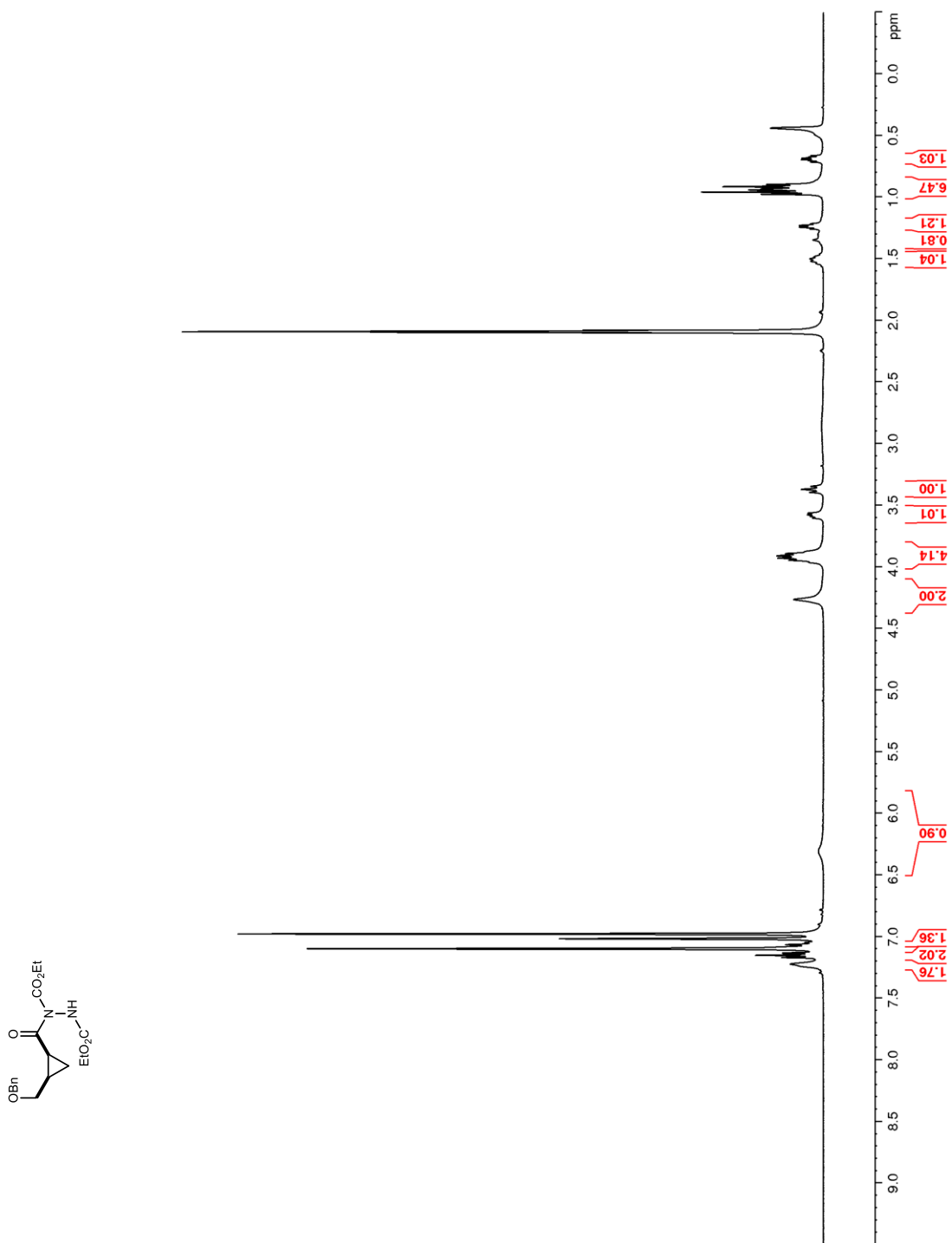


Figure 98. ^{13}C NMR (150 MHz, toluene- d_8) of **108**

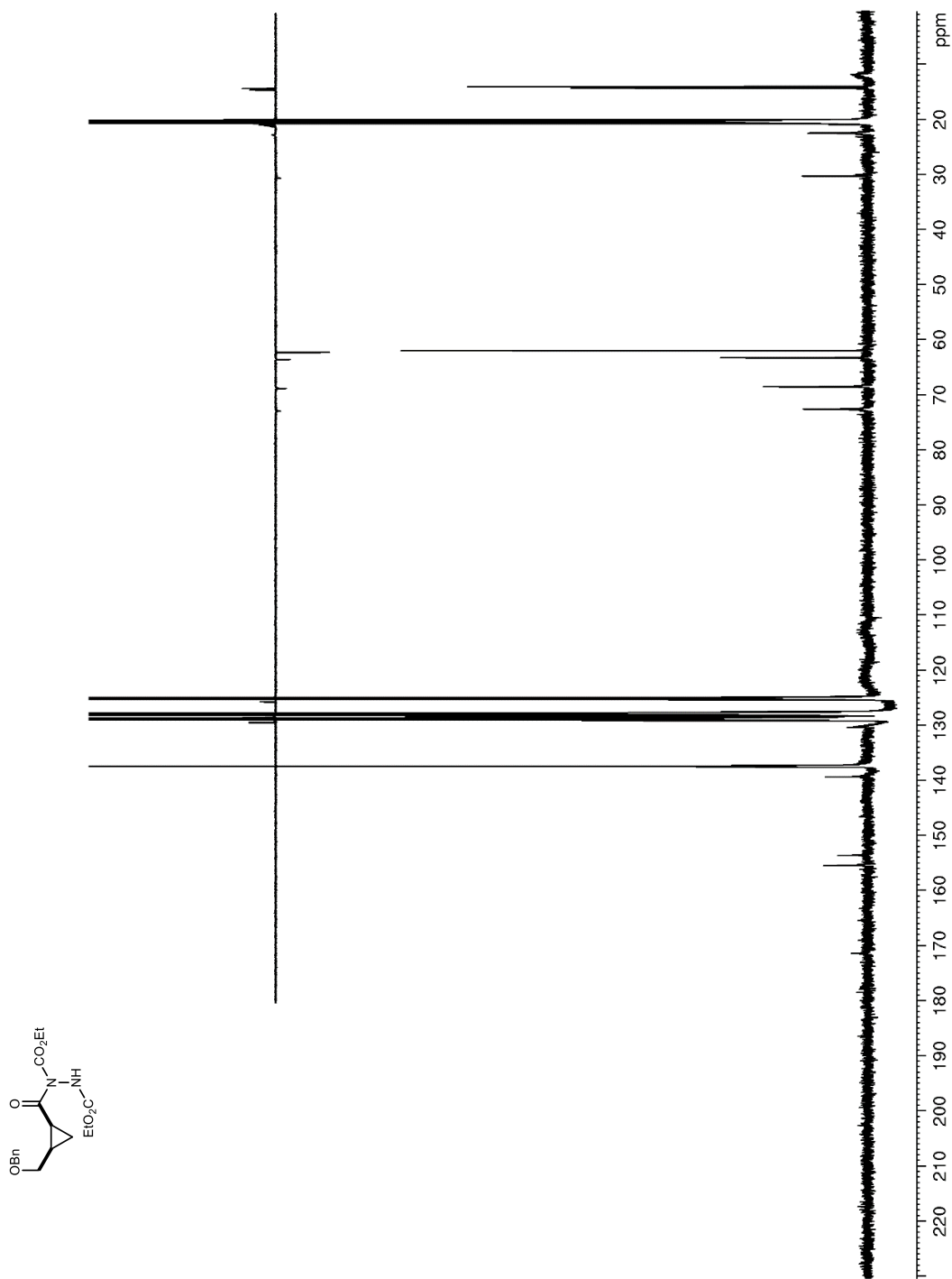


Figure 99. ^1H NMR (600 MHz, CDCl_3) of **120**

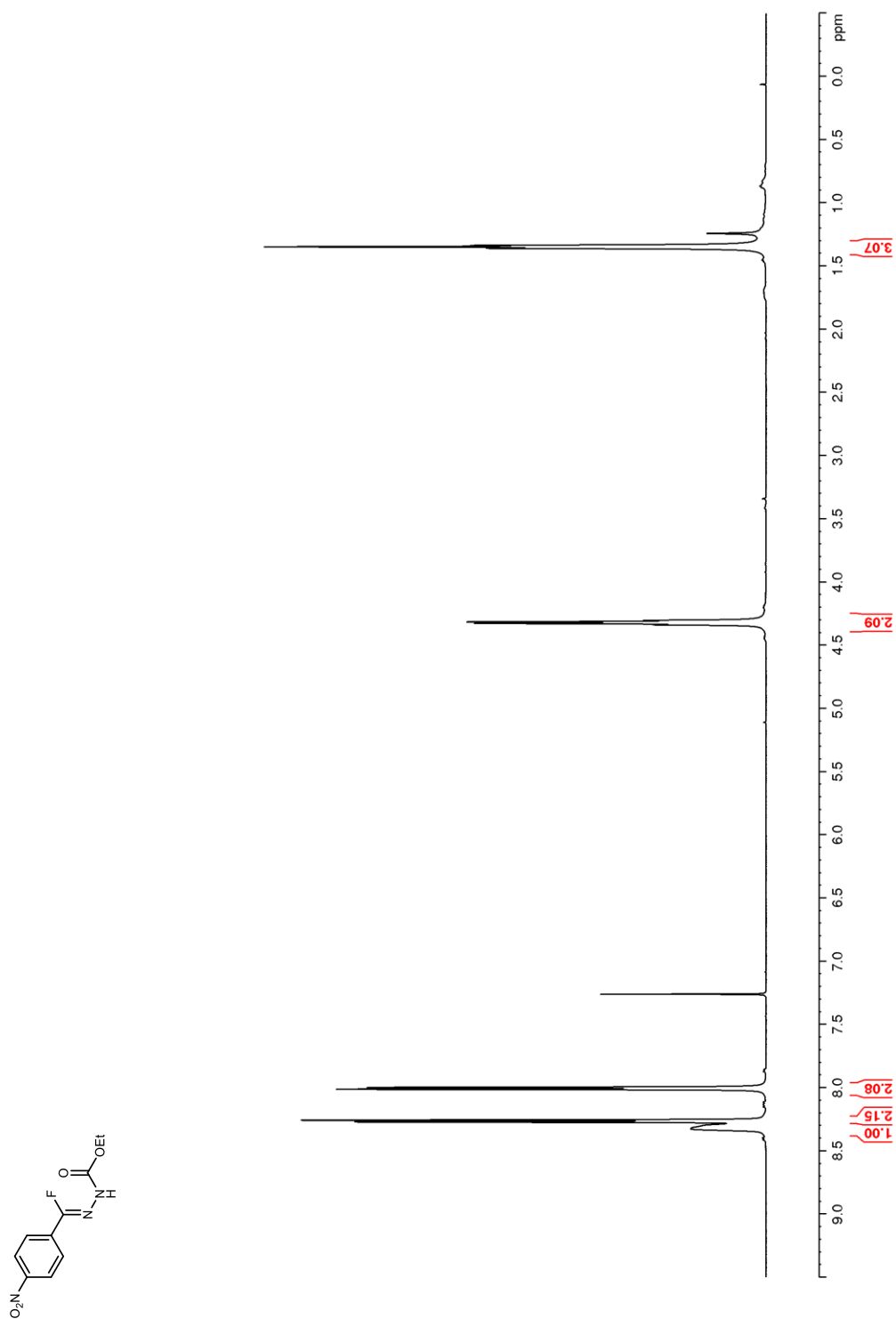


Figure 100. ^{13}C NMR (150 MHz, CDCl_3) of **120**

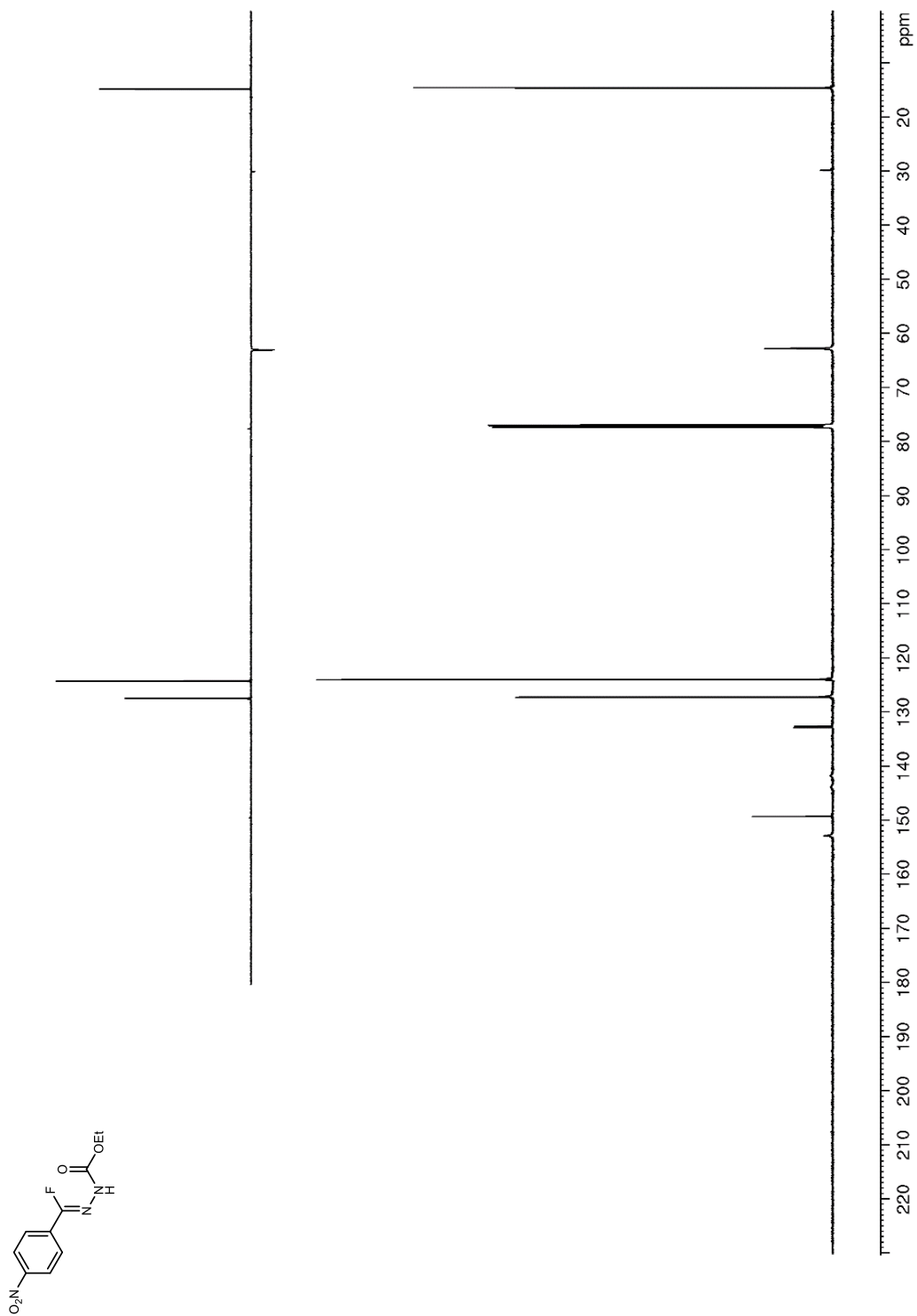


Figure 101. ^{19}F NMR (376 MHz, CDCl_3) of **120**

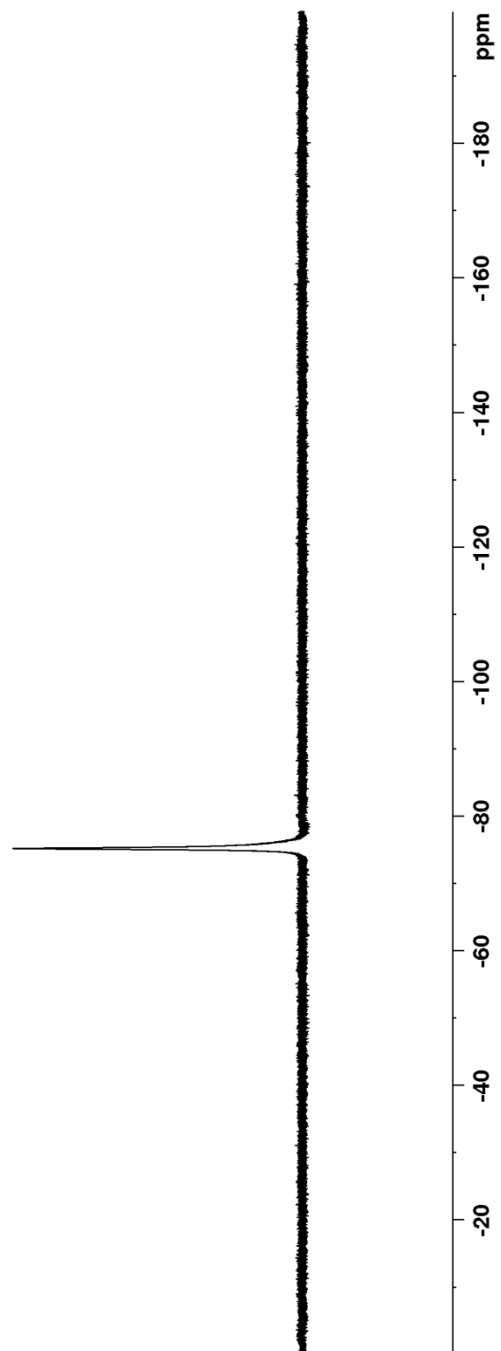
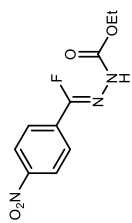


Figure 102. ^1H NMR (600 MHz, CDCl_3) of **121**

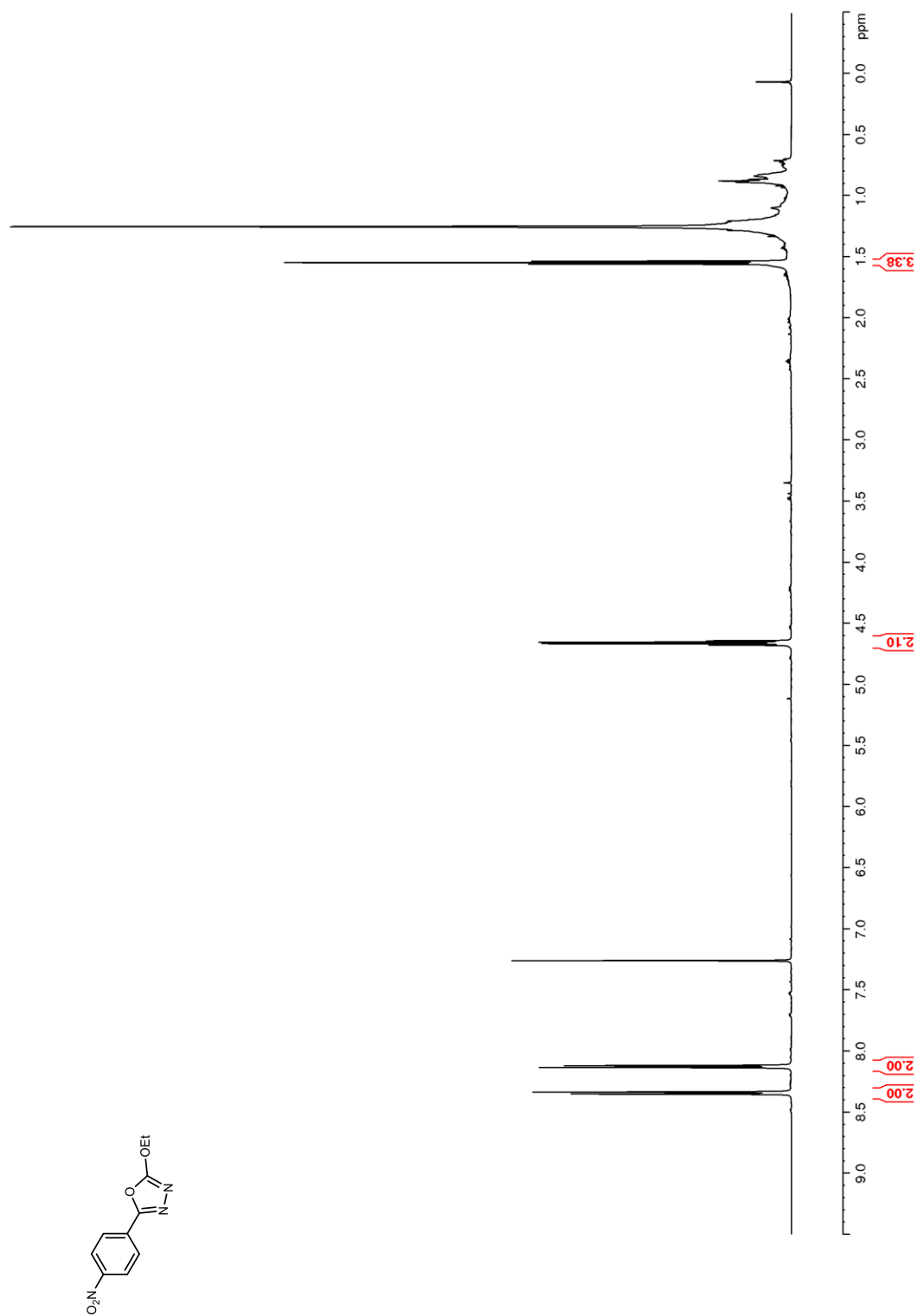


Figure 103. ^{13}C NMR (150 MHz, CDCl_3) of **121**

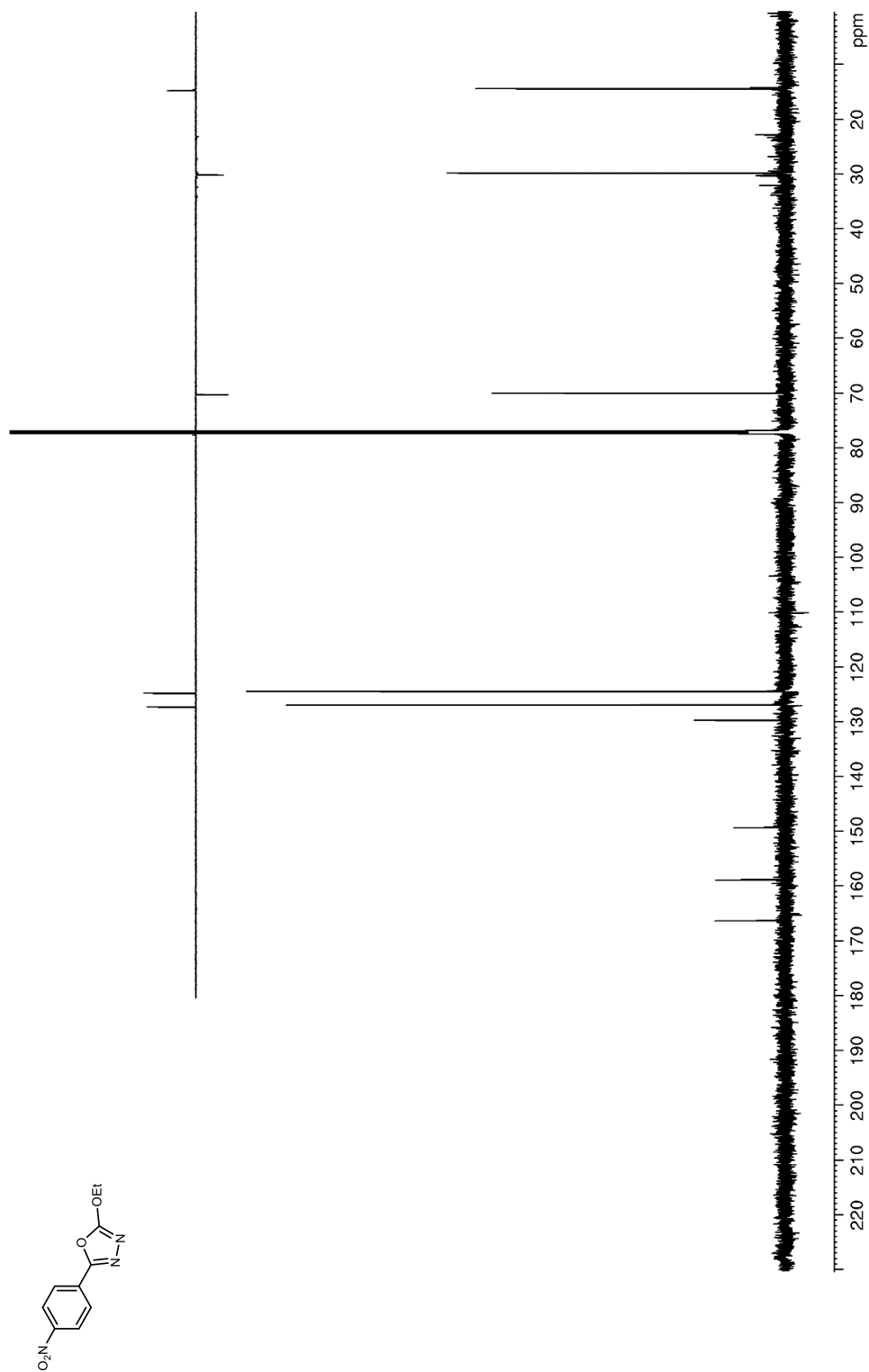


Figure 104. ^1H NMR (600 MHz, CDCl_3) of **138**

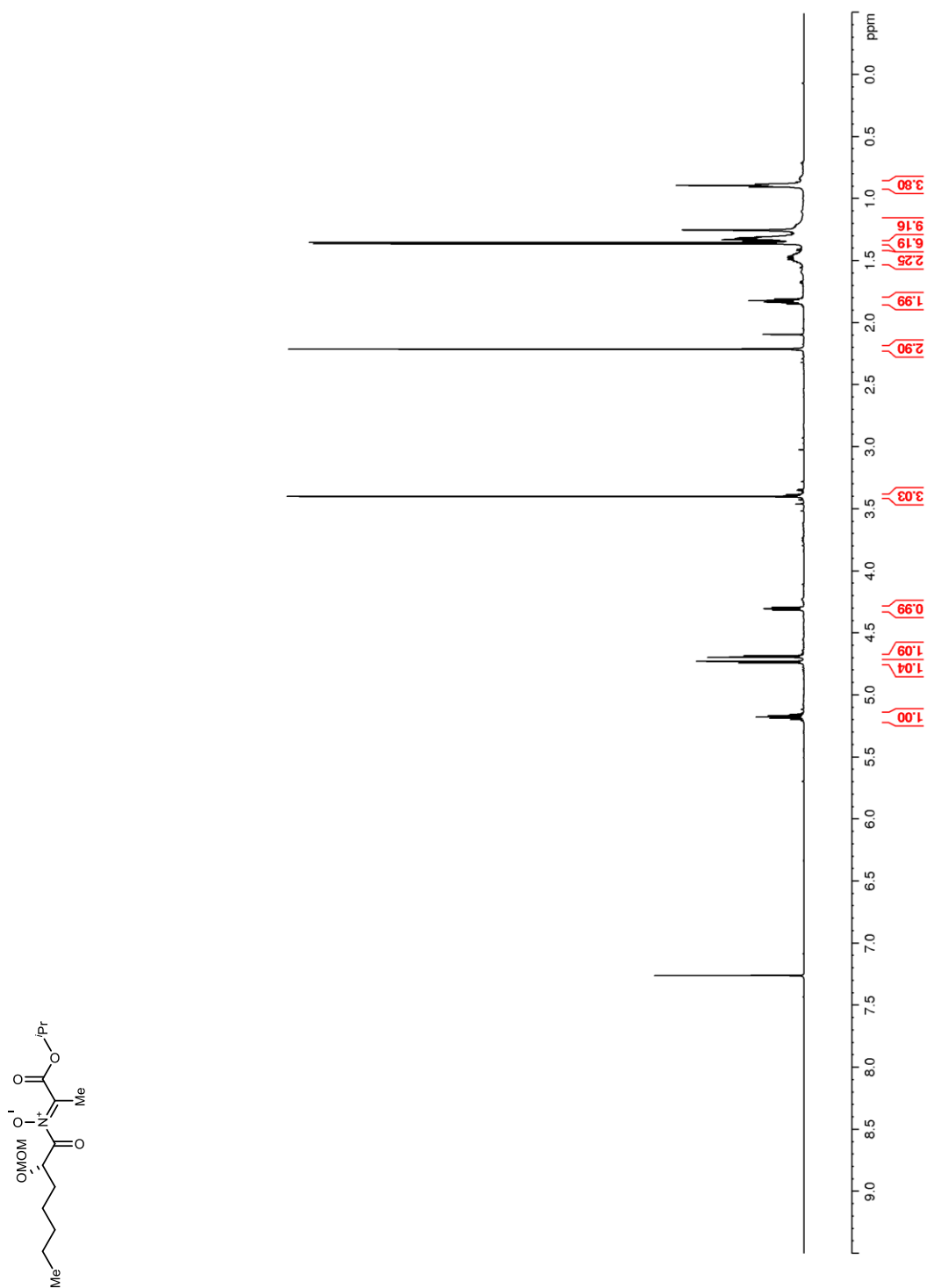


Figure 105. ^{13}C NMR (150 MHz, CDCl_3) of **138**

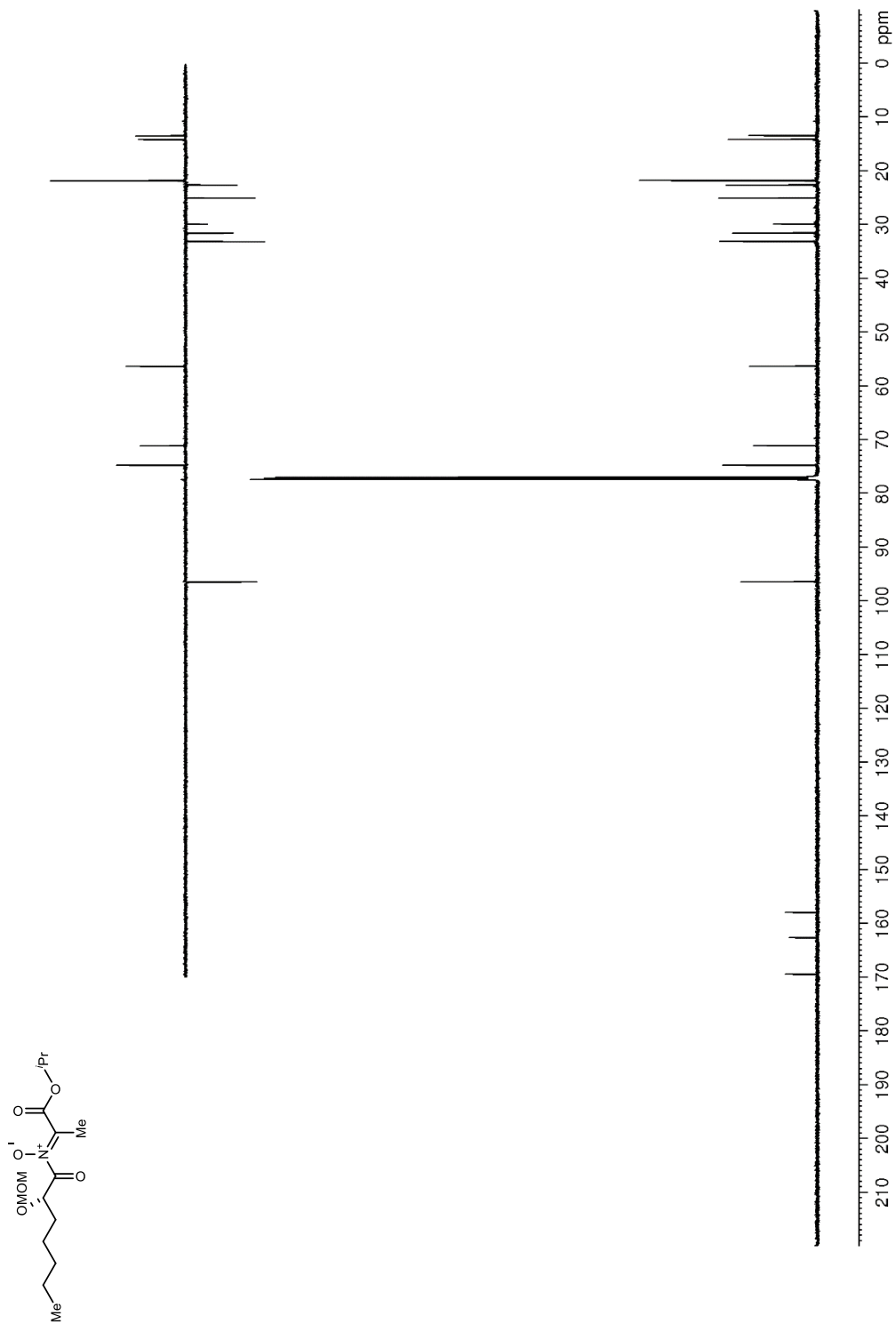


Figure 106. ^1H NMR (400 MHz, CDCl_3) of **151**

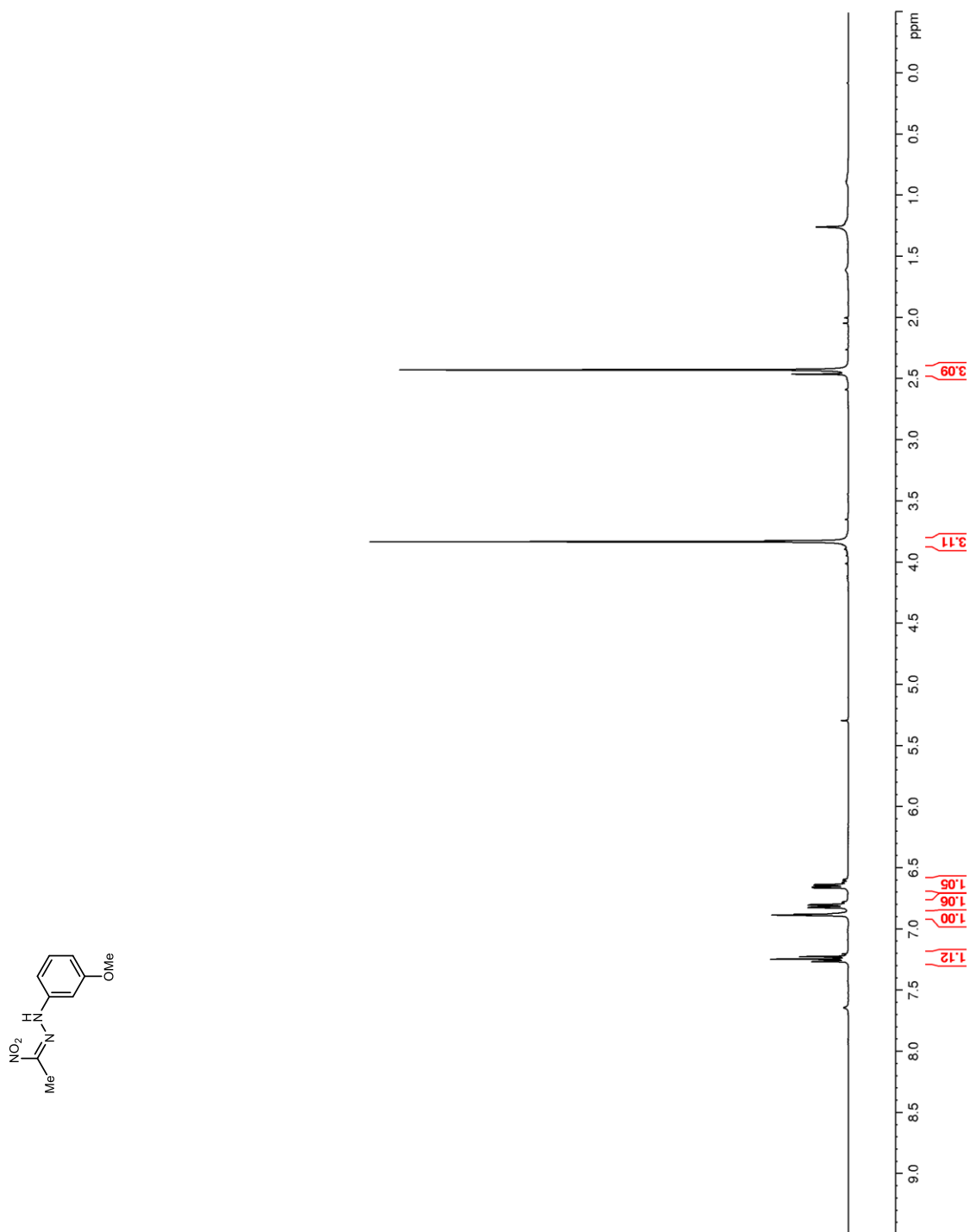


Figure 107. ^{13}C NMR (100 MHz, CDCl_3) of **151**

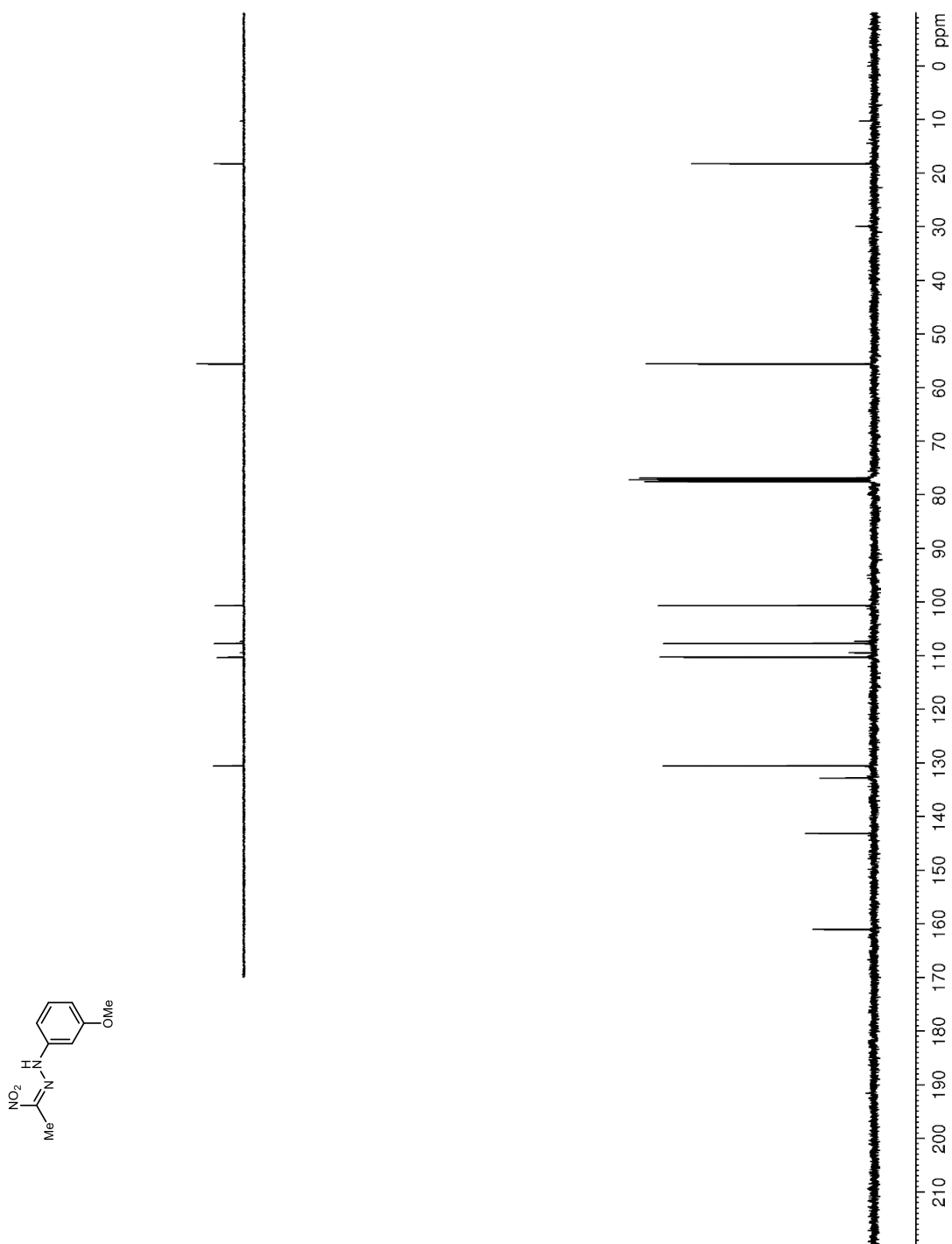


Figure 108. ^1H NMR (400 MHz, CDCl_3) of **171**

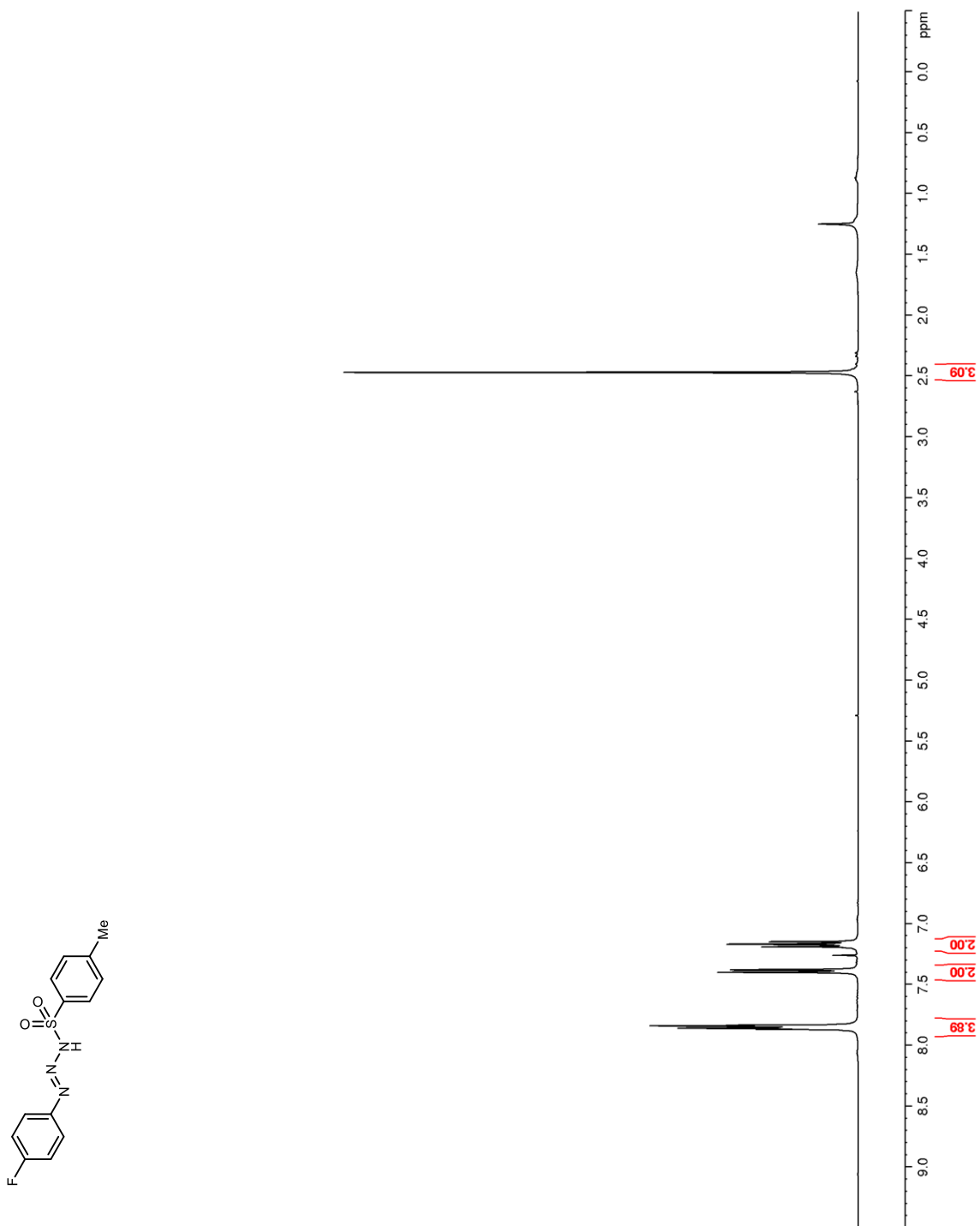


Figure 109. ^{13}C NMR (100 MHz, CDCl_3) of **171**

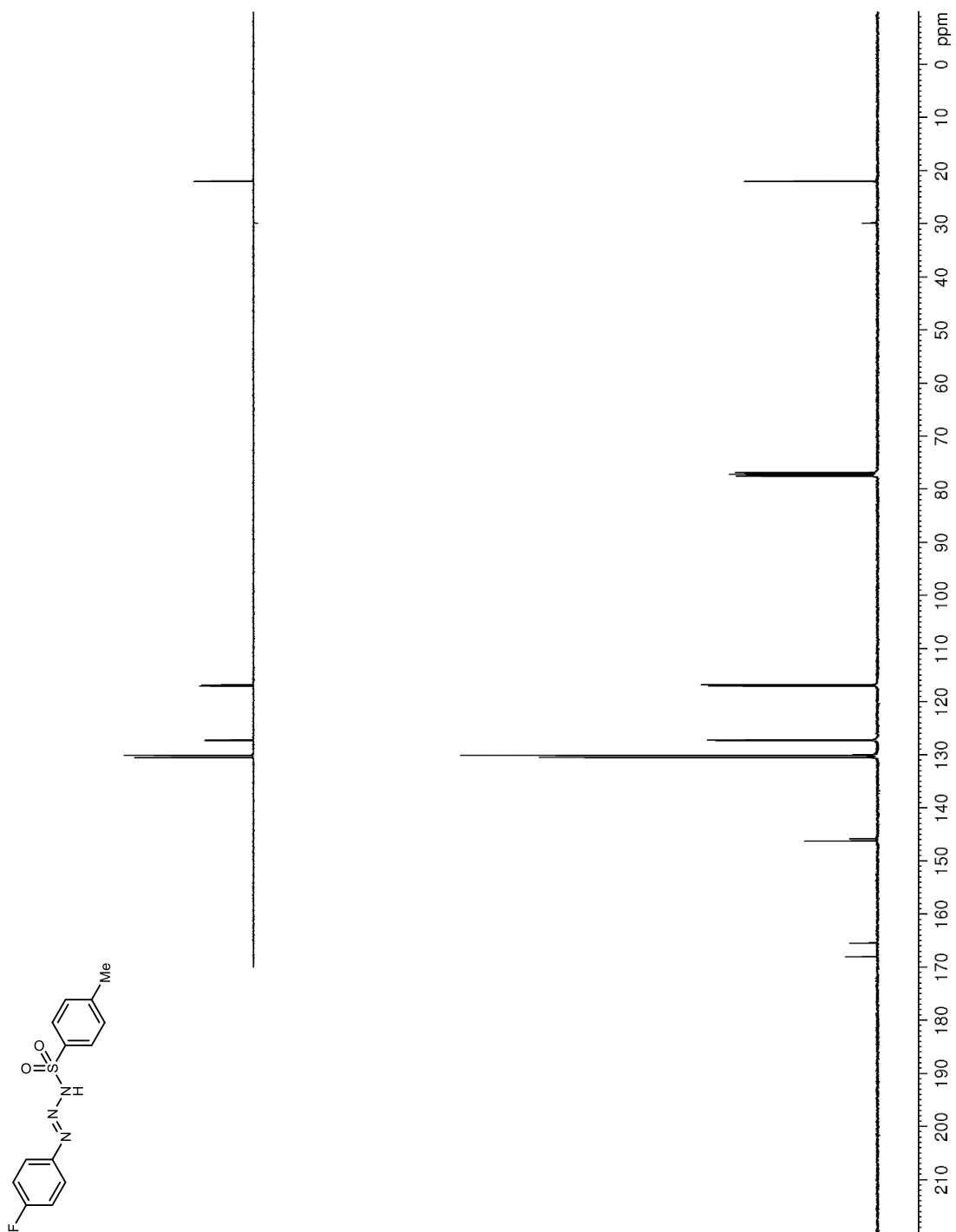


Figure 110. ^{19}F NMR (376 MHz, CDCl_3) of **171**

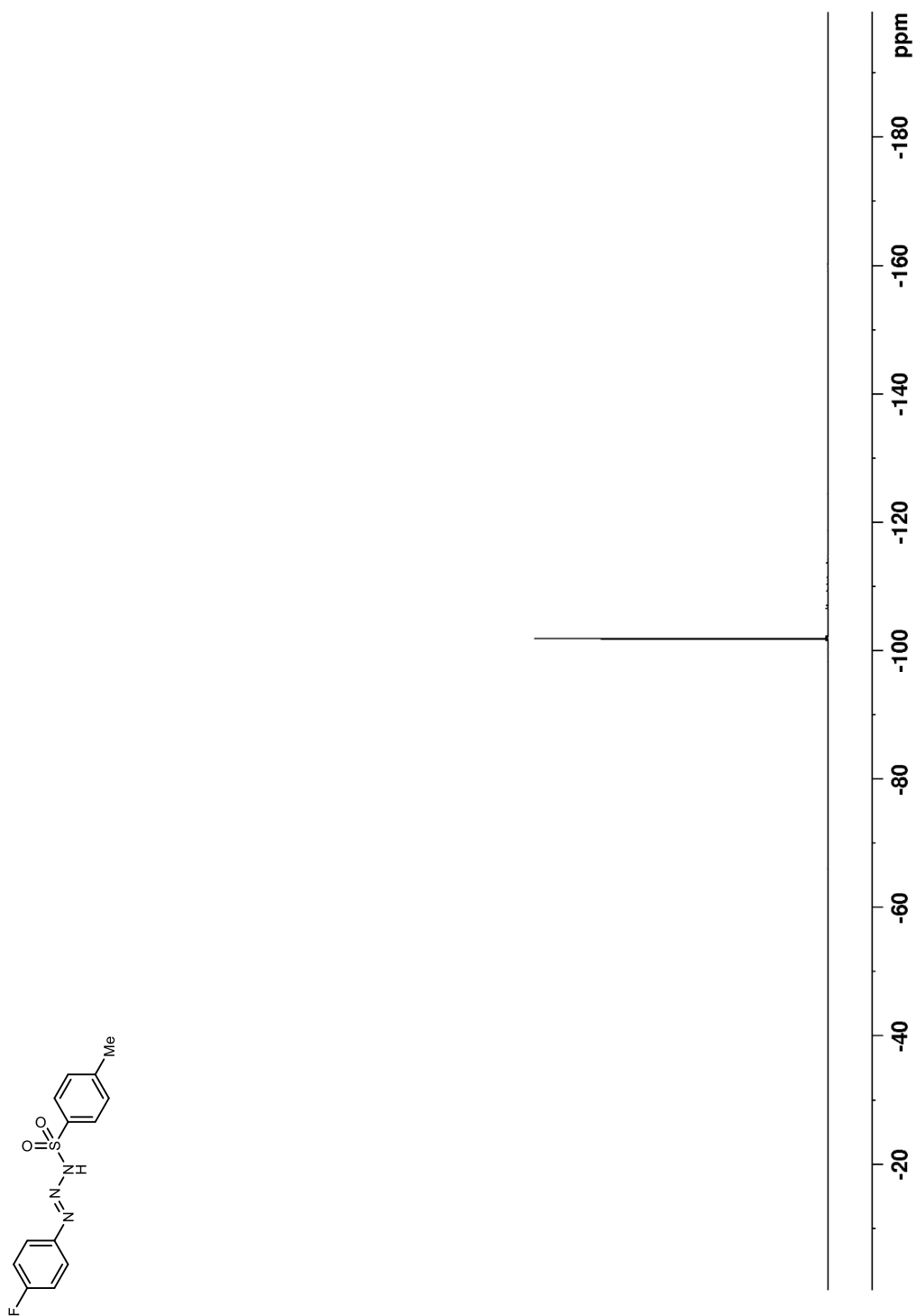


Figure 111. ^1H NMR (600 MHz, CDCl_3) of **179**

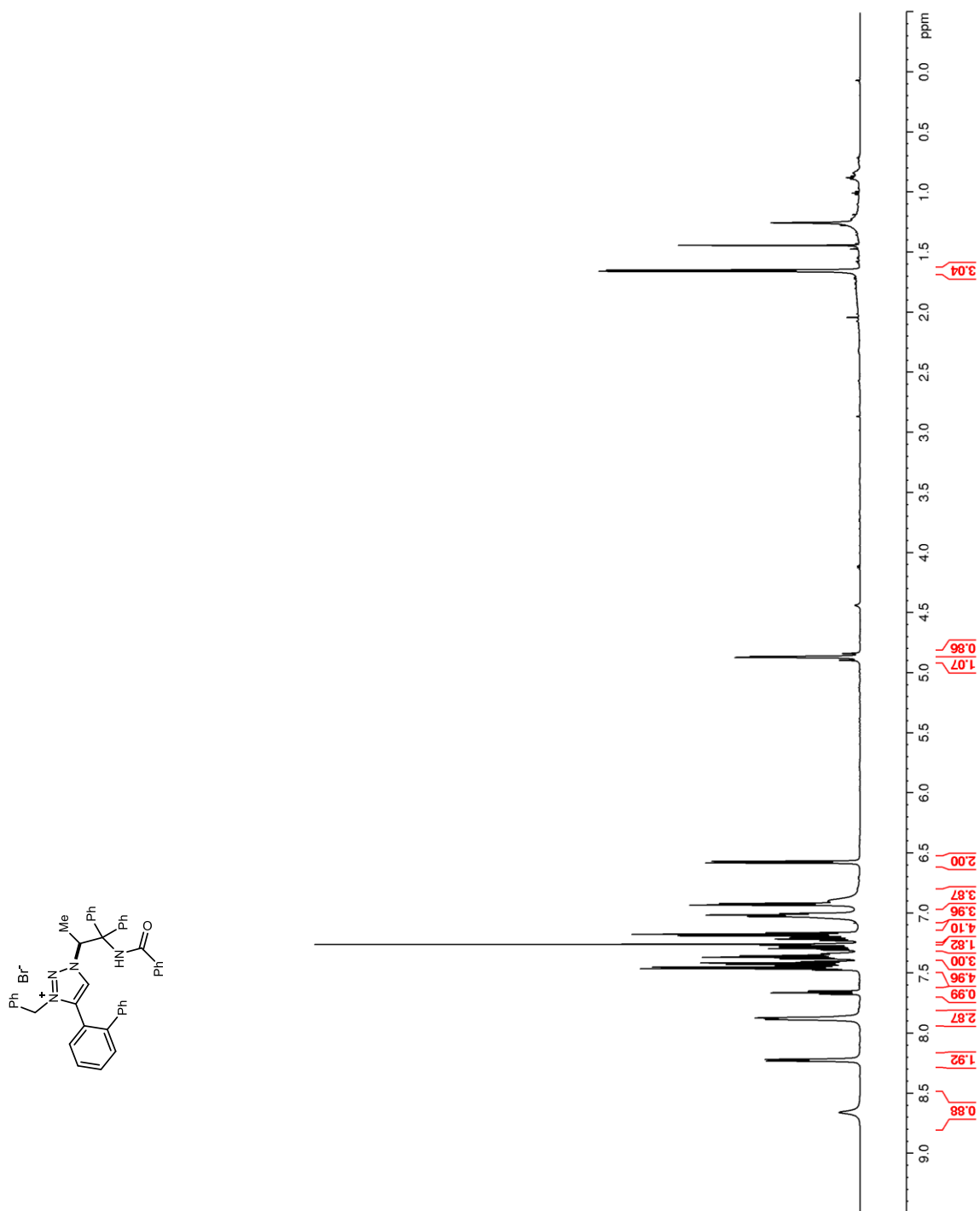


Figure 112. ^{13}C NMR (150 MHz, CDCl_3) of **179**

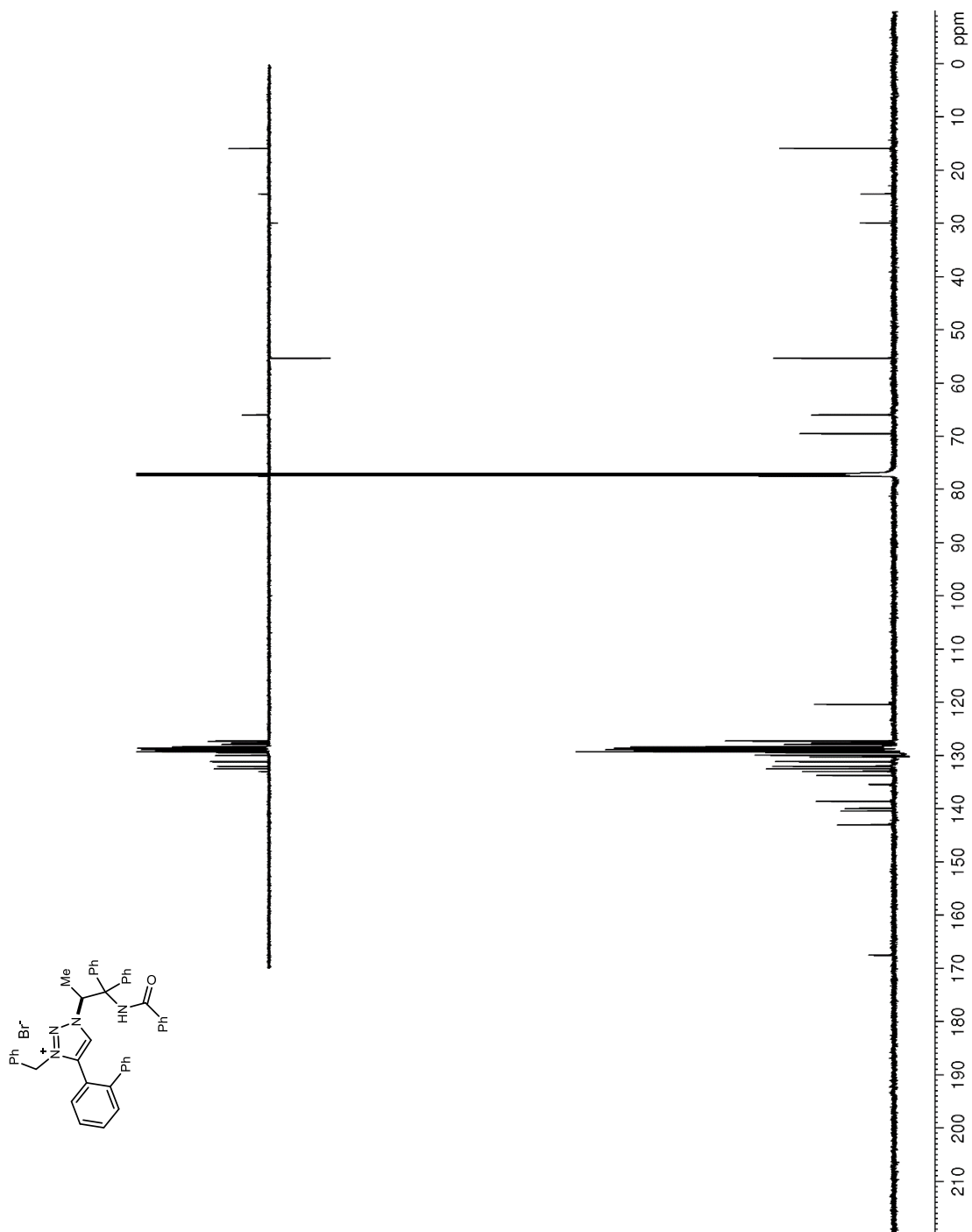


Figure 113. ^1H NMR (400 MHz, CDCl_3) of **183**

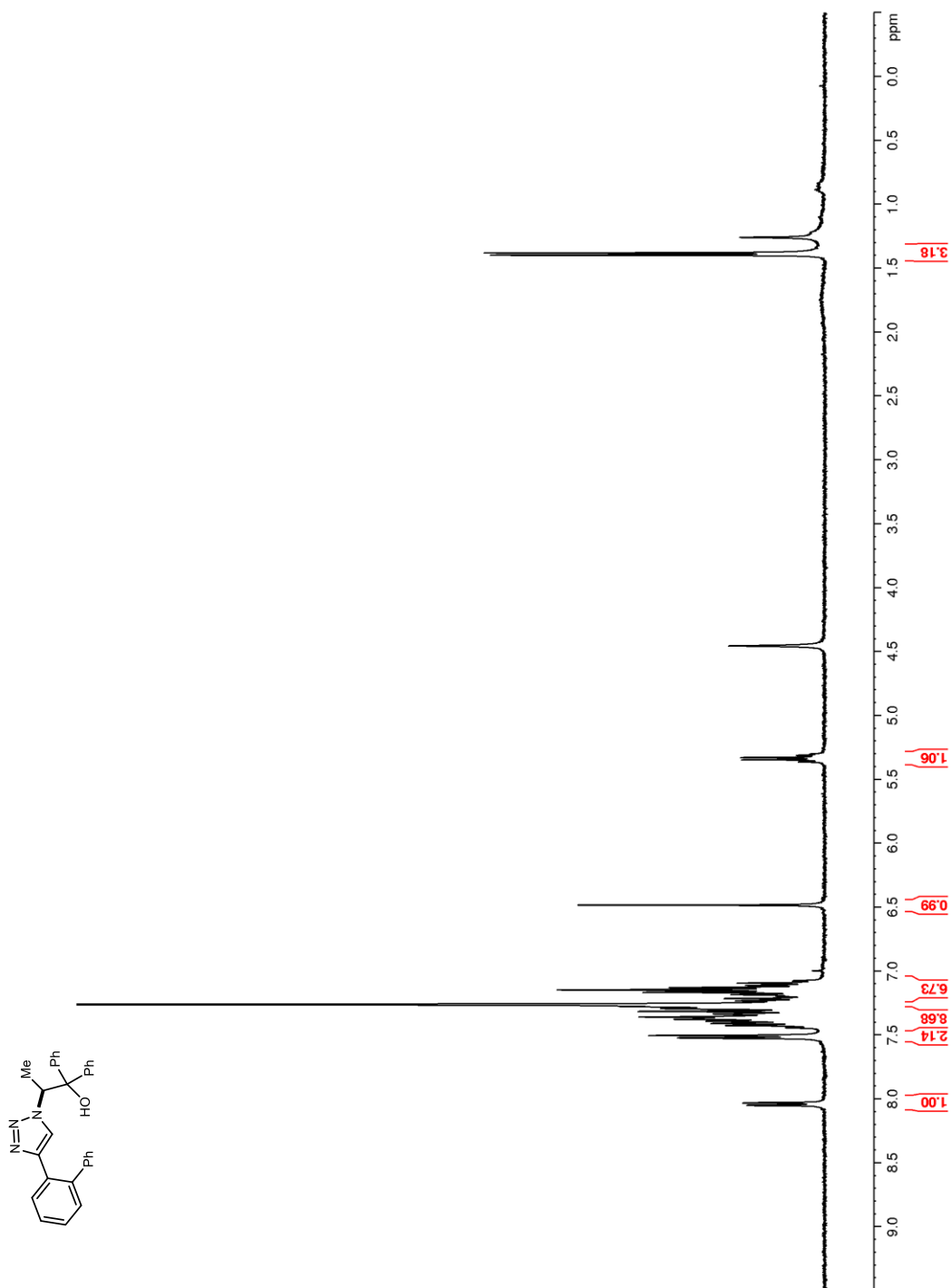


Figure 114. ^{13}C NMR (100 MHz, CDCl_3) of **183**

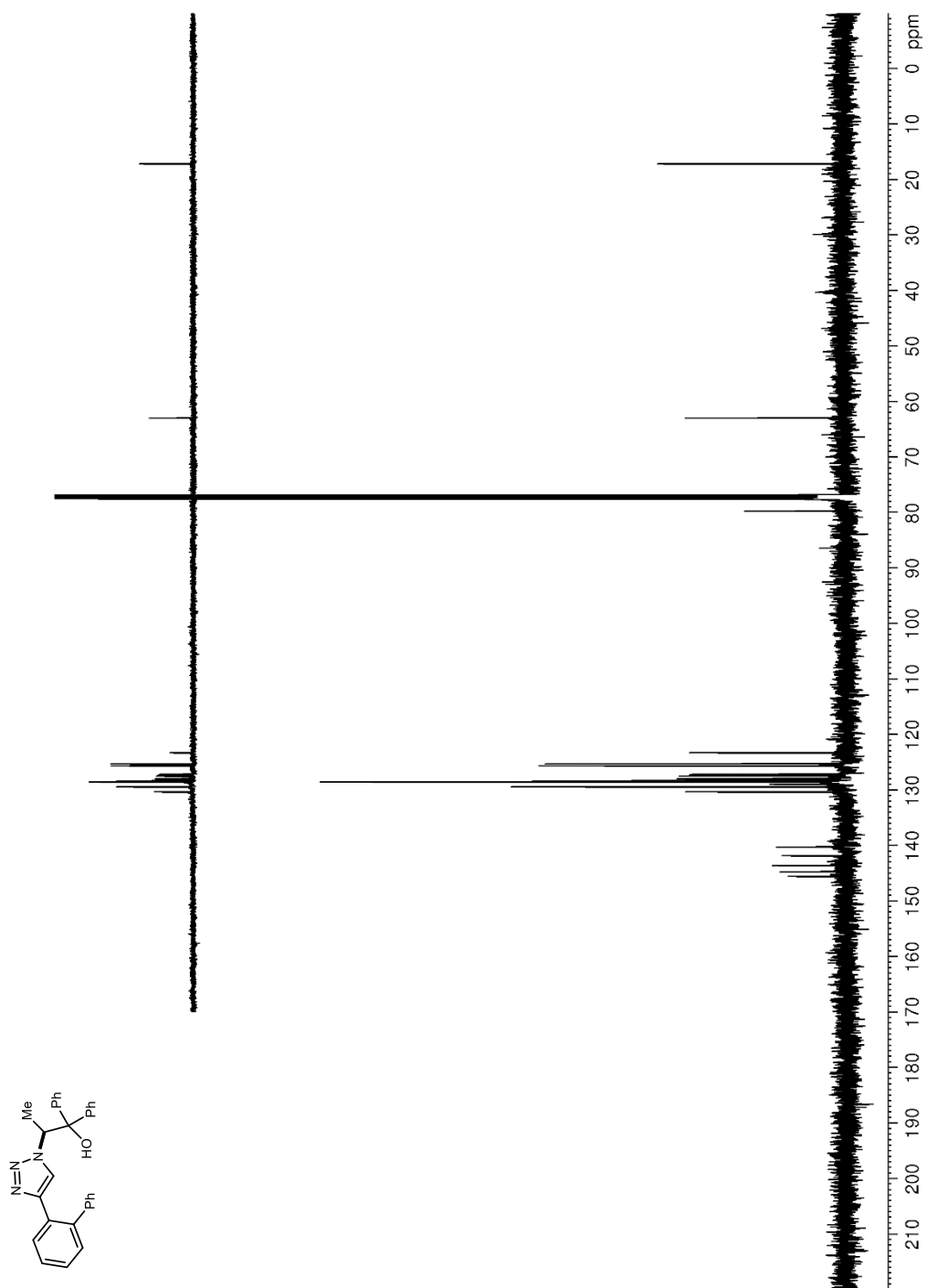


Figure 115. ^1H NMR (400 MHz, CDCl_3) of **187**

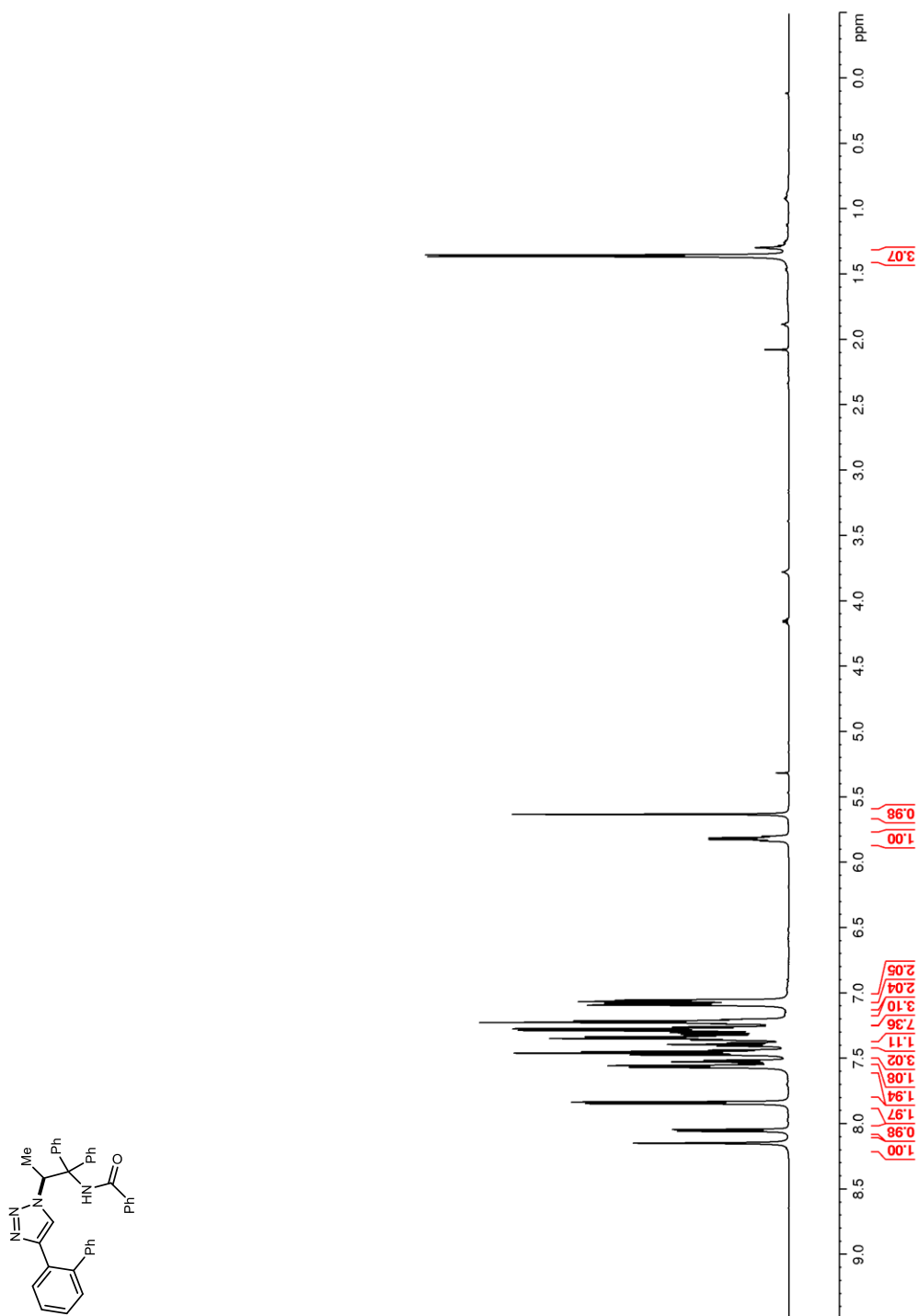


Figure 116. ^{13}C NMR (100 MHz, CDCl_3) of **187**

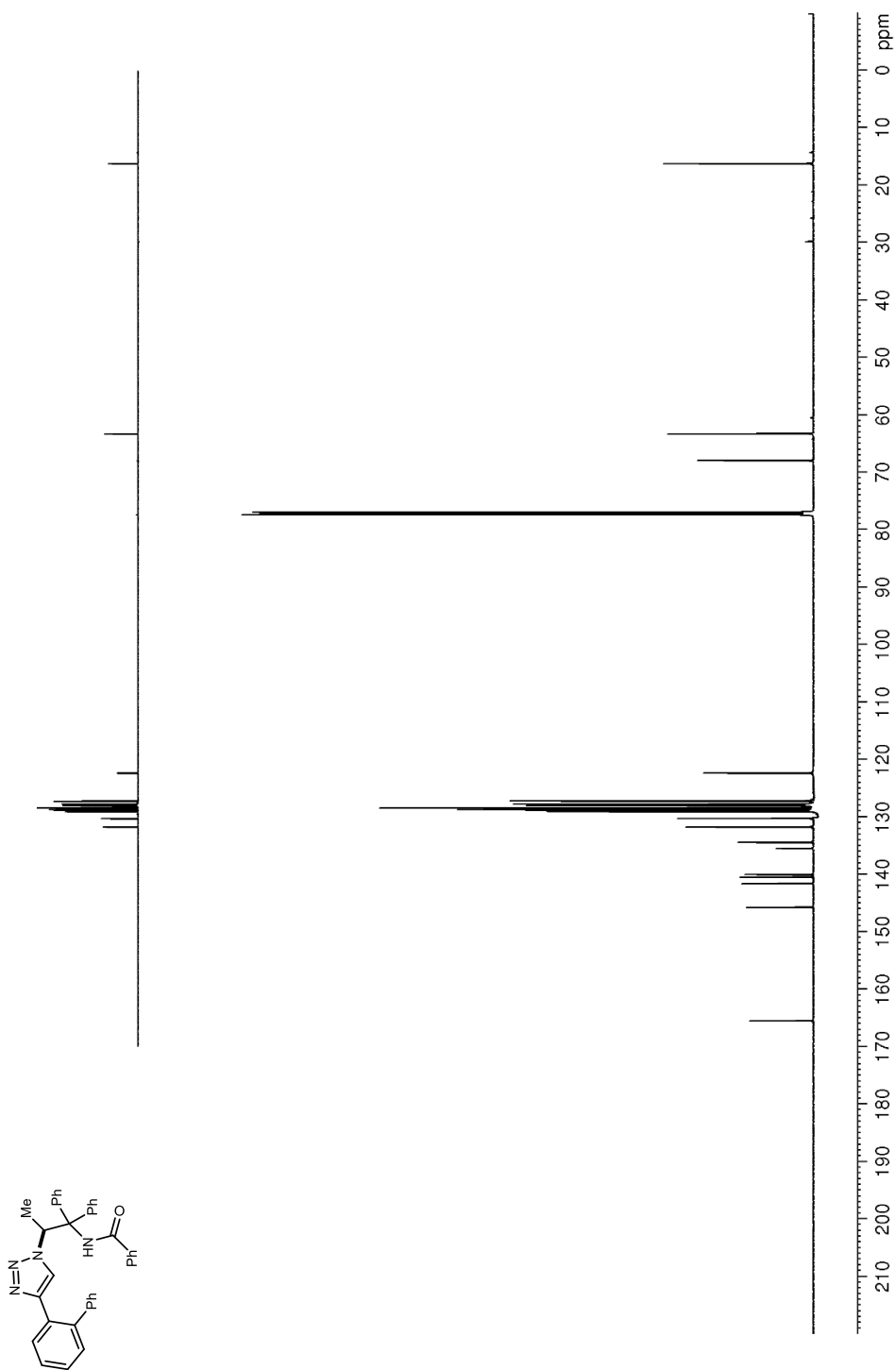


Figure 117. ^1H NMR (400 MHz, $\text{DMSO-}d_6$) of **196**

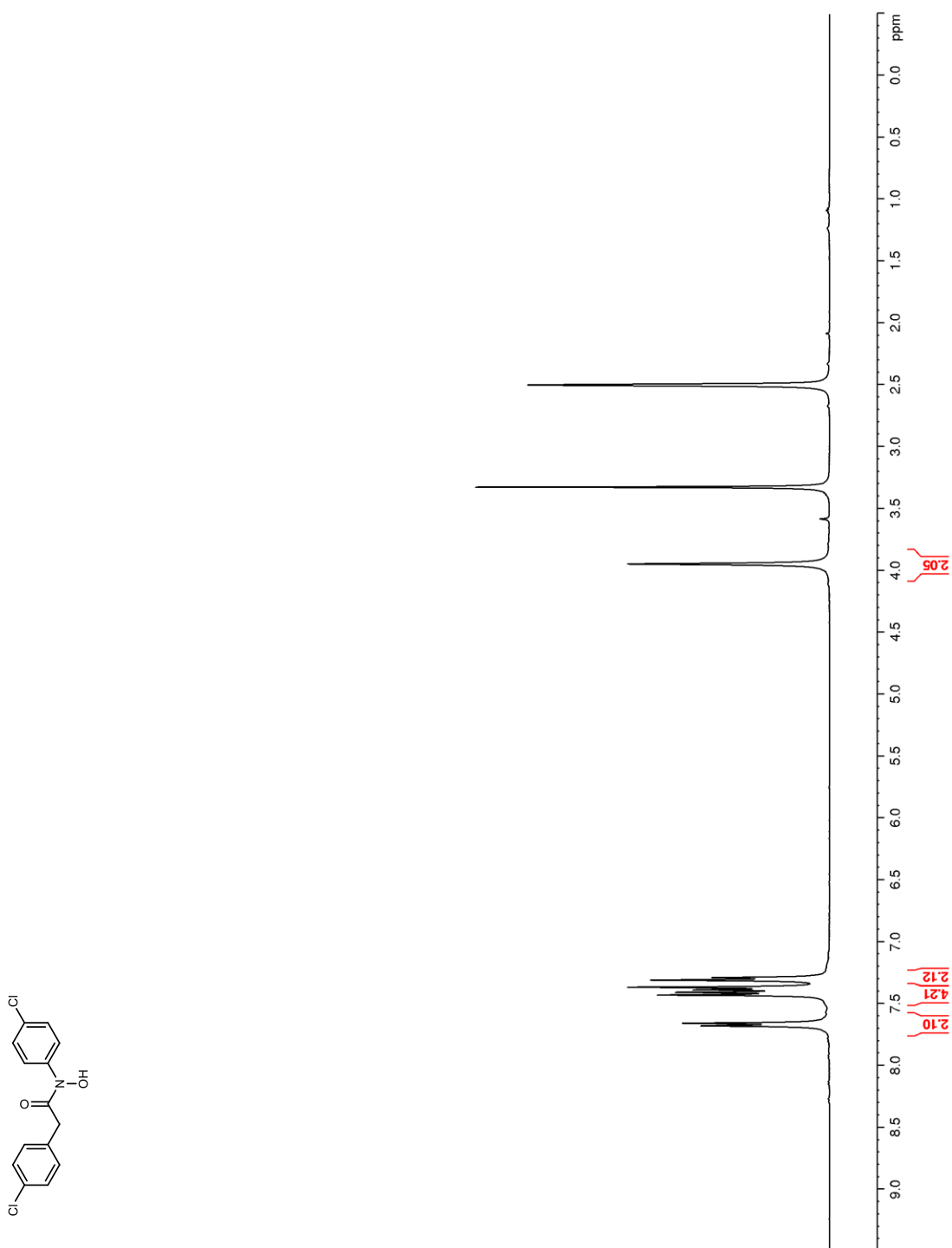


Figure 118. ^{13}C NMR (100 MHz, $\text{DMSO-}d_6$) of **196**

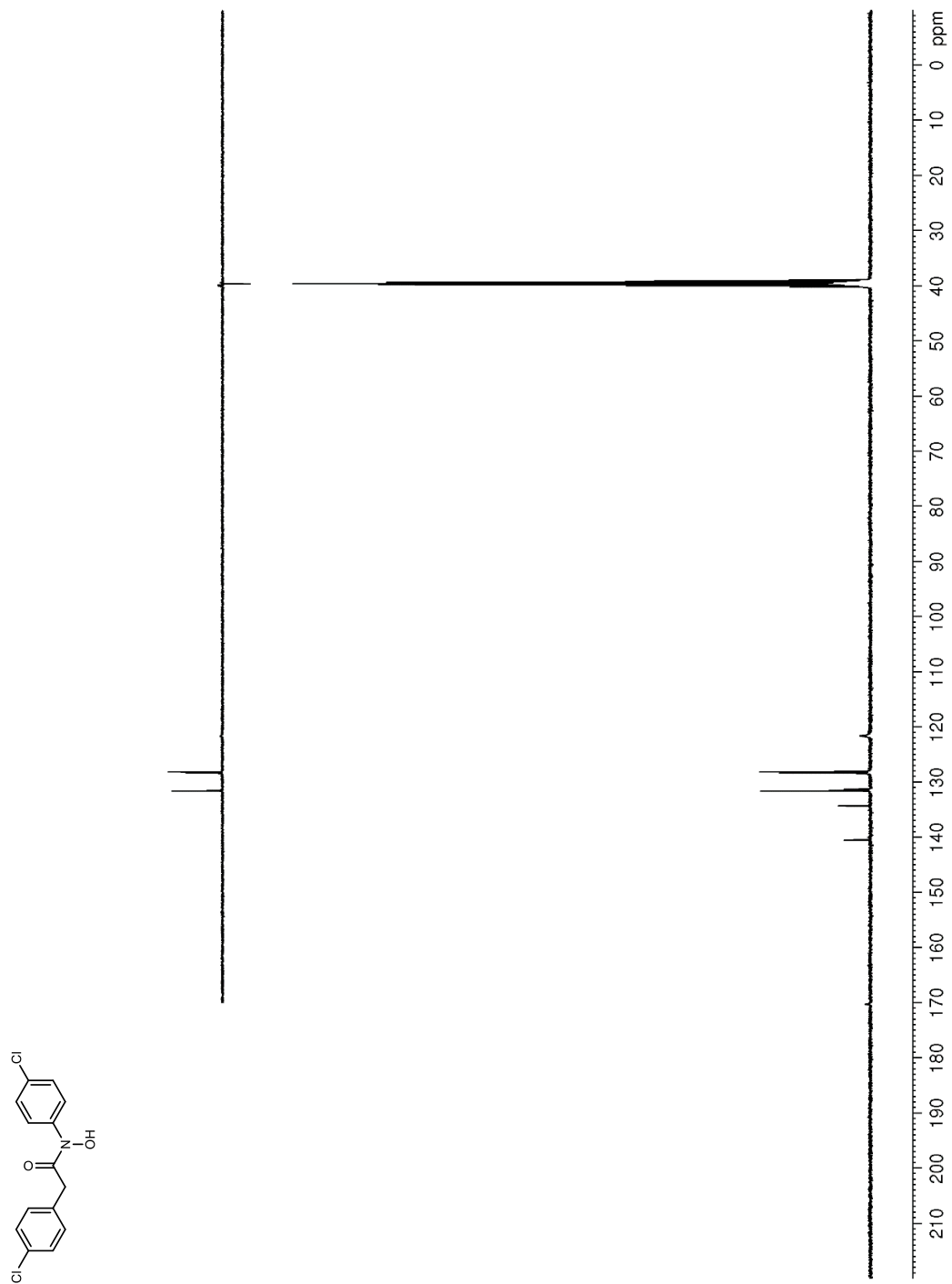


Figure 119. ^1H NMR (400 MHz, acetone- d_6) of **215**

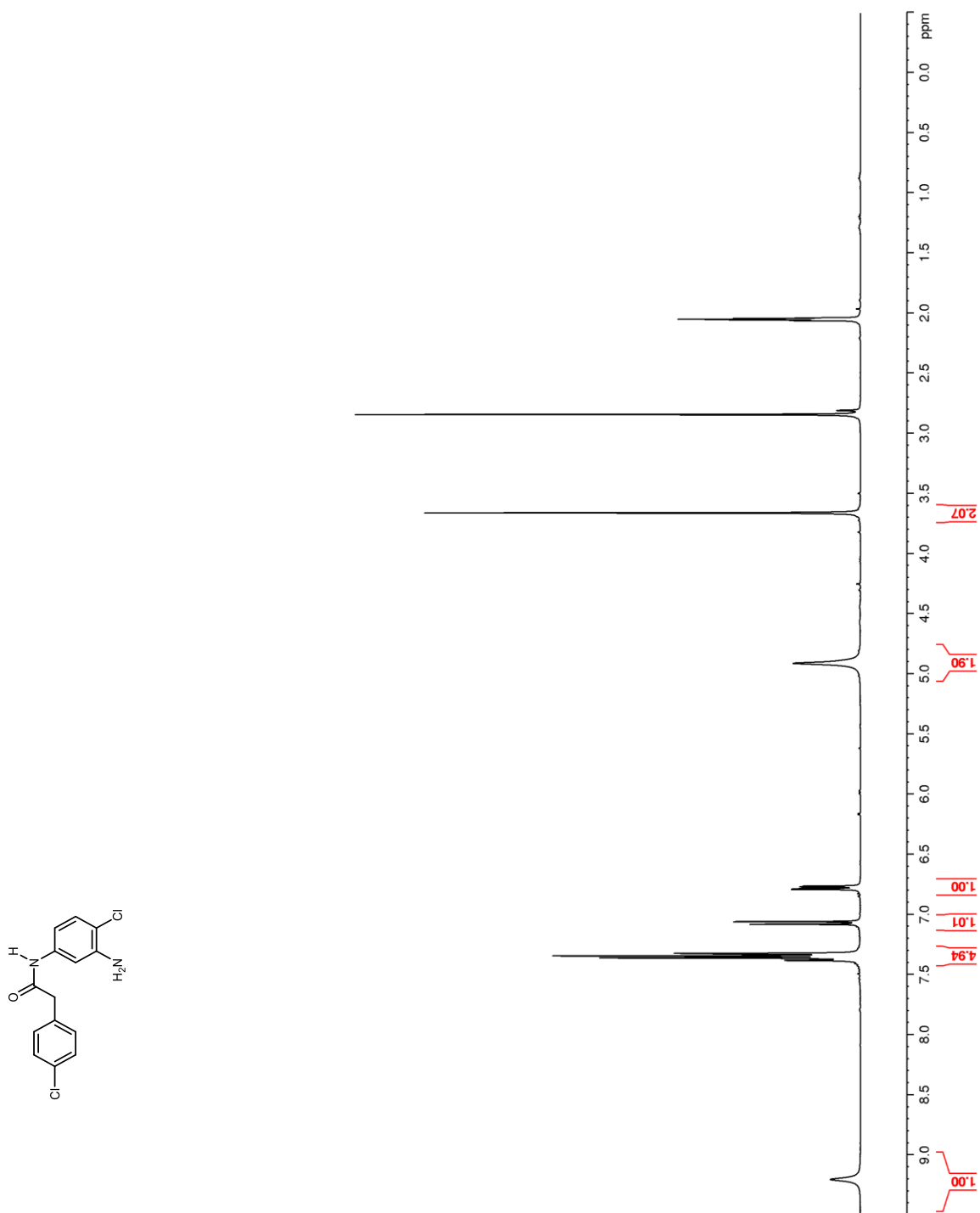


Figure 120. ^{13}C NMR (100 MHz, acetone- d_6) of **215**

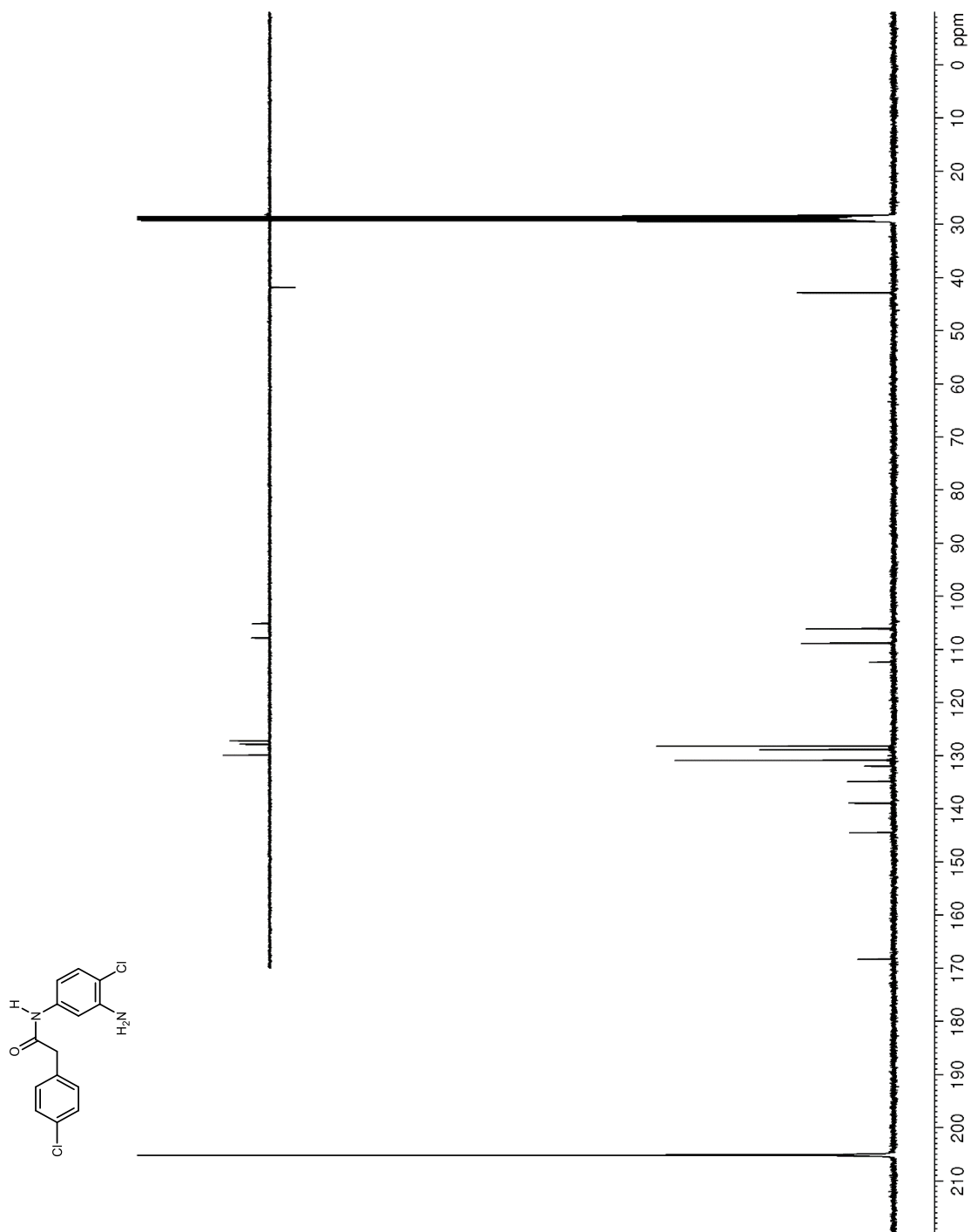


Figure 121. ^1H NMR (400 MHz, $\text{DMSO-}d_6$) of **216**

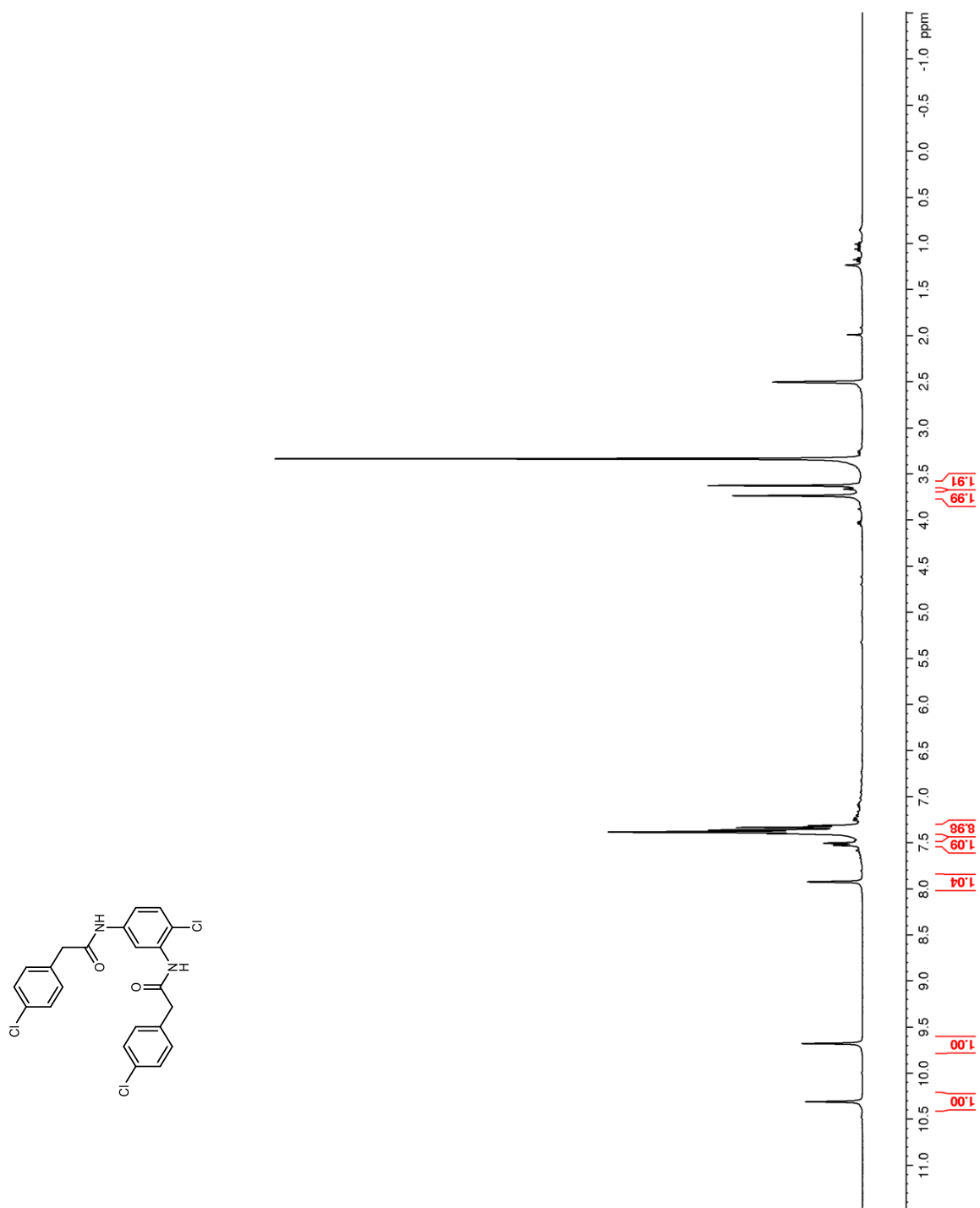


Figure 122. ^{13}C NMR (100 MHz, $\text{DMSO-}d_6$) of **216**

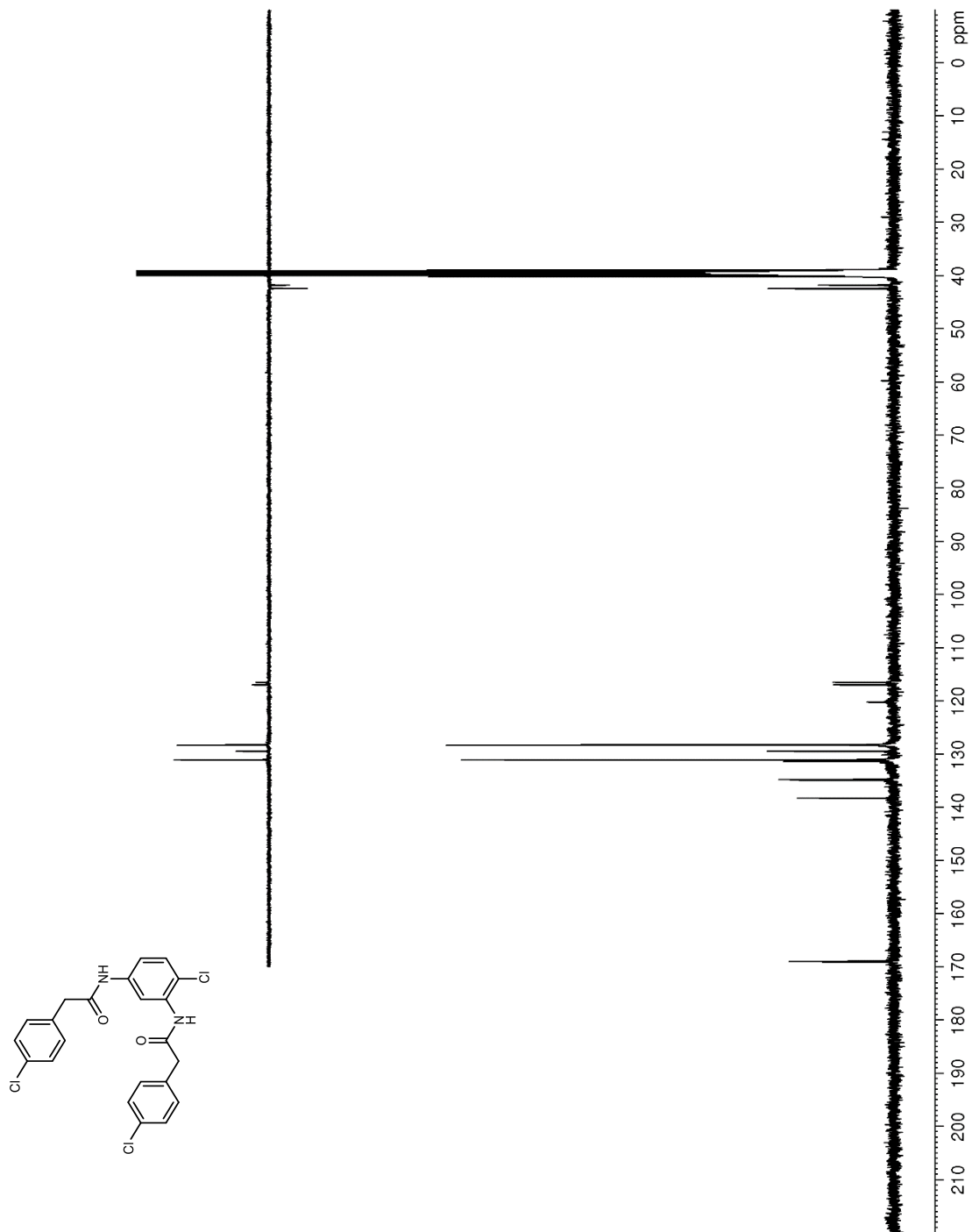


Figure 123. ^1H NMR (400 MHz, CDCl_3) of **220**

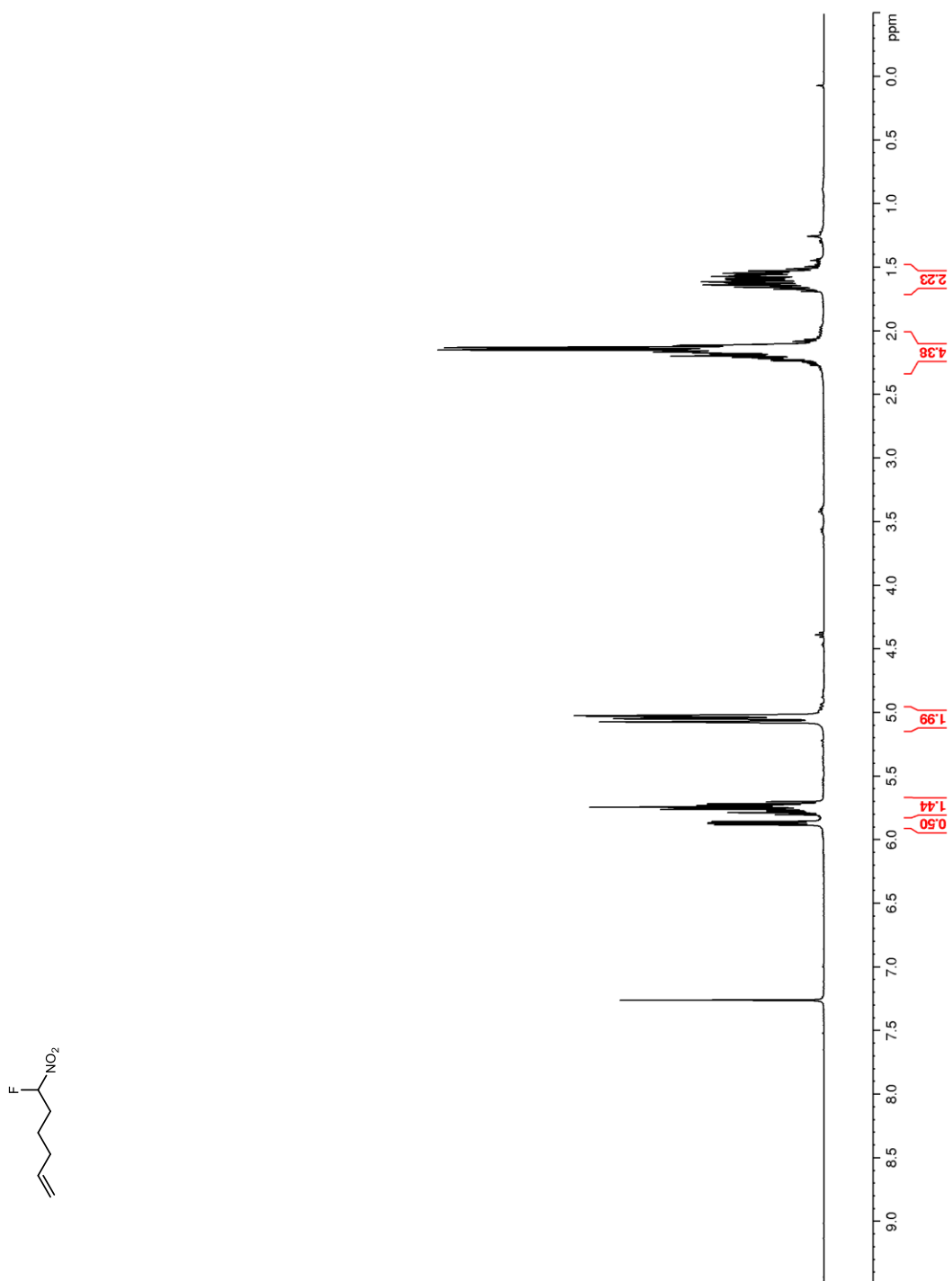


Figure 124. ^{13}C NMR (100 MHz, CDCl_3) of **220**

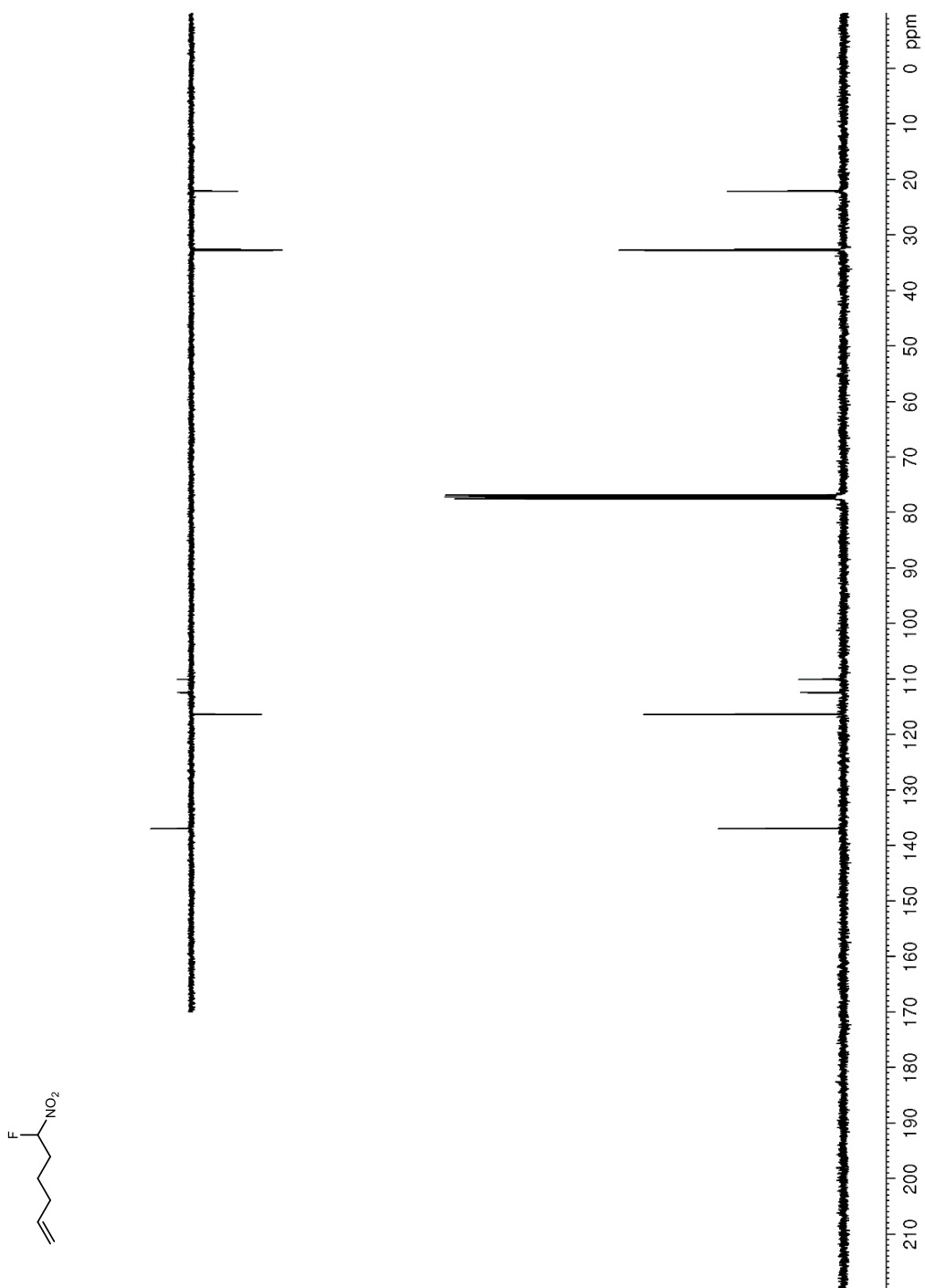


Figure 125. ^{19}F NMR (376 MHz, CDCl_3) of **220**

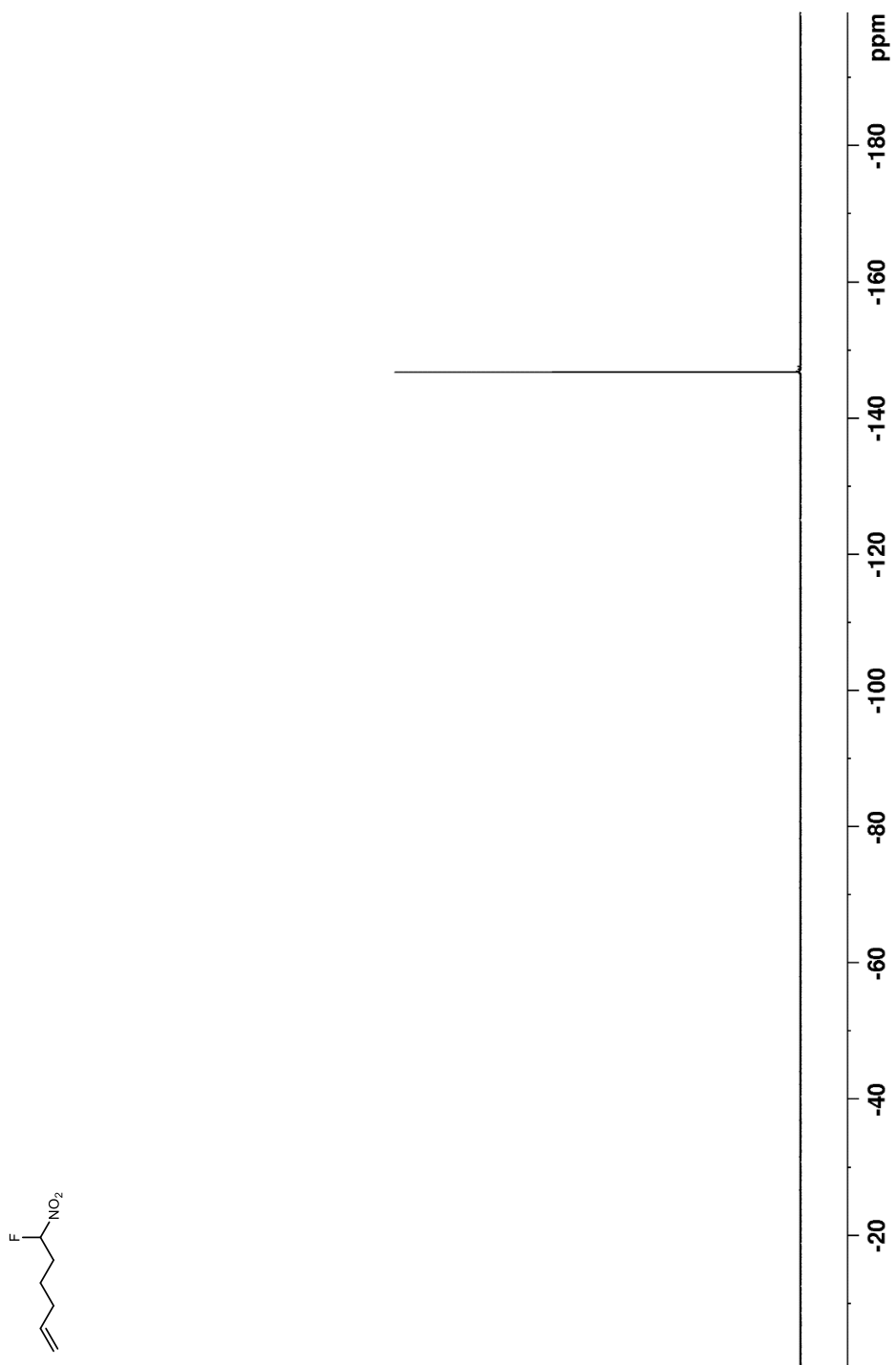


Figure 126. ^1H NMR (400 MHz, CDCl_3) of **222**

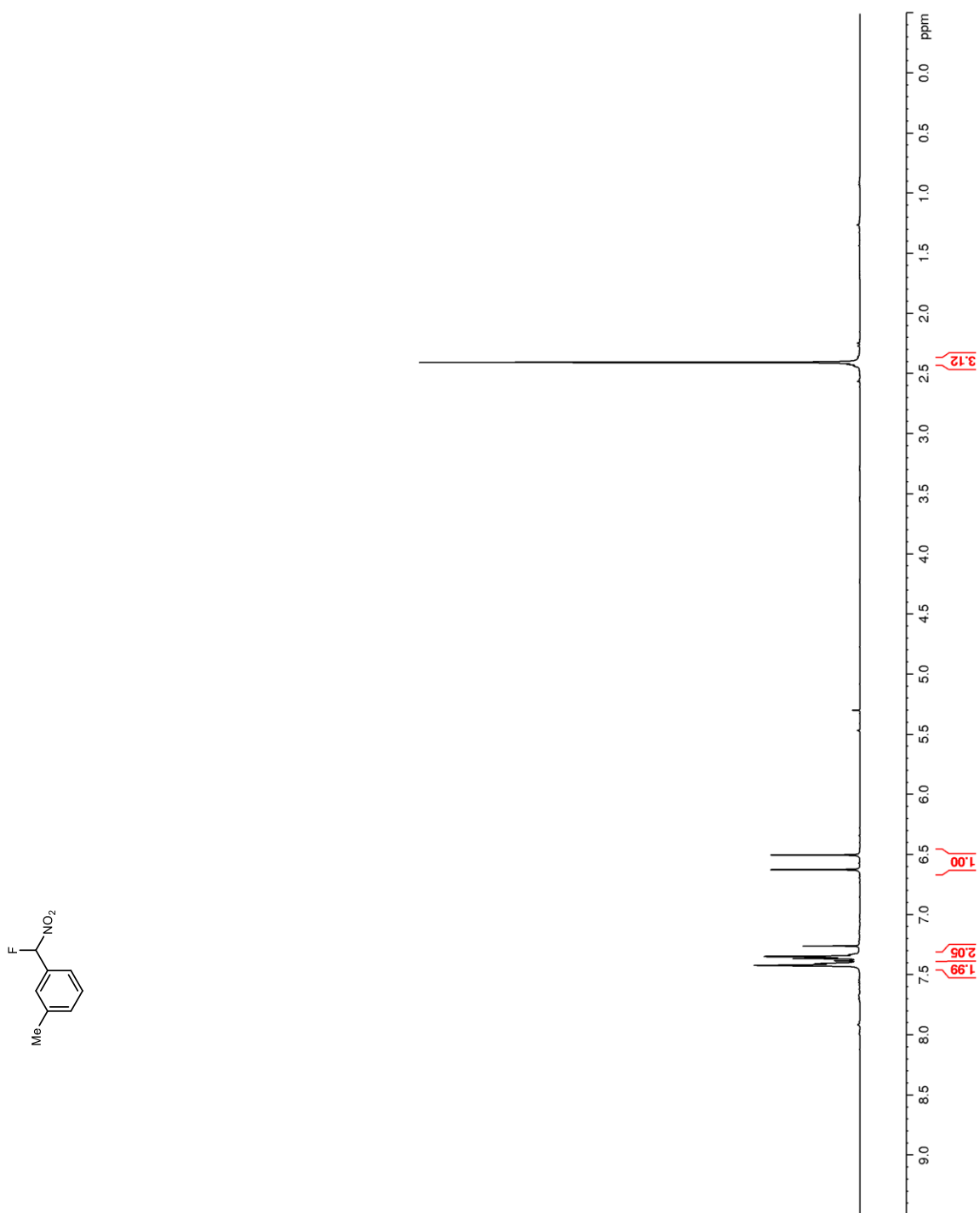


Figure 127. ^{13}C NMR (100 MHz, CDCl_3) of **222**

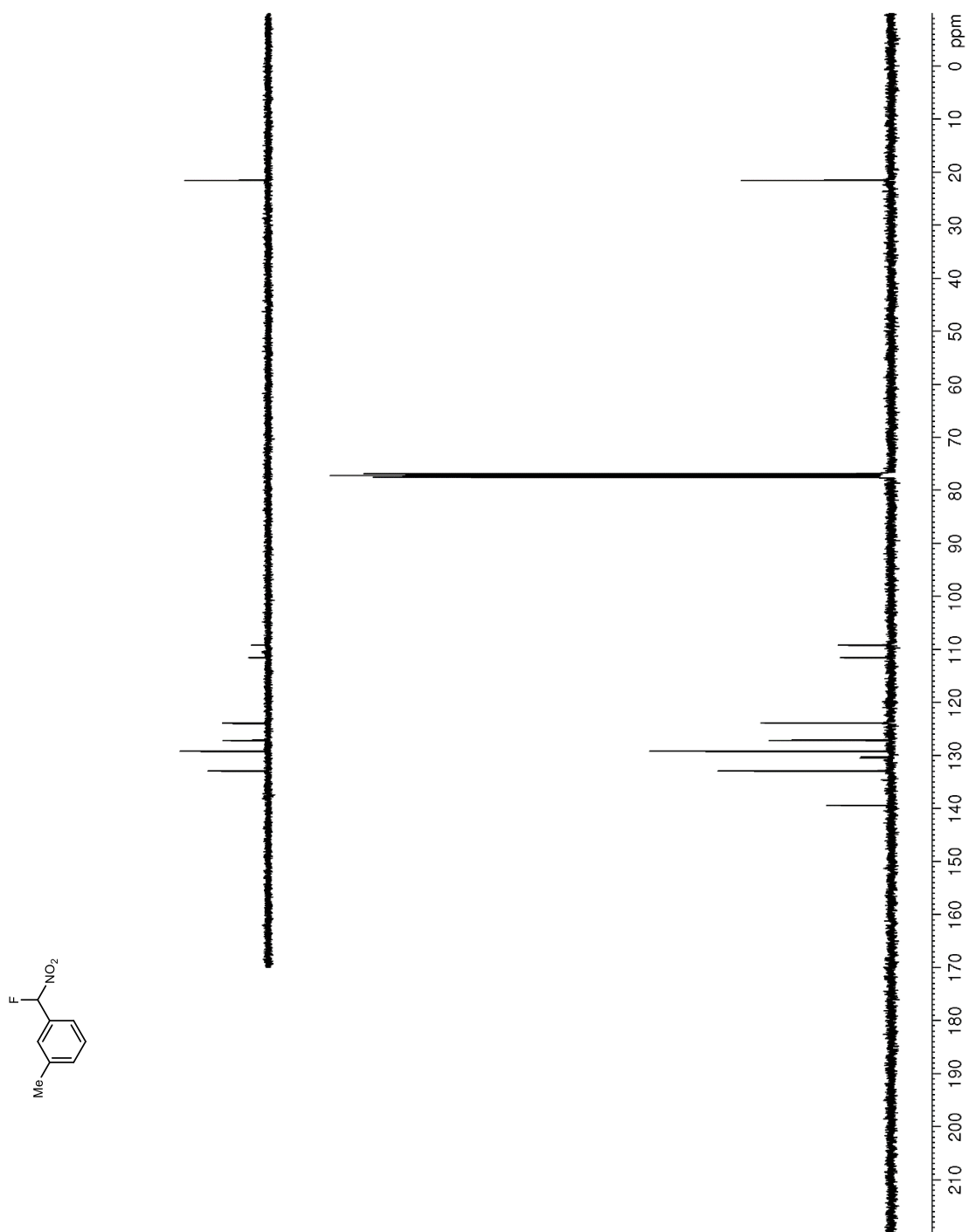


Figure 128. ^{19}F NMR (376 MHz, CDCl_3) of **222**

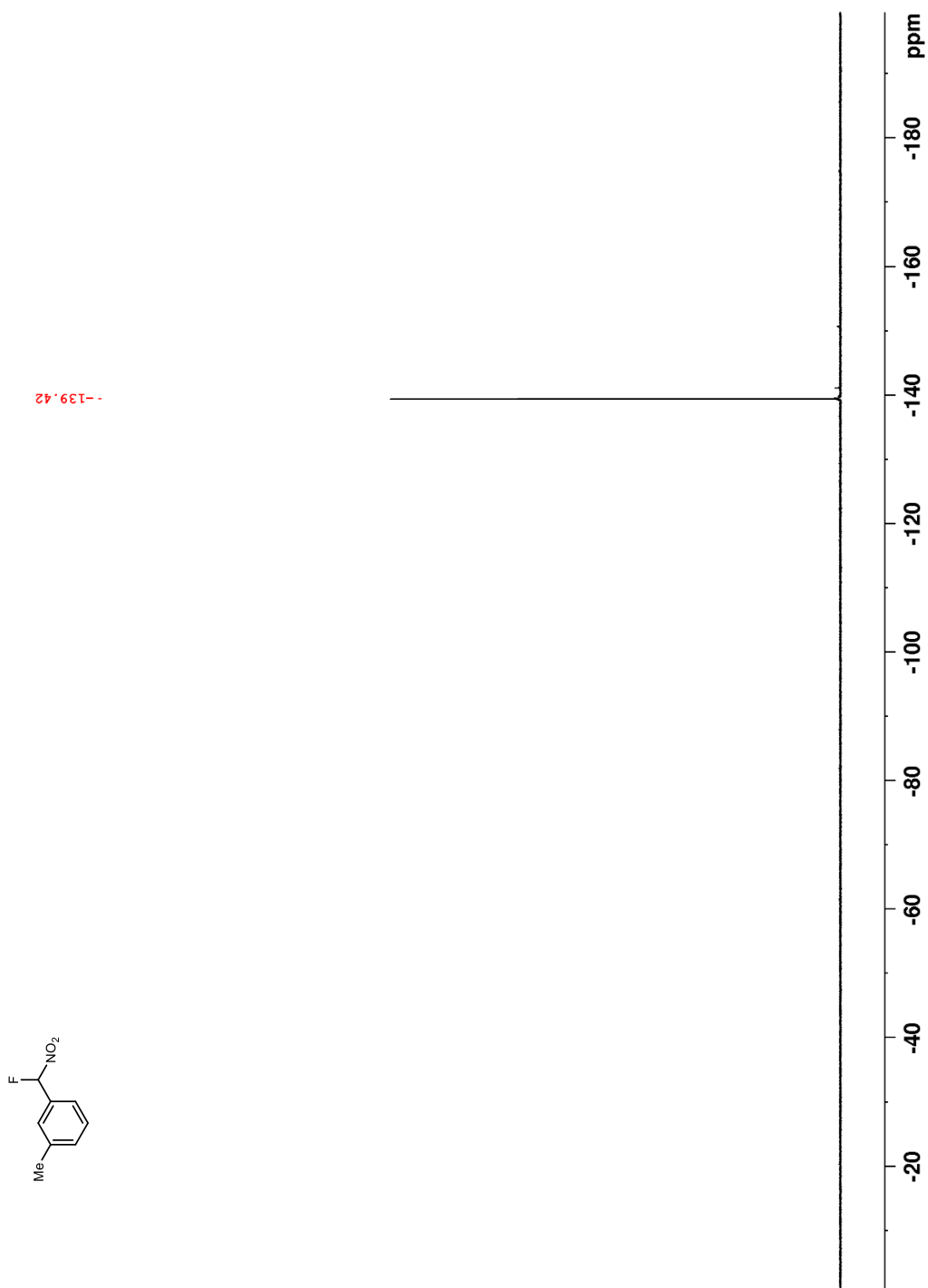


Figure 129. ^1H NMR (400 MHz, CDCl_3) of **223**

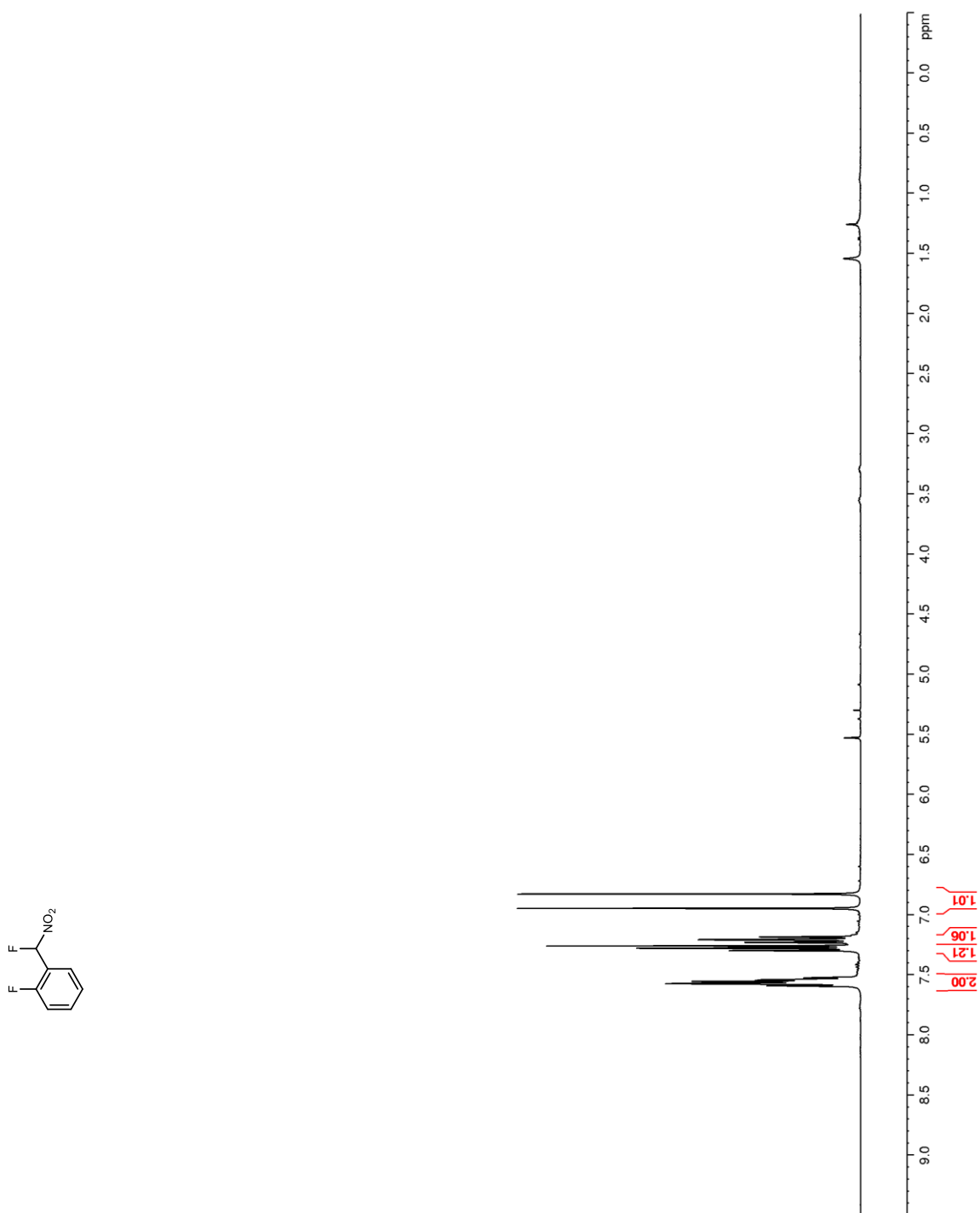


Figure 130. ^{13}C NMR (100 MHz, CDCl_3) of **223**

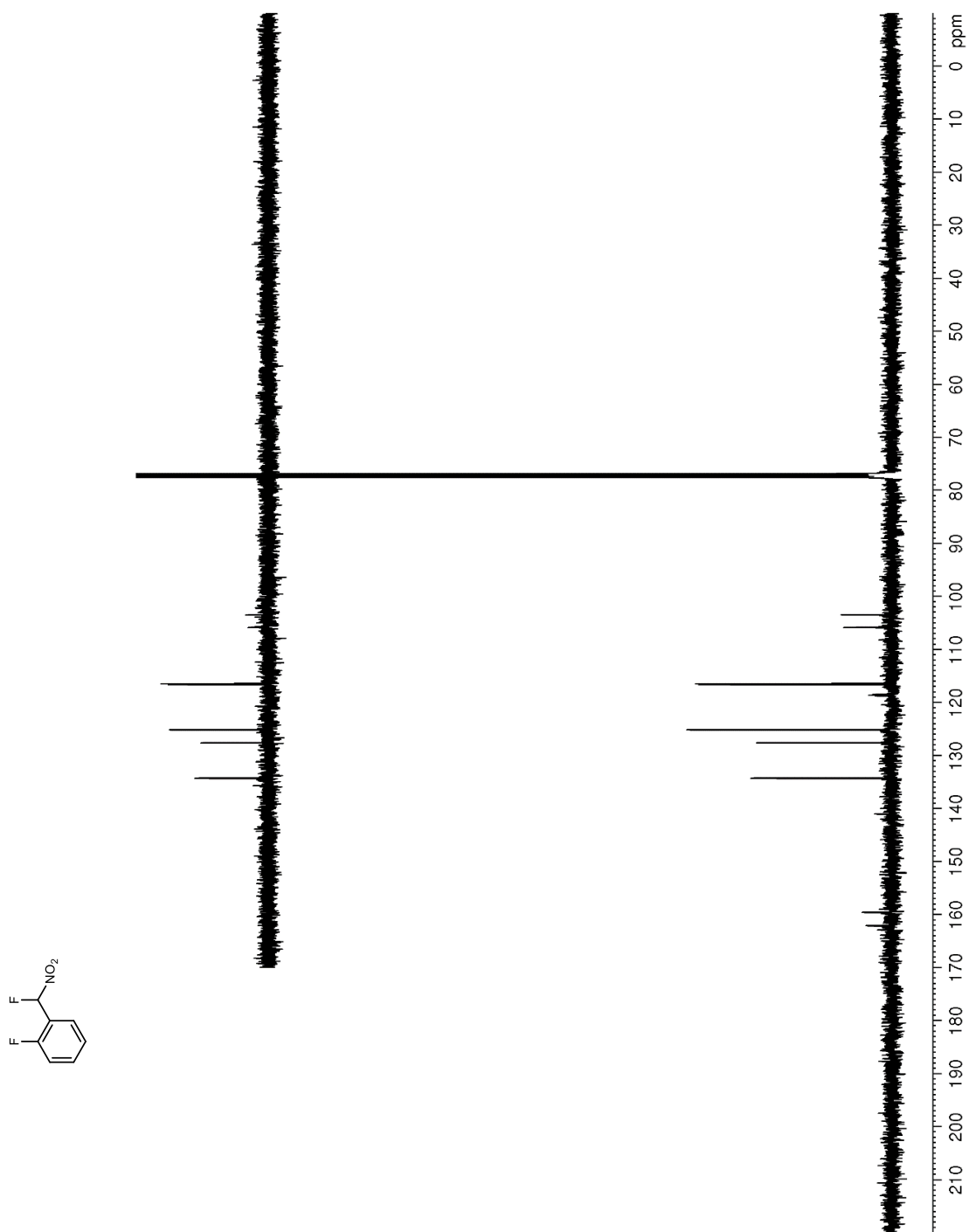


Figure 131. ^{19}F NMR (376 MHz, CDCl_3) of **223**

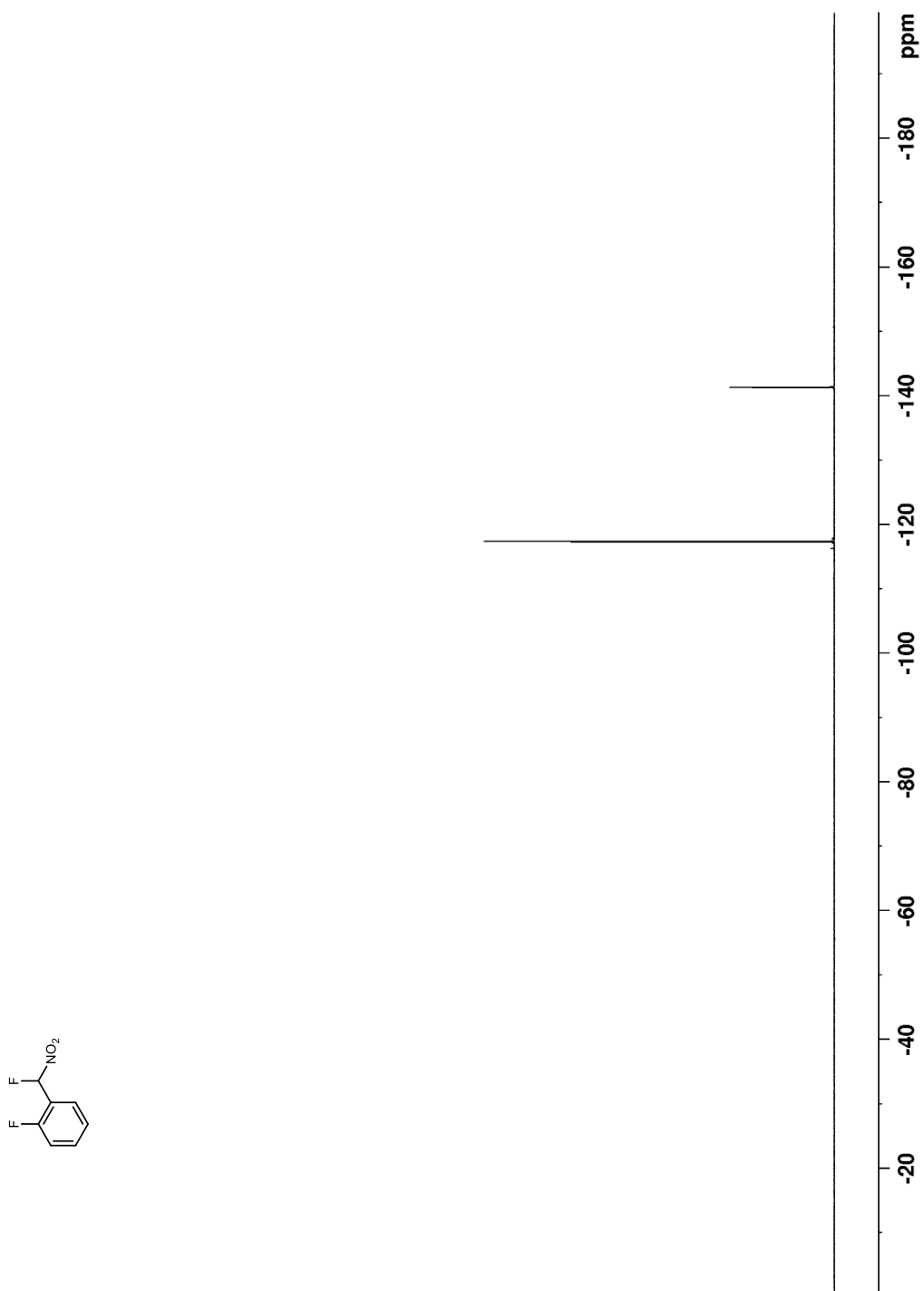


Figure 132. ^1H NMR (400 MHz, $\text{DMSO-}d_6$) of **230**

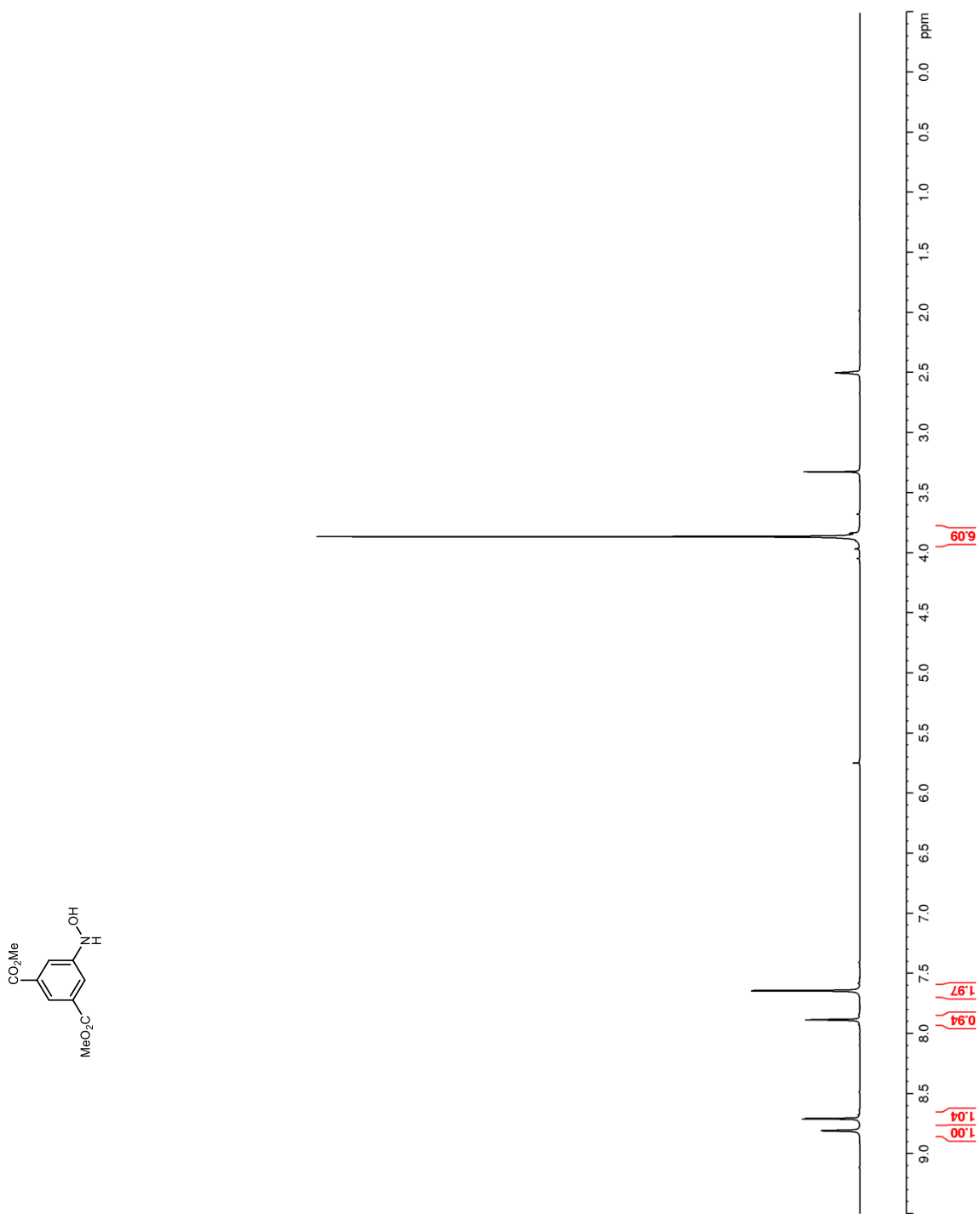


Figure 133. ^{13}C NMR (100 MHz, $\text{DMSO-}d_6$) of **230**

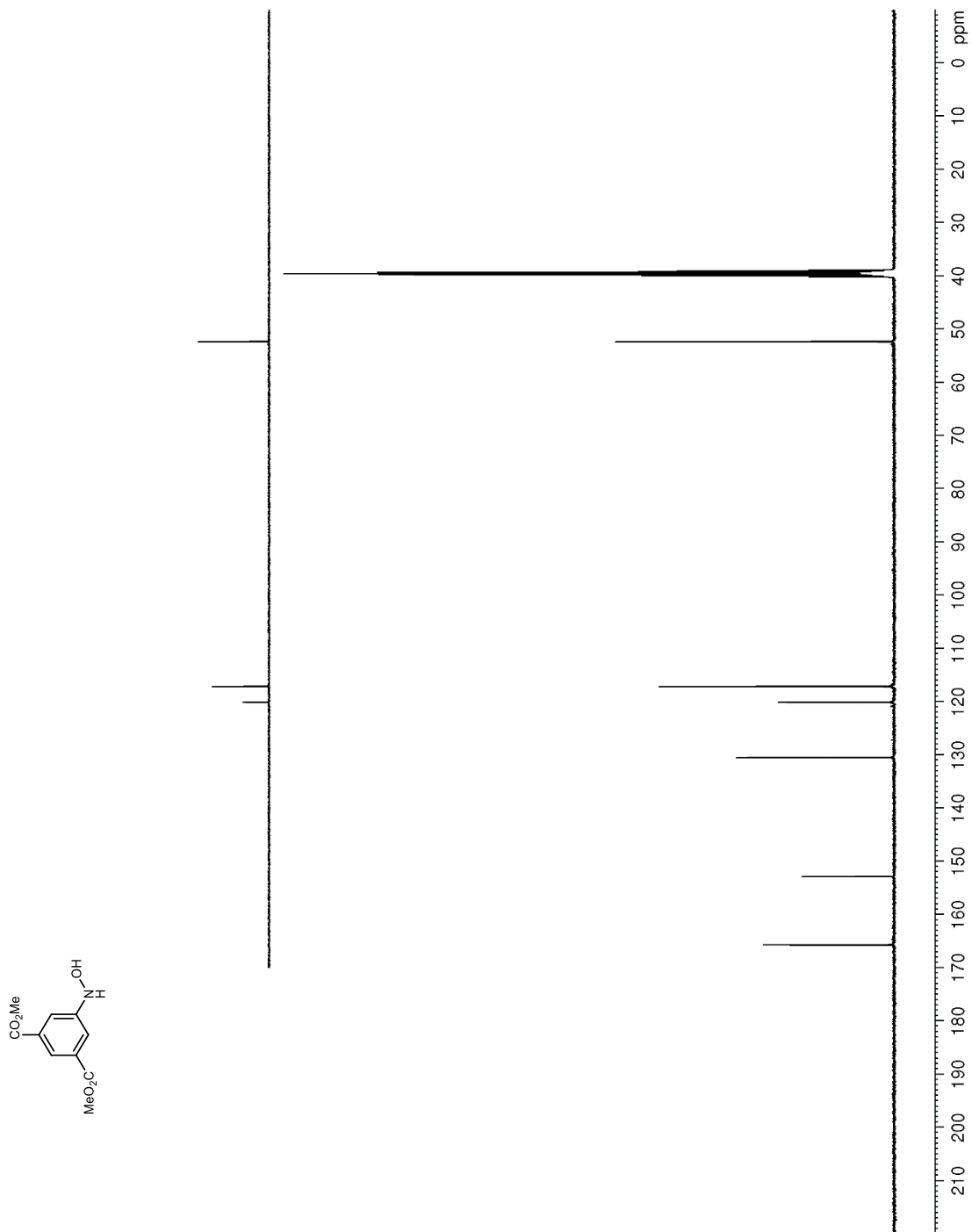


Figure 134. ^1H NMR (400 MHz, $\text{DMSO-}d_6$) of **232**

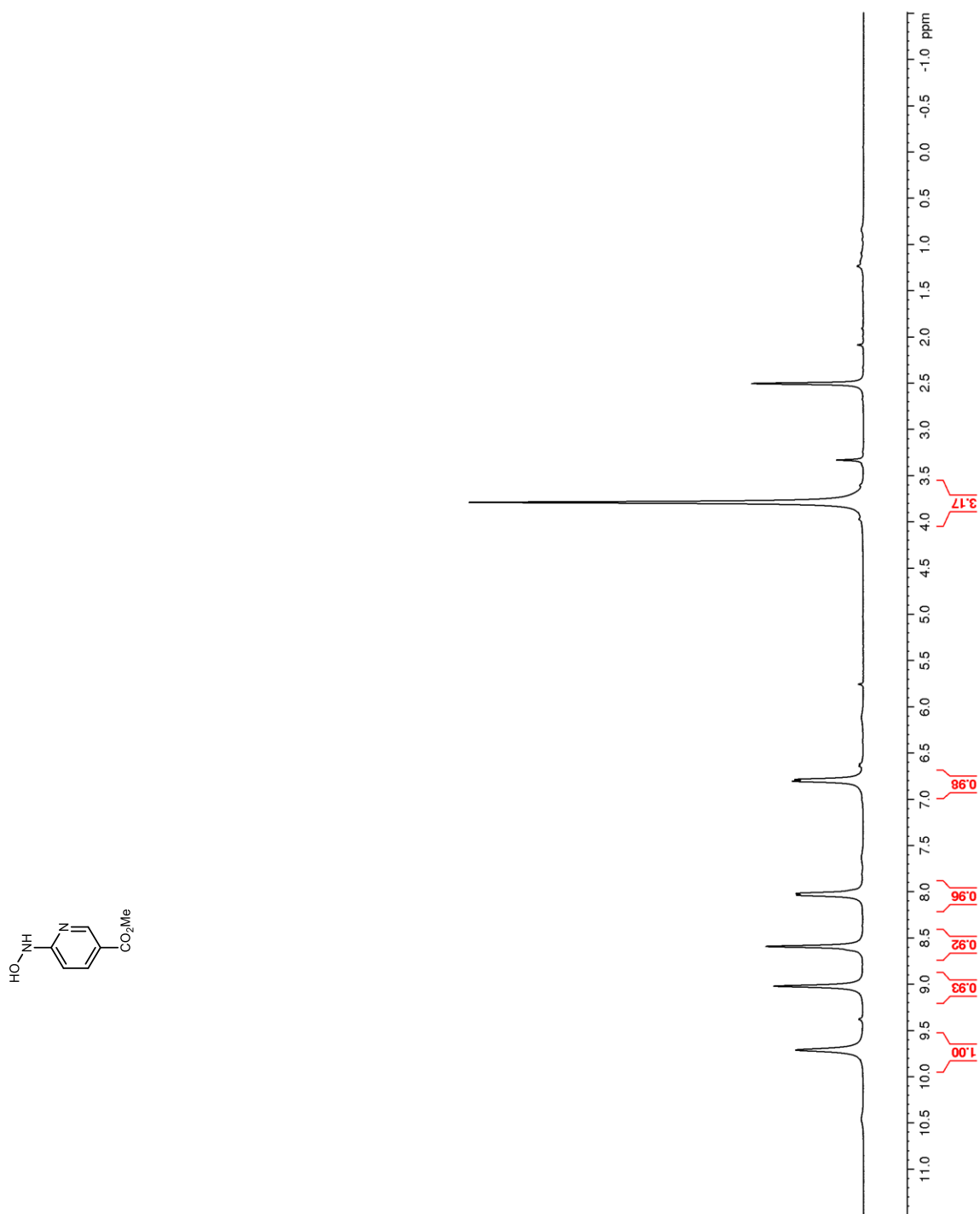


Figure 135. ^{13}C NMR (100 MHz, $\text{DMSO-}d_6$) of **232**

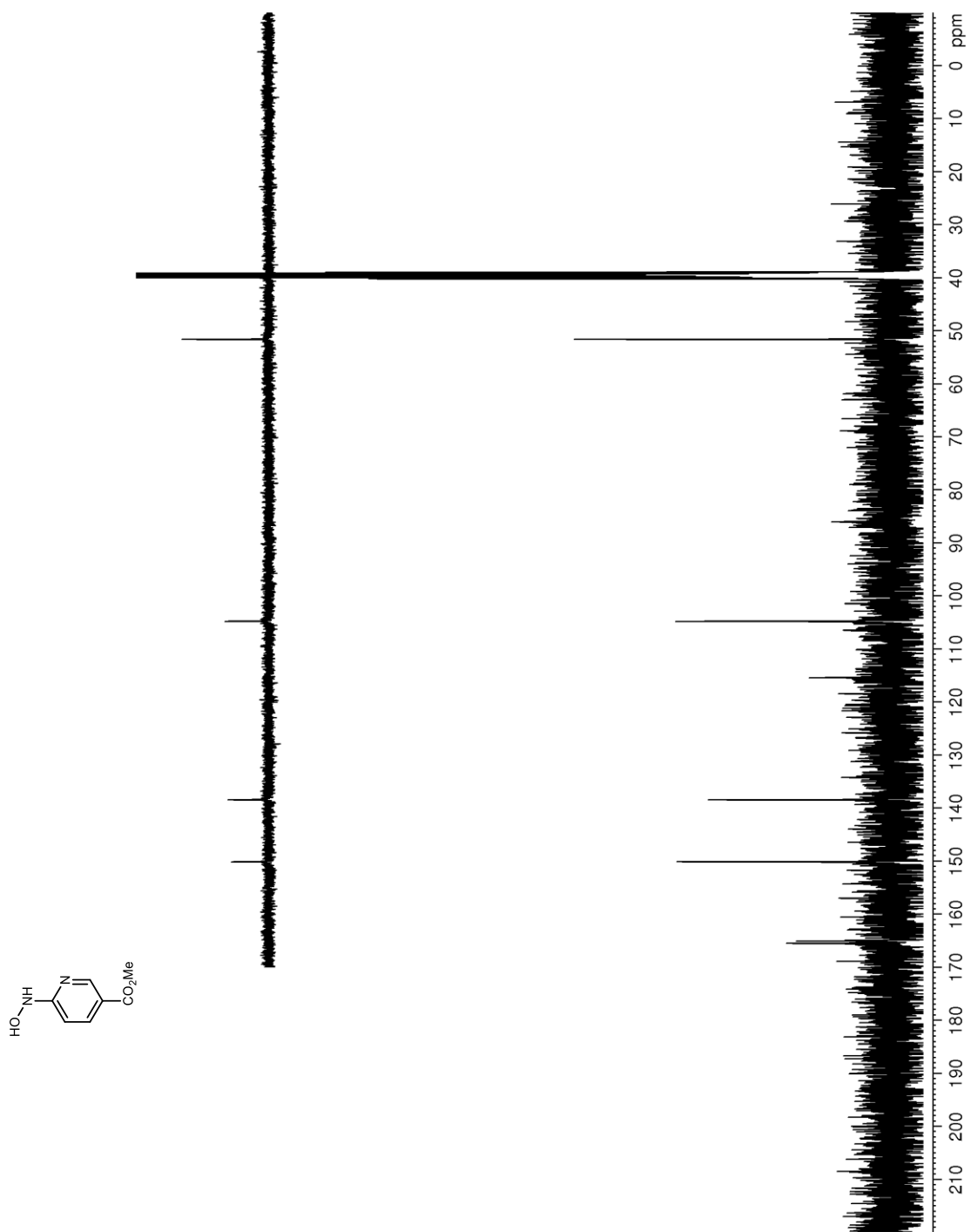


Figure 136. ^1H NMR (400 MHz, $\text{DMSO-}d_6$) of **233**

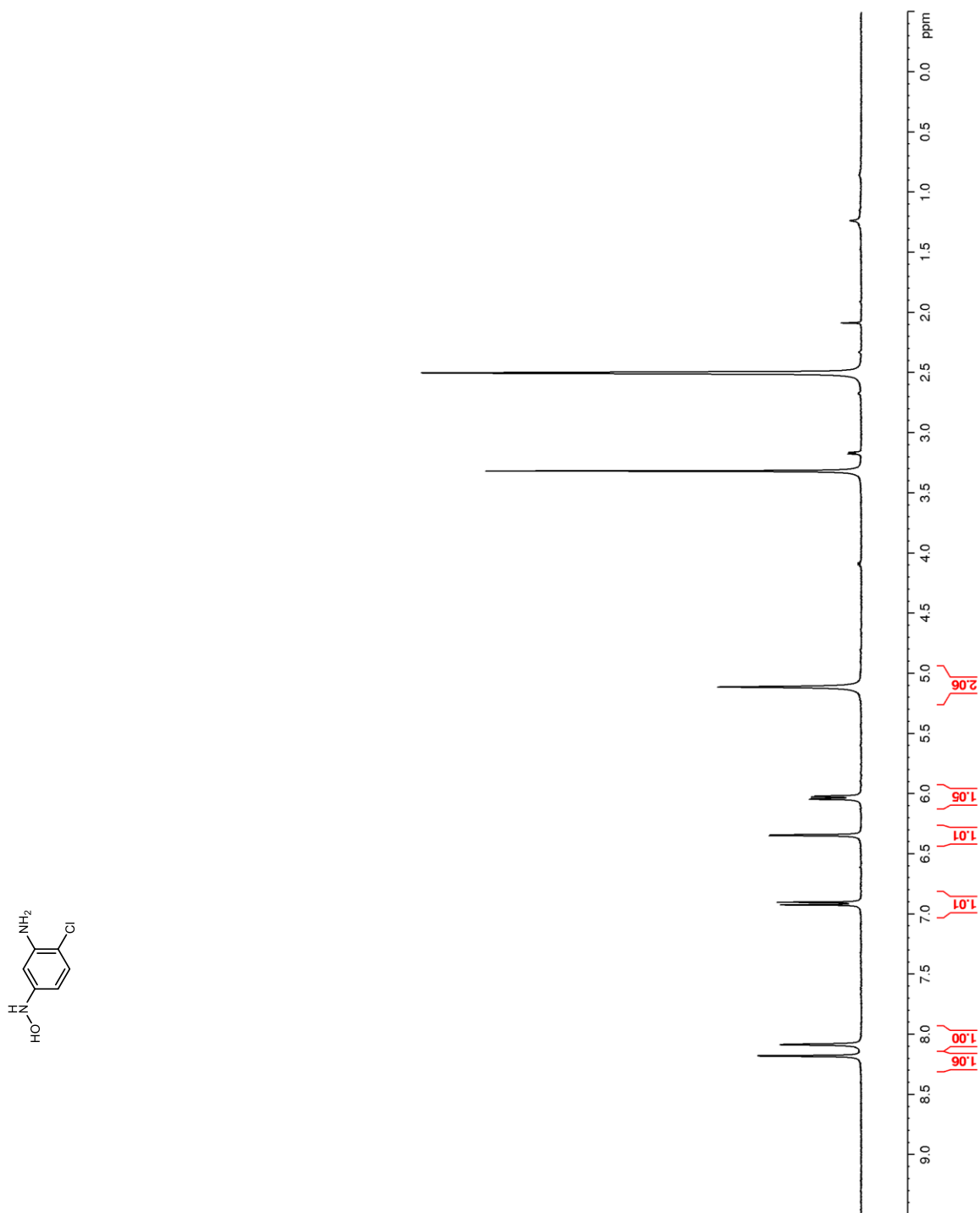


Figure 137. ^{13}C NMR (100 MHz, $\text{DMSO-}d_6$) of **233**

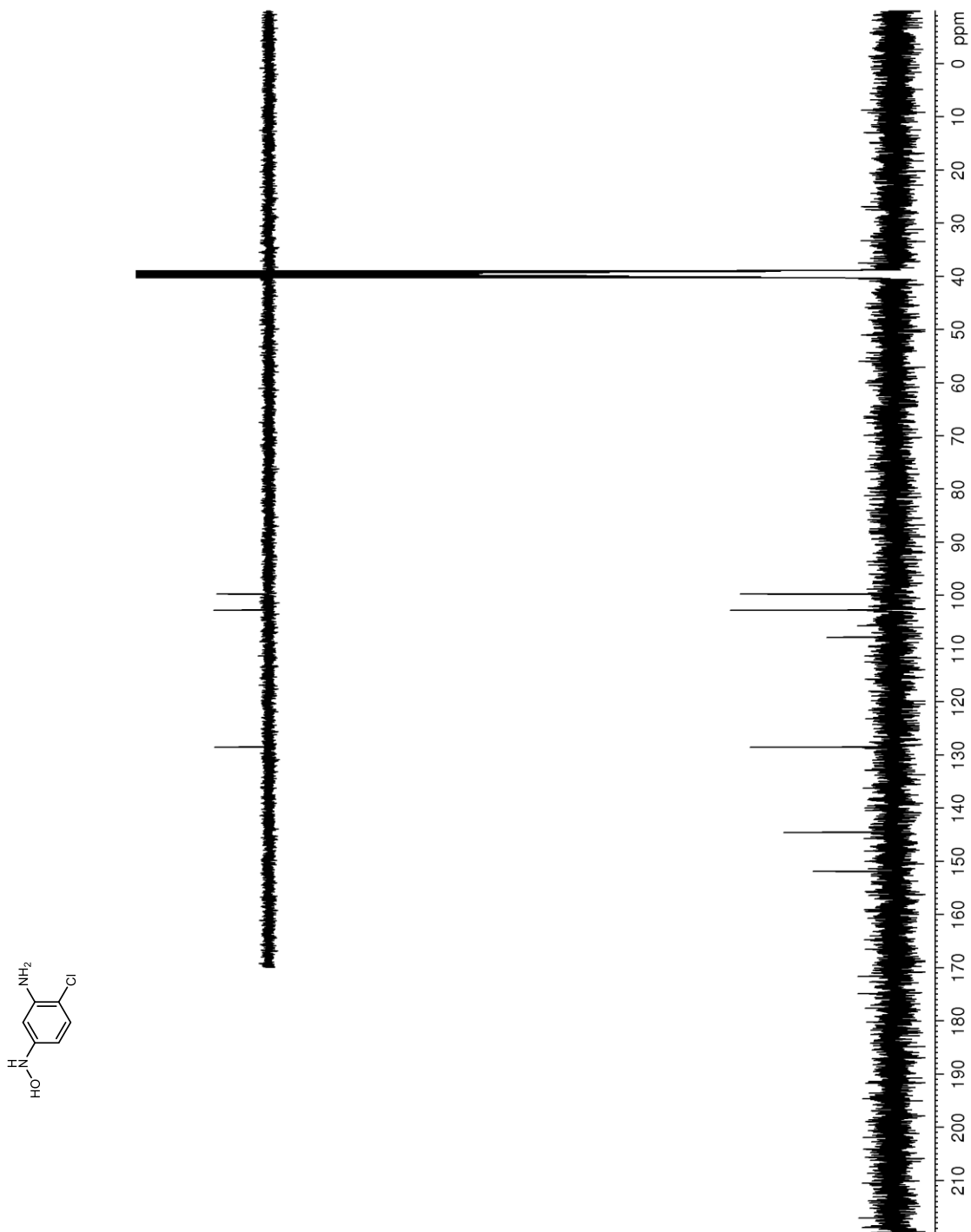


Figure 138. ^1H NMR (400 MHz, $\text{DMSO-}d_6$) of **234**

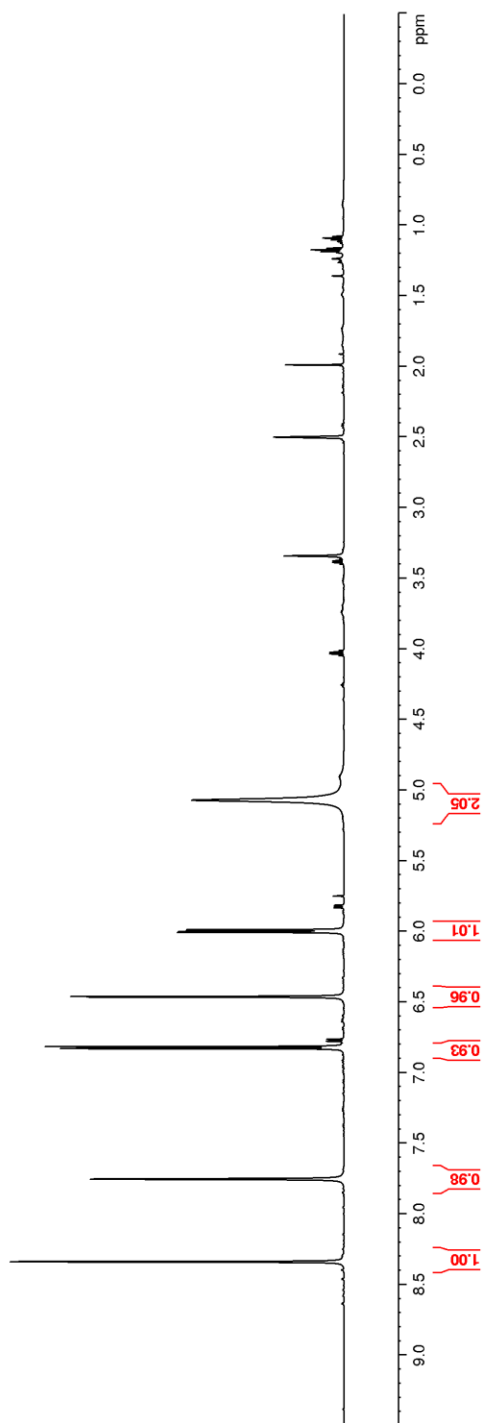
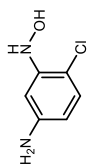


Figure 139. ^{13}C NMR (100 MHz, $\text{DMSO-}d_6$) of **234**

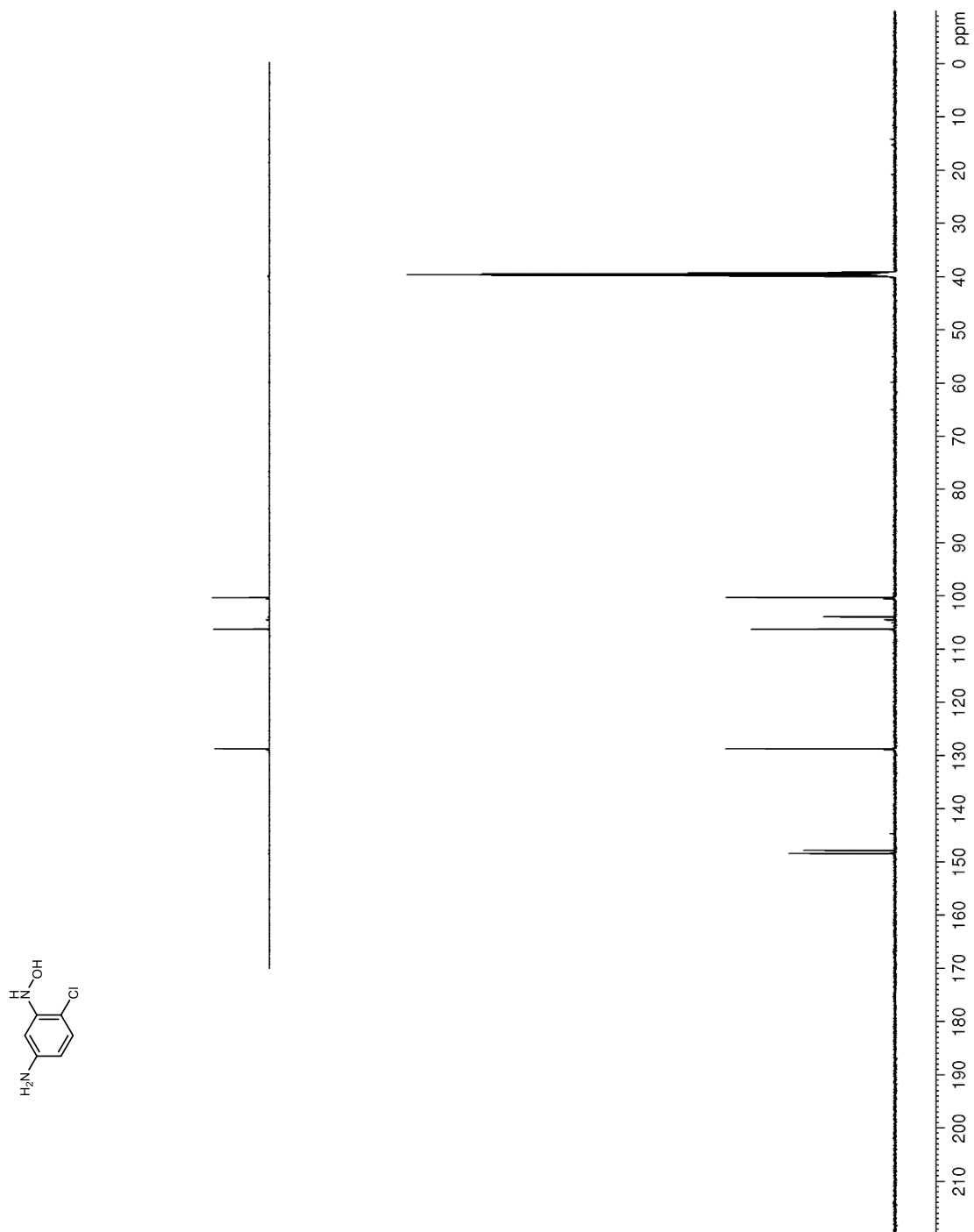


Figure 140. ^1H NMR (400 MHz, $\text{DMSO-}d_6$) of **237**

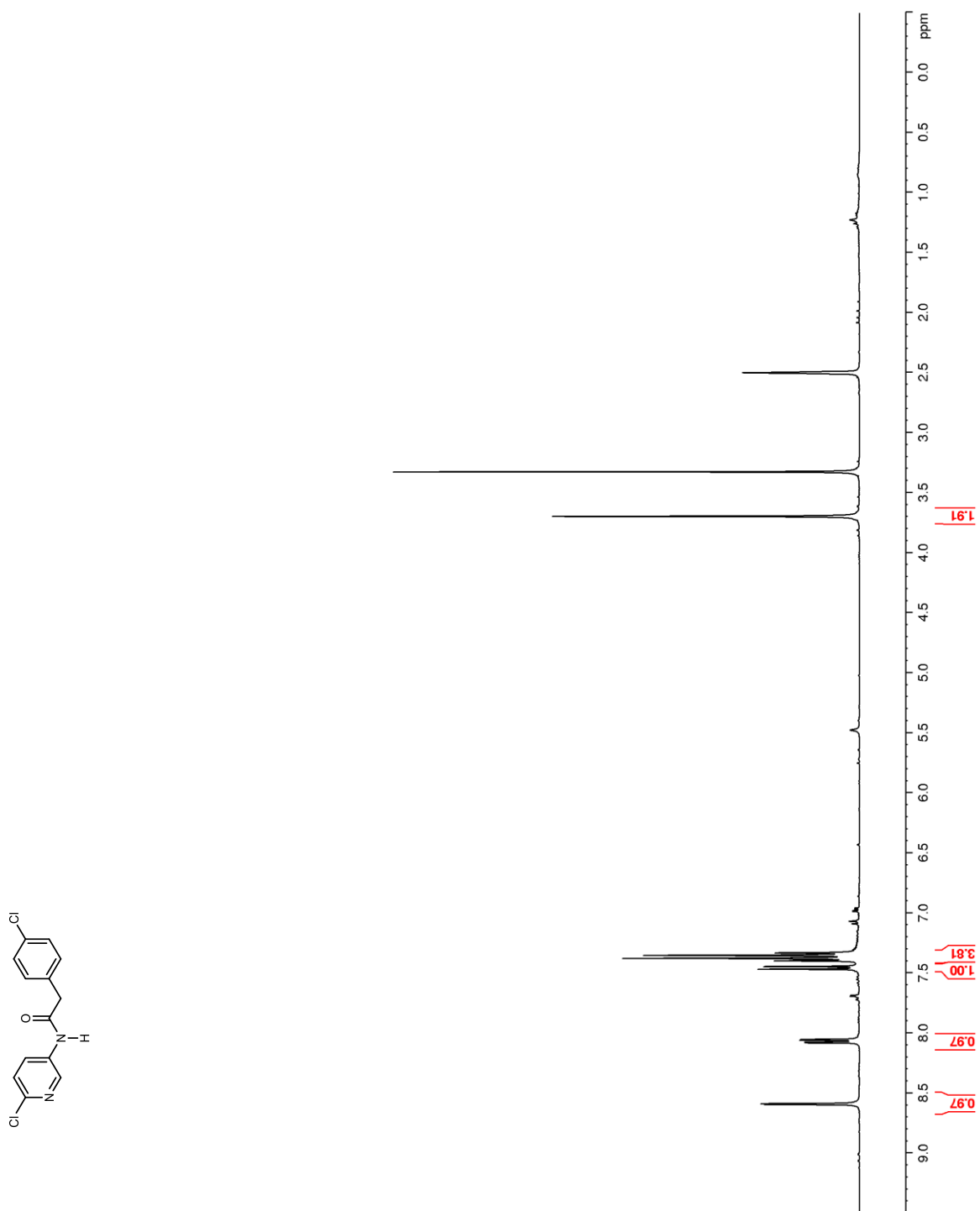


Figure 141. ^{13}C NMR (100 MHz, $\text{DMSO-}d_6$) of **237**

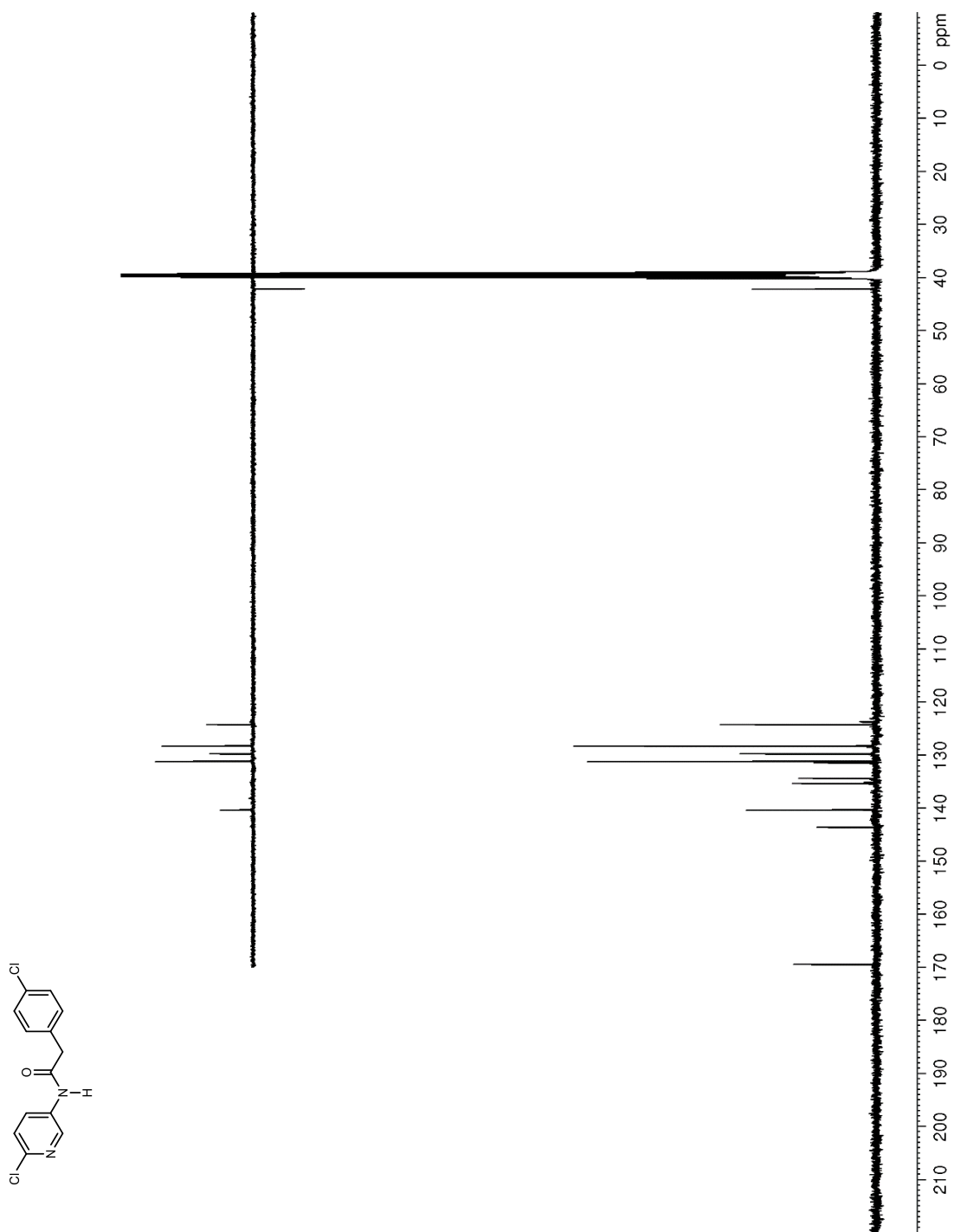


Figure 142. ^1H NMR (600 MHz, $\text{DMSO-}d_6$) of **238**

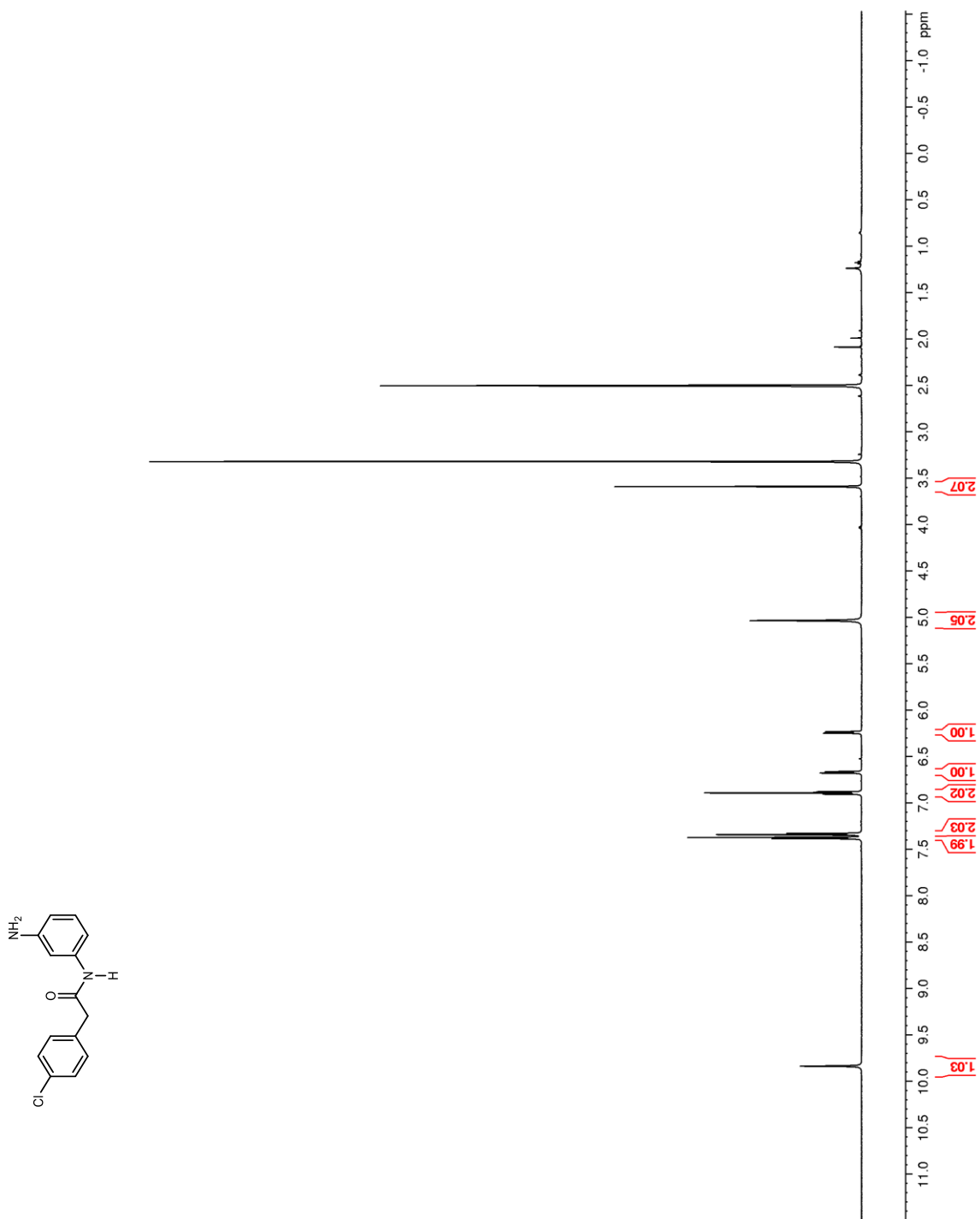


Figure 143. ^{13}C NMR (150 MHz, $\text{DMSO-}d_6$) of **238**

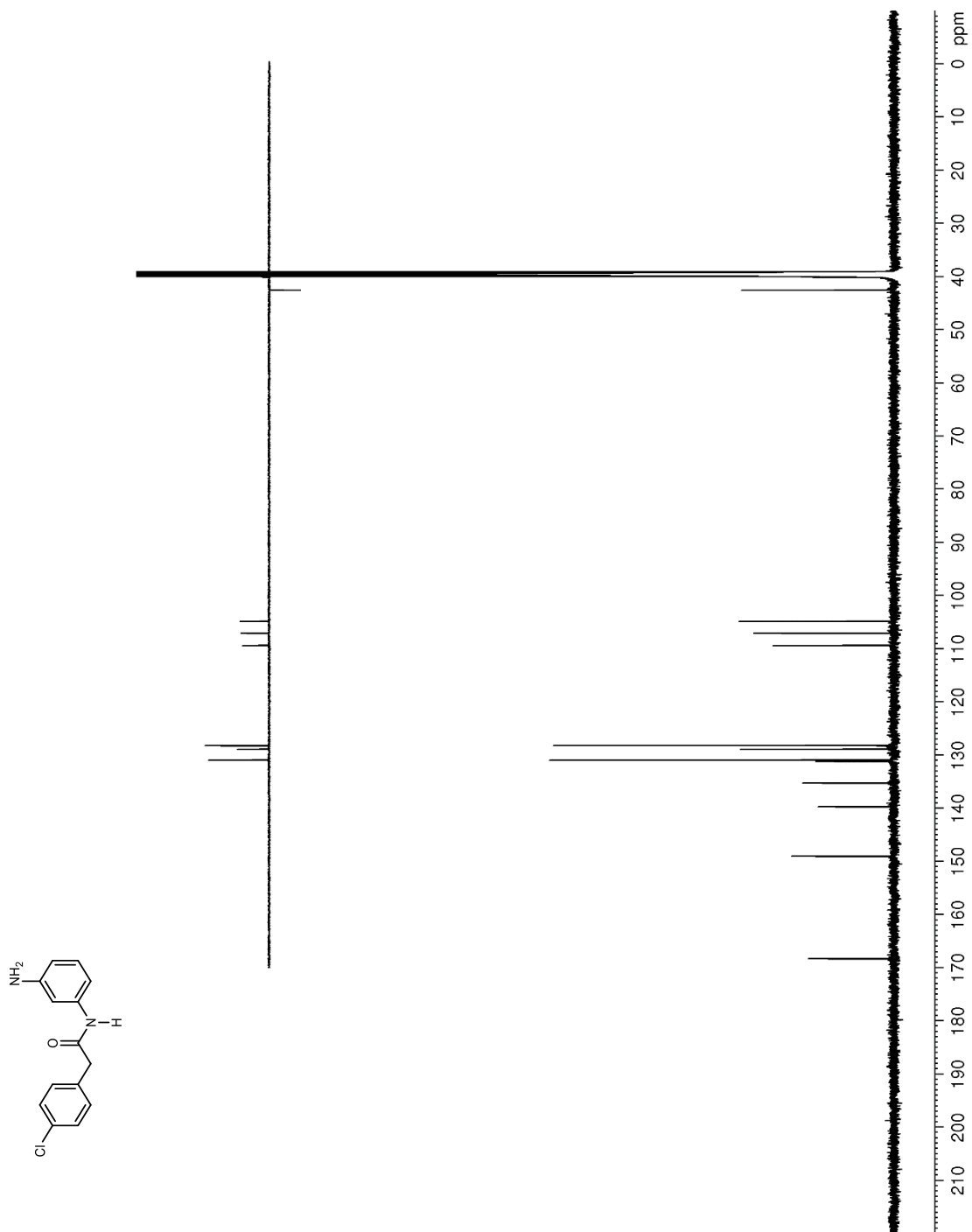


Figure 144. ^1H NMR (400 MHz, $\text{DMSO-}d_6$) of **239**

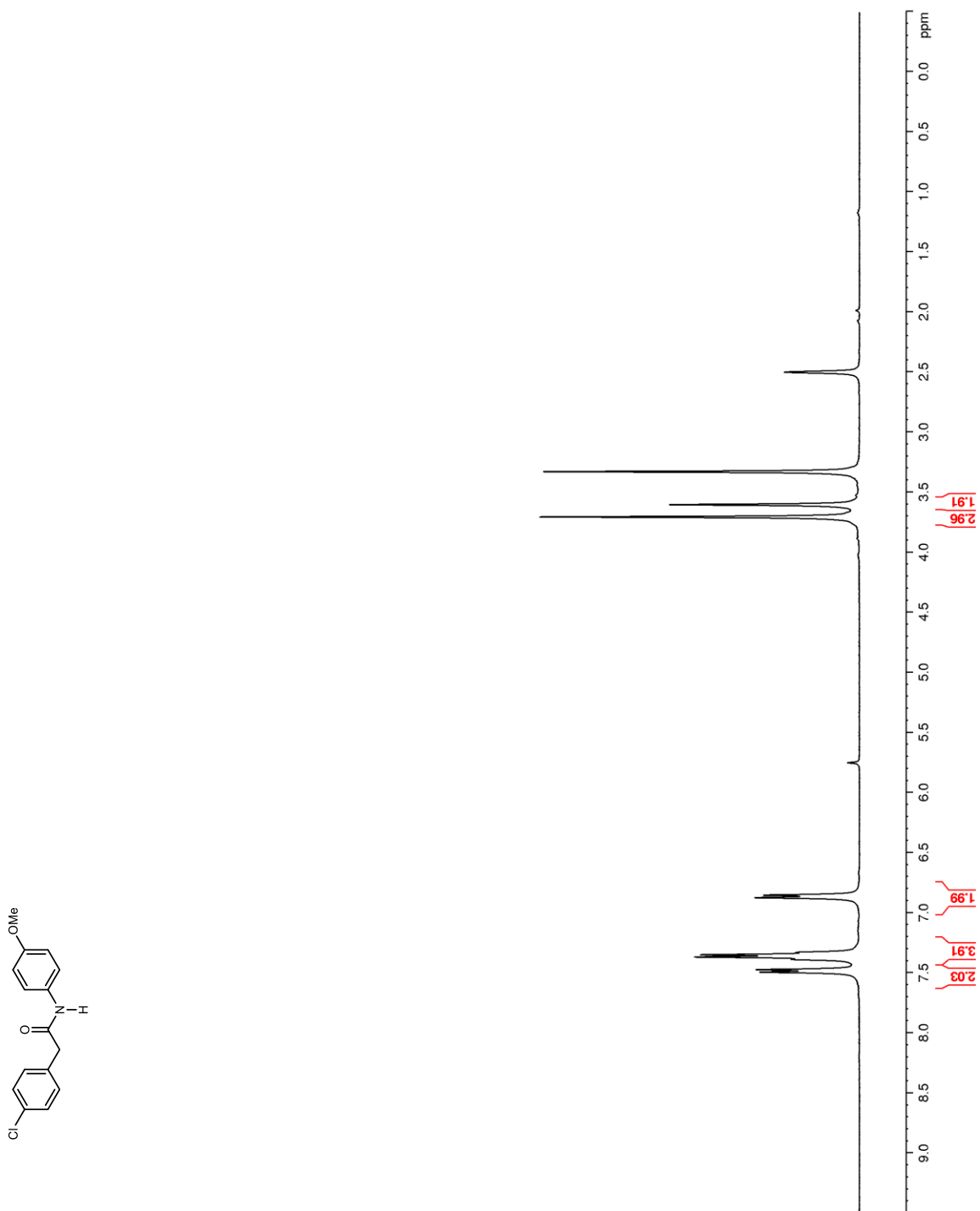


Figure 145. ^{13}C NMR (100 MHz, $\text{DMSO-}d_6$) of **239**

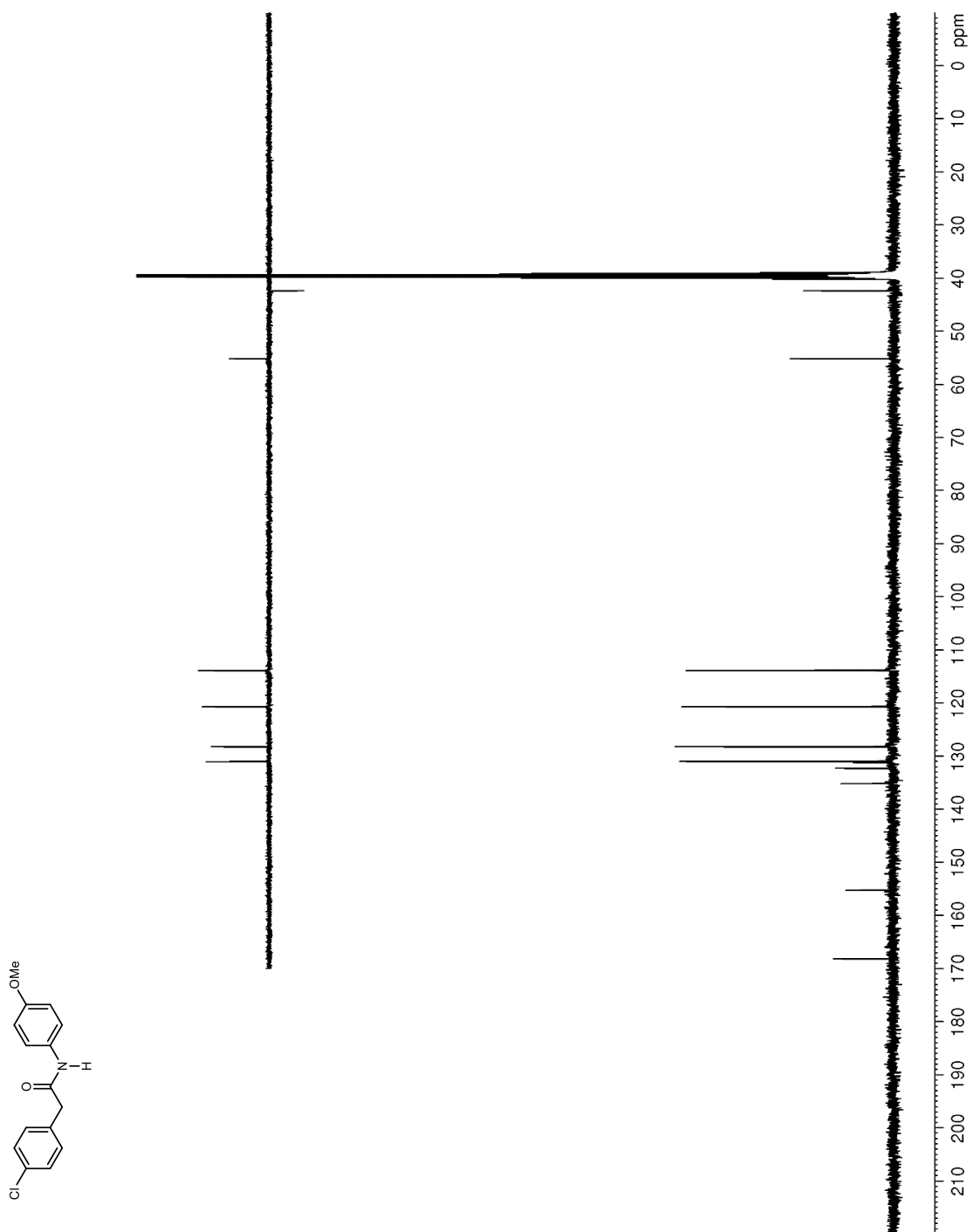


Figure 146. ^1H NMR (400 MHz, $\text{DMSO-}d_6$) of **24**

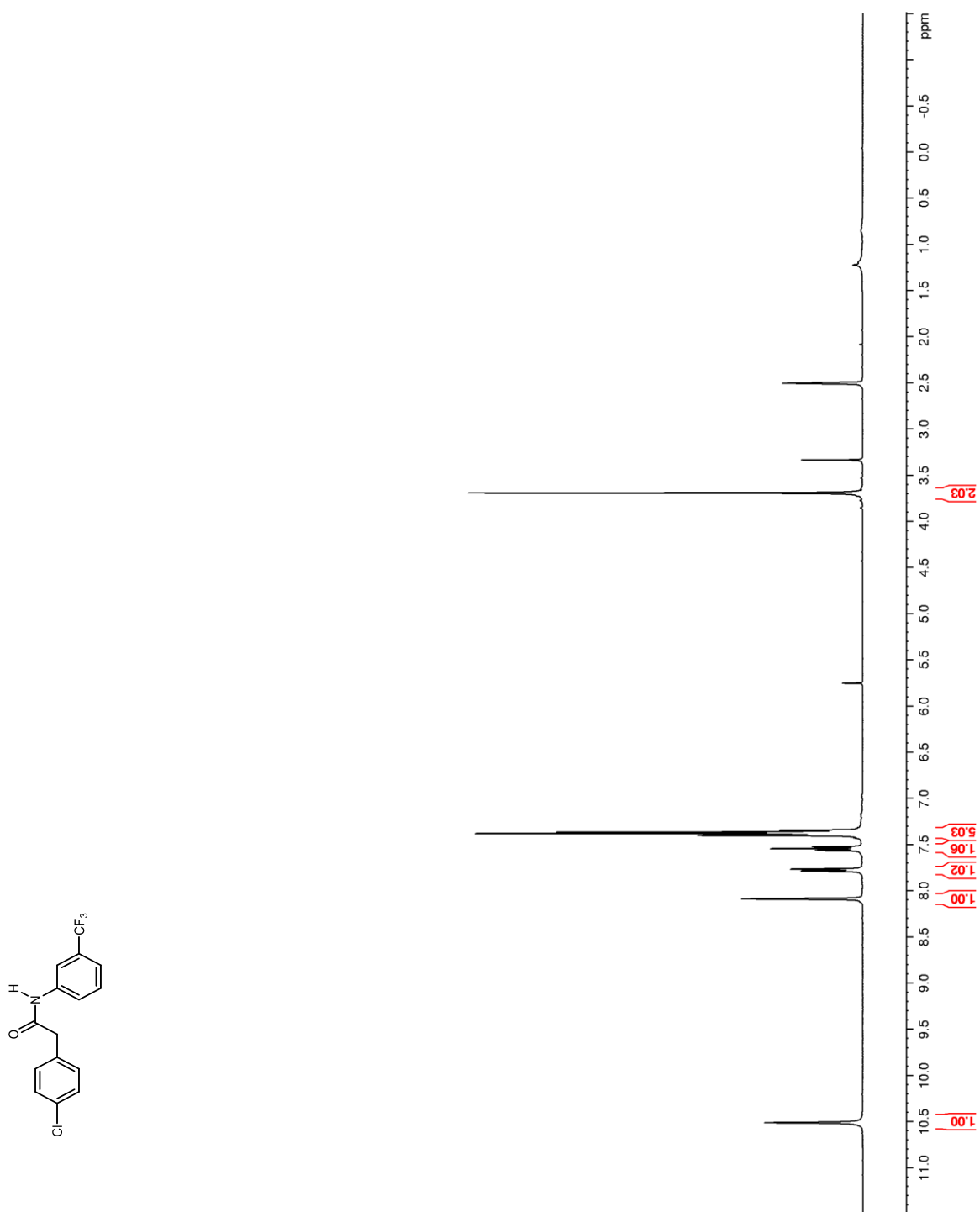


Figure 147. ^{13}C NMR (100 MHz, $\text{DMSO-}d_6$) of **24**

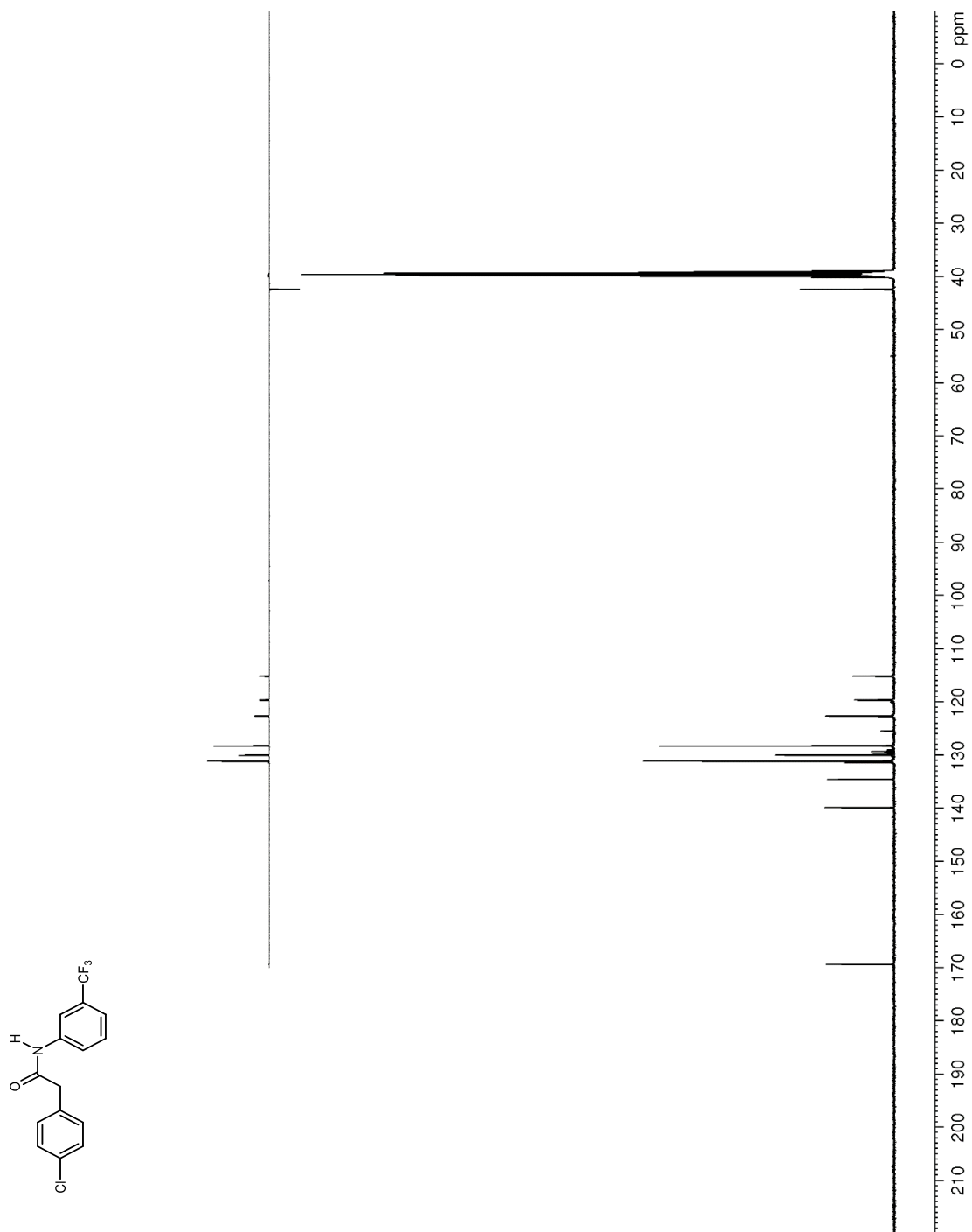


Figure 148. ^{19}F NMR (376 MHz, $\text{DMSO-}d_6$) of **240**

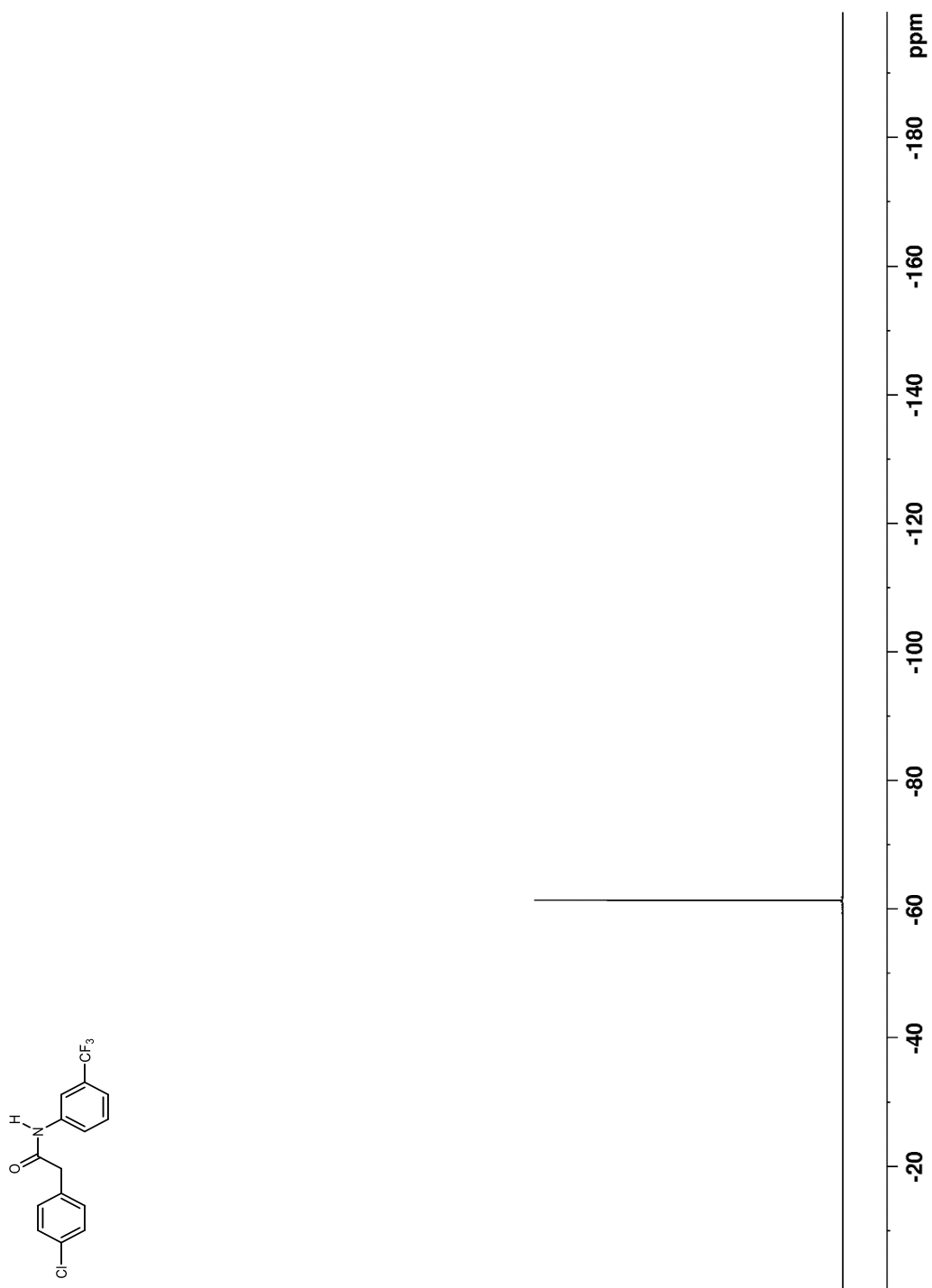


Figure 149. ^1H NMR (400 MHz, $\text{DMSO-}d_6$) of **241**

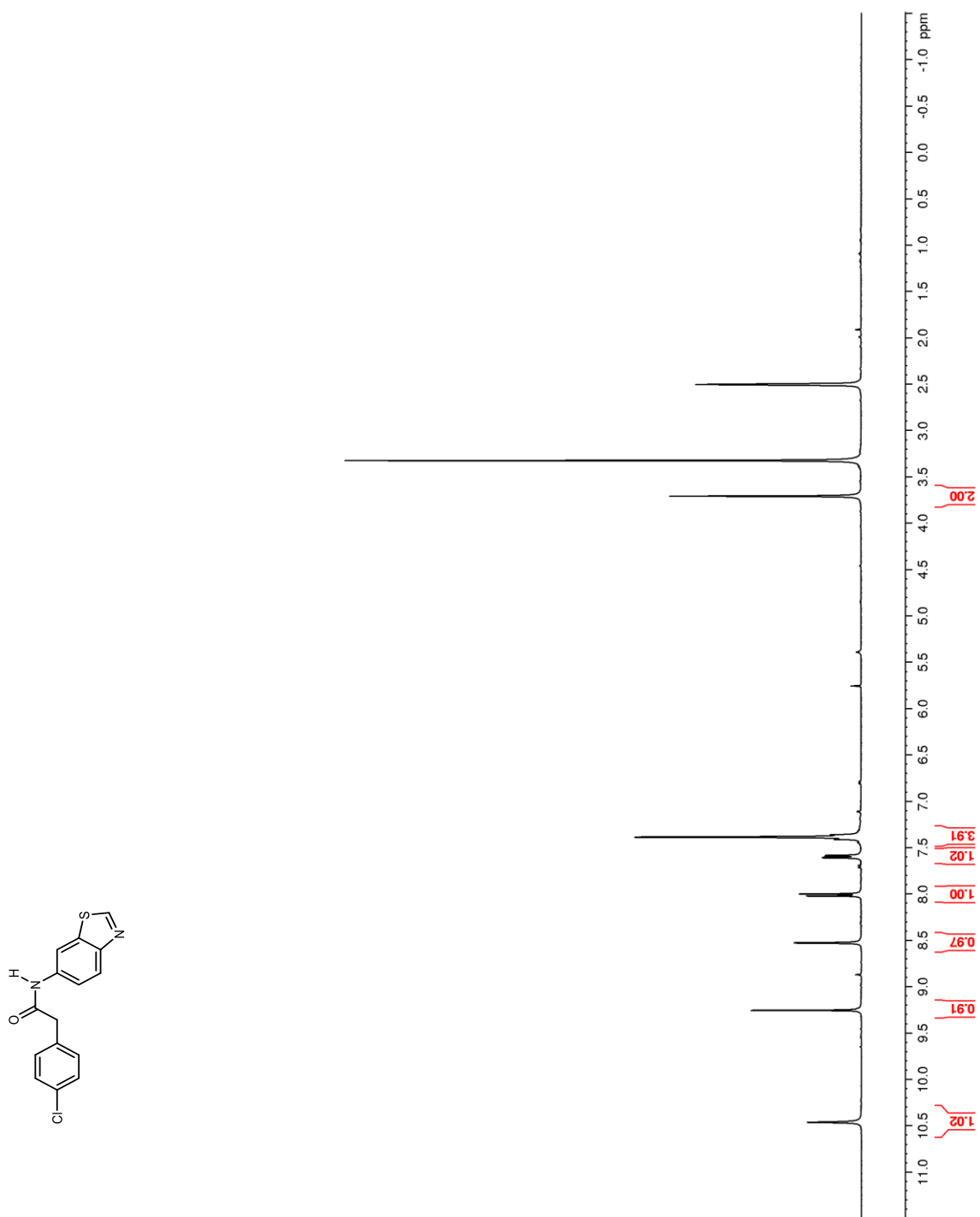


Figure 150. ^{13}C NMR (100 MHz, $\text{DMSO-}d_6$) of **241**

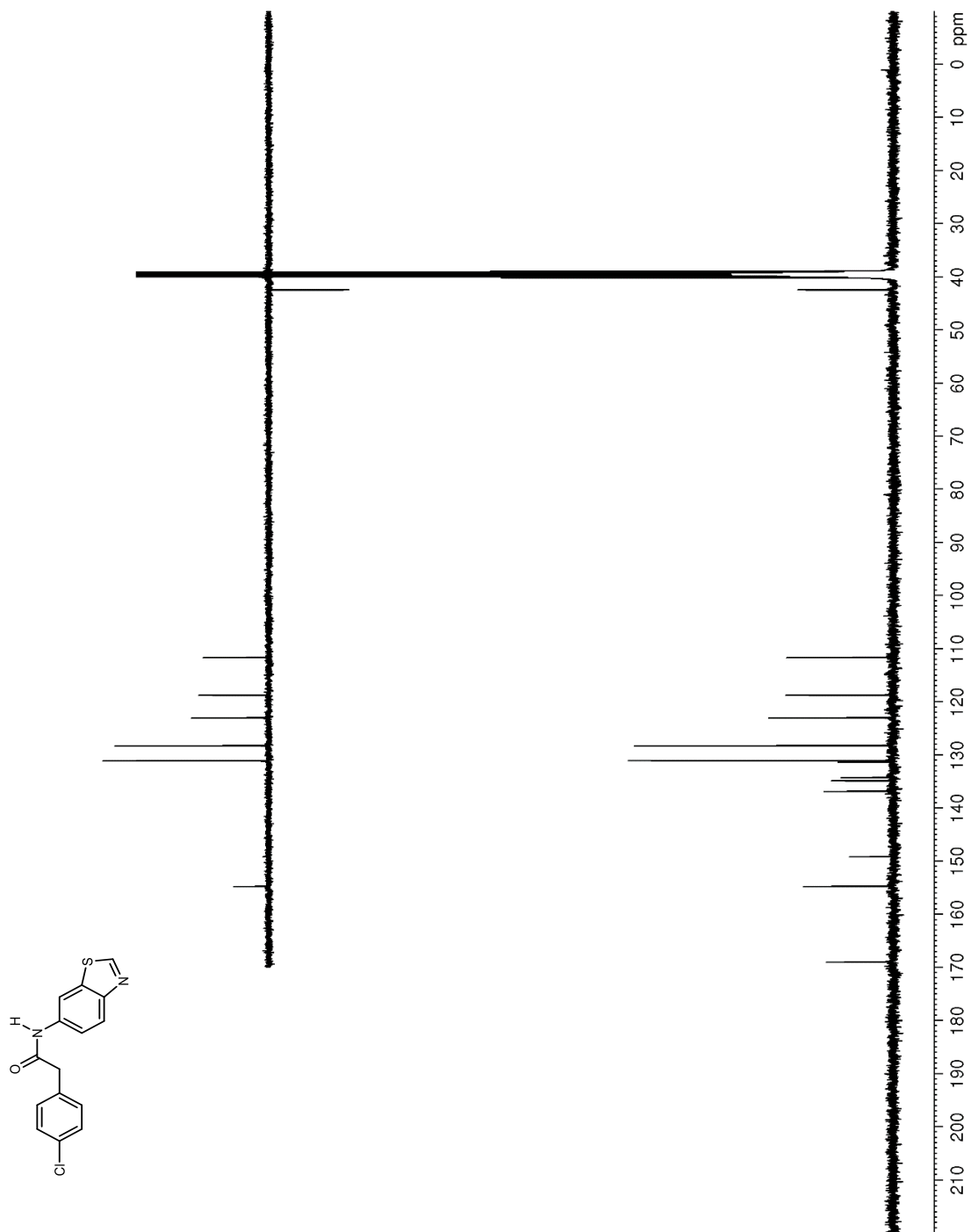


Figure 151. ^1H NMR (400 MHz, $\text{DMSO-}d_6$) of **24**

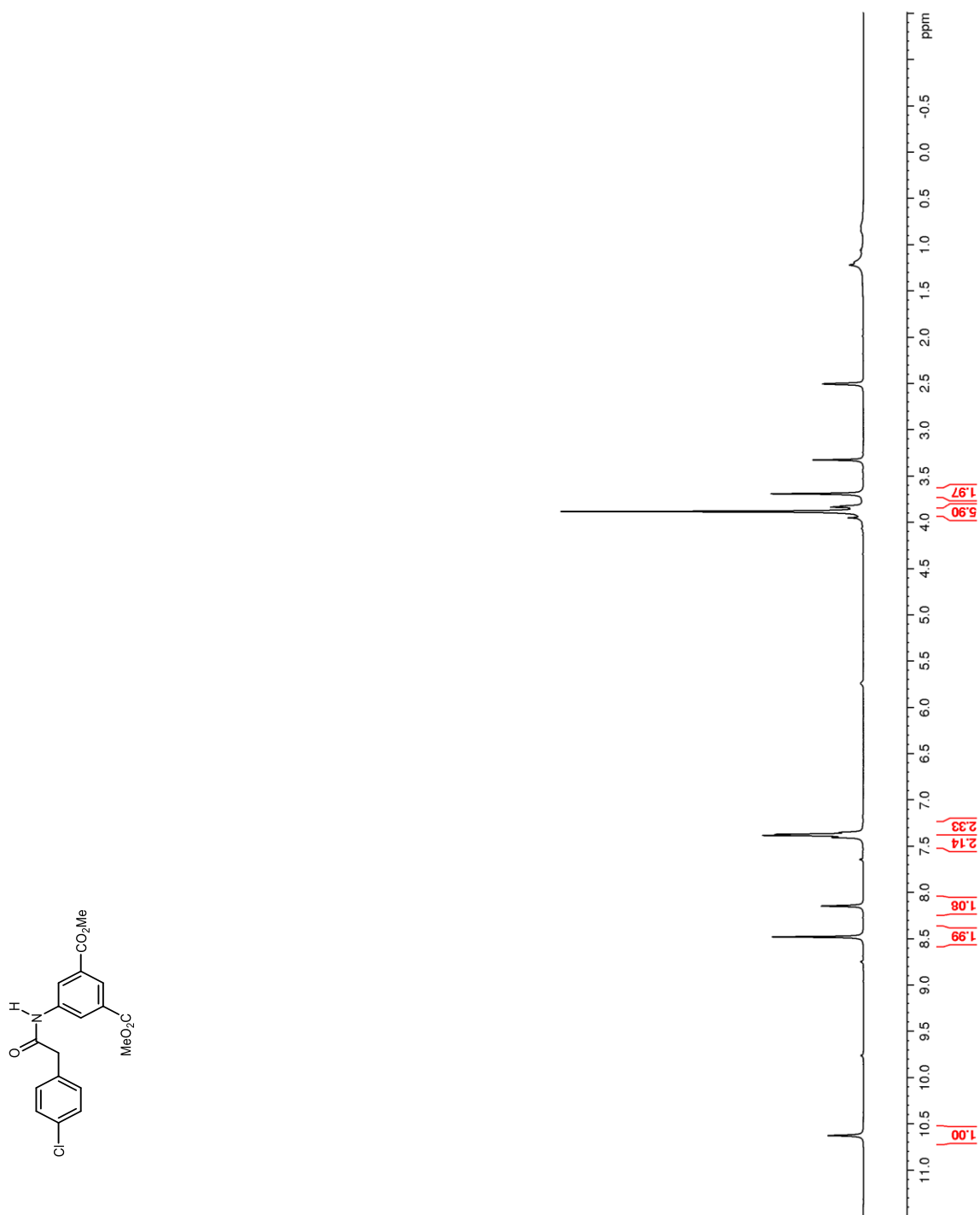


Figure 152. ^{13}C NMR (100 MHz, $\text{DMSO-}d_6$) of **24**

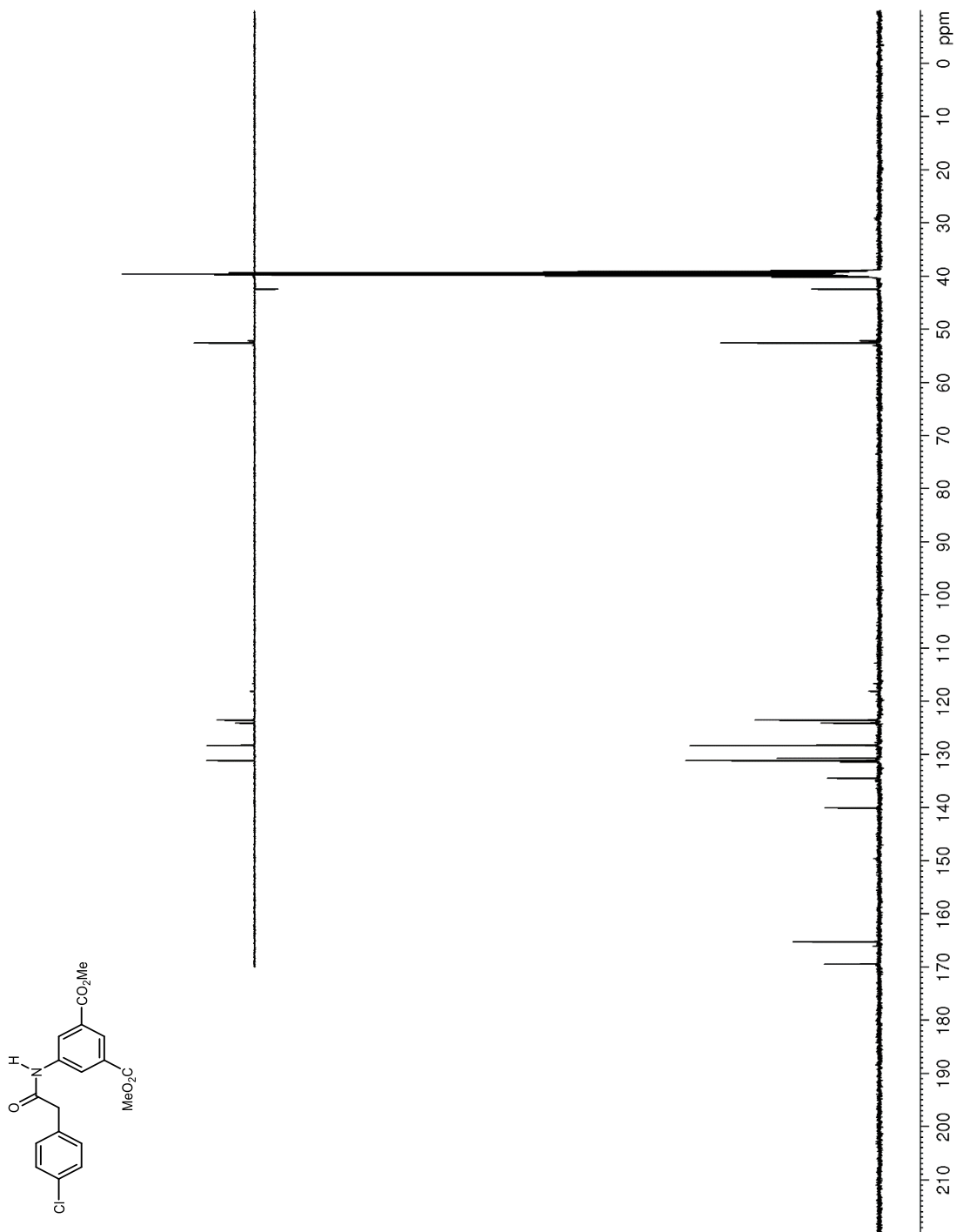


Figure 153. ^1H NMR (400 MHz, $\text{DMSO-}d_6$) of **244**

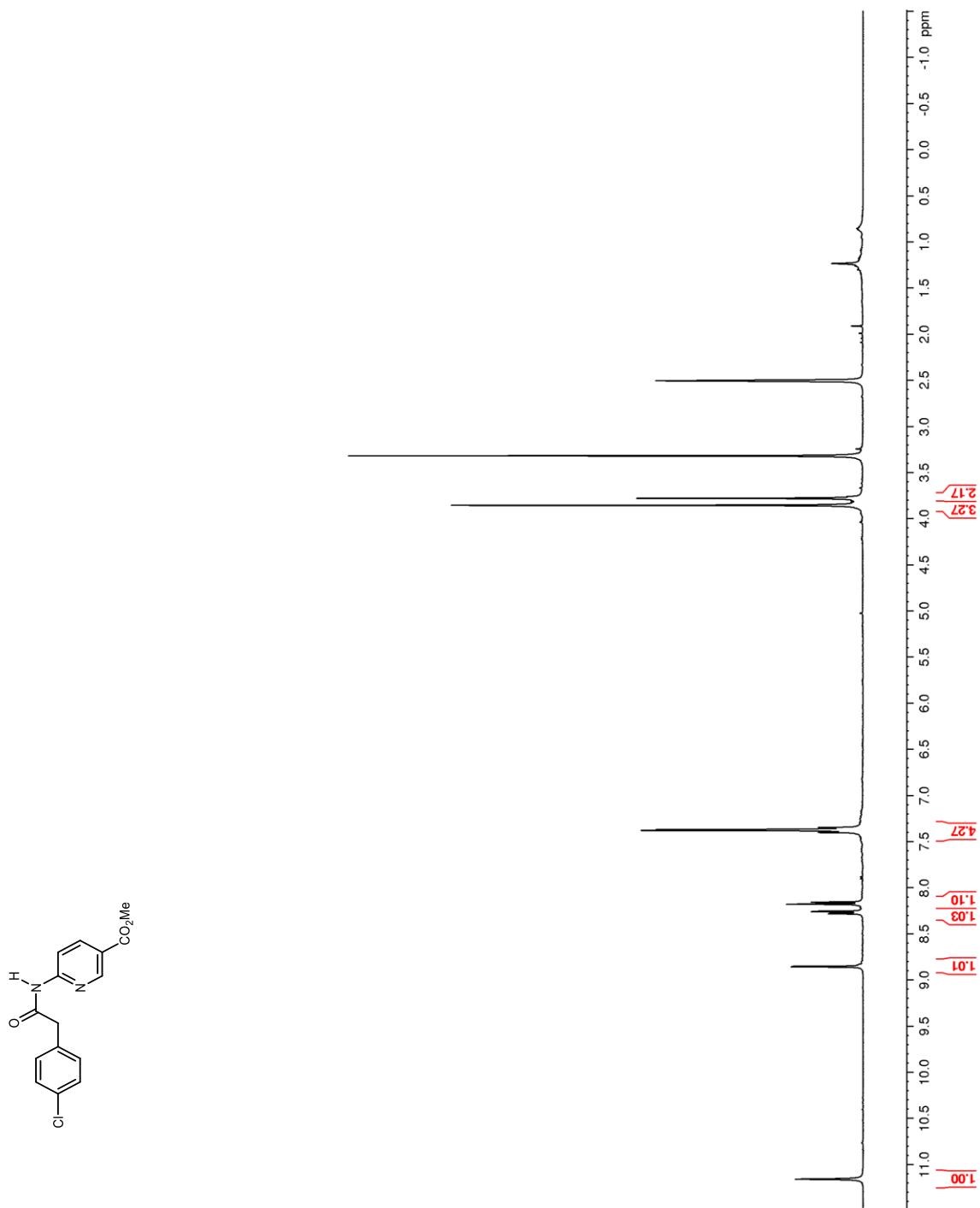


Figure 154. ^{13}C NMR (100 MHz, $\text{DMSO-}d_6$) of **24**

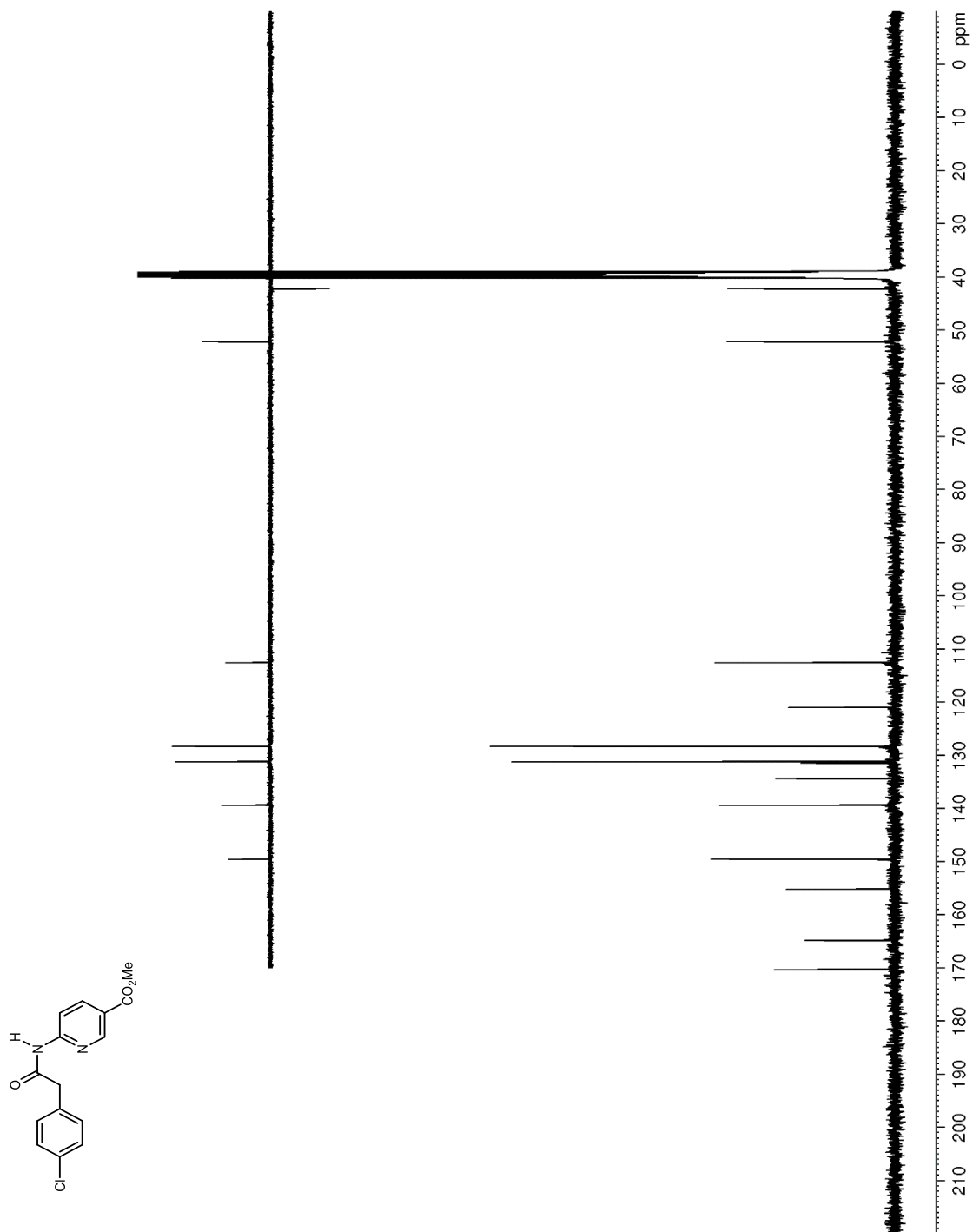


Figure 155. ^1H NMR (400 MHz, $\text{DMSO-}d_6$) of **245**

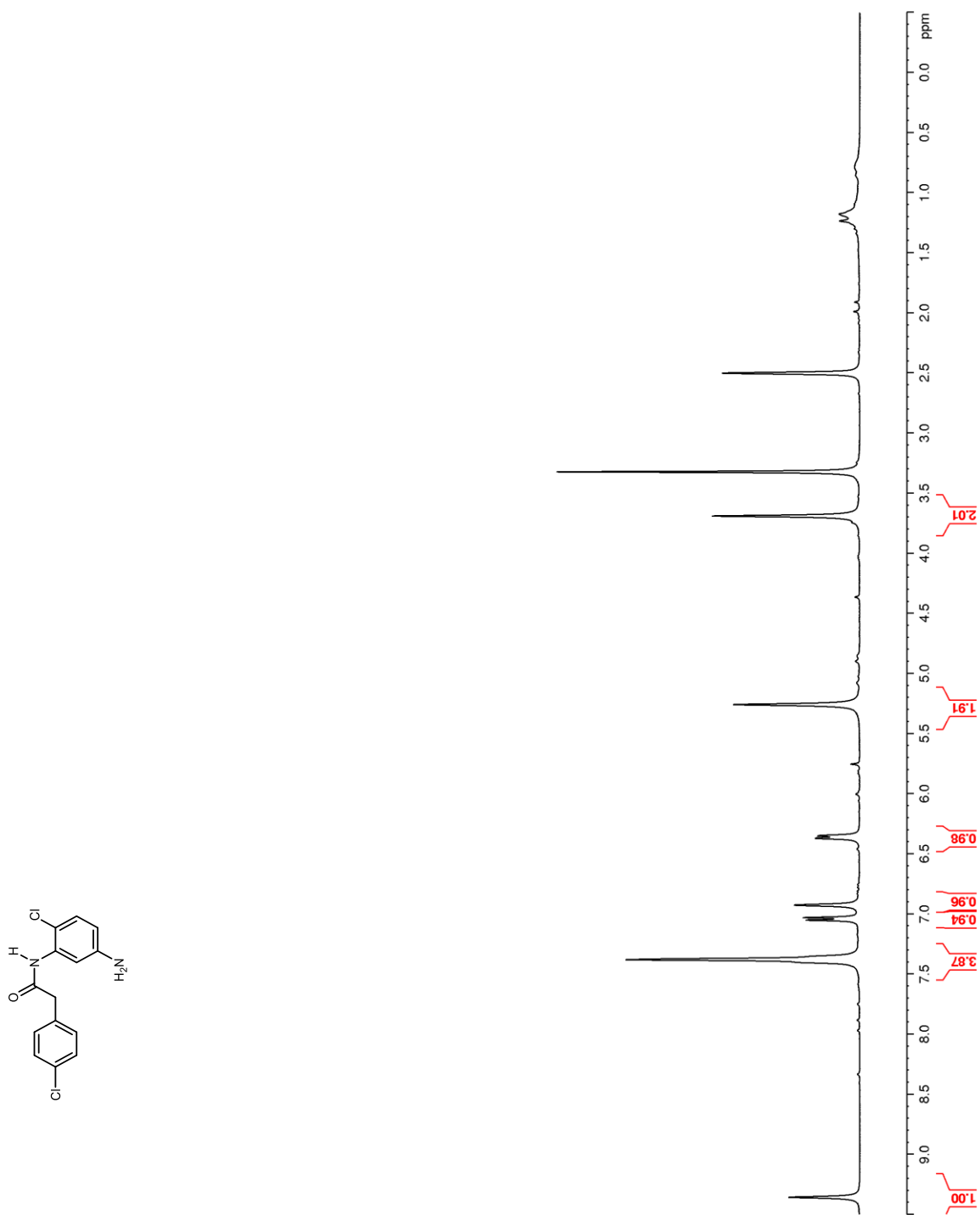


Figure 156. ^{13}C NMR (100 MHz, $\text{DMSO-}d_6$) of **245**

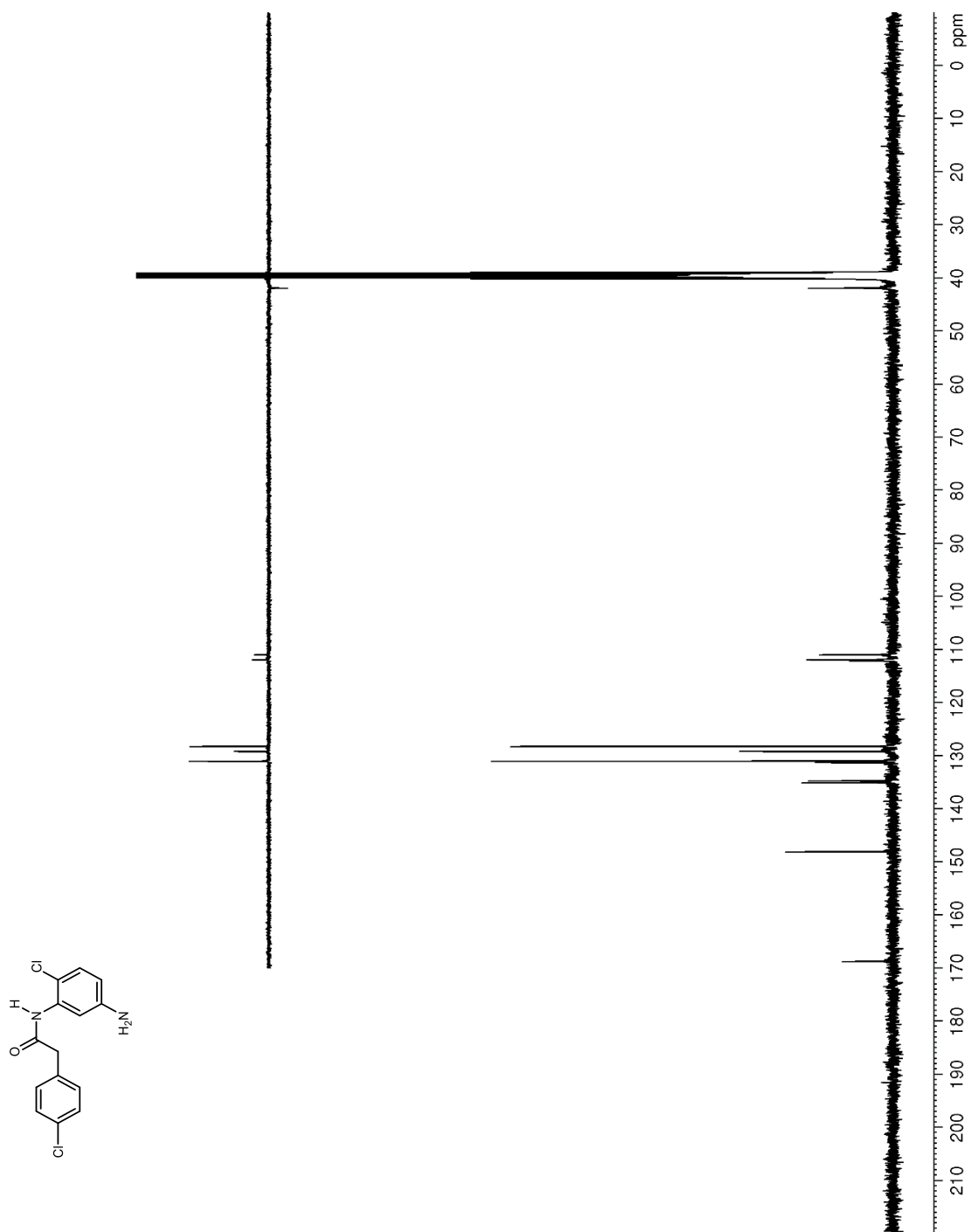


Figure 157. ^1H NMR (600 MHz, $\text{DMSO-}d_6$) of **24**

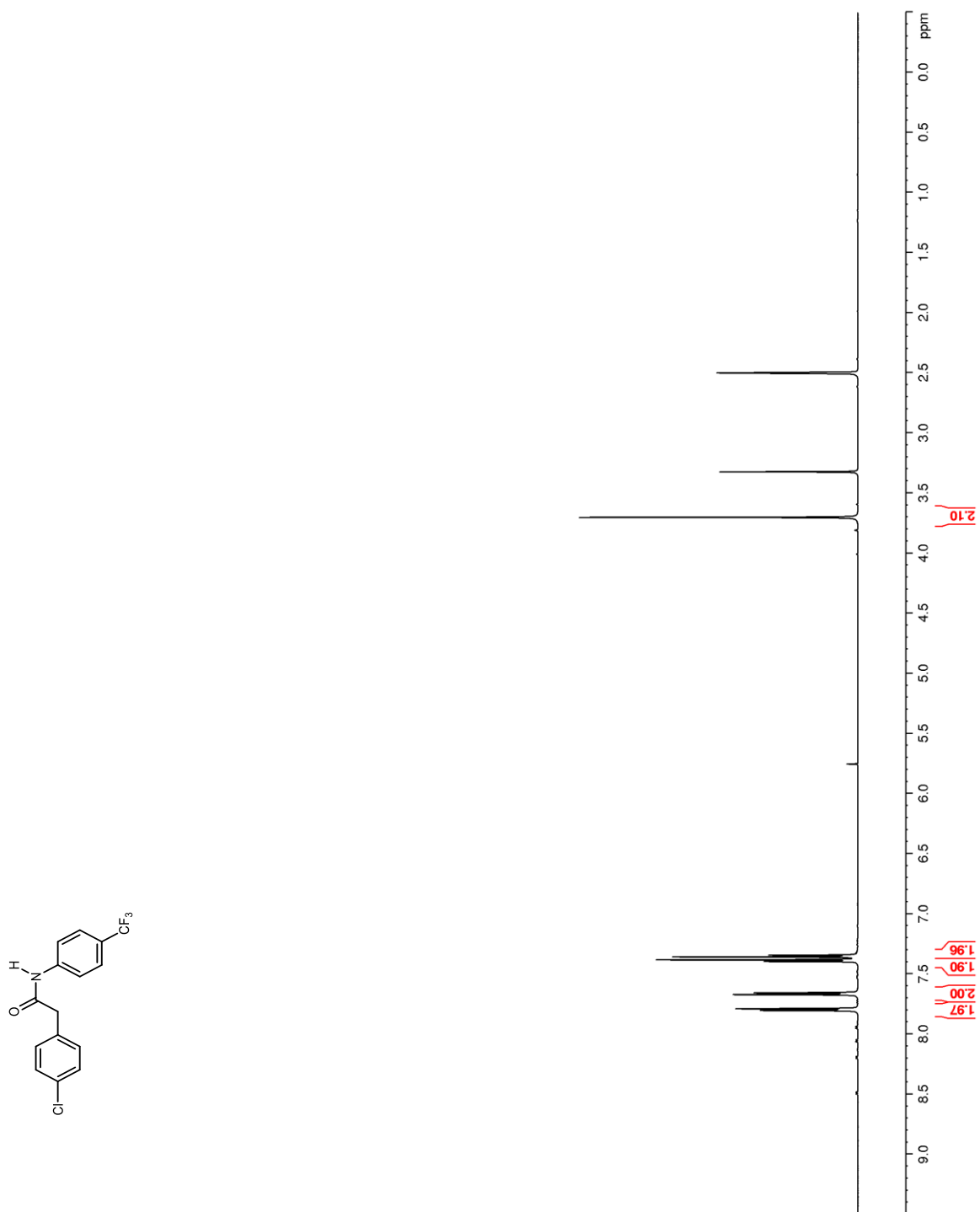


Figure 158. ^{13}C NMR (150 MHz, $\text{DMSO-}d_6$) of **24**

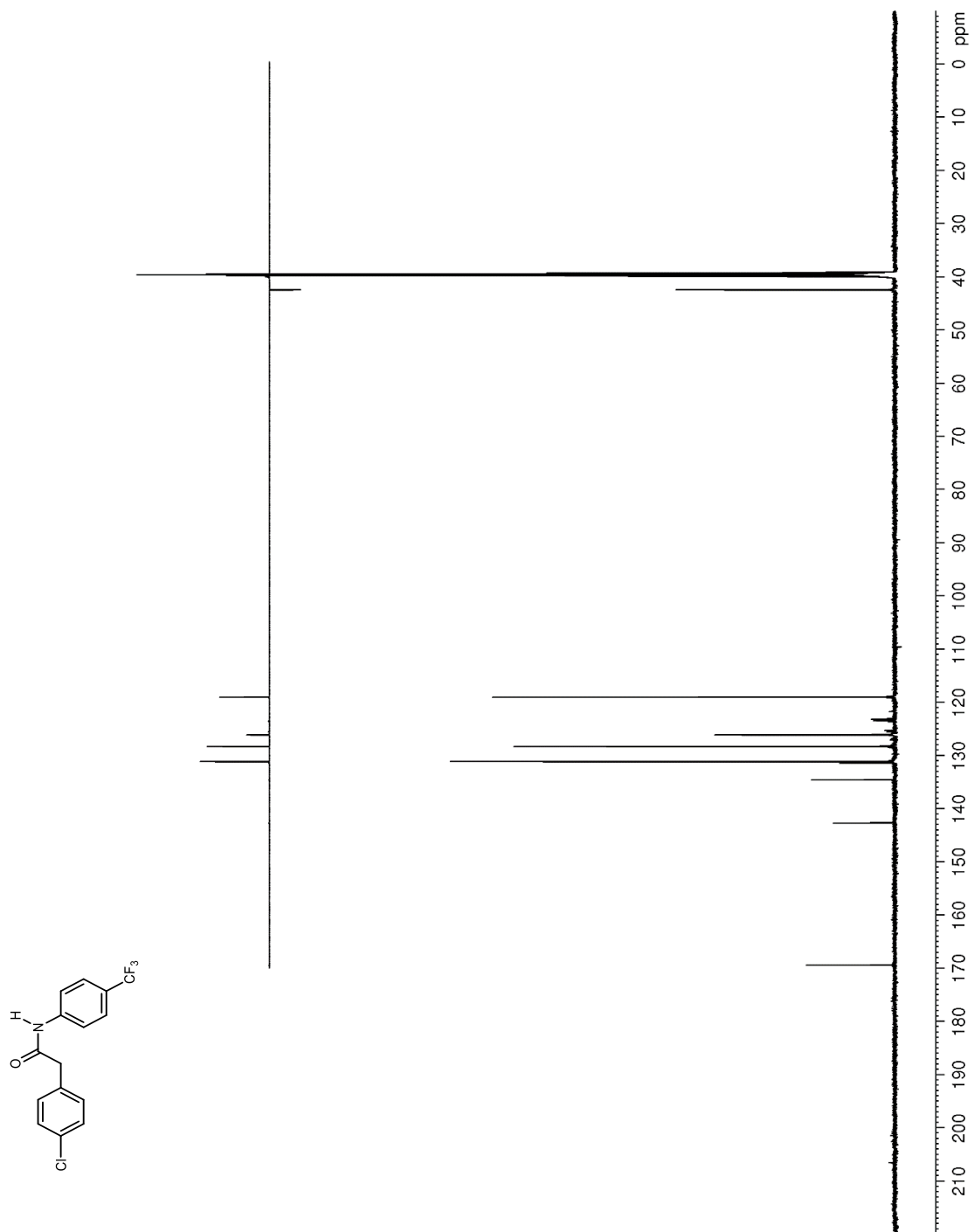


Figure 159. ^{19}F NMR (376 MHz, $\text{DMSO-}d_6$) of **246**

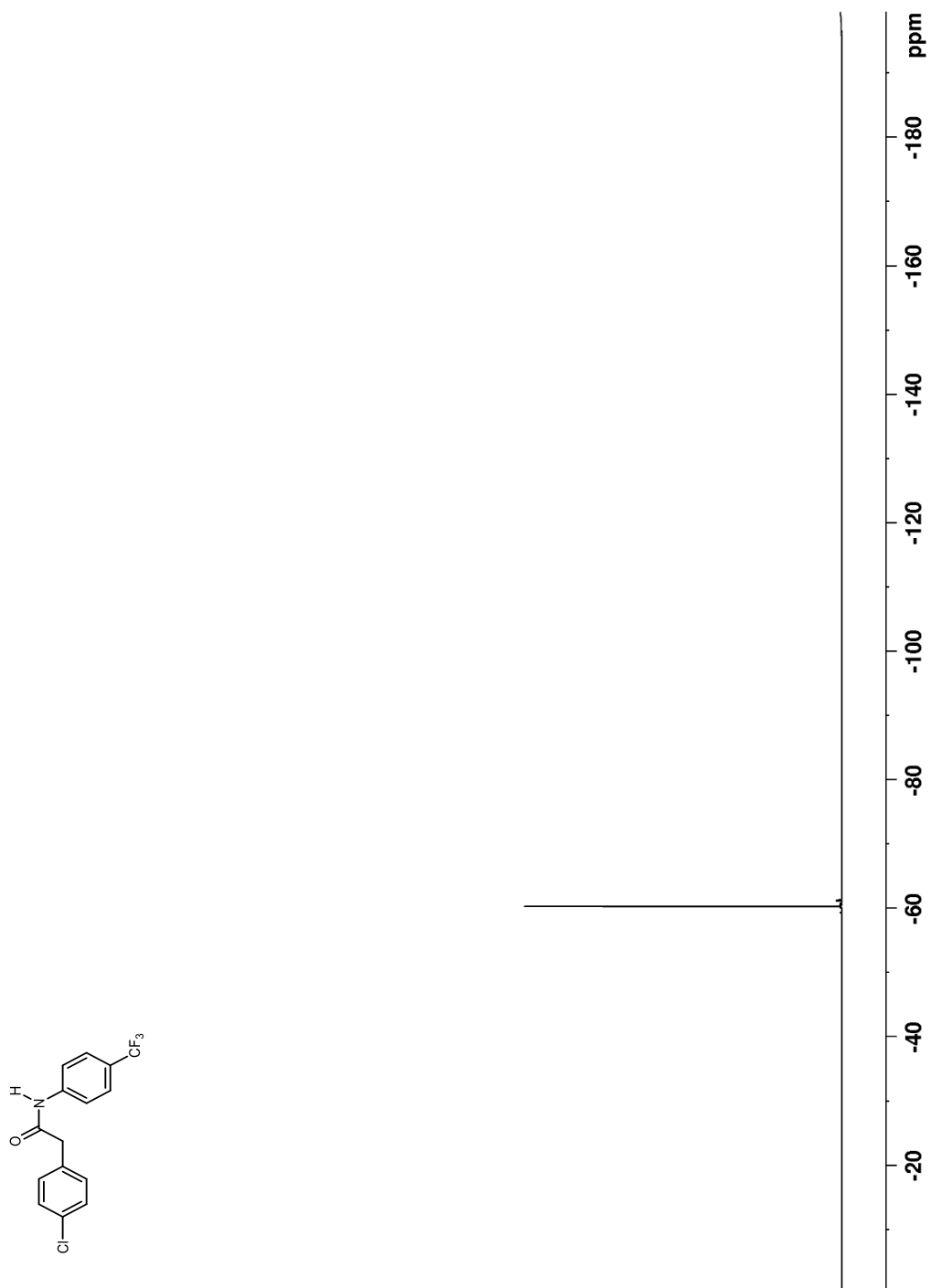


Figure 160. ^1H NMR (400 MHz, $\text{DMSO-}d_6$) of **247**

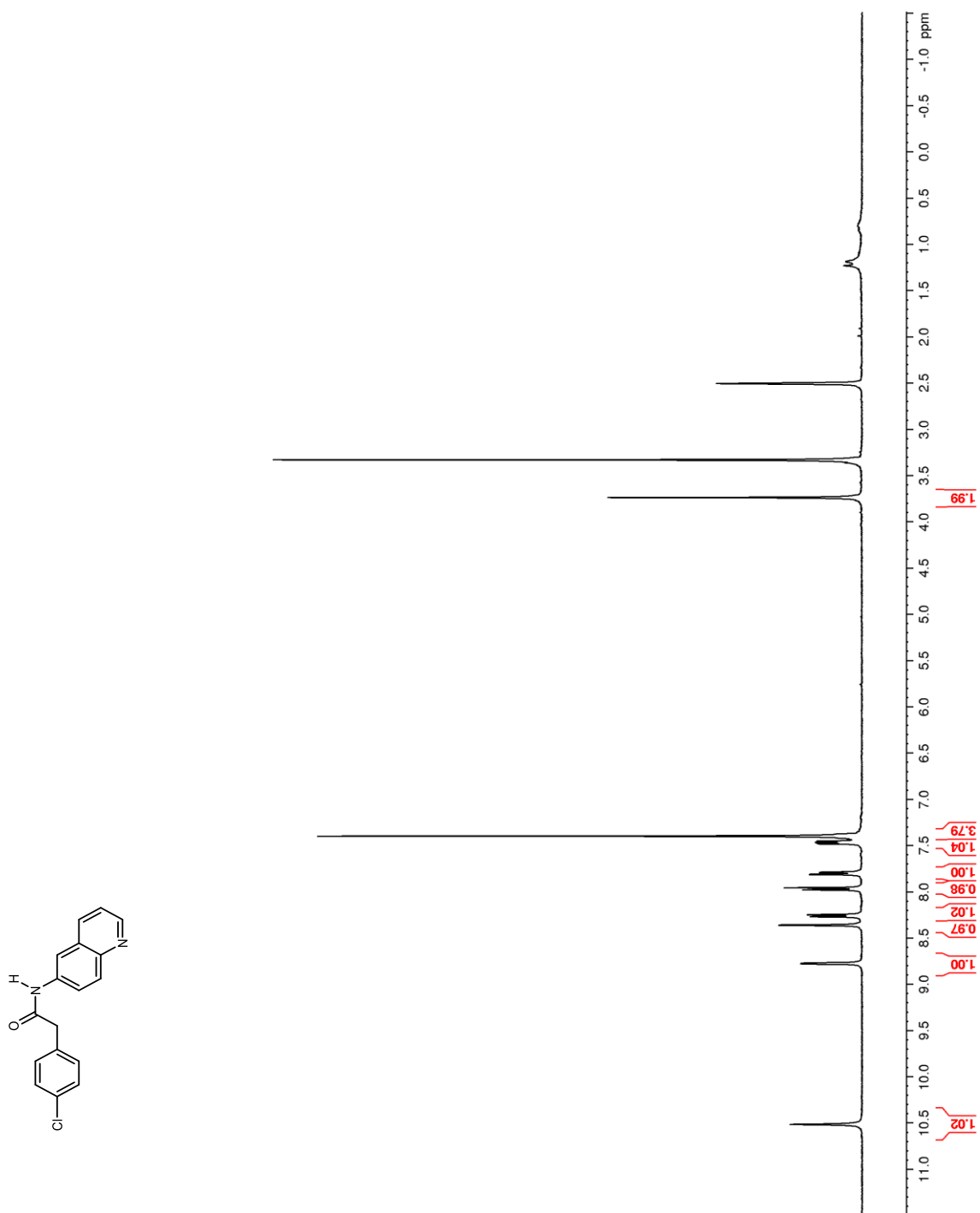


Figure 161. ^{13}C NMR (100 MHz, $\text{DMSO-}d_6$) of **247**

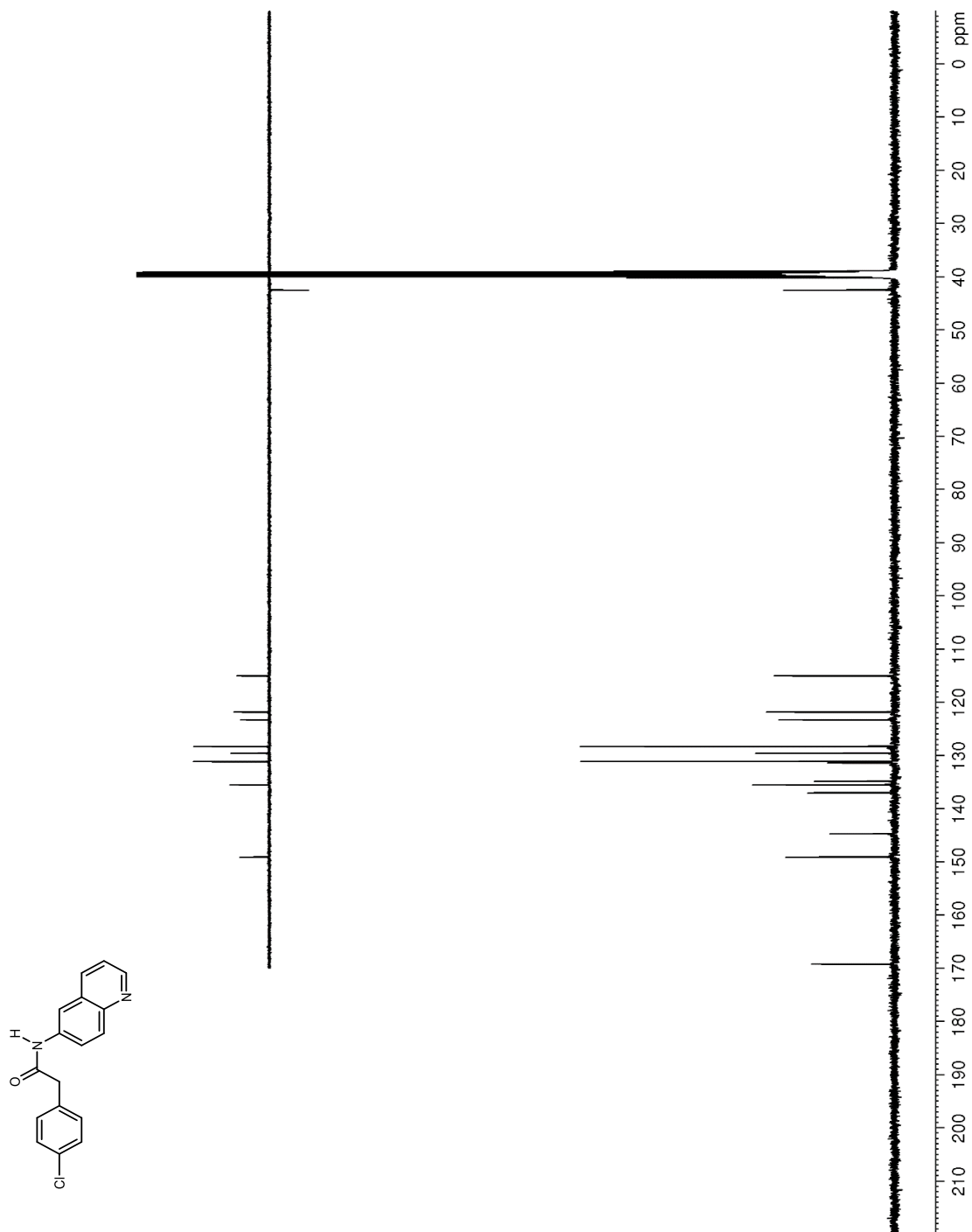


Figure 163. ^{13}C NMR (150 MHz, CDCl_3) of **249**

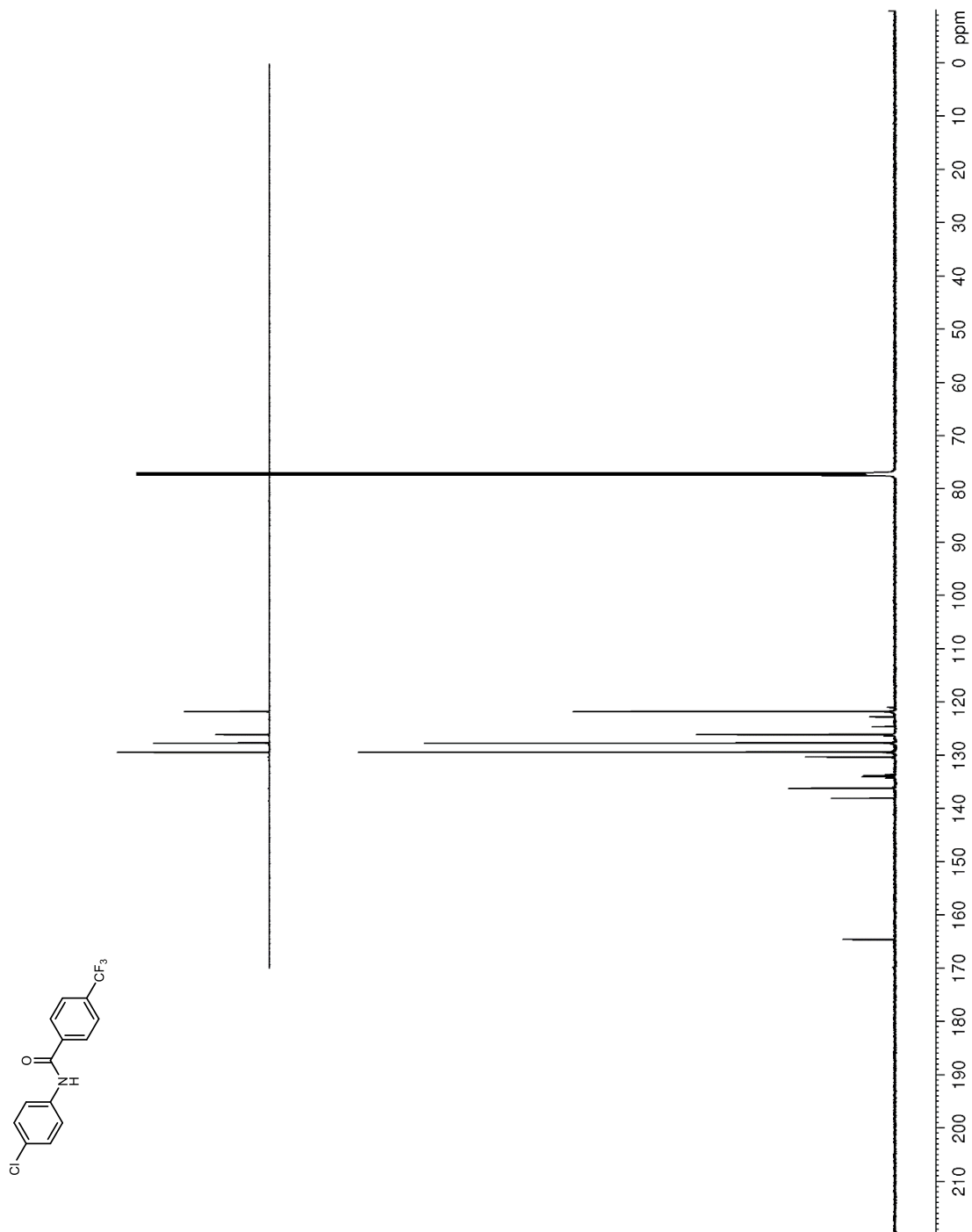


Figure 164. ^{19}F NMR (376 MHz, CDCl_3) of **249**

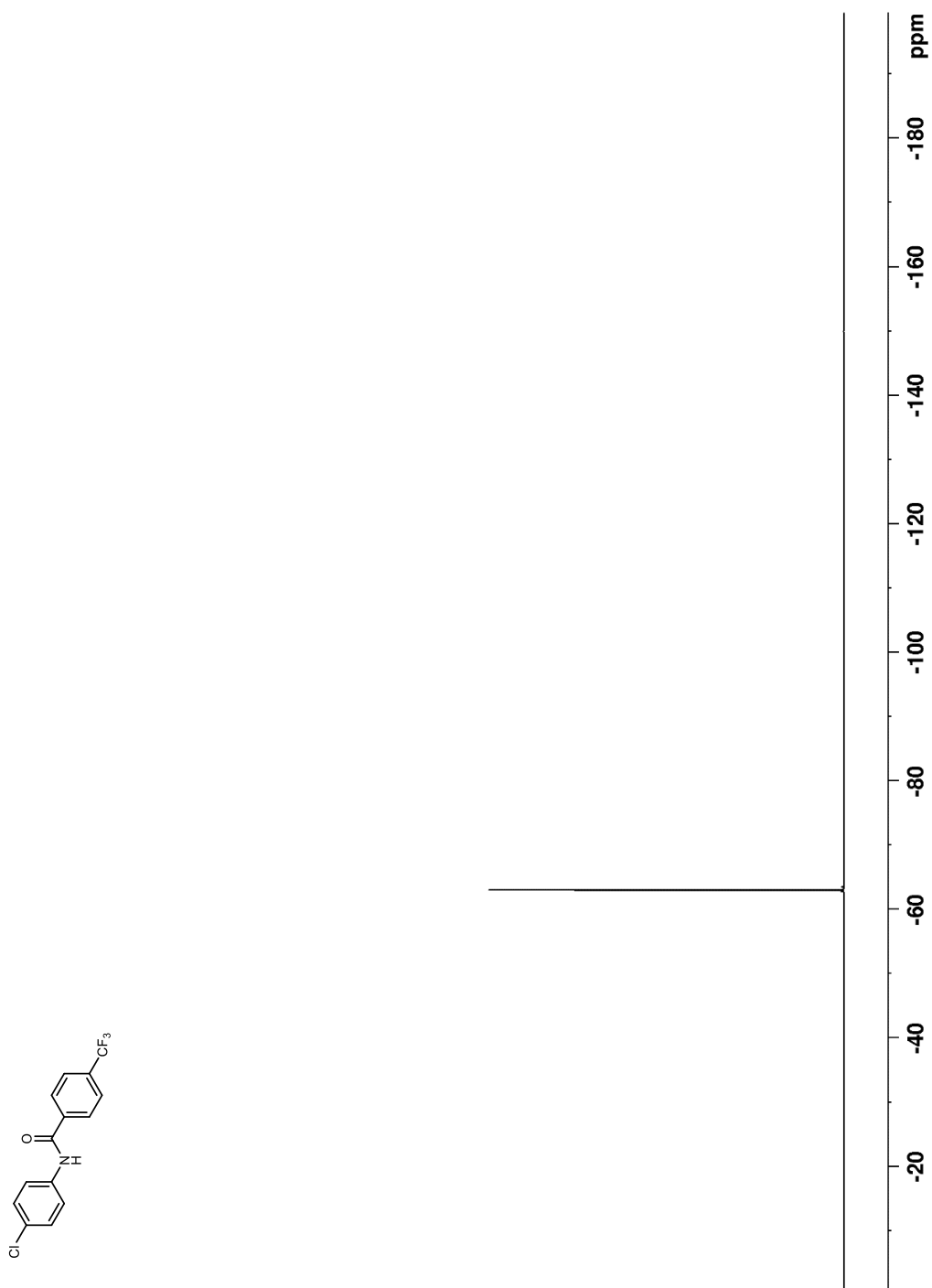


Figure 165. ^1H NMR (400 MHz, CDCl_3) of **25**

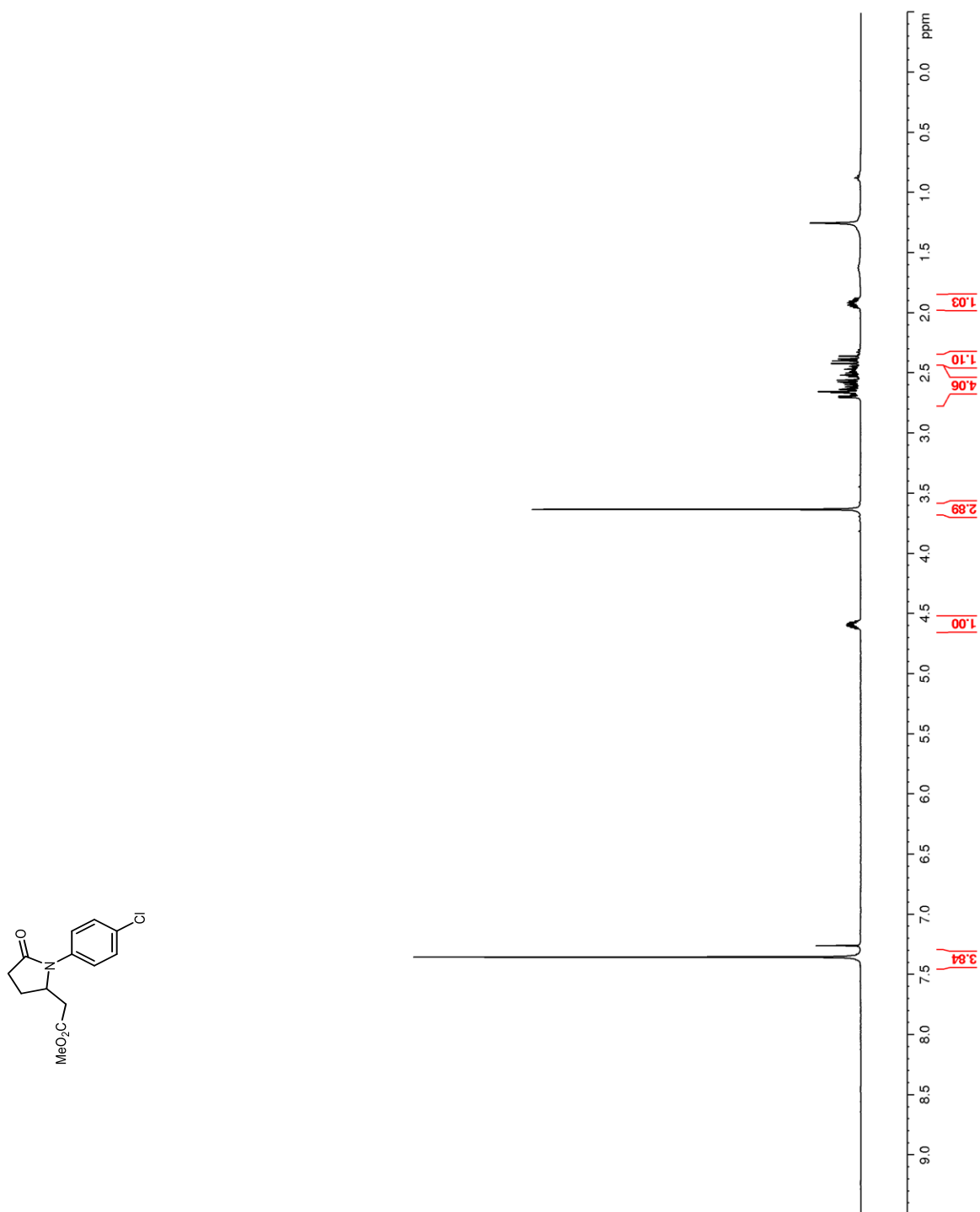


Figure 166. ^{13}C NMR (100 MHz, CDCl_3) of **25**

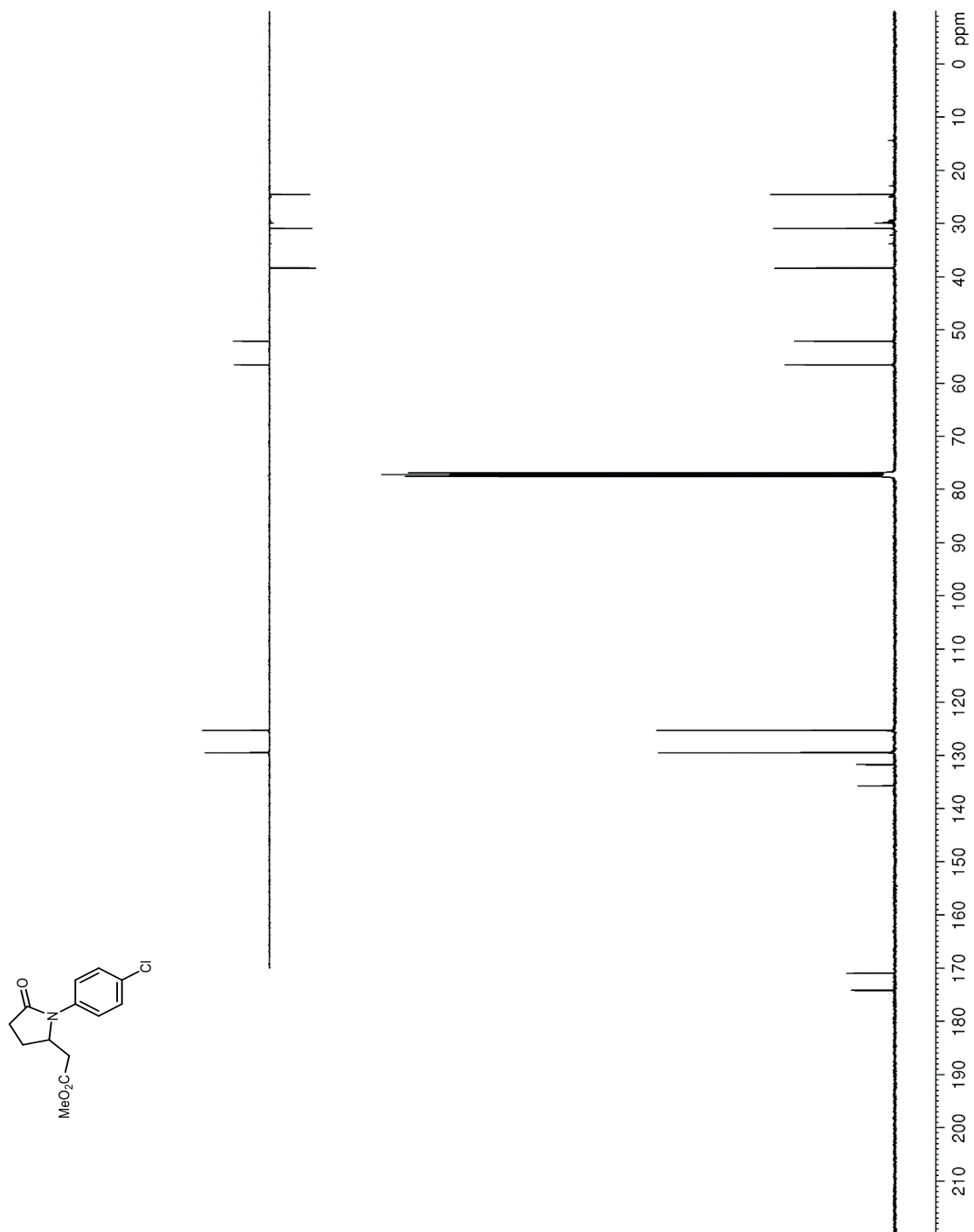


Figure 167. ^1H NMR (600 MHz, CDCl_3) of **253**

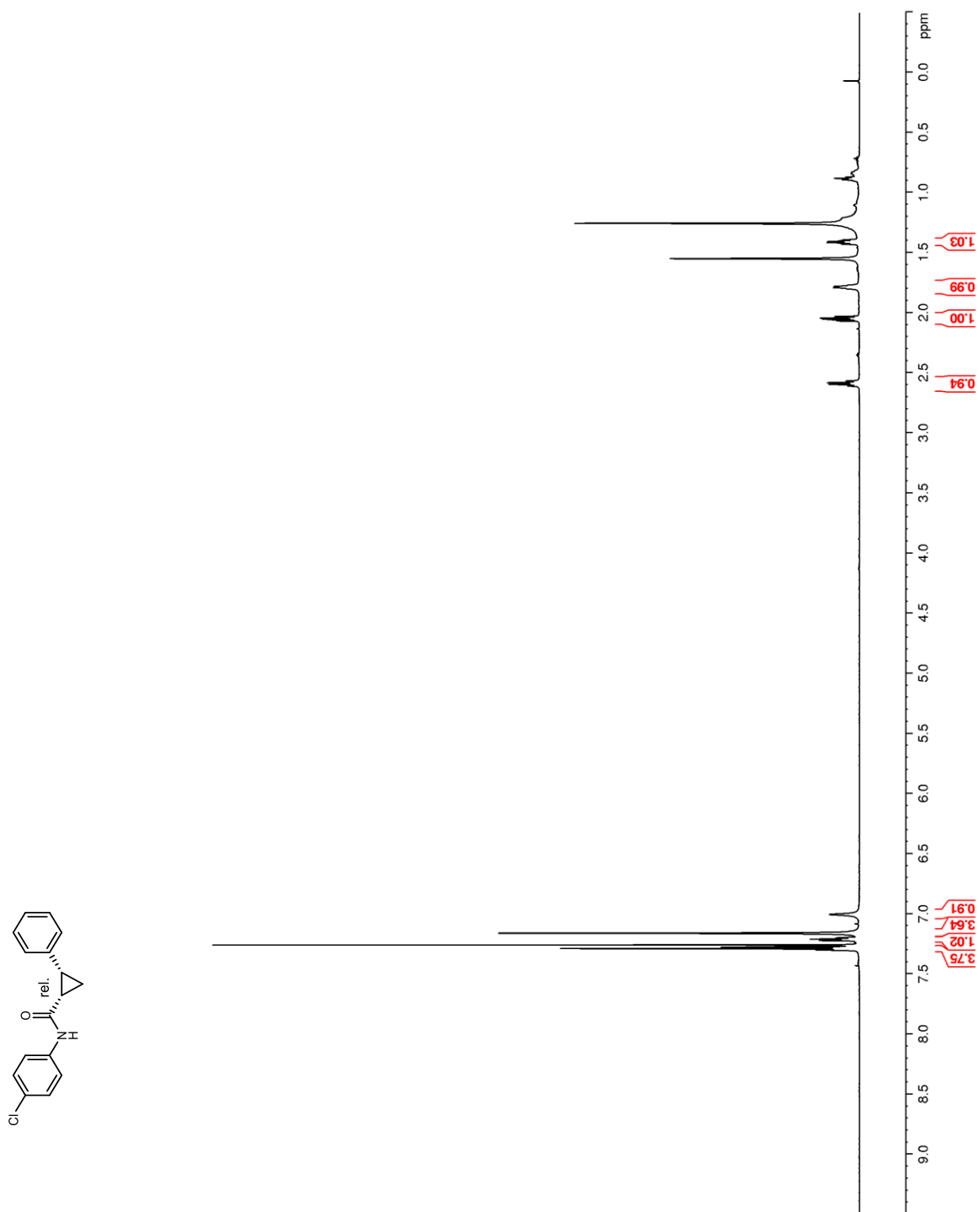


Figure 168. ^{13}C NMR (150 MHz, CDCl_3) of **253**

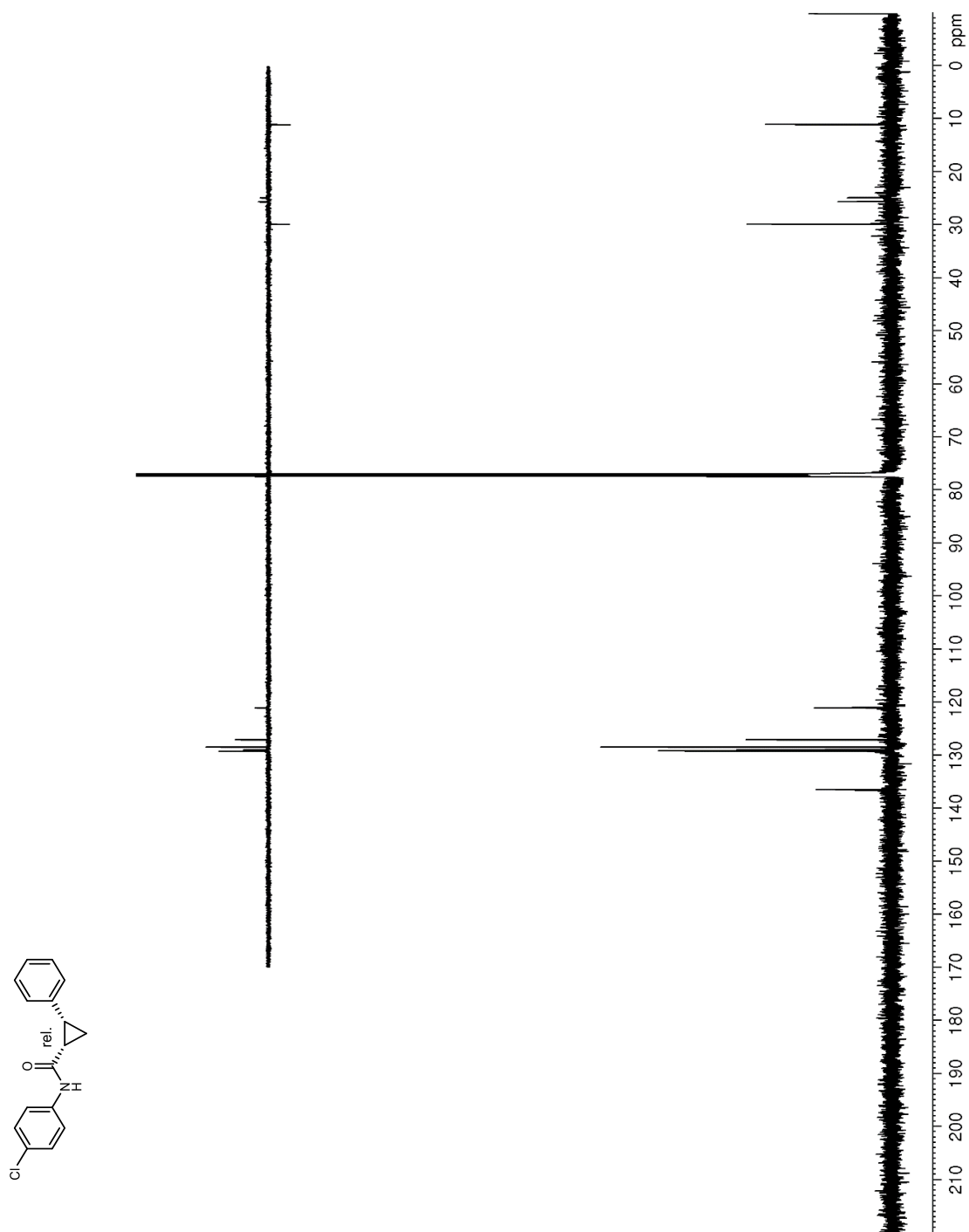


Figure 169. ^1H NMR (400 MHz, CDCl_3) of **254**

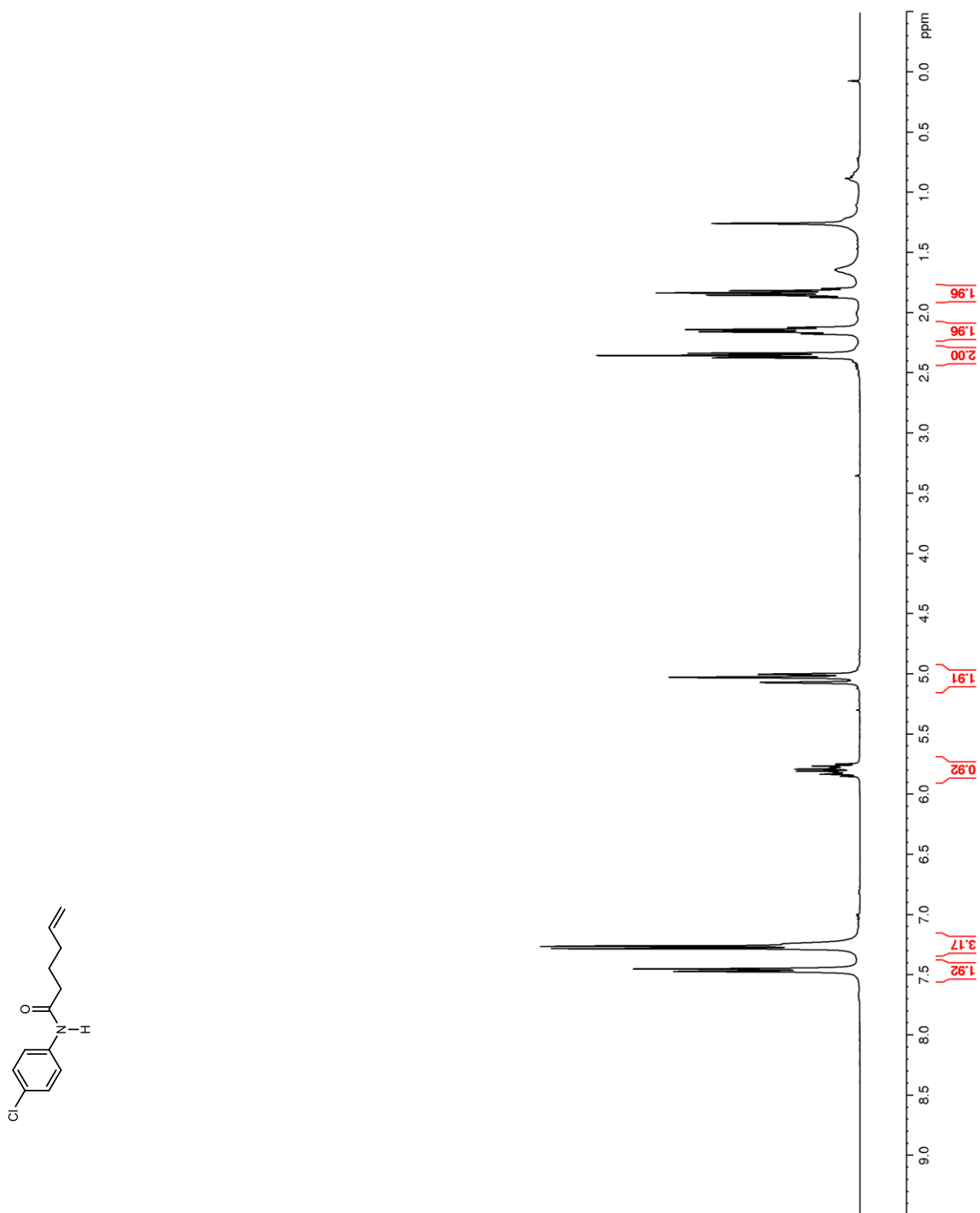


Figure 170. ^{13}C NMR (100 MHz, CDCl_3) of **254**

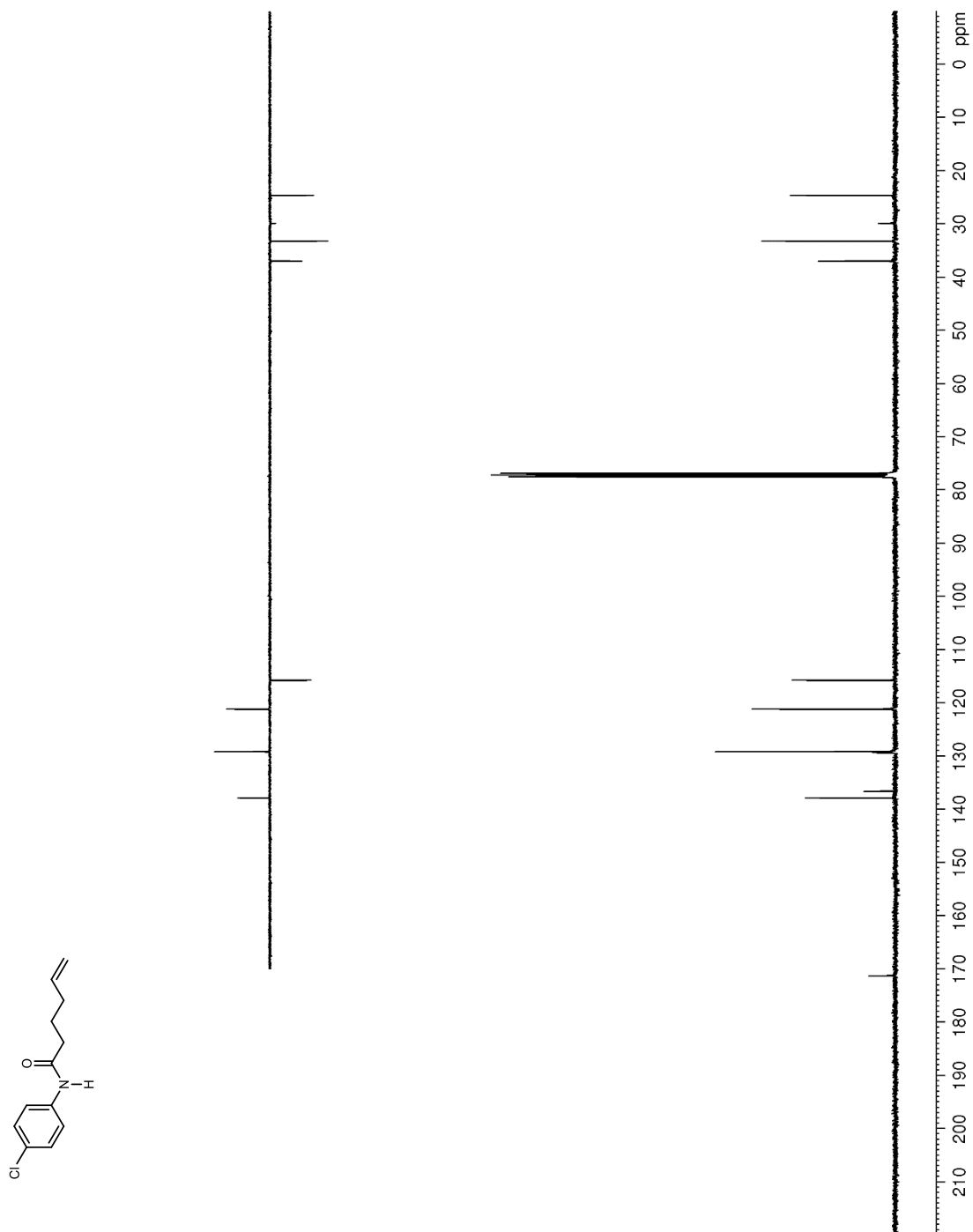


Figure 171. ^1H NMR (400 MHz, CDCl_3) of **25**

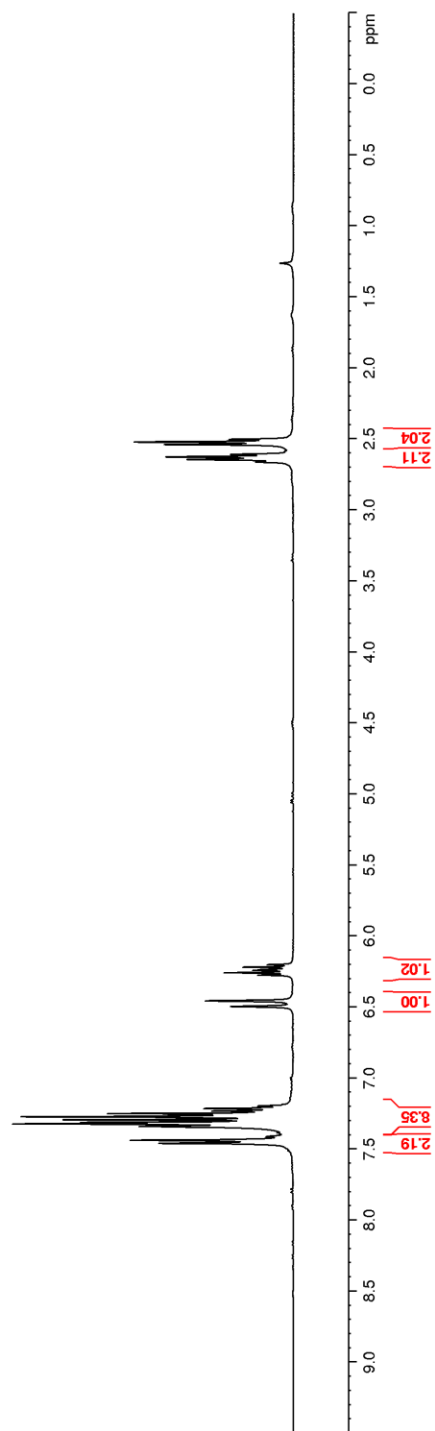
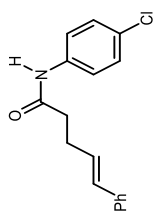


Figure 172. ^{13}C NMR (100 MHz, CDCl_3) of **25**

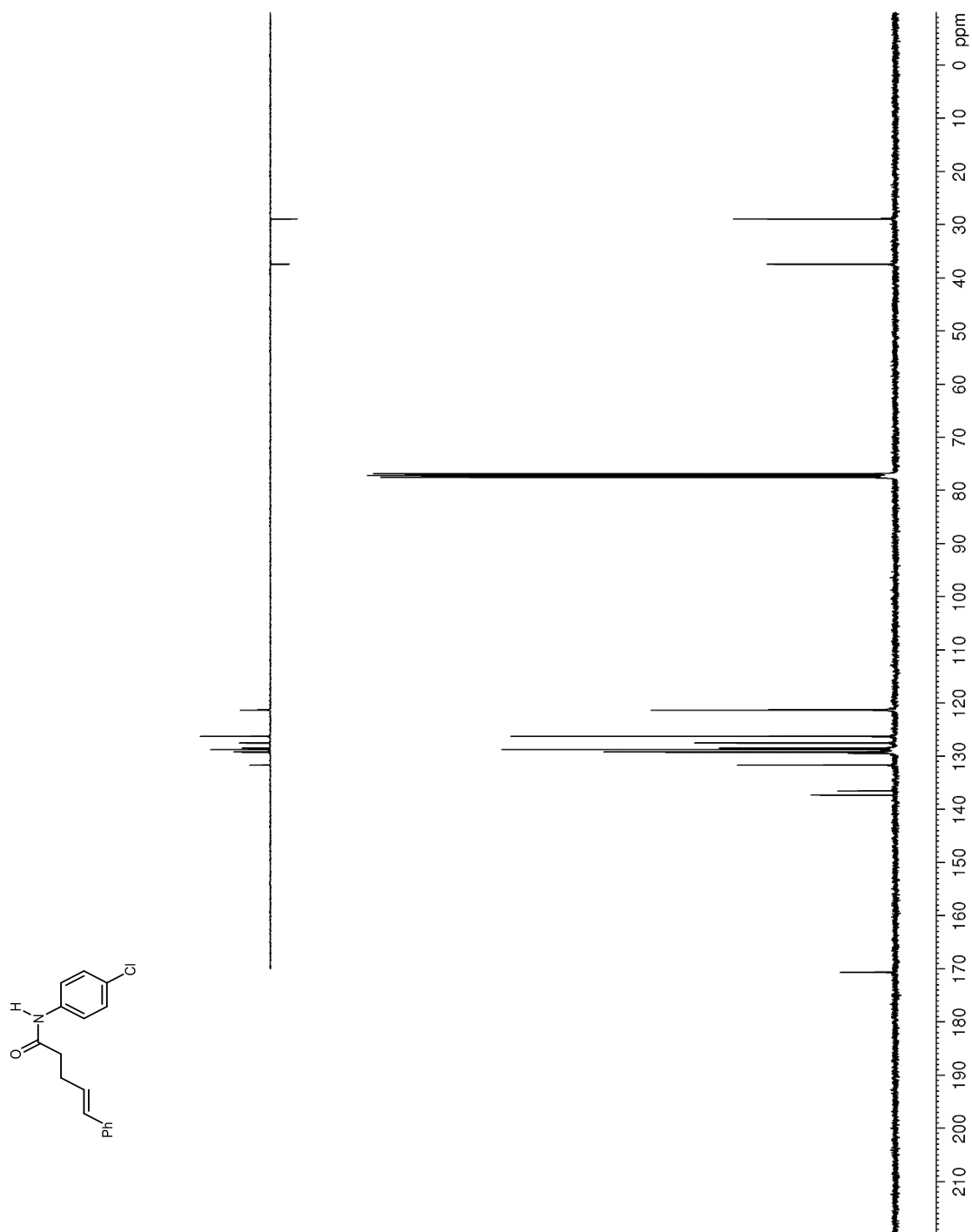


Figure 173. ^1H NMR (600 MHz, CDCl_3) of **260**

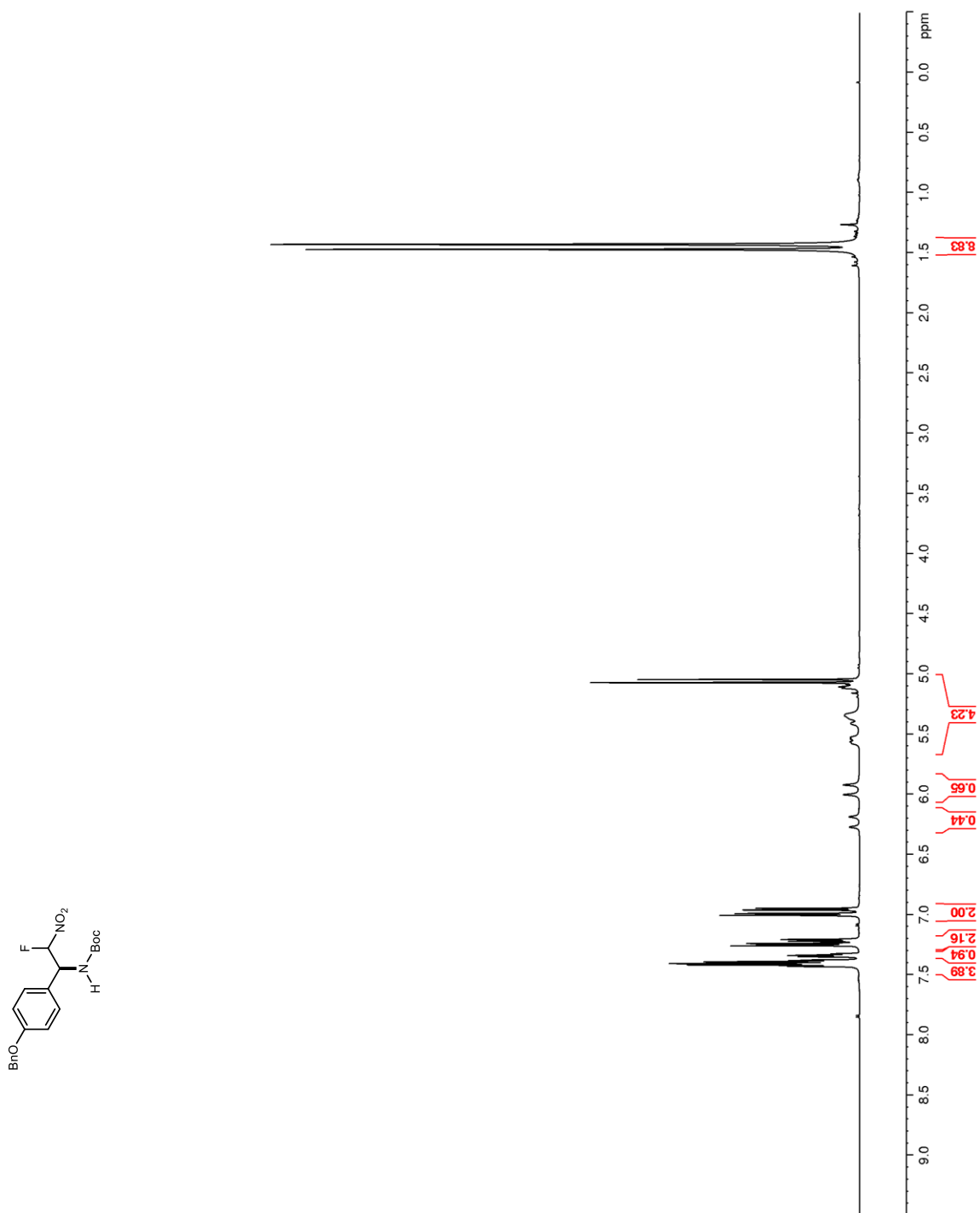


Figure 174. ^{13}C NMR (150 MHz, CDCl_3) of **260**

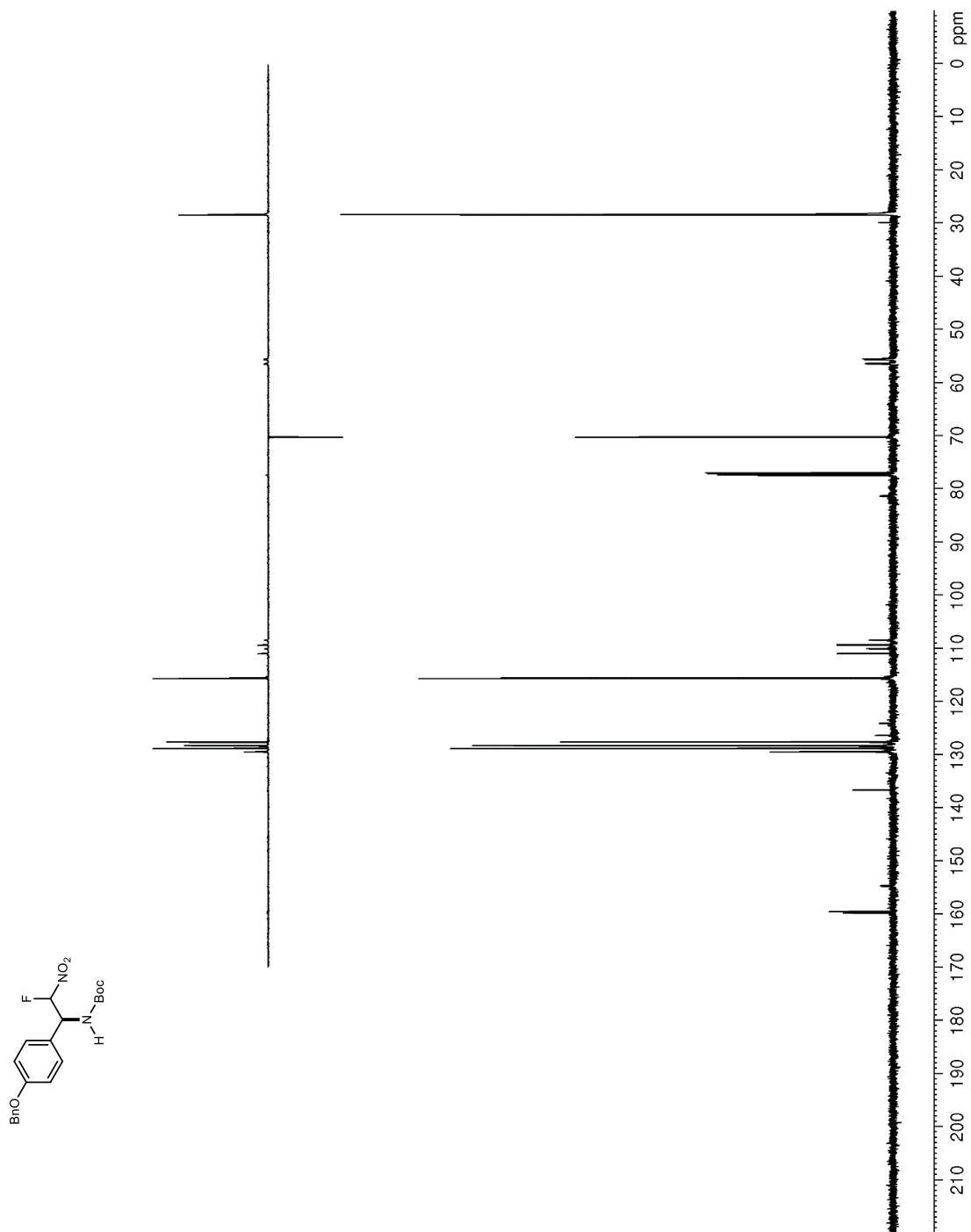


Figure 175. ^{19}F NMR (376 MHz, CDCl_3) of **260**

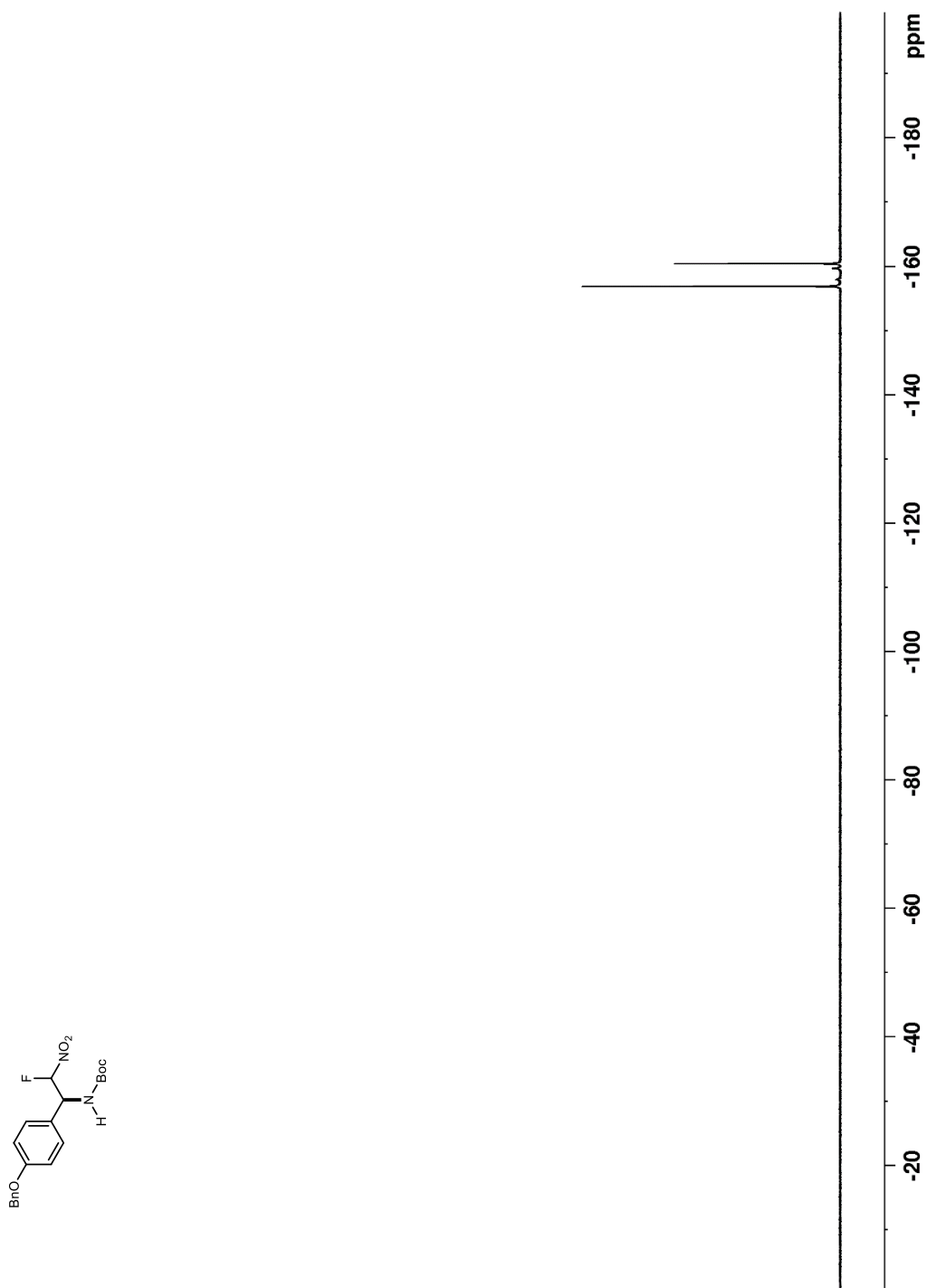


Figure 176. ^1H NMR (600 MHz, CDCl_3) of **261**

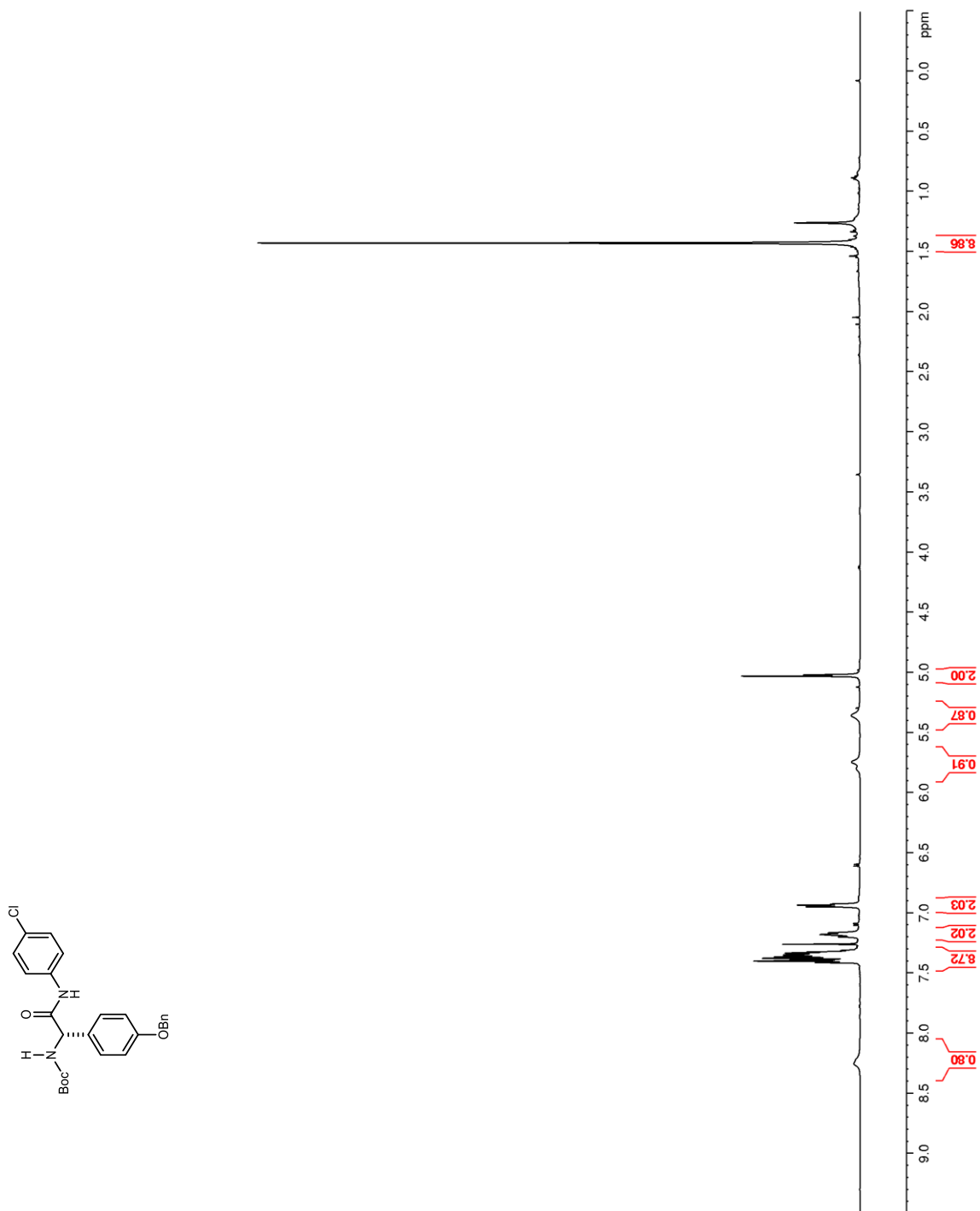


Figure 177. ^{13}C NMR (150 MHz, CDCl_3) of **261**

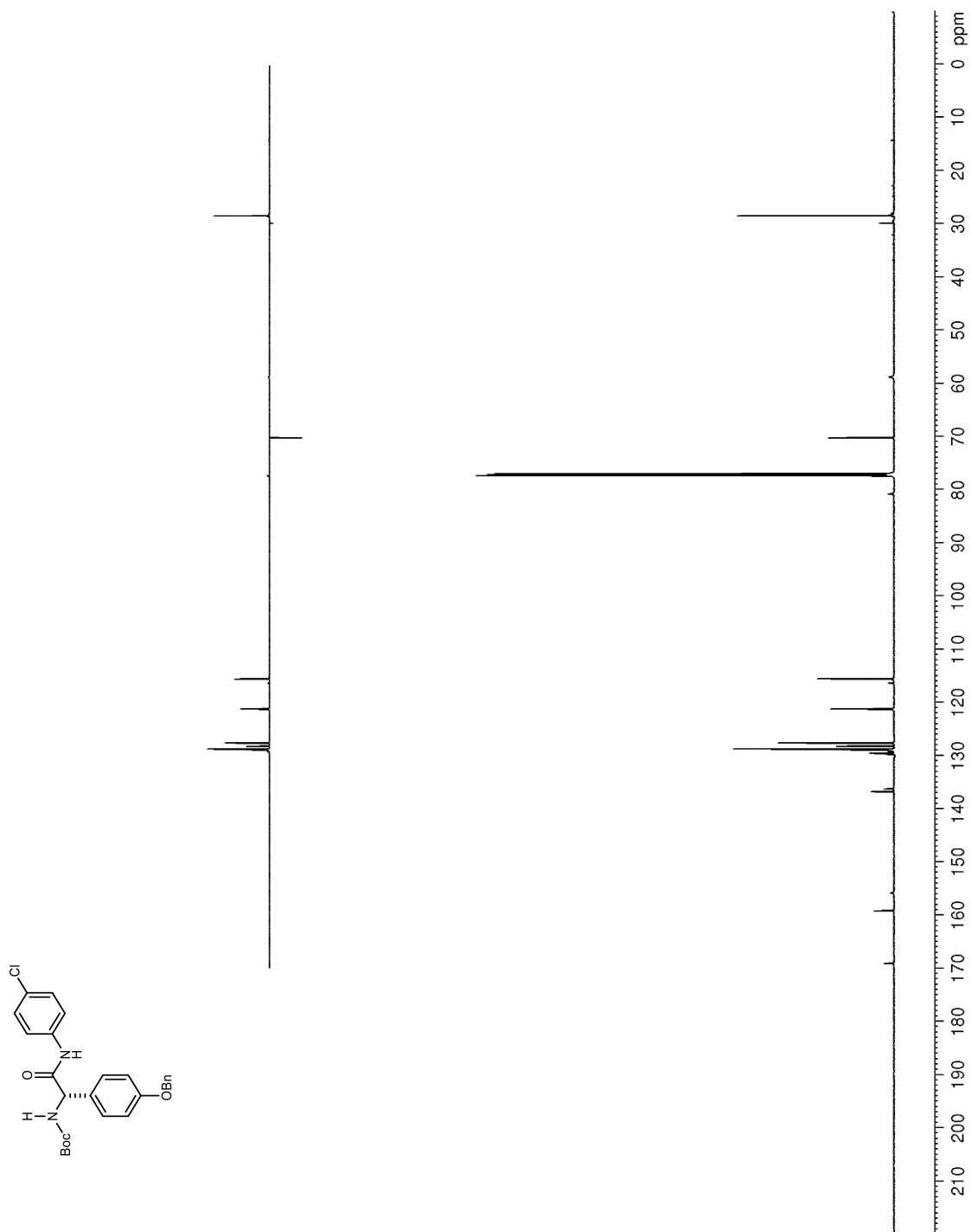


Figure 178. ^1H NMR (600 MHz, CDCl_3) of **263**

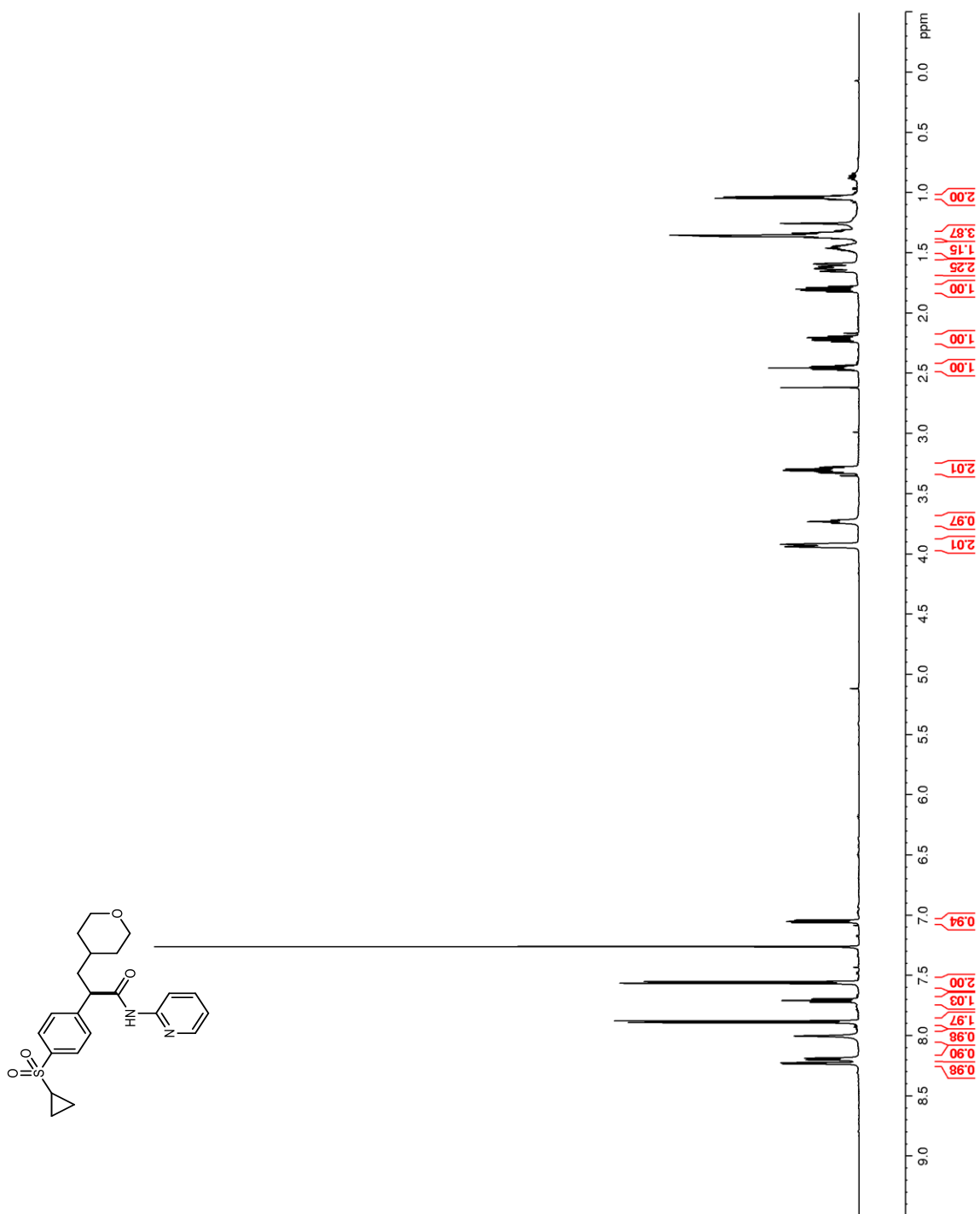


Figure 179. ^{13}C NMR (150 MHz, CDCl_3) of **263a**

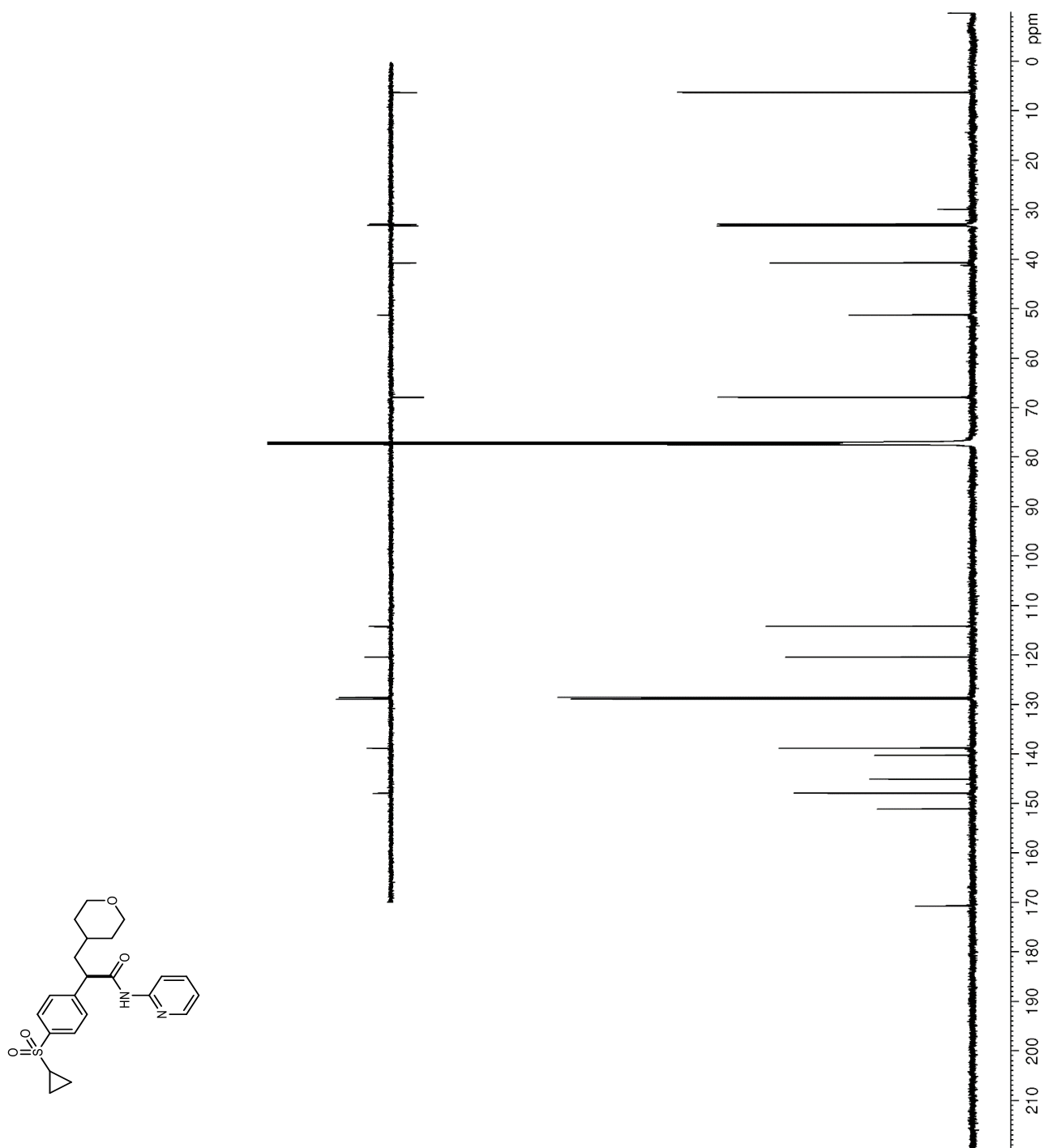


Figure 180. ^1H NMR (400 MHz, CDCl_3) of **27**

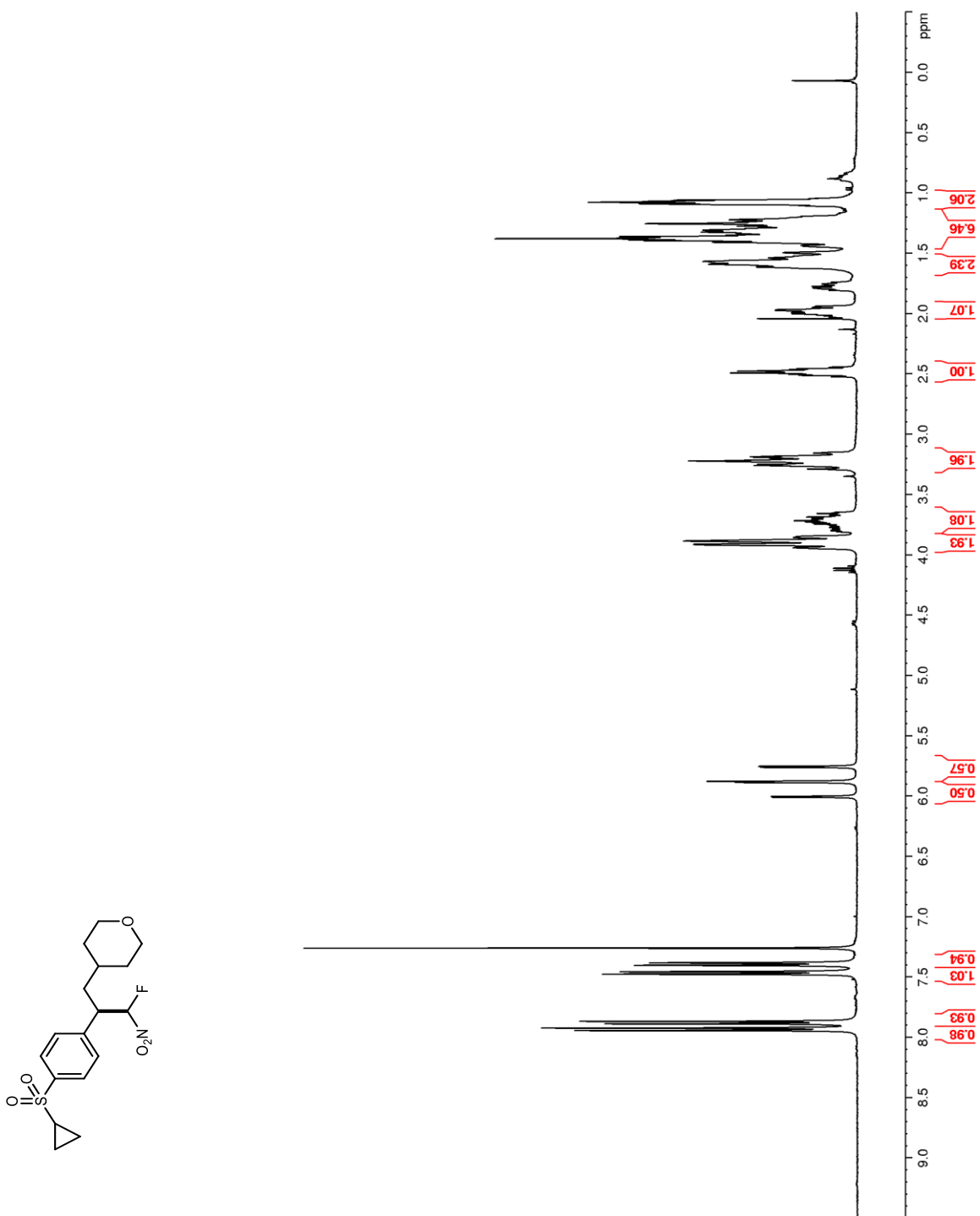


Figure 181. ^{13}C NMR (100 MHz, CDCl_3) of **27**

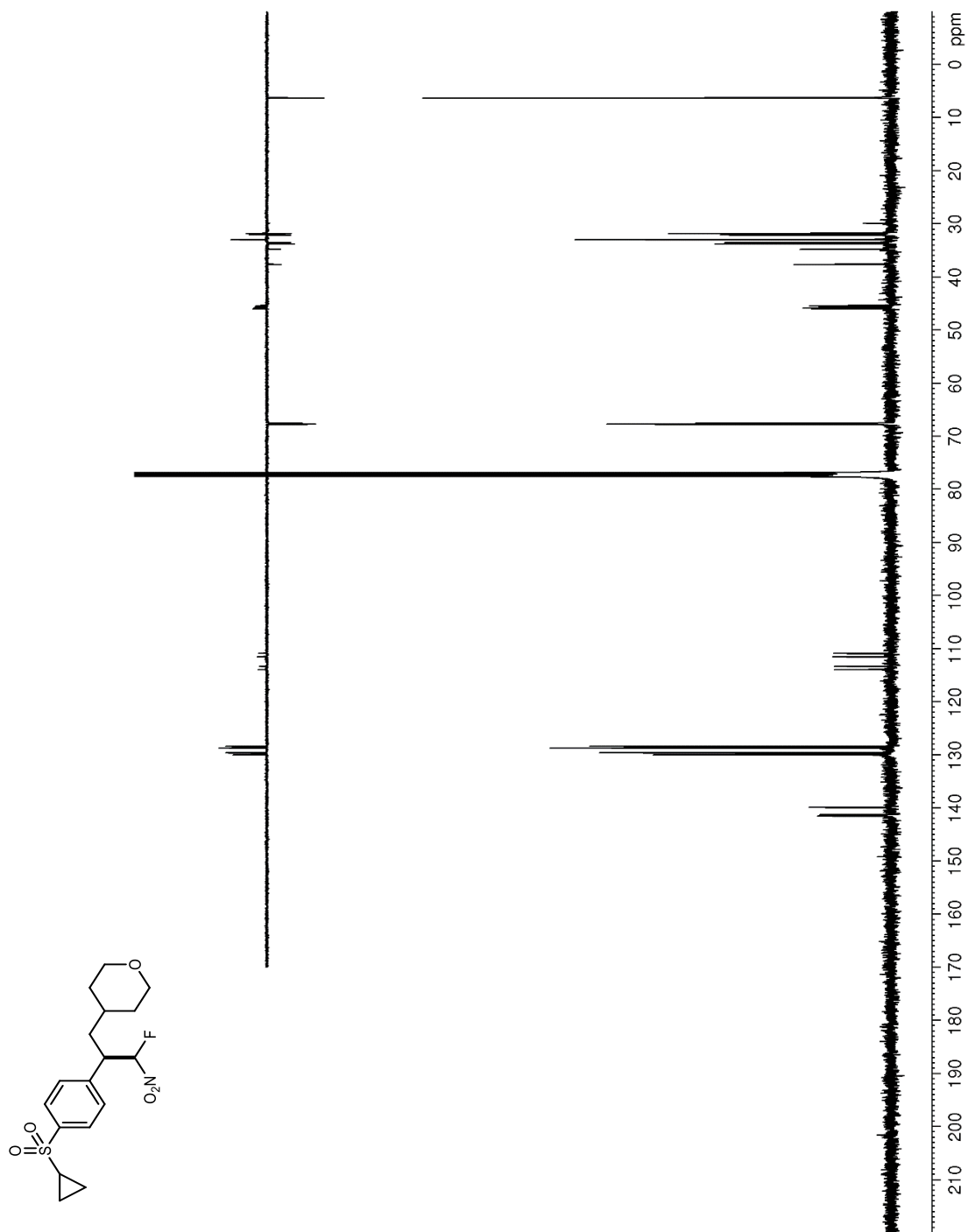


Figure 182. ^{19}F NMR (376 MHz, CDCl_3) of **271**

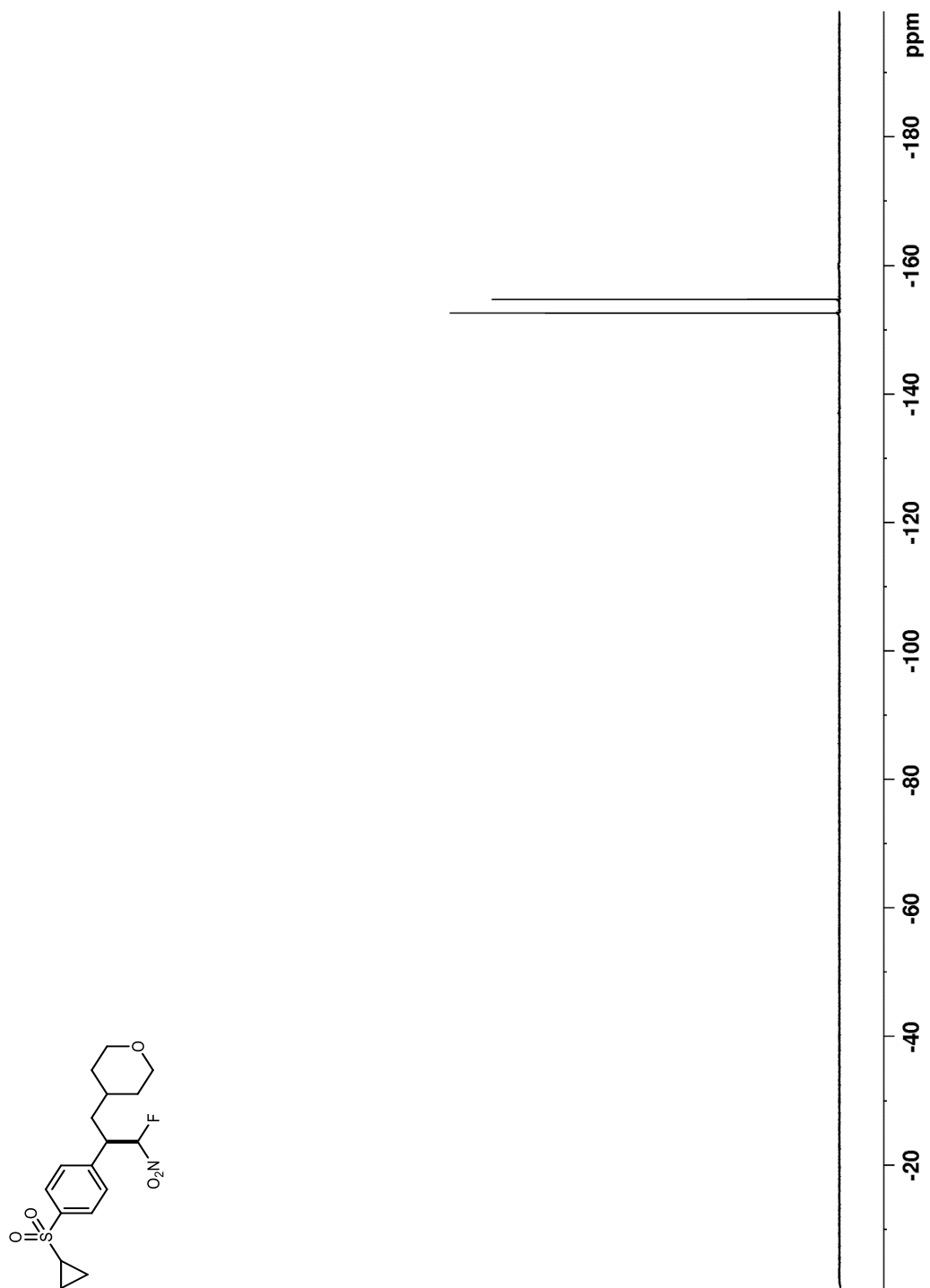


Figure 183. ^1H NMR (400 MHz, CDCl_3) of **27**

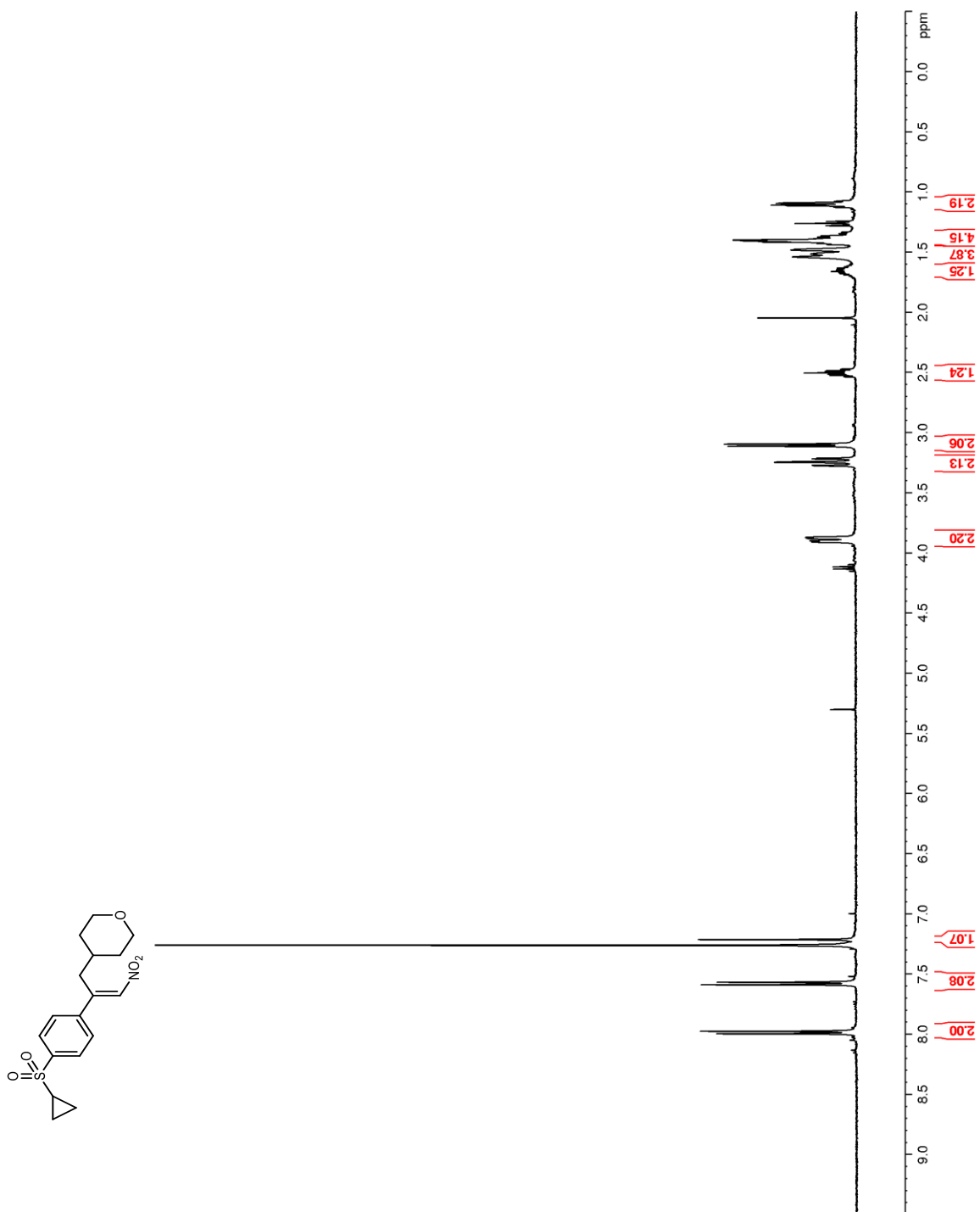


Figure 185. ^1H NMR (400 MHz, CDCl_3) of **27**

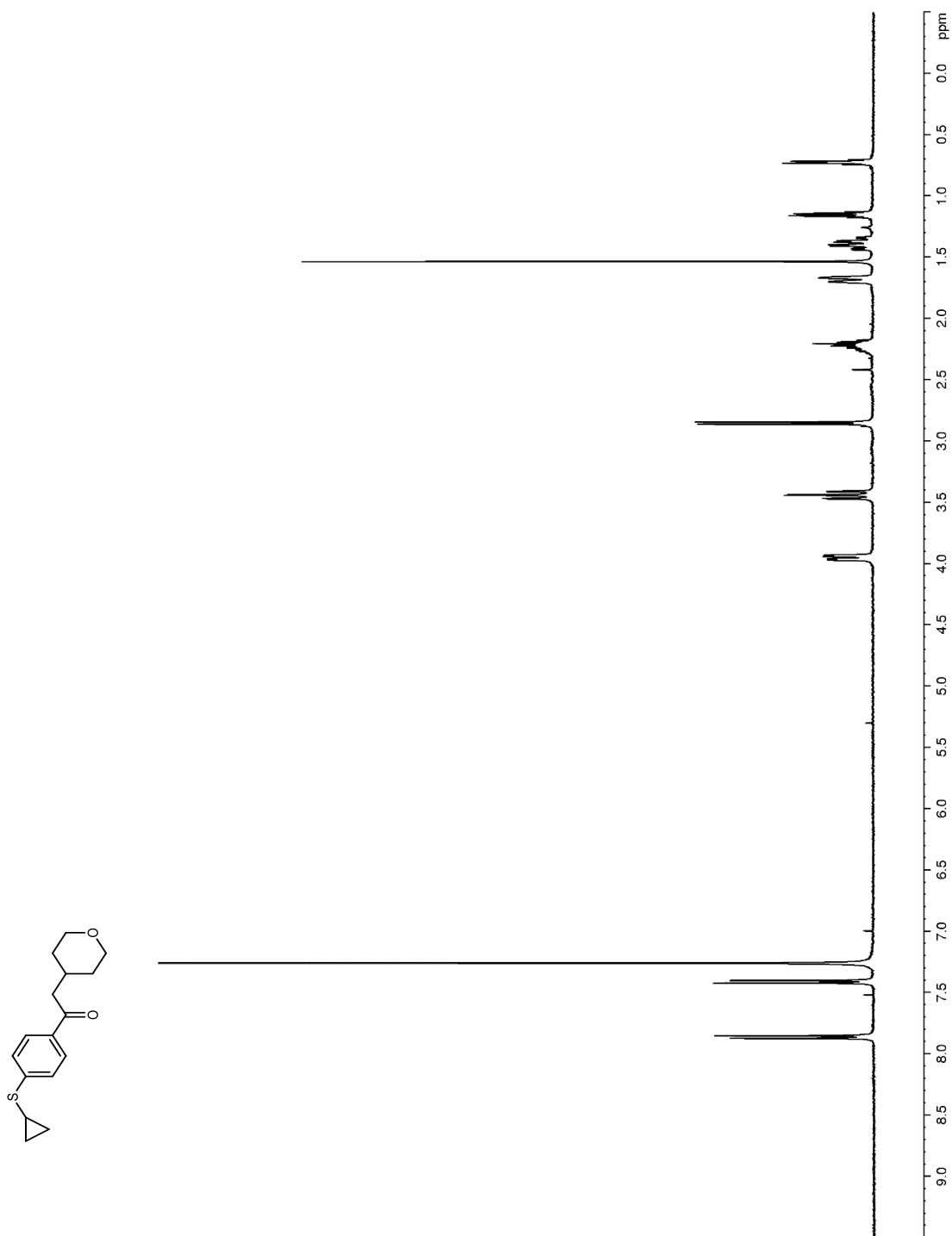


Figure 186. ^{13}C NMR (100 MHz, CDCl_3) of **27**

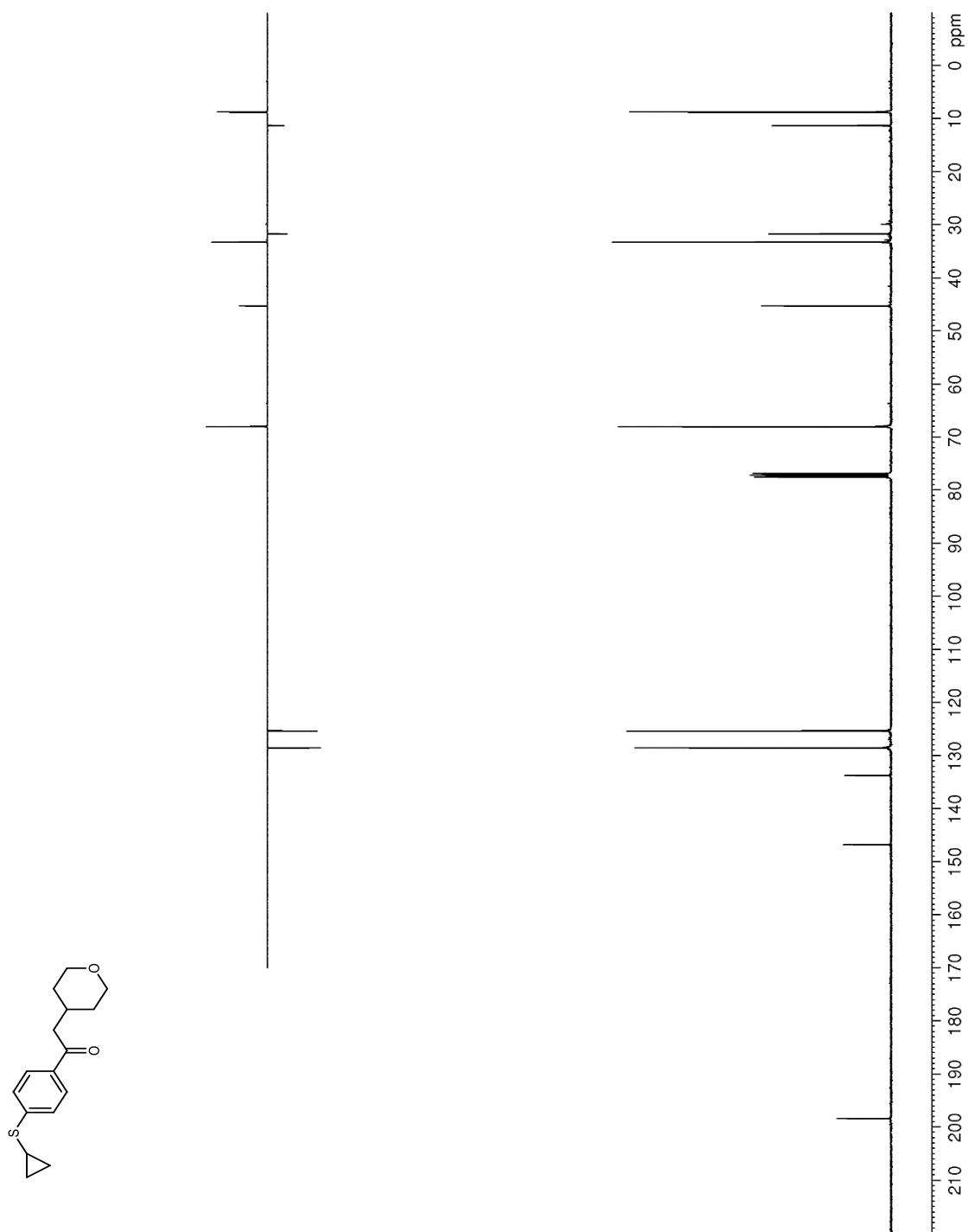


Figure 187. ^1H NMR (400 MHz, CDCl_3) of **27**

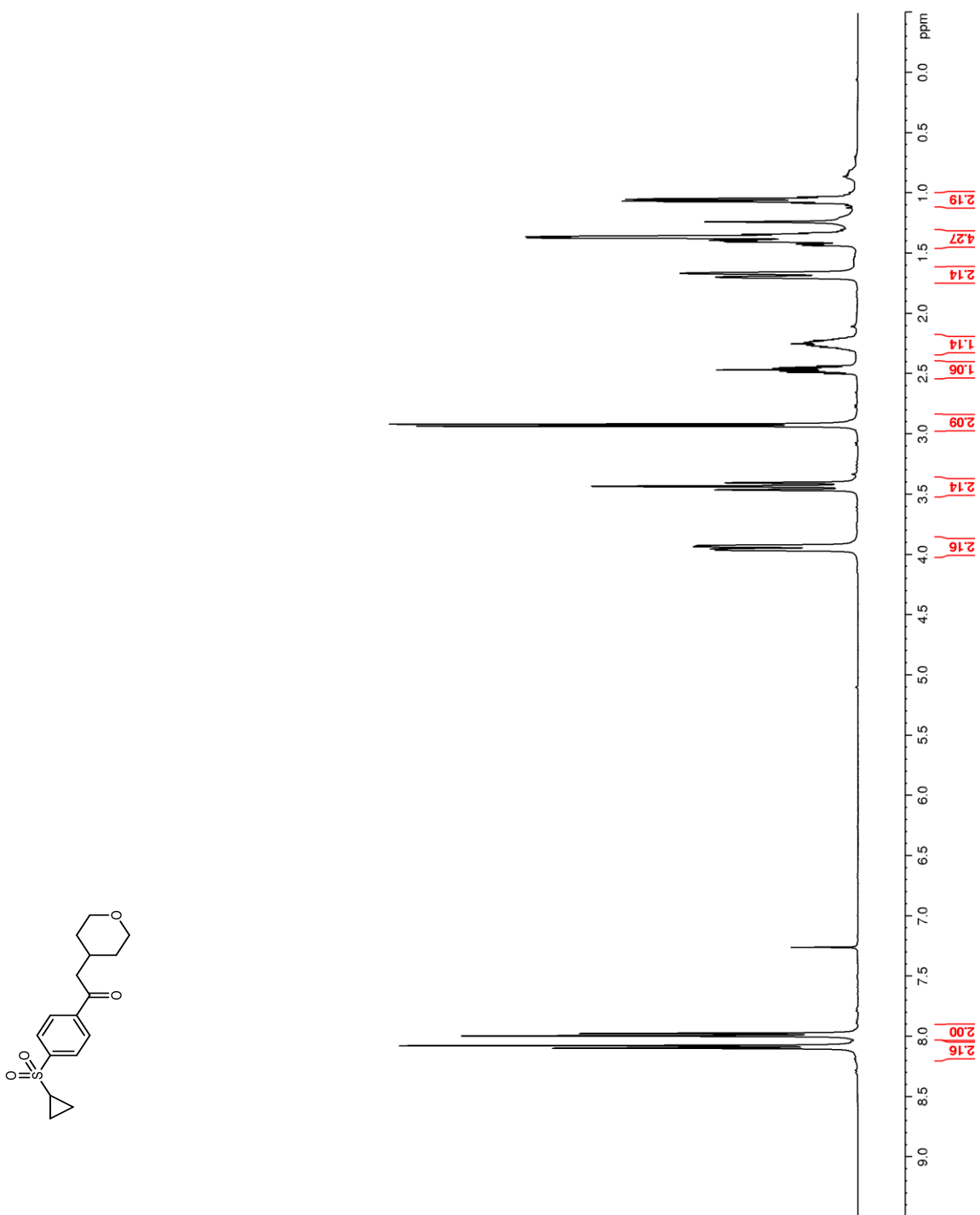


Figure 188. ^{13}C NMR (100 MHz, CDCl_3) of **27**

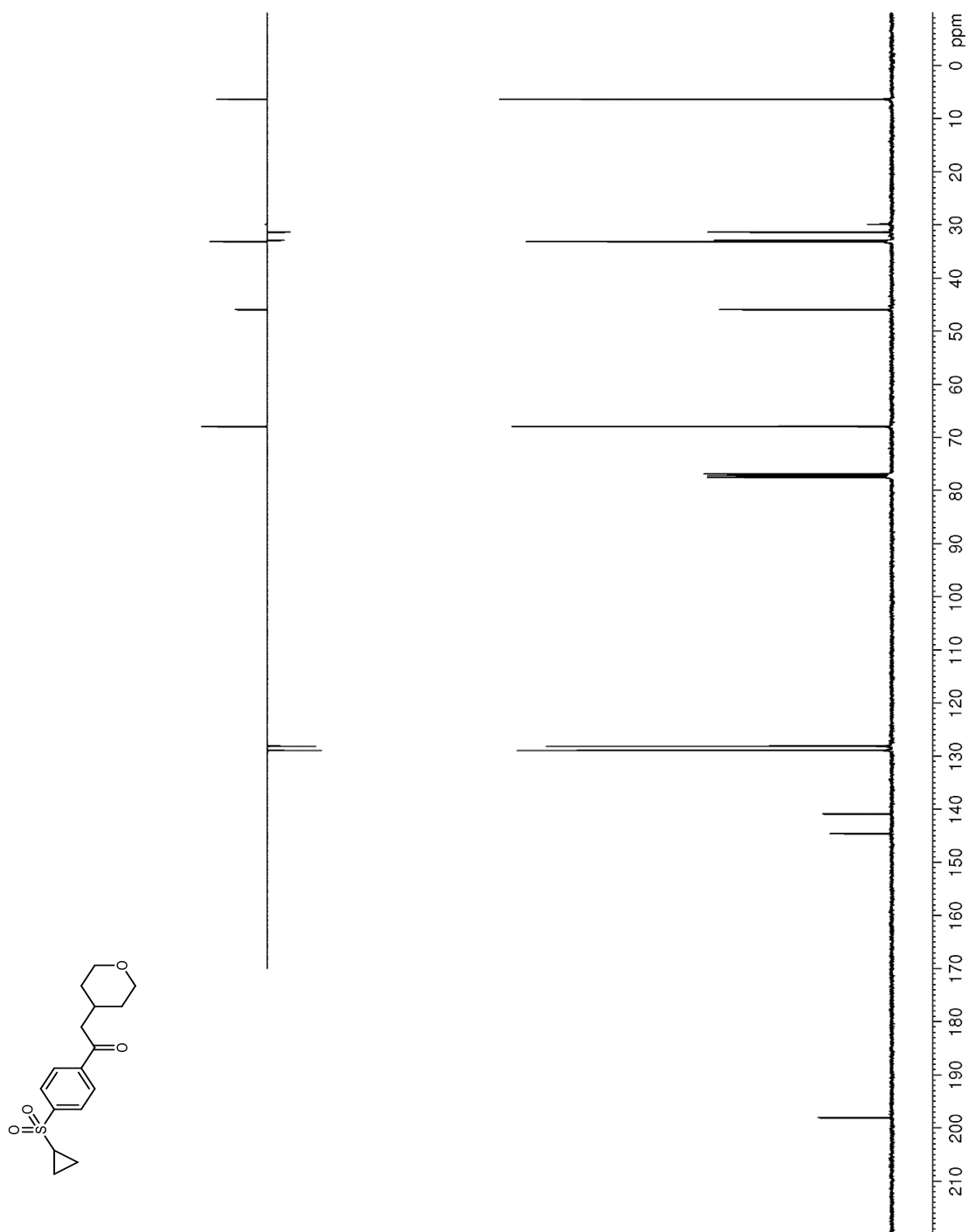


Figure 189. ^1H NMR (400 MHz, CDCl_3) of **28**

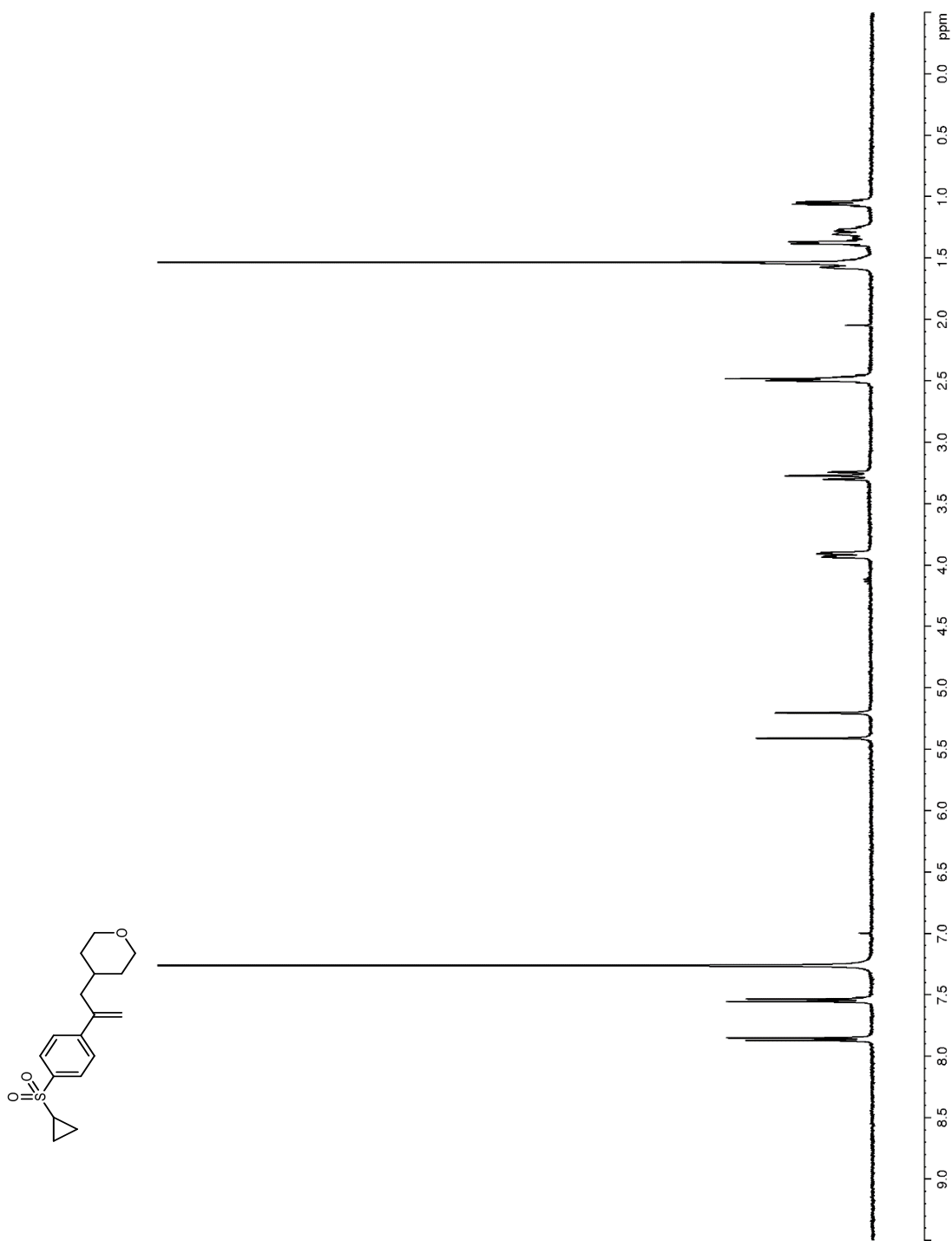


Figure 190. ^{13}C NMR (100 MHz, CDCl_3) of **28**

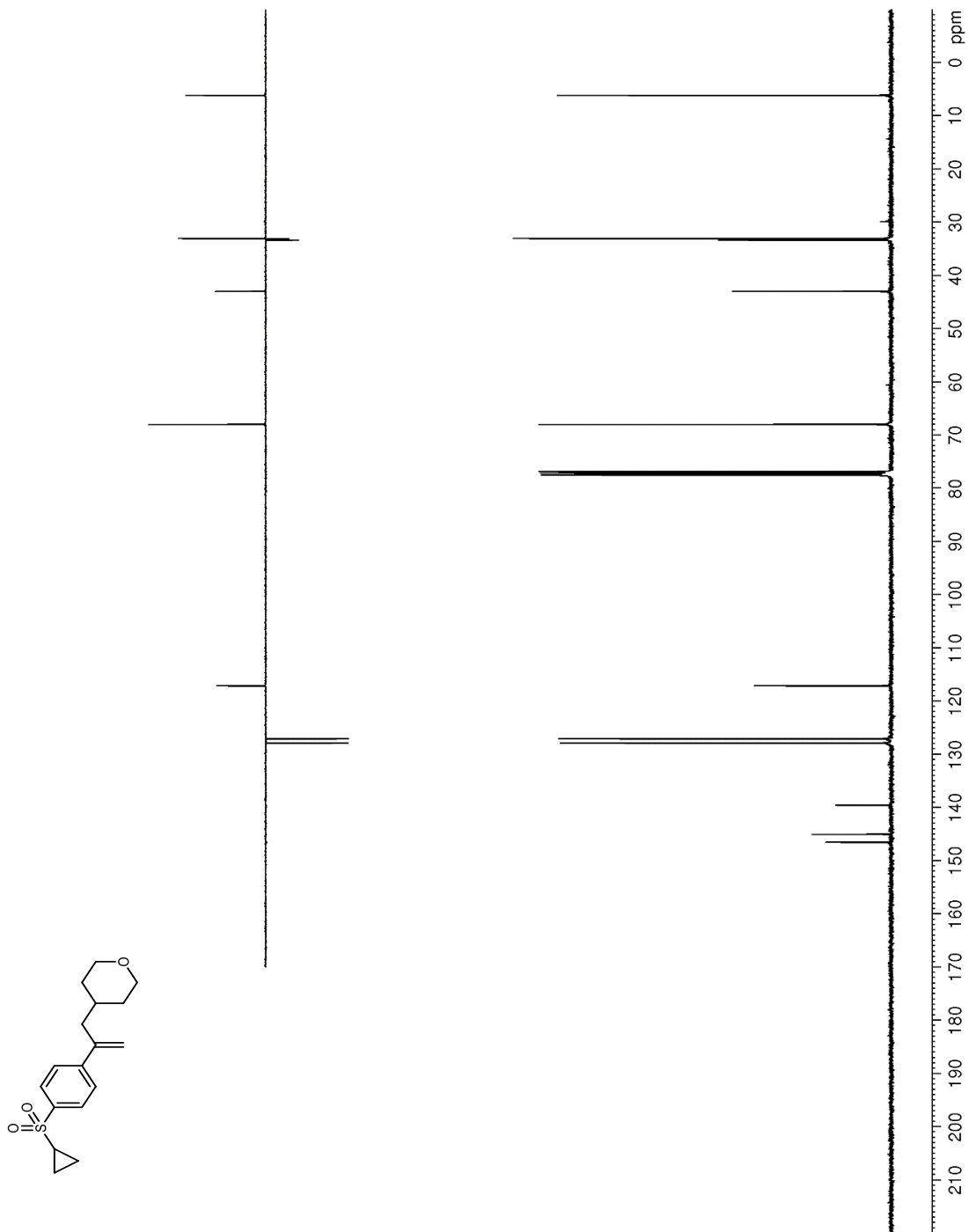


Figure 191. ^1H NMR (400 MHz, CDCl_3) of **28**

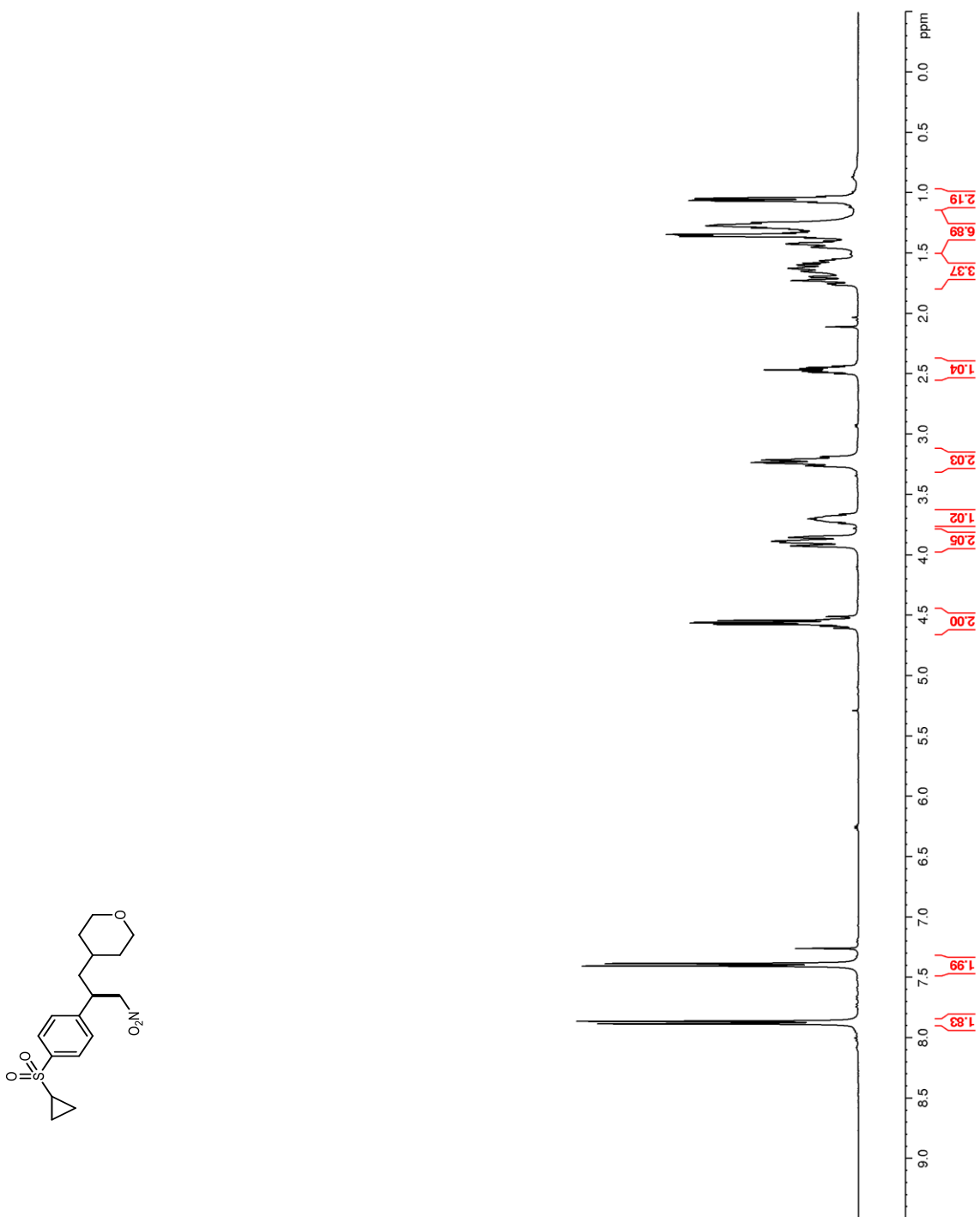


Figure 192. ^{13}C NMR (100 MHz, CDCl_3) of **28**

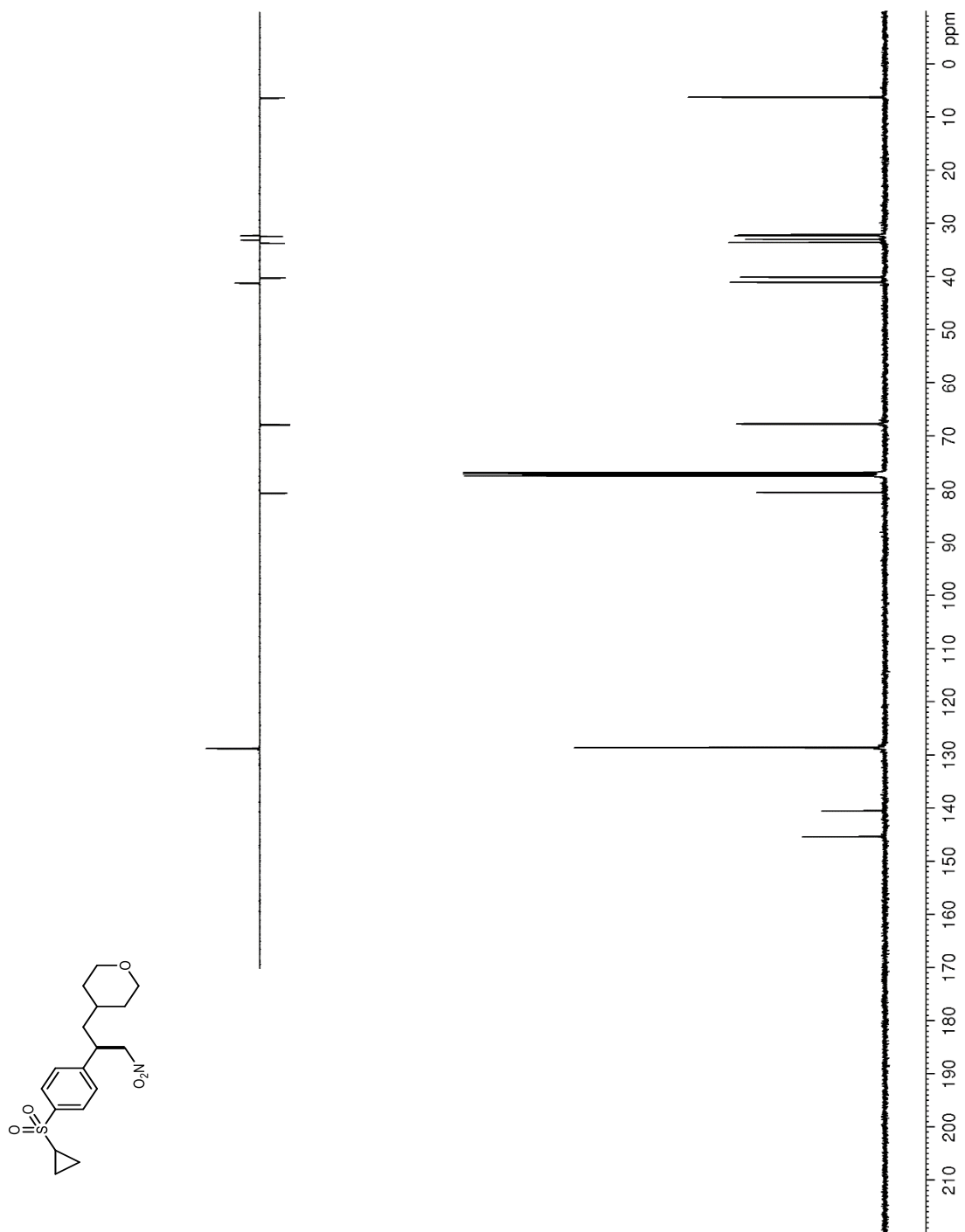


Figure 193. ^1H NMR (600 MHz, CDCl_3) of **29**

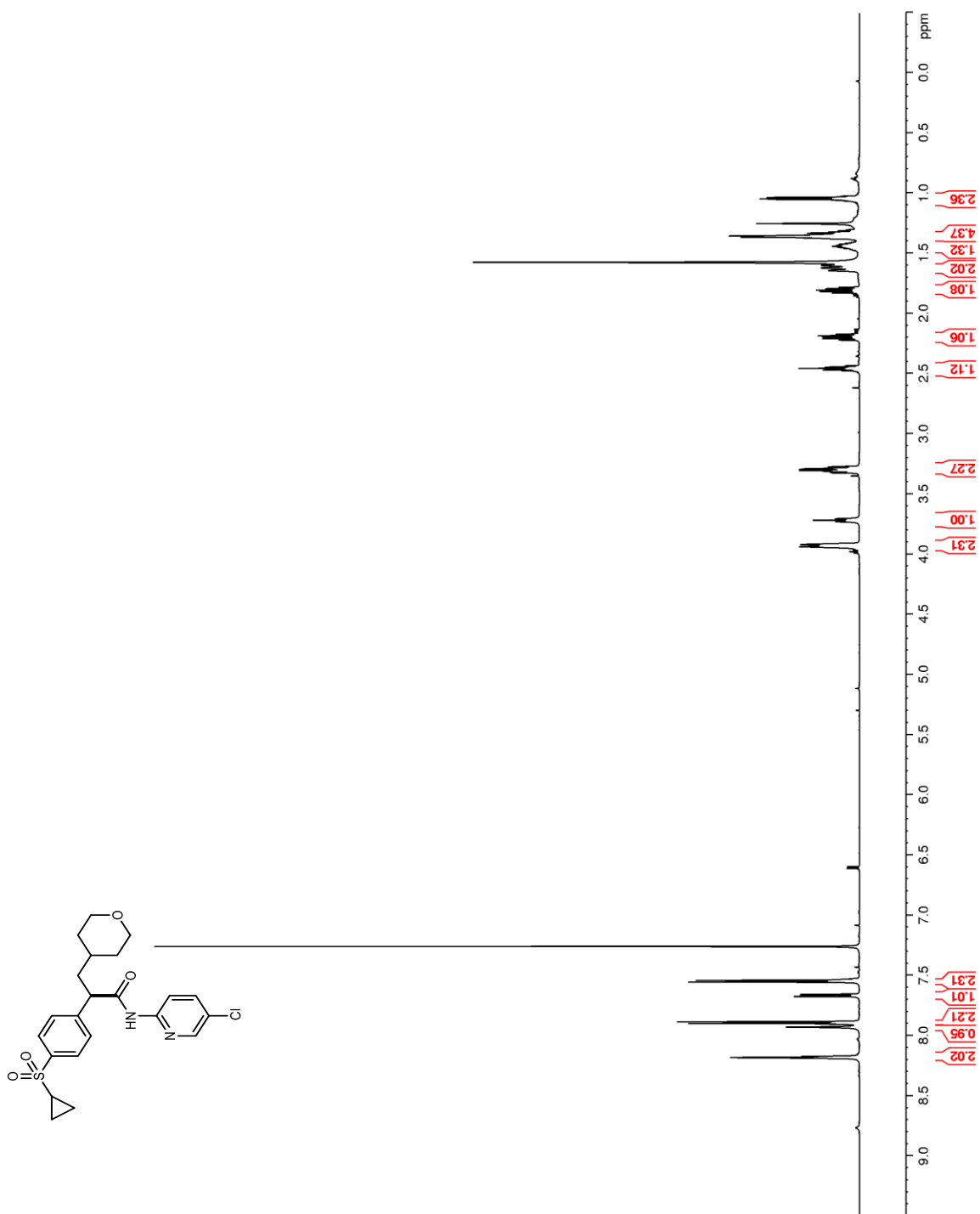


Figure 194. ^{13}C NMR (150 MHz, CDCl_3) of **29**

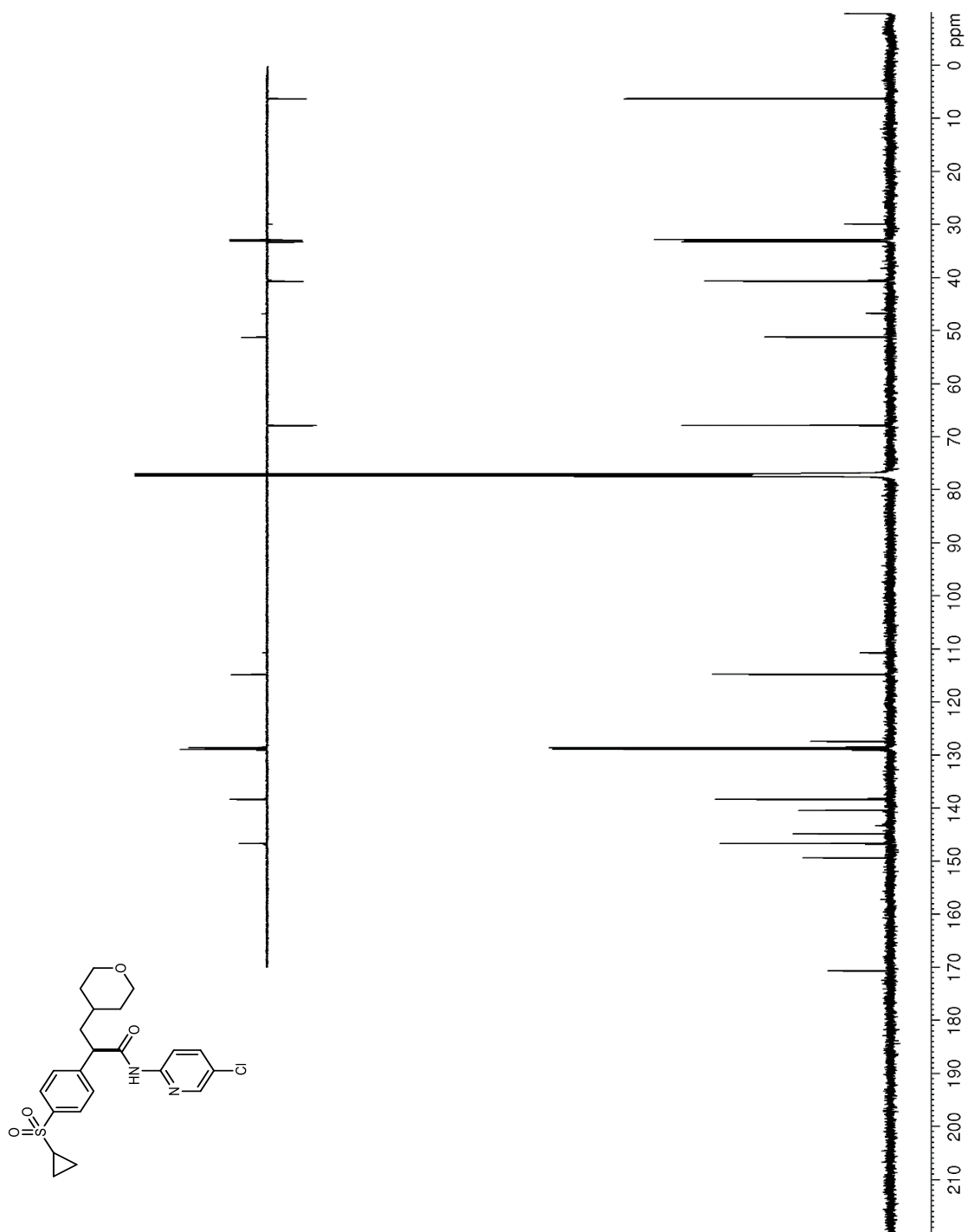


Figure 195. ^1H NMR (600 MHz, CDCl_3) of **29**

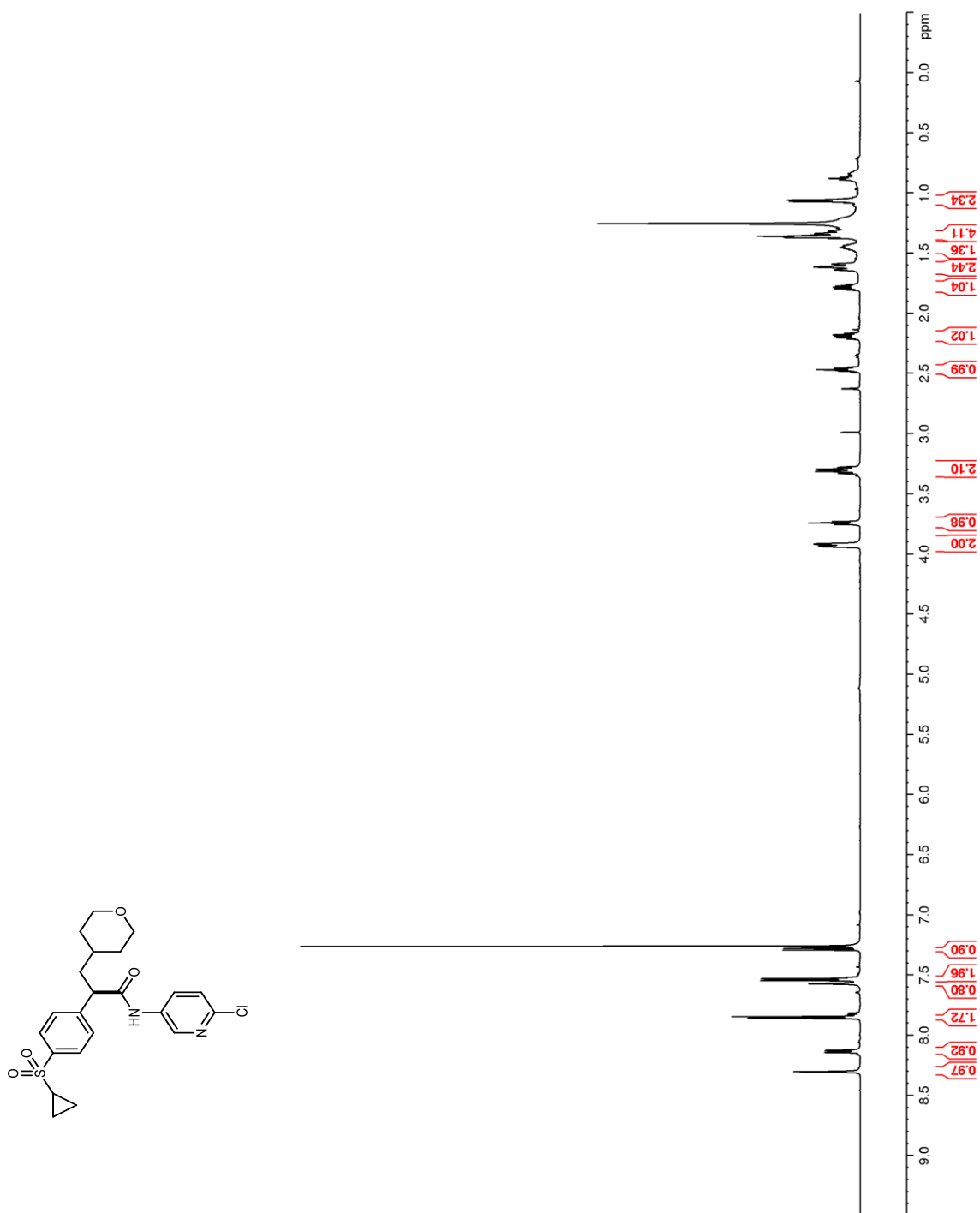


Figure 196. ^{13}C NMR (150 MHz, CDCl_3) of **29**

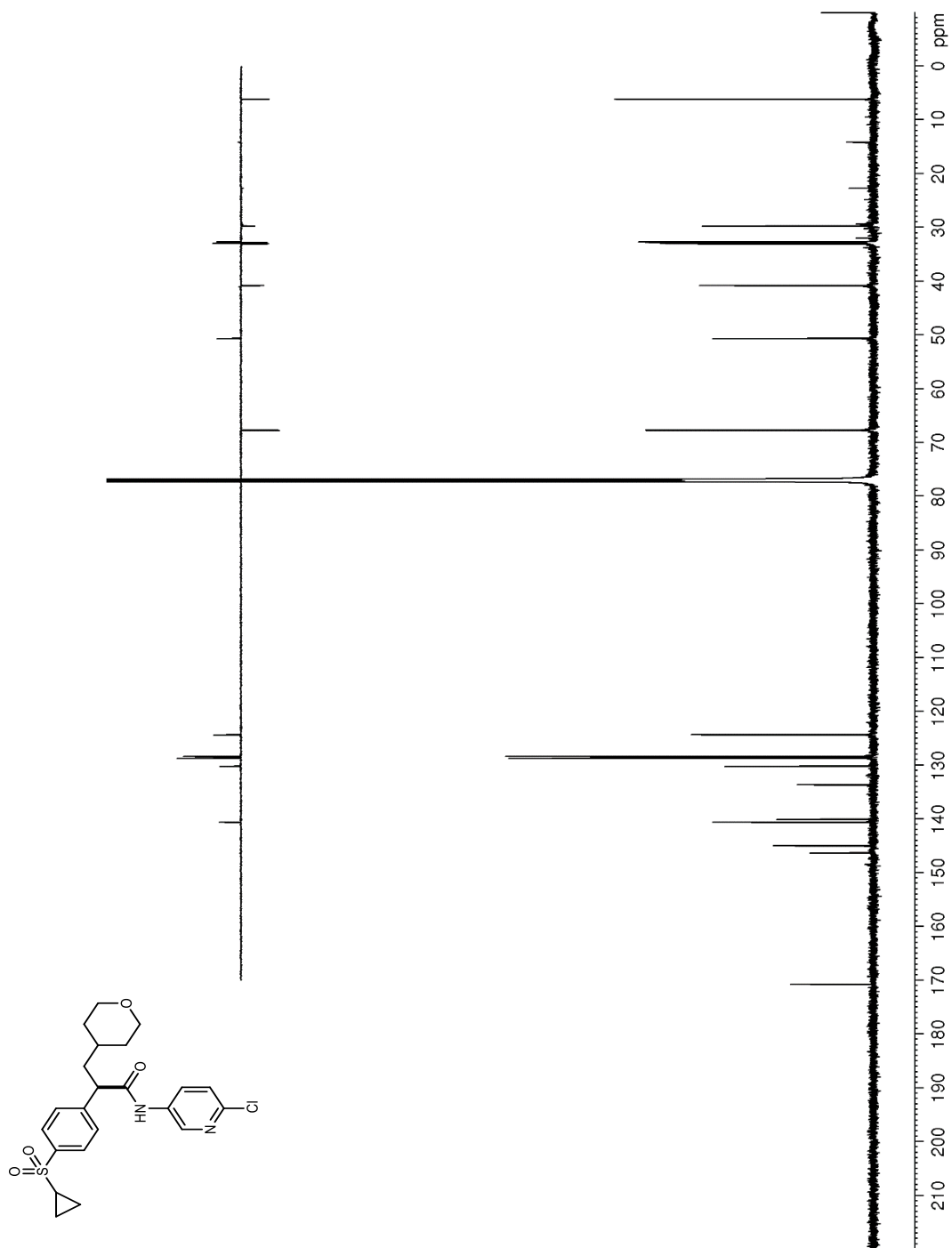


Figure 197. ^1H NMR (600 MHz, CDCl_3) of **29**

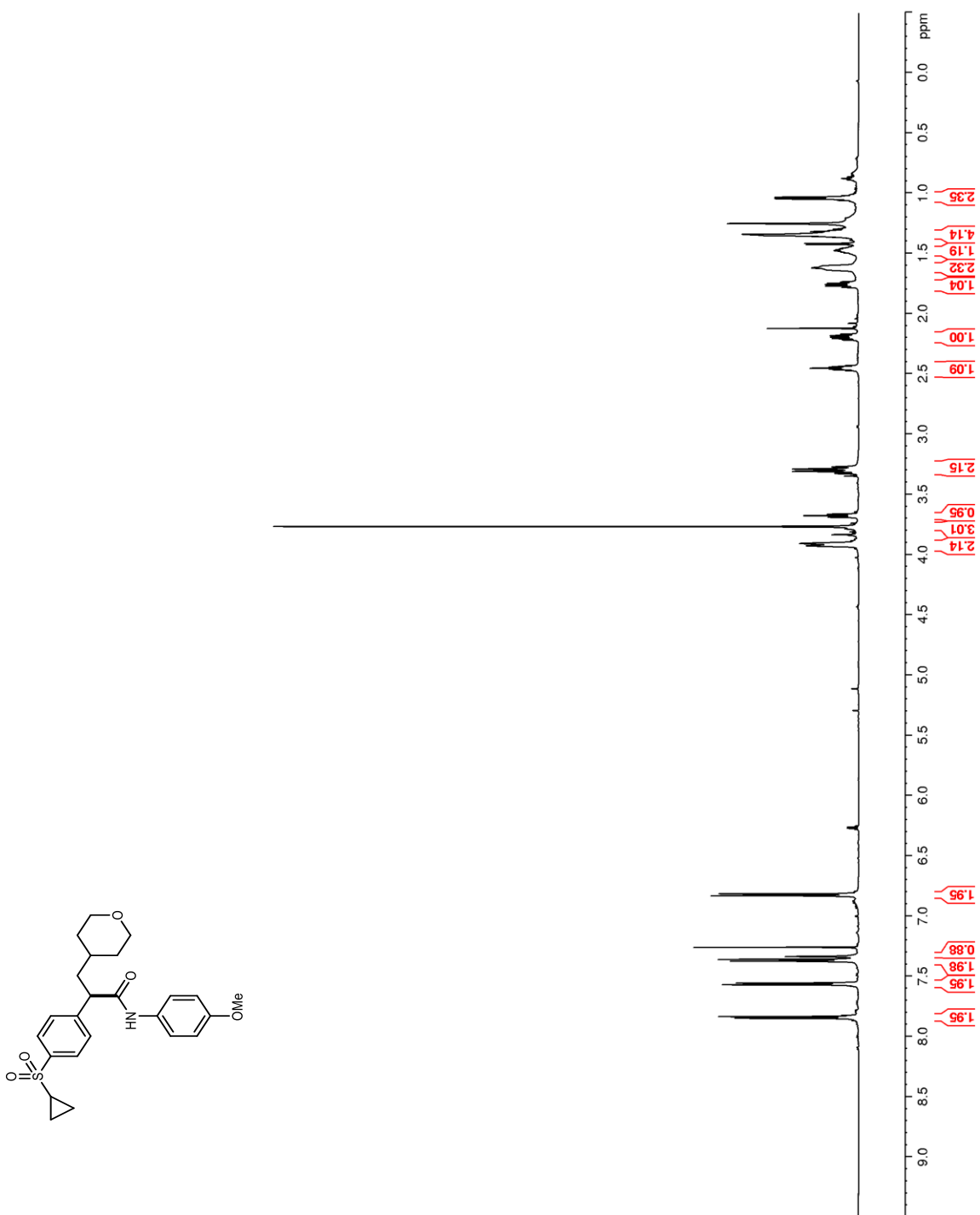


Figure 198. ^{13}C NMR (150 MHz, CDCl_3) of **29**

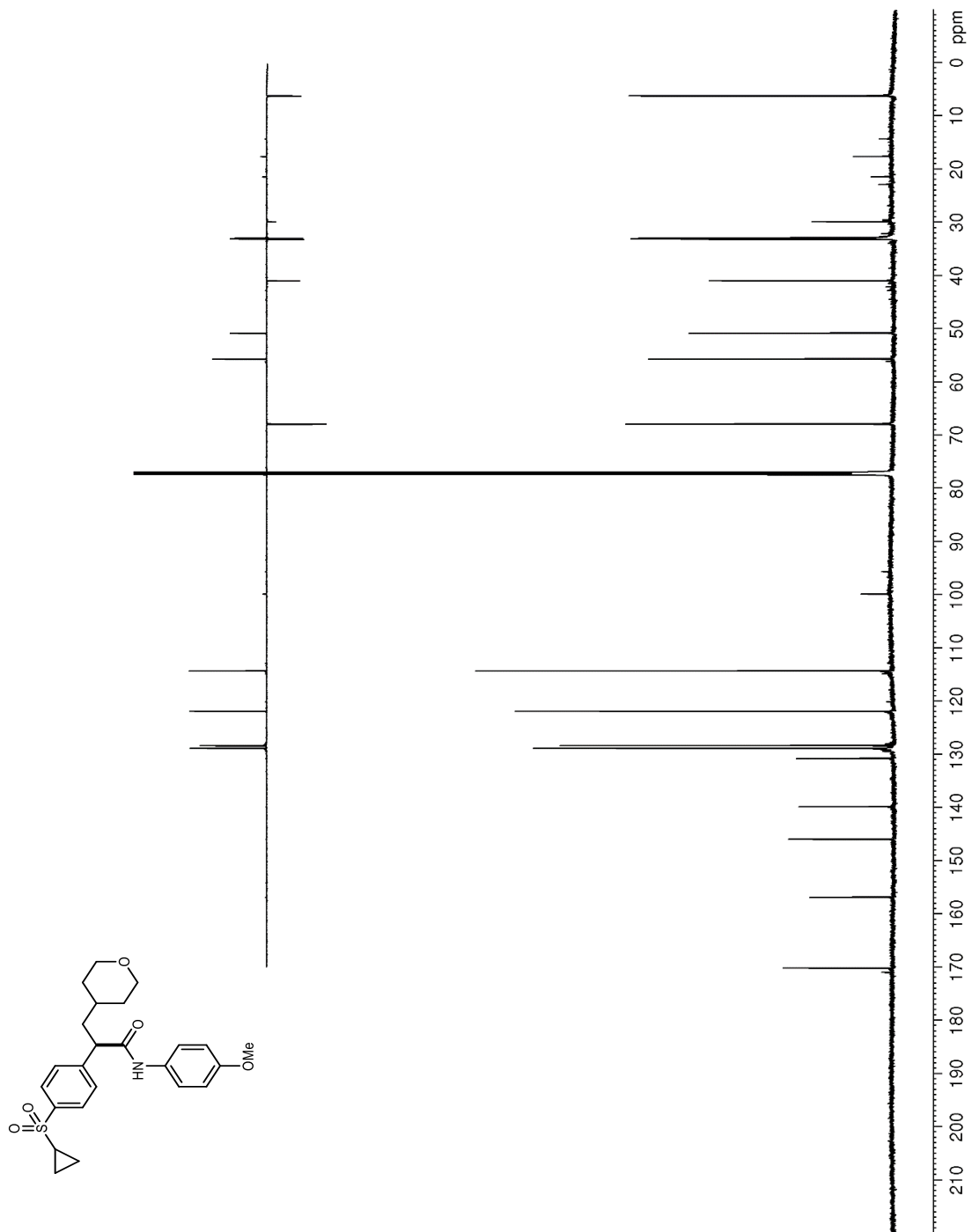


Figure 199. ^1H NMR (400 MHz, CDCl_3) of **S1**

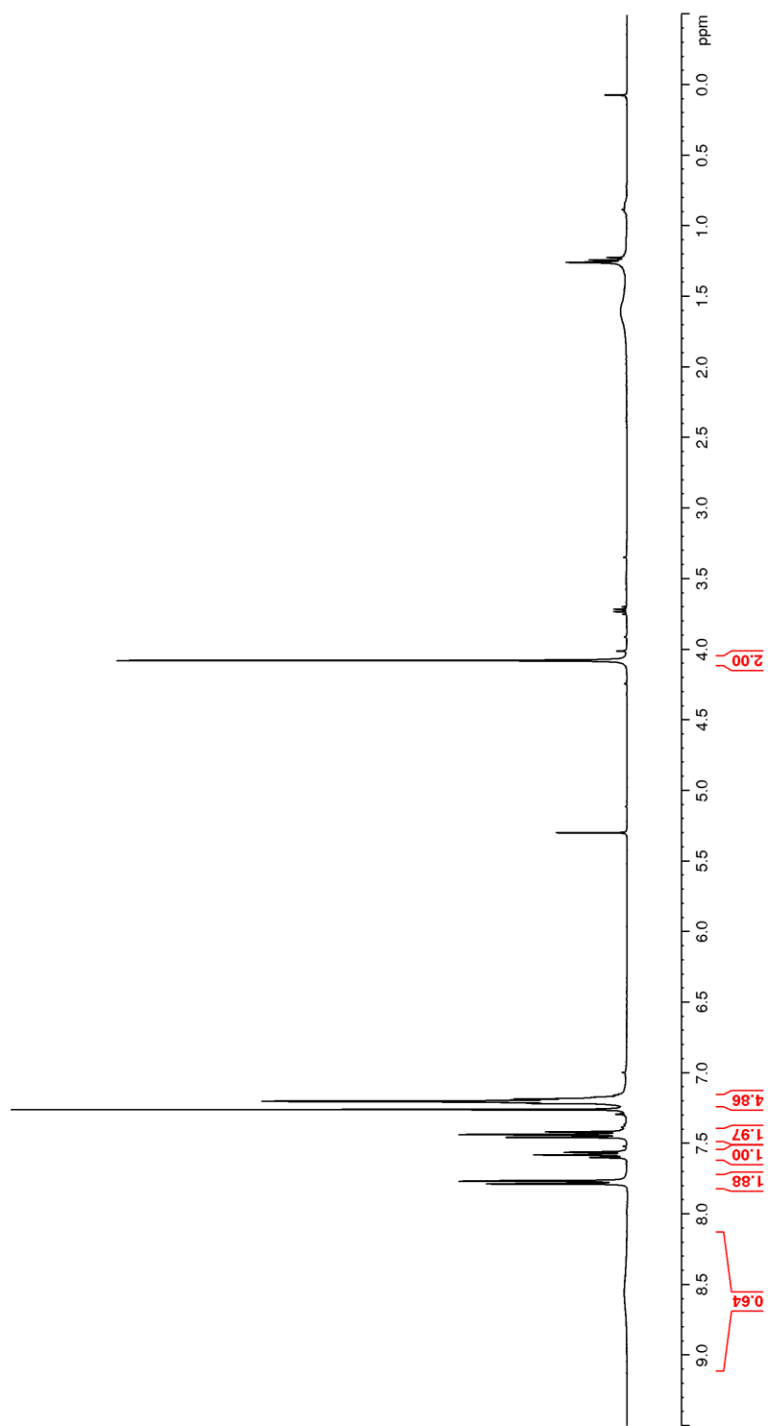
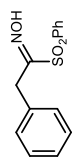


Figure 200. ^{13}C NMR (100 MHz, CDCl_3) of **S1**

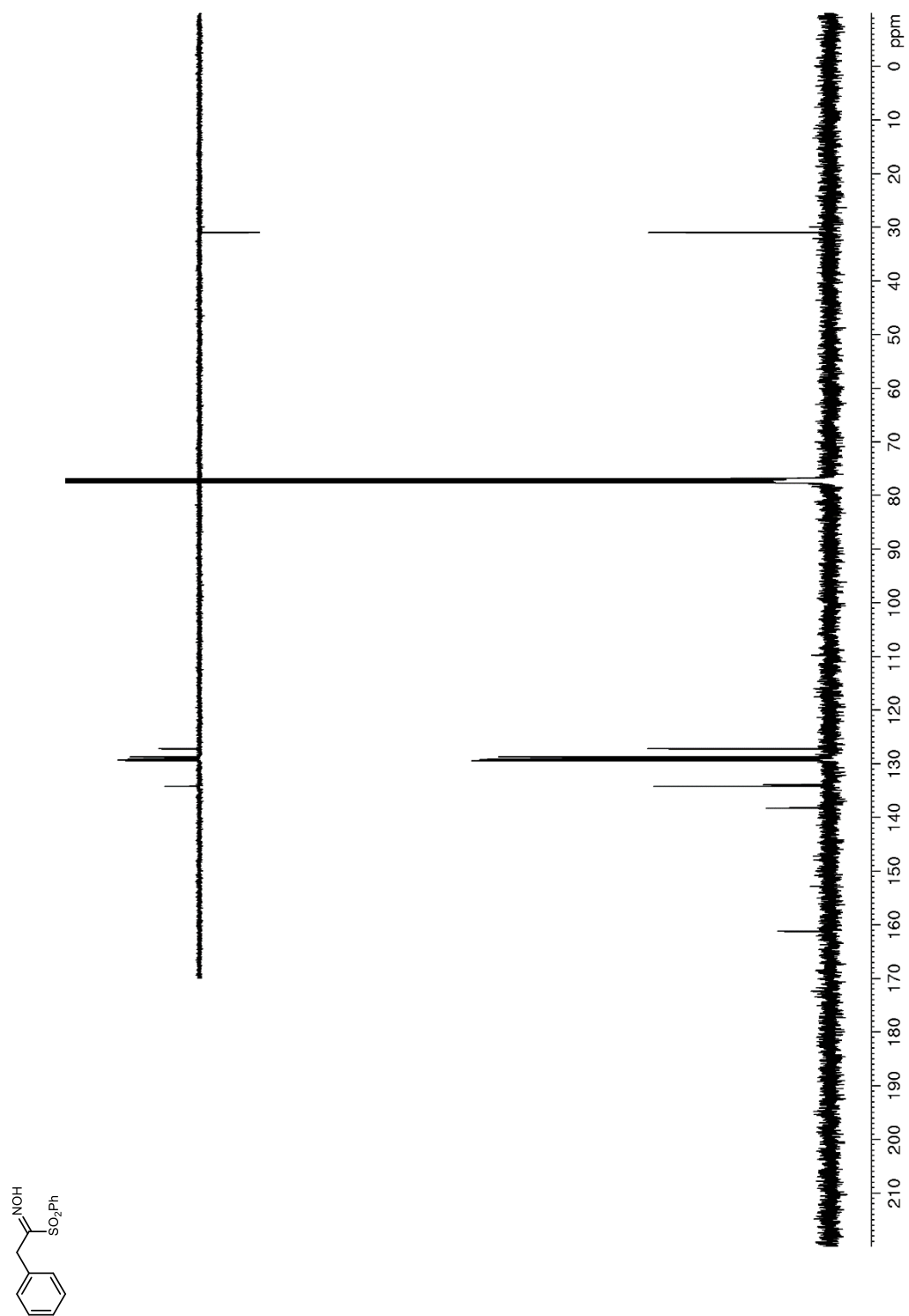


Figure 201. ^1H NMR (400 MHz, CDCl_3) of **S2**

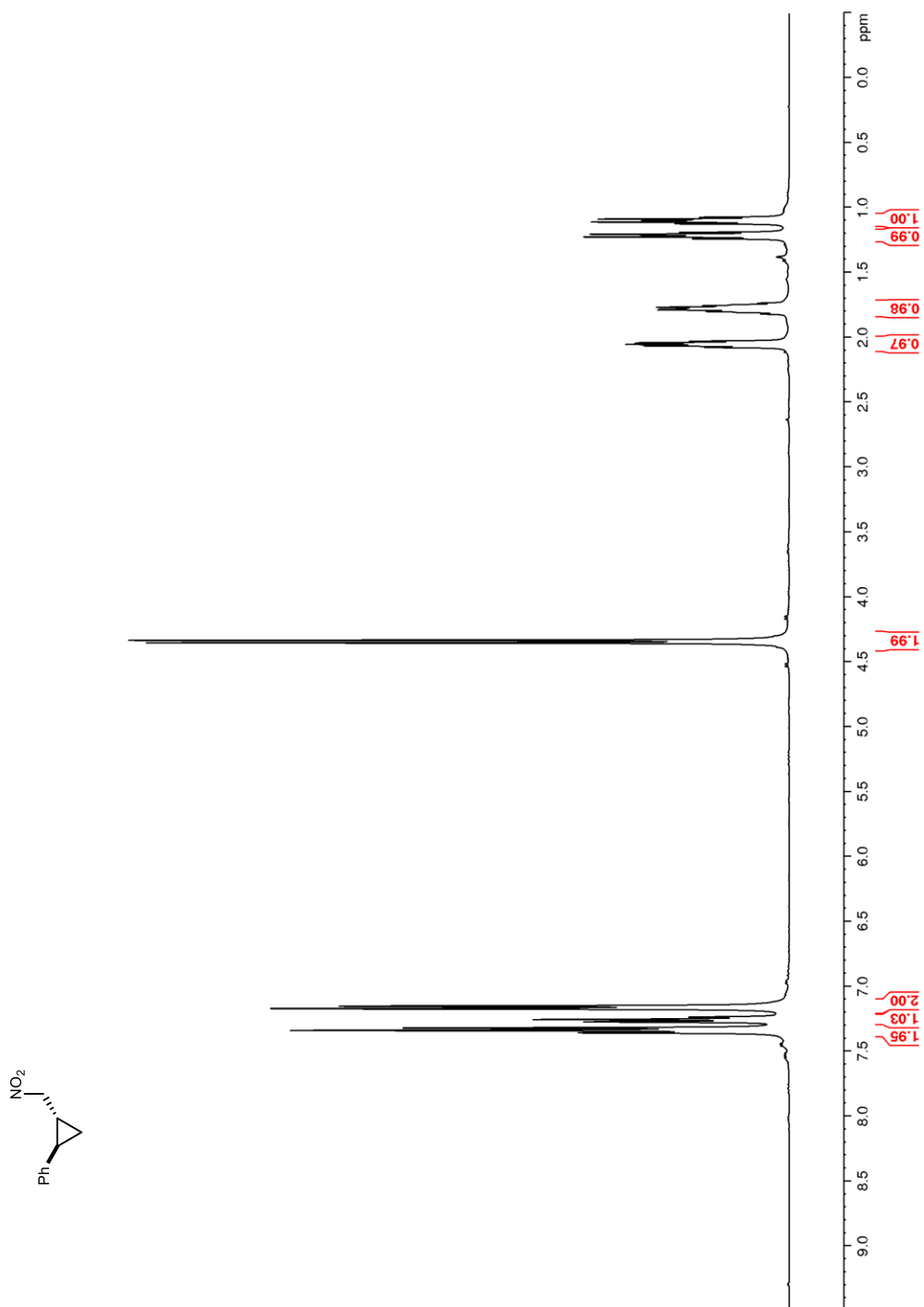


Figure 202. ^{13}C NMR (100 MHz, CDCl_3) of **S2**

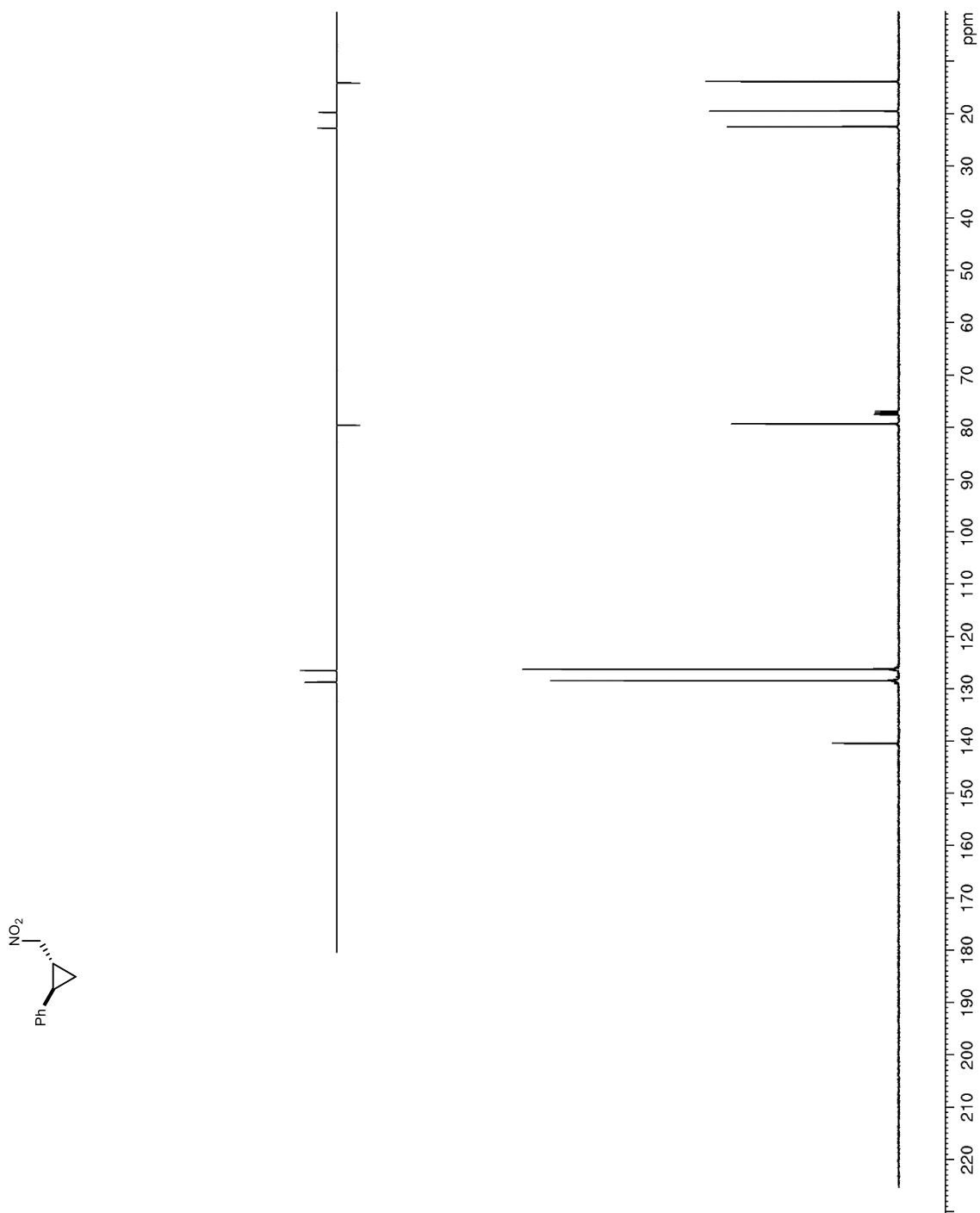


Figure 203. ^1H NMR (400 MHz, CDCl_3) of **S3**

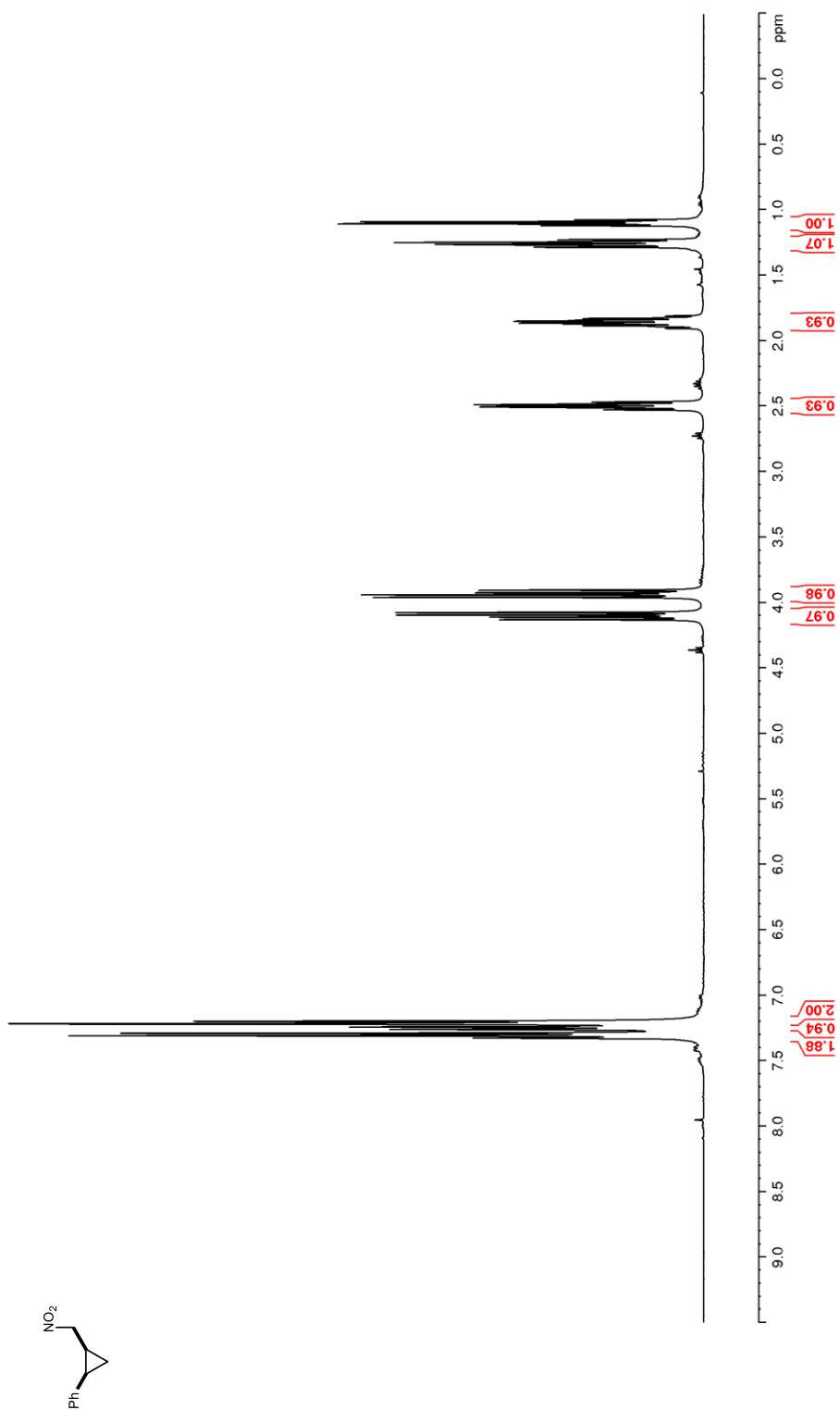


Figure 204. ^{13}C NMR (100 MHz, CDCl_3) of **S3**

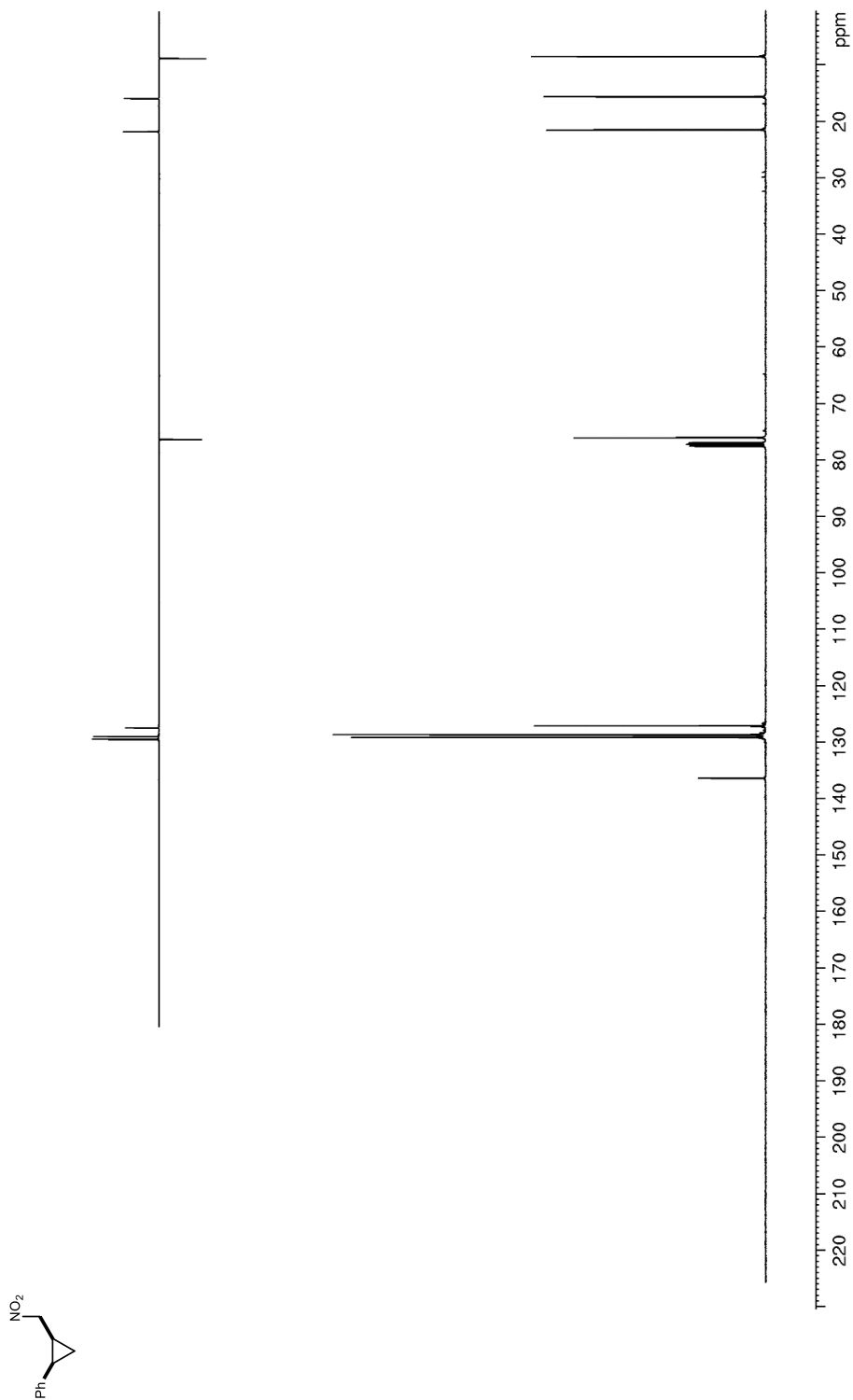


Figure 205. ^1H NMR (400 MHz, CDCl_3) of **S4**

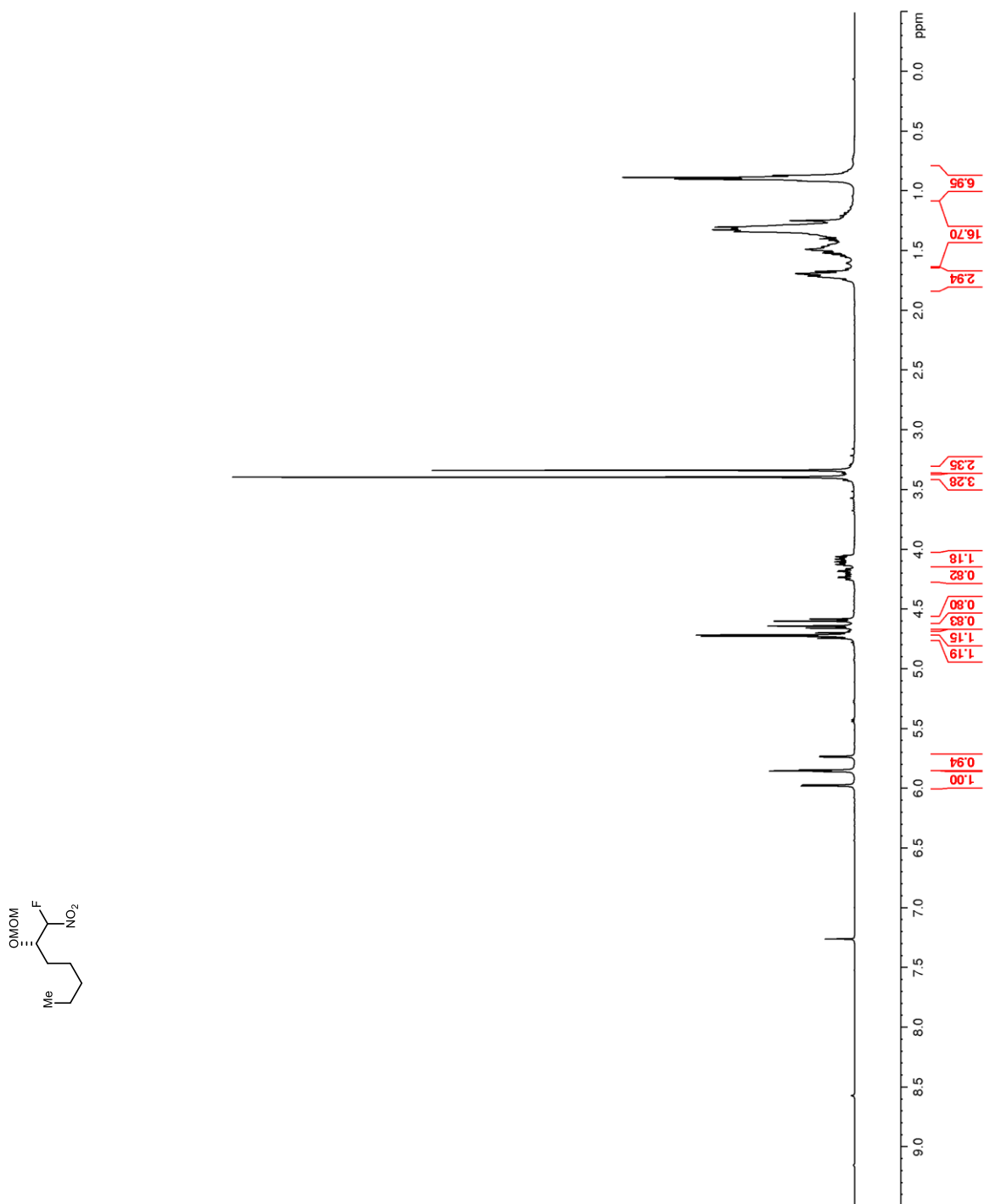


Figure 206. ^{13}C NMR (100 MHz, CDCl_3) of **S4**

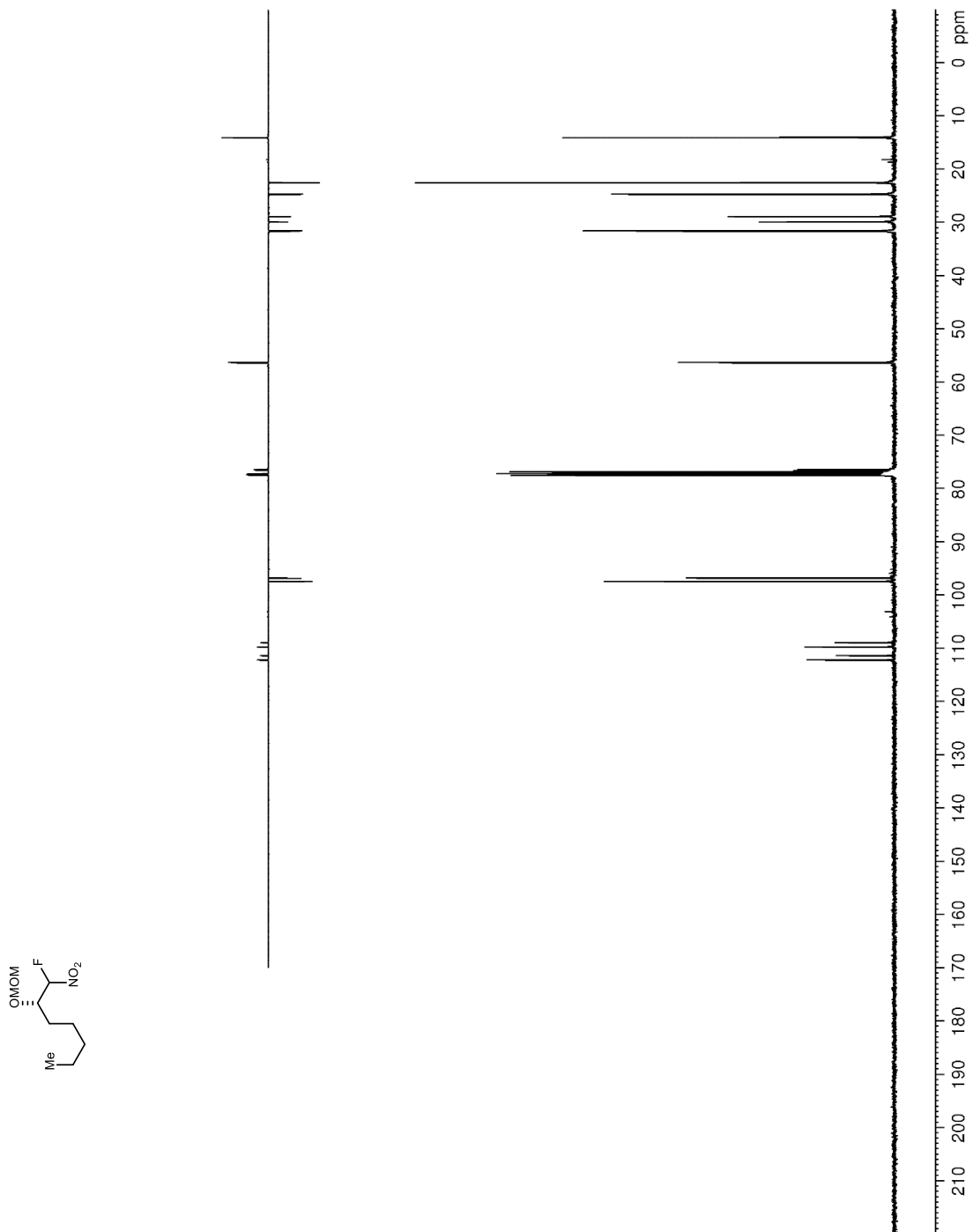


Figure 207. ^{19}F NMR (376 MHz, CDCl_3) of **S4**

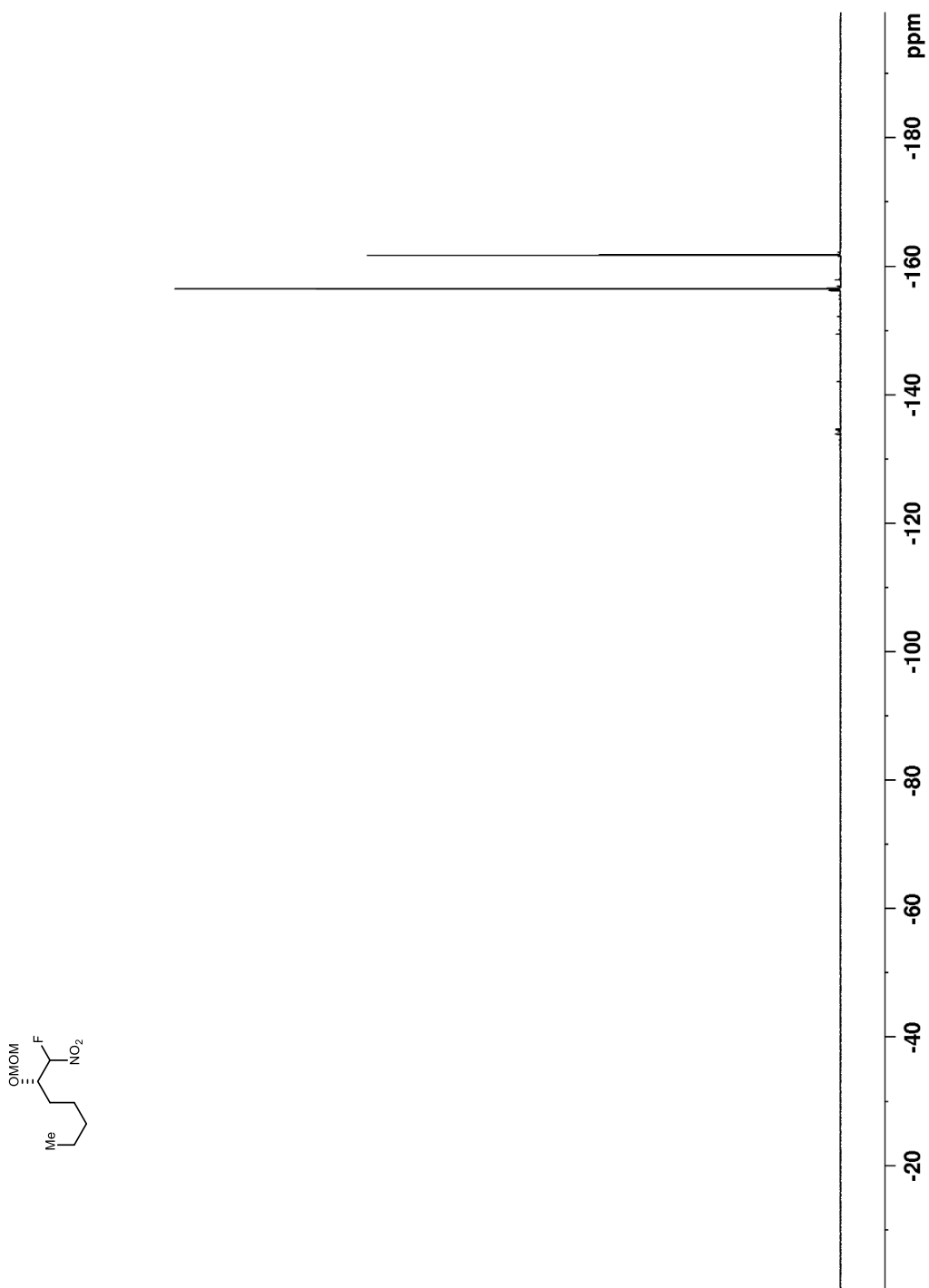


Figure 208. ^1H NMR (400 MHz, CDCl_3) of **S5**

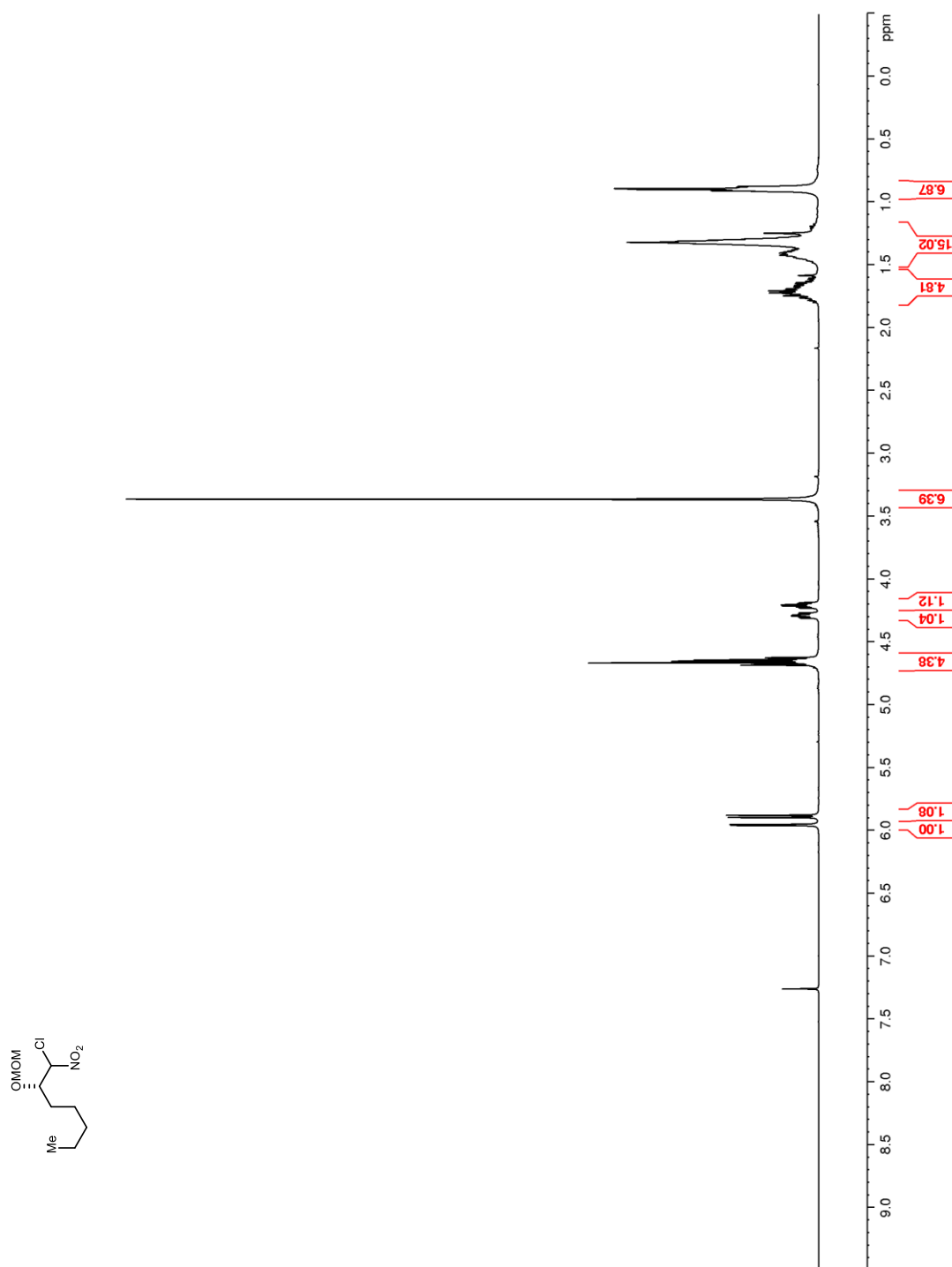


Figure 209. ^{13}C NMR (100 MHz, CDCl_3) of **S5**

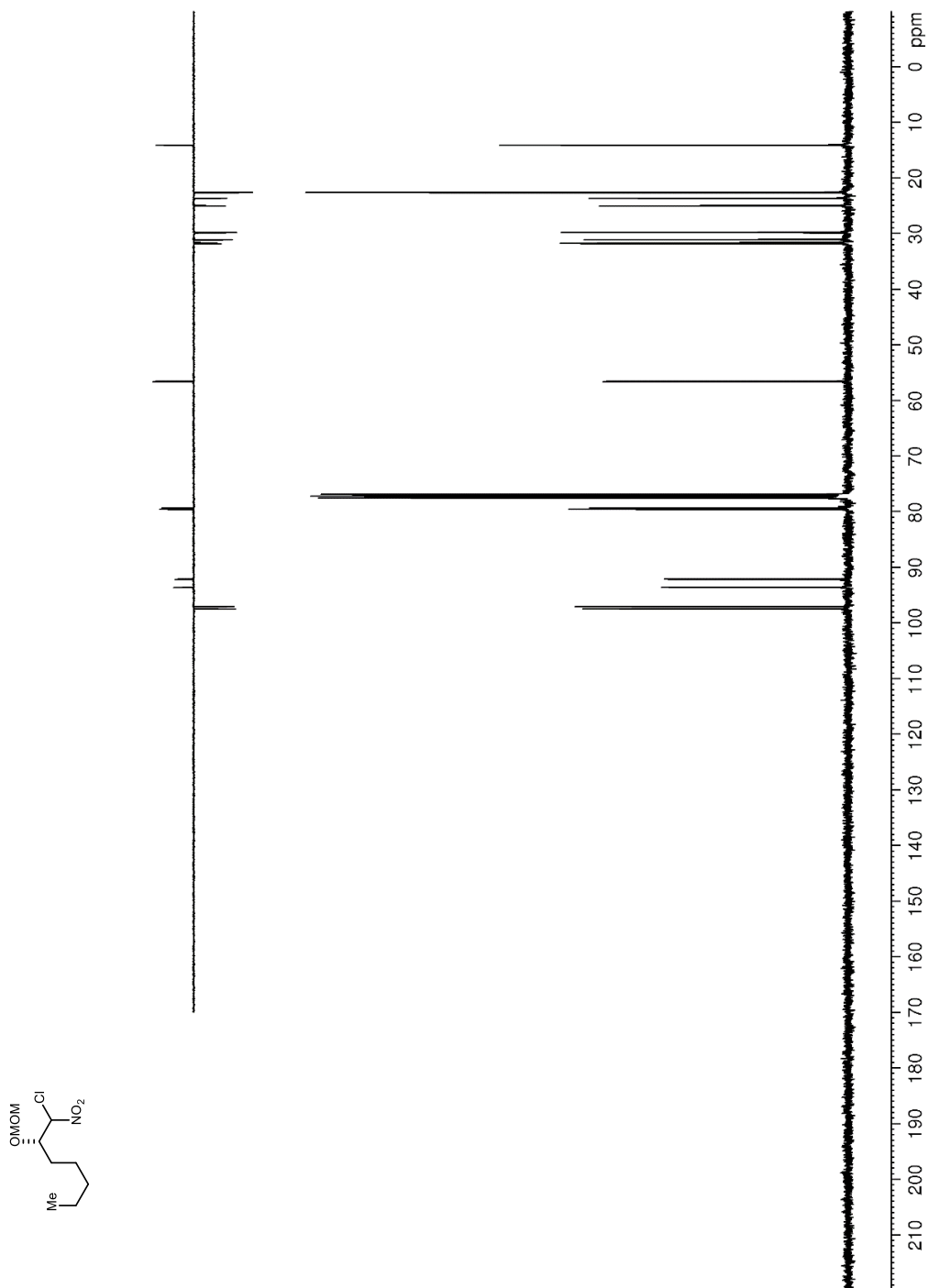


Figure 210. ^1H NMR (600 MHz, CDCl_3) of **S6**

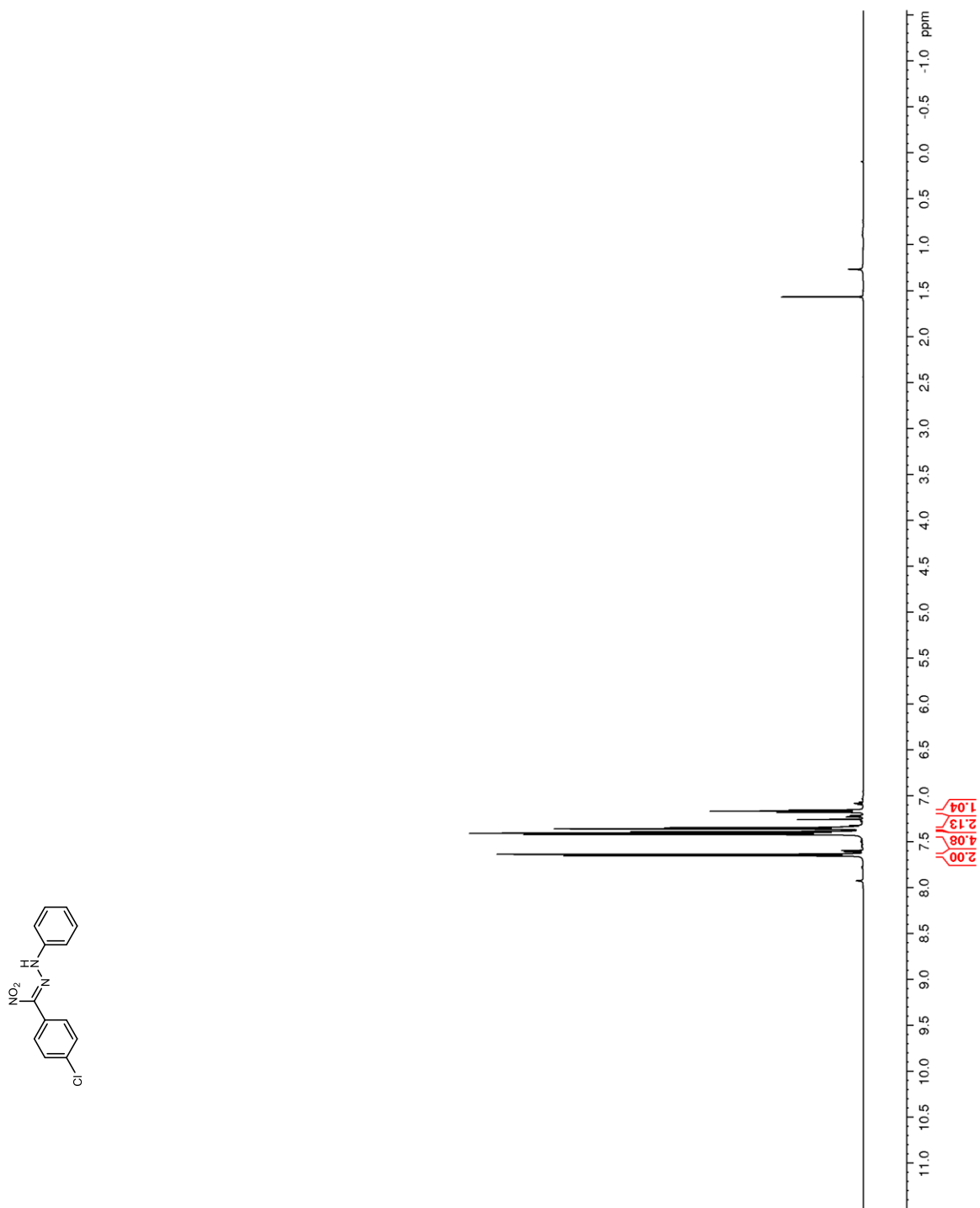


Figure 211. ^{13}C NMR (150 MHz, CDCl_3) of **S6**

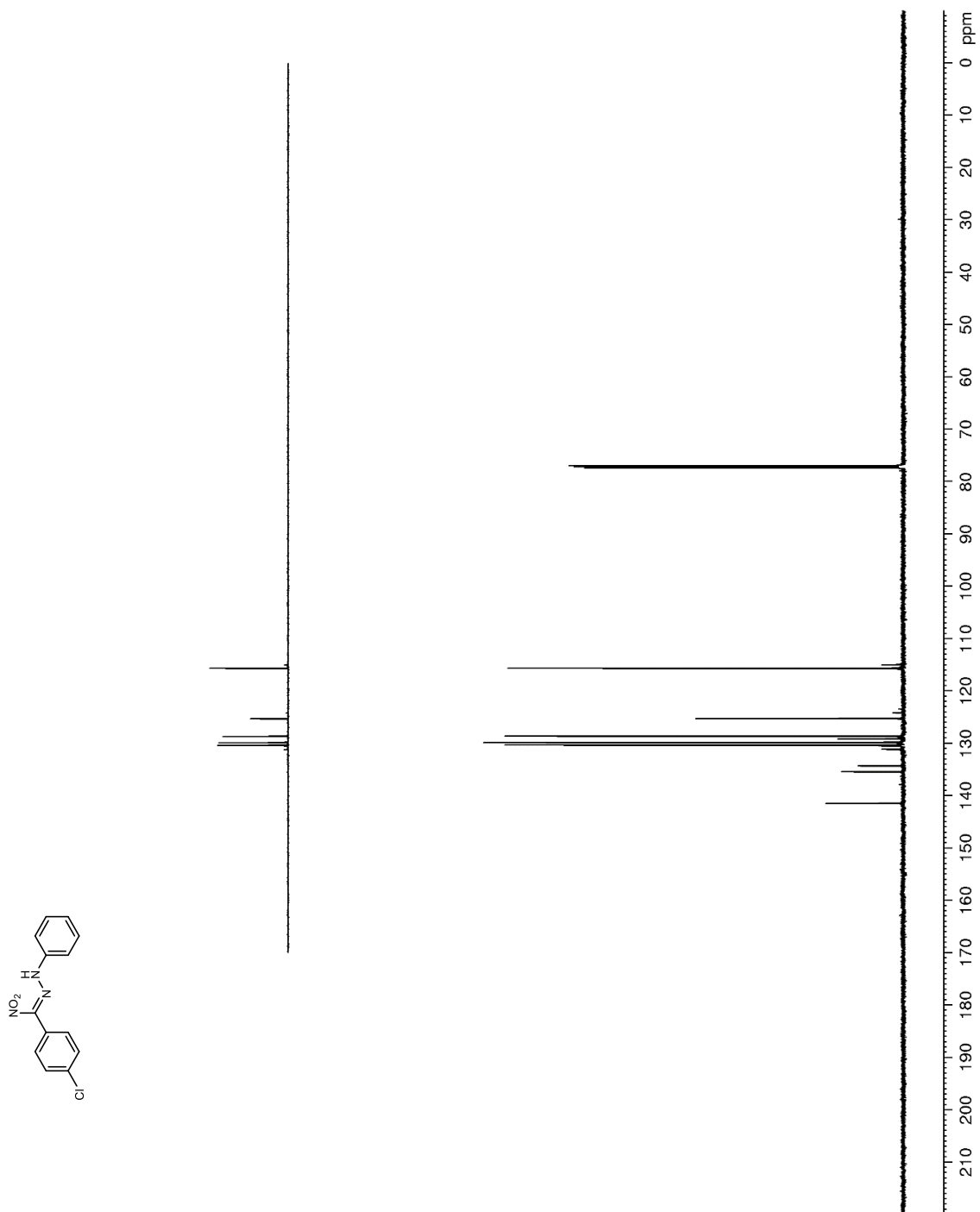


Figure 212. ^1H NMR (600 MHz, $\text{DMSO-}d_6$) of **S7**

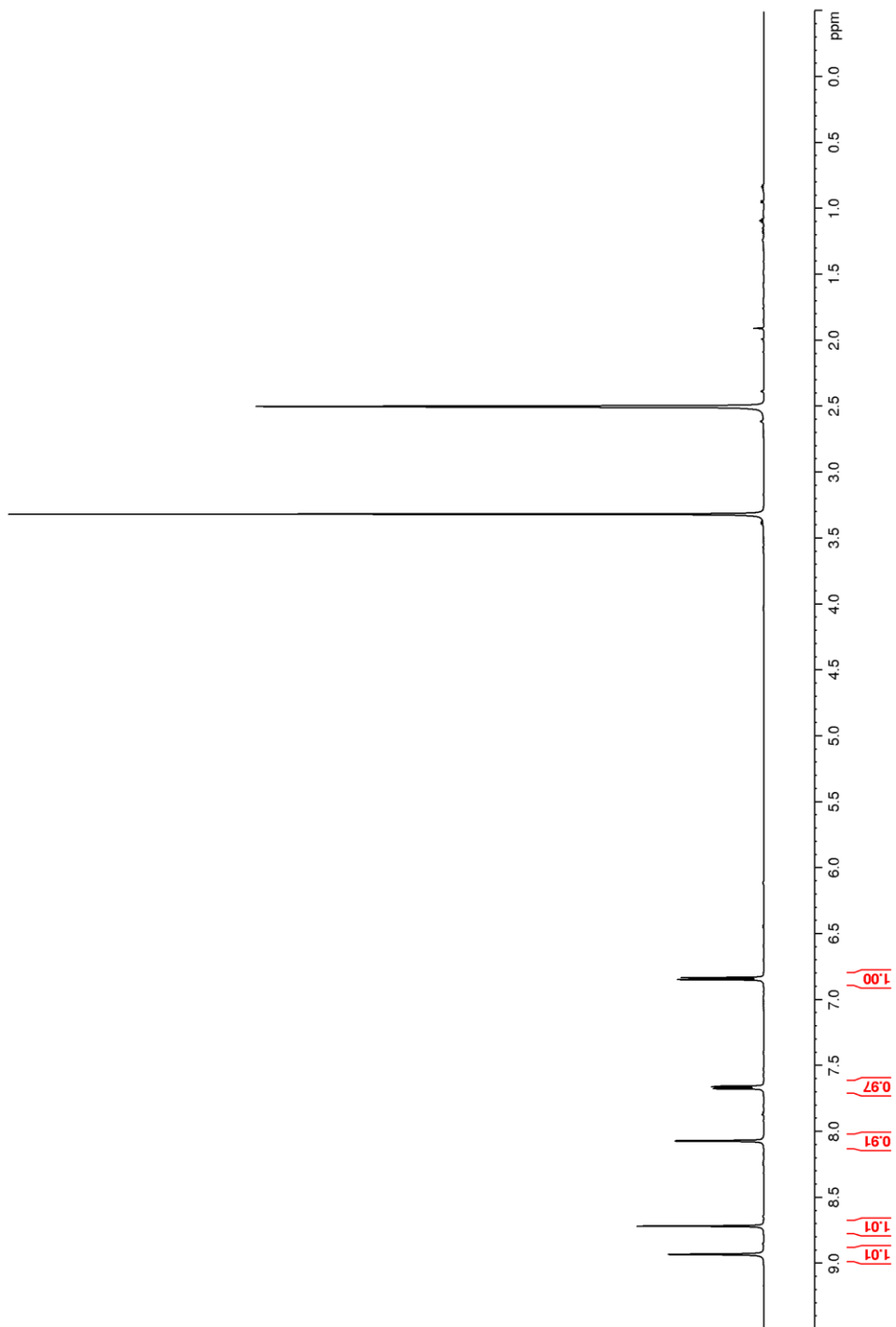
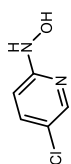


Figure 213. ^{13}C NMR (150 MHz, $\text{DMSO-}d_6$) of **S7**

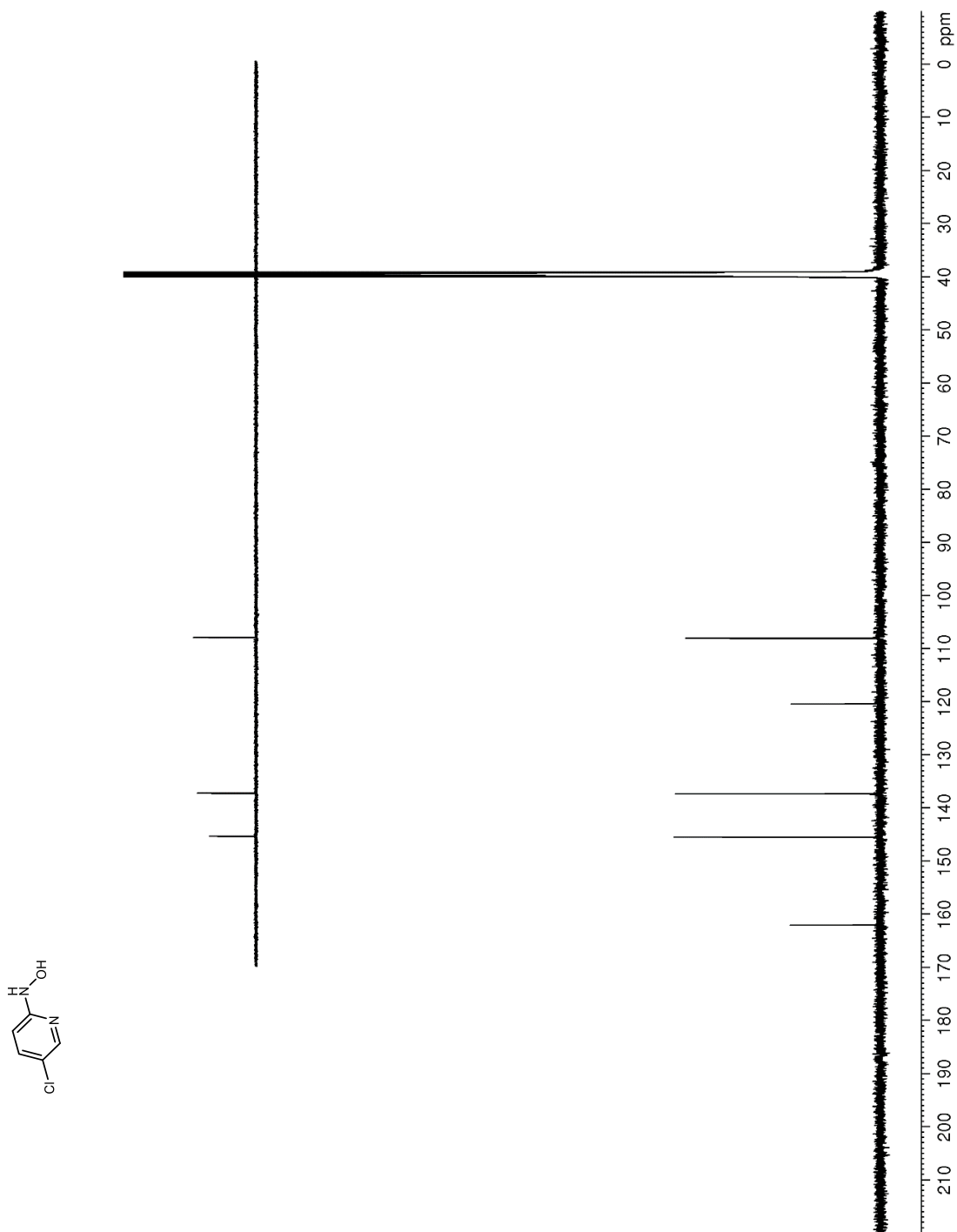


Figure 214. ^1H NMR (400 MHz, DMSO-d_6) of Conversion of **85a** in degassed solvent; t = 0, 15, 60, 180, 240 minutes (bottom to top)

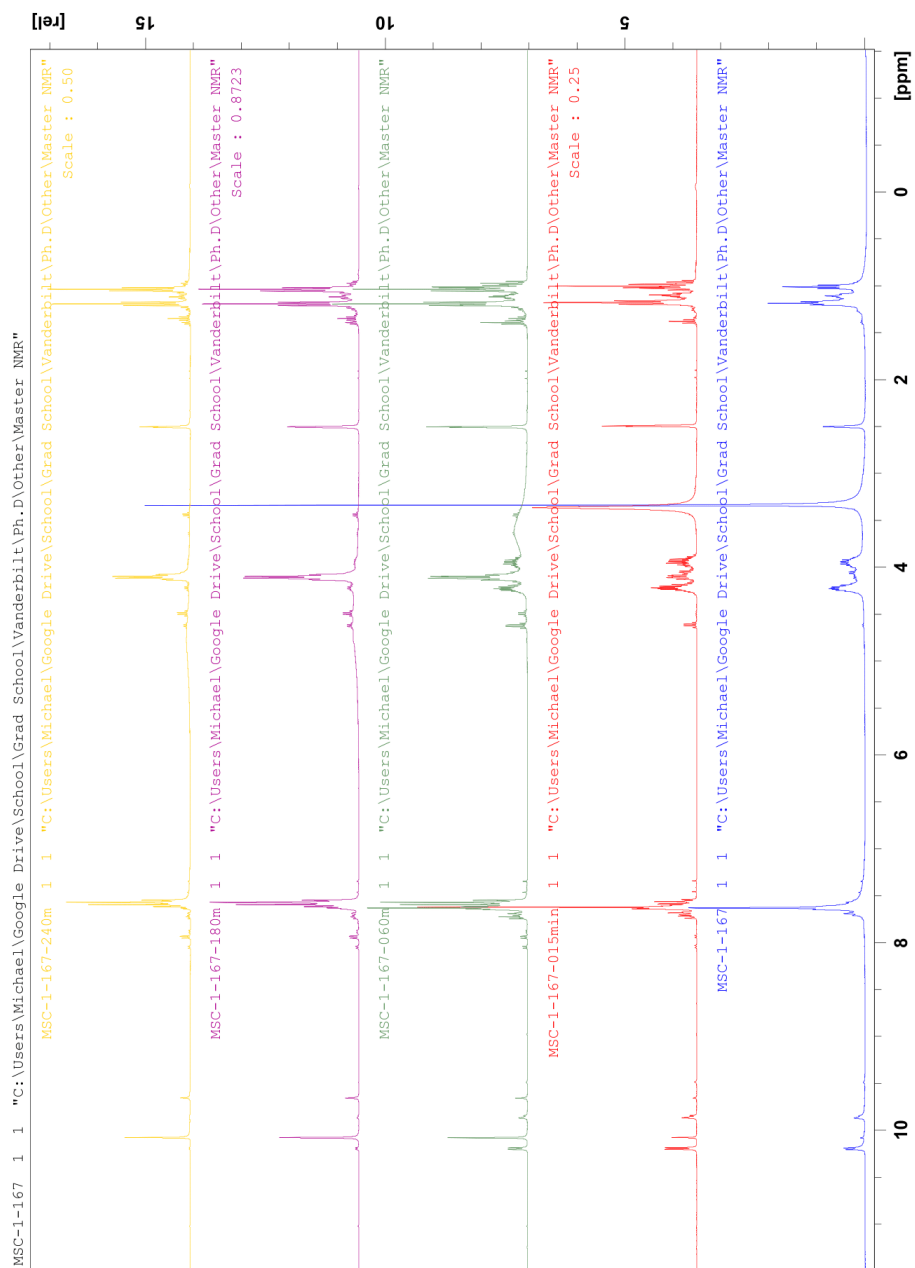


Figure 215. ^1H NMR (400 MHz, DMSO-d_6) of Conversion of **85b** in degassed solvent; $t = 0, 15, 60, 120$ minutes (bottom to top)

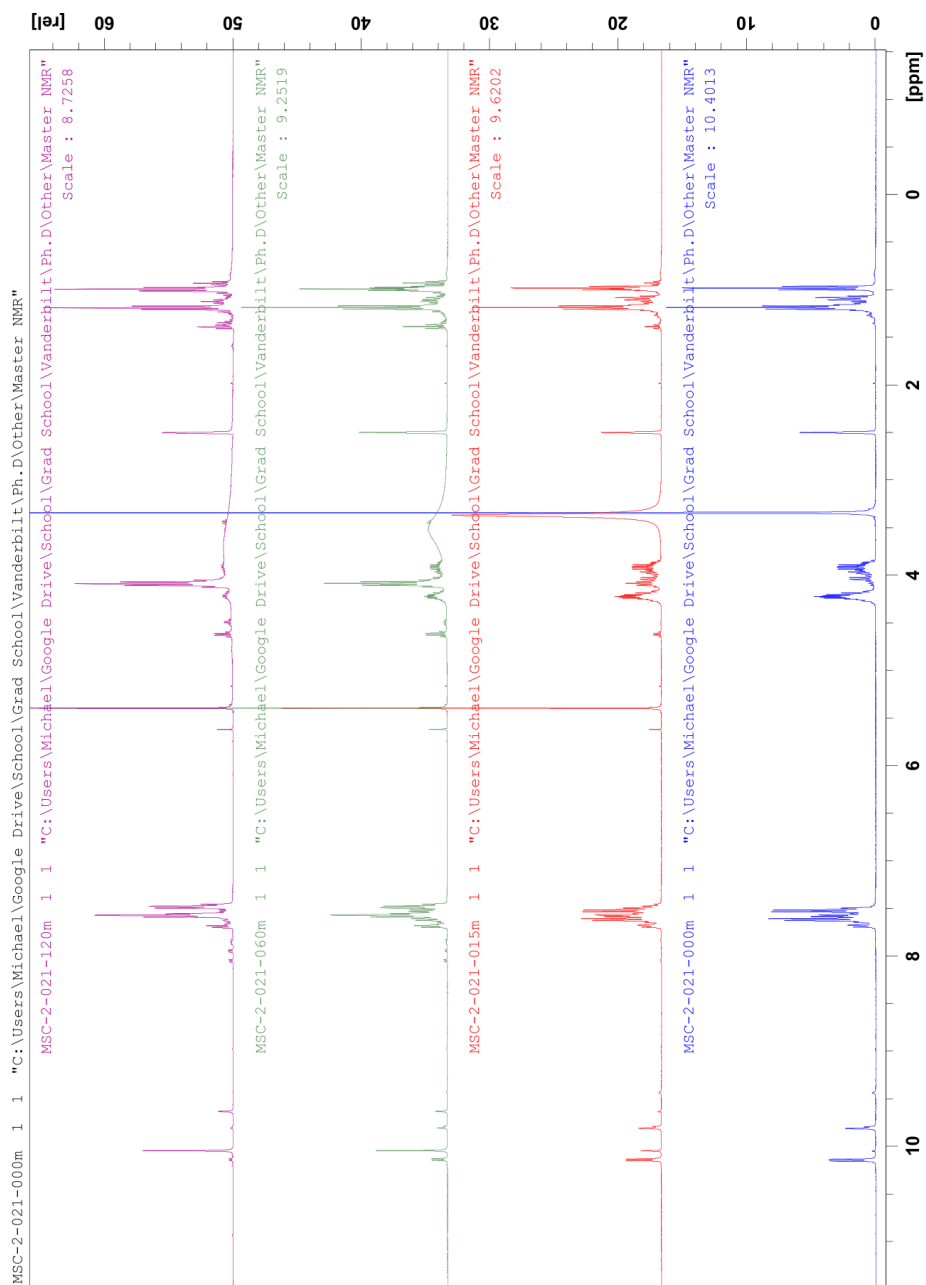


Figure 216. ^1H NMR (400 MHz, DMSO-d_6) of Conversion of **85c** in dry degassed solvent; $t = 0, 15, 60, 150$ minutes (bottom to top)

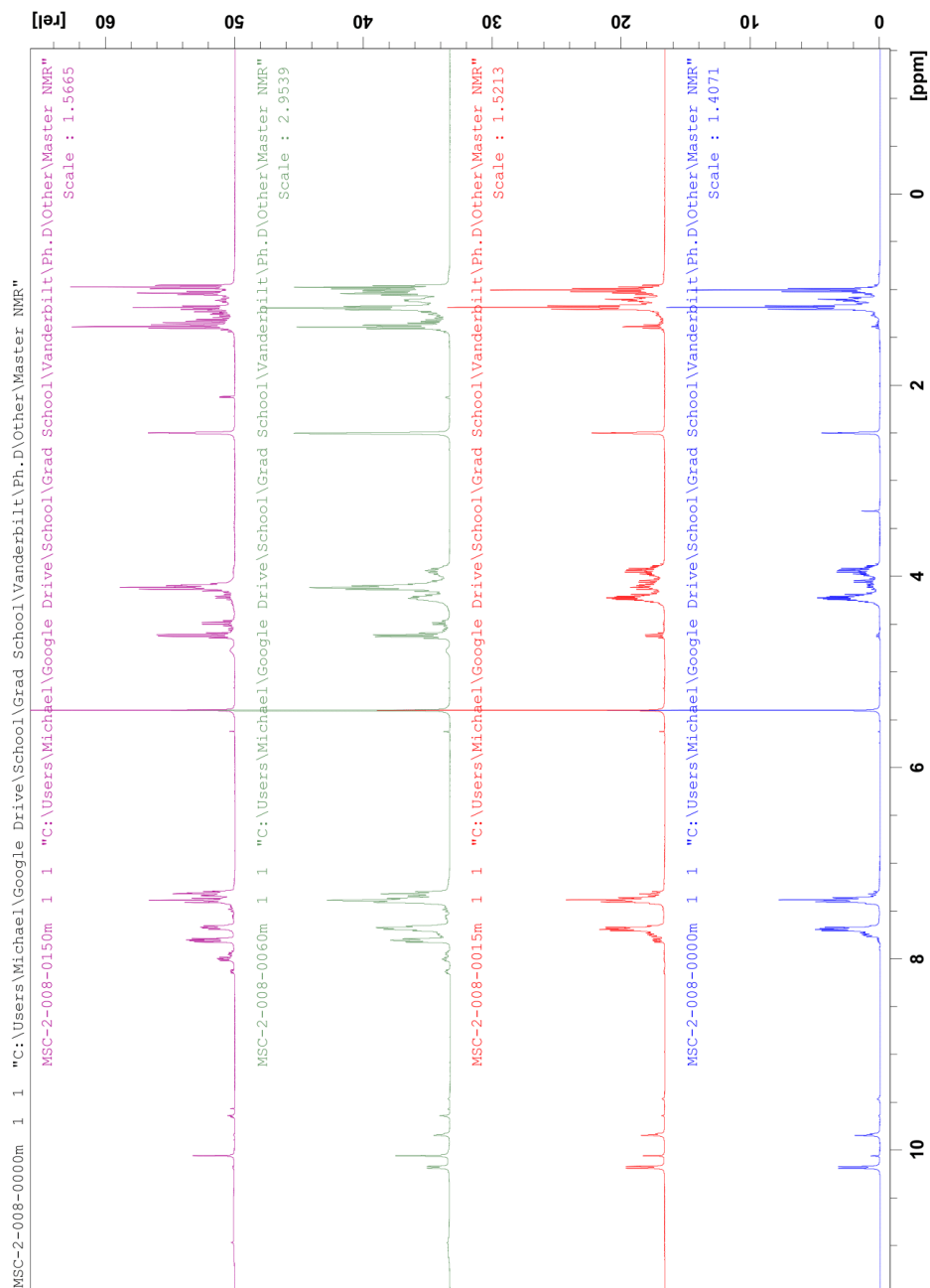


Figure 217. ^1H NMR (400 MHz, DMSO-d_6) of Conversion of **85c** in degassed solvent; t = 0, 15, 60, 150 minutes (bottom to top)

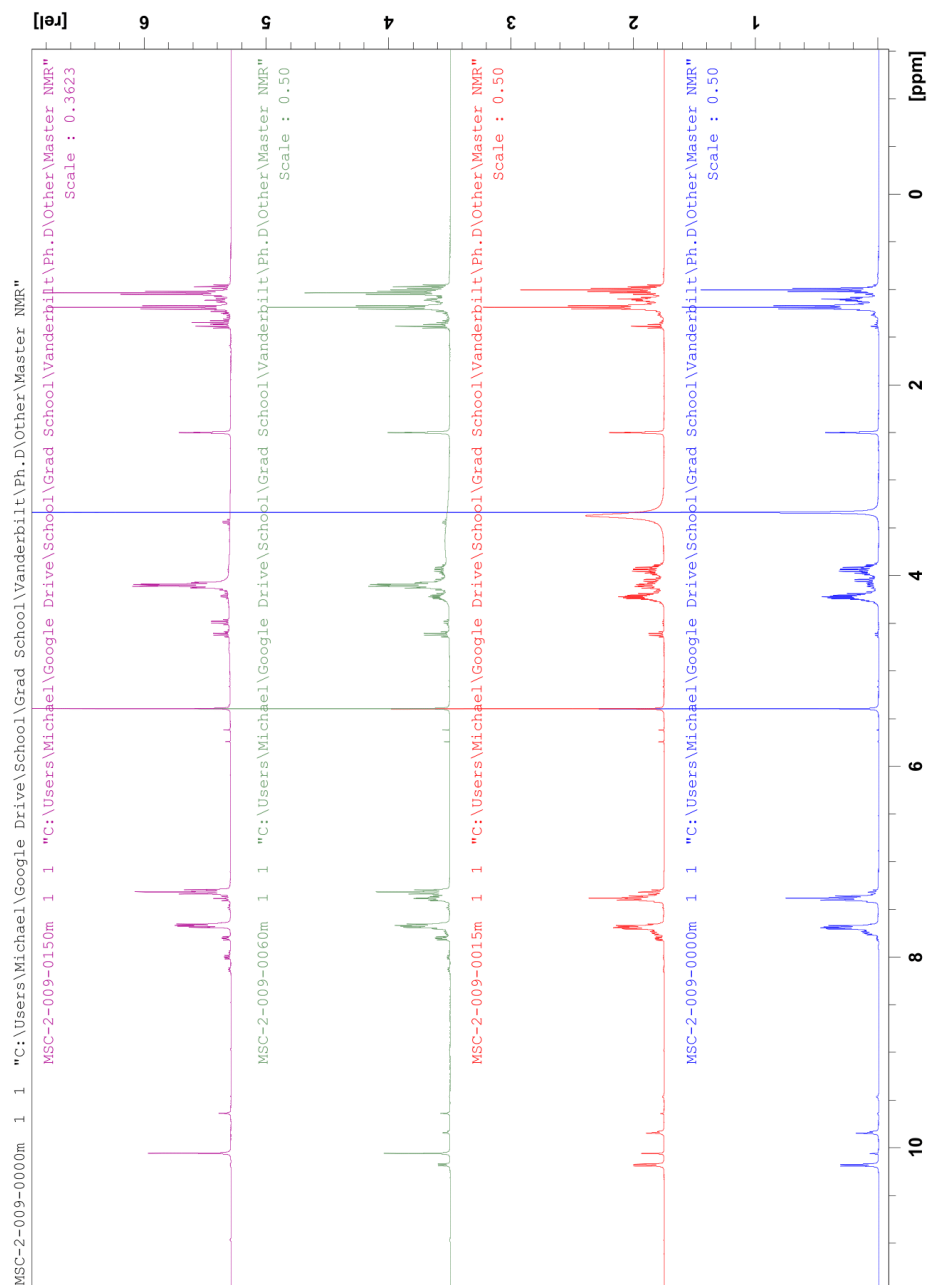


Figure 218. ^1H NMR (400 MHz, DMSO-d_6) of Conversion of **85c** in dry oxygenated solvent; $t = 0, 15, 60, 150$ minutes (bottom to top)

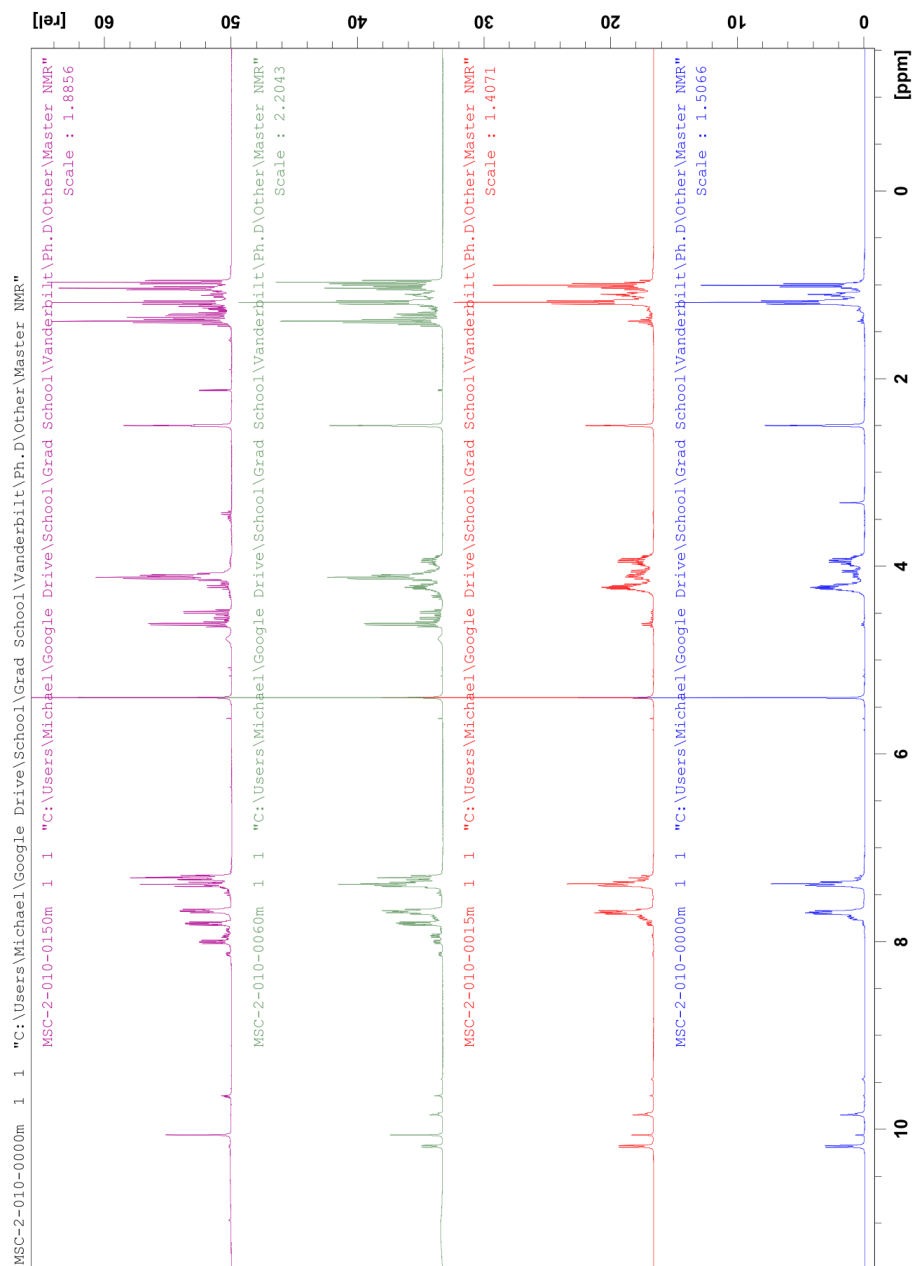


Figure 219. ^1H NMR (400 MHz, DMSO-d_6) of Conversion of **85d** in degassed solvent; $t = 0, 90, 360, 950$ minutes (bottom to top)

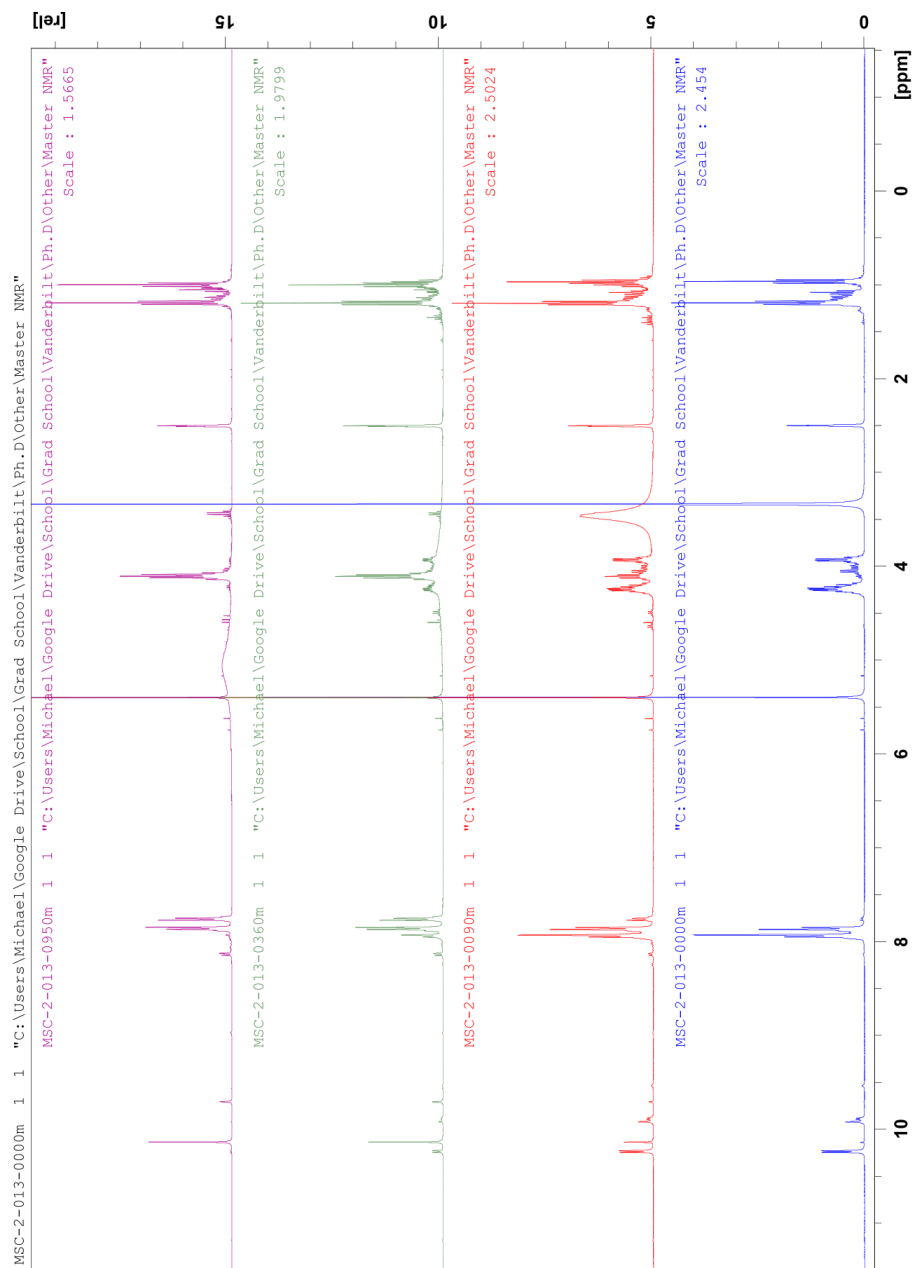


Figure 220. ^1H NMR (400 MHz, DMSO-d_6) of Conversion of **85e** in degassed solvent; t = 0, 90, 270, 520, 2240 minutes (bottom to top)

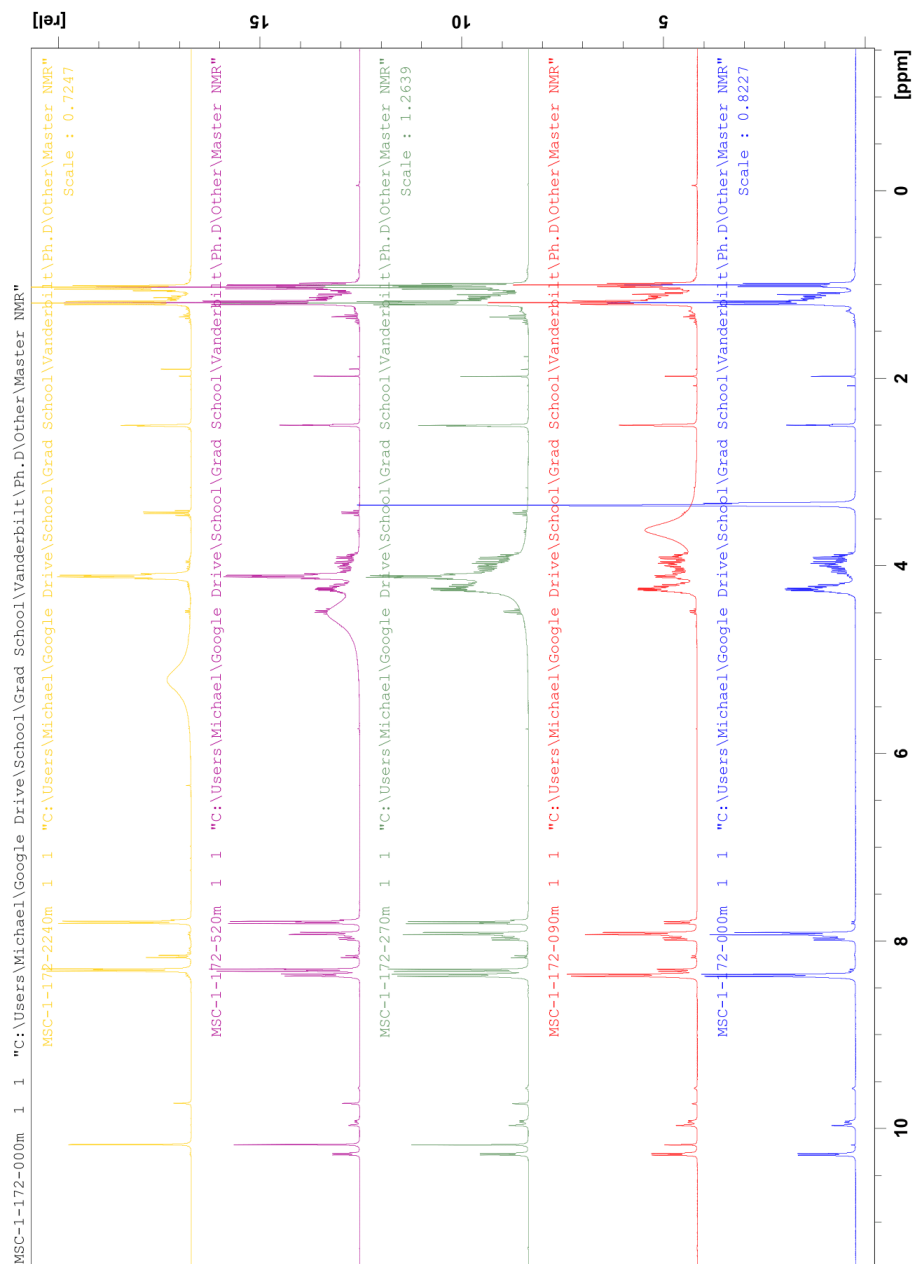
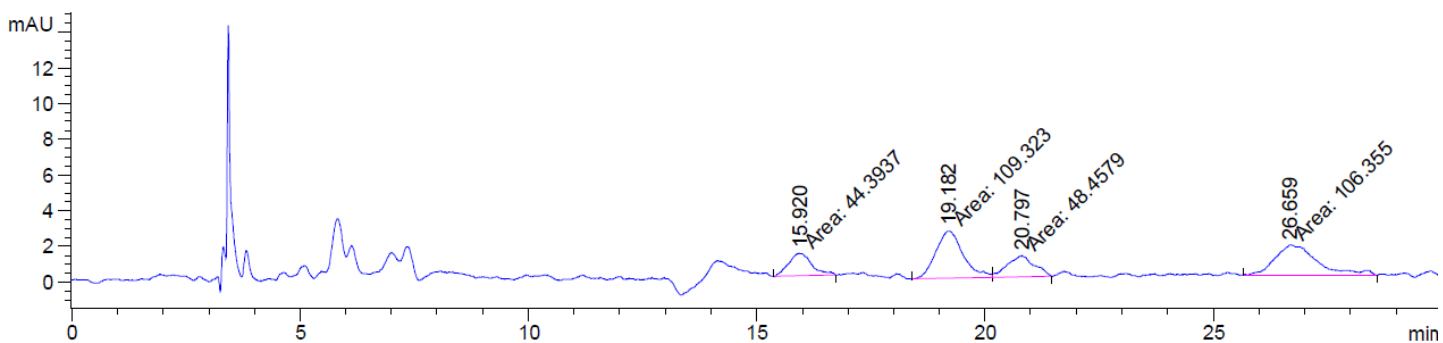


Figure 221. Selective ^1H NMR NOE on a mixture of **272** and **291** (600 MHz, CDCl_3) irradiating minor (purple, *Z*, 3% enhancement) and major (green, *E*, 3% enhancement) isomers with isolated minor (red, *Z*) and major (blue, *E*) for reference



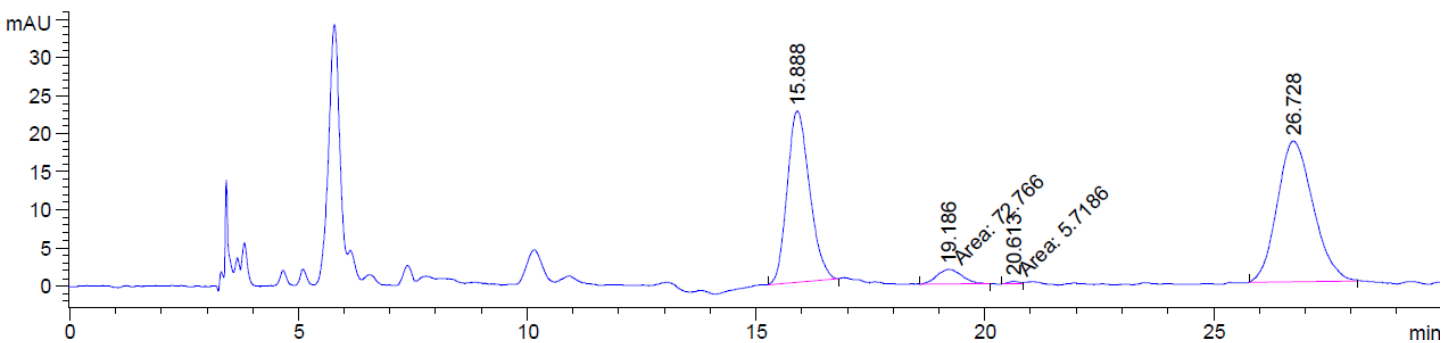
Figure 222. HPLC traces of **19** (racemic top; enantioenriched bottom)



Signal 3: DAD1 D, Sig=230,16 Ref=360,100

Peak #	RetTime [min]	Type	Width [min]	Area [mAU*s]	Height [mAU]	Area %
1	15.920	MM	0.5867	44.39373	1.26117	14.3888
2	19.182	MF	0.6896	109.32272	2.64234	35.4335
3	20.797	FM	0.6867	48.45794	1.17613	15.7061
4	26.659	MM	1.0540	106.35511	1.68183	34.4716

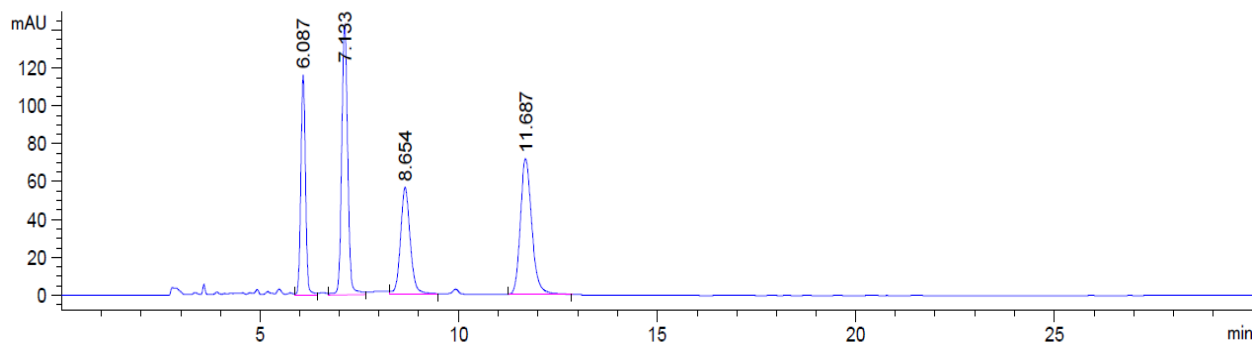
Totals : 308.52950 6.76147



Peak #	RetTime [min]	Type	Width [min]	Area [mAU*s]	Height [mAU]	Area %
1	15.888	BB	0.5182	767.50446	22.48567	41.2604
2	19.186	MM	0.6351	72.76604	1.90947	3.9118
3	20.613	MM	0.2672	5.71860	3.56729e-1	0.3074
4	26.728	BB	0.7181	1014.15668	18.54084	54.5203

Totals : 1860.14577 43.29270

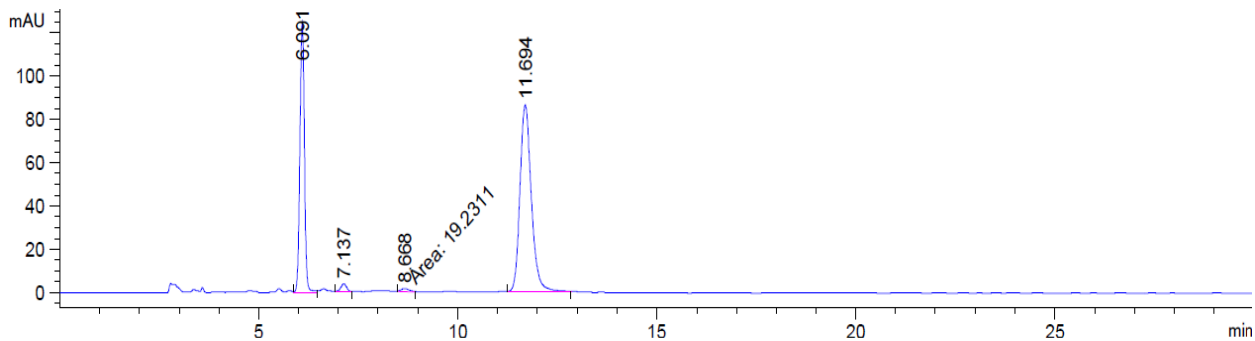
Figure 223. HPLC traces of **22** (racemic top; enantioenriched bottom)



Signal 3: MWD1 D, Sig=230,16 Ref=360,100

Peak #	RetTime [min]	Type	Width [min]	Area [mAU*s]	Height [mAU]	Area %
1	6.087	VV	0.1231	927.87726	116.30401	19.1642
2	7.133	VB	0.1595	1485.05945	142.55965	30.6721
3	8.654	VB	0.2632	982.23596	56.94144	20.2869
4	11.687	BB	0.3088	1446.55176	71.88275	29.8768

Totals : 4841.72443 387.68785

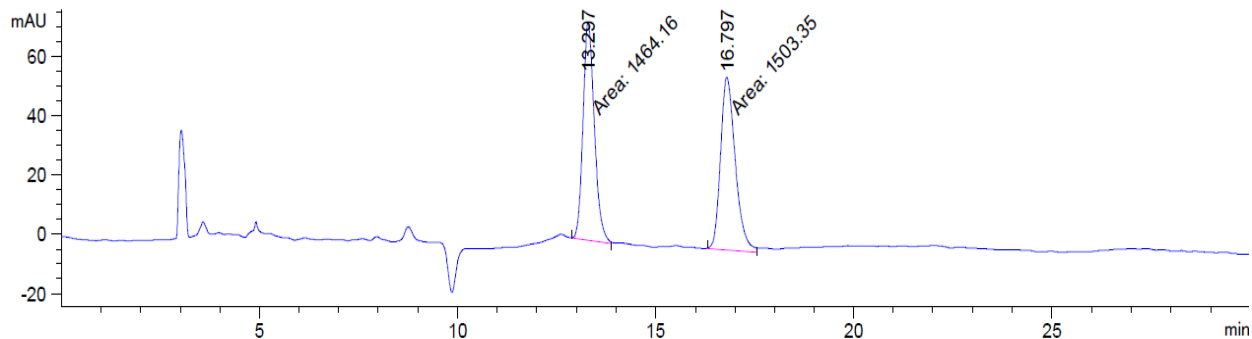


Signal 3: MWD1 D, Sig=230,16 Ref=360,100

Peak #	RetTime [min]	Type	Width [min]	Area [mAU*s]	Height [mAU]	Area %
1	6.091	VV	0.1242	986.92200	124.88849	35.6888
2	7.137	VV	0.1717	43.59702	3.86294	1.5765
3	8.668	MM	0.2463	19.23114	1.30136	0.6954
4	11.694	BB	0.3061	1715.60339	86.22401	62.0392

Totals : 2765.35355 216.27679

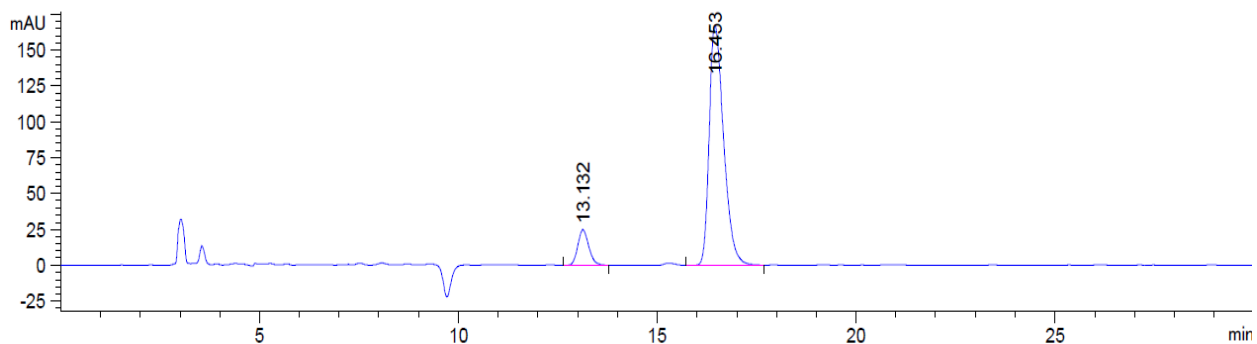
Figure 224. HPLC traces of **24** (racemic top; enantioenriched bottom)



Signal 3: MWD1 D, Sig=230,4 Ref=360,100

Peak #	RetTime [min]	Type	Width [min]	Area [mAU*s]	Height [mAU]	Area %
1	13.297	MM	0.3323	1464.15808	73.42778	49.3396
2	16.797	MM	0.4295	1503.35400	58.33090	50.6604

Totals : 2967.51208 131.75868

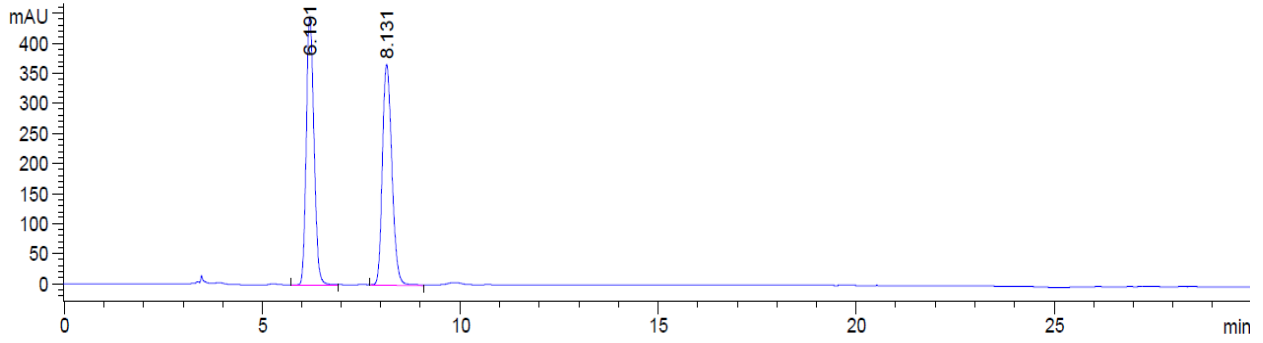


Signal 3: MWD1 D, Sig=230,4 Ref=360,100

Peak #	RetTime [min]	Type	Width [min]	Area [mAU*s]	Height [mAU]	Area %
1	13.132	VB	0.2950	473.96915	24.80183	10.0698
2	16.453	VB	0.3888	4232.86279	167.50143	89.9302

Totals : 4706.83194 192.30327

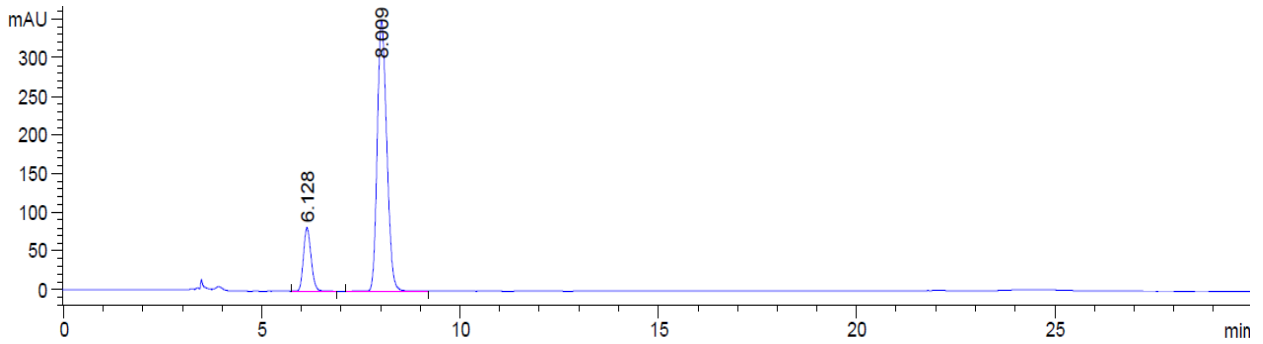
Figure 225. HPLC traces of **25** (racemic top; enantioenriched bottom)



Signal 3: DAD1 D, Sig=230,16 Ref=360,100

Peak #	RetTime [min]	Type	Width [min]	Area [mAU*s]	Height [mAU]	Area %
1	6.191	VB	0.2163	6091.75781	443.27155	49.7664
2	8.131	VB	0.2681	6148.93604	365.91440	50.2336

Totals : 1.22407e4 809.18594

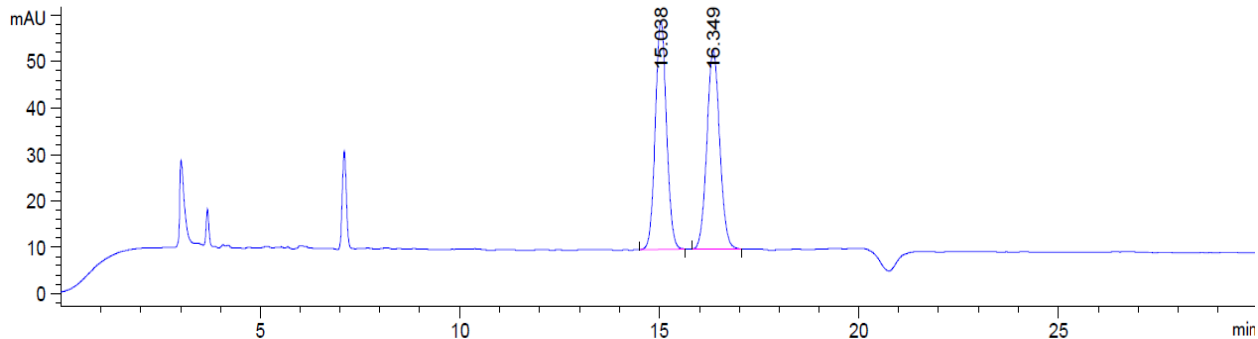


Signal 3: DAD1 D, Sig=230,16 Ref=360,100

Peak #	RetTime [min]	Type	Width [min]	Area [mAU*s]	Height [mAU]	Area %
1	6.128	VB	0.2069	1124.84363	82.57008	16.0354
2	8.009	BB	0.2684	5889.91064	349.83838	83.9646

Totals : 7014.75427 432.40845

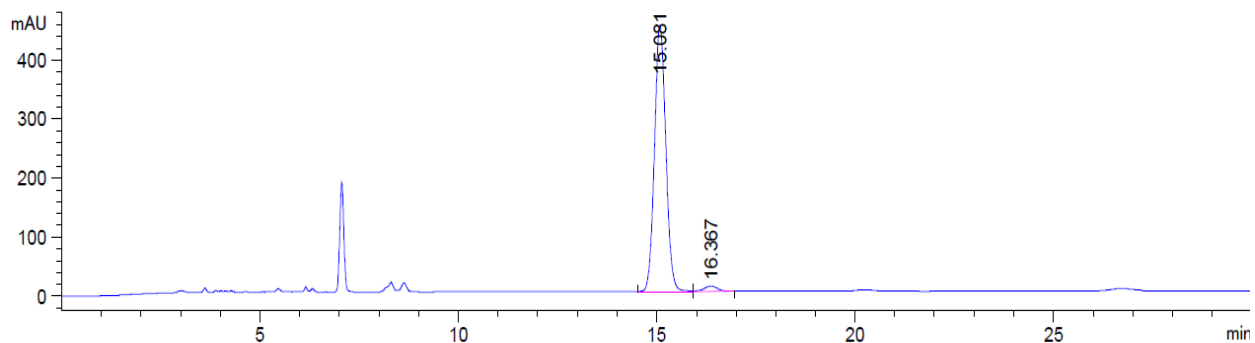
Figure 226. HPLC traces of **69** (racemic top; enantioenriched bottom)



Signal 3: MWD1 D, Sig=230,16 Ref=360,100

Peak #	RetTime [min]	Type	Width [min]	Area [mAU*s]	Height [mAU]	Area %
1	15.038	BB	0.3021	965.36786	49.37095	50.1379
2	16.349	BB	0.3473	960.05792	42.86669	49.8621

Totals : 1925.42578 92.23764

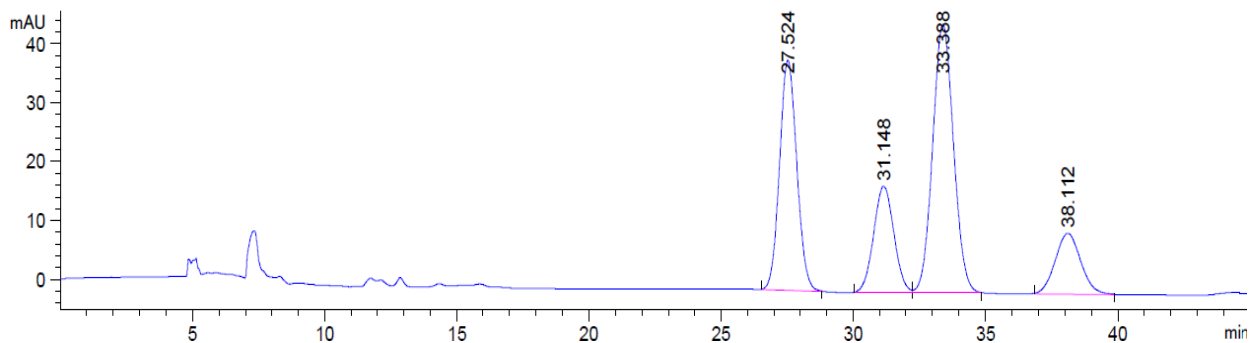


Signal 3: MWD1 D, Sig=230,16 Ref=360,100

Peak #	RetTime [min]	Type	Width [min]	Area [mAU*s]	Height [mAU]	Area %
1	15.081	BV	0.3077	8958.32129	451.12570	97.6781
2	16.367	VB	0.3583	212.94435	9.12247	2.3219

Totals : 9171.26564 460.24818

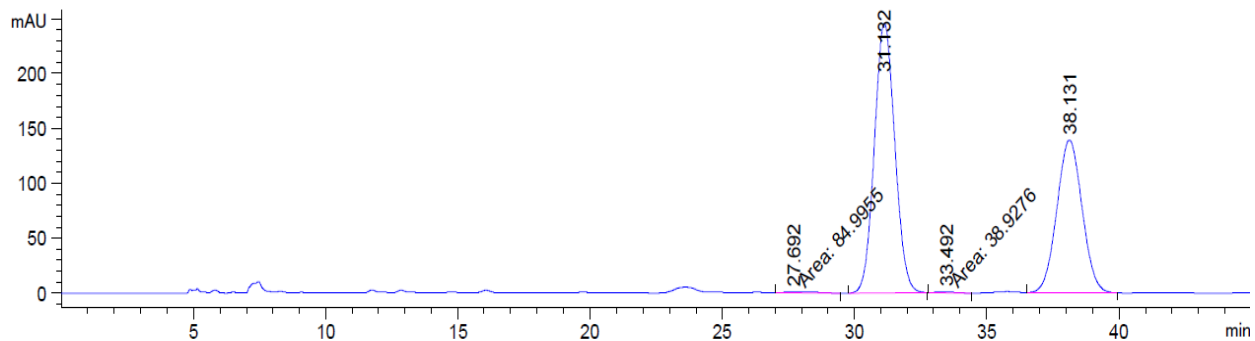
Figure 227. HPLC traces of **260** (racemic top; enantioenriched bottom)



Signal 3: MWD1 D, Sig=230,16 Ref=360,100

Peak #	RetTime [min]	Type	Width [min]	Area [mAU*s]	Height [mAU]	Area %
1	27.524	BB	0.7006	1768.23328	39.02407	29.8475
2	31.148	BV	0.8189	963.49896	18.04520	16.2637
3	33.388	VB	0.8551	2504.19873	45.57300	42.2704
4	38.112	BB	0.9800	688.30219	10.29463	11.6184

Totals : 5924.23315 112.93690

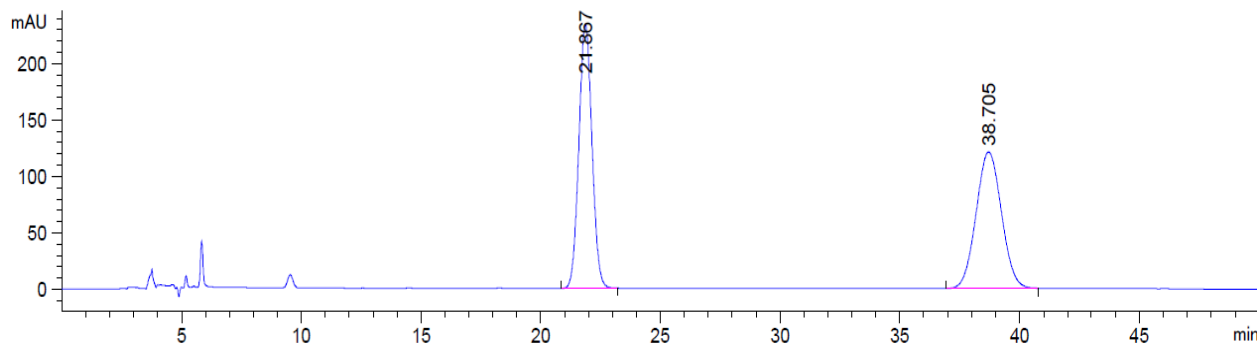


Signal 3: MWD1 D, Sig=230,16 Ref=360,100

Peak #	RetTime [min]	Type	Width [min]	Area [mAU*s]	Height [mAU]	Area %
1	27.692	MM	1.5180	84.99554	9.33180e-1	0.3761
2	31.132	BB	0.8374	1.32132e4	245.72008	58.4603
3	33.492	MM	0.8296	38.92765	7.82033e-1	0.1722
4	38.131	VB	1.0304	9264.89941	139.21654	40.9914

Totals : 2.26021e4 386.65183

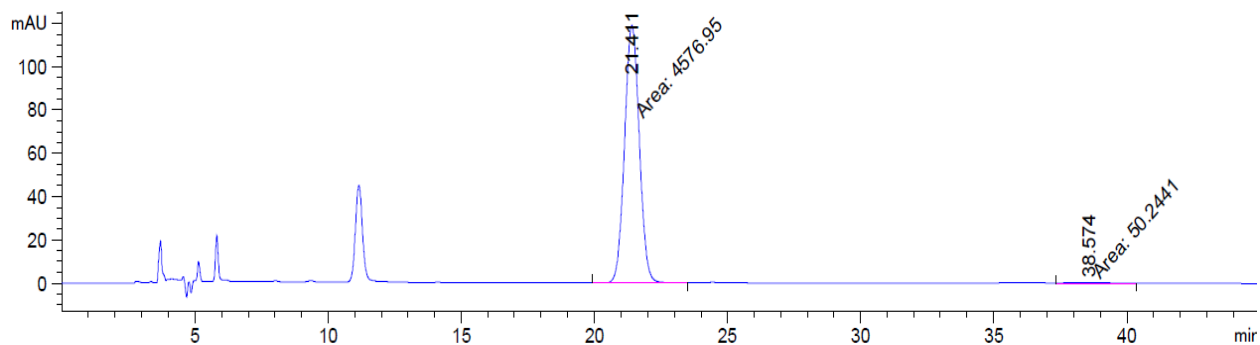
Figure 228. HPLC traces of **261** (racemic top; enantioenriched bottom)



Signal 1: MWD1 B, Sig=254,16 Ref=360,100

Peak #	RetTime [min]	Type	Width [min]	Area [mAU*s]	Height [mAU]	Area %
1	21.867	BB	0.5953	8955.94434	234.65605	50.0461
2	38.705	BB	1.1442	8939.43848	121.24214	49.9539

Totals : 1.78954e4 355.89819

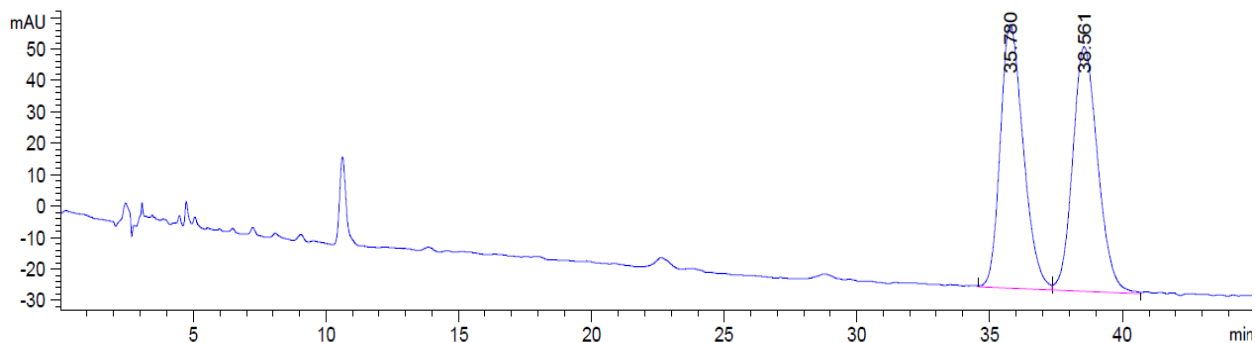


Signal 1: MWD1 B, Sig=254,16 Ref=360,100

Peak #	RetTime [min]	Type	Width [min]	Area [mAU*s]	Height [mAU]	Area %
1	21.411	MM	0.6405	4576.94971	119.08941	98.9142
2	38.574	FM	1.7177	50.24408	4.87526e-1	1.0858

Totals : 4627.19379 119.57693

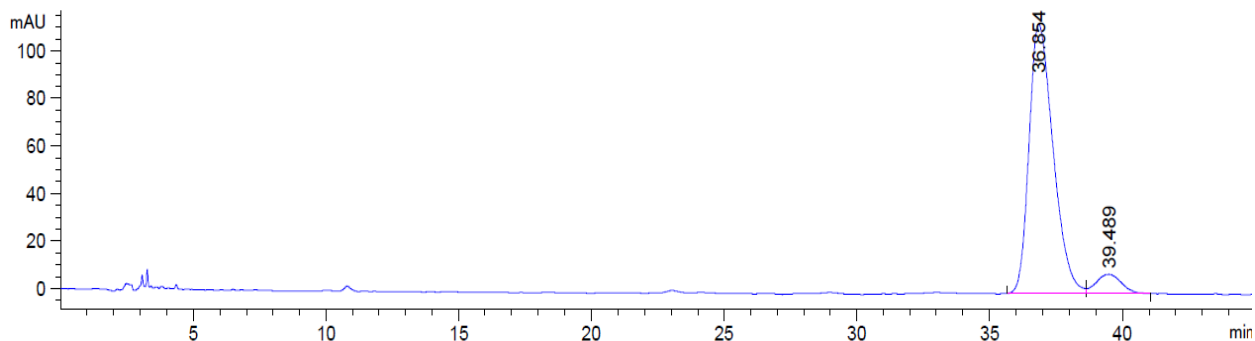
Figure 230. HPLC traces of **282** (racemic top; enantioenriched bottom)



Signal 3: MWD1 D, Sig=230,16 Ref=360,100

Peak #	RetTime [min]	Type	Width [min]	Area [mAU*s]	Height [mAU]	Area %
1	35.780	VV	0.9261	5075.76416	83.86234	49.7496
2	38.561	VV	1.0162	5126.86572	77.86403	50.2504

Totals : 1.02026e4 161.72637

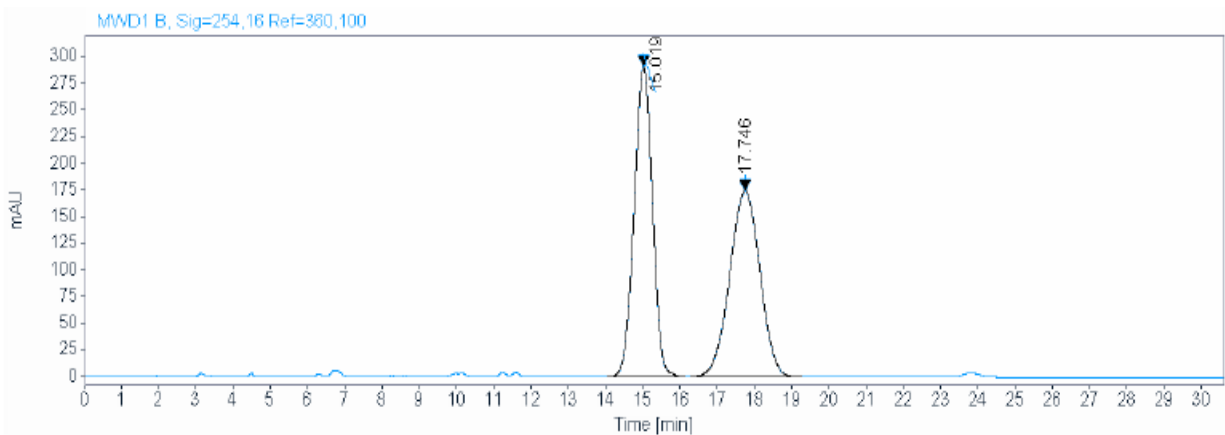


Signal 3: MWD1 D, Sig=230,16 Ref=360,100

Peak #	RetTime [min]	Type	Width [min]	Area [mAU*s]	Height [mAU]	Area %
1	36.854	BV	0.9758	7177.37549	113.49945	92.9098
2	39.489	VB	1.0193	547.72308	8.17861	7.0902

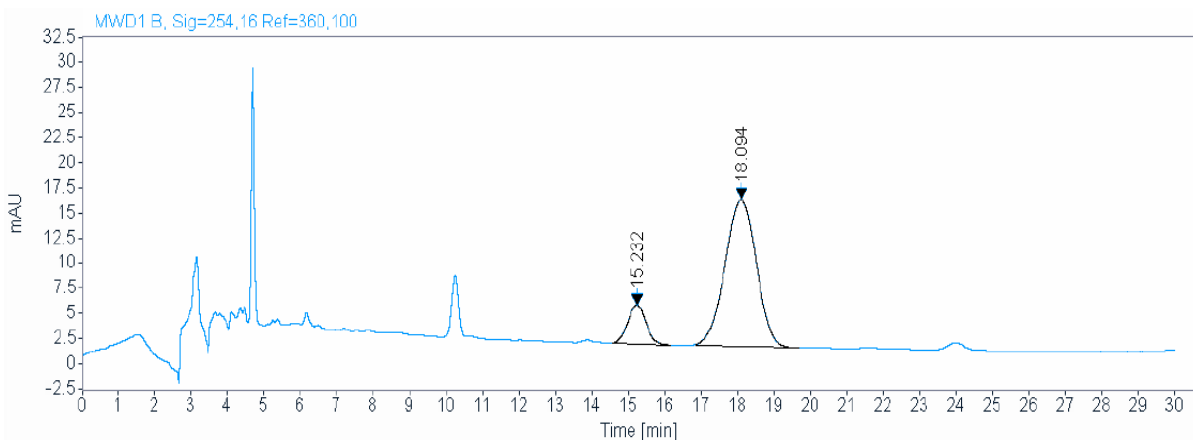
Totals : 7725.09857 121.67806

Figure 231. HPLC traces of **85e** (racemic top; t=0 min bottom)



Signal: MWD1 B, Sig=254,16 Ref=360,100

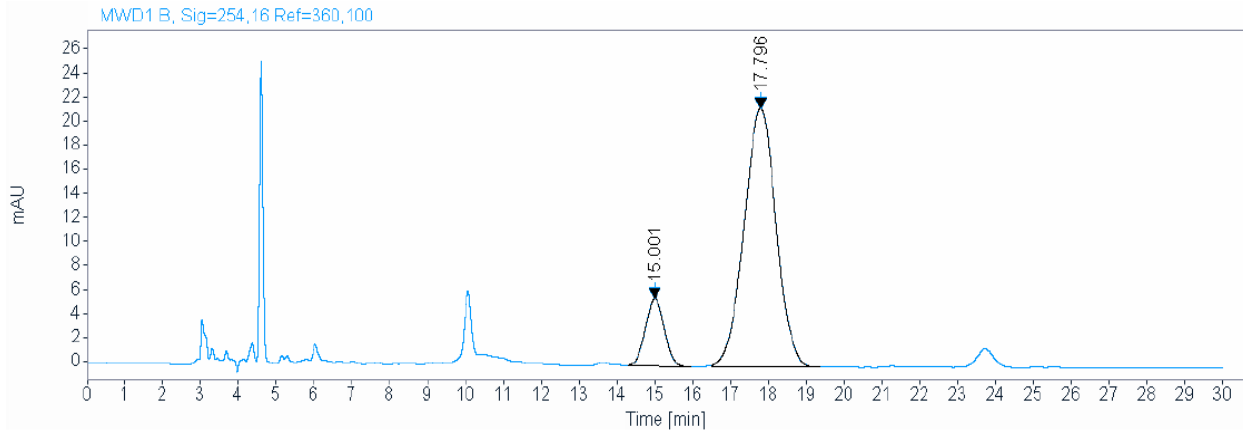
RT [min]	Type	Width [min]	Area	Height	Area%	Name
15.019	BB	0.5352	9975.0391	291.4989	50.1417	
17.746	BB	0.8907	9918.6523	174.6134	49.8583	
Sum			19893.6914			



Signal: MWD1 B, Sig=254,16 Ref=360,100

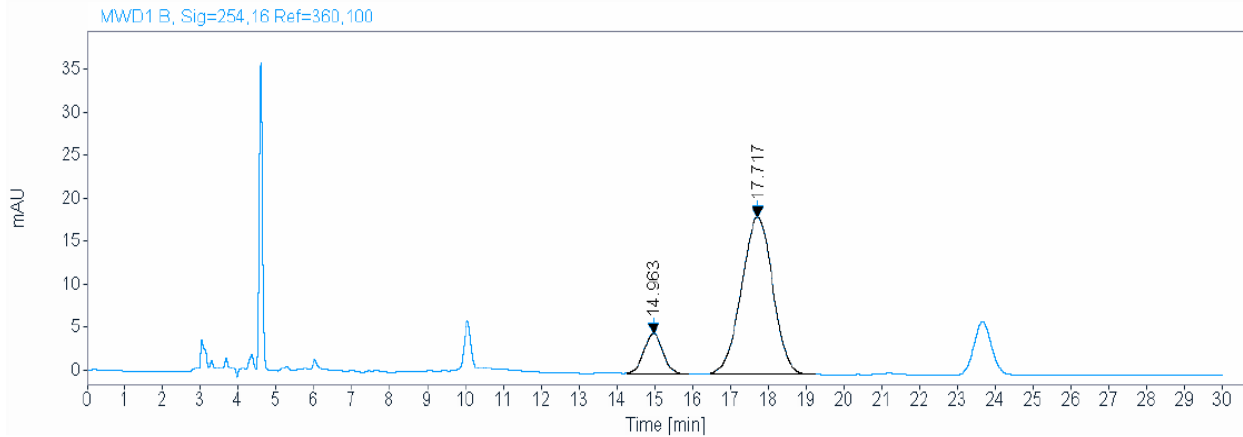
RT [min]	Type	Width [min]	Area	Height	Area%	Name
15.232	BB	0.5372	134.7093	3.8790	13.3844	
18.094	BB	0.9102	871.7538	14.5662	86.6156	
Sum			1006.4631			

Figure 232. HPLC traces of **85e** continued (t=20 top; t=140 min bottom)



Signal: MWD1 B, Sig=254,16 Ref=360,100

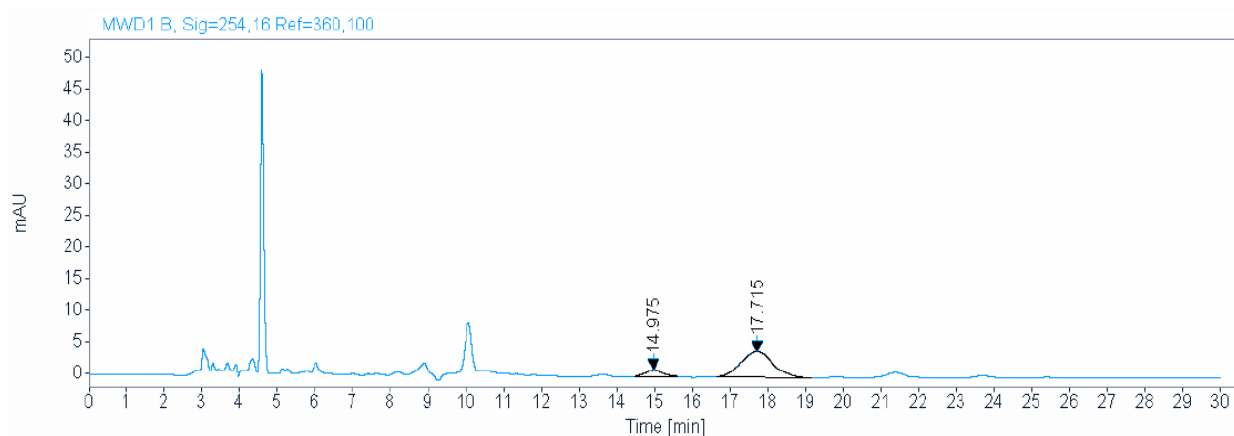
RT [min]	Type	Width [min]	Area	Height	Area%	Name
15.001	BB	0.5326	193.4166	5.5777	13.2719	
17.796	BB	0.9095	1263.9269	21.4498	86.7281	
Sum			1457.3435			



Signal: MWD1 B, Sig=254,16 Ref=360,100

RT [min]	Type	Width [min]	Area	Height	Area%	Name
14.963	BB	0.5448	164.6648	4.6767	13.5110	
17.717	BB	0.8981	1054.0822	18.2434	86.4890	
Sum			1218.7470			

Figure 233. HPLC traces of **85e** continued (t=1400 min)



Signal: MWD1 B, Sig=254,16 Ref=360,100

RT [min]	Type	Width [min]	Area	Height	Area%	Name
14.975	MF	0.5783	34.4762	0.9936	12.7585	
17.715	FM	0.9817	235.7455	4.0025	87.2415	
	Sum		270.2217			